

ADVANCES IN LATE TRANSITION METAL CATALYSIS, OLEFINATION REACTIONS AND APPLICATIONS

By KUNAL KESKAR, M.Sc.

A

Thesis Submitted to the School of Graduate Studies in
Partial Fulfilment of the Requirements for the
Degree of
Doctor of Philosophy

McMaster University © Copyright by Kunal Keskar, December 2014,
Hamilton, ON

McMaster University DOCTOR OF PHILOSOPHY (2014) Hamilton, Ontario
(Chemistry)

TITLE: Advances in Late Transition Metal Catalysis, Olefination Reactions and
Applications

AUTHOR: Kunal Keskar, M.Sc. (McMaster University, Canada and Pune
University, India)

SUPERVISOR: Professor James McNulty

NUMBER OF PAGES: XXIX, 299.

Abstract:

Two series of stable palladium and silver complexes ligated with hemilabile ligands were prepared. The stability, structure and application of these well-defined complexes in promoting various reactions (cycloaddition reactions, hydroamination reactions, cross-coupling reactions, etc.) was investigated.

A novel, well-defined silver (I) acetate complex, ligated to 2-diphenylphosphino-*N,N*-diisopropylcarboxamide, was prepared and characterized. Reactivity of this homogeneous complex was investigated and examples of the first purely silver catalyzed azide-alkyne cycloaddition (AgAAC) were discovered. The hemilabile nature of the ligand was observed to play a major role in this cycloaddition. Structure-activity studies with a series of related ligands revealed a pronounced ligand effect on the AgAAC reaction. The ligand 2-ditertiarybutylphosphino-*N,N*-diisopropylcarboxamide was identified as the most efficient ligand in the AgAAC reaction. The catalyst was found to be effective even at loadings as low as 0.5 mol%, permitting a regioselective synthesis of 1,4 triazoles in good yield. Additionally, this catalyst was found to be thermally stable with no silver mirror precipitation, commonly observed during silver(I) catalyzed thermal reactions.

A highly efficient method was developed for intramolecular hydroamination reactions of 2-alkynylanilines using AgOAc complexes of ligands such as 2-ditertiarybutylphosphino-*N,N*-diisopropylcarboxamide, leading to functionalized indole derivatives. The reactions were performed at low loadings (1.0 mol%) in benign solvents such as methanol at room temperature. These hydroamination reactions were observed to be first order with respect to the catalyst. Optimization on a series of related ligands allowed identification of a thermally stable homogeneous catalyst for the intramolecular hydroamination reaction.

The economical and readily available lactone phthalide was used as a building block for construction of a novel series of homologous hemilabile ligands. These ligands were isolated as their hydrohalide salts, which allowed for ease of handling and storage. Application of homogeneous Pd-complexes of these hemilabile ligands was investigated and they were found to be highly effective for the Suzuki-Miyaura cross-coupling reaction with sterically hindered, deactivated aryl chlorides.

The reaction of dimethyl acetals with trialkyl phosphine hydrobromide salt was found to give α -alkoxy phosphonium salts. The Wittig-type reaction of these α -alkoxy phosphonium salts with ethyl glyoxylate gave a series of methoxycinnamates in good yields. A highly efficient thermal cycloaddition of these methoxycinnamates with benzyl azides was carried out, yielding regioselective 1,4,5 trisubstituted cinnamyl-triazoles in good yields. A few of these triazoles displayed potent anticancer (aromatase) inhibitory activity up to 0.02 μ M.

A corresponding diethyl acetal, prepared from ethyl glyoxylate was found to react with a trialkylphosphonium hydrohalide salt yielding a related α -alkoxy phosphonium salt. The reaction of this functionalized phosphonium salt with a variety of aldehydes gave α -alkoxy acrylates. The α -alkoxy acrylate derived from paraformaldehyde was found to undergo an "On-Palladium" Heck-Jeffery-Amination cyclization sequence with a variety of *ortho*-iodoanilines. This process provided ready easy access to a series of differentially functionalized ethyl-2-indolecarboxylates. The mechanism was observed to be distinct from the usual Heck reaction and a catalytic cycle was proposed.

An efficient, diversity-oriented total synthesis of the cyanobacterial natural product nostodione A was developed in eight chemical steps and with 21.6% overall yield from ethyl-2-indolecarboxylates. The synthesis of a mini-panel of

structural analogs allowed for the discovery of anti-parasitic biological activity of nostodione A and its analogues for the first time.

Acknowledgements:

It would be impossible to write this thesis without the support of the many kind people around me.

First, I would like to express my sincere gratitude to my advisor Prof. James McNulty for allowing me to work in his group. I would like to thank him for his constant advice, guidance and motivation throughout this work. His extensive knowledge of chemistry has always been inspiring. I would also like to recognize the patience and understanding that Jim has shown towards me. I would like to thank the entire McNulty group (current and past) for their friendship and support over the past years, especially Ramesh, Carlos, David, Sean, Alex, Carla, Chanti, Venketesan, Janice, Priyabrata, Amol and Ehsan. I also enjoyed my time working with undergraduate students during my studies, especially Spencer, Mike, Angela and Rebecca

I would like to thank my committee members, Prof. Fred Capretta and Prof. Paul Harrison for their insightful reviews of my work. Their feedback and suggestions were always constructive. I am also thankful to the Department of Chemistry and Chemical Biology, McMaster University and Cytec Industries-Canada for providing funding for this work. I would also like to thank OGS-Canada for awarding me a scholarship during the 2013-2014 academic year.

Beyond my studies, I have been blessed with a huge circle of friends in my daily life that helped me to remain human during my time at Hamilton. They made my stay enjoyable and cherished. Special thanks go to my friends Amol, Aditi, Nishad, Prajyot, Manraj, Rahul, Chinar, Prasanna, Nilesh, Dharmesh and Yuvraj for being there for me. I am thankful to my mother, late father and brother for loving and supporting me all the way. I would like to appreciate the support shown by my in-laws and last but not least, I would like to thank my lovely wife,

Sneha, for being so understanding and patient. I am sure she now understands a few things related to practical organic chemistry due to my lengthy talks with her, trying to explain what went wrong in lab on a given day, when she would listen patiently to everything. I appreciate that.

Finally, I would like to share a saying that kept me motivated during these years. Gary Kirsten, the former Indian cricket coach, shared his thoughts on his ideal world. He said, *"I don't think life needs to be easy. Life needs to be challenging and that's how we keep ourselves alive... If life becomes easy, then you need to re-evaluate where you are in life. Life should be just living on the edge of your comfort zone... If it becomes easy, we stop thinking, we stop learning, we stop growing as people. If life becomes easy, it's a dangerous place to be."*

Table of Contents:

List of Schemes, Tables, Figures and Abbreviations.....	XIII
List of Publications.....	XXVI
Preface.....	XXVII

CHAPTER I: Introduction: Catalysis and the Wittig Reaction

1.1 Catalysis: Overview.....	1
1.1.1 Heterogeneous Catalysts.....	1
1.1.2 Homogeneous Catalysts.....	2
1.2 Transition Metals.....	3
1.3 Palladium.....	4
1.3.1 Pd(II)-Catalyzed Reactions.....	5
1.3.2 Pd(0)-Catalyzed Reactions.....	9
1.4 Ligand Effects in Homogeneous Pd(0)-Catalyzed Reactions.....	11
1.4.1 Suzuki-Miyaura Reaction.....	12
1.4.2 Buchwald-Hartwig Amination.....	17
1.5 Gold.....	23
1.5.1 Ligand Effects in Homogeneous Gold Catalysis.....	25
1.6 Multicatalysis.....	30
1.6.1 Merging Organocatalysis with Homogeneous Metal Catalysis.....	31
1.7 Silver.....	34

1.8 Homogeneous Silver Catalysis.....	38
1.8.1 Hemilabile Ligands: SHOP (Shell higher olefin process) Ligand.....	39
1.9 Objectives(I).....	42
1.10 The Wittig Reaction: Overview.....	42
1.11 Wittig Chemistry Development in McNulty Lab.....	47
1.12 Objectives(II).....	49
1.13 References.....	50

CHAPTER II: The first well-defined silver(I)-complex catalyzed cycloaddition of azides onto terminal alkynes at room temperature

2.1 Introduction.....	58
2.2 Results and Discussion.....	60
2.3 Conclusion.....	66
2.4 References.....	66
2.5 Experimental Section.....	69
2.6 NMR Spectra.....	76

CHAPTER III: Discovery of a robust and efficient homogeneous silver(I) catalyst for the cycloaddition of azides onto terminal alkynes

3.1 Introduction.....	96
3.2 Results and Discussion.....	97

3.3 Conclusion.....	104
3.4 References.....	104
3.5 Experimental Section.....	109
3.6 NMR Spectra.....	121

CHAPTER IV: A robust, well-defined homogeneous silver(I) catalyst for mild intramolecular hydroamination of 2-ethynylanilines leading to indoles

4.1 Introduction.....	132
4.2 Results and Discussion.....	134
4.3 Conclusion.....	141
4.4 References.....	142
4.5 Experimental Section.....	143
4.6 NMR Spectra.....	151

CHAPTER V: Phthalide: a direct building-block towards P,O and P,N hemilabile ligands: Application in the palladium-catalysed Suzuki-Miyaura cross-coupling of aryl chlorides

5.1 Introduction.....	166
5.2 Results and Discussion.....	168
5.3 Conclusion.....	173

5.4 References.....	174
5.5 Experimental Section.....	177
5.6 NMR Spectra.....	185

CHAPTER VI: Discovery of a new class of cinnamyl-triazole as potent and selective inhibitors of aromatase (cytochrome P450 19A1)

6.1 Introduction.....	203
6.2 Results and Discussion.....	205
6.3 Conclusion.....	208
6.4 References.....	210
6.5 Experimental Section.....	213
6.6 NMR Spectra.....	222

CHAPTER VII: A tandem “on-palladium” Heck-Jeffery Amination route toward the synthesis of functionalized indole-2-carboxylates

7.1 Introduction.....	228
7.2 Results and Discussion.....	229
7.3 Conclusion.....	237
7.4 References.....	238
7.5 Experimental Section.....	241
7.6 NMR Spectra.....	248

CHAPTER VIII: Total synthesis of the cyanobacterial metabolite nostodione A: discovery of its antiparasitic activity against *Toxoplasma gondii*

8.1 Introduction.....	259
8.2 Results and Discussion.....	260
8.3 Conclusion.....	268
8.4 References.....	269
8.5 Experimental Section.....	271
8.6 NMR Spectra.....	280
CHAPTER IX: Conclusion.....	297

List of Schemes, Figures and Tables

CHAPTER I: Schemes, Figures and Tables

Scheme 1-1. Examples of heterogeneous catalysis.....	2
Scheme 1-2. Examples of homogeneous catalysis.....	3
Scheme 1-3. Wacker oxidation.....	6
Scheme 1-4. Pd(II)-catalyzed intramolecular cyclization from alkenes.....	6
Scheme 1-5. Pd(II)-catalyzed intramolecular cyclization from alkynes.....	7
Scheme 1-6. SM cross-coupling reaction of 2,4-dibromobenzoic acid.....	16
Scheme 1-7. SM cross-coupling reaction of 1,2-dichloro-benzene.....	17
Scheme 1-8. Typical BHA reaction.....	18
Scheme 1-9. Buchwald's ligand for asymmetrical triarylamine synthesis.....	20
Scheme 1-10. Pd-catalyzed synthesis of annulated heterocycles.....	21
Scheme 1-11. Pd-catalyzed BHA in tandem with SM cross-coupling reactions.	22
Scheme 1-12. Synthesis of 2-bromoindoles, effect of $t\text{Bu}_3\text{P}$ ligand.....	23
Scheme 1-13. Gold-catalyzed cycloisomerization of 1,6-enyne.....	26
Scheme 1-14. Gold-catalyzed synthesis of 7- <i>exo-dig</i> vs 8- <i>endo-dig</i> cyclization.	26
Scheme 1-15. Gold-catalyzed cascade cyclization.....	27
Scheme 1-16. Gold-catalyzed Conia-ene cyclization.....	28
Scheme 1-17. Gold-catalyzed hydroamination: Inter- and intramolecular.....	28

Scheme 1-18. Au-catalyzed intermolecular addition of carboxylic acids to alkynes.....	29
Scheme 1-19. Crucial synthetic step: Neurymenolide-A synthesis.....	30
Scheme 1-20. Merging organocatalysis with gold catalysis.....	32
Scheme 1-21. Merging organocatalysis with Pd catalysis.....	32
Scheme 1-22. Merging organocatalysis with Pd catalysis: Introduction of asymmetry.....	33
Scheme 1-23. Silver(I) catalyzed activation of alkynes.....	34
Scheme 1-24. Silver(I) catalyzed activation of alkenes.....	35
Scheme 1-25. Ag(I) catalyzed three component coupling reaction.....	36
Scheme 1-26. Role of Ag(I) catalyst in Sonogashira reaction.....	37
Scheme 1-27. Homogeneous AgX catalysis with hemilabile ligands: Mechanism of action.....	41
Scheme 1-28. Vitamin A acetate synthesis.....	43
Scheme 1-29. Use of trialkylphosphines in the Wittig reaction.....	47
Figure 1-1. Cross-coupling reaction: Types and general mechanism.....	10
Figure 1-2. Examples of ligands used in SM cross-coupling reactions.....	14
Figure 1-3. Buchwald's ligands: Monoarylation of ammonia.....	19
Figure 1-4. Examples of ligands used in BHA reactions.....	21
Figure 1-5. Organocatalysis, mode of reactivity: Enamine and iminium activation.....	31

Figure 1-6. SHOP ligand and mode of reactivity of hemilabile ligands.....	40
Figure 1-7. General Wittig reaction.....	43
Figure 1-8. Mechanism of Wittig reaction.....	44
Figure 1-9. Vedejs's model explaining the stereochemical outcome of the Wittig reaction.....	46
Figure 1-10. Dichotomous reactivity of dialkyl vs. diaryl-phosphonium salts with dimethyl acetals.....	48

CHAPTER II: Schemes, Figures and Tables

Scheme 2-1. Previous work on Ag (I) catalyzed AAC reaction. a) AAC reaction in the presence of Cu^{I} . b) Ag^{I} -mediated AAC reaction. c) Other Ag (I)-catalyzed AAC reaction.....	59
Scheme 2-2. Synthesis of the SHOP amide: AgOAc (1:1) complex 5 and ORTEP plot (lower).....	60
Scheme 2-3. Silver-catalyzed AAC reaction.....	61
Scheme 2-4. AgAAC reaction with deuterium labelling.....	65
Scheme 2-5. Silver phenylacetylide control reactions under the standard condition.....	65
Figure 2-1. Generally accepted mechanism for the copper(I)-catalyzed azide-alkyne cycloaddition (AAC) reaction.....	58
Table 2-1. Scope of azide participation in the Ag-AAC reaction.....	62
Table 2-2. Scope of the alkyne participation in the Ag-AAC reaction.....	63

CHAPTER III: Schemes, Figures and Tables

Scheme 3-1. Synthesis of AgOAc complexes of ligands 5e and 5g (top) and ball and stick plots of 6e (CCDC 843618) and 6g (CCDC 882589) (bottom).....	103
Scheme 3-2. Proposed catalytic cycle for the homogeneous Ag(I)-catalyzed AAC reaction.....	103
Figure 3-1. The general CuAAC reaction.....	96
Figure 3-2. Scope of the aryl alkyne in AgAAC reaction.....	100
Table 3-1. Pronounced ligand effects on the AgAAC reaction.....	98
Table 3-2. Optimization with catalyst 6g in the AgAAC reaction.....	99

CHAPTER IV: Schemes, Figures and Tables

Scheme 4-1. Postulated reactivity of homogeneous silver(I)-promoted alkyne hydroamination.....	134
Scheme 4-2. General method for preparation of aminoalkynes.....	137
Figure 4-1. Ligand optimization (top) identifying complex D as optimal (100% conversion after 2.5 h) and kinetic data for complexes A , D (three concentrations) and comparison with the heterogeneous AgOAc promoted reaction, room temp. in methanol.....	135
Figure 4-2. Postulated catalytic cycle for the hemilabile ligand accelerated intramolecular hydroamination promoted by catalyst D	140
Table 4-1. Silver salt-promoted intramolecular hydroamination.....	133
Table 4-2. Scope of the homogeneous intramolecular hydroamination of 2-alkylanilines promoted with 1.0 mol-% complex D at room temperature.....	138

Figure 4-3. Photographs taken after the hydroamination reaction in toluene showing silver metal deposition in the heterogeneous reactions (A and B) but not in the homogeneous reaction (C).....	143
---	-----

CHAPTER V: Schemes, Figures and Tables

Scheme 5-1. Synthesis of P,O & P,N-type hemilabile ligands from phthalide 1 ...	168
Scheme 5-2. Synthesis of ligand 3b from <i>N,N</i> -diisopropyl-benzamide.....	169
Figure 5-1. Hemilabile Examples of P,O and P,N type ligands employed in metal-mediated cross-coupling and other processes.....	167
Table 5-1. SM cross coupling reaction of chlorobenzene with Pd-complexes of ligand 2	170
Table 5-2. Screening phthalide-derived ligands 3a-3d in the Suzuki-Miyaura cross coupling reaction.....	171
Table 5-3. SM cross coupling reaction of aryl halides with ligand 3c	172

CHAPTER VI: Schemes, Figures and Tables

Scheme 6-1. Synthesis of alkoxyphosphonium salts 14a-14h	206
Figure 6-1. Structures of currently used AIs 1-3 , and the SERM agent tamoxifen 4 . Example of aromatase conversion of 5 to 6 and structure of recently described potent AIs 7 employing aryl halide ketone bioisosteres.....	203
Figure 6-2. Cinnamyl-triazole core structure 8 and retrosynthetic analysis based on the Wittig reaction of alkoxyphosphonium salt 12	204
Table 6-1. Conversion of α -methoxy phosphonium salts to β -methoxycinnamate “alkyne equivalents”	206

Table 6-2. Regiocontrolled thermal Huisgen cycloaddition of benzyl azides onto β -methoxycinnamates leading to potent Als.....	209
--	-----

CHAPTER VII: Schemes, Figures and Tables

Scheme 7-1. Synthesis of α -alkoxyacrylates and cinnamates using functionalized ylides.....	229
Scheme 7-2. Annulation of ortho-iodoanilines with alkoxy acrylate 3 via a standard Heck and the tandem “on-palladium” Heck-Jeffery-amination process (isolated yields given).....	230
Scheme 7-3. Proposed catalytic cycle for annulation of ortho-iodoanilines with alkoxy acrylate 3 via the tandem “on-palladium” heck-Jefferey-amination process.....	231
Scheme 7-4. Independent synthesis of the α -ethoxy cinnamate 5 and conversion to 6 thermally and under Heck-Jeffery-Amination conditions.....	234
Scheme 7-5. Scope of olefination reaction with phosphonium salt 2	247
Table 7-1. Optimization of the Heck-Jeffery-amination process for the synthesis of indole-2-carboxylate 7	233
Table 7-2. Synthesis of functionalized Indole-2-carboxylates.....	236

CHAPTER VIII: Schemes, Figures and Tables

Scheme 8-1. Synthesis of the 3-oxalyl-indole-2-phosphonomethyl intermediates (13) and (14).....	262
Scheme 8-2. Completion of the synthesis of nostodione A (1) employing the HWE strategy.....	264
Figure 8-1. Structure of the cyanobacterial secondary metabolite nostodione A (1) and related biosynthetic alkaloids.....	260

Figure 8-2. Retrosynthetic analysis of nostodione A (1).....	261
Figure 8-3. Quantification of invasion inhibition of nostodione A and mini panel using red/green assay.....	268
Table 8-1. Optimization of the intramolecular phosphonate acylation.....	262
Table 8-2. Assembly of nostodione A mini-panel (1) and (17)-(22) via the HWE strategy and anti-toxoplasmosis biological activity.....	266

List of Abbreviations:

AAC = Azide-Alkyne Cycloaddition

Ac₂O = acetic anhydride

AgOTf = silver triflate

AgOAc = silver(I) acetate

AgI = silver(I) iodide

AgNO₃ = silver(I) nitrate

AgClO₄ = silver(I) perchlorate

Ag₂O = silver(I) oxide

Ag₂CO₃ = silver(I) carbonate

AgOSO₂CF₃ = silver triflate

Ag₂SO₄ = silver sulphate

AgAAC = Silver(I) catalyzed Azide-Alkyne Cycloaddition

AI = aromatase inhibitor

AlCl₃ = aluminum(III) chloride

AuCl = gold(I) chloride

AuCl₃ = gold(III) chloride

BHA = Buchwald-Hartwig Amination

BINAP = (2,2'-bis(diphenylphosphino)-1,1'-binaphthyl)

Boc = tert-butoxycarbonyl

CaCO_3 = calcium carbonate

CCDC = Cambridge Crystallographic Data Centre

CDCl_3 = deuterated chloroform

CH_2Cl_2 = dichloromethane

CI = chemical ionization

Cs_2CO_3 = cesium carbonate

CO = carbon monoxide

CO_2 = carbon dioxide

$(\text{COCl})_2$ = oxalyl chloride

CuCl_2 = copper(II) chloride

CuI = copper(I) iodide

CuAAC = Copper(I) catalyzed Azide-Alkyne Cycloaddition

CsF = cesium Fluoride

CYTOP-292 = 1,3,5,7-tetramethyl-6-phenyl-2,4,8-trioxa-6-phosphaadamantane

de = diastereomeric excess

DFT = Density Functional Theory

DIBAL-H = diisobutylaluminium hydride

DMF = dimethylformamide

DMSO-d_6 = deuterated dimethyl sulphoxide

DPEPhos = bis[(2-diphenylphosphino)phenyl] ether

Et_2Zn = diethyl zinc

EtOH = ethanol

Et_2O = diethylether

EtOAc = ethyl acetate

ee = enantiomeric excess

EI = electron ionization

ES+/ESI+ = Electrospray Mass Spectrometry, positive mode

H_2O = water

HBr = hydrobromic acid

HCl = hydrochloric acid

$\text{Hg}(\text{OAc})_2$ = mercury(II) acetate

Hunigs base = diisopropylethylamine

HOAc = acetic acid

HMPA = hexamethyl phosphoramidate

HJA = Heck-Jeffery Amination

HWE = Horner–Wadsworth–Emmons reaction

IC_{50} = The concentration of an inhibitor that is required for 50% inhibition of an enzyme in vitro.

K_3PO_4 = potassium phosphate

K_2CO_3 = potassium carbonate

KF = potassium fluoride

KI = potassium iodide

LDA = lithium diisopropylamide

LHMDS = lithium bis(trimethylsilyl)amide

LiOH = lithium hydroxide

MeNO₂ = nitromethane

MeCN/ACN = acetonitrile

M.P. = melting point

MeOH = methanol

NMP = N-methyl pyrrolidine

Na/KO^tBu = sodium/Potassium tertiary butoxide

NaOH = sodium hydroxide

NaH = sodium hydride

NaBH₄ = sodium borohydride

NaOAc = sodium acetate

NaHCO₃ = sodium hydrogen carbonate

NH₄Cl = ammonium Chloride

NCS = N-chloro succunamide

nM = nanomolar

*n*BuLi = *n*-Butyllithium

OPA = oxaphosphetane

PtO₂ = platinum dioxide

Pd = palladium

PdOAc₂ = palladium(II) acetate

PdCl₂ = palladium (II) chloride

PhMe = toluene

PMB = *p*-Methoxybenzyl bromide

*p*TSA = *p*-toluenemethane sulphonic acid

PCy₃ = tricyclohexylphosphine

Pd₂(dba)₃ = tris(dibenzylideneacetone)dipalladium(0)

PPh₃ = triphenylphosphine

P \ddot{y} = pyridine

P(OMe)₃ = trimethyl phosphite

PBr₃ = phosphorous(III) bromide

SHOP = Shell Higher Olefin Process

SM = Suzuki-Miyaura cross-coupling

THF = tetrahydrofuran

TEA/Et₃N = triethylamine

Tol-d₈ = deuterated toluene

TsCl = tosyl chloride

TS = transition state

TMS = tetramethylsilane

TBAF = tetra butyl ammonium fluoride

TBAB = tetra butyl ammonium bromide

$t\text{Bu}_3\text{P}$ = tributylphosphine

$t\text{Bu}_2\text{PH}$ = ditertiarybutylphosphine

TLC = Thin Layer Chromatography

Xantphos = 4,5-Bis(diphenylphosphino)-9,9-dimethylxanthene

ZnBr_2 = Zinc(II) bromide

μM = micromolar

List of Publications:

This thesis is based on the following papers, which are referred to by their Roman numerals. Reprints were made with permission from the publishers. These are attached at the beginning of each chapter where applicable

- I. "The First Well-Defined Silver(I)-Complex-Catalyzed Cycloaddition of Azides onto Terminal Alkynes at Room Temperature"- ***Chemistry – A European Journal***, 2011, 17, 14727–14730.- James McNulty, Kunal Keskar and Ramesh Vemula.
- II. "Discovery of a Robust and Efficient Homogeneous Silver(I) Catalyst for the Cycloaddition of Azides onto Terminal Alkynes"- ***European Journal of Organic Chemistry***, 2012, 5462-5470.- James McNulty and Kunal Keskar.
- III. "A Robust, Well-Defined Homogeneous Silver(I) Catalyst for Mild Intramolecular Hydroamination of 2-Ethynylanilines Leading to Indoles."- ***European Journal of Organic Chemistry***, 2014, 1622-1629.- James McNulty and Kunal Keskar.
- IV. "Phthalide: a direct building-block towards P,O and P,N-hemilabile ligands: Application in the palladium-catalysed Suzuki-Miyaura cross-coupling of aryl chlorides."- ***Organic Biomolecular Chemistry***, 2013, 11, 2404-2407.- James McNulty and Kunal Keskar.
- V. "Discovery of a new class of cinnamyl-triazole (from alkoxy cinnamates) as a potent and selective inhibitors of aromatase (cytochrome P450 19A1)"- ***Bioorganic & Medicinal Chemistry Letters***, 2014, 24, 4586-4589.- James McNulty, Kunal Keskar, Dennis J. Crankshaw and Alison C. Holloway.

- VI. "A Tandem "On-Palladium" Heck–Jeffery Amination Route Toward the Synthesis of Functionalized Indole-2-carboxylates"- ***European Journal of Organic Chemistry***, **2011**, 6902–6908."- James McNulty and Kunal Keskar.
- VII. "Total synthesis of the cyanobacterial metabolite Nostodione: discovery of its antiparasitic and anti-invasion activity to *Toxoplasma gondii*."- ***Chemical Communications***, **2014**, 50, 8904-8907.- James McNulty, Kunal Keskar, Lorraine Jones-Brando, Claudia Bordón and Robert Yolken.
- VIII. "High Yielding Synthesis of Carboranes Under Mild Conditions Using a Homogeneous Silver(I) Catalyst. Direct Evidence of a Bimetallic Intermediate." - ***Angewandte. Chemie. International. Edition***, 2014, 53, 5156-5160.- Mohamed E. El-Zaria, Kunal Keskar, Afaf R. Genady, Joseph A. Ioppolo, James McNulty and John F. Valliant. (**Highlighted in Synfacts**: A Mild Method to Access Functionalized Carboranes. ***Synfacts*** **2014**, 10(6), 585). (*Work described in this publication is not included in the thesis*)

Preface:

1. The research reported in chapter 2 was published in 2011: McNulty, J., Keskar, K., and Vemula, R. "The First Well-Defined Silver(I)-Complex-Catalyzed Cycloaddition of Azides onto Terminal Alkynes at Room Temperature., *Chem. Eur. J.* **2011**, 17 (52), 14727-14730." I performed all the synthesis, purification and characterization of compounds reported in this chapter. Dr. R. Vemula synthesized the complex **5** (**Scheme3, Chapter 1**) for the first time in our laboratory. X-Ray crystallographic analysis was performed by Dr. Hilary Jenkins, McMaster University.
2. The research reported in chapter 3 was published in 2012: McNulty, J., and Keskar, K. "Discovery of a Robust and Efficient Homogeneous Silver(I) Catalyst for the Cycloaddition of Azides onto Terminal Alkynes., *Eur. J. Org. Chem.* **2012**, 5462-5470." I performed all the synthesis, purification and characterization of compounds reported in this chapter. X-Ray crystallographic analysis was performed by Dr. Hilary Jenkins, McMaster University.
3. The research reported in chapter 4 was published in 2014: McNulty, J., Keskar, K. "A Robust, Well-Defined Homogeneous Silver(I) Catalyst for Mild Intramolecular Hydroamination of 2-Ethynylanilines Leading to Indoles., *Eur. J. Org. Chem* **2014**, 1622-1629." I performed all the synthesis, purification and characterization of compounds reported in this chapter.
4. The research reported in chapter 5 was published in 2013: McNulty, J., and Keskar, K. "Phthalide derived new ligands and Their Pd Catalyzed Efficient Suzuki Cross-Coupling reactions with Aryl Chlorides. *Org. Biomol. Chem.* **2013**, 11, 2404-2407." I performed all the synthesis, purification and characterization of compounds reported in this chapter.

5. The research reported in chapter 6 was published in 2014: McNulty, J., Keskar, K., Crankshaw, D. J., Holloway, A. C. "Discovery of a new class of cinnamyl-triazole (from alkoxy cinnamates) as a potent and selective inhibitors of aromatase (cytochrome P450 19A1), *Bioorg. Med. Chem. Lett.* **2014**, 24, 4586-4589." I performed all the synthesis, purification and characterization of compounds reported in the article. The biological activities were measured by Dr. D. Crankshaw and Dr. A. C. Holloway, McMaster University.
6. The research reported in chapter 7 was published in 2011: McNulty, J. and Keskar, K. "A Tandem "On-Palladium" Heck-Jeffery Amination Route Toward the Synthesis of Functionalized Indole-2-carboxylates. *Eur. J. Org. Chem.* **2011**, 6902–6908." I performed all the synthesis, purification and characterization of compounds reported in this article.
7. The research reported in chapter 8 was published in 2014: McNulty, J., Keskar, K., Bordón, C., Yolken R., Jones-Brando, L. "Total synthesis of the cyanobacterial metabolite Nostodione A: discovery of its antiparasitic and anti-invasion activity to *Toxoplasma gondii*., *Chem. Commun.* **2014**, 50, 8904-8907." I performed all the synthesis, purification and characterization of compounds reported in the article. The biological activities were measured by C. Bordón, R. Yolken and L. Jones-Brando at John Hopkins University School of Medicine, Baltimore, USA.

CHAPTER I: Introduction to Catalysis and Wittig reaction

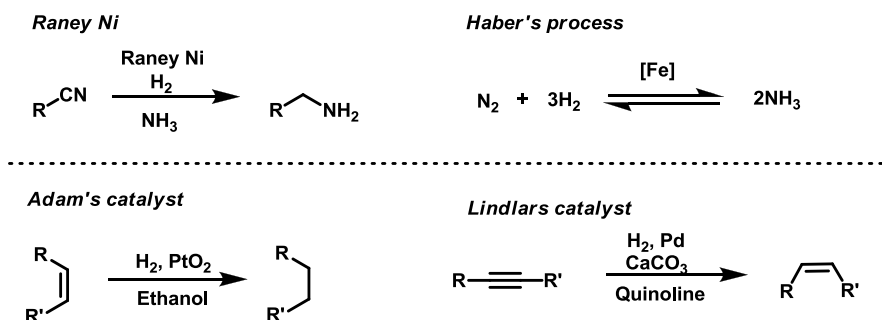
1.1 Catalysis

“Catalysis” is the term coined by Berzelius to describe the process by which the rate of a chemical reaction is increased through the use of a non-stoichiometric amount of a facilitator known as the “catalyst.” The catalyst itself does not undergo any permanent change during the catalytic process. A catalyst provides an alternate route for the reaction, which has a lower activation energy. Catalysts themselves can be categorized as homogeneous or heterogeneous based on their solubility in the reaction medium in question.¹

1.1.1 Heterogeneous Catalysts

Heterogeneous catalysts are those that remain completely insoluble in the reaction media. Heterogeneous catalysts have certain advantages, the main ones being their easy separation from the reaction media and the fact that they are often economical, have good thermal stability and can often be reused with little processing. Although they are a popular choice for use in industry, there are several disadvantages associated with their use.¹ Active sites are poorly defined and not distributed uniformly on the catalyst surface, therefore there is a lack of control over the reaction site which can make it difficult to obtain the desired product, can affect reproducibility, and limits applicability to asymmetric catalysis.² Early examples of successful heterogeneous catalysts and processes include the Raney nickel catalyzed reduction of nitriles into their corresponding amines in the presence of ammonia (**Scheme 1-1, top left**) and Haber’s process in producing ammonia using hydrogen and nitrogen in the presence of an iron catalyst (**Scheme 1-1, top right**).^{3a} In addition, Adam’s catalyst (PtO_2/H_2), which was discovered in 1922, proved very successful for the hydrogenation of alkenes, alkynes and nitro compounds and in hydrogenolysis reactions (**Scheme 1-1, bottom left**).^{3b} The Lindlar supported catalyst ($\text{Pd}/\text{CaCO}_3/\text{quinoline}$) selectively reduces alkynes to *cis*-alkenes and is

another example of a widely used heterogeneous catalyst (**Scheme 1-1, bottom right**).^{3c}

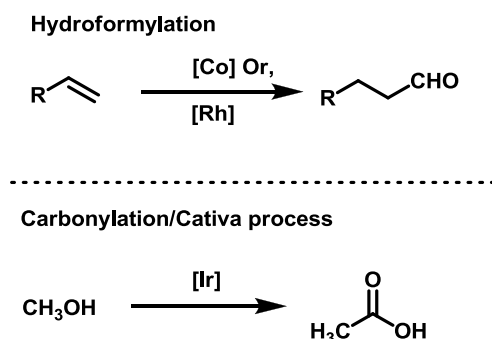


Scheme 1-1. Examples of heterogeneous catalysis.

1.1.2 Homogeneous Catalysts

Homogeneous catalysts on the other hand are completely soluble in the reaction media. As the catalyst is soluble in the reaction media, it is possible to study the reaction mechanism of product formation in more detail, follow kinetics in a quantitative manner and investigate intermediates through different spectroscopic techniques. Active sites are often well defined, therefore a high level of understanding and control over reaction sites is possible. Homogeneous catalysts often involve the addition of a stabilizing “ligand” that solubilizes the metal in a defined oxidation state. These may be investigated spectroscopically, including X-ray crystal structural analysis, providing a well-defined, molecular-level understanding of their structure. Active sites can also be modified using designer ligands, including chiral versions where applicable, in order to modify reactivity and any desired selectivity, including substrate scope, regiocontrol, and stereoselectivity. However, homogeneous catalysts do possess several disadvantages, with the foremost factor usually being cost. Catalyst recovery is often difficult, as it is often hard to separate the catalyst from the product mechanically without extensive work-up and recovery protocols. Homogeneous catalysts can also

have low thermal stability and may precipitate reduced metals or halide salts. Although homogeneous catalysis is expensive, the unmatched advantages in comparison to heterogeneous catalysis has rendered their use increasingly popular for industry (pharmaceutical, fine chemical, agrochemical, etc.) in order to produce high value intermediates, and have been cornerstones of academic research for the last five decades. As an early example of homogeneous catalysis, hydroformylation employing $\text{HCo}(\text{CO})_4$ as a catalyst, as originally discovered by Otto Roelen in 1938, is still an important industrial process producing aldehydes and detergent alcohols from terminal alkenes (α -olefins) (**Scheme 1-2, top**). Subsequently, Wilkinson reported rhodium-based hydroformylation by using $\text{RhCl}(\text{PPh}_3)_4$ as a catalyst, which occurs under milder conditions and with higher chemo- and regioselectivity.⁴ The Cativa process, which is used for the production of acetic acid through the carbonylation of methanol, uses an iridium-containing catalyst; $[\text{Ir}(\text{CO})_2\text{I}_2]^-$ and is another early example of homogeneous catalysis (**Scheme 1-2, bottom**).⁵



Scheme 1-2. Examples of homogeneous catalysis.

1.2 Transition Metals

According to IUPAC, a transition metal is “an element whose atom has a partially filled *d* sub-shell or, which can give rise to cations with an incomplete *d* sub-shell.” These are usually divided into early transition metals, middle

transition metals, and late transition metals. Late transition metals are those that are in groups 8–11. They can often access many oxidation states as well as permit facile ligand association and dissociation, these unique and distinctive properties are fundamental to their development in homogeneous catalysis.⁶

The following section will provide a brief introduction to “late” transition metals and their reactivity in particular, palladium [Pd], gold [Au] and silver [Ag]. An overview of the reactions involving ligated homogeneous late transition metal complexes (Pd, Au, Ag) in organic synthesis is also presented.

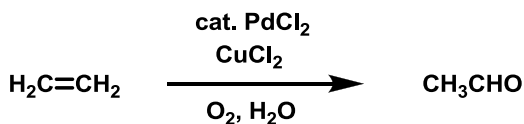
1.3 Palladium

Palladium, with the atomic symbol Pd and an atomic number 46, belongs to group 10 with [Xe] $4d^{10} 5s^0$ as its electronic configuration.⁷ Owing to its “unique combination of various properties,”^{7e} palladium-based catalysts are used in a variety of chemical reactions, including hydrogenation, cross-coupling reactions, electrophilic cyclization, etc. Palladium has many oxidation states; the most common are 0, +2, and +4. These oxidation states are easily accessible. The Pauling electronegativity of palladium is 2.20 as compared to the electronegativity of carbon, which is 2.55; therefore, the Pd-C bond is relatively nonpolar and shows low reactivity toward polar groups like ketones, esters, aldehydes, etc., which are reactive toward reagents prepared from alkali metals and alkaline earth metals, for example, organolithium and Grignard reagents. High levels of chemoselectivity are thus achievable using palladium catalysis. Reactions involving organopalladium species are usually cleaner due to fewer side reactions, as palladium does not enter into a one electron transfer reaction in the same way that its competitor, nickel metal [Ni to Ni(I)], does. Pd(II) intermediates can undergo facile reductive elimination to regenerate Pd(0), an important phenomenon that does not occur readily with metals like magnesium. Because of these superior properties, palladium

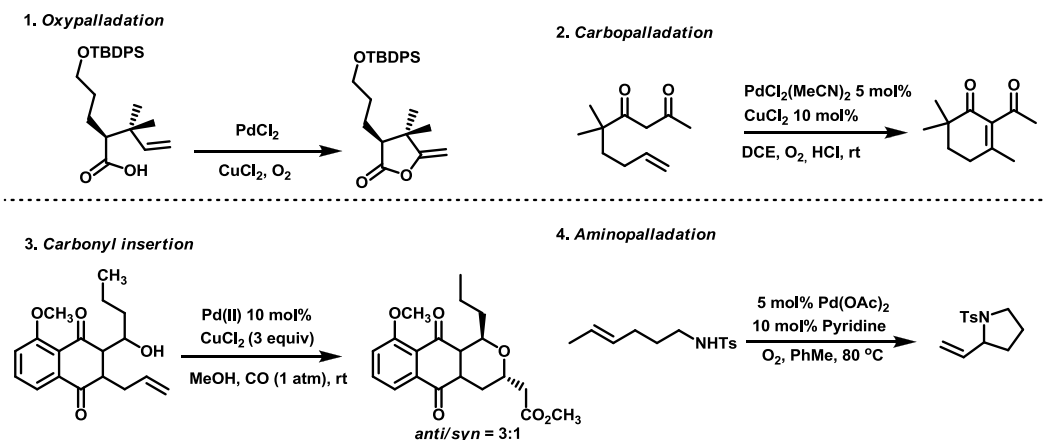
catalysts are also often used in domino reactions where multiple Pd-catalyzed reactions are possible in one pot. They are compatible with other transition metals so they can also be used in dual-metal catalyzed transformations. Typically, reactions involving Pd are divided into oxidative reactions, which involve Pd(II) salts and catalytic reactions with Pd(0) complexes.⁷

1.3.1 Pd(II)-Catalyzed Reactions

Coordinationally unsaturated Pd(II) complexes are highly electrophilic and can bind to electron-rich functional groups, forming π -complexes. For example, Pd(II)-catalyst, upon coordination with alkene, the π -electron density generates a π -complex. Any subsequent attack by a nucleophile (water, ammonia, enamines, alcohol, carboxylic acids, etc.) on this complex generates an intermediate involving a Pd-C σ bond. Since these intermediates are less stable, they can undergo β -hydride elimination, nucleophilic displacement, or hydride shift depending on the reaction conditions. Essentially, all these pathways produce an inactive Pd(0) species in a reaction mixture, making them useful only for stoichiometric reactions. However, such reactions can be made catalytic under reaction conditions that include stoichiometric terminal oxidants (molecular oxygen, benzoquinone, copper(II) salts, etc.). These are used to regenerate active Pd(II) from Pd(0).⁷ One of the classic examples involving such a process, where the nucleophile is water, is seen in the Wacker oxidation. This process is based on Pd(II)-alkene complexation and is regarded as the first industrial application of palladium in homogeneous catalysis. Originally described in 1894, the process involved ethylene oxidation into acetic acid, which was mediated by stoichiometric PdCl₂. It took more than 60 years to realize that Pd(II) can be regenerated from Pd(0). CuCl₂ was added as an oxidant in order to make the reaction catalytic; the Cu(I) was re-oxidized through molecular oxygen (**Scheme 1-3**).⁷

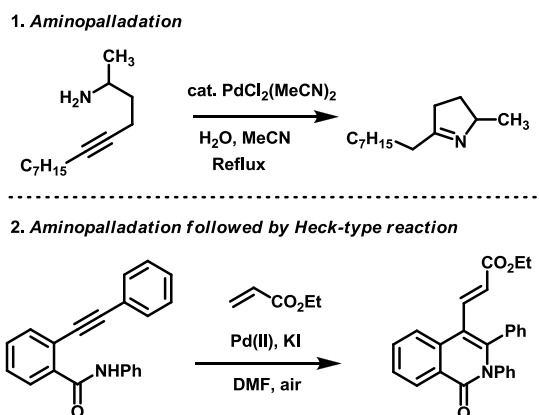
**Scheme 1-3.** Wacker oxidation.

The intramolecular version, where the nucleophile is present within the molecule, provides access to various high-value heterocycles or carbocycles. For example, a PdCl₂-catalyzed intramolecular oxypalladation of alkene acids occurs in the presence of CuCl₂ and molecular oxygen (**Scheme 1-4, top left**).^{8a} Carbopalladation (**Scheme 1-4, top right**), where the activated methylene is added across the double bond,^{8b} and intramolecular aminopalladation using Pd(OAc)₂ in the presence of molecular oxygen for the synthesis of pyrrolidine derivative^{8c} (**Scheme 1-4, bottom right**), are also examples. The intermediate with the Pd-C σ bond can also undergo various insertion reactions. For example, an insertion with CO to form an acylpalladium intermediate upon alcoholysis can generate the corresponding carboxylic acid ester (**Scheme 1-4, bottom left**).^{8d}

**Scheme 1-4.** Pd(II)-catalyzed intramolecular cyclization from alkenes.

In all of the above cases, overall oxidation of the organic molecule occurs in association with the Pd(II)-Pd(0) reduction. However, the presence of a β -heteroatom with respect to Pd in the σ -alkylpalladium(II) intermediate leads to its preferential elimination while generating Pd(II) species. There are also examples where protonolysis of the Pd-C σ bond occurs, generating the Pd(II) species and avoiding the use of stoichiometric oxidant in the reaction.⁷

In a similar fashion, electrophilic Pd(II)-catalysts coordinate with triple bonds and reduce the electron density of alkyne, which allows for nucleophilic attack by different heteroatoms (intra-/intermolecular) or by carbon-centred nucleophiles, leading to functionalized molecules. However, the major difference here is that the vinylpalladium intermediate undergoes protonolysis with the regeneration of the Pd(II)-catalyst (**Scheme 1-5, top**).^{8e} The vinylpalladium intermediate can also react with CO/alkene via an insertion mechanism to produce a corresponding carbonylated product or a Heck-type product. For example, the reaction of the vinylpalladium intermediate with alkene (Heck type), followed by β -hydride elimination, provides an alkenylated product with the generation of Pd(0), which obviously needs to oxidize back to Pd(II) (**Scheme 1-5, bottom**).^{8f}



Scheme 1-5. Pd(II)-catalyzed intramolecular cyclization from alkynes.

Direct use of Pd(II)-catalysts in the C-H bond alkenylation is also known. Fuziwara and Moritani developed the efficient coupling of arenes and alkenes (styrene, methyl acrylate) through an oxidative Pd(II)-catalyzed process. Initial reactions were stoichiometric however, later these reactions were made catalytic using an external oxidant. In this mechanism, a Pd(II) catalyst is used for the initial C-H bond functionalization of the arene. This is followed by olefin coordination and 1,2-migratory insertion and then β -hydride elimination to give the arylated olefin. A Pd-H bond is subsequently formed, which yields Pd(0) after reductive elimination. Re-oxidation of the Pd(0) catalyst to Pd(II) completes the catalytic cycle. Alternatively, the alkene can be activated through the Pd(II) catalyst, which is followed by the nucleophilic attack of an arene, causing insertion and subsequent β -hydride elimination. This is followed by reductive elimination, which generates the arylated olefin and Pd(0) species. Again, re-oxidation of the Pd(0) catalyst to Pd(II) completes the catalytic cycle.⁹

In a similar fashion, Pd(II) catalyzed C-H arylation can be achieved using a Pd(II) catalyst, where the highly electrophilic Pd(II) catalyst is used for the initial C-H bond functionalization of an arene. Depending on the subsequent oxidative addition with Ar-X, or transmetalation with R-M, a Pd(II)-Pd(IV)-Pd(II) or Pd(II)-Pd(0)-Pd(II) catalytic cycle operates to create a new C-C bond.^{10a} The introduction of a suitable directing group often helps to promote regioselective Pd(II)-catalyzed C-H functionalization of arenes. In addition, the Pd(II)-mediated oxidative coupling of arenes and organometallic compounds is also known.^{10a} For example, a stoichiometric version of arene homocoupling has been known since 1965; this particular case involved the Pd(OAc)₂-catalyzed homocoupling of two molecules of benzene.^{10b,c}

Heck reactions are typically conducted in the presence of phosphine ligands; however, Jeffery's ligandless condition, which typically uses a Pd(II) precursor like Pd(OAc)₂ with a combination of an inorganic base and tetraalkylammonium

salts, observes a large rate of acceleration with aryl iodides.¹¹ Although the stabilizing effect of tetraalkylammonium salts on Pd colloids was recommended, a Pd(II)-Pd(IV) catalytic cycle cannot be ruled out.

Overall, the majority of reactivity from Pd(II) catalysts lies in the electrophilic activation of π -bonds, much like Lewis acid activation and C-H functionalization reactions.

1.3.2 Pd(0)-Catalyzed Reactions

The reactivity of Pd(0) catalysts differs from Pd(II) because the former involves the oxidative addition of organic halides (or pseudohalides) as a key step in the reaction cycle. For the purpose of this discussion, well-known homogeneous Pd-catalyzed hydrogenation reactions, employing oxidative addition of hydrogen, will be excluded. Oxidative addition of $\text{LnPd}(0)$ (where Ln denotes n coordinating ligands) to the organo halide generates a reactive intermediate in which Pd(II) is attached to the organic group via a σ bond. This species further reacts with a nucleophile such as an organometallic reagent, or a heteroatom-containing species (amine, alcohol, etc.) through a transmetalation (or ligand exchange) process and subsequently via a reductive elimination, that expels the product and regenerates the original $\text{LnPd}(0)$ species to continue the catalytic cycle. The cases involving ligand exchange with carbon-based nucleophiles have become exceedingly important. Overall these cross-coupling reactions represent a powerful strategy in the construction of C-C and C-heteroatom bonds. $\text{LnPd}(0)$ -catalyzed cross-coupling reactions are now routinely used by scientists within academia and various industries.⁷

The mechanistic cycle for all the Pd(0)-catalyzed cross-coupling reactions is similar, and some general details of the steps can be described. Oxidative addition of $\text{LnPd}(0)$ is generally faster into C-I than C-Br or C-Cl bond due to the lower bond dissociation energy of C-I (lower lying σ^*). In the

transmetalation step, the transfer of ligands occurs from one metal to another, resulting from a difference in electronegativity between two metals.

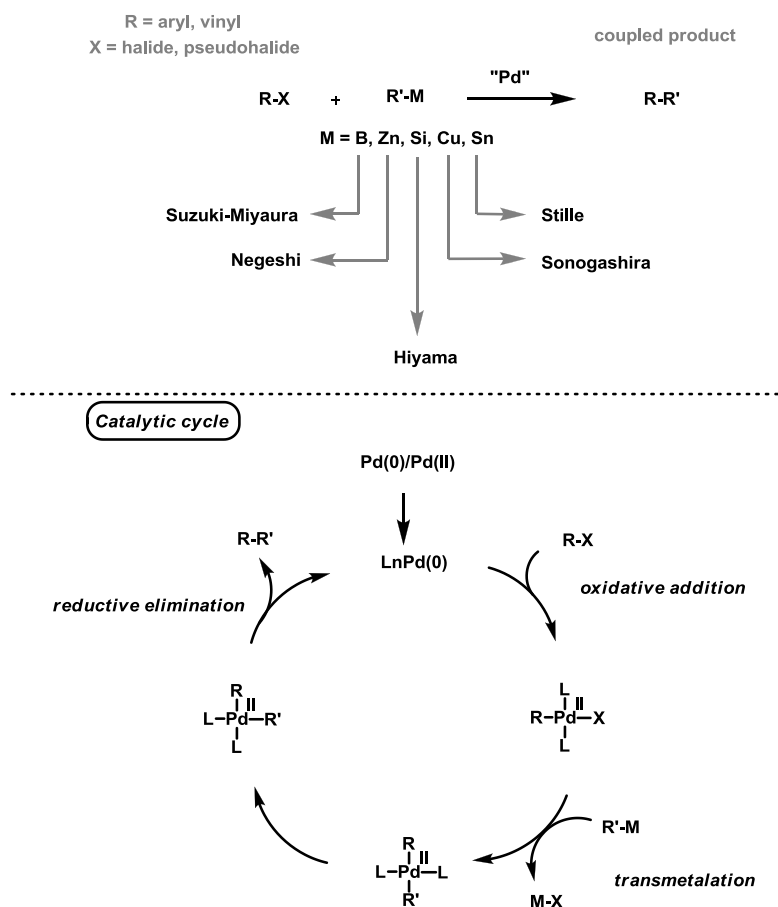


Figure 1-1. Cross-coupling reaction: Types and general mechanism.

The transmetalation can proceed through an associative, dissociative or concerted interchange pathway. This step is followed by the isomerization step, where the two groups being eliminated in the last step occupy a *cis* position, which is a prerequisite for the reductive elimination step. In the final step, the catalytically active LnPd(0) species is regenerated through the reductive elimination of the coupling product (**Figure 1-1**). The mechanism operates similarly in the Buchwald-Hartwig amination (BHA), where the nucleophile is an amine. These LnPd(0)-catalyzed reactions have provided a

valuable tool to chemists for the creation of complex molecules. In recognition of their contributions in the development of Pd-catalyzed reactions, the 2010 Nobel Prize in Chemistry was awarded to Suzuki (Suzuki-Miyaura [SM] reaction), Negishi (Negishi coupling), and Heck (Heck coupling).¹²

1.4 Ligand Effects in Homogeneous Pd(0)-Catalyzed Reactions

In general, the use of homogeneous catalysis has transformed organic synthesis beyond imagination. Ligands play an important role in homogeneous catalysis. Ligands donate electron density to the metal center, thereby stabilizing the metal center in different oxidation states. Small changes in ligand structure, such as in the steric bulk or electronic properties can bring changes to the reactivity of the catalyst. This in turn changes the regioselectivity and stereoselectivity in the final product and increases the stability and solubility of the catalyst itself. Phosphine ligands have emerged as one of the most used ligands in homogeneous catalysis. When coordinated, the metal center provides superior reactivity and selectivity in comparison to the metal alone.⁶

Ligands play a crucial role in Pd-catalyzed cross-coupling reactions. Overall, oxidative addition is nucleophilic in nature and facilitated with more electron density on Pd. Thus, electron-rich phosphines accelerate the oxidative addition step. Bulky ligands promote ligand dissociation prior to oxidative addition in order to form the active monoligated LPd(0) species. The reduced electron density of Pd and bulky ligands with a large bite angle facilitate the reductive elimination step. Bulky ligands help the reductive elimination step by relieving the strain.^{7, 13}

In the following sections, an overview of the ligand effects in homogeneous Pd(0) catalysis is provided with respect to the Suzuki-Miyaura and Buchwald-Hartwig coupling reactions.

1.4.1 Suzuki-Miyaura Reaction

The transition metal cross-coupling reactions of organic halides (pseudohalides) with organoboron compounds are known as Suzuki-Miyaura coupling reactions. This reaction represents a simple and effective route toward the synthesis of substituted biphenyls. In 1975, Heck observed the first transmetalation reaction with a vinyl boronic acid on Pd, which adds to methyl acrylate via a Heck type process to give conjugated diene.^{14a} However, Suzuki and coworkers reported the Pd-catalyzed cross-coupling reaction between alkenyl boranes and alkenyl bromides for the first time in 1979.^{14b} Since then, many researchers have made significant contributions to this field. Aryl iodides and bromides are the most common halide partners used in SM cross-coupling reactions. Coupling reactions of aryl chlorides are more attractive from an industrial point of view, as these are economical and readily available. However, aryl chlorides are challenging substrates and often require optimized reaction conditions with a suitable ligand and Pd source. Over the years, extensive research has been carried out in this field in order to find a general ligand for the activation of aryl chlorides. As described earlier, sterically hindered, electron-rich phosphines have proved to be useful in affecting both the oxidative addition and reductive elimination processes in catalytic cycles. In addition, ligands increase the lifespan of Pd(0), preventing it from forming inactive Pd black.^{7, 13}

In 1997, Shen and coworkers reported the use of PCy₃ as a ligand in the Pd-catalyzed coupling of activated aryl chlorides with arylboronic acids in NMP using CsF as a base at 100°C.¹⁵ Shortly after that, in 1998, Fu used a P(^tBu)₃/Pd₂dba₃ catalyst system for the Pd-catalyzed coupling of inactivated aryl chlorides with boronic acids at 90°C in dioxane with Cs₂CO₃ as a base and at room temperature with KF as base in THF.¹⁶ Since then, trialkylphosphines have become the popular choice for ligands in SM cross coupling. However, these trialkylphosphine are quite prone to oxidation; hence, they are very

unstable in air. Numerous research groups, including those run by Buchwald and Fu, are actively involved in the development of more air stable ligands that are effective in activating difficult aryl chloride substrates. Buchwald reported ligands derived from a biaryl-based scaffold (DavePhos, JohnPhos) for SM cross-coupling reactions (**Figure 1-2**). Ligands derived from a biaryl scaffold carry several advantages, as they are crystalline, air and thermal stable, and most importantly are tunable.¹³ For example, the catalyst derived from JohnPhos (**2**, **Figure 1-2**) was highly active at room temperature for coupling reactions of aryl bromide and chloride at 0.5–1.0 mol% Pd loading. Catalytic activity of DavePhos (**1**, X = NMe₂, **Figure 1-2**) was inferior to JohnPhos, supporting the idea that the dimethylamino group was not required for catalytic activity. Further, the dicyclohexyl version of the JohnPhos and DavePhos ligand was found to be more active than JohnPhos for sterically hindered substrates at low catalyst loading (**Figure 1-2**).¹⁷ The success of Buchwald's ligands is attributed mainly to the perfect combination of steric bulk and electronic factors. The basic phosphine (trialkylphosphine > triphenylphosphine) is important for the acceleration of oxidative addition. These phosphines bind strongly to Pd, which increases the shelf life of a catalyst and ensures that the catalyst remains in the solution for a longer time. The steric bulk of the ligand ensures facile reductive elimination and favors the formation of monoligated Pd species at room temperature.¹³ Highly efficient ligands also translate to a very low catalyst loading for a reaction for example, Buchwald showed that for a cross coupling between 4'-bromoacetophenone and phenylboronic acid, 100,000,000 turnovers were obtained in < 24 h at 100 °C using JohnPhos. The same reaction was repeated with just Pd(OAc)₂ and in the absence of JohnPhos gave only 100,000 turnovers. This result clearly illustrates the effect of ligands on the Pd-catalyzed SM cross-coupling reaction.^{17c} Later, Buchwald also introduced X-Phos and S-Phos ligands (**3** and **4**, **Figure 1-2**) and presented their applicability in the production of

heterobiaryl compounds from corresponding heteroaryl boronic acids, which are often challenging.¹⁸

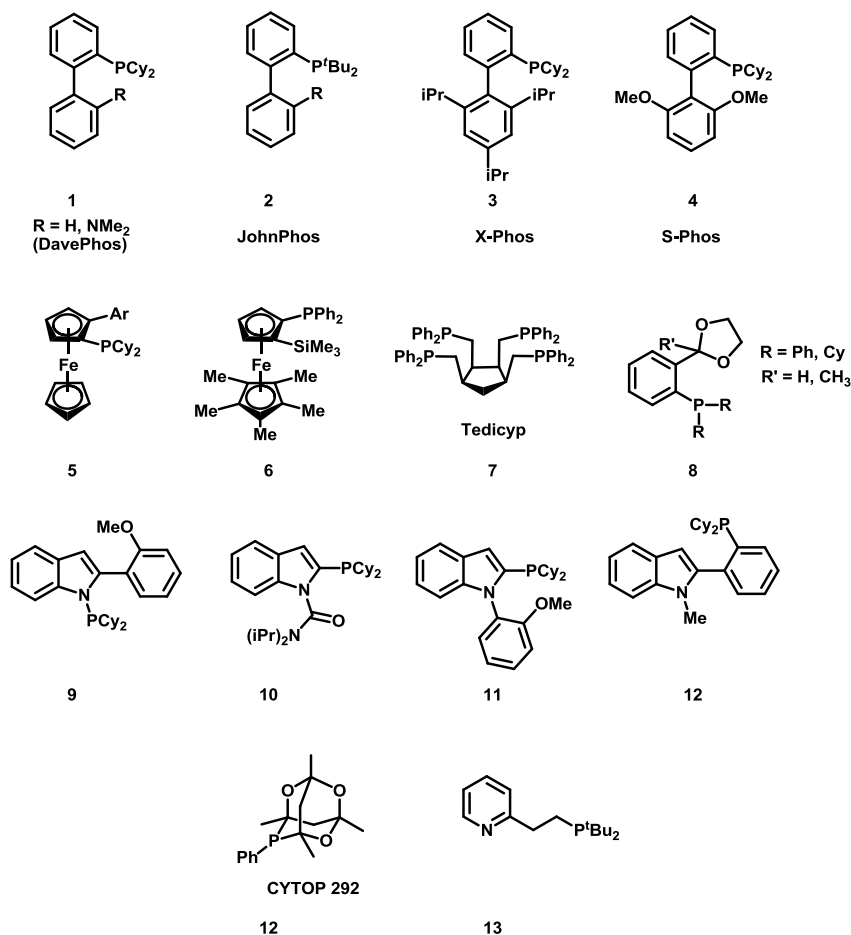


Figure 1-2. Examples of ligands used in SM cross-coupling reactions.

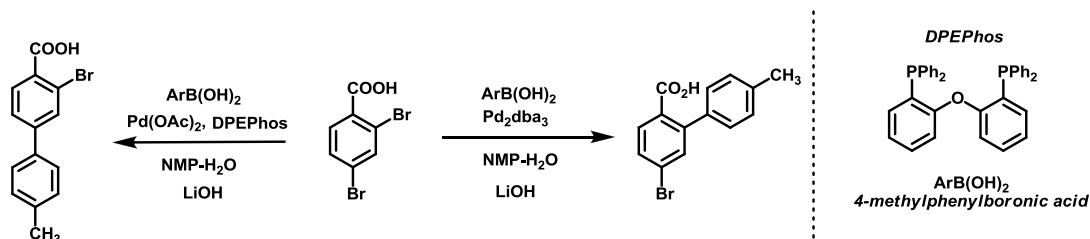
Buchwald reported X-Phos and Kwong reported on the use of indolylphosphine ligands for the SM cross-coupling reaction of aryl tosylates (**Figure 1-2**).¹⁹ Kwong also reported that these ligands were successfully employed in the coupling of potassium aryltrifluoroborates and aryl mesylates as well as in the coupling of aryl chlorides and heteroaryl chlorides with aryl boronic acids.²⁰ Johannsen reported ferrocene ligands for the coupling range of aryl chlorides at room temperature (**5**, **Figure 1-2**).^{21a} Fu reported that silylated ferrocene

ligands (**6**, **Figure 1-2**) are effective in the SM cross coupling of inactivated aryl chlorides at a mild temperature. Surprisingly, the silyl group was found to be essential in the catalytic activity of the ligand.^{21b} The use of the tetrapodal phosphine ligand, Tedicyp, was reported by Santelli (**7**, **Figure 1-2**). The Tedicyp ligand has been successfully utilized due to the 4-diphenylphosphino arms that bind strongly to Pd, ensuring high catalytic activity. Santelli was able to carry out a SM cross-coupling reaction with as low as 0.0000005% catalyst loading.²² P-O and P-N type ligands represent an important class of hemilabile ligands, which use a weak and tunable donor substituent along with a sterically hindered, electron-rich phosphine. The weak/hemilabile donor helps stabilize the metal center by using an “on and off”-type interaction with Pd. Guram and coworkers described several P-O type ligands for a SM cross-coupling reaction (**8**, **Figure 1-2**).²³ In another report, it was shown that a sterically hindered phosphine, CYTOP 292, was used for effective SM cross-coupling reactions of aryl chlorides, alkyl halide/tosylates with boronic acids, and alkylboranes at mild conditions (**12**, **Figure 1-2**). The ligand is based upon a phosphadamantate skeleton, and is crystalline and air stable, making it a good choice for SM cross-coupling reactions.^{24a-c} McNulty and coworkers introduced the pyridine-based ligand, which was also effective for sterically hindered aryl chlorides and sterically hindered boronic acids (**13**, **Figure 1-2**).^{24d}

The site-selective cross coupling of dihaloarenes represents a great prospect for synthesizing multisubstituted arenes in a short amount of time. However, the site-selective mono-functionalization of dihalobenzenes poses a unique challenge, as the required ligand must only activate the specific C-X bond in the presence of other C-X bonds within the same molecule. Site-selective SM coupling for the substrate with two different halo groups is less challenging because the bond dissociation energy difference between C-I, C-Br, and C-Cl offers enough energy barriers for chemo-selective activation. Such an advantage is not present in substrates with identical halo groups, for example,

with dichlorobenzenes or dibromobenzenes. Such selective coupling could be achieved via substrate control, which takes advantage of the inherent reactivity of the substrate and the corresponding C-X bond. Lately, the use of a catalyst to achieve such mono-functionalization has gained a lot of attention. A few examples pertaining to the catalyst-based site-selective mono-functionalization of arenes are provided below.

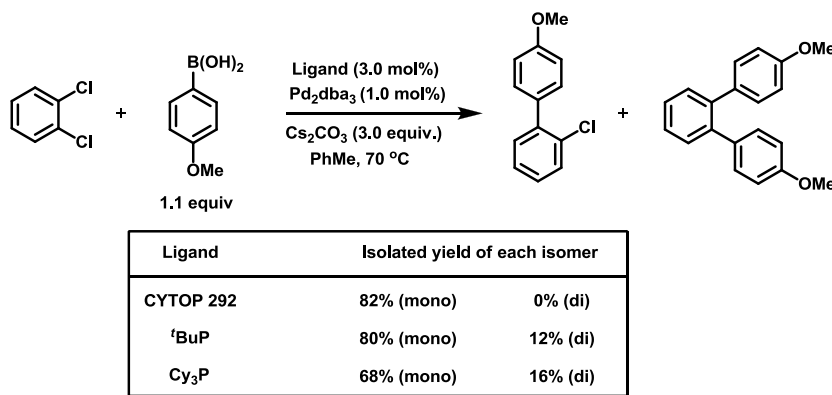
The site-selective SM cross-coupling reaction of 2,4-dibromobenzoic acid was reported by Houpis and coworkers (**Scheme 1-6**). Ortho-selective coupling occurred under phosphine-free conditions, giving 80% of the product, whereas use of the bulky bidentate phosphine ligand, DPEPhos, gave the para-selective coupling in 68% isolated yield. It was assumed that under ligand-free conditions the carboxylic group would coordinate with Pd, thereby leading to the oxidative addition of the ortho bromo group. Use of a sterically bulky phosphine ligand with greater ligating properties does not allow such coordination, hence the para-selectivity.²⁵



Scheme 1-6. SM cross-coupling reaction of 2,4-dibromobenzoic acid.

McNulty and coworkers were able to couple all three isomers of dichlorobenzene with phenylboronic acid (**Scheme 1-7**). High yields of monoarylations were obtained in each case. For example, the SM cross-coupling reaction between 1,2-dichlorobenzene with 1.1 equivalent of 4-methoxyphenylboronic acid under the reaction condition using CYTOP 292 gave 82% of the monoarylated product. In comparison, ligands such as ^tBu₃P

and Cy_3P generated a mixture of mono and di-aryl coupling products. Increasing the concentration of 4-methoxyphenylboronic acid to 2.2 equivalents also led to a higher concentration of monoarylated product (74% monoarylation and 5% diarylation) with CYTOP 292.^{24c}

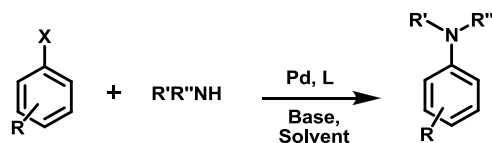


Scheme 1-7. SM cross-coupling reaction of 1,2-dichlorobenzene.

Overall, developing ligands for SM cross-coupling reactions is still being actively pursued in academia. Often, criteria such as ease of synthesis, high stability, ease of manipulation, and its usefulness in activating hindered and deactivated aryl chloride are considered in the development process. In addition to the above challenges, compatibility with other catalytic systems is also considered when creating new domino reactions.

1.4.2 Buchwald-Hartwig Amination

A $\text{Pd}(0)$ -catalyzed cross-coupling reaction of amine with aryl halide leading to a C-N bond has become a standard tool for the construction of amines (**Scheme 1-8**). Buchwald-Hartwig Amination (BHA) has revolutionized the field of amination, as classic protocols like Ullmann reactions, which use copper salts, suffer from severe drawbacks such as high loading, long reactions times, high temperatures, etc.²⁶

**Scheme 1-8.** Typical BHA reaction.

Once again, bulky and electron-rich ligands form an active catalyst with Pd and catalyze BHA very efficiently with aryl chlorides. The coupling partner often includes a primary and secondary amine, NH-containing heterocycle (indole, morpholine, etc.), ammonia, hydrazine, and amides.

Some of the challenging BHA include the monoarylation of ammonia and hydrazine as well as the regioselective arylation of imidazoles and 1,2,3-triazoles. Out of all the examples, BHA with ammonia is most important from an industrial point of view since ammonia is available at low cost, is abundant, and is easily accessible. But the BHA of ammonia is usually very difficult to achieve, and there are obvious reasons for it: 1) Ammonia can displace the ligands on Pd and form an inactive catalyst. 2) Reductive elimination from the Ar-Pd-NH₂ complex has never been observed as it forms a stable bridging structure. 3) The reaction's product can act as a substrate toward the reaction itself, producing diarylamines.²⁷ In 2006, Hartwig screened a variety of sterically hindered ligands, including P^tBu₃, Q-Phos, X-Phos, IPr, DPPF, BINAP, and the JosiPhos ligand. Surprisingly, a reaction only occurred with the JosiPhos ligand. He reported that the complex generated from JosiPhos (CyPF-^tBu), i.e., 1.0 mol% of CyPF-^tBuPdCl₂ in DME with 80 psi of ammonia at 90 °C and using NaO^tBu as a base, converted 4-tert-butylbromobenzene to 4-tert-butylaniline. The reaction showed excellent selectivity for monoarylation (17:1). Hartwig screened a variety of substrates, including aryl chloride, iodides, and sterically hindered aryl halides. He also used lithium amide as a source of ammonia, and all of these considerations resulted in a good to

excellent yield with high monoarylation selectivity under mild conditions.²⁸ In 2007, Buchwald came up with the designer catalyst system based upon the ligand structure, which for the first time allowed the synthesis of symmetrical and nonsymmetrical di- and triarylamines in addition to the monoarylation. The coupling of chlorobenzene was attempted with 5 equivalents of ammonia in the presence of $\text{Pd}_2(\text{dba})_3$, with NaO^tBu as the base in 1,4 dioxane solvent. Buchwald observed that with 5.0 mol% of the ligand, **1**, **3** and **5** yielded mostly diarylamine as a product (**Figure 1-3**), whereas ligands with a $^t\text{Bu}_3\text{P}$ group (**2**, **4** and **6**, **Figure 1-3**) produced monoarylation as the chief product.²⁹

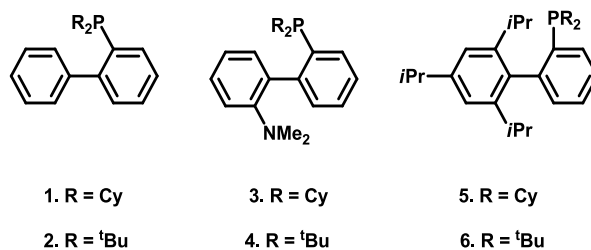
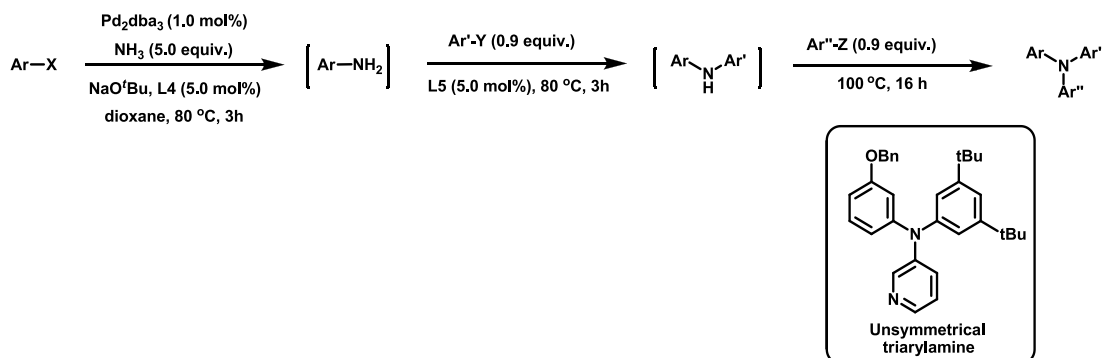


Figure 1-3. Buchwald's ligands: Monoarylation of ammonia.

In perhaps the most challenging synthesis of a one-pot nonsymmetrical triarylamine synthesis, Buchwald used the sequential addition of three different aryl halides to ammonia (**Scheme 1-9**). The success of the reaction was attributed to the use of different ligand at each stage. The synthesis of symmetrical diarylamine and triarylamine was achieved by using ligand **5** (**Figure 1-3**) and by changing the reaction temperature as well as the concentration of aryl halide.²⁹

In a similar fashion, the synthesis of asymmetrical diarylamine was also accomplished using ligand **4** (**Figure 1-3**).²⁹ Later, Hartwig also developed a similar protocol and applied the monoarylation of tosylates for the first time.³⁰ Stradiotto described the use of Mor-DalPhos (**3**, **Figure 1-4**) for the

monoarylation with ammonia using aryl chlorides and tosylate at room temperature.³¹



Scheme 1-9. Buchwald's ligand for asymmetrical triarylamine synthesis.

Overall, various bulky and electron-rich ligands exist that can catalyze the BHA for aryl chlorides effectively. A selection of some of the important ligands for catalyzing BHA is shown below.

In 2013, Stradiotto compared existing landmark catalyst systems for BHA and described BippyPhos/[Pd(cinnamyl)Cl]₂ as a single catalyst system for BHA that can operate over a broad range of substrates, including primary/secondary amine, NH heterocycles, ammonia, amides, and hydrazines (**12**, **Figure 1-4**).^{31c} Stradiotto and coworkers were able to show that existing BHA catalyst systems are task specific. When screened, they found that the majority of the landmark catalyst systems, including cataCXium A, XantPhos, JosiPhos, BrettPhos, and RuPhos, were effective for some but not all of the BHA reactions, like the arylation of primary and secondary amines, the N-arylation of indoles, the monoarylation of ammonia, etc.^{31c}

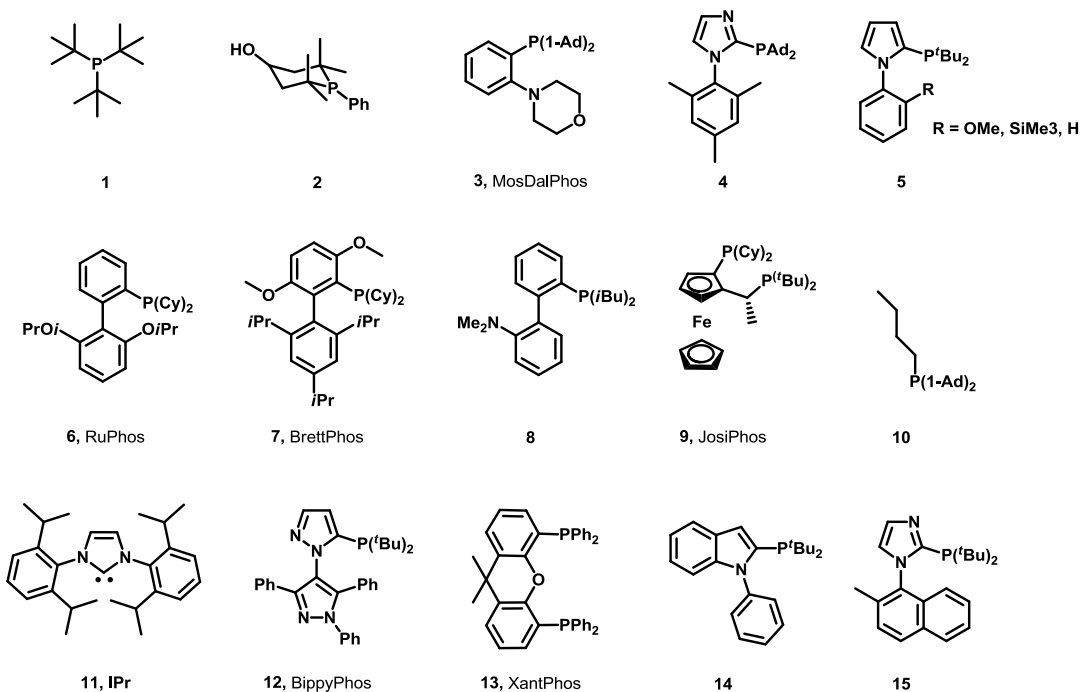
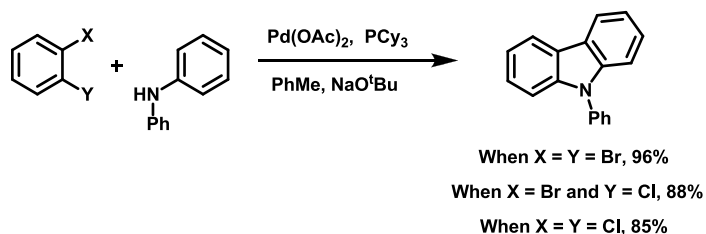


Figure 1-4. Examples of ligands used in BHA reactions.

Amination represents an important organic reaction used in the synthesis of nitrogen-containing heterocyclic molecules like indoles. The following section will provide a few examples from recent literature for the synthesis of indole type molecules where ligand effect played a crucial role in the BHA reaction.



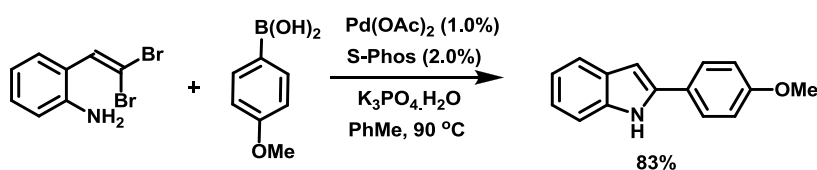
Scheme 1-10. Pd-catalyzed synthesis of annulated heterocycles.

Ackermann reported a Pd-catalyzed domino synthesis of annulated heterocycles. Starting from anilines and various dihaloarenes, authors have

been able to construct carbazoles. The synthesis includes successive amination and direct C-H bond arylation (**Scheme 1-10**).³²

Ackermann screened a variety of conditions and found PCy₃ to be a suitable ligand for an efficient process. Fortunately, the approach worked equally well for all 1,2-dichlorobenzenes, producing an 85% isolated yield of corresponding carbazole. Ackermann was also able to show the synthesis of carbazoles with free NH groups being generated in a good yield (57–81%). Before this report, there was no approach for direct arylation based on domino carbazole synthesis.³²

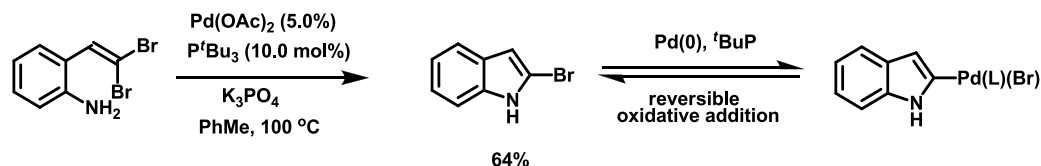
In 2005, Lautens and coworkers demonstrated the use of a Pd-catalyzed intramolecular BHA and an intermolecular SM cross-coupling reaction in tandem, leading to 2-substituted indoles. Starting from *ortho-gem*-dibromovinylanilines and various boronic acids, and using a catalytic system that consisted of 1.0 mol% Pd(OAc)₂ and 2.0 mol% of an S-Phos ligand, good yields of 2-substituted indoles were obtained (**Scheme 1-11**).^{33a}



Scheme 1-11. Pd-catalyzed BHA in tandem with SM cross-coupling reactions.

In 2010, Lautens and coworkers presented a remarkable ligand effect in the synthesis of 2-bromoindoles. When screened, they found that except for ^tBu₃P no other ligand (BINAP, R₃P, SPhos, JohnPhos, etc.) was able to catalyze this reaction. The researchers proposed that with ^tBu₃P, there is a reversible oxidative addition into the carbon-bromine bond of the product. With other ligands, in the absence of boronic acids, the oxidative addition product of the 2-bromoindole resulted in a catalytically inactive/dead complex. Whereas, with

bulky $t\text{Bu}_3\text{P}$, under similar reaction conditions, the $\text{LnPd}(0)$ can be released back into the catalytic cycle (**Scheme 1-12**).^{33b}



Scheme 1-12. Synthesis of 2-bromoindoles, effect of $t\text{Bu}_3\text{P}$ ligand.

Overall, the majority of $\text{Pd}(\text{II})$ -catalyzed chemistry is initiated through π -activation from substrates like alkenes, alkynes, etc., and often requires an oxidant to make these reactions catalytic; whereas the fundamental reaction as initiated by $\text{LnPd}(0)$ chemistry involves oxidative addition. Ligands have played a tremendous role in the success of these new C-C bond-forming reactions.

1.5 Gold

Gold has an atomic number of 79 and belongs to group 11 of the periodic table. It has $[\text{Xe}] 4f^{14} 5d^{10} 6s^1$ for its electronic configuration and can exist in different oxidation states, but the most common are +1 and +3. Gold exhibits a relativistic effect and the lanthanide contraction, which decreases the size of its 6s orbital and increases the size of its 5d orbital. As a result, electrons in 6s orbitals are drawn closer to the nucleus therefore they have greater ionization energy; whereas electrons in 5d orbitals, being shielded by 6s orbitals, experience weaker nuclear attraction. Low lying valence s or p orbitals (LUMO) along with high electronegativity is responsible for higher Lewis acidity for gold.³⁴

Homogeneous gold catalysis occurs with gold(I) and gold(III) compounds. $\text{Au}(\text{III})$ possesses a +3 oxidation state, with a d^8 electronic configuration. It has square planar geometry. $\text{Au}(\text{III})$ prefers hard Lewis basic ligands, for example, dichloro(2-pyridinecarboxylato)gold. $\text{Au}(\text{I})$ displays a d^{10} electronic

configuration with a preference for a linear geometry. It favors soft ligands such as π -bonds, phosphines, etc. Due to the higher oxidation potential of Au(I) to Au(III) relative to Pd(0) to Pd(II), Au(I) catalysis are generally highly tolerant toward air and moisture; as a result, open flask reactions can be carried out. Gold(I) catalysts have L_2Au^+ , or a $LAuX$ composition. The most common source of Au(I) catalyst is AuCl; however its use is limited as it can easily undergo reduction to Au(0). Hence, in order to stabilize the Au(I) center, strong sigma-donor ligands like phosphine are required. In the case of a $LAuX$ complex, the ligand X is generally a weaker coordinating group. However the $LAuX$ complex can be covalent or ionic depending on the nature of the X. Cationic gold is accessed by treating the complex with a silver activator that has a weakly coordinating counter anion, For example, $LAuCl$ treated with $AgOTf$ produces $LAu^+(OTf^-)$ and $AgCl$. In some cases, it was observed that the added silver salt can take part in the apparent Au(I) catalyzed reaction; hence in order to avoid the use of silver salts altogether, a labile ligand strategy was developed. Gagosz developed the triphenylphosphinegold(I)triflimide catalyst, where the triflimide group is labile enough that it easily dissociates in a solution to create the catalytically active Au(I) species.³⁵

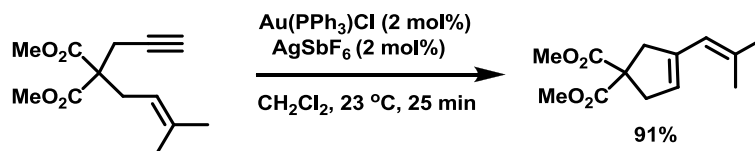
Interestingly, although ligated Pd(0) and Au(I) catalysts both utilize metals with isoelectronic d^{10} configurations, for Pd(0) catalysis, the principle mode of reactivity proceeds via oxidative addition, whereas Au(I) initiates processes via π -activation in view of its π -Lewis acidity and resistant to undergo oxidative addition. A scarce number of reports do exist in the literature claiming cross-coupling reactions with Au(I) species that proceed through oxidative addition. Corma and coworkers developed a catalytic system based on Au(I) for a SM reaction between aryl iodide and aryl boronic acids.^{36a,b} Subsequently, Corma and You reported that Au(I) catalyzed Sonogashira reaction.^{36c,d} Nevertheless, Echavarren and coworkers were able to show that the presence of 0.1 mol%

Pd contaminants could successfully drive the so-called Au(I) catalyzed Sonogashira reaction.^{36e} After a thorough investigation, Corma and coworkers were able to show that the Sonogashira reaction was catalyzed by Au nanoparticles; hence a homogeneous Au(I) mechanism was ruled out.^{36f}

On the other hand, gold-catalyzed reactions have enjoyed unparalleled success, being a mild Lewis acid. Gold-catalyzed reactions can be broadly classified as a nucleophilic/heteroatom functionalization of C-C multiple bonds, cycloaddition, coupling reactions, and cycloisomerization reactions of polyunsaturated substrates. The most common type of reaction observed in the literature for gold catalysis is the nucleophilic/heteroatom functionalization of C-C multiple bonds. In general, gold-catalyzed reactions are mild and selective, have short reaction times, tolerate a variety of other functional groups in the molecules, can easily create complex structures from relatively simple molecules, minimize the number of steps needed, and are very efficient. This last consideration is the most important, as the reaction can be performed with a lower catalyzed loading at ambient temperature. For these reasons, although gold catalysts are expensive, they are still very popular in the industry and academia.³⁷

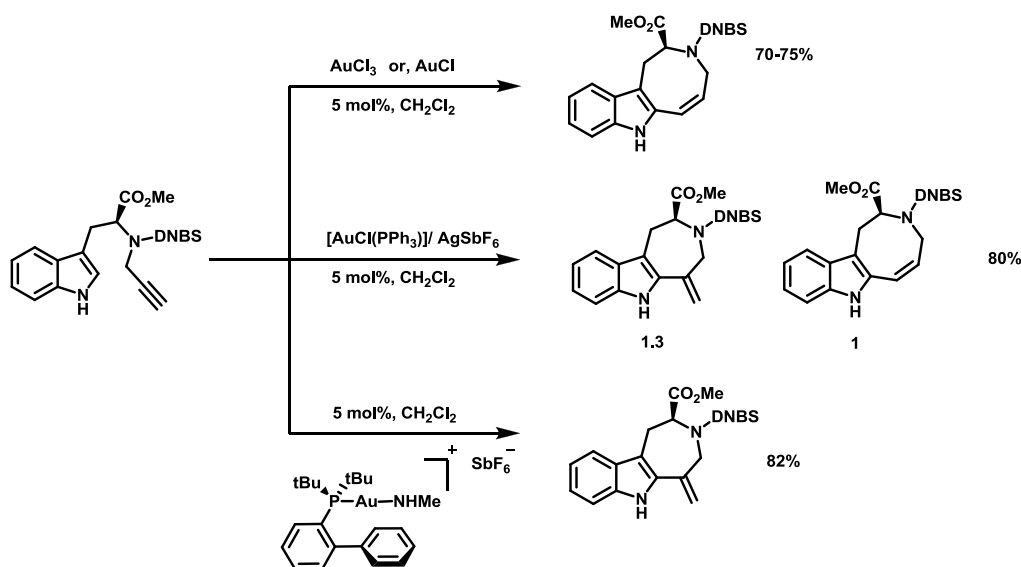
1.5.1 Ligand Effects in Homogeneous Gold Catalysis

The following section will explain the importance of the ligand effect in gold catalysis using various examples. Echavarren and coworkers described an intramolecular enyne cycloisomerization of 1,6-enynes. Under the catalytic system employed, an exclusive *5-exo-dig* cyclization was observed over a *6-endo-dig* cyclization. The use of Au(PPh₃)Cl or AgSbF₆ alone did not yield the product, highlighting the importance of silver salts in gold catalysis. Cationic gold species coordinate exclusively to alkyne, leaving alkene for the nucleophilic attack (**Scheme 1-13**).³⁸



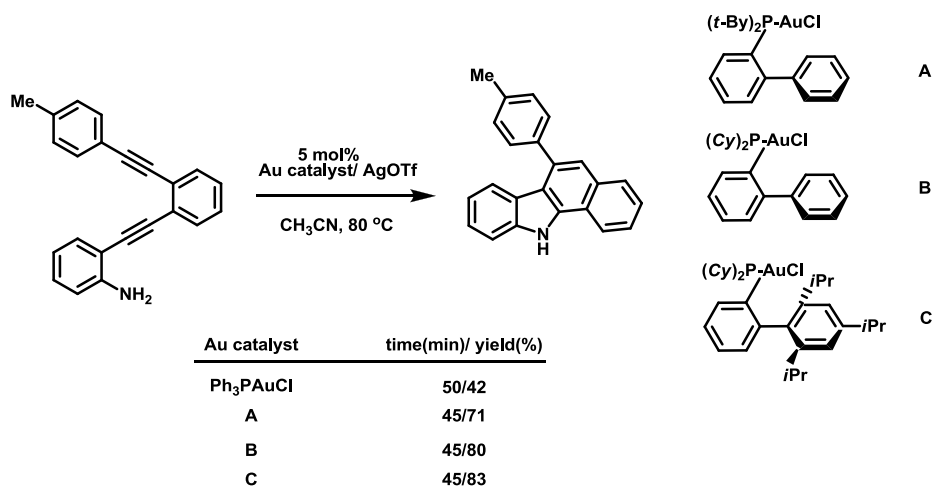
Scheme 1-13. Gold-catalyzed cycloisomerization of 1,6-enyne.

In another interesting work, Echavarren and coworkers showed that the intramolecular reaction of indole with alkyne is dependent upon the nature of the gold catalyst. They were able to show that with the cationic gold(I) complex (JohnPhosAu-MeCN) SbF_6 , an exclusive seven-member ring with an exocyclic double bond, azepino[4,5-*b*] indole, forms the core. Whereas, AuCl_3 or AuCl produced an azocino[4,5-*b*] indole core. The reaction using a chloride abstraction strategy yielded a mixture of products (**Scheme 1-14**).³⁹



Scheme 1-14. Gold-catalyzed synthesis of 7-*exo-dig* vs. 8-*endo-dig* cyclization.

Ohno and Fujii synthesized fused indoles via a gold-catalyzed cascade cyclization of diynes that resulted in functionalized carbazoles.

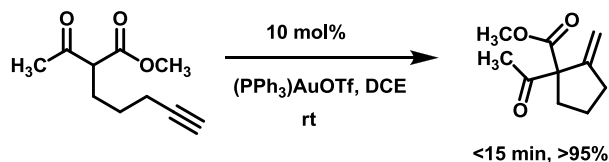


Scheme 1-15. Gold-catalyzed cascade cyclization.

This involves *5-endo-dig* hydroamination, followed by a *6-endo-dig* hydroarylation strategy (**Scheme 1-15**). In the model substrate, the initial reaction was conducted using Ph₃PAuCl; however only 42% yield was obtained. It was assumed that the electron-rich alkyne was strongly bonded to the cationic gold complex, thereby hindering the hydroamination step. In order to improve the yields, the researchers used bulky, biaryl-containing phosphine ligands with Au(I) complexes in order to improve the dissociation of an active gold complex from the alkyne. As expected, the Au complexes B and C showed greater activity and gave higher yields for the overall cascade reaction (**Scheme 1-15**).⁴⁰

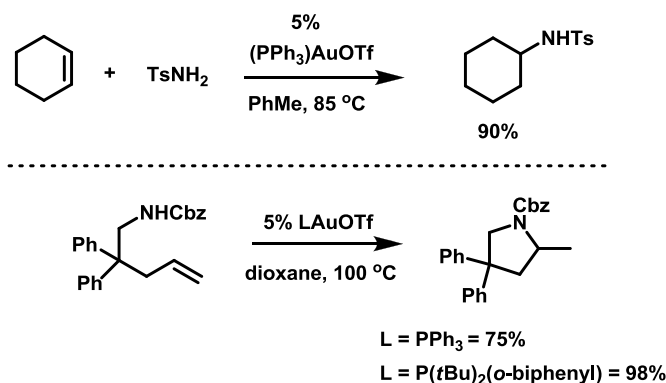
Gold catalysts were shown to be effective in catalyzing the addition of 1,3-dicarbonyl compounds to C-C multiple bonds. The Au(I)-catalyzed Conia-ene reaction developed by Toste and coworkers is an excellent example of this.⁴¹ In this case, β -ketoesters tethered to alkynes reacts under Au(I)-catalyzed conditions to produce α -vinylketones in excellent yield. It is important to note that before this discovery, such reactions were carried out thermally or with other transition metals that operate at lower temperatures, requiring the use of

an acid or a base to form the enolate for a successful reaction. The Au(I)-catalyzed version operates at ambient temperature under neutral conditions (**Scheme 1-16**).



Scheme 1-16. Gold-catalyzed Conia-ene cyclization.

The triphenylphosphinegold(I) triflate catalyzed the reaction in less than 15 minutes with a clean conversion into the product. On the other hand, use of triphenylphosphinegold(I) chloride led to no conversion, highlighting the importance of a cationic active species. The proposed mechanism involves an attack from 1,3-dicarbonyl nucleophiles on the Au(I)-alkyne complex.⁴¹

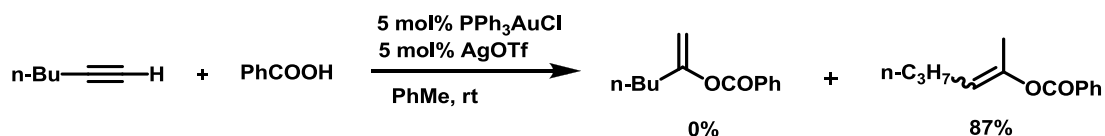


Scheme 1-17. Gold-catalyzed hydroamination: Inter- and intramolecular.

The Au(I)-catalyzed hydroamination of alkenes was first carried out by He and coworkers. Excellent yields were obtained when the intra- and intermolecular addition of tosylamide to alkenes was catalyzed using 5% Ph₃PAuOTf at 85 °C (**Scheme 1-17, top**). Subsequently the reaction scope was extended and

Widenhoefer found that bulkier ligands like $P(t\text{-Bu})_2(o\text{-biphenyl})$ increase the yields for the hydroamination of carbamates, carboxamides, and ureas (**Scheme 1-17, bottom**).⁴²

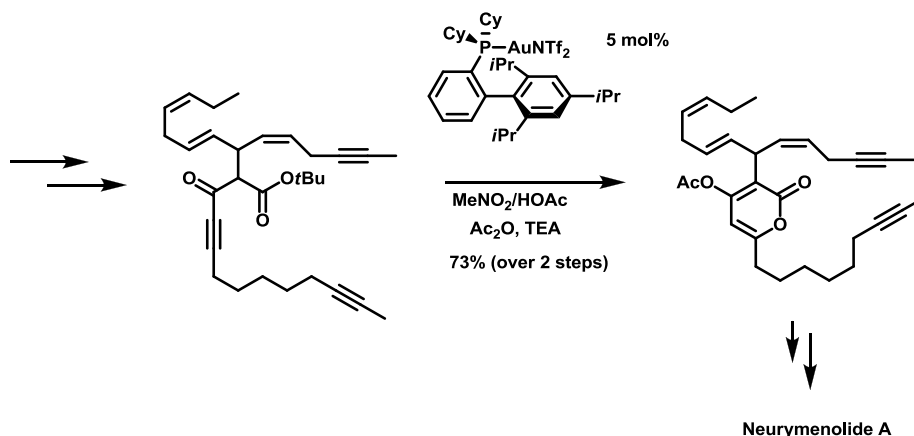
In 2006, the intramolecular gold-catalyzed addition of acids to alkynes was reported by Mechelet.⁴³ However, it took five years to identify the intermolecular version. In 2010, Kim and coworkers discovered the gold(I)-catalyzed intermolecular addition of carboxylic acids and esters to terminal alkynes. When 1-hexyne was treated with benzoic acid in toluene in the presence of a $\text{Ph}_3\text{PAuCl}/\text{AgOTf}$ catalyst, the *E*- and *Z*-mixture of a more stable enol benzoate was obtained. Initially, the formed Markonikov addition product was completely isomerized to a more thermodynamically stable product under the reaction conditions (**Scheme 1-18**).⁴³



Scheme 1-18. Gold-catalyzed intermolecular addition of carboxylic acids to alkynes.

Gold-catalyzed reactions are exceptionally mild and chemoselective; hence, they can be applied for the total synthesis of complex natural products even in late stages.⁴⁴ These reactions have proven to be mild and high yielding with no side reactions. A classic example of this is the total synthesis of Neurymenolide A by Fürstner and coworkers.⁴⁵ Neurymenolide A is an α -pyrone-derived natural product that exhibits activity against methicillin-resistant *Staphylococcus aureus* and vancomycin-resistant *Enterococcus faecium*. Fürstner and coworkers synthesized the important α -pyrone core by using gold-catalyzed cyclization. The precursor represents several challenges as it includes a polyunsaturated system. However, the use of a Xphos-ligated gold complex led to the proposed α -pyrone synthesis. The cyclization occurs at

room temperature, producing α -pyrone in 73% yield. This represents the chemoselectivity and mildness of the gold-catalyzed reaction (**Scheme 1-19**).⁴⁵



Scheme 1-19. Crucial synthetic step: Neurymenolide-A synthesis.

1.6 Multicatalysis

Homogeneous metal catalysis has revolutionized the field of organic synthesis. Due to extensive research in this area, it now has applications in various fields ranging from natural product synthesis to the synthesis of privileged structures. At the same time, in the last decade there has been explosive growth in the area of organocatalysis, a field in which small organic molecules are used as a catalyst to bring about a chemical transformation.

In an effort to find efficient ways to build complex molecular structures with excellent overall selectivity and to enhance the extent of chemical transformations, scientists have taken advantage of multicatalysis, which allows them to construct highly functionalized molecules rapidly using simple starting materials. Such reactions usually involve two or more different types of catalytic processes. Multicatalysis can be divided into three main categories: dual metal catalysis, a combination of two organocatalysts, and

organocatalysis with metal catalysis.⁴⁶ Of these, the latter one is described below with a few examples.

1.6.1 Merging Organocatalysis with Homogeneous Metal Catalysis⁴⁷

Organocatalysis involves either enamine activation or iminium activation. It entails the activation of carbonyl compounds using amines. Enamine behaves as nucleophiles whereas iminium behaves as electrophiles (**Figure 1-5**).

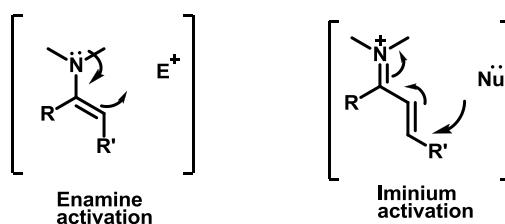
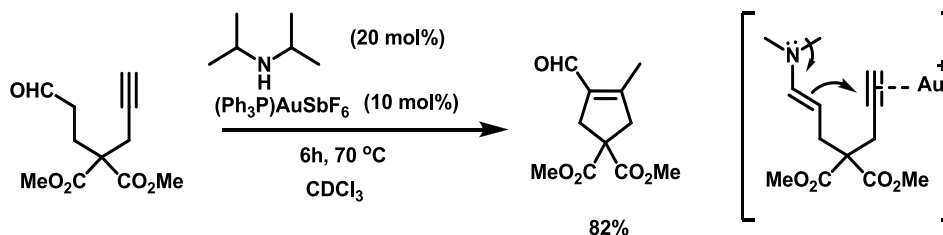


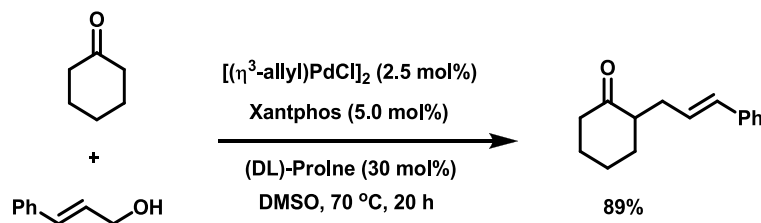
Figure 1-5. Organocatalysis, mode of reactivity: Enamine and iminium activation.

It is well known that carbonyl compounds can be activated as enamines, which perform as nucleophiles. Their reaction with the activated electrophiles (catalyzed by transition metal) represents an excellent opportunity. One of the ways to activate the alkyne is by using cationic gold complexes. The participation of such a gold-activated alkyne in the overall reaction with enamine nucleophiles represents a unique opportunity. The addition of activated methylene compounds across unactivated alkynes is well known. However, a less enolizable carbonyl compound struggles to react with alkynes. In 2008, Kirsch and coworkers described a successful recipe where they successfully combined organocatalysis with gold(I) catalysis. They described the 5 *exo-dig* intramolecular cyclization of terminal alkynes (**Scheme 1-20**).⁴⁸

**Scheme 1-20.** Merging organocatalysis with gold catalysis.

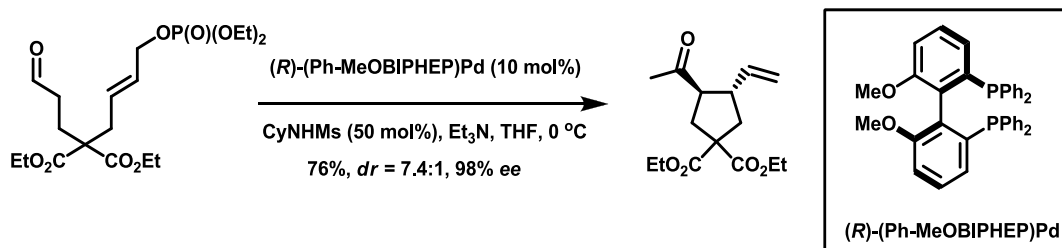
The formyl alkyne was treated with $(\text{PPh}_3)\text{AuSbF}_6$ (10 mol%) and diisopropylamine (20 mol%) in CDCl_3 at 70°C , which resulted in a thermodynamic product with an 82% yield from the 5 *exo-dig* cyclization (**Scheme 1-20**). Based on the control reactions, it was concluded that the absence of either reagent does not produce the required product. Kirsch proposed a mechanism in which the enamine nucleophile attacks the Au(I)-activated alkyne followed by a double bond migration as depicted in **Scheme 1-20**.⁴⁸

Breit and coworkers reported a dual proline and homogeneous palladium-catalyzed allylic alkylation of enolizable carbonyl compounds with allylic alcohol. They asserted that an intermolecular proline catalyzed enamine addition to a palladium π -allyl complex was occurring (**Scheme 1-21**).⁴⁹

**Scheme 1-21.** Merging organocatalysis with Pd catalysis.

Breit conducted an extensive search for the perfect source of an amine and ligand and found that a combination of proline and Xantphos along with Pd

was the best for the catalytic system. It was believed that the Xantphos provided the biggest bite angle, which is required to form the Pd π -allyl complex. In support of this assumption, reactions conducted with other ligands such as PPh_3 , dppe, dppf, and DPEphos produced inferior yields as a result of their low bite angle in comparison to the Xantphos bite angle (111°). Breit also observed that employing enantiomerically pure proline did not provide enough induction for this allylation reaction, which is a drawback of this approach (**Scheme 1-21**).⁴⁹



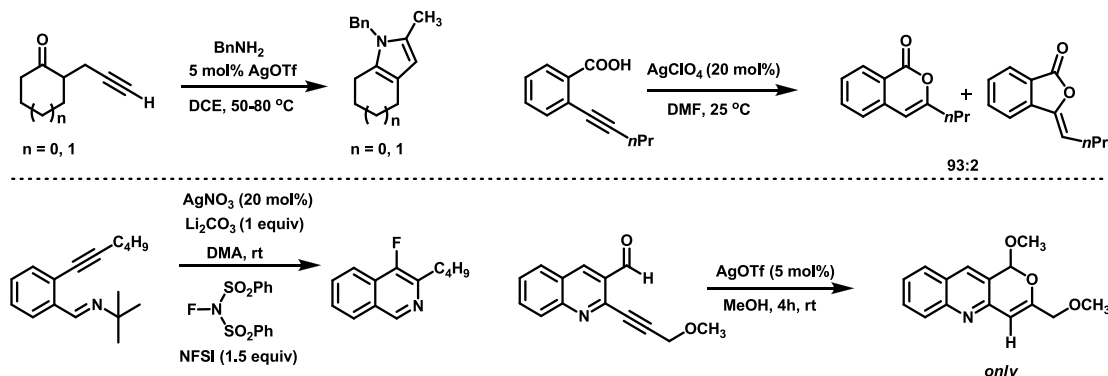
Scheme 1-22. Merging organocatalysis with Pd catalysis: Introduction of asymmetry.

In 2009, Saicic successfully reported an asymmetric version for a similar reaction. Saicic used allyl phosphate as a substrate with palladium ligated to (R) -(Ph-MeOBIPHEN)Pd (10 mol%), which resulted in a five-membered ring with good yield, and most importantly, with good dr and ee . Other bidentate ligands gave either a poor yield or poor selectivity (**Scheme 1-22**).⁵⁰

Gold catalysis was neglected for a long time due to cost, insolubility of gold salts and lack of development of homogeneous catalysis. However, the last decade or so, has seen a tremendous growth in their applicability in catalysis, especially homogeneous catalysis. Today, gold catalysts are among the most popular choices of organic chemists for the synthesis of various heterocycles under mild conditions.

1.7 Silver

Silver, with the atomic symbol Ag and an atomic number of 47, belongs to group 11 with $[\text{Kr}]4d^{10} 5s^1$ as its electronic configuration. Naturally occurring silver has two stable isotopes: ^{107}Ag and ^{109}Ag , the former exists in slightly higher proportion (51.8%). The most common oxidation state of silver is +1, although +2 and +3 also exist. Silver has a long history in organic chemistry. For example, reactions such as the Arndt-Eistert rearrangement and the Wolff rearrangement were known in the early 20th century. In addition, there is the stoichiometric use of Ag(I) salts in Tollens' reaction, where carboxylic acids can be synthesized from aldehydes. Although, Ag(I)-catalyzed reactions are well established, the last two decades have seen a renaissance in Ag(I) catalysis. It has primarily played a crucial role in Au and Pd catalysis, where silver salts are added purely to drive silver-halide precipitation, thereby opening a vacant site in the coordination sphere of the metal. Silver-mediated reactions, especially with Ag(I), are possible because of its mild Lewis acidity.⁵¹

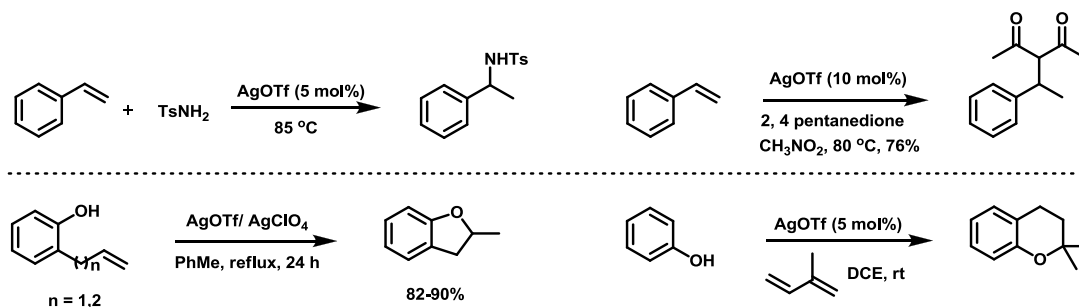


Scheme 1-23. Silver(I) catalyzed activation of alkynes.

Ag(I) salts can behave as σ -Lewis acids and π -Lewis acids. Similar to Au(I), when coordinated to the π -electrons, the π -system (olefin, alkyne, etc.) become susceptible to a nucleophilic attack. Such nucleophilic attacks can be

intramolecular or intermolecular. With an intramolecular nucleophilic attack, a variety of heterocycles can be synthesized.⁵¹

The Ag(I)-catalyzed activation of alkynes has seen great success. This approach is used to synthesize various *O*- and *N*-heterocycles. **Scheme 1-23** illustrates a few examples. Functionalized pyrroles were synthesized by the intramolecular cyclization of in situ generated imine on to alkyne, which was activated by silver triflate (**Scheme 1-23, top left**).⁵² The AgClO₄/DMF catalytic system was used for the selective synthesis of pyranones (**Scheme 1-23, top right**). This selective *endo*-lactonization strategy was achieved using an intramolecular carboxylic acid addition to the Ag(I)-activated alkyne. Negishi and coworkers also showed that the *exo* and *endo* mode of lactonization can be selectively achieved using specific Ag(I) salts (**Scheme 1-23, top right**).⁵³

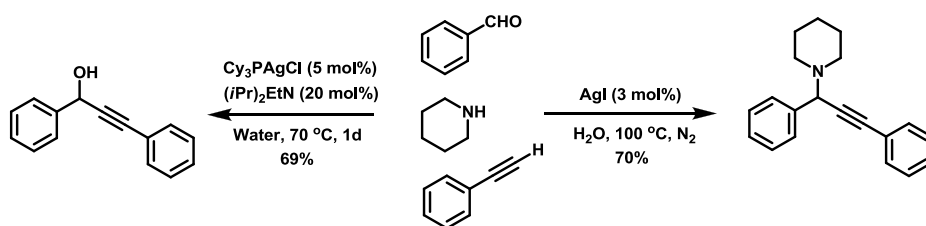


Scheme 1-24. Silver(I) catalyzed activation of alkenes.

Liu and coworkers described the Ag(I)-catalyzed intramolecular oxidative aminofluorination of alkynes. Researchers have shown that the presence of a base is crucial for the inhibition of the hydroamination product (**Scheme 1-23, bottom left**).⁵⁴ Belmont and coworkers selectively synthesized pyranoquinolines using silver triflate. Carbonyl oxygen adds to the Ag(I)-activated alkynes through 6-*exo-dig* cyclization, generating a pyrylium intermediate. Methanol addition and protonation produce the pyranoquinoline product. Similarly, 5-*endo-dig* was also created using silver oxide as the

source of silver. They explained the observed dichotomy by using the pK_a values of the conjugate acid of the silver counterion (**Scheme 1-23, bottom right**).⁵⁵

Compared to alkynes, Ag(I)-catalyzed reactions of alkenes are less studied. **Scheme 1-24** presents a few examples. The silver triflate catalyzed hydroamination of styrene was achieved with tosylamide by Nájera and coworkers (**Scheme 1-24, top left**).⁵⁶ In one case, Li and coworkers reported the silver triflate catalyzed addition of activated methylene compounds (malonates) to styrene in refluxing CH_3NO_2 (**Scheme 1-24, top right**).⁵⁷ In another example, the intramolecular cyclization of phenol derivatives on the terminal alkene was achieved in refluxing toluene (**Scheme 1-24, bottom left**).⁵⁸ Silver triflate catalyzed sequential C-C and C-O bond formation was realized between phenol and diene (**Scheme 1-24, bottom right**).⁵⁹

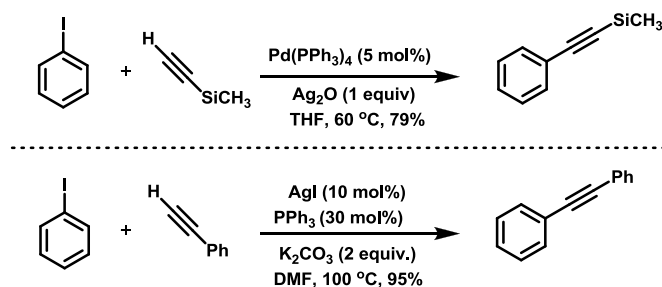


Scheme 1-25. Ag(I) catalyzed three component coupling reaction.

In the case of terminal alkyne, after initial π -coordination, the corresponding silver acetylide could be formed. Such silver acetylides are mild, are stable, can be easily stored, and are nucleophilic in nature; moreover, they can be added to activated carbonyl groups and imines.^{51a} For example, Li and coworkers reported a three-component coupling of aldehydes, alkynes, and amines catalyzed by AgI in refluxing water.^{60a} Additionally, the first catalytic nucleophilic addition of alkynyl silver to aldehydes was achieved using AgCl, Cy₃P, and ethyldiisopropylamine in water. It was found that the water and

phosphine activated the silver acetylide toward the nucleophilic addition (**Scheme 1-25**).^{60b}

Silver acetylides can be used in trapping experiments as well as with electrophiles such as deuterium, halogens, CO₂, etc. They can also be used in cross-coupling reactions where silver acetylide can transmetalate to vinyl, or aryl palladium species, formed after the initial oxidative addition reaction between the Pd(0) catalyst and vinyl or aryl iodide, for example, when Ag(I) assists in a Pd(0)-mediated Sonogashira reaction (**Scheme 1-26, top**).^{51e}



Scheme 1-26. Role of Ag(I) catalyst in the Sonogashira reaction.

On the other hand, recently, Wang and Li reported on a Pd-free, Ag(I)-catalyzed Sonogashira reaction (**Scheme 1-26, bottom**). The researchers successfully carried out a Sonogashira reaction using aryl iodide and various aryl and alkyl acetylenes, using AgI/PPh₃, potassium carbonate, and DMF. Although the reaction mechanism was not clear, the involvement of silver acetylide has been suggested.⁶¹

The last decade has seen increasing interest toward homogeneous silver(I)-catalyzed reactions involving phosphine ligands. The Ag(I)-BINAP catalyst system was introduced by Yamamoto and coworkers for an enantioselective allylation reaction between aldehydes and allyltributyltin. For example, a 5 mol% AgOTf (S)-BINAP catalyst catalyzed the allylation reaction between benzaldehyde and allyltributyltin with 88% yield and 96% ee.⁶² A similar

allylation reaction using allylsilanes was also reported using (R)-BINAP and AgF, with good yields and enantioselectivities.^{63a} Apart from allylation reactions, the Ag(I)-BINAP catalyst system was also used in reactions such as the Mukiyama-aldol reaction, Nitroso-aldol reactions, etc.^{51b,g}

Hoveyda and Snapper reported amino acid based ligands for a Ag(I)-catalyzed hetero-Diels-Alder reaction of imines and Danishefsky diene, which produced cycloadducts in high yields with > 89% ee.⁶⁴ Hoveyda also described an enantioselective Mannich reaction between silyl enol ethers and aldimines catalyzed by an *iso*-Leu-derived phosphine ligand and AgOAc in the presence of 2-propanol.⁶⁴ Apart from these reports, several reactions including [3 + 2] cycloadditions, silyene transfer, Nitrene transfer, and carbene transfer reactions are known to be catalyzed by homogeneous Ag(I) catalysts.^{51b,g}

The synthetic community has begun to realize the efficiency of Ag catalysis in various organic reactions. Its mild Lewis acidity (σ and π) has played a significant role in its success. Silver catalysis does not necessarily require special reaction conditions such as an inert atmosphere, dry solvents, etc. Reaction times are often short, conversions are clean, and product isolation is easy. Silver salts are readily available and are economical. In the field of homogeneous Ag(I) catalysis, there are early signs of success with a few catalysts, such as Yamamoto's BINAP-based silver catalysts. However, the application of such catalysts is still sparse.^{63b-e} Despite its success, the low solubility of silver salts in organic media and thus the requirement of high temperatures for a Ag(I)-catalyzed organic reaction is often a concern. Such a high temperature reaction often precipitates the inactive silver mirror/Ag(0), which is difficult to get rid of.⁵¹

1.8 Homogeneous Silver Catalysis

The chemistry of homogenous ligated Pd(0) complexes has occupied center stage in transition metal mediated bond forming reactions over the last four

decades. In the last decade or so, the chemistry of gold(I) species of general type $L-Au^+X^-$ has emerged. As described above, while such species have isoelectronic s^0d^{10} configurations, their reactivity differs considerably, with Pd entering many processes via oxidative addition reactions while Au^+ complexes initiate reactions with alkynes, allenes, etc., via initial Lewis acid complexation. A series of comprehensive reviews on organosilver chemistry drew our attention for several reasons.⁵¹ These include the above-mentioned use of silver salts, as catalysts in organic reactions, despite the low solubility in organic media. In many cases for both Au and Pd catalysis, silver salts are added purely to drive silver-halide precipitation.

Given the pronounced ligand effects observed in L_2Pd chemistry and gold chemistry, it became of interest for us to investigate well-defined *homogeneous catalytic species* of type $L_2Ag^+X^-$ and to probe their reactivity. Would they initiate via Lewis acid activation like Au^+ ? Could they be tuned with the appropriate ligand to enter oxidative addition reactions, a holy grail in organosilver and gold chemistry,⁶⁵ or to perform other chemistries involving dual-metal catalysis or organocatalysis/transition metal co-catalyzed reactions? The increasing cost⁶⁶ for both Pd and Au precursors is another practicality warranting a closer look at the possibilities available with isoelectronic Ag(I)-species.

1.8.1 Hemilabile Ligands: SHOP (Shell higher olefin process) Ligand

Ligands containing both weakly and strongly coordinating appendages are classified as hemilabile ligands. Typically, homogenous catalysis involves the use of strong ligands, leading to stable complexes.^{6,67} Often, the literature reports the ineffectiveness of the catalytic system due to the absence of a vacant site.⁶⁸ However, hemilabile ligands have both hard and soft donors; as a result, when bound to a given metal, they can induce different electronic properties on substrate reactivity through their “on-off” polarization (**Figure 1-**

6). Due to such polarization, a vacant site is often created on the metal center for substrate binding and further reaction. These ligands play a crucial role in various reactions catalyzed by transition metals. There are a variety of hemilabile ligands reported in the literature, including P,O- and P,N-type ligands. They have enjoyed a lot of success in transition metal catalyzed cross-coupling reactions.^{6,67}

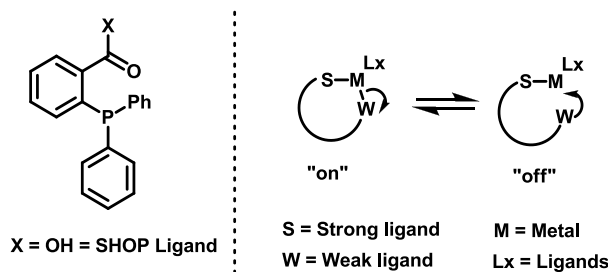
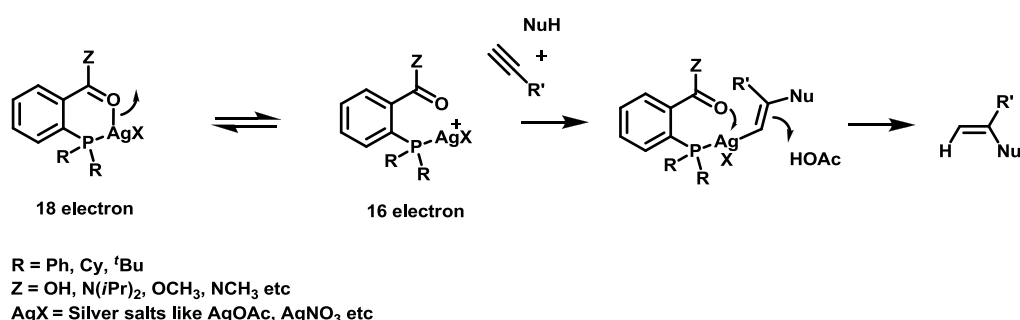


Figure 1-6. SHOP ligand and mode of reactivity of hemilabile ligands.

The applications of hemilabile ligands in transition metal chemistry are well documented. Perhaps the most important application for the P,O-type hemilabile ligand is the SHOP, which applies to the oligomerization of ethylenes. This novel catalytic system makes use of nickel salt and a bidentate (P,O) ligand. It was found to be very efficient in terms of the selective production of linear alpha olefins and today forms one of the most important industrial applications for homogeneous catalysis (**Figure 1-6**).⁶⁹

We assert that a scaffold based on the SHOP-type ligand could offer many advantages and be versatile in the development of progressively useful homogeneous silver(I) catalysts, including eventually the development of chiral versions. We envisioned that a (1:1) SHOP amide/acid and silver salt should form a stable 18-electron complex. This complex would have both a strong donor in the form of phosphine and a weak donor such as oxygen or nitrogen. As a result of this ligation, the resultant $L_2Ag(I)X^-$ complex should be readily

soluble in a variety of organic solvents. It would also be thermally stable, which would allow high temperature reactions without/with minimal silver metal deposition. The basic concept of the hemilabile SHOP amide/acid-AgX (X = anion) complex is to instill sequential acceptor/donor properties, i.e., activation of the alkyne (or, other π –system) via the 16-electron intermediate and the addition of a nucleophile, followed by the back donation from the weak donor before protonation.



Scheme 1-27. Homogeneous AgX catalysis with hemilabile ligands:
 Mechanism of action.

It is well known that silver salts can act as a σ -Lewis acid and/or a π -Lewis acid. Upon coordination with silver salts, the π -system should become more susceptible to nucleophilic attack. Gold catalysts are considered to be the most promising activators for triple bonds. One of the factors responsible for this is the binding energy of the active catalyst. The binding energy of gold compounds upon coordination with triple bond is 28–39 kcal mol⁻¹, whereas silver salts are in the region of 18–30 kcal mol⁻¹, clearly making the former superior. However, cationic species of the class AgPR₃⁺ can exhibit binding energies of 30 kcal mol⁻¹ which is similar to gold, potentially rendering them as effective mild Lewis acid catalysts.⁷⁰ We expect the modulation of the R, Z, and X groups to significantly affect π -activation with the eventual goal of developing ligated Ag(I) catalysts that can perform as Au(I)-type catalysis (**Scheme 1-27**).

1.9 Objective

The objective of the work described in this thesis was to synthesize SHOP-type P,O-, and, P,N-type hemilabile ligands and to synthesize new transition metal complexes (mainly Ag and Pd) containing mixed donor ligands, allowing us to study their catalytic activities in transition metal catalyzed reactions.

In chapter two, the successful synthesis of the first well-defined SHOP amide, the AgOAc complex, is described. The stability and applicability of this complex toward the first example of homogeneous silver(I)-catalyzed azide-alkyne cycloaddition (AgAAC) is described. Further, the logical optimization of the ligand structure, which resulted in a more active catalyst system and subsequent improvement in the catalytic activity of the AgAAC reaction, is also reported.

In chapter three, homogeneous silver(I)-catalyzed intramolecular hydroamination leading to 2-substituted indoles is described.

In chapter four, a new class of hemilabile ligands is synthesized from commercially available, low-cost phthalide is described. The successful application of these ligands in activating aryl chlorides for an SM cross-coupling reaction is discussed.

1.10 The Wittig Reaction

The direct conversion of aldehydes or ketones to olefins was a key fundamental problem for synthetic organic chemists until Wittig and coworkers published their landmark papers in the early 1950s. Only a few years after its discovery, the Wittig reaction began to play a major role in synthetic organic chemistry. Olefination reactions, including the classic Wittig and later Horner, Horner-Wadsworth-Emmons, and Peterson chemistry, are considered highly reliable regio- and stereo-controllable reactions and are now regarded as strategic C-C bond forming reactions frequently encountered in complex organic synthesis.

A typical Wittig reaction involves the condensation reaction of a phosphorus ylide with an aldehyde or ketone followed by an elimination yielding an olefin and phosphine oxide (**Figure 1-7**).⁷¹

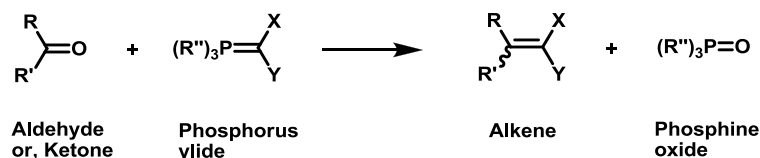
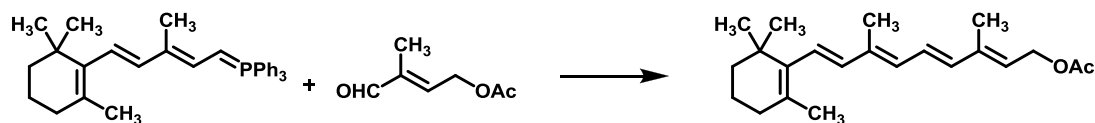


Figure 1-7. General Wittig reaction.

By virtue of its effectiveness, the Wittig reaction has been applied by scientists in many natural product syntheses, both in academia and in the industry. For example, the synthesis of vitamin “A,” acetate, was the first example of the Wittig reaction on an industrial scale (**Scheme 1-28**).⁷²



Scheme 1-28. Vitamin A acetate synthesis.

The Wittig reaction involves phosphorus ylides as the nucleophilic carbon component. The ylides are prepared through the deprotonation of the phosphonium salts. These phosphonium salts are usually prepared through a reaction of triphenylphosphine and an alkyl halide. Alkyltriphenyl phosphonium halides are weakly acidic; therefore strong bases like sodium hydride, organolithium reagents, substituted amide anions like hexamethyldisilylamide (HMDS), etc., must be used. The ylides generated are then quenched with the carbonyl compounds.⁷³ The synthetic utility of phosphorus ylides was first

developed by the Wittig group. Their reaction with aldehydes or ketones allows a carbon-carbon double bond formation with complete positional control.⁷⁴

The reaction mechanism for the Wittig reaction is one of the most discussed topics in the literature and active research is still being conducted in this area.⁷⁵

The mechanism proposed involved the addition of the nucleophilic ylide carbon to the carbonyl group of the aldehyde/ketone to produce a dipolar intermediate called a betaine. This was followed by the elimination of phosphine oxide to yield the olefin. This syn-periplanar elimination is believed to occur after the formation of a four-member oxaphosphetane (OPA) intermediate. Alternatively, the reaction might proceed through initial direct formation of the OPA intermediate, involving a formal polar [2+2] cycloaddition of the ylide and carbonyl group (**Figure 1-8**). Research at the theoretical level has been carried out to study such OPA intermediates.

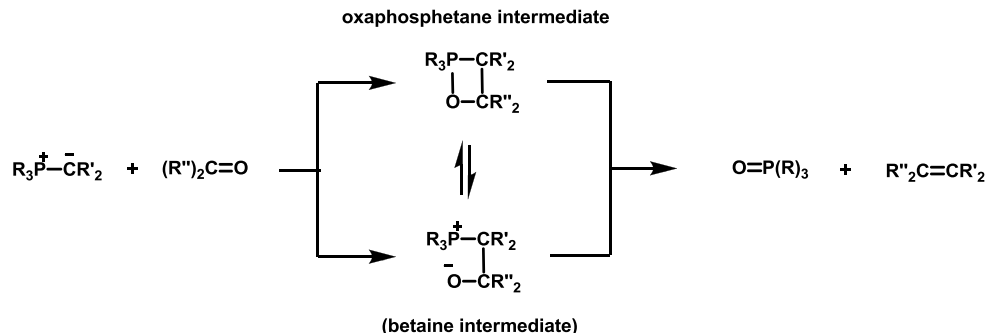


Figure 1-8. Mechanism of Wittig reaction.

In general, ylides can be classified as non-stabilized ($R' = \text{alkyl}$), semi (moderately) stabilized ($R' = \text{aryl}$), or stabilized ($R' = \text{CO}_2R, \text{CN}$) based on the charge delocalization. Non-stabilized ylides are highly reactive and their Wittig reactions often provide (*Z*)-olefins. The Wittig reactions of semi-stabilized ylides are not selective and give a 1:1 mixture of (*E*)- and (*Z*)-olefin isomers. Use of resonance-stabilized ylides often leads to *threo* betaine/OPA and thus to the

(*E*)-olefin.⁷³ However, the outcome of the Wittig reaction largely depends upon the use of solvent, base, aldehyde, and substituents on stationary phosphorus during the reaction itself.

The stereochemical outcome of the olefins generated from the Wittig reaction can be affected by the solvent concentration, the cation of the base used for deprotonation, the temperature of the reaction, and the type of aldehyde. Scientists have attempted to explain the stereochemical outcome of the Wittig reaction and whether an intermediary reaction involves betaine or OPA.^{74,75} Several studies have proposed the existence of betaine as an intermediate for the Wittig reaction under certain reaction conditions⁷⁶ and some conclusions should be made from such studies, as the presence of lithium salts does favor the formation of betaines. However, efforts have been made to distinguish between “salt” and “salt free” Wittig reactions. Vedejs studied the Wittig reaction mechanism and provided evidence in favor of an OPA intermediate. He reviewed low-temperature NMR studies and characterized the OPA intermediates; all the while, he was unable to detect betaine intermediates. In 1988, Vedejs highlighted the importance of 1,2 and 1,3 interactions in “salt free” Wittig chemistry. He states that “*Typical non-stabilized or, moderate ylides react via an early transition state and under kinetic control. The subtle interplay of 1,2 and 1,3 steric interactions is responsible for cis and trans selectivity and puckered transition states are increasingly important as the 1,3 interactions associated with the bulk α to the carbonyl group become dominant.*” Thus the non-stabilized ylides react via an early puckered *cis* TS that minimizes 1,2 and 1,3 steric interaction while *trans* TS is more planar. Although *trans* TS has an unfavorable 1,3 interaction, subsequent puckering would lead to an increase in the 1,2 interaction. Therefore with regard to non-stabilized ylides, *cis* TS is favored over *trans* TS, whereas for stabilized ylides, planar TS is favored since 1,2 steric hindrance plays a more important role in *cis* TS (**Figure 1-9**).⁷⁷

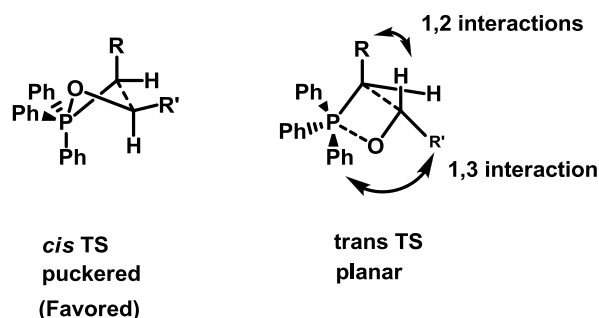


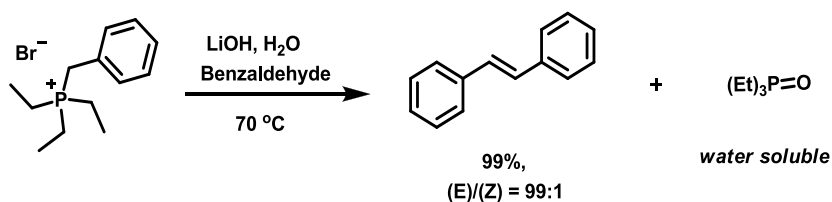
Figure 1-9. Vedejs's model explaining the stereochemical outcome of the Wittig reaction.

Although the Wittig reaction has several advantages, it suffers from a serious problem of isolation with regard to the olefin from the reaction mixture. At the end of the Wittig reaction, the reaction mixture consists of a corresponding product and equimolar phosphine oxide by-product. Isolating the olefin in such a situation is a real challenge.

Phosphine oxides can be removed from the reaction mixture through filtration; however, difficulties were encountered when filtration was practiced at an industrial scale due to the expensive specialized facilities required.⁷⁸ To date, various methods have been reported to address the problem of phosphine oxide. Solutions generally include the use of phosphine, having the formula PPh_2Ar , where Ar is a phenyl group with 4-COOH, or they include the use of 4- NR_2 , which facilitates the removal of phosphine oxide after the Wittig reaction has occurred by washing it with a base or an acid.⁷⁸ It is also possible to distill the required olefin out of the reaction mixture.⁷⁸ These remedies have certain advantages but they also suffer from drawbacks, such as the lengthy procedures involved in making special phosphines or the loss of stereochemical information about olefin due to distillation. Alternatively, phosphine oxide can be isolated and converted back to a phosphine through a reduction with alane.⁷⁹

1.11 Wittig Chemistry Development in McNulty Lab

McNulty Lab has been working in the field of Wittig olefination for the past seven to eight years. Our lab has enjoyed a lot of success in this field, particularly in using trialkylphosphonium salts for the Wittig reaction and in removing phosphine oxide from the Wittig reaction mixture. In 2009, McNulty and coworkers demonstrated that semi-stabilized ylides can be formed in water from the reaction of trialkylbenzylphosphonium salts and sodium hydroxide/lithium hydroxide.⁸⁰ The generated ylide reacted with aromatic aldehydes in the water and resulted in the precipitation of trans-stilbene with good selectivity. The success of this approach is attributed to the chemoselective deprotonation of the benzylic C-H protons. In addition to this success, trialkylphosphine oxide, a by-product from the reaction, was shown to be completely water-soluble (**Scheme 1-29**).



Scheme 1-29. Use of trialkylphosphines in the Wittig reaction.

Since then, McNulty and coworkers have extended the scope of this aqueous Wittig chemistry in order to access 1,3-dienes and 1,3,5-trienes.⁸⁰ Shortly after that, the thermal reaction of trialkylphosphine hydrohalide with benzylic alcohol and allylic alcohol was shown to directly yield a corresponding phosphonium salt without accessing the corresponding toxic halides. The microwave-assisted synthesis of stilbenes and heterostilbenes generated from these ylides in water proved beneficial. It not only reduced the overall time required for the synthesis but was also chemoselective in the presence of aldehydes containing other

acidic functionality like phenol, indole, pyrroles, etc.⁸⁰ In 2010, McNulty and coworkers reported the dichotomous reactivity of triphenylphosphine and triethylphosphine hydrobromide salts in their reactions with dimethyl acetals (Figure 1-10).⁸¹

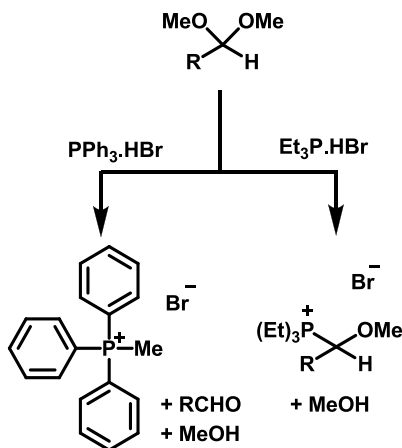


Figure 1-10. Dichotomous reactivity of dialkyl vs. diarylphosphonium salts with dimethyl acetals.

Triphenylphosphine hydrobromide was found to react with dimethyl acetals, but the reaction proceeded to yield the corresponding quaternary methyl(triphenyl) phosphonium salt. Remarkably, the reaction of triethylphosphine hydrobromide with dimethyl acetals was found to produce the corresponding α -methoxy phosphonium salt. In addition, the thermal reaction of benzaldehyde dimethyl acetal with triethylphosphonium hydrobromide gave the corresponding α -methoxy phosphonium salt. This new process was found to be quite general and allowed the high-yielding synthesis of a range of α -methoxy functionalized phosphonium salts under mild conditions.

The proposed mechanism involved an initial protonation and the loss of methanol molecules in order to generate an oxonium cation. Due to the sterics and soft nature of triphenylphosphine, it attacks the methyl group yielding P-

methyl phosphonium. In contrast, the strong and not-so-bulky triethylphosphine nucleophile directly attacks the cationic site producing alkoxy phosphonium salt. Ylides generated from these α -alkoxyphosphonium salts under classical Wittig conditions were able to react with a variety of aldehydes, producing vinyl ethers in good yields.

1.12 Objectives

In order to extend the utility of these α -alkoxyphosphonium salts beyond simple stilbene formation, we wish to use ylides generated from α -alkoxyphosphonium salts with other carbonyl groups (such as ethyl glyoxylate). We desire to engage dialkyl acetals derived from ethyl glyoxylate with triethylphosphonium hydrohalides. Subsequently, we want to take advantage of these olefination products and further use them in transition metal catalyzed chemistry and/or other applications.

In chapter five, successful reactions of α -alkoxyphosphonium salts with ethyl glyoxylate are described. The use of these olefination products as “alkyne surrogates” in a Cu-free click reaction to produce 1,5-substituted 1,2,3 triazoles, which inhibit human aromatase (CYP 450 19A1), is also described.

In chapter six, the synthesis of α -alkoxy acrylates and cinnamates from a reaction of dialkylacetals derived from ethyl glyoxylate with carbonyl compounds is presented. The use of α -alkoxy acrylates in the Pd-catalyzed synthesis of indole-2-carboxylates is also discussed.

In chapter seven, the synthesis of a natural product, nostodione A, and its analogs is described. using earlier methodology of synthesizing indole-2-

carboxylates. A novel antiparasitic activity against *Toxoplasma gondii* is also described.

1.13 References

1. Crabtree, R. H. *The Organometallic Chemistry of the Transition Metals*. Wiley-VCH: Hoboken, New Jersey, **2009**.
2. Heitbaum, M.; Glorius, F.; Escher, I. *Angew. Chem. Int. Ed.* **2006**, *45*, 4732-4762.
3. (a) Appl, M. *Ullmann's Encyclopedia of Industrial Chemistry*, **2006**. (b) Voorhees, V.; Adams, R. *J. Am. Chem. Soc.* **1922**, *44*, 1397-1405. (c) Lindlar, H. *Helv. Chim. Acta*, **1952**, *35*, 446-450.
4. Pospech, J.; Fleischer, I.; Franke, R.; Buchholz, S.; Beller, M. *Angew. Chem. Int. Ed.* **2013**, *52*, 2852-2872.
5. Sunley, G. J.; Watson, D. J. *Catalysis Today*, **2000**, *58*, 293-307.
6. Kamer, Paul C. J.; Van Leeuwen, Piet W. N. M. *Phosphorus(III)Ligands in Homogeneous Catalysis: Design and Synthesis*. Wiley-VCH: **2012**.
7. (a) Negishi, E-I. *Handbook of Organopalladium Chemistry for Organic Synthesis*. John Wiley and Sons, Inc, New York, USA. (Ed) **2003**. (b) Tsuji, J. *Palladium in Organic Synthesis*, Springer: Berlin (Ed) **2005**. (c) Tsuji, J. *Palladium Reagents and Catalysts: Innovations in Organic Synthesis*. Wiley and Sons: New York, **1995**. (d) Molander, G. A. *Handbook of Reagents for Organic Synthesis, Catalyst Components for Coupling Reactions*. Wiley and Sons, **2008**. (e) Molnar, A. *Palladium-Catalyzed Coupling Reactions: Practical Aspects and Future*. John Wiley and Sons, **2013**.
8. (a) Jacobi, P. A.; Li, Y. *Org. Lett.* **2003**, *5*, 701-704. (b) Pei, T.; Wang, X.; Widenhoefer, R. A. *J. Am. Chem. Soc.* **2003**, *125*, 648-649. (c) Fix, S. R.; Brice, J. L.; Stahl, S. S. *Angew. Chem. Int. Ed.* **2002**, *41*, 164-166. (d) Semmelhack, M. F.; Zask, A. *J. Am. Chem. Soc.* **1983**, *105*, 2034-2043. (e) Wolf, L. B.; Tjen, K. C. M. F.; Brink, H. T.; Blaauw, R. H.; Hiemstra, H.;

- Schoemaker, H. E.; Rutjes, F. P. J. T. *Adv. Synth. Catal.* **2002**, *344*, 70-83.
- (f) Álvarez, R.; Martínez, C.; Madich, Y.; Denis, J. G.; Aurrecoechea, J. M.; de Lera, Á. R. *Chem. Eur. J.* **2010**, *16*, 12746-12753.
9. (a) Fujiwara, Y.; Moritani, I.; Danno, S.; Asano, R.; Teranishi, S. *J. Am. Chem. Soc.* **1969**, *91*, 7166-7169. (b) Oestreich, M. *The Mizoroki-Heck Reaction*. Wiley-VCH, **2009**.
10. (a) Yu, J.; Shi, Z. *C-H activation: Topics in Current Chemistry*, **2011**, 292. (b) van Helden, R.; Verberg, G. *Recl. Trav. Chim. Pays-Bas*, **1965**, *84*, 1263-1273. (c) Iataaki, H.; Yoshimoto, H. *J. Org. Chem.* **1973**, *38*, 76-79.
11. Reetz, M. T.; de Vries, J. G. *Chem. Commun.* **2004**, 1559-1563.
12. Colacot, T. J. *Platinum Metals Rev.* **2011**, *55*, 84-90.
13. Martin, R.; Buchwald, S. L. *Acc. Chem. Res.* **2008**, *41*, 1461-1473.
14. (a) Dieck, H. A.; Heck, R. F. *J. Org. Chem.* **1975**, *40*, 1083-1090. (b) Miyaura, N.; Yamada, K.; Suzuki, A. *Tetrahedron Lett.* **1979**, *20*, 3437-3440.
15. Shen, W. *Tetrahedron Lett.* **1997**, *38*, 5575-5578.
16. (a) Littke, A. F.; Fu, G. C. *Angew. Chem. Int. Ed.* **1998**, *37*, 3387-3388. (b) Fu, G. C. *Acc. Chem. Res.* **2008**, *41*, 1555-1564.
17. (a) Old, D. W.; Wolfe, J. P.; Buchwald, S. L. *J. Am. Chem. Soc.* **1998**, *120*, 9722-9723. (b) Wolfe, J. P.; Buchwald, S. L. *Angew. Chem. Int. Ed.* **1999**, *38*, 2413-2416. (c) Wolfe, J. P.; Singer, R. A.; Yang, B. H.; Buchwald, S. L. *J. Am. Chem. Soc.* **1999**, *121*, 9550-9561.
18. Billingsley, K.; Buchwald, S. L. *J. Am. Chem. Soc.* **2007**, *129*, 3358-3366.
19. (a) So, C. M.; Lau, C. P.; Chan, A. S. C.; Kwong, F. Y. *J. Org. Chem.* **2008**, *73*, 7731-7734. (b) Nguyen, H. N.; Huang, X.; Buchwald, S. L. *J. Am. Chem. Soc.* **2003**, *125*, 11818-11819.
20. (a) So, C. M.; Lau, C. P.; Kwong, F. Y. *Org. Lett.* **2007**, *9*, 2795-2798. (b) So, C. M.; Yeung, C. C.; Lau, C. P.; Kwong, F. Y. *J. Org. Chem.* **2008**, *73*, 7803-7806. (c) Chow, W. K.; So, C. P.; Lau, C. P.; Kwong, F. Y. *J. Org. Chem.* **2010**, *75*, 5109-5112.

21. (a) Jensen, J. F.; Johannsen, M. *Org. Lett.* **2003**, 5, 3025-3028. (b) Liu, S-Y.; Choi, M. J.; Fu, G. C. *Chem. Commun.* **2001**, 2408-2409.
22. Kondolff, I.; Doucet, H.; Santelli, M. *Tetrahedron*, **2004**, 60, 3813-3818.
23. Bei, X.; Turner, H. W.; Weinberg, H.; Guram, A. S. *J. Org. Chem.* **1999**, 64, 6797-6803.
24. (a) Adjabeng, G.; Brenstrum, T.; Wilson, J.; Frampton, C.; Robertson, A.; Hillhouse, J.; McNulty, J.; Capretta, A. *Org. Lett.* **2003**, 5, 953-955. (b) Brenstrum, T.; Gerristman, D. A.; Adjabeng, G. M.; Frampton, C. S.; Britten, J.; Robertson, A. J.; McNulty, J.; Capretta, A. *J. Org. Chem.* **2004**, 69, 7635-7639. (c) Ullah, E.; McNulty, J.; Robertson, A. *Eur. J. Org. Chem.* **2012**, 2127-2131. (d) Ullah, E.; McNulty, J.; Kennedy, C.; Robertson, A. *Org. Biomol. Chem.* **2011**, 9, 4421.
25. (a) Manabe, K.; Yamaguchi, M. *Catalysis*, 2014, 4, 307-320.
26. Ley, S. V.; Thomas, A. W. *Angew. Chem. Int. Ed.* **2003**, 42, 5400-5449.
27. van der Vlugt, J. I. *Chem. Soc. Rev.* **2010**, 39, 2302-2322.
28. Shen, Q.; Hartwig, J. F. *J. Am. Chem. Soc.* **2006**, 128, 10028-10029.
29. Surry, D. S.; Buchwald, S. L. *J. Am. Chem. Soc.* **2007**, 129, 10354-10355.
30. Vo, G. D.; Hartwig, J. F. *J. Am. Chem. Soc.* **2009**, 131, 11049-11061.
31. (a) Alsabeh, P. G.; Lundgren, R. J.; McDonald, R.; Johansson Seechurn, C. C. C.; Colacot, T. J.; Stradiotto, M. *Chem. Eur. J.* **2013**, 19, 2131-2141. (b) Lundgren, R. J.; Stradiotto, M. *Aldrichimica Acta*, **2012**, 45, 59-66. (c) Crawford, S. M.; Lavery, C. B.; Stradiotto, M. *Chem. Eur. J.* **2013**, 19, 16760-16771.
32. Ackermann, L.; Althammer, A. *Angew. Chem. Int. Ed.* **2007**, 46, 1627-1629.
33. (a) Fang, Y.; Lautens, M. *Org. Lett.* **2005**, 7, 3549-3552. (b) Newman, S. G.; Lautens, M. *J. Am. Chem. Soc.* **2010**, 132, 11416-11417.
34. (a) Gorin, D. J.; Toste, F. D. *Nature*, **2007**, 446, 395-403. (b) Pyykkö, P. *Angew. Chem. Int. Ed.* **2004**, 43, 4412-4456. (c) Pyykkö, P. *Inorg. Chim. Acta*. **2005**, 358, 4113-4130.

35. (a) Mezailles, N.; Ricard, L.; Gagosz, F. *Org. Lett.* **2005**, 7, 413-4136. (b) Ricard, L.; Gagosz, F. *Organometallics*, **2007**, 26, 4704-4707.
36. (a) González-Arellano, C.; Corma, A.; Iglesias, M.; Sánchez, F. *J. Catal.* **2006**, 238, 497-501. (b) Corma, A.; Gutiérrez-Puebla, E.; Iglesias, M.; Monge, A.; Pérez-Ferreras, S.; Sánchez, F. *Adv. Synth. Catal.* **2006**, 348, 1899-1907. (c) González-Arellano, C.; Abad, A.; Corma, A.; García, H.; Iglesias, M.; Sánchez, F. *Angew. Chem. Int. Ed.* **2007**, 46, 1536-1538. (d) Li, P.; Wang, L.; Wang, M.; You, F. *Eur. J. Org. Chem.* **2008**, 5946-5951. (e) Lauterbach, T.; Livendahl, M.; Rosellón, A.; Espinet, P.; Echavarren, A. M. *Org. Lett.* **2010**, 12, 3006-3009. (f) Corma, A.; Juárez, R.; Boronat, M.; Sánchez, F.; Iglesias, M.; García, H. *Chem. Commun.* **2011**, 47, 1446-1448.
37. (a) Hashmi, A. S. K. *Chem. Rev.* **2007**, 107, 3180-3211. (b) Arcadi, A. *Chem. Rev.* **2008**, 108, 3266-3325. (c) Li, Zigang.; Brouwer, C.; He, C. *Chem. Rev.* **2008**, 108, 3239-3265. (d) Gorin, D. J.; Sherry, B. D.; Toste, F. D. *Chem. Rev.* **2008**, 108, 3351-3378. (e) Corma, A.; Leyva-Pérez, A.; Sabater, M. J. *Chem. Rev.* **2011**, 111, 1657-1712. (d) Krause, N.; Winter, C. *Chem. Rev.* **2011**, 111, 1994-2009. (e) Hashmi, A. S. K. *Angew. Chem. Int. Ed.* **2010**, 49, 5232-5241. (f) Hashmi, A. S. K.; Bührle, M. *Aldrichim. Acta.* **2010**, 43, 27-33.
38. Nieto-Oberhuber, C.; Paz Muñoz, M.; Buñuel, E.; Nevado, C.; Cárdenas, D. J.; Echavarren, A. M. *Angew. Chem. Int. Ed.* **2004**, 43, 2402-2406.
39. Ferrer, C.; Echavarren, A. M. *Angew. Chem. Int. Ed.* **2006**, 45, 1105-1109.
40. Hirano, K.; Inaba, Y.; Takahashi, N.; Shimano, M.; Oishi, S.; Fujii, N.; Ohno, H. *J. Org. Chem.* **2011**, 76, 1212-1227.
41. Kennedy-Smith, J. J.; Staben, S. T.; Toste, F. D. *J. Am. Chem. Soc.* **2004**, 126, 4526-4527.
42. (a) Zhang, J.; Yang, C.; He, C. *J. Am. Chem. Soc.* **2006**, 128, 1798-1799. (b) Han, X.; Widenhoefer, R. A. *Angew. Chem. Int. Ed.* **2006**, 45, 1747-1749. (c) Widenhoefer, R. A.; Han, X. *Eur. J. Org. Chem.* **2006**, 4555-4563.

43. (a) Genin, E.; Toullec, P. Y.; Antoniotti, S.; Brancour, C.; Genêt, J.; Michelet, V. *J. Am. Chem. Soc.* **2006**, *128*, 3112-3113. (b) Chary, B. C.; Kim, S. *J. Org. Chem.* **2010**, *75*, 7928-7931.
44. (a) Zhang, Y.; Luo, T.; Yang, Z. *Nat. Prod. Rep.* **2014**, *31*, 489-503. (b) Hashmi, A. S. K.; Toste, F. D. *Modern Gold Catalyzed Synthesis: Wiley-VCH*, **2012**.
45. Chaladaj, W.; Corbet, M.; Fürstner, A. *Angew. Chem. Int. Ed.* **2012**, *51*, 6929-6933.
46. Patil, N. T.; Shinde, V. S.; Gajula, B. *Org. Biomol. Chem.* **2012**, *10*, 211-224.
47. (a) Zhong, C.; Shi, X. *Eur. J. Org. Chem.* **2010**, 2999-3025. (b) Loh, C. C. J.; Enders, D. *Chem. Eur. J.* **2012**, *18*, 10212-10225. (c) Duschek, A.; Kirsch, S. F.; *Angew. Chem. Int. Ed.* **2008**, *31*, 5703-5705. (d) Hashmi, A. S. K.; Hubbert, C.; *Angew. Chem. Int. Ed.* **2010**, *49*, 1010-1012.
48. Binder, J. T.; Crone, B.; Haug, T. T.; Menz, H.; Kirsch, S. F. *Org. Lett.* **2008**, *10*, 1025-1028.
49. Usui, I.; Schmidt, S.; Breit, B. *Org. Lett.* **2009**, *11*, 1453-1456.
50. Vulovic, B.; Bihelevic, F.; Matovic, R.; Saicic, R. N. *Tetrahedron*, **2009**, *65*, 10485-10494.
51. (a) Halbes-Letinois, U.; Weibel, J.; Pale, P. *Chem. Soc. Rev.* **2007**, *36*, 759-769. (b) Naodovic, M.; Yamamoto, H. *Chem. Rev.* **2008**, *108*, 3132-3148. (c) Yamamoto, Y. *Chem. Rev.* **2008**, *108*, 3199-3222. (d) Alvarez-Corral, M.; Munoz-Dorado, M.; Rodriguez-Garcia, I. *Chem. Rev.* **2008**, *108*, 3174-3198. (e) Weibel, J. M.; Blanc, A.; Pale, P. *Chem. Rev.* **2008**, *108*, 3149-3173. (f) Hirner, J. J.; Shi, Y.; Blum, S. A. *Acc. Chem. Res.* **2011**, *44*, 603-613. (g) Harmata, M. *Silver in Organic Chemistry*: John Wiley and Sons, Inc. **2010**.
52. Harrison, T. J.; Kozak, J. A.; Corbella-Pane, M.; Dake, G. R. *J. Org. Chem.* **2006**, *71*, 4525-4529.
53. Negeshi, E.; Kotora, M. *Tetrahedron*, **1997**, *53*, 6707-6738.
54. Xu, T.; Liu, G. *Org. Lett.* **2012**, *14*, 5416-5419.

55. Godet, T.; Vaxelaire, C.; Michel, C.; Milet, A.; Belmont, P. *Chem. Eur. J.* **2007**, *13*, 5632-5641.
56. Giner, X.; Najera, C. *Synlett*, **2009**, 3211-3213.
57. Yao, X.; Li, C. J. *J. Org. Chem.*, **2005**, *70*, 5752-5755.
58. Ito, Y.; Kato, R.; Hamashima, K.; Kataoka, Y.; Oe, Y.; Ohta, T.; Furukawa, I. *J. Organomet. Chem.* **2007**, *692*, 691-697.
59. Youn, S. W.; Eom, J. I. *J. Org. Chem.* **2006**, *71*, 6705-6707.
60. (a) Wei, C.; Li, Z.; Li, C. J. *Org. Lett.* **2003**, *5*, 4473-4475. (b) Yao, X.; Li, C. J. *Org. Lett.* **2005**, *7*, 4395-4398.
61. Li, P.; Wang, L. *Synlett*, **2006**, *14*, 2261-2265.
62. (a) Yanagisawa, A.; Nakashima, H.; Ishiba, A.; Yamamoto, H. *J. Am. Chem. Soc.* **1996**, *118*, 4723-4724. (b) Yanagisawa, A.; Nakashima, H.; Nakatsuka, Y.; Ishiba, A.; Yamamoto, H. *Bull. Chem. Soc. Jpn.* **2001**, *74*, 1129-1137.
63. (a) Yanagisawa, A.; Kageyama, H.; Nakatsuka, Y.; Asakawa, K.; Matsumoto, Y.; Yamamoto, H. *Angew. Chem. Int. Ed.* **1999**, *38*, 3701-3703. (b) Momiyama, N.; Yamamoto, H. *J. Am. Chem. Soc.* **2004**, *126*, 5360-5361. (c) Najera, C.; Retamosa, M. de G.; Sansano, J. M. *Org. Lett.* **2007**, *9*, 4025-4028. (d) Ohkouchi, M.; Masui, D.; Yamaguchi, M.; Yamagishi, T. *J. Mol. Cat. A: Chem.* **2001**, *170*, 1-16. (e) Lettko, L.; Wood, J. S.; Rausch, M. D. *Inorg. Chim. Acta.* **2000**, *308*, 37-44.
64. (a) Josephsohn, N. S.; Snapper, M. L.; Hoveyda, A. H. *J. Am. Chem. Soc.* **2003**, *125*, 4018-4019. (b) Josephsohn, N. S.; Snapper, M. L.; Hoveyda, A. H. *J. Am. Chem. Soc.* **2004**, *126*, 3734-3735. (c) Josephsohn, N. S.; Carswell, E. L.; Snapper, M. L.; Hoveyda, A. H. *Org. Lett.* **2005**, *7*, 2711-2713.
65. Wegner, H. A.; Auzias, M. *Angew. Chem. Int. Ed.* **2011**, *50*, 8236-8247.
66. Gold: 1266 US\$/oz, Palladium: 885 US\$/oz, Silver: 19 US\$/oz (Price on 2 September 2014. Source KITCO Ltd.)
67. Kwong, F. Y.; Chan, A. S. C. *Synlett*, **2008**, 1440-1448. (references therein)

68. Inoguchi, K.; Sakuraba, S.; Achiwa, K. *Synlett*, **1992**, 169-178.
69. Keim, W. *Angew. Chem. Int. Ed.* **2013**, 52, 12492-12496.
70. Yamamoto, Y.; Gridnev, I. D.; Patil, N. T. *Chem. Commun.* **2009**, 5075-5087.
71. Cary and Sundberg, *Advance Organic Chemistry-Part B*, 4th Edition.
72. Wittig, G.; Geissler, G. *Justus Liebigs Ann. Chem.* **1953**, 580, 44-57.
73. Pommer, H. *Angew. Chem. Int. Ed.* **1977**, 16, 423-429.
74. Schlosser, M. *Topics in Stereochemistry*, **1970**, 5, 1-30.
75. (a) Bestman, H.; Vostrowsky, O. *Topics in Current Chem.* **1983**, 109, 85-163.
(b) Vedejs, E. *Topics in Stereochemistry*, **1994**, 21, 1-158. (c) Byrne, P. A.; Gilheany, D. G. *Chem. Soc. Rev.* **2013**, 42, 6670-6696 (and ref therein).
76. (a) Schröder, U.; Berger, S. *Eur. J. Org. Chem.* **2000**, 2601-2604. (b) Neumann, R. A.; Berger, S. *Eur. J. Org. Chem.* **1998**, 1085-1087. (c) Subramanyam, C. *Tetrahedron Lett.* **1995**, 36, 9249-9252. (d) McNulty, J.; Keskar, K. *Tetrahedron Lett.* **2008**, 49, 7054-7057.
77. (a) Vedejs, E.; Snoble, K. A. *J. Am. Chem. Soc.* **1973**, 95, 5778-5780. (b) Vedejs, E.; Meier, G. P.; Snoble, K. A. *J. Am. Chem. Soc.* **1981**, 103, 2823-2831. (c) Vedejs, E.; Marth, C. F. *J. Am. Chem. Soc.* **1988**, 110, 3948-3958. (d) Vedejs, E.; Marth, C. F. *J. Am. Chem. Soc.* **1990**, 112, 3905-3909.
78. Fukumoto, T.; Yamamoto, A. *US patent 5292973*, **1994**,
79. (a) Griffin, S.; Heath, L.; Wyatt, P. *Tetrahedron Lett.* **1998**, 39, 4405-4406. (b) Bootle-Wilbraham, A.; Head, S.; Longstaff, J.; Wyatt, P. *Tetrahedron Lett.* **1999**, 40, 5267-5270.
80. (a) McNulty, J.; Das, P. *Eur. J. Org. Chem.* **2009**, 4031-4035. (b) McNulty, J.; Das, P. *Tetrahedron Lett.* **2009**, 50, 5737-5740. (c) McNulty, J.; Das, P.; McLeod, D. *Chem. Eur. J.* **2010**, 16, 6756-6760.
81. McNulty, J.; Das, P. *Eur. J. Org. Chem.* **2010**, 3587-3591.

JOHN WILEY AND SONS LICENSE
TERMS AND CONDITIONS

Sep 30, 2014

This is a License Agreement between Kunal Keskar ("You") and John Wiley and Sons ("John Wiley and Sons") provided by Copyright Clearance Center ("CCC"). The license consists of your order details, the terms and conditions provided by John Wiley and Sons, and the payment terms and conditions.

All payments must be made in full to CCC. For payment instructions, please see information listed at the bottom of this form.

License Number	3462570740887
License date	Sep 05, 2014
Licensed content publisher	John Wiley and Sons
Licensed content publication	Chemistry - A European Journal
Licensed content title	The First Well-Defined Silver(I)-Complex-Catalyzed Cycloaddition of Azides onto Terminal Alkynes at Room Temperature
Licensed copyright line	Copyright © 2011 WILEY-VCH Verlag GmbH & Co. KGaA, Weinheim
Licensed content author	James McNulty, Kunal Keskar, Ramesh Vemula
Licensed content date	Nov 28, 2011
Start page	14727
End page	14730
Type of use	Dissertation/Thesis
Requestor type	Author of this Wiley article
Format	Print and electronic
Portion	Full article
Will you be translating?	No
Title of your thesis / dissertation	"Advances in Late Transition Metal Catalysis, Olefination Reactions and Applications"
Expected completion date	Dec 2014
Expected size (number of pages)	300

Chapter II: The first well-defined silver(I)-complex catalyzed cycloaddition of azides onto terminal alkynes at room temperature

2.1 Introduction

The copper(I)-catalyzed Huisgen dipolar cycloaddition of terminal alkynes **1** with azides **2**^[1] to yield 1,4- and 1,4,5-substituted 1,2,3-triazoles **3** (AAC reaction) has been transformed in recent years since its description as the prototype “click” reaction,^[2] to become a general process with applications in diverse areas ranging from functional materials^[3] to biological chemistry.^[4,5] The generally accepted mechanism for the reaction, outlined in **Figure 2-1**,^[5,6] involves a stepwise process initiated through generation of a copper(I) acetylide **I** which complexes to the azide **2**, undergoes the cycloaddition, generating a metalated triazole **III**, which is then protonated^[6e] to yield the product **3**, regenerating the catalyst.

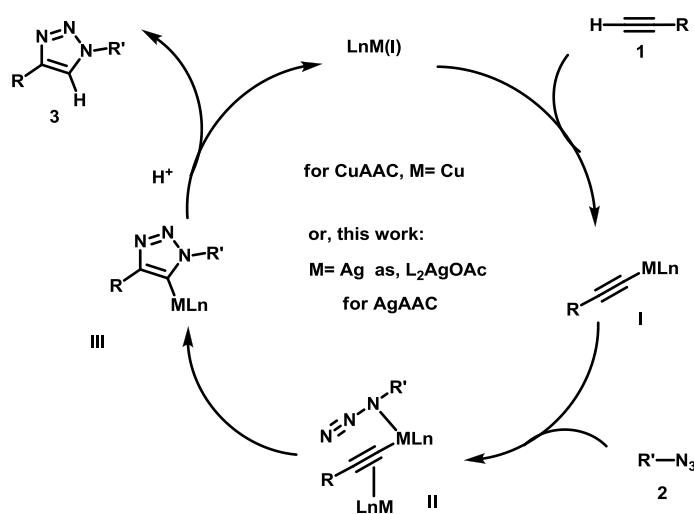
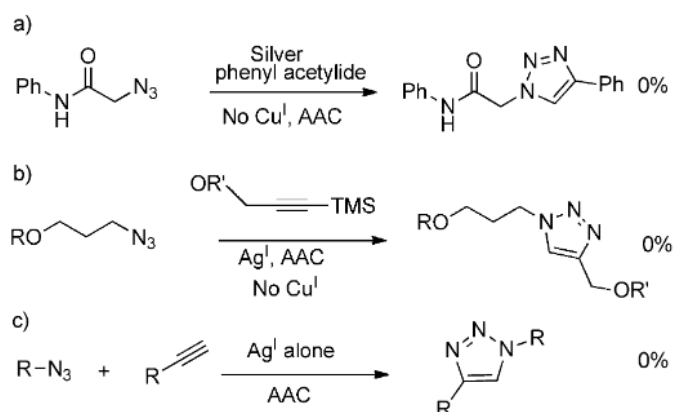


Figure 2-1. Generally accepted mechanism for the copper(I)-catalyzed azide-alkyne cycloaddition (AAC) reaction.

A bimetallic pathway has been proposed for the cycloaddition step involving π -complexation of the copper(I) catalyst to the Cu-acetylide/azide yielding the intermediate **II** (and variations thereof), prior to the cycloaddition. The

intermediacy of higher order Cu-oligomer complexes and involvement of copper(II) species have also been reported.^[6c,d]

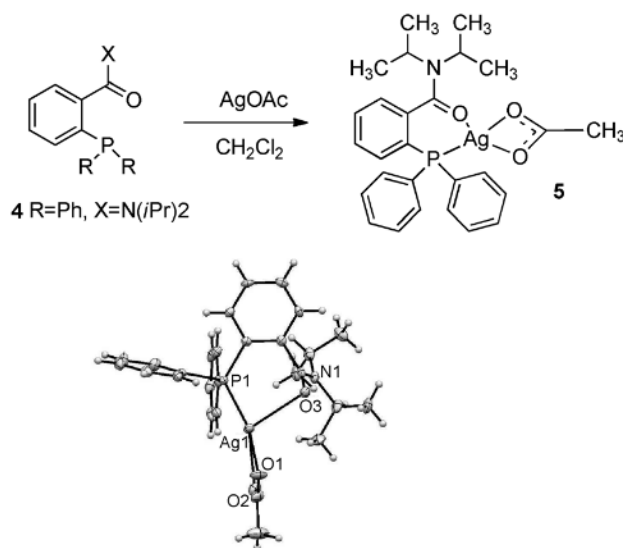
While gold(I),^[7a] silver(I)^[6d,7c] and other^[7b] acetylides are known to participate in the AAC reaction, the addition of copper(I) salts is required to effect the cycloaddition, in accord with the π -complexation step. No competent silver(I) or gold(I) species has been reported to catalyze the catalytic cycle alone, and several failed attempts at copper-free AAC reactions with silver acetylides have been reported (**Scheme 2-1**). For example, the stoichiometric addition of silver phenylacetylide to azides failed to promote cyclization in the absence of copper.^[6d] The silver mediated desilylation of a trimethylsilyl alkyne, producing the Ag-acetylide intermediate, also did not enter reaction with azides on their own accord.^[7c-e] These and other reports^[3a,5b] have shown that despite the efficacy of silver(I) species catalyzing other processes,^[8] they do not catalyze the AAC reaction. In this work, we report the first example of a well-defined silver(I) complex as a viable catalyst for the copper-free, room temperature AAC reaction.



Scheme 2-1. Previous work on Ag(I) catalyzed AAC reaction. a) AAC reaction in the presence of Cu^I . b) Ag^I -mediated AAC reaction. c) Other Ag^I -catalyzed AAC reaction.

2.2 Results and Discussion

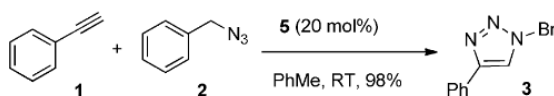
Our research group has recently investigated the development of hemilabile and bidentate P,O- and P,N-type ligands for a variety of $[\text{Pd}(\text{L}_2)]$ -catalyzed reactions.^[9] Parallel to this work, we became interested in the reactivity of isoelectronic s^0d^{10} silver(I) species. Well defined species of type $[\text{Ag}^+(\text{L}_2)(\text{X}^-)]$ have been reported with 2,2'-bis(diphenyl-phosphino)-1,1'-binaphthyl (BINAP) and thiaphosphines.^[10] We focused on generating P,O-type silver complexes from reaction of silver(I) species with amides of the tunable 2-diphenylphosphinobenzoic acid (SHOP) ligand **4** ($\text{R}=\text{Ph}$, $\text{X}=\text{OH}$).^[11] We were able to form a crystalline 1:1 complex of the diisopropylamide ligand **4** ($\text{R}=\text{Ph}$, $\text{X}=\text{N}(\text{iPr})_2$) with silver acetate.



Scheme 2-2. Synthesis of the SHOP amide: AgOAc (1:1) complex **5** and ORTEP plot (lower).

Crystals suitable for X-ray diffraction were readily deposited from dichloromethane-pentane and the resulting structure depicted in **Scheme 2-2**. The complex is tetragonal, exhibiting a shorter Ag-P contact (2.345 Å) than the reported BINAP-complex (2.449 Å).^[10a] The Ag-atom was also coordinated to

the oxygen atom of the amide as expected (2.680 Å), and asymmetrically bound to the acetate counter-anion (Ag-O contacts 2.167 and 2.669 Å). Complex **5** proved to be highly soluble in standard organic media (CH₂Cl₂, PhMe, THF etc) and poorly soluble in water. The complex did not deposit silver chloride when shaken with brine and was very stable thermally, melting with decomposition at 170-190 °C. The crystals proved to be very air stable, non hygroscopic and contain no solvate. The ³¹P-NMR spectrum of complex **5** exhibited sharp signals even at room temperature in CDCl₃ (δ 4.57, d, ²J_{P-Ag} = 712 Hz), fully in accord with a tightly coordinated mononuclear species in solution.^[10e]



Standard reaction conditions: Phenylacetylene (0.19 mmol, 1.0 eq), benzyl azide (0.93 mmol, 4.8 eq), catalyst (**5**) 20 mol%, caprylic acid 20 mol%, PhMe, rt, 48 h.

Scheme 2-3. Silver-catalyzed AAC reaction.

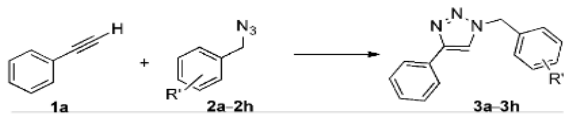
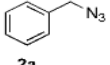
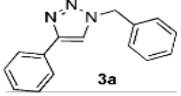
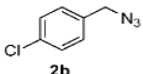
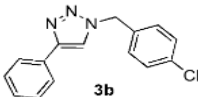
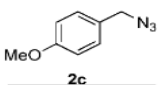
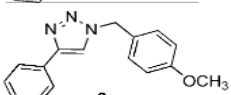
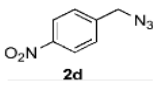
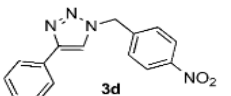
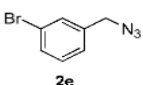
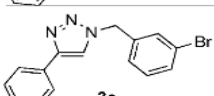
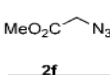
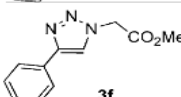
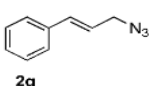
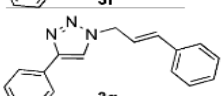
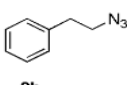
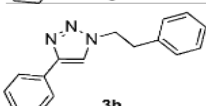
We initially investigated the AAC reaction of phenylacetylene and benzyl azide (1:1 ratio) in the presence of 10 mol% of various silver(I) salts (AgOAc, Ag₂O, AgNO₃, AgOTf) as well as complex **5** at room temperature in toluene. While the salts alone did not provide any adduct, to our surprise, complex **5** was observed to catalyze the AAC reaction regioselectively, at room temperature, slowly forming the 1,4 triazole regioisomer **3** selectively in 9-10% yield., **Scheme 2-3**.

Encouraged by this result, we screened several additives known from the Cu-AAC process^[6b,6e], in particular the addition of 10 mol% of benzoic acid or 20 mol% of caprylic acid was found to facilitate the AgAAC reaction. This process provided the 1,4-triazole in 43-52% yield over 48h at room temperature. Increasing the catalyst loading to 20 mol% and excess azide (4.8 eq) allowed

the reaction to go to completion and the triazole was isolated in 98% yield (**Table 2-1**, entry 1).

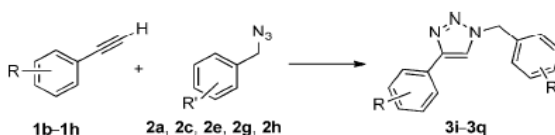
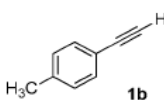
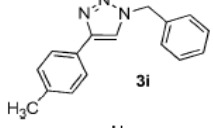
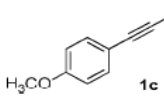
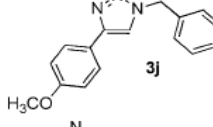
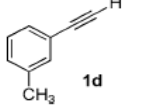
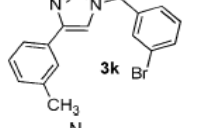
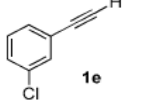
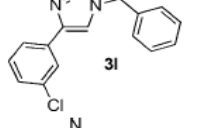
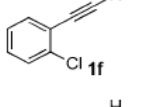
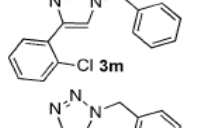
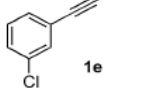
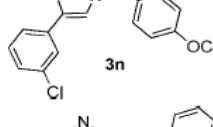
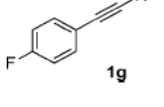
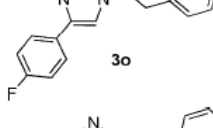
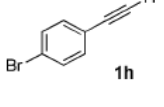
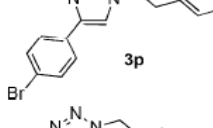
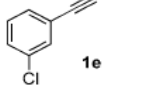
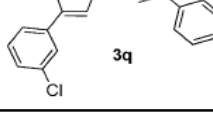
These parameters were chosen as the “standard condition” and a wide range of functionalized azides (**Table 2-1**) and phenylacetylenes (**Table 2-2**) were found to successfully undergo the AgAAC process efficiently under these mild conditions. In all the cases, exclusive formation of the 1,4 regioisomer was observed in 72-99% yield.

Table 2-1. Scope of azide participation in the Ag-AAC reaction.^[a]

		
	Azide	Product
		Yield [%]
1		 98
2		 95
3		 99
4		 99
5		 99
6		 90
7		 99
8		 99

[a] Reaction conditions: Phenyl acetylene (0.19 mmol), benzyl azide (0.93 mmol, 4.8 eq), Catalyst **5** (20 mol%), caprylic acid (20 mol%), PhMe (1mL), 48 h, rt.

Table 2-2. Scope of the alkyne participation in the Ag-AAC reaction.^[a]

			
Phenylacetylene	Azide	Product	Yield [%]
1			
 1b	2a	 3i	72
2			
 1c	2a	 3j	90
3			
 1d	2e	 3k	99
4			
 1e	2a	 3l	99
5			
 1f	2a	 3m	99
6			
 1e	2c	 3n	99
7			
 1g	2h	 3o	97
8			
 1h	2h	 3p	99
9			
 1e	2g	 3q	99

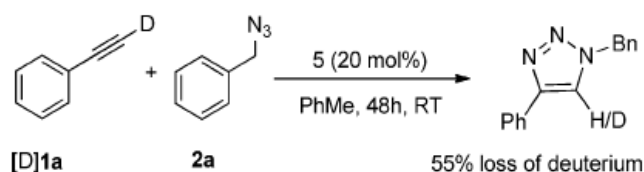
[a] Reaction conditions: Phenyl acetylene (0.19 mmol), benzyl azide (0.93 mmol, 4.8 eq.), Catalyst **5** (20 mol%), caprylic acid (20 mol%), PhMe (1mL), 48 h, rt.

The general reaction was investigated in a series of control experiments. The reaction of phenylacetylene with benzyl azide 1:1 in toluene at room temperature in the presence of 20 mol% caprylic acid, but absence of complex **5**, yielded no triazole product over 48h. The same experiment with the addition of silver acetate (20 mol%) led to no reaction while the silver triflate complex of ligand **4** (10 mol%) gave only 5% isolated yield of the triazole. In contrast, the addition of 10 mol% of complex **5** resulted in 52% conversion to the triazole in 48h.

These results indicate that a silver(I) source alone is not sufficient, but that complex **5** is required for catalytic activity. Furthermore, the results are basically in agreement with the earlier negative results shown in **Scheme 2-1** and indicate that catalyst **5** is exceptional in its ability to promote the AgAAC reaction. In a further control experiment (**Scheme 2-4**), deuterated phenyl acetylene ($\text{C}_6\text{H}_5\text{CCD}$, >99% D) was used in place of phenylacetylene under our standard conditions yielding the triazole with 55% loss of deuterium.

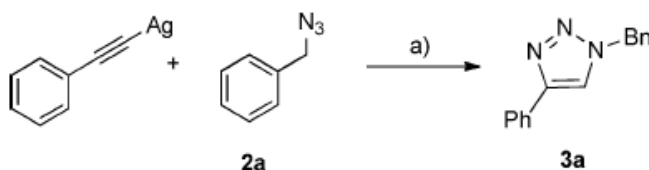
This result is in accord with the intermediacy of a silver acetylide, as opposed to an alkyne π -complexation pathway, wherein deuterium should be retained. Lastly, silver acetylide was prepared quantitatively and several control reactions investigated with benzyl azide under standard conditions (**Scheme 2-5**). In the absence of catalyst **5**, no reaction occurs, demonstrating that the role of **5** is not simply acetylide formation, but that it plays a role in further activation of the intermediate in order to effect cyclization. This result is in accord with a bimetallic π -complex species of type II (**Figure 2-1**), in which both metals are silver. In the absence of catalyst **5**, but addition of caprylic acid (0.20 equivalents) very slow conversion to the 1,4- triazole is observed, leading to 14% isolated yield after 48h. This result demonstrates that the carboxylic acid can play a minor role in the cyclization reaction itself as well as the final triazole protonation step, most likely through activation of the alkyne bond in the azide-acetylide complex. Although this acid catalyzed pathway is not efficient, to our

knowledge this is the first report on the role of acid in promoting the AAC reaction with silver acetylide. Finally, preformed silver acetylide reacted under the standard conditions with addition of caprylic acid (0.20 equiv.) and catalyst **5** (0.20 equiv.) to generate the 1,4-triazole in 32% yield, contrasting to 98% yield when catalyst **5** is used alone. This result indicates that the SHOP-amide ligand plays a pivotal role on both the terminal acetylide component in addition to further π -complexation to the alkyne (**Figure 2-1**, II where $L_n = N,N$ -diisopropyl-2-phenylphosphinobenzamide **4**).



Reaction conditions: a) Phenylacetylene (0.19 mmol, 1.0 eq), benzyl azide (0.93 mmol, 4.8 eq), **5** (20 mol%) rt, 48 h in PhMe, Isolated yield 55%.

Scheme 2-4. AgAAC reaction with deuterium labelling.



Reaction conditions: a) Silver phenyl acetylide (**7**, 0.09 mmol, 1.0 eq), benzyl azide (0.45 mmol, 4.8 eq), r.t. 48h in PhMe. 1) No catalyst **5**; 0% **3a**. 2) Caprylic acid (0.20 eq), no catalyst **5**; 14% **3a**. 3. Caprylic acid (0.20 eq), catalyst **5** (0.20 eq); 32% **3a**.

Scheme 2-5. Silver phenylacetylide control reactions under the standard condition.

2.3 Conclusion

In summary, we report the synthesis of a novel silver(I)acetate complex ligated to a 2-diphenylphosphino-*N,N*-diisopropylcarboxamide ligand and identified the first general purely silver azide-alkyne cycloaddition (AgAAC) process catalyzed by this well-defined species. Control experiments show that the reaction proceeds via silver acetylide formation but that further activation of the acetylide-azide intermediate is necessary to effect cyclization. These features are in accord with the generally accepted mechanism of the copper(I)-catalyzed process described in **Figure 2-1**. Silver(I)-salts alone are not sufficient to promote the cycloaddition indicating that an important role is played by the hemilabile P,O-type ligand. The hemilabile nature of this ligand may play a role in opening coordination sites on silver for azide complexation (cleavage of the Ag-O bond) and returning electron density to the alkyne bond through the metal to effect the cyclization. Structure-activity studies with a series of related ligands to probe the ligand effect and applications of this mildly Lewis-acidic silver(I)-species soluble on organic solvents in promoting other reactions are in progress.

2.4 Reference

- [1]. (a) C. W. Tornøe, C. Christensen, M. Meldal, *J. Org. Chem.* **2002**, *67*, 3057-3064. (b) V. V. Rostovtsev, L. G. Green, V. V. Fokin, K. B. Sharpless, *Angew. Chem. Int. Ed.* **2002**, *41*, 2596-2599.
- [2]. H. C. Kolb, M. G. Finn, K. B. Sharpless, *Angew. Chem. Int. Ed.* **2001**, *40*, 2004-2021.
- [3]. (a) M. Juricek, P. H. J. Kouwer, A. E. Rowan, *Chem. Comm.* **2011**, *47*, 8740-8749. (b) J. M. Casas-Solvas, E. Ortiz-Salmerón, I. Fernández, L. García-Fuentes, F. Santoyo-González, A. Vargas-Berenguel, *Chem. Eur. J.* **2009**, *15*, 8146-8162. (c) J. F. Lutz, *Angew. Chem. Int. Ed.* **2007**, *46*, 1018-1025.

- [4]. (a) A. Wang, N. W. Nairn, R. S. Johnson, D. A. Tirrell, K. Grabstein, *Chem. Bio. Chem.* **2008**, 9, 324-330. (b) F. Amblard, J. H. Cho, R. F. Schinazi, *Chem. Rev.* **2009**, 109, 4207-4220. (c) T. Fekner, X. Li, M. M. Lee, M. K. Chan, *Angew. Chem. Int. Ed.* **2009**, 48, 1633-1635. (d) E. M. Sletten, C. R. Bertozzi, *Acc. Chem. Res.* **2011**, 44, 666-676. (e) M. D. Best, M. M. Rowland, H. E. Bostic, *Acc. Chem. Res.* **2011**, 44, 686-698.
- [5]. For a selection of recent reviews and contributions see: (a) L. Ackermann, H. K. Potukuchi, *Org. Biomol. Chem.* **2010**, 8, 4503-4513. (b) J. E. Hein, V. V. Fokin, *Chem. Soc. Rev.* **2010**, 39, 1302-1315. (c) M. Meldal, C. W. Tornøe, *Chem. Rev.* **2008**, 108, 2952-3015. (d) V. D. Bock, H. Hiemstra, J. H. van Maarseveen, *Eur. J. Org. Chem.* **2006**, 51-68. (e) S. Diez-Gonzalez, *Catal. Sci. Technol.* **2011**, 1, 166-178. (f) E. J. Yoo, M. Ahlquist, S. H. Kim, I. Bae, V. V. Fokin, K. B. Sharpless, S. Chang, *Angew. Chem. Int. Ed.* **2005**, 46, 1730-1733.
- [6]. For select mechanistic and theoretical investigations see: (a) O. R. Valentin, V. F. Valery, M. G. Finn, *Angew. Chem. Int. Ed.* **2005**, 44, 2210-2215. (b) B. F. Straub, *Chem. Comm.* **2007**, 3868-3870. (c) B. R. Buckley, S. E. Dann, D. P. Harris, H. Heaney, E. C. Stubbs, *Chem. Comm.* **2010**, 2274-2276. (d) I. P. Silvestri, F. Andemarian, G. N. Khairallah, S. W. Yap, T. Quach, S. Tsegay, C. M. Williams, R. A. R. O'Hair, P. S. Donnelly, S. J. Williams, *Org. Biomol. Chem.* **2011**, 9, 6082-6088. (e) C. Shao, X. Wang, J. Xu, J. Zhao, Q. Zhang, Y. Hu, *J. Org. Chem.* **2010**, 75, 7002-7005.
- [7]. (a) Gold acetylide: D. V. Partyka, L. Gao, T. S. Teets, J. B. Updegraff III, N. Deligonul, T. G. Gray, *Organometallics* **2009**, 28, 6171-6182. (b) Aluminum acetylide: Y. Zhou, T. Lecourt, L. Micouin, *Angew. Chem. Int. Ed.* **2010**, 49, 2607-2610. (c) V. Aucagne, D. A. Leigh, *Org. Lett.* **2006**, 8, 4505-4507. (d) F. Himo, T. Lovell, R. Hilgraf, V. V. Rostovtsev, L. Noodleman, K. B. Sharpless, V. V. Fokin, *J. Am. Chem. Soc.* **2005**, 127, 210-216..

- [8]. (a) U. Halbes-Letinois, J. Weibel, P. Pale, *Chem. Soc. Rev.* **2007**, 36, 759-769. (b) M. Naodovic, H. Yamamoto, *Chem. Rev.* **2008**, 108, 3132-3148. (c) Y. Yamamoto, *Chem. Rev.* **2008**, 108, 3199-3222. (d) M. Alvarez-Corral, M. Munoz-Dorado, I. Rodriguez-Garcia, *Chem. Rev.* **2008**, 108, 3174-3198.
- [9]. (a) E. Ullah, J. McNulty, A. Robertson, C. Kennedy, *Org. Biomol. Chem.* **2011**, 9, 4421-4424. (b) E. Ullah, J. McNulty, V. Larichev, A. Robertson, *Eur. J. Org. Chem.* **2010**, 6824-6830. (c) E. Ullah, J. McNulty, A. Robertson, *Tetrahedron Lett.* **2009**, 50, 5599-5602.
- [10]. (a) N. Momiyama, H. Yamamoto, *J. Am. Chem. Soc.* **2004**, 126, 5360-5361. (b) C. Najera, M. de G. Retamosa, J. M. Sansano, *Org. Lett.* **2007**, 9, 4025-4028. (c) M. Ohkouchi, D. Masui, M. Yamaguchi, T. J. Yamagishi, *Mol. Cat. A: Chem.* **2001**, 170, 1-15. (d) L. Lettko, J. S. Wood, M. D. Rausch, *Inorg. Chim. Acta* **2000**, 308, 37-44.
- [11]. The parent ligand was first developed at Shell for the Ni-mediated higher olefins process (ethylene oligomerization) and is known as the SHOP ligand, see: (a) R. S. Bauer, P. W. Glockner, W. Keim, H. van Zwet, H. Chung, U.S. Pat. 3,644,563, **1972**. (b) W-M. Dai, Y. Zhang, *Tetrahedron Lett.* **2005**, 46, 1377-1381. (c) F. Y. Kwong, W. H. Lam, C. H. Yeung, K. S. Chan, A. S. C. Chan, *Chem. Comm.* **2004**, 1922-1923. (d) B. M. Trost, F. D. Toste, *J. Am. Chem. Soc.* **1998**, 120, 815-816.
- [12]. F. Alonso, Y. Moglie, G. Radivoy, M. Yus, *Eur. J. Org. Chem.* **2010**, 1875-1884.
- [13]. B. Pal, P. Jaisankar, V. S. Giri, *Syn Commun.* **2004**, 34, 1317-1323.
- [14]. M. Maddani, K. R. Prabhu, *Tetrahedron Lett.* **2008**, 49, 4526-4530.
- [15]. H. Ankati, E. Biehl, *Tetrahedron Lett.* **2009**, 50, 4677-4682.
- [16]. J. Ritschel, F. Sasse, M. E. Maier, *Eur. J. Org. Chem.* **2007**, 78-87.
- [17]. A. Lüth, W. Löwe, *Eur. J. Med. Chem.* **2008**, 43, 1478-1488.
- [18]. J. McNulty, J. J. Nair, S. Cheekoori, V. Larichev, A. Capretta, A. J. Robertson, *Chem. Eur. J.* **2006**, 12, 9314-9322.

- [19]. S. Chassaing, A. Sido, A. Alix, M. Kumarraja, P. Pale, J. Sommer, *Chem. Eur. J.* **2008**, *14*, 6713-6721.
- [20]. P. Appukkuttan, W. Dehaen, V. V. Fokin, E. Van der Eycken, *Org. Lett.* **2004**, *6*, 4223–4225.
- [21]. X. Meng, X. Xu, T. Gao, B. Chen, *Eur. J. Org. Chem.*, **2010**, 5409–5414.
- [22]. L. Zhao, W-Y. Wong, T. C. W. Mak, *Chem. Eur. J.* **2006**, *12*, 4865-4872.
- [23]. M. Rubina, V. Gevorgyan, *J. Am. Chem. Soc.* **2001**, *123*, 44, 11107-11108.

2.5 Experimental section

All reactions were carried out under nitrogen atmosphere in oven dried glassware. Toluene (dry) was distilled over sodium/benzophenone. AgOAc (purity \geq 99.0%) and AgOTf (purity = 99.95%) were purchased from Fluka Chemica, Switzerland and SigmaAldrich, Canada respectively. DMSO (dry) was obtained from SigmaAldrich. Phenyl acetylenes were obtained from SigmaAldrich, AlfaAesar, Canada. Melting points were recorded in open capillary using a calibrated Büchi melting point B540 apparatus and are corrected. Thin layer chromatography (TLC) was carried out using aluminium sheets pre-coated with silica gel 60F₂₅₄ (Merck) and was visualized under 254 nm UV light. ¹H, ¹³C spectra were recorded on a AV 600 spectrometer in CDCl₃ with TMS as internal standard. Chemical shifts (δ) are reported in ppm downfield of TMS and coupling constants (*J*) are expressed in hertz (Hz).

General procedure for the preparation of starting azides:^[12] (Table 2-1, 2a-2h) Sodium azide (1.0 g, 15.3 mmol, 1 eq.) was dissolved in DMSO (25 mL) by stirring in a flame-dried 100 mL round bottom flask under nitrogen for 12 h. A solution of corresponding benzyl bromide/chloride (13.8 mmol, 0.9 eq) was added and the reaction was stirred for 10 h. Water (20 mL) was added slowly to quench the reaction (exothermic process) and stirred until it cooled to room temperature. The mixture was poured into water (50 mL) and extracted with diethyl ether (3 x 30 mL). The organic layer was separated, washed with brine,

dried with sodium sulphate, filtered, and concentrated in *vacuo* to afford azide (**2a-2h**) as a oil.

1-(azidomethyl)benzene:^[12] (Table 2-1, **2a**) ¹H NMR (200 MHz, CDCl₃) δ 7.43-7.25 (m, 5H), 4.35 (s, 2H).

1-(azidomethyl)-4-chlorobenzene:^[13] (Table 2-1, **2b**) ¹H NMR (600 MHz, CDCl₃) δ 7.39 (d, *J* = 8.3 Hz, 2H), 7.28 (d, *J* = 8.3 Hz, 2H), 4.35 (s, 2H).

1-(azidomethyl)-4-methoxybenzene:^[14] (Table 2-1, **2c**) ¹H NMR (600 MHz, CDCl₃) δ 7.28 (d, *J* = 8.6 Hz, 2H), 6.94 (d, *J* = 8.6 Hz, 2H), 4.30 (s, 2H), 3.85 (s, 3H).

1-(azidomethyl)-4-nitrobenzene:^[15] (Table 2-1, **2d**) ¹H NMR (600 MHz, CDCl₃) δ 8.27 (d, *J* = 8.6 Hz, 2H), 7.53 (d, *J* = 8.5 Hz, 2H), 4.53 (s, 2H).

1-(azidomethyl)-3-bromobenzene:^[16] (Table 2-1, **2e**) ¹H NMR (600 MHz, CDCl₃) δ 7.51 (d, *J* = 1.9 Hz, 2H), 7.28 (d, *J* = 1.4 Hz, 2H), 4.35 (s, 2H).

Methyl 2-azidoacetate:^[17] (Table 2-1, **2f**) ¹H NMR (600 MHz, CDCl₃) δ 3.91 (s, 2H), 3.83 (s, 3H).

Cinnamyl azide:^[12] (Table 2-1, **2g**) ¹H NMR (600 MHz, CDCl₃) δ 7.44 (d, *J* = 7.4 Hz, 2H), 7.37 (t, *J* = 7.7 Hz, 2H), 7.34 – 7.29 (m, 1H), 6.69 (d, *J* = 15.8 Hz, 1H), 6.28 (dt, *J* = 15.7, 6.6 Hz, 1H), 3.98 (d, *J* = 6.6 Hz, 2H).

1-(2-azidoethyl)benzene:^[18] (Table 2-1, **2h**) ¹H NMR (600 MHz, CDCl₃) δ 7.37 (t, *J* = 7.4 Hz, 2H), 7.33 – 7.28 (m, 1H), 7.28 – 7.24 (m, 2H), 3.55 (t, *J* = 7.3 Hz, 2H), 2.94 (t, *J* = 7.3 Hz, 2H).

General Procedure for Ag(I)-catalyzed synthesis of 1,2,3 -Triazole: To a mixture of phenyl acetylene (0.020 g, 0.19 mmol, 1 eq) and benzyl azide (0.125 g, 0.93 mmol, 4.8 mmol) in 1 mL of toluene were added sequentially catalyst (**5**) (20 mol%) and caprylic acid (20 mol%). The mixture was then stirred at room

temperature for 48 h. The reaction mixture was diluted and extracted with ethyl acetate (2 X 20 mL) washed with sodium bicarbonate (5 mL), brine and dried over anhydrous sodium sulphate and concentrated under reduced pressure. The resulting residue was purified through silica gel column chromatography (10-20% ethyl acetate: hexanes) to afford the desired product.

1-Benzyl-4-phenyl-1*H*-1,2,3-triazole:^[6e] (Table 2-1, Entry 1, 3a)

¹H NMR (600 MHz, CDCl₃) δ 7.79 (dd, *J* = 8.2, 1.1 Hz, 2H), 7.65 (s, 1H), 7.43 – 7.34 (m, 5H), 7.34 – 7.27 (m, 3H), 5.57 (s, 2H). ¹³C NMR (151 MHz, CDCl₃) δ 148.2, 134.6, 130.5, 129.1, 128.8, 128.2, 128.0, 125.7, 119.4, 54.2.

1-(4-Chlorobenzyl)-4-phenyl-1*H*-1,2,3-triazole:^[19] (Table 2-1, Entry 2, 3b)

¹H NMR (600 MHz, CDCl₃) δ 7.84 – 7.76 (m, 2H), 7.66 (s, 1H), 7.43 – 7.38 (m, 2H), 7.38 – 7.34 (m, 2H), 7.32 (dt, *J* = 9.1, 4.3 Hz, 1H), 7.25 (s, 2H), 5.55 (s, 2H). ¹³C NMR (151 MHz, CDCl₃) δ 149.1, 135.5, 133.8, 131.1, 130.1, 130.1, 129.5, 128.9, 126.3, 120.1, 54.1.

1-(4-Methoxybenzyl)-4-phenyl-1*H*-1,2,3-triazole:^[19] (Table 2-1, Entry 3, 3c)

¹H NMR (600 MHz, CDCl₃) δ 7.79 – 7.71 (m, 2H), 7.58 (s, 1H), 7.35 (t, *J* = 7.6 Hz, 2H), 7.27 (d, *J* = 7.4 Hz, 1H), 7.23 (d, *J* = 8.7 Hz, 2H), 6.87 (d, *J* = 8.7 Hz, 2H), 5.47 (s, 2H), 3.77 (s, 3H). ¹³C NMR (151 MHz, CDCl₃) δ 159.9, 148.0, 130.5, 129.6, 128.7, 128.1, 126.5, 125.6, 119.2, 114.5, 55.3, 53.8.

1-(4-Nitrobenzyl)-4-phenyl-1*H*-1,2,3-triazole:^[19] (Table 2-1, Entry 4, 3d)

¹H NMR (600 MHz, CDCl₃) δ 8.27 (d, *J* = 8.8 Hz, 2H), 7.84 (dd, *J* = 8.1, 1.0 Hz, 2H), 7.77 (s, 1H), 7.51 – 7.42 (m, 4H), 7.41 – 7.33 (m, 1H), 5.73 (s, 2H). ¹³C NMR (151 MHz, CDCl₃) δ 148.7, 148.1, 141.7, 130.0, 128.9, 128.5, 128.5, 125.7, 124.3, 119.6, 53.2.

1-(3-Bromobenzyl)-4-phenyl-1*H*-1,2,3-triazole:^[6e] (Table 2-1, Entry 5, 3e)

¹H NMR (600 MHz, CDCl₃) δ 7.87 – 7.80 (m, 2H), 7.72 (s, 1H), 7.53 (d, *J* = 7.7 Hz, 1H), 7.50 (s, 1H), 7.44 (t, *J* = 7.6 Hz, 2H), 7.39 – 7.33 (m, 1H), 7.32 – 7.23 (m, 2H), 5.58 (s, 2H). ¹³C NMR (151 MHz, CDCl₃) δ 148.4, 136.8, 131.9, 131.0, 130.7, 130.3, 128.8, 128.3, 126.5, 125.7, 123.1, 119.4, 53.4.

Ethyl 2-(4-Phenyl-1*H*-1,2,3-triazol-1-yl)acetate:^[6c] (Table 2-1, Entry 6, 3f)

¹H NMR (600 MHz, CDCl₃) δ 7.94 (s, 1H), 7.90 – 7.85 (m, 2H), 7.46 (t, *J* = 7.7 Hz, 2H), 7.38 (t, *J* = 7.4 Hz, 1H), 5.26 (s, 2H), 3.86 (s, 3H). ¹³C NMR (151 MHz, CDCl₃) δ 166.7, 148.3, 130.3, 128.8, 128.3, 125.8, 120.9, 53.1, 50.8.

1-Cinnamyl-4-phenyl-1*H*-1,2,3-triazole:^[12] (Table 2-1, Entry 7, 3g)

¹H NMR (600 MHz, CDCl₃) δ 7.87 (d, *J* = 1.3 Hz, 2H), 7.84 (s, 1H), 7.48 – 7.41 (m, 4H), 7.35 (m, 4H), 6.75 (d, *J* = 15.8 Hz, 1H), 6.43 (dt, *J* = 15.8, 6.7 Hz, 1H), 5.22 (dd, *J* = 6.7, 1.2 Hz, 2H). ¹³C NMR (151 MHz, CDCl₃) δ 148.1, 135.5, 130.5, 128.8, 128.7, 128.6, 128.2, 126.7, 125.7, 121.9, 119.3, 52.4.

1-(2-phenylethyl)-4-phenyl-1*H*-1,2,3-triazole:^[20] (Table 2-1, Entry 8, 3h)

¹H NMR (600 MHz, CDCl₃) δ 7.79 (dd, *J* = 8.3, 1.1 Hz, 2H), 7.49 (s, 1H), 7.43 (t, *J* = 7.7 Hz, 2H), 7.38 – 7.31 (m, 3H), 7.31 – 7.26 (m, 1H), 7.17 (d, *J* = 7.4 Hz, 2H), 4.67 (t, *J* = 7.3 Hz, 2H), 3.29 (t, *J* = 7.2 Hz, 2H). ¹³C NMR (151 MHz, CDCl₃) δ 147.4, 137.0, 130.6, 128.8, 128.8, 128.7, 128.1, 127.1, 125.7, 119.9, 51.7, 36.8.

1-Benzyl-4-p-tolyl-1*H*-1,2,3-triazole:^[6e] (Table 2-2, Entry 1, 3i)

¹H NMR (600 MHz, CDCl₃) δ 7.71 (d, *J* = 8.1 Hz, 2H), 7.64 (s, 1H), 7.45 – 7.37 (m, 3H), 7.36 – 7.31 (m, 2H), 7.23 (d, *J* = 7.9 Hz, 2H), 5.60 (s, 2H), 2.39 (s, 3H). ¹³C NMR (151 MHz, CDCl₃) δ 148.3, 138.0, 134.7, 129.4, 129.1, 128.7, 128.0, 127.6, 125.6, 119.1, 54.2, 21.2.

1-Benzyl-4-(4-methoxyphenyl)-1*H*-1,2,3-triazole:^[6e] (Table 2-2, Entry 2, 3j)

¹H NMR (600 MHz, CDCl₃) δ 7.65 (d, *J* = 8.9 Hz, 2H), 7.50 (s, 1H), 7.36 – 7.27 (m, 3H), 7.26 – 7.21 (m, 2H), 6.86 (d, *J* = 8.9 Hz, 2H), 5.49 (s, 2H), 3.76 (s, 3H). ¹³C NMR (151 MHz, CDCl₃) δ 159.6, 148.1, 134.7, 129.1, 128.7, 128.0, 127.0, 123.2, 118.6, 114.2, 55.3, 54.2.

1-(3-Bromobenzyl)-4-(3-methylphenyl)-1*H*-1,2,3-triazole: (Table 2-2, Entry 3, 3k)

M.P. 96-97 °C. ¹H NMR (600 MHz, CDCl₃) δ 7.70 (s, 1H), 7.69 (s, 1H), 7.61 (d, *J* = 7.7 Hz, 1H), 7.52 (d, *J* = 7.8 Hz, 1H), 7.49 (s, 1H), 7.32 (t, *J* = 7.6 Hz, 1H), 7.30 – 7.23 (m, 2H), 7.17 (d, *J* = 7.6 Hz, 1H), 5.57 (s, 2H), 2.41 (s, 3H). ¹³C NMR (151 MHz, CDCl₃) δ 148.5, 138.5, 136.9, 131.9, 130.9, 130.7, 130.2, 129.0, 128.7, 126.5, 126.4, 123.1, 122.8, 119.4, 53.4, 21.4. HRMS (M)⁺ calc for C₁₆H₁₄N₃Br: 327.0398, found 327.0371.

1-Benzyl-4-(3-chlorophenyl)-1*H*-1,2,3-triazole:^[16] (Table 2-2, Entry 4, 3l)

¹H NMR (600 MHz, CDCl₃) δ 7.81 (t, *J* = 1.7 Hz, 1H), 7.74 – 7.70 (m, 1H), 7.69 (s, 1H), 7.45 – 7.39 (m, 3H), 7.38 – 7.30 (m, 4H), 5.61 (s, 2H). ¹³C NMR (151 MHz, CDCl₃) δ 146.9, 134.7, 134.4, 132.3, 130.1, 129.2, 128.9, 128.1, 128.1, 125.7, 123.7, 119.8, 54.3.

1-Benzyl-4-(2-chlorophenyl)-1*H*-1,2,3-triazole:^[21] (Table 2-2, Entry 5, 3m)

¹H NMR (600 MHz, CDCl₃) δ 8.18 (dd, *J* = 7.9, 1.6 Hz, 1H), 8.04 (s, 1H), 7.37 – 7.27 (m, 5H), 7.26 – 7.22 (m, 2H), 7.19 (m, 1H), 5.54 (s, 2H). ¹³C NMR (151 MHz, CDCl₃) δ 144.4, 134.6, 131.1, 130.1, 129.8, 129.2, 129.1, 129.0, 128.7, 127.9, 127.1, 123.1, 54.2.

1-(4-methoxybenzyl)-4-(3-chlorophenyl)-1*H*-1,2,3-triazole: (Table 2-2, Entry 6, 3n)

M.P. 134-136 °C. ¹H NMR (600 MHz, CDCl₃) δ 7.80 (s, 1H), 7.71 (d, *J* = 7.7 Hz, 1H), 7.65 (s, 1H), 7.35 (t, *J* = 7.8 Hz, 1H), 7.30 (d, *J* = 8.7 Hz, 3H), 6.95 (d, *J* = 8.6 Hz, 2H), 5.54 (s, 2H), 3.85 (s, 3H). ¹³C NMR (151 MHz, CDCl₃) δ 160.0, 146.8, 134.7, 132.3, 130.0, 129.7, 128.1, 126.3, 125.7, 123.7, 119.6, 114.6, 55.3, 53.9. HRMS (M)⁺ calc for C₁₆H₁₄N₃OCl: 299.0823, found 299.0825.

1-(2-phenylethyl)-4-(4-fluorophenyl)-1*H*-1,2,3-triazole: (Table 2-2, Entry 7, 3o)

M.P. 142-143 °C. ¹H NMR (600 MHz, CDCl₃) δ 7.78 – 7.73 (m, 2H), 7.44 (s, 1H), 7.36 – 7.31 (m, 2H), 7.31 – 7.27 (m, 1H), 7.19 – 7.15 (m, 2H), 7.12 (t, *J* = 8.7 Hz, 2H), 4.66 (t, *J* = 7.3 Hz, 2H), 3.28 (t, *J* = 7.2 Hz, 2H). ¹³C NMR (151 MHz, CDCl₃) δ 162.7 (d, *J* = 247.2 Hz), 146.7, 137.1, 128.9 (d, *J* = 21.0 Hz), 127.5 (d, *J* = 8.1 Hz), 127.3, 127.0, 115.9 (d, *J* = 21.8 Hz), 51.9, 36.9. HRMS (M)⁺ calc for C₁₆H₁₄N₃F: 267.1171, found 267.1172.

1-(2-phenylethyl)-4-(4-bromophenyl)-1*H*-1,2,3-triazole: (Table 2-2, Entry 8, 3p)

M.P. 153-154 °C. ¹H NMR (600 MHz, CDCl₃) δ 7.66 (d, *J* = 8.5 Hz, 2H), 7.56 (d, *J* = 8.5 Hz, 2H), 7.47 (s, 1H), 7.33 (t, *J* = 7.2 Hz, 2H), 7.28 (m, 1H), 7.16 (d, *J* = 6.9 Hz, 2H), 4.66 (t, *J* = 7.2 Hz, 2H), 3.28 (t, *J* = 7.2 Hz, 2H). ¹³C NMR (151 MHz, CDCl₃) δ 146.4, 136.9, 131.9, 129.6, 128.8, 128.7, 127.2, 121.9, 119.9, 51.8, 36.7. HRMS (M)⁺ calc for C₁₆H₁₄N₃Br: 327.0360, found 327.0371.

1-Cinnamyl-4-(3-chlorophenyl)-1*H*-1,2,3-triazole: (Table 2-2, Entry 9, 3q)

M.P. 117-119 °C. ¹H NMR (600 MHz, CDCl₃) δ 7.89 – 7.82 (m, 2H), 7.78 – 7.73 (m, 1H), 7.49 – 7.41 (m, 2H), 7.38 (td, *J* = 7.4, 2.5 Hz, 3H), 7.35 – 7.30 (m, 2H), 6.75 (d, *J* = 15.8 Hz, 1H), 6.42 (dt, *J* = 15.8, 6.7 Hz, 1H), 5.22 (dd, *J* = 6.7, 1.2

Hz, 2H). ^{13}C NMR (151 MHz, CDCl_3) δ 146.8, 135.7, 135.3, 134.8, 132.3, 130.1, 128.8, 128.7, 128.1, 126.7, 125.8, 123.7, 121.6, 119.6, 52.5. HRMS (M)⁺ calc for $\text{C}_{17}\text{H}_{14}\text{N}_3\text{Cl}$: 295.0863, found 295.0876.

1-Benzyl-5-deuterium-4-phenyl-1*H*-1,2,3-triazole:^[7b] (Scheme 2-4, 3r)

^1H NMR (200 MHz, CDCl_3) δ 7.82-7.79 (m, 2H), 7.41-7.32 (m, 8H), 5.59 (s, 2H).

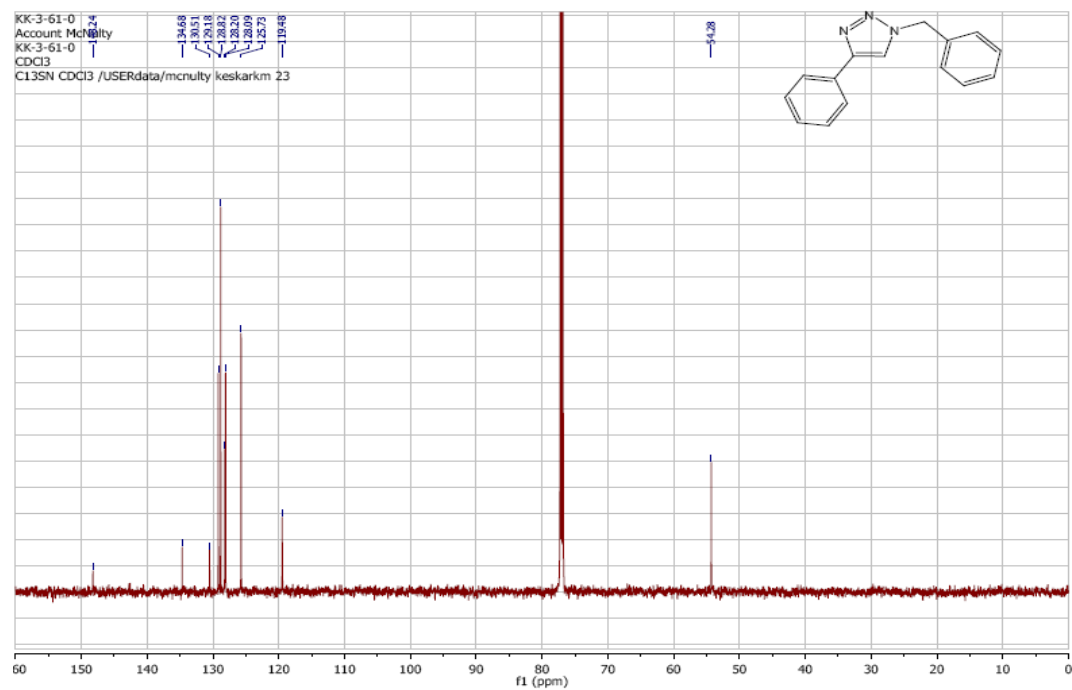
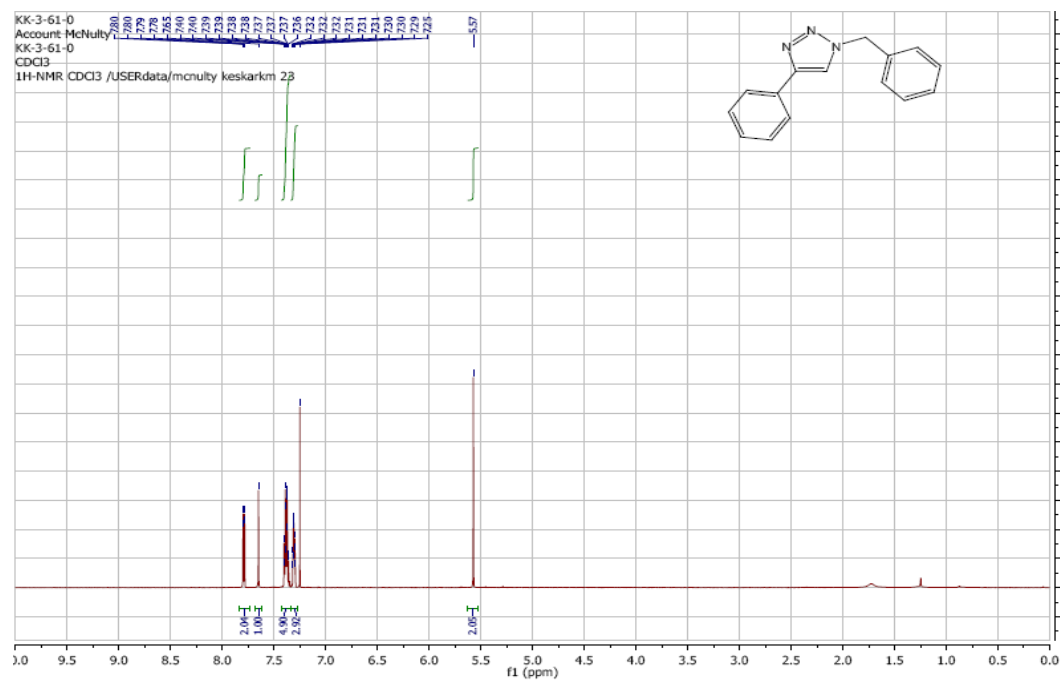
Synthesis of Silver phenyl acetylide:^[22] (Scheme 2-5, 7) Compound **7** was prepared according to the literature method.

Synthesis of Phenylacetylene-*d*:^[23] (Scheme 2-4, 1a-D) Compound **1a-D** was prepared according to the literature method. deuterium purity >98%.

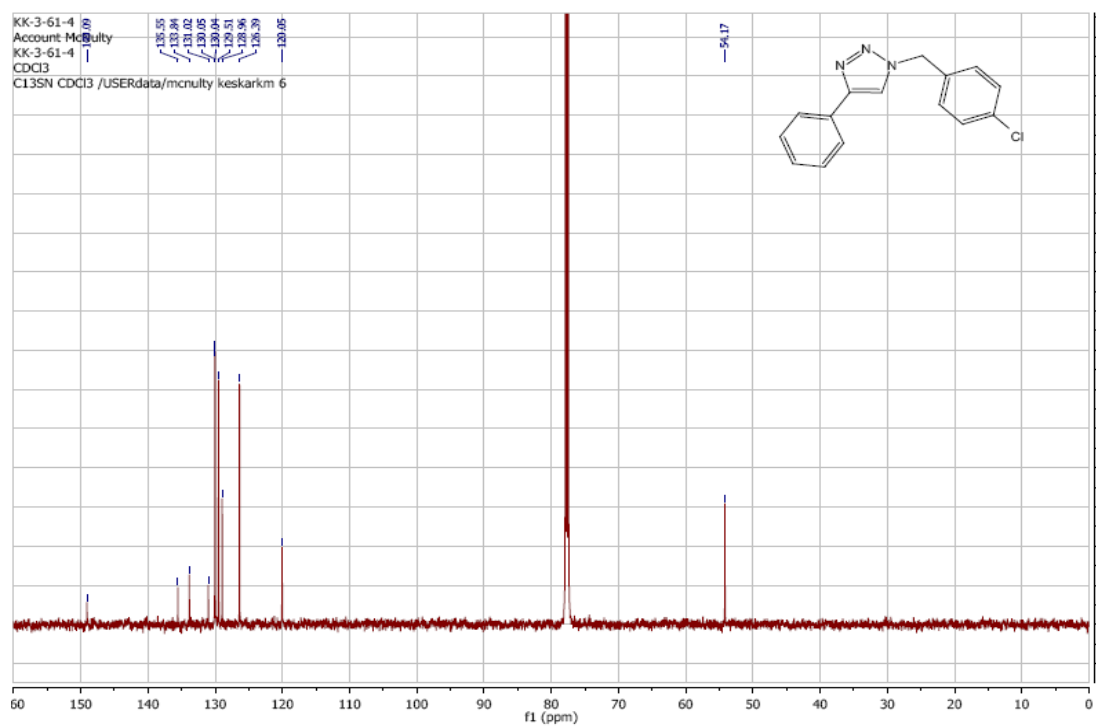
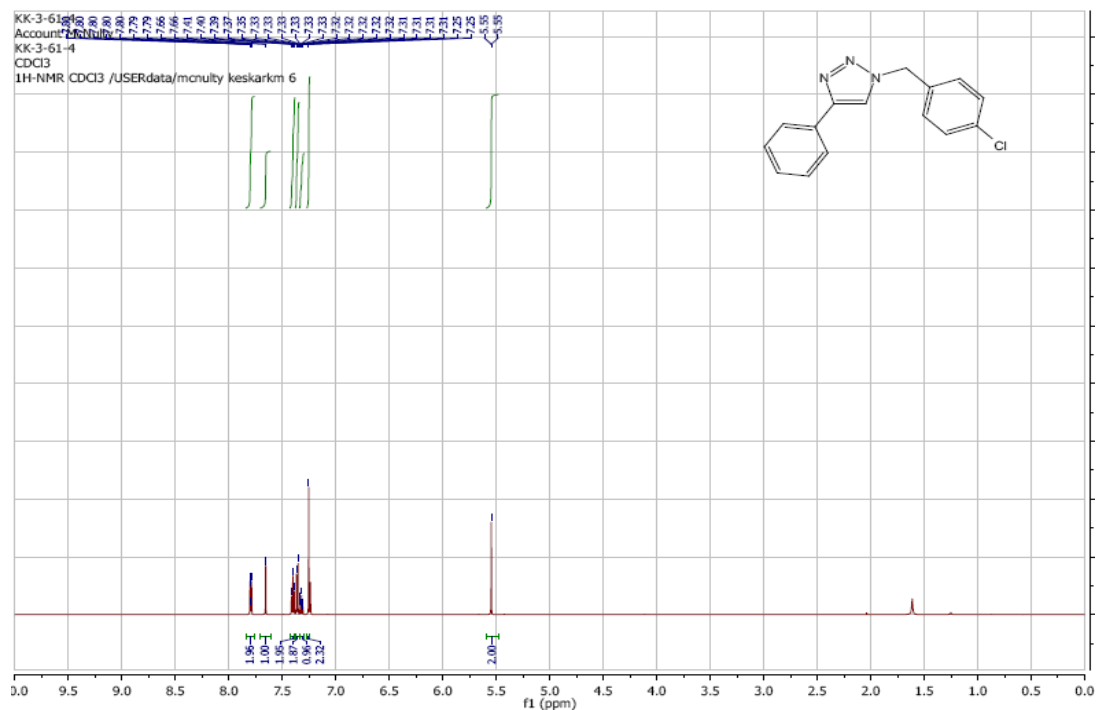
Preparation of AgOAc-SHOP Amide (*N,N*-diisopropyl-2-diphenylphosphinobenzamide), complex **5: (Scheme 2-2)** *N,N*-diisopropyl-2-diphenylphosphinobenzamide (SHOP amide) was prepared according to the literature method.^[11b] To an oven dried flask SHOP amide **4** (0.5g, 1.28 mmol, 1 eq), silver acetate (0.2 g, 1.28 mmol, 1 eq), dry dichloromethane (10 mL) and distilled water (10 mL) were added and stirred at room temperature for 30 mins. The organic and aqueous layers were separated and the aqueous layer was extracted with dichloromethane (3 x 10 mL). The organic layer was dried on MgSO_4 , filtered and concentrated in *vacuo* to afford the silver complex **5**. Crystals of complex **5** were developed for X-ray studies by dissolving **5** in dichloromethane-pentane and allowing the solvents to evaporate slowly. M.P. Complex **5** decomposes at 170-190 °C. HRMS (M)⁺ calc for $\text{C}_{25}\text{H}_{28}\text{AgNOP}$: 496.0953, found 496.0959. ^{31}P NMR (243 MHz, CDCl_3) δ 4.57 (d, J = 712.3 Hz). X-Ray data can be found online (Reference I, List of publication. CCDC 843618).

2.6 NMR Spectra (^1H and ^{13}C NMR spectra of final triazoles)

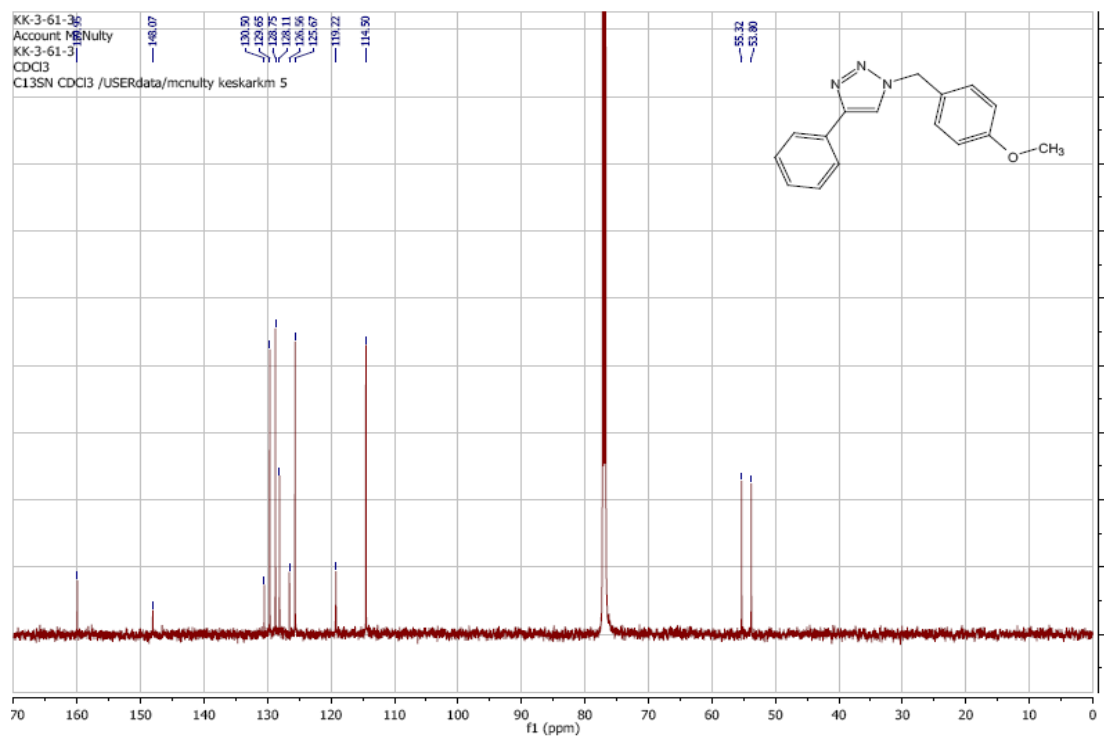
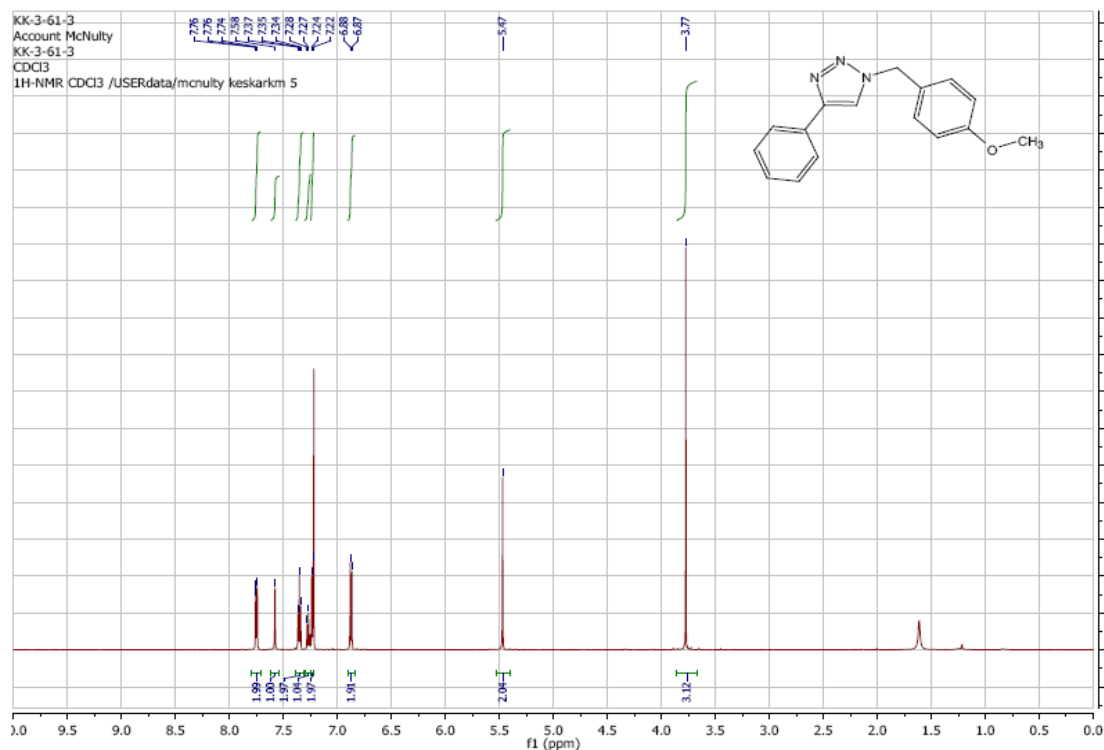
1-Benzyl-4-phenyl-1*H*-1,2,3-triazole: (Table 2-1, Entry 1, 3a)



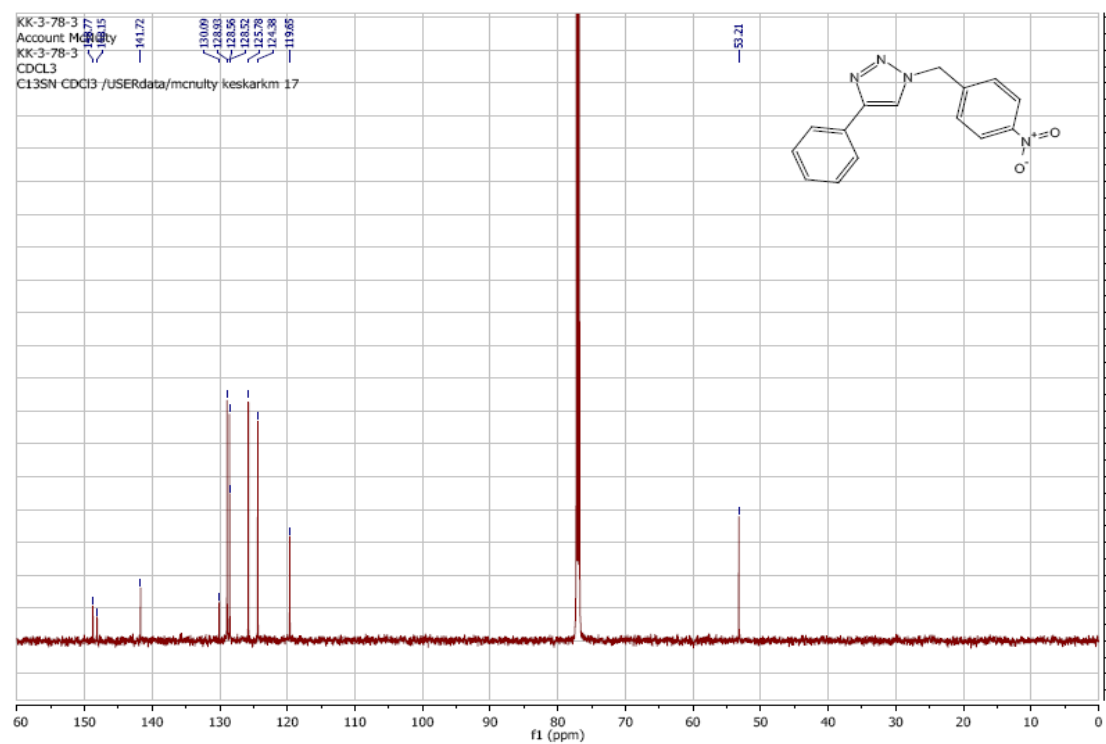
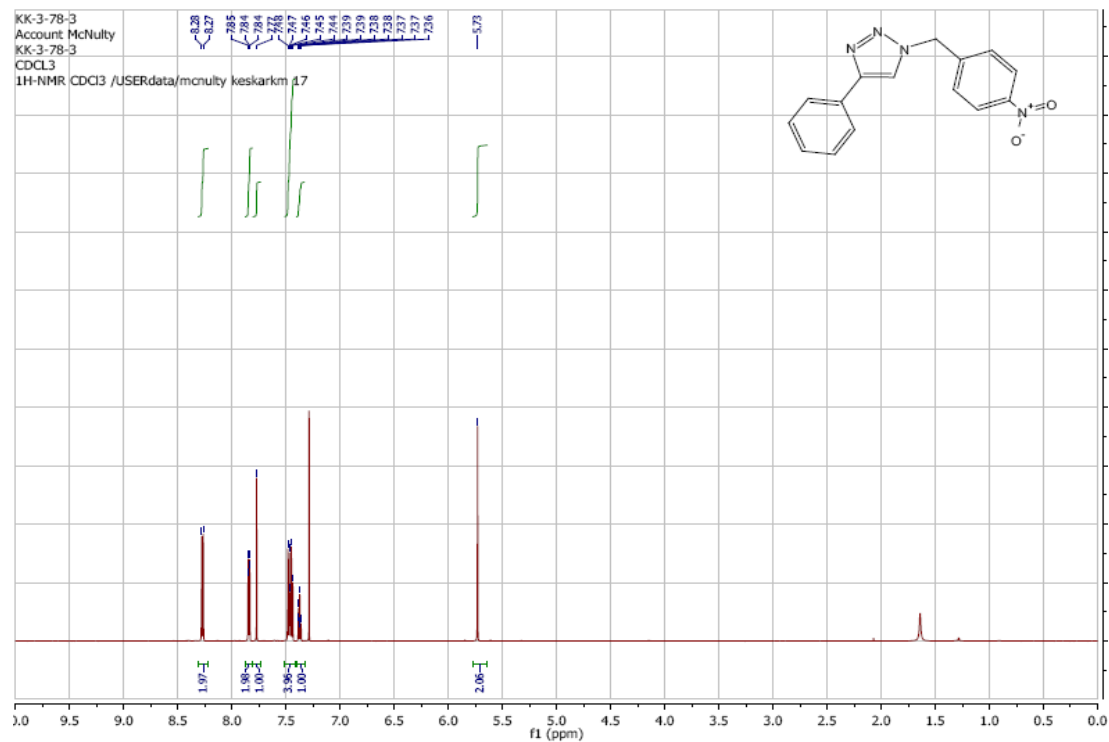
1-(4-Chlorobenzyl)-4-phenyl-1*H*-1,2,3-triazole: (Table 2-1, Entry 2, 3b)



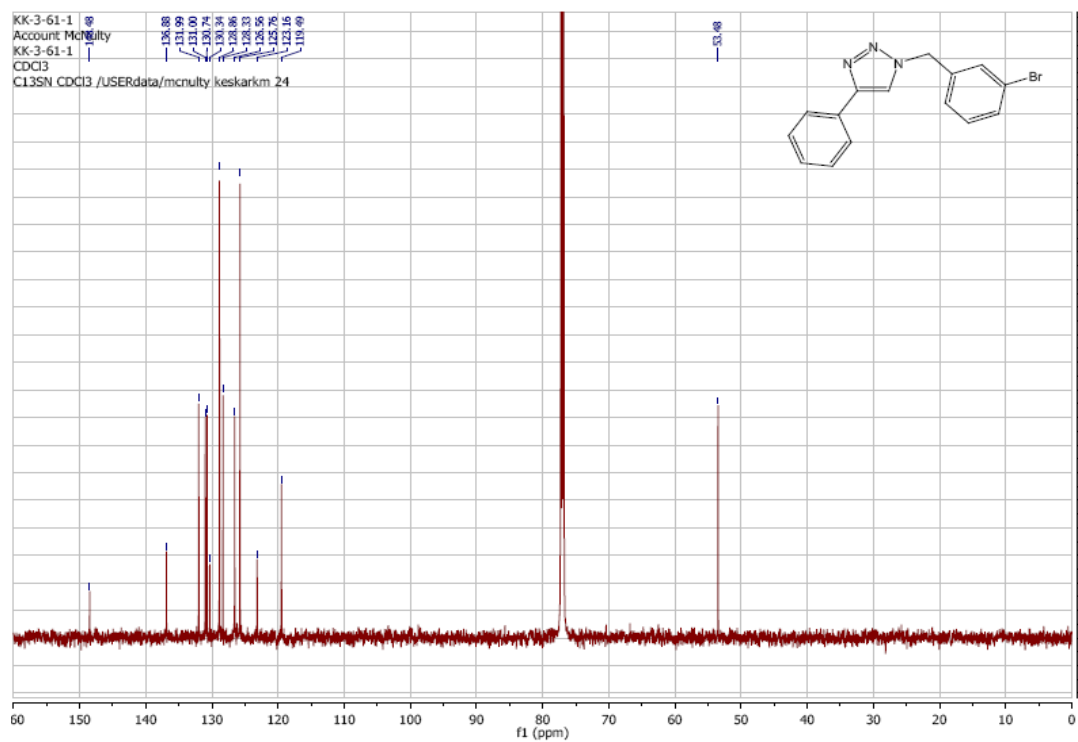
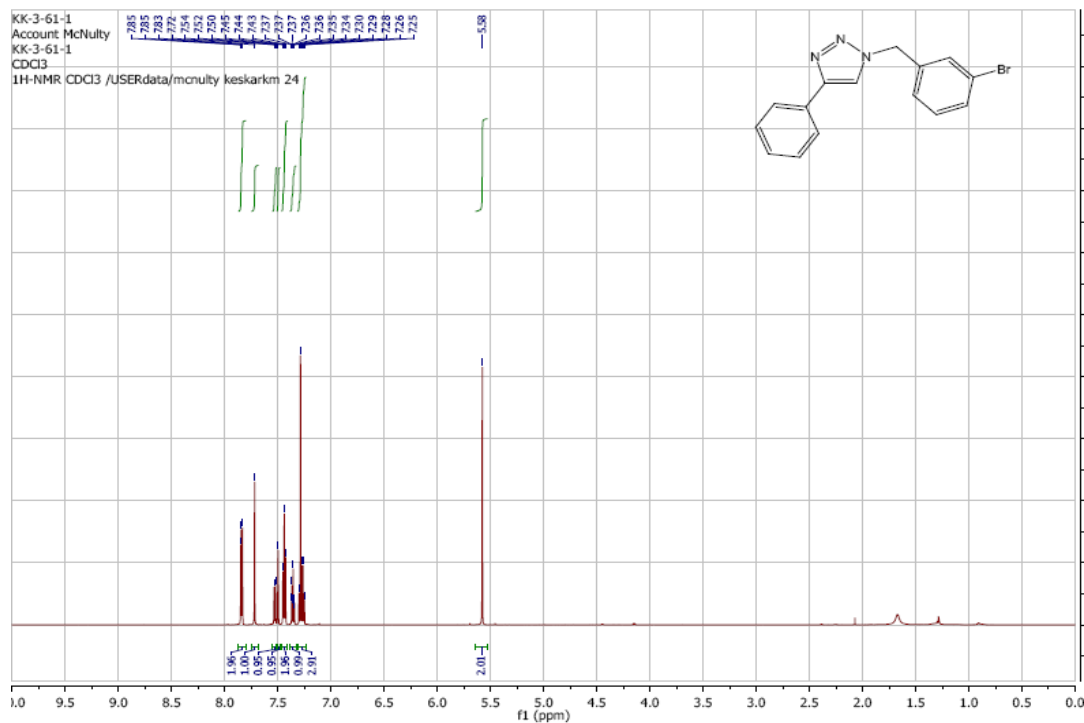
1-(4-Methoxybenzyl)-4-phenyl-1*H*-1,2,3-triazole: (Table 2-1, Entry 3, 3c)



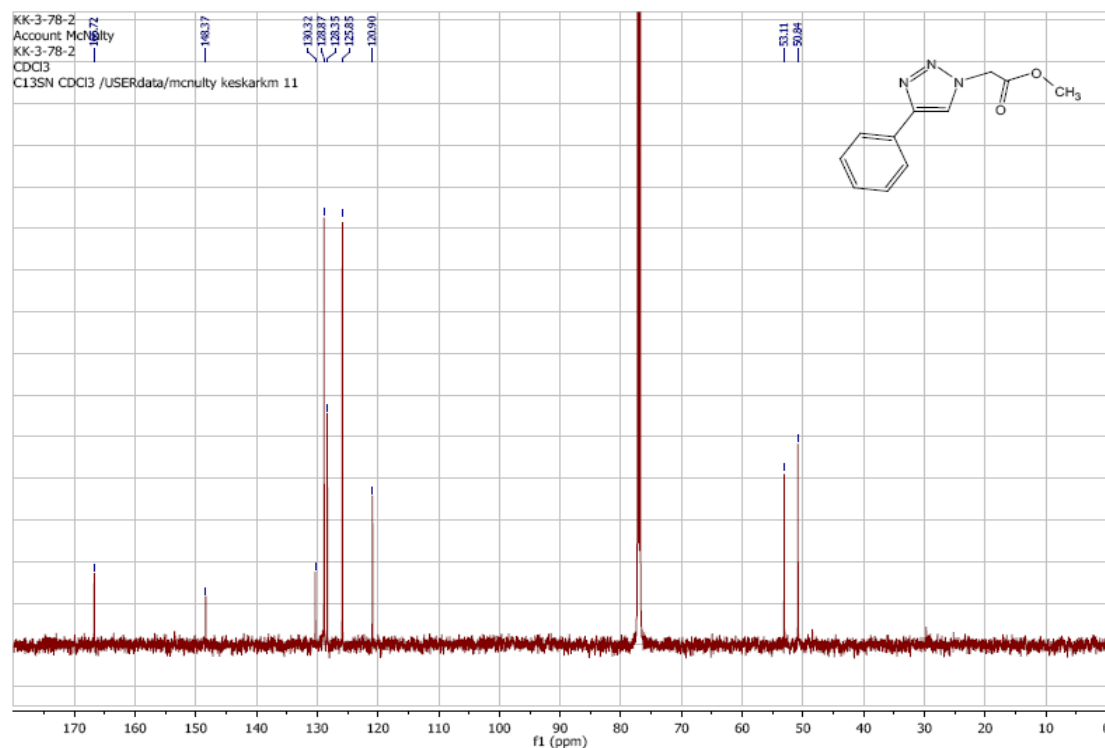
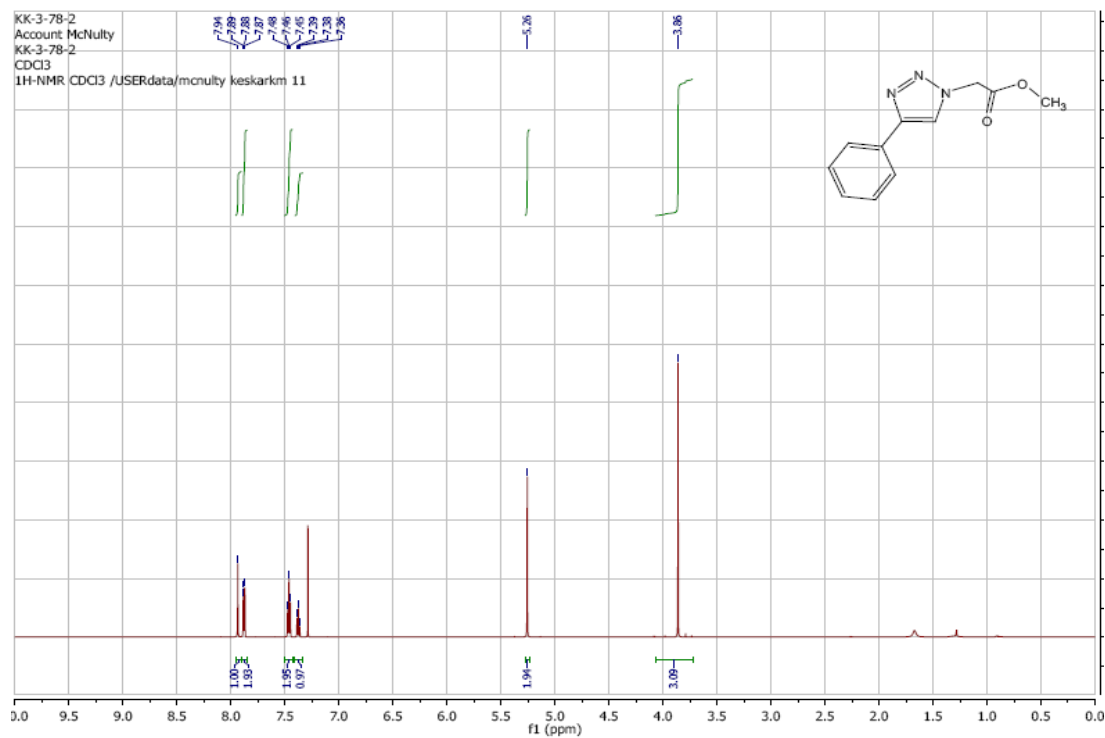
1-(4-Nitrobenzyl)-4-phenyl-1*H*-1,2,3-triazole: (Table 2-1, Entry 4, 3d)



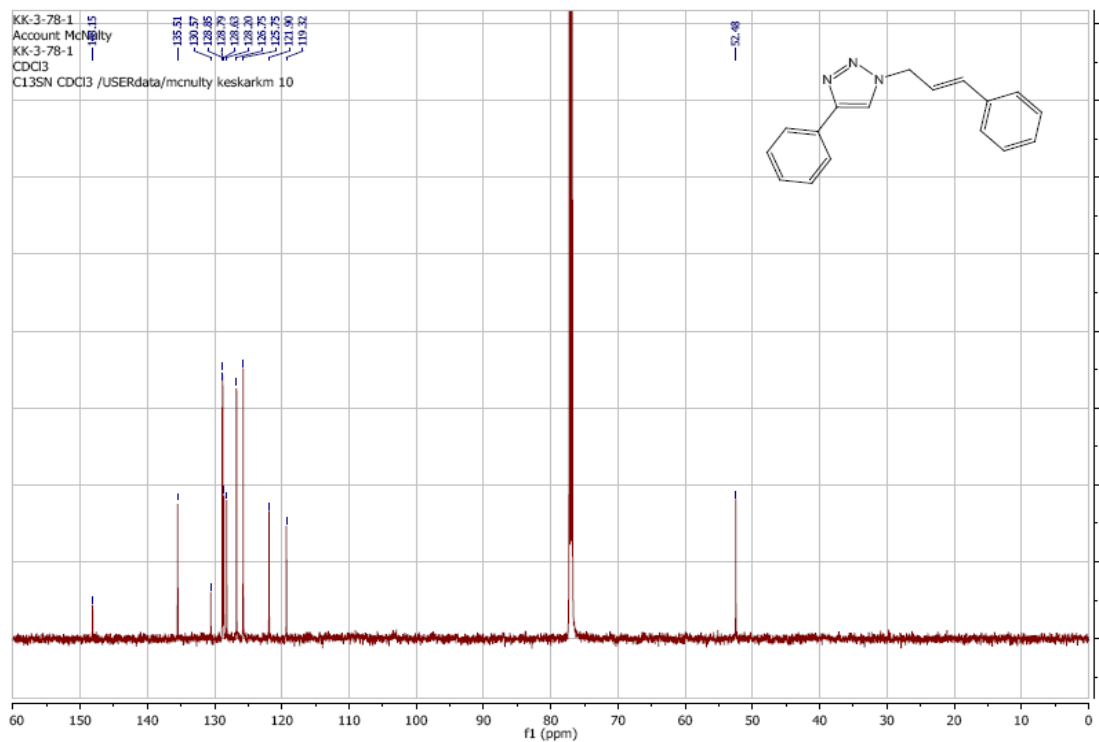
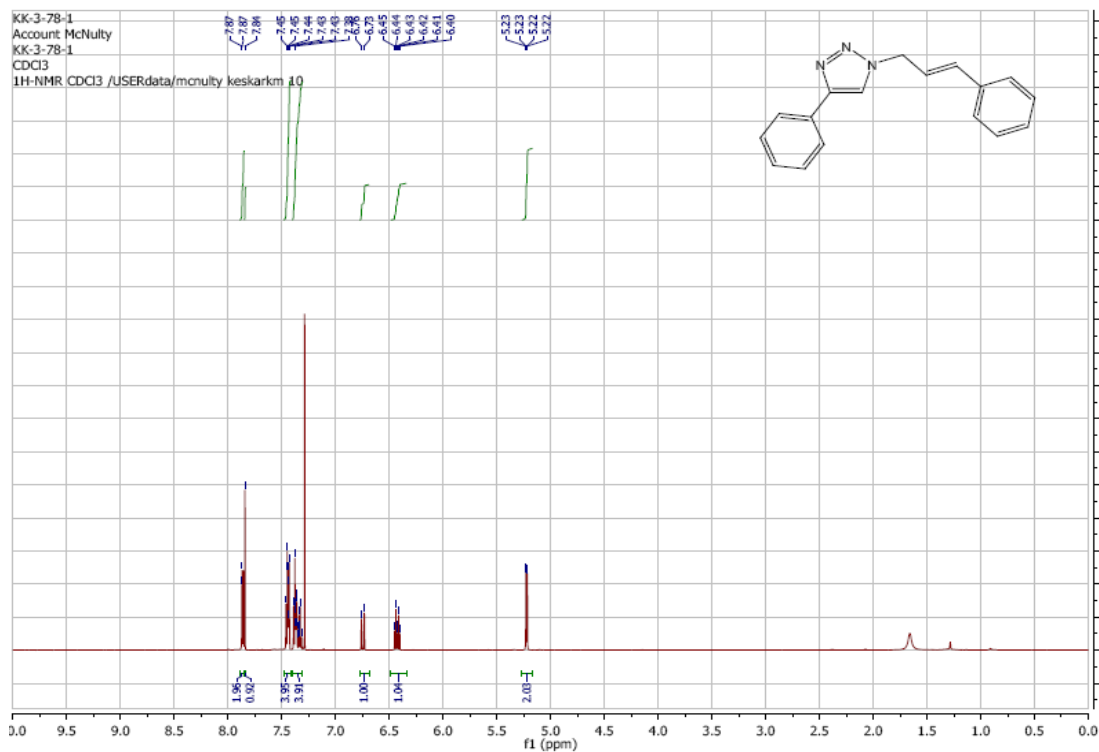
1-(3-Bromobenzyl)-4-phenyl-1*H*-1,2,3-triazole: (Table 2-1, Entry 5, 3e)



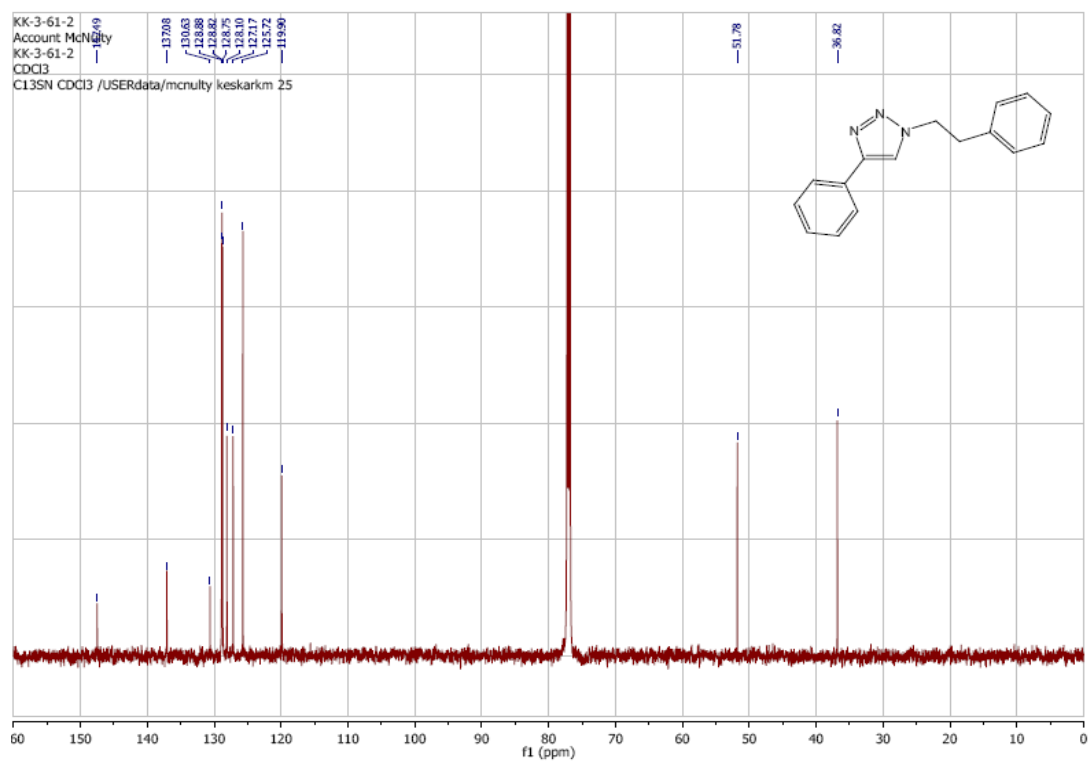
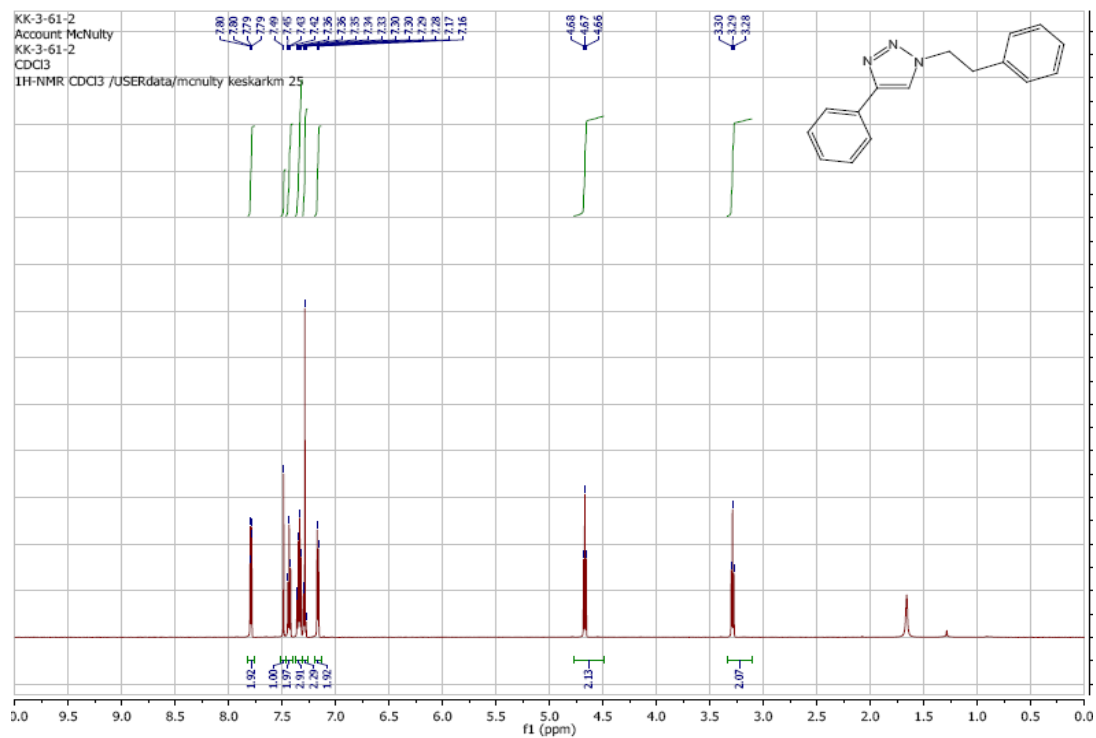
Ethyl 2-(4-Phenyl-1*H*-1,2,3-triazol-1-yl)acetate: (Table 2-1, Entry 6, 3f)



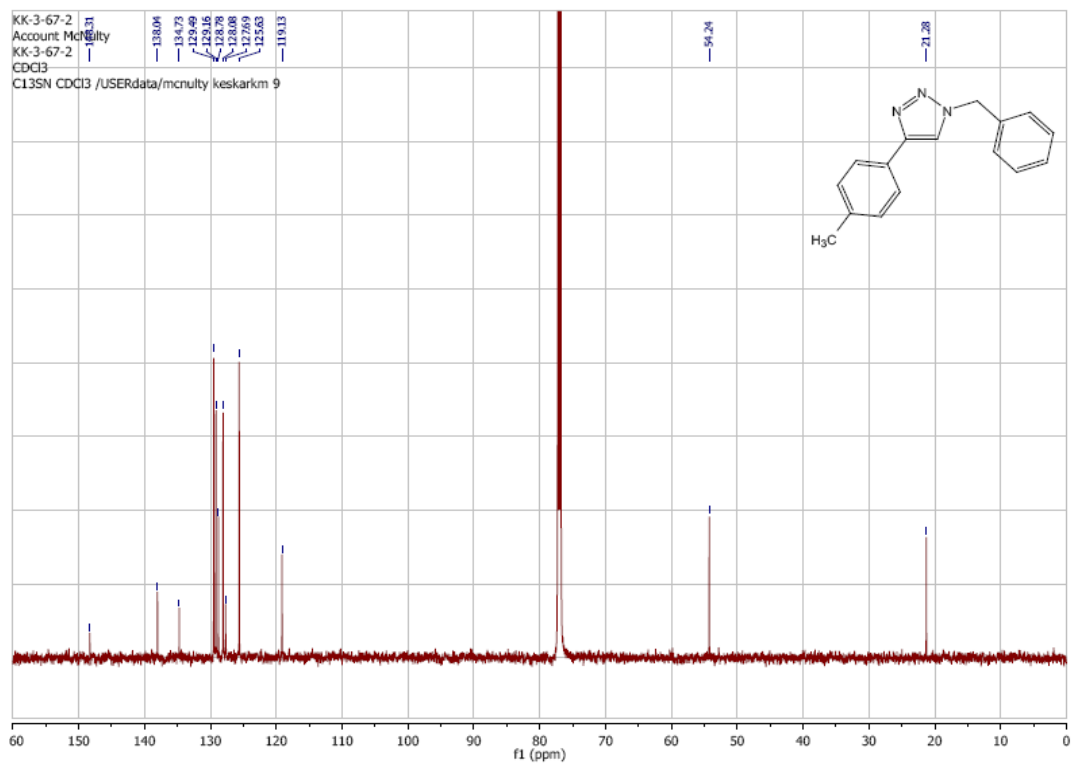
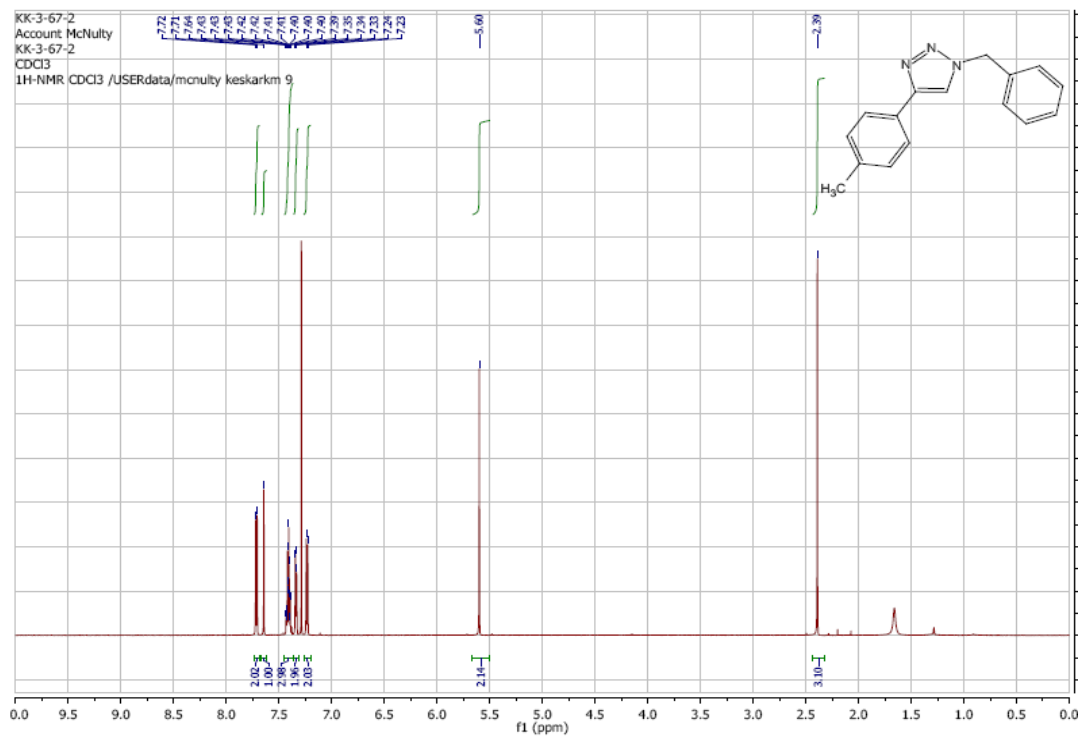
1-Cinnamyl-4-phenyl-1*H*-1,2,3-triazole: (Table 2-1, Entry 7, 3g)



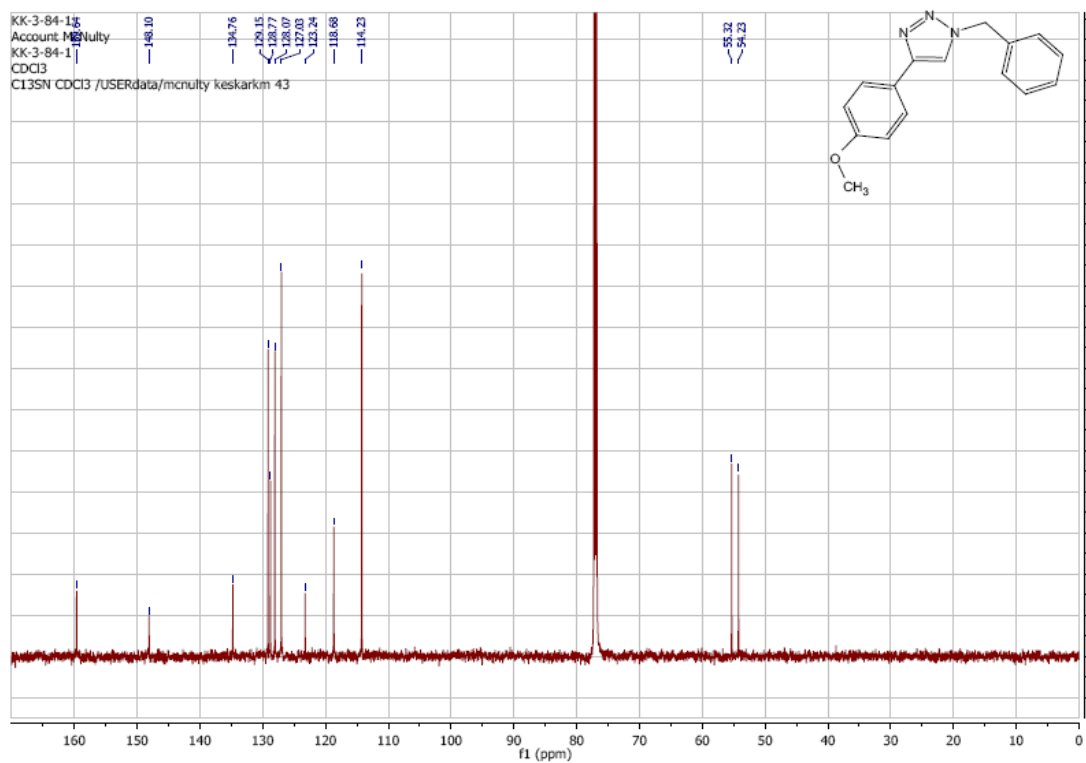
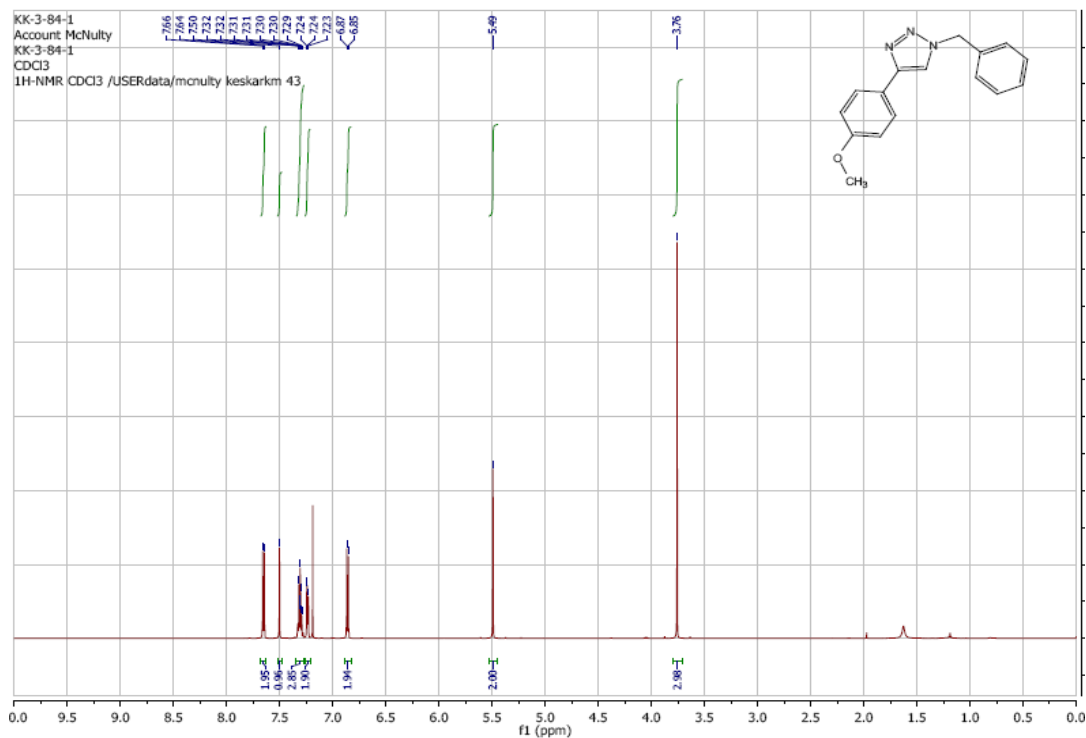
1-(2-phenylethyl)-4-phenyl-1*H*-1,2,3-triazole: (Table 2-1, Entry 8, 3h)



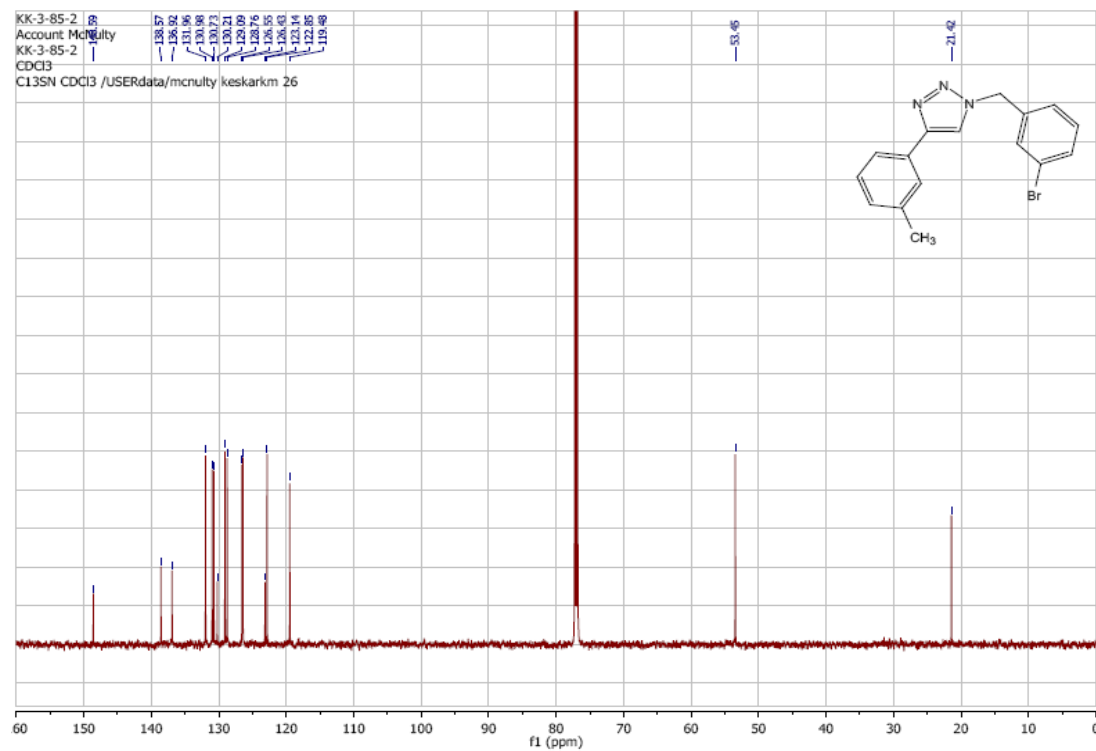
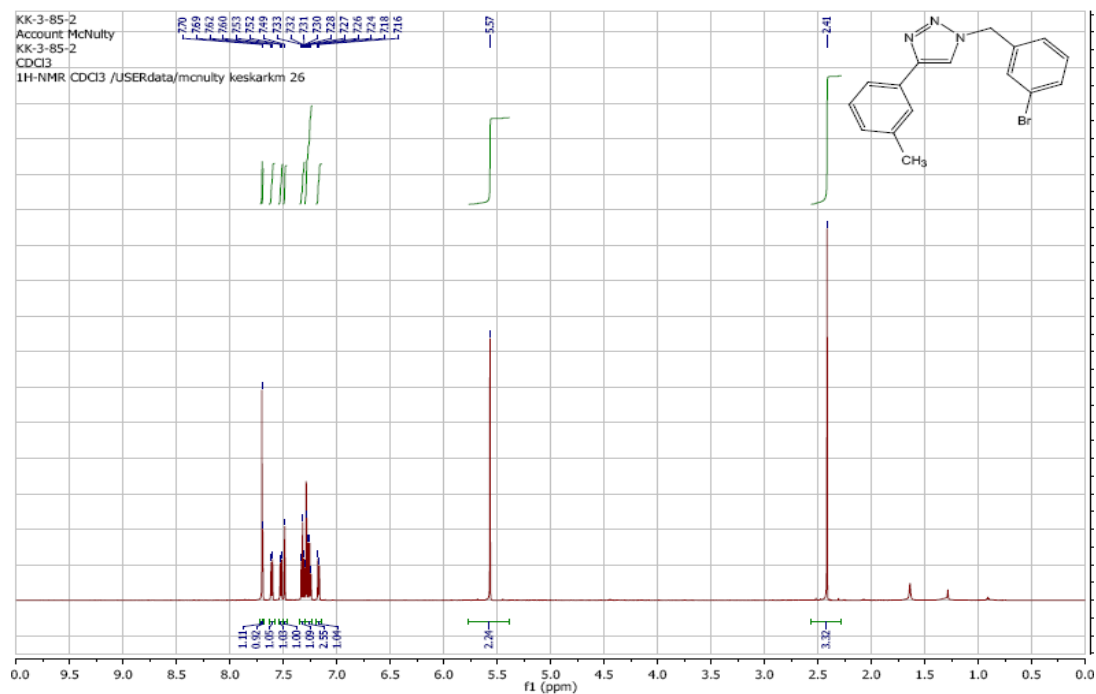
1-Benzyl-4-*p*-tolyl-1*H*-1,2,3-triazole: (Table 2-2, Entry 1, 3i)



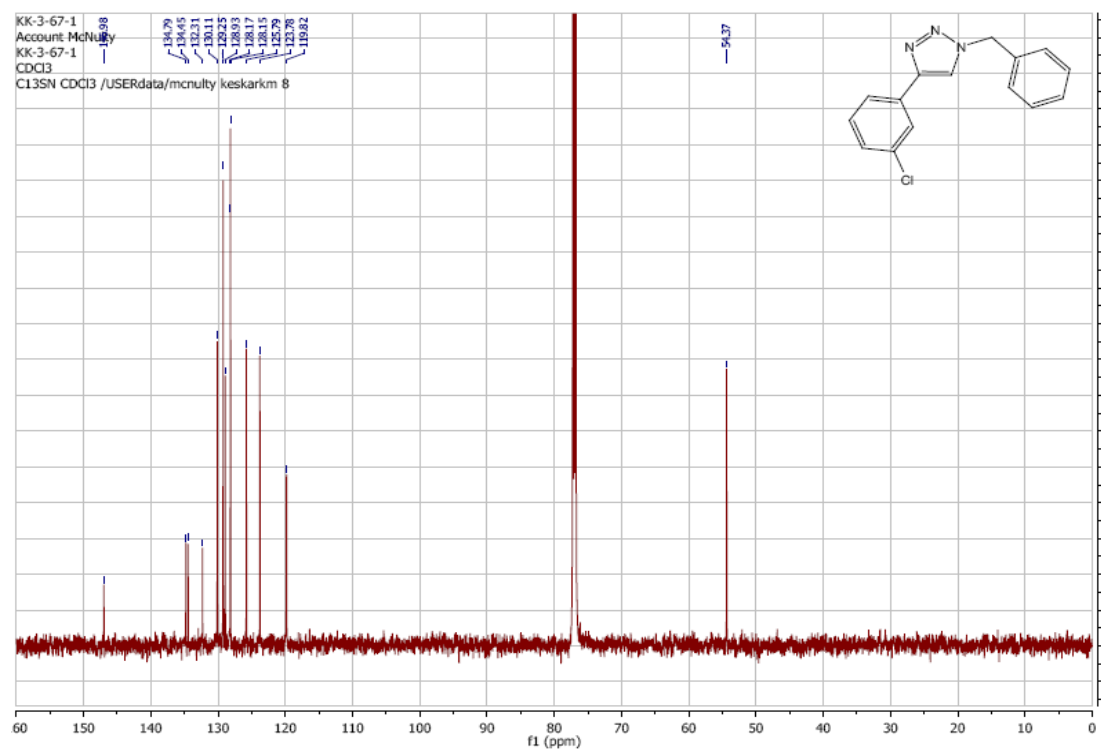
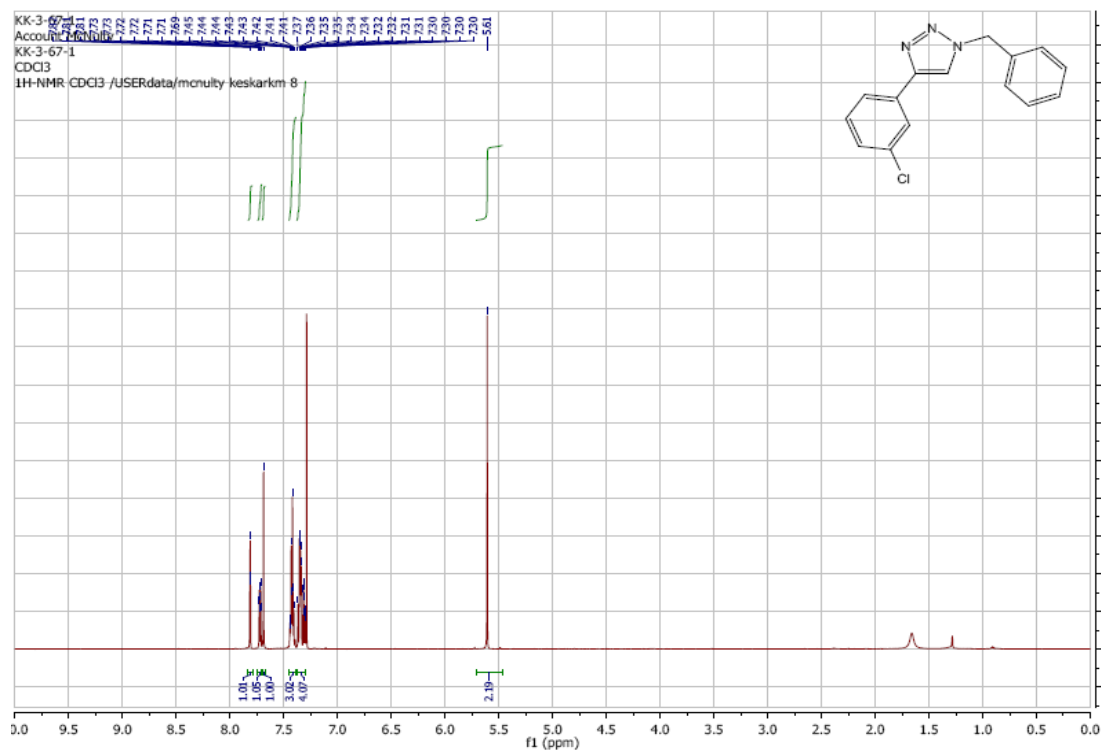
1-Benzyl-4-(4-methoxyphenyl)-1*H*-1,2,3-triazole: (Table 2-2, Entry 2, 3j)



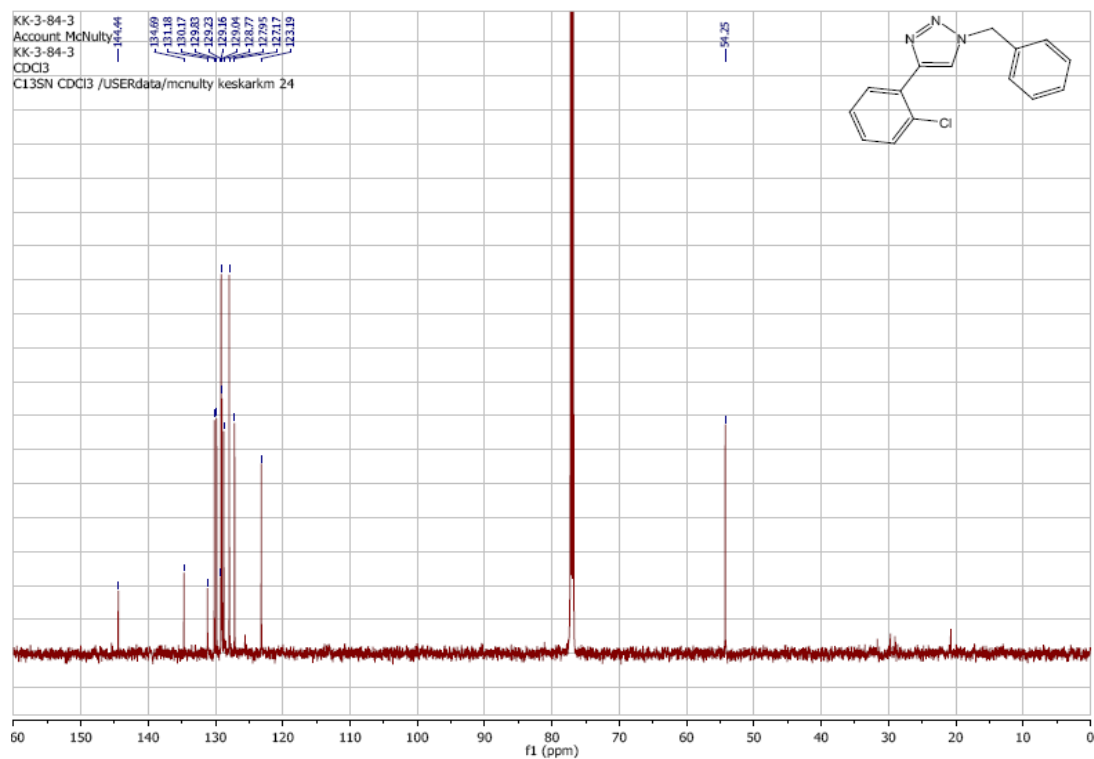
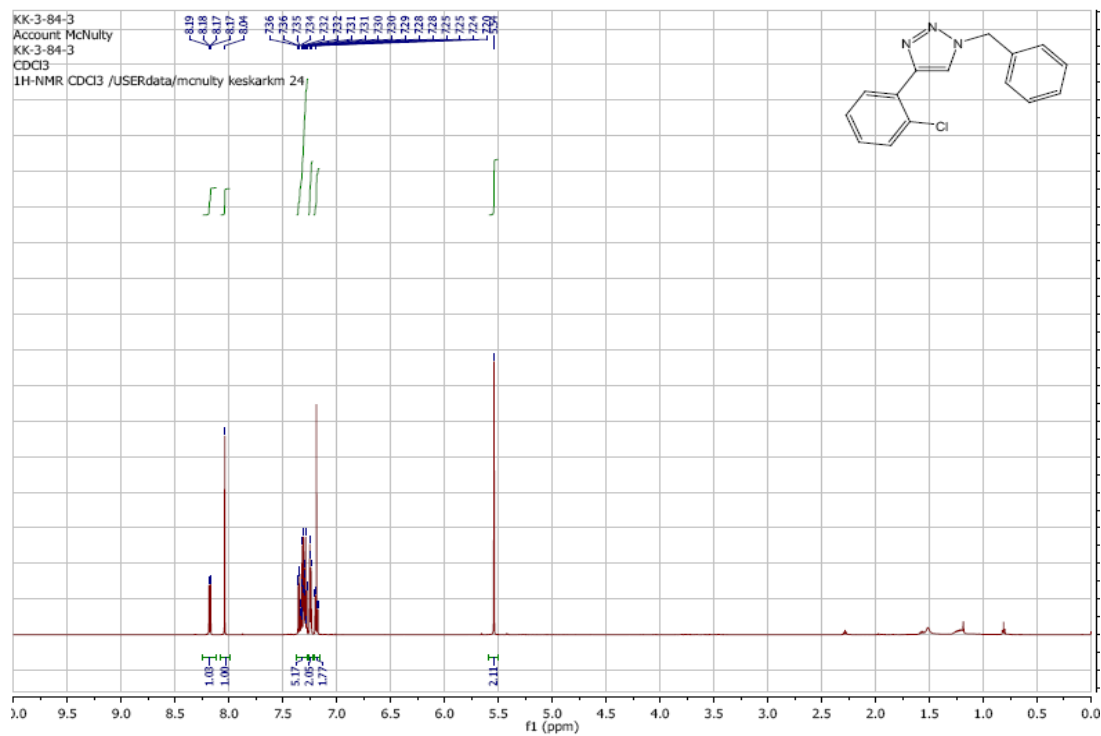
1-(3-Bromobenzyl)-4-(3-methylphenyl)-1*H*-1,2,3-triazole: (Table 2-2, Entry 3, 3k)



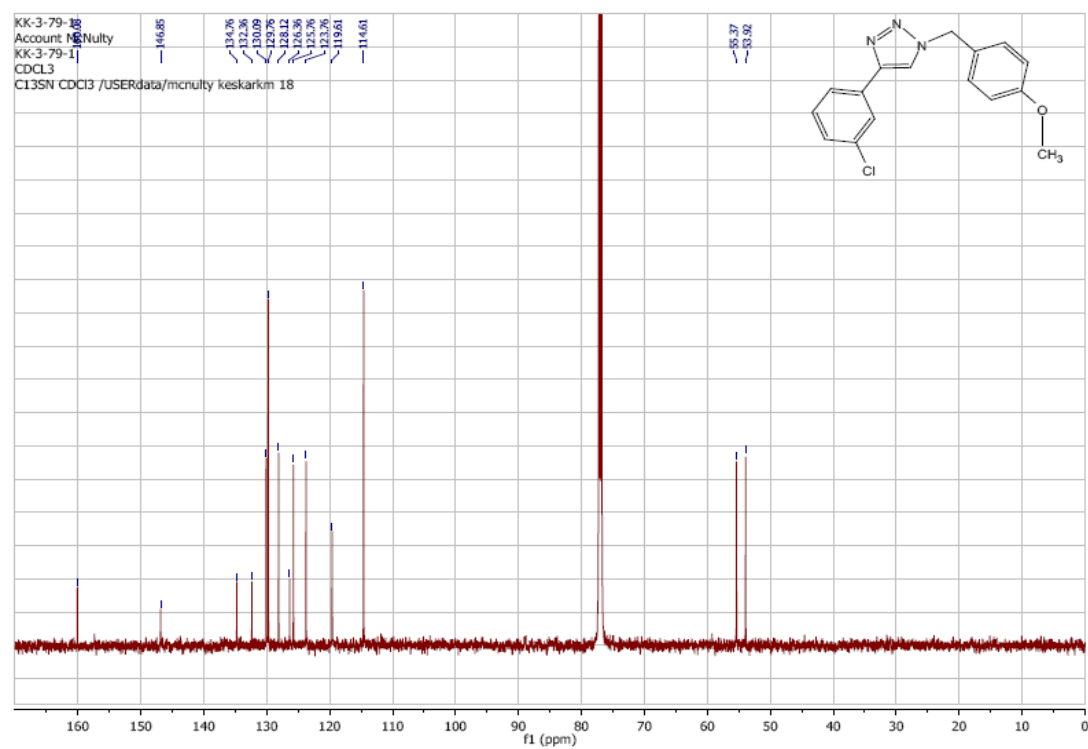
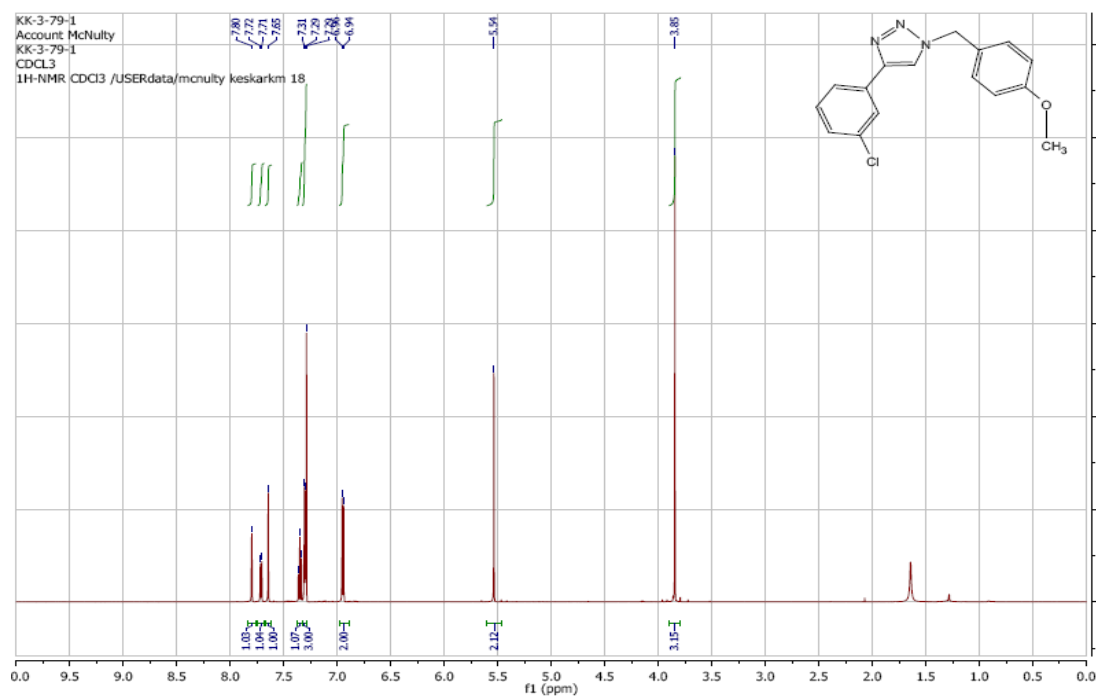
1-Benzyl-4-(3-chlorophenyl)-1*H*-1,2,3-triazole: (Table 2-2, Entry 4, 3l)

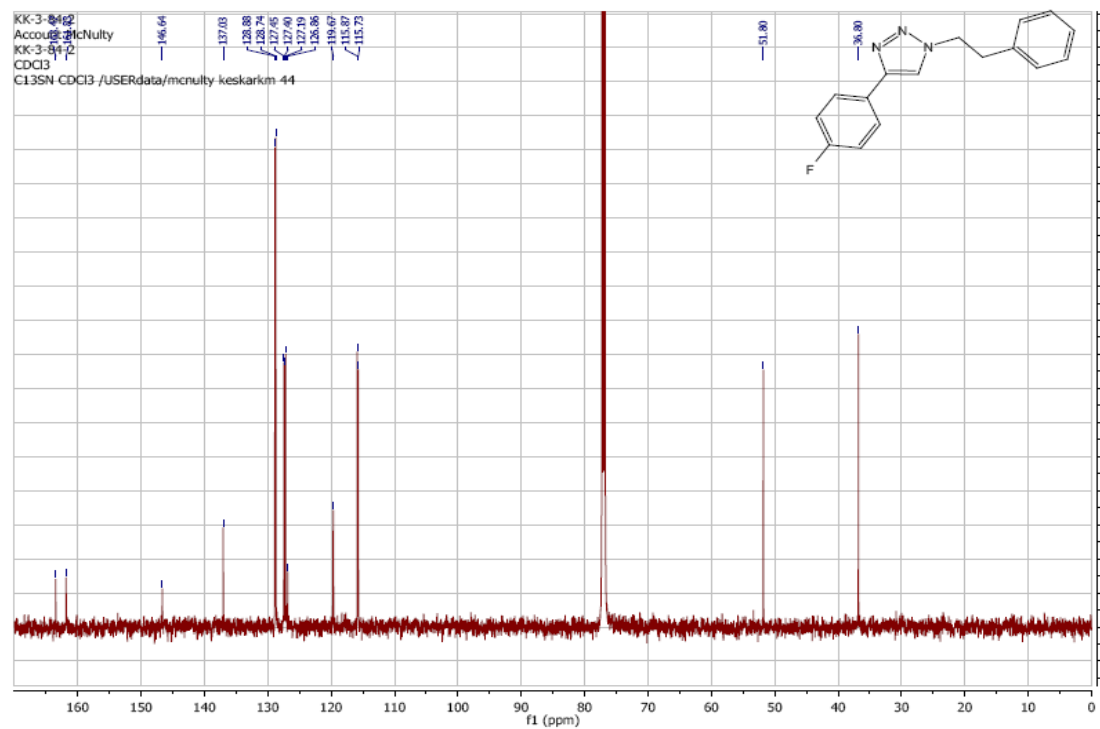
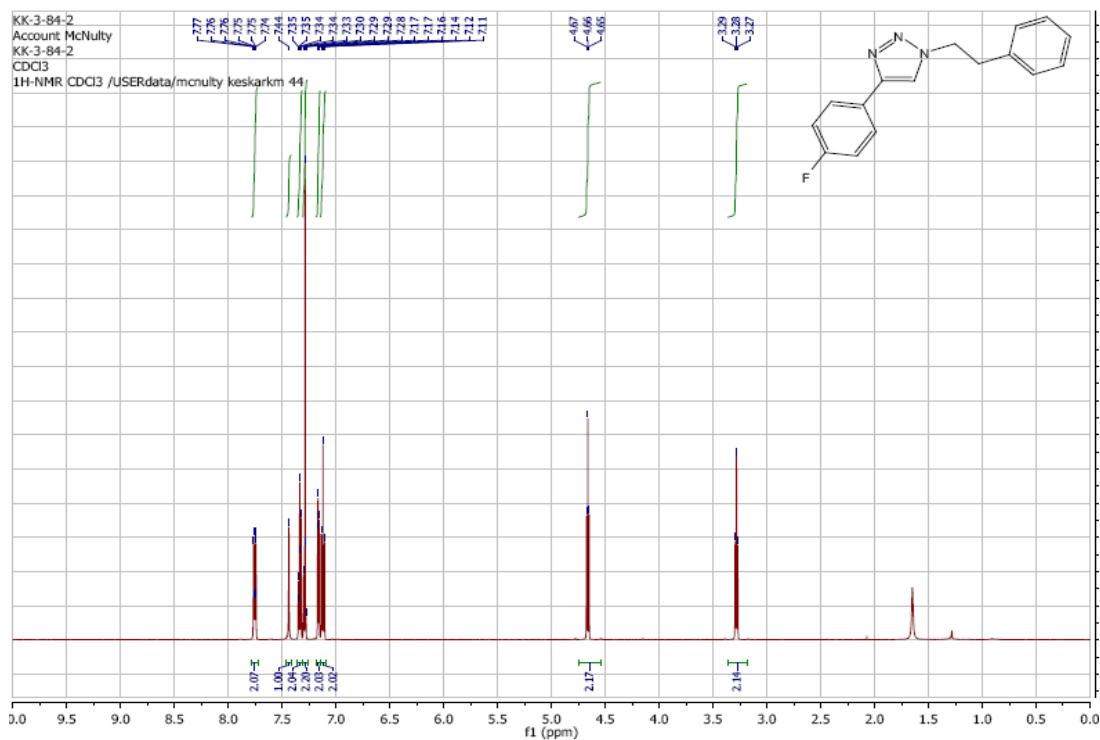


1-Benzyl-4-(2-chlorophenyl)-1*H*-1,2,3-triazole: (Table 2-2, Entry 5, 3m)

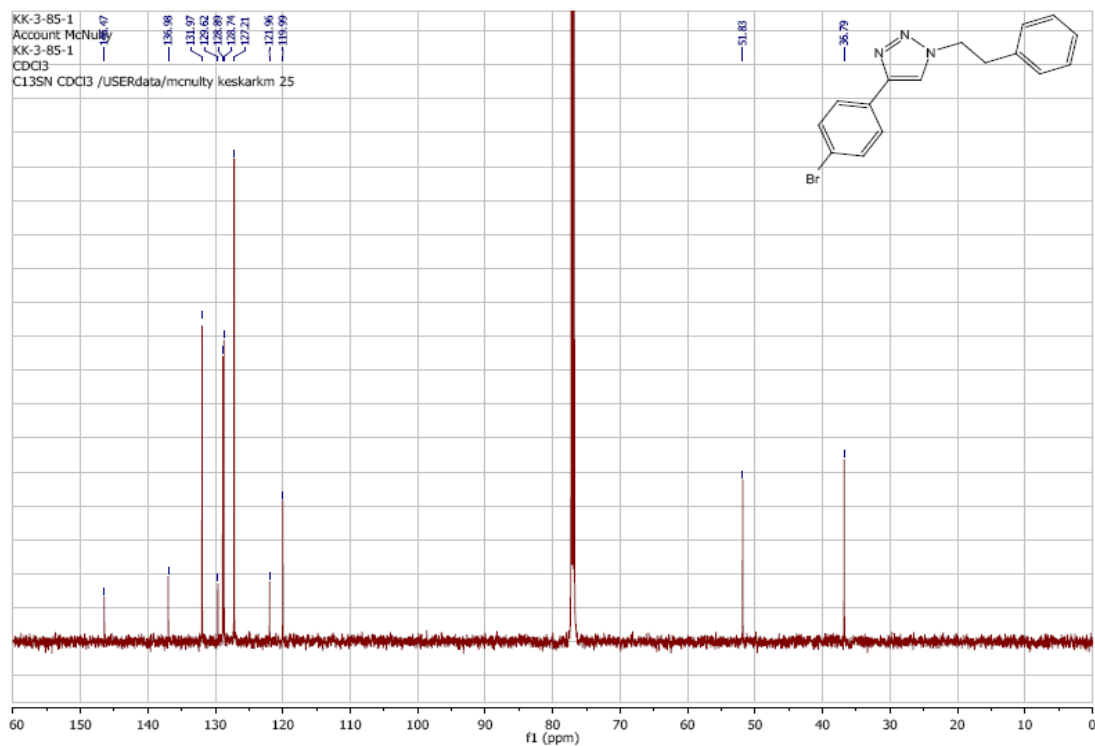
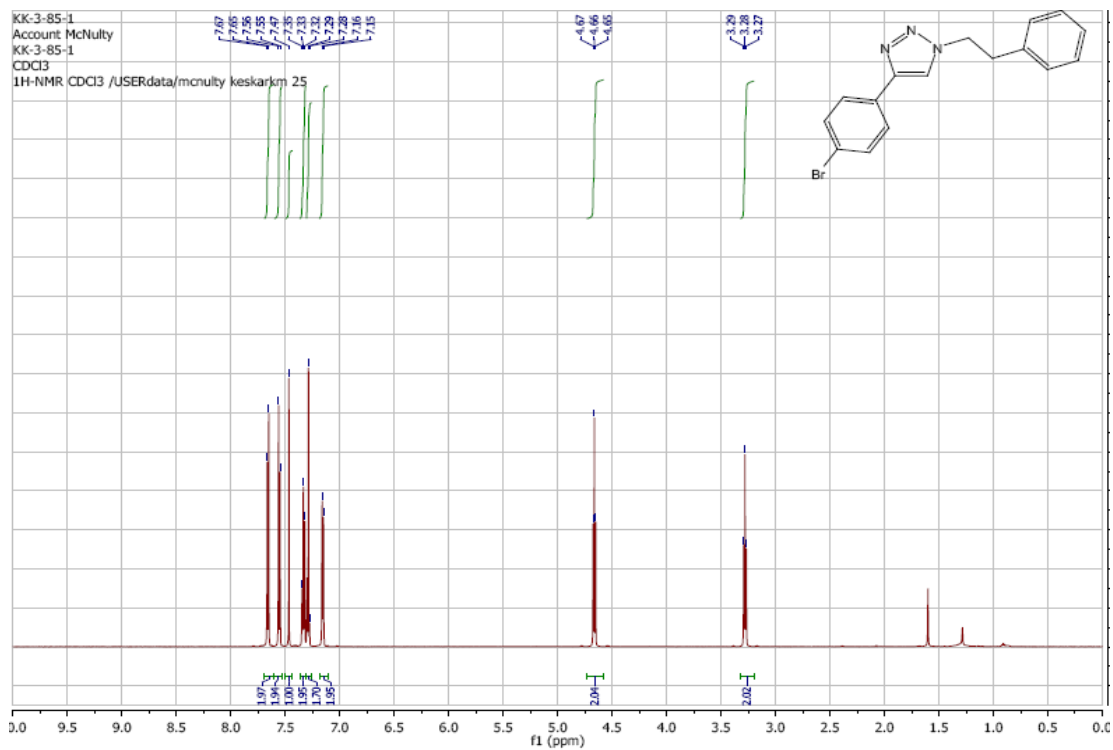


1-(4-methoxybenzyl)-4-(3-chlorophenyl)-1*H*-1,2,3-triazole: (Table 2-2, Entry 6, 3n)

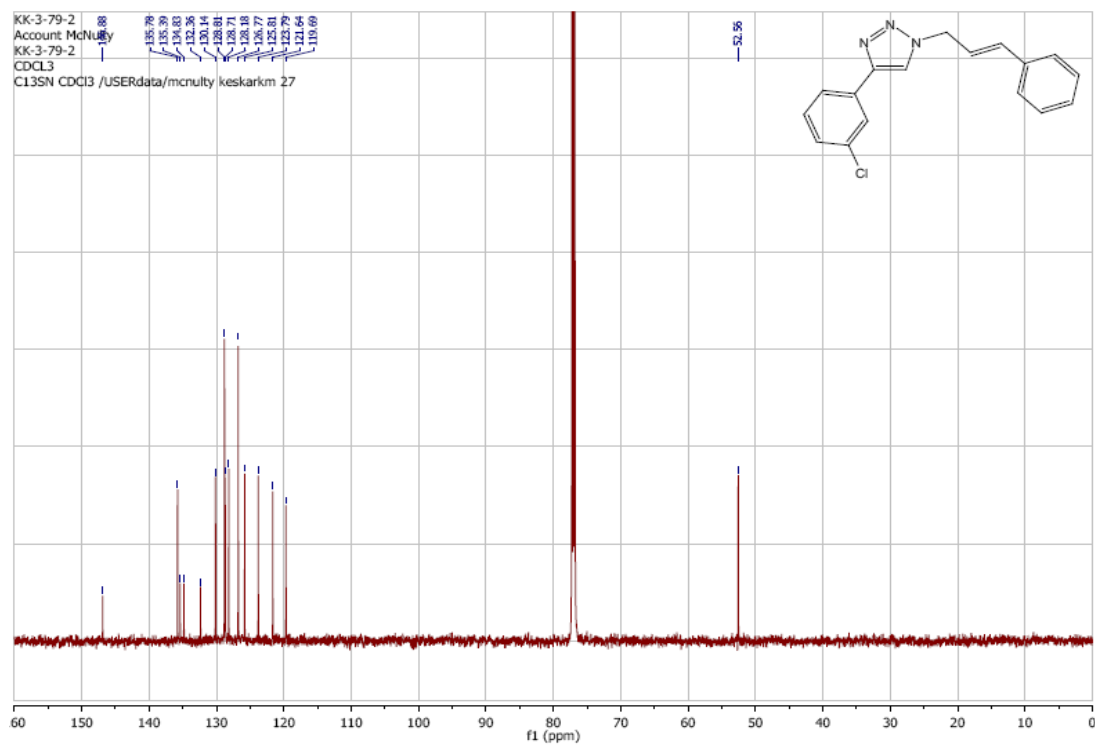
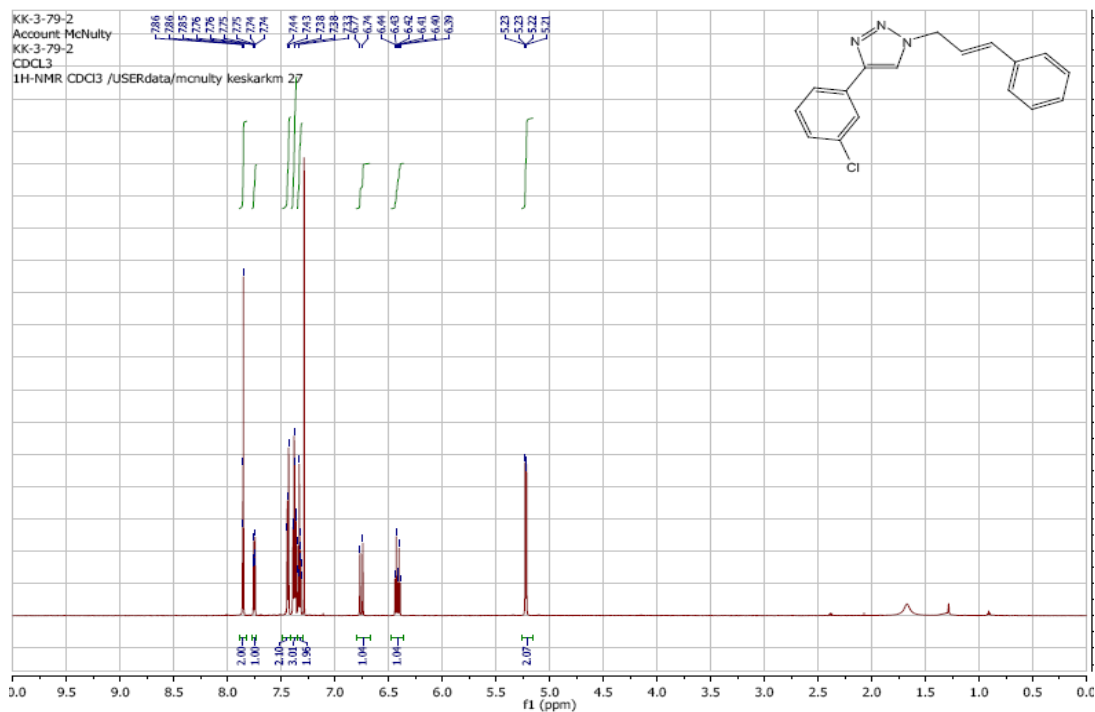


1-(2-phenylethyl)-4-(4-fluorophenyl)-1*H*-1,2,3-triazole: (Table 2-2, Entry 7, 3o)

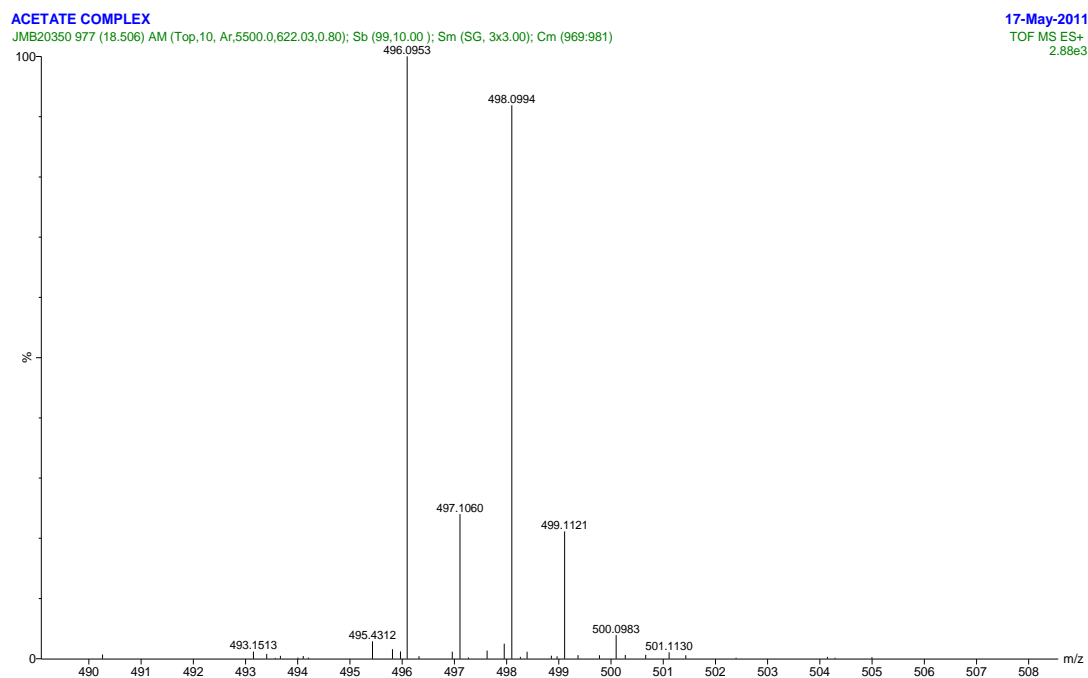
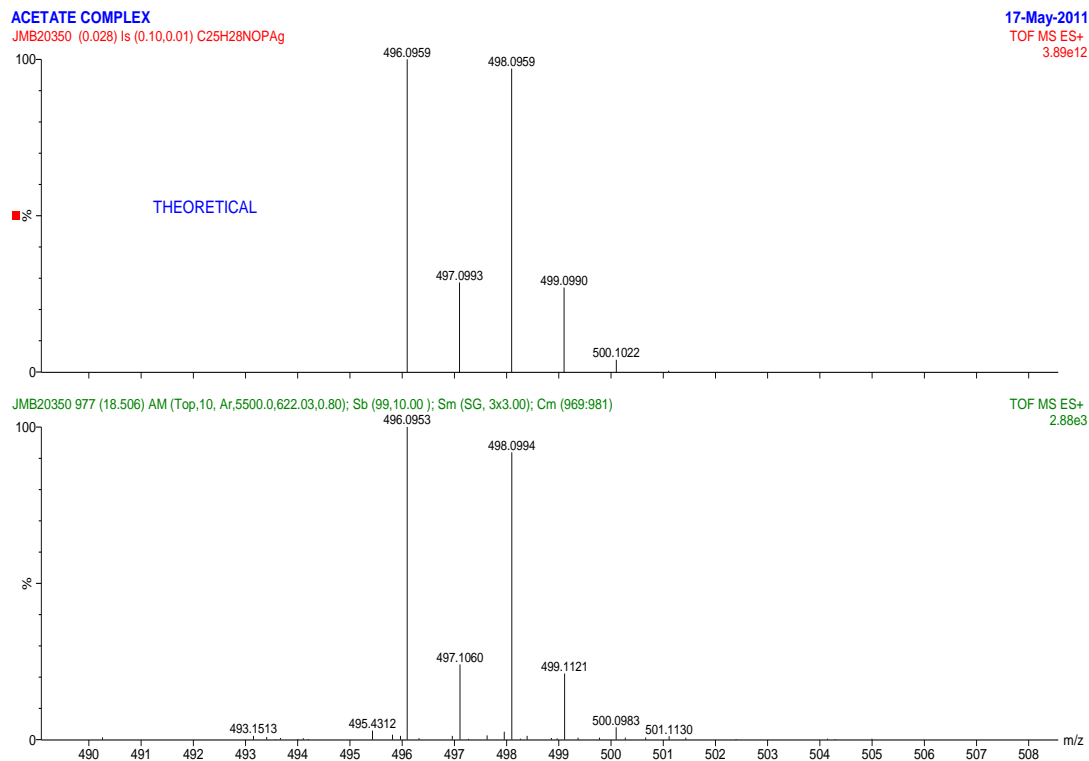
1-(2-phenylethyl)-4-(4-bromophenyl)-1*H*-1,2,3-triazole: (Table 2-2, Entry 8, 3p)

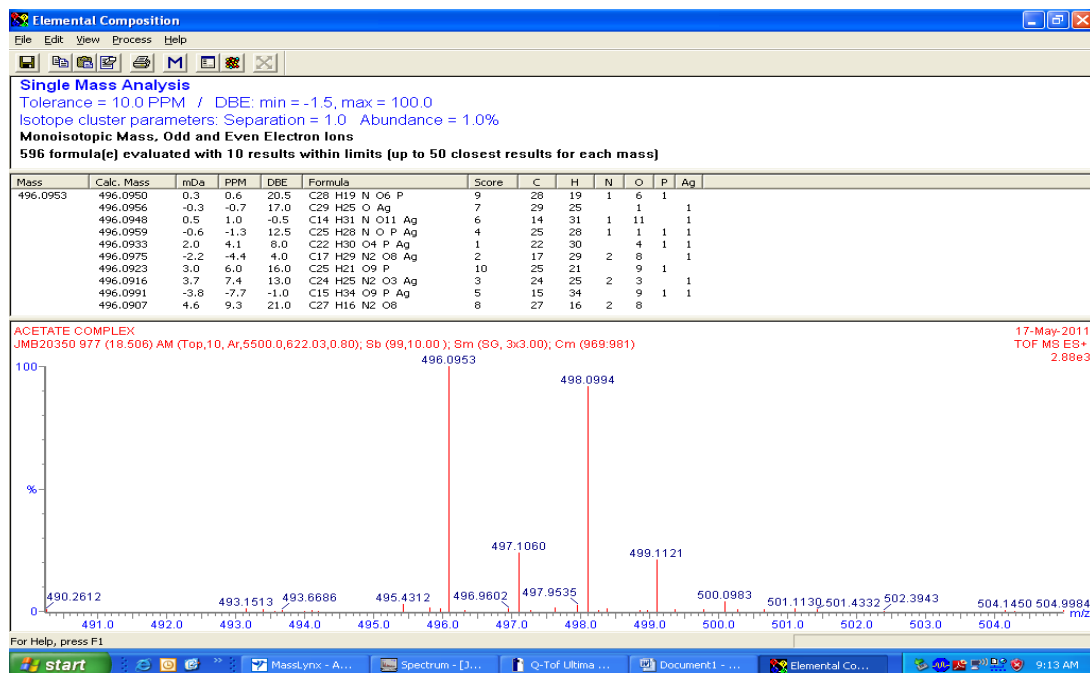


1-Cinnamyl-4-(3-chlorophenyl)-1*H*-1,2,3-triazole: (Table 2-2, Entry 9, 3q)

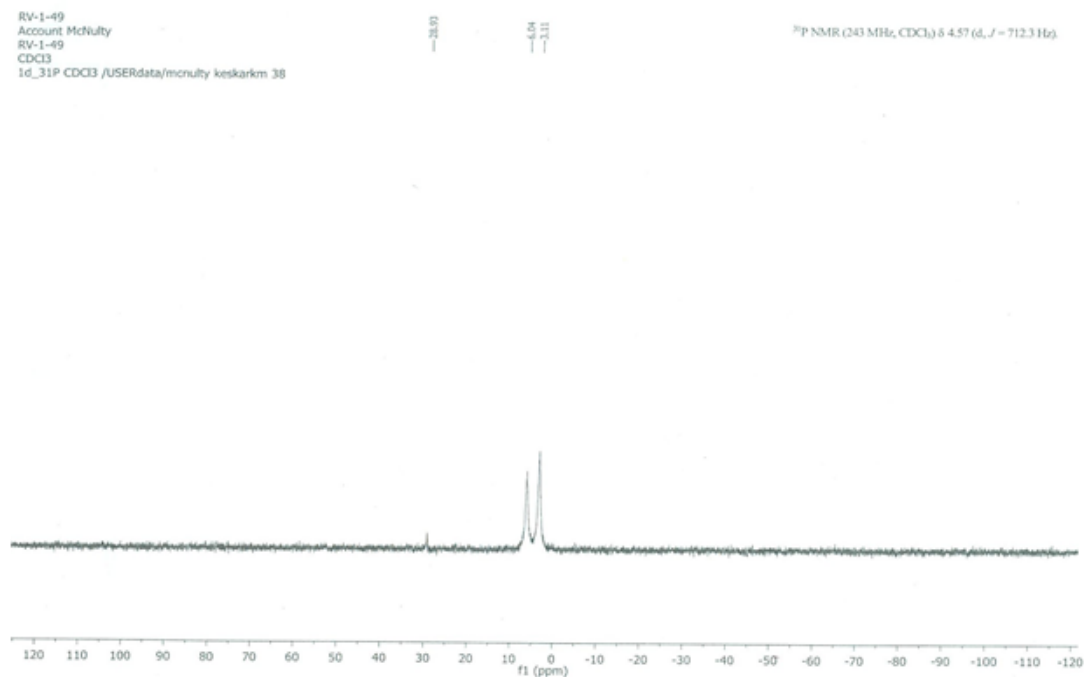


HRMS (M^+) of complex 5 (Scheme 2-2):





³¹P of Complex 5 (Scheme 2-2)



JOHN WILEY AND SONS LICENSE
TERMS AND CONDITIONS

Sep 30, 2014

This is a License Agreement between Kunal Keskar ("You") and John Wiley and Sons ("John Wiley and Sons") provided by Copyright Clearance Center ("CCC"). The license consists of your order details, the terms and conditions provided by John Wiley and Sons, and the payment terms and conditions.

All payments must be made in full to CCC. For payment instructions, please see information listed at the bottom of this form.

License Number	3462571004366
License date	Sep 05, 2014
Licensed content publisher	John Wiley and Sons
Licensed content publication	European Journal of Organic Chemistry
Licensed content title	Discovery of a Robust and Efficient Homogeneous Silver(I) Catalyst for the Cycloaddition of Azides onto Terminal Alkynes
Licensed copyright line	Copyright © 2012 WILEY-VCH Verlag GmbH & Co. KGaA, Weinheim
Licensed content author	James McNulty, Kunal Keskar
Licensed content date	Aug 17, 2012
Start page	5462
End page	5470
Type of use	Dissertation/Thesis
Requestor type	Author of this Wiley article
Format	Print and electronic
Portion	Full article
Will you be translating?	No
Title of your thesis / dissertation	"Advances in Late Transition Metal Catalysis, Olefination Reactions and Applications"
Expected completion date	Dec 2014
Expected size (number of pages)	300

Chapter III: Discovery of a Robust and Efficient Homogeneous Silver(I) Catalyst for the Cycloaddition of Azides onto Terminal Alkynes

3.1 Introduction

Since the concept of “click” chemical reactions was described by Sharpless,^[1a] the copper(I)-catalyzed Huisgen dipolar cycloaddition (CuAAC: i.e., the copper-catalyzed Huisgen cycloaddition) reaction has emerged as the most extensively investigated and applied. This reaction permits the chemoselective, regiocontrolled conjugation of a functionalized alkyne **1** to a functionalized azide **2**^[1] yielding a 1,4- or 1,4,5-substituted 1,2,3-triazole **3** and occasionally the 1,5-regioisomer **4** (**Figure 3-1**). Applications in many areas ranging from functional materials, drug discovery, biological and hybrid bioconjugate areas have increased exponentially over the last decade.^[2,3] The reaction (**Figure 3-1**) mechanism is complex, proceeding through a stepwise process initiated via a copper(I) acetylide **A**, which complexes to the azide **2**. Complexation of the copper(I) catalyst to the Cu-acetylide/azide leads to intermediate **B**, which undergoes the cycloaddition to generate a metalated triazole **C**,^[4,5] and this intermediate, upon protonation,^[5e] yields the 1,4-triazole **3**.

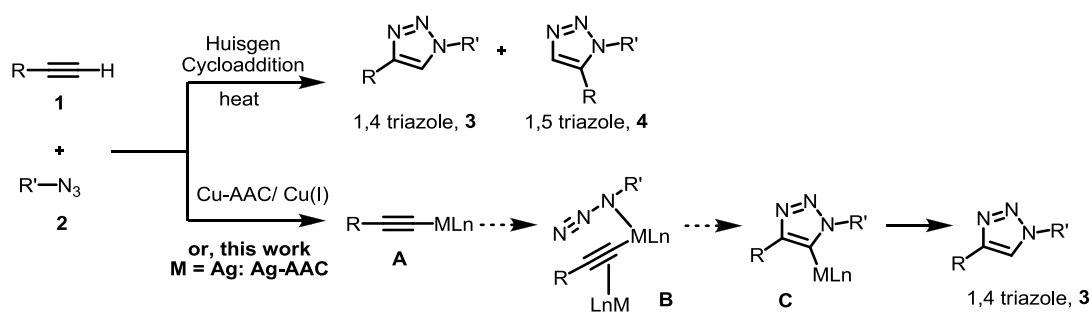


Figure 3-1. The general CuAAC reaction.

Despite the positive attributes of the 1,4-regioselective Cu-AAC process, several problems persist. From a fundamental viewpoint, isoelectronic gold(I),^[6a] silver(I)^[5d,6b] acetylides are known to participate in the AAC reaction,

however the addition of copper(I) salts is *required* to effect the cycloaddition. No competent silver(I) or gold(I) species has been reported to promote the AAC-reaction alone,^[5d, 5f 6b-6d] The rationale for the failure of a competent silver(I) catalyst is not clear.

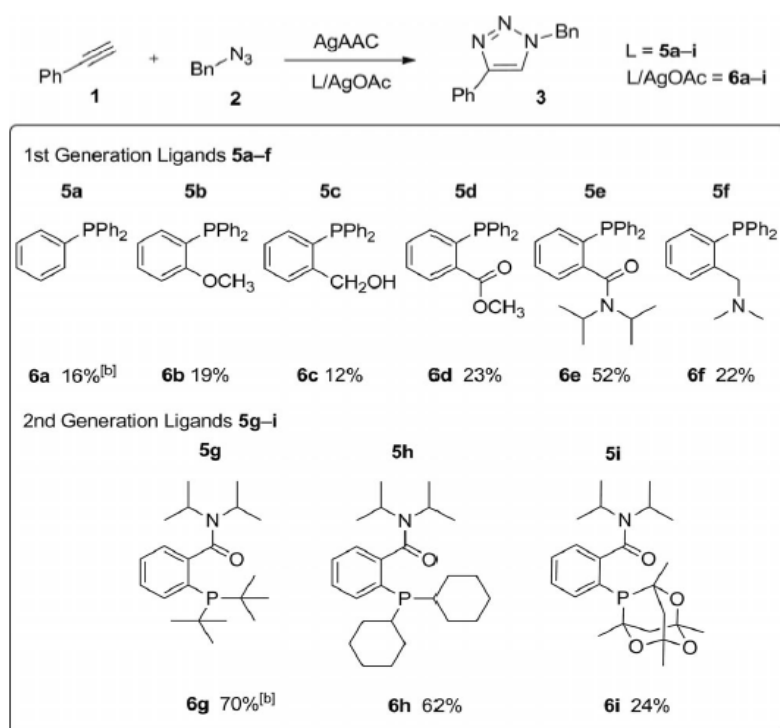
In addition, reports of problematic Cu-AAC reactions^[5g, 7a-7f] and the toxicity (including genotoxicity) of redox-active copper(I) species have arisen in relation to biological applications.^[9] Many copper catalyzed processes are heterogeneous and suffer from aggregation problems. Homogeneous copper catalysis has been achieved using amine and phosphine ligands, allowing low catalyst loadings (<1%).^[7g-7j] Despite the unpromising precedents reported for a possible AgAAC process, we became interested in exploring homogeneous complexes of type $[\text{Ag}^+(\text{L}_2)(\text{X}^-)]$ for several applications and recently discovered the first homogeneous silver(I) catalyst for the AAC reaction.^[8] In accord with issues of copper toxicity, concern has been raised over the potential toxicity of silver nanoparticles.^[10a] Silver complexes have been shown to be significantly less cytotoxic than silver salts.^[10b] Silver complexes are not expected to participate in analogous ($\text{Cu}^{\text{I}}\text{-Cu}^{\text{II}}$) one electron transfer processes and we were confident that a stable, catalytically efficient suitably ligated silver(I) species could be developed which would not precipitate metallic silver or silver halide under the conditions required. In view of these concerns and initial success,^[8] we have systematically evaluated structural effects of the ligand in the Ag-mediated AAC process. Here in, we report the development of an optimized, chemically stable, highly efficient silver(I) homogeneous catalyst for the AgAAC process.

3.2 Result and Discussion

We recently reported a homogeneous, well-defined silver(I) complex derived from silver acetate and *N,N*-diisopropyl-(2-diphenylphosphino)-benzamide (**5e**) competent in affecting the AgAAC process. Whereas these reactions

proceeded at room temperature in toluene, the catalyst was inefficient. Full conversion of the alkyne/azide to triazole required the use of 20 mol-% catalyst and a 4.8-fold excess of azide relative to alkyne. Our vision in developing the hemilabile ligand **5e** was to enable push-pull effects on the metal centre allowing progression through the cycle by electrophilic 14-electron to 18-electron intermediates effecting cyclization through nucleophilic ligand-mediated polarization of the complexed alkyne onto the azide (*vide infra*).

Table 3-1. Pronounced ligand effects on the AgAAC reaction.^[a]



[a] Reaction conditions: Phenyl acetylene (0.18 mmol, 1.2 equiv.), benzyl azide (0.15 mmol, 1.0 equiv.), catalyst (10 mol-%), caprylic acid (20 mol-%), PhMe (1.0 mL), 48 h, r.t. [b] Yield of triazole **3**.

To probe ligand effects in the AgAAC process, ligands **5a-5i** (Table 3-1) were synthesized by using standard methods by employing nucleophilic and electrophilic phosphane coupling (see Experimental Section). Crystalline complexes **6a-6i** (Table 3-1) of ligands **5a-5i** were formed with silver acetate

(1:1) in all cases. The AgAAC process was investigated under a standard set of conditions (10 mol% catalyst, 48h, r.t. in toluene) with all nine silver complexes (**Table 3-1**). The first generation of ligands **5a-5f** consisted of modifications to the weak donor ability of the *ortho*-substituent on the ligand. A slight excess of alkyne (azide:alkyne ratio 1.0:1.2) was used in contrast to our earlier requirement of excess azide (4.8 equivalents). The overall results of screening catalysts **6a-6f** demonstrated the clear superiority of the *N,N*-diisopropylamide substituent, which, fortuitously, the first ligand investigated in the series.^[8]

Table 3-2. Optimization with catalyst **6g** in the AgAAC reaction.^[a]

Reaction scheme: Phenyl acetylene (1) + Benzyl azide (2) $\xrightarrow[\text{AgAAC reaction}]{\text{6g conditions}}$ 3 + 4

Entry	Cat. loading [mol-%]	Temp. [°C]	Time [h]	Conversion 3/4 (% isolated yield of 3)
1	10	25	48	70:0 (70)
2	10	70	48	93:0 (92)
3	10	110	48	95:5 (94)
4	10	110	24	95:5 (92)
5	10	70	24	82:0 (80)
6	10	90	24	89:0 (86)
7	5	110	24	95:5 (92)
8	5	90	24	90:0 (ND)
9	5	90	24	93:0 (ND)
10	2	90	24	62:0 (ND)
11	2	90	24	99:0 (98)
12	2	90	12	79:0 (ND)
13	1	90	24	92:0 (ND)
14	0.5	90	24	79:0 (ND)
15	1	90	48	99:0 (ND)
16	0.5	90	48	99:0 (ND)

[a] Reaction conditions for entries 1–8, 10: Phenyl acetylene (0.18 mmol, 1.2 equiv.), benzyl azide (0.15 mmol, 1.0 equiv.), caprylic acid (20 mol-%), PhMe (1.0 mL). Reaction conditions for entries 9, 11–16: Phenyl acetylene (0.09 mmol, 1.0 equiv.), benzyl azide (0.14 mmol, 1.5 equiv.), caprylic acid (20 mol-%), PhMe (1.0 mL).

The effect of the *ortho* substituent is sharp both on catalytic activity and overall stability of the complex. Complex **6e** (most stable) showed only minor silver metal deposition after one reaction cycle, while catalyst **6c** (least stable) decomposed rapidly and gave poor conversion. Also, stronger and weaker donor appendages at the *ortho* position appear detrimental with the amide substituent alone exhibiting a superior effect on catalyst stability and turnover. The second generation of ligands **5g-5i** was therefore prepared retaining the *N,N*-diisopropylamide substituent and modulating the phosphine substituent from diphenyl- (i.e., **5e**) to ditertbutyl- (i.e., **5g**), dicyclohexyl- (i.e., **5h**) and the phosphadamantane derivative **5i**.^[11] Screening the new complexes **6g-6i** derived from the second-generation ligands in the AgAAC reaction (**Table 3-1**) demonstrated the superiority of the di-*tert*-butyl- and dicyclohexyl-containing ligands.

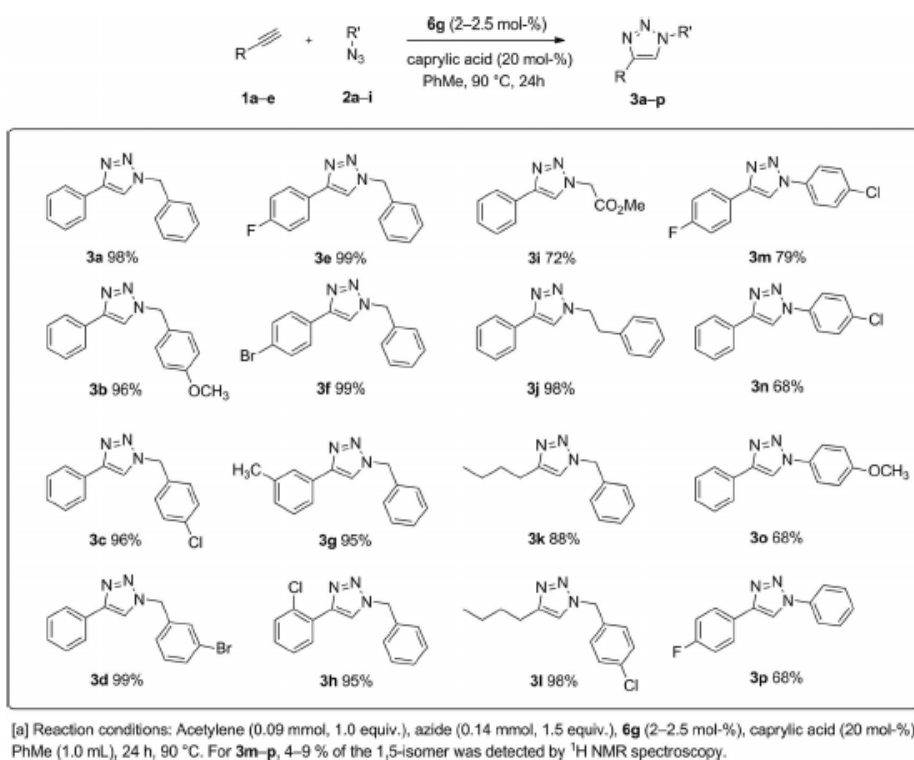


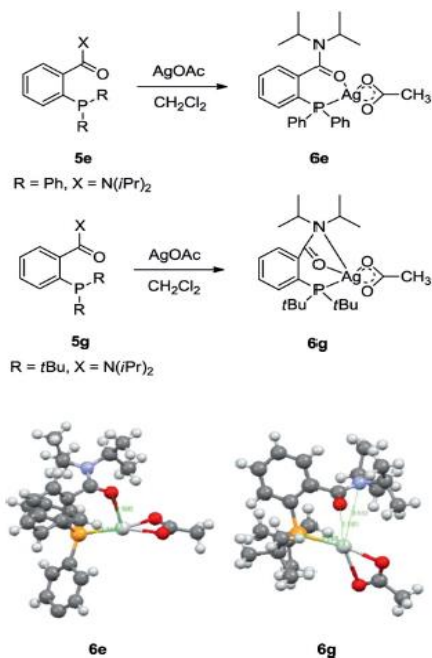
Figure 3-2. Scope of the aryl alkyne in AgAAC reaction.^[a]

On the basis of these ligand effects, catalyst **6g** was chosen with the goals of increased catalyst efficiency and expanding scope in the reaction. The silver complex **6g** is a solvate-free, air-stable white crystalline solid (m.p. 190-200 °C decomp.) that is very soluble in toluene and most other organic solvents. It produces clear colourless solutions in organic solvents that remain unaffected for weeks under normal laboratory conditions and through various heating/cooling cycles. No precipitation of silver metal is observed at all. The optimization results for catalyst **6g** are summarized in **Table 3-2**. The initial reaction provided seven catalyst turnovers at room temperature over 48 hours (**Table 3-2**, entry 1). Increasing the temperature allowed higher conversion; however trace formation of the minor 1,5-regioisomeric triazole **4** was observed at temperatures above 100 °C while formation of this product was totally suppressed at 90 °C (**Table 3-2**, entries 2-7). All other reactions were therefore conducted at 90 °C and catalyst loading was now reduced (**Table 3-2**, entries 8-16). Modification of the alkyne:azide stoichiometry showed that a slight excess of azide (alkyne:azide, 1.0:1.5) was superior to a slight excess of alkyne (**Table 3-2**, entries 10 and 11). Overall, catalyst **6g** proved to be highly active with loadings as low as 0.5 mol-% providing quantitative conversion (200 turnovers) within 48 hours. Using 2-2.5 mol-% of catalyst **6g** under otherwise conditions of **Table 3-2** (entry 11), >99% conversion to the 1,4-triazole was observed after 24h at 90 °C. To check the efficiency of the catalyst, the above reaction was repeated three times further on the initial catalyst charge using identical quantities of azide and alkyne providing >99%, 96% and 95% conversion on subsequent runs. The solution remained completely clear, colourless and homogeneous, showing no sign of silver metal precipitation after the fourth cycle. Control experiments also demonstrated that no Staudinger-type azide reduction occurred between catalyst **6g** and benzyl azide under the AgAAC reaction conditions, demonstrating further the exceptional stability of this complex. The silver mediated AAC reaction proved broad in scope with

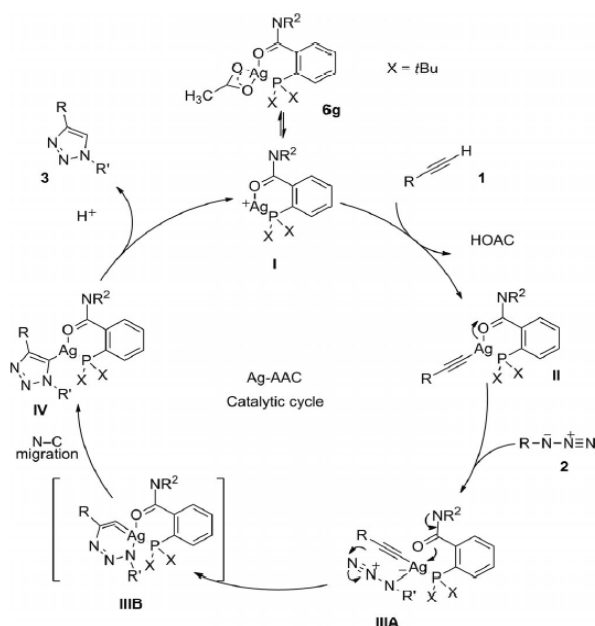
complex **6g**, as summarized in **Figure 3-2**. These reactions were conducted using 2-2.5 mol-% of catalyst **6g** in order to achieve high conversions in a 24 h reaction period (i.e. similar to **Table 3-2**, entry 11). The AgAAC reaction catalyzed by **6g** is successful with a wide range of substrates including aryl-, benzyl- and alkyl azides coupling with both phenyl- and aliphatic acetylenes. No restrictions on the generality have been identified on the process so far.

Earlier, we reported the X-ray crystal structure for the complex **6e**.^[8] In order to gain potential insights into the reactivity of complex **6g**, crystals suitable for X-ray were grown and the crystal structure shown in **Scheme 3-1**. The silver atom of complex **6e** proved ligated to the amide donor via one of the non-bonding lone pairs of the oxygen atom (2.680 Å). In contrast, the highly active complex **6g** showed weak ligation to the amide HOMO with contacts between Ag-O (3.163 Å) and Ag-N (3.632 Å), while other contacts (Ag-P and Ag-acetate) were very similar.

The reaction could readily be followed by NMR in [D₈]toluene. Interruption at various times during progress of the standard reaction and analysis by ³¹P-NMR showed only the presence of complex **6g**, with no other aggregate species observable. In addition, ¹H-NMR showed only clean conversion of azide/alkyne to triazole. The role of the ligand in complex **6g** is clearly significant and we postulate the following stepwise catalytic cycle (**Scheme 3-2**). The proposed catalytic cycle for the AgAAC process provides a rationale for the effectiveness of the hemilabile ligand on complex **6g**. Loss of acetate from the 18-electron species **6g** yields the active catalyst **I** (14e⁻) which forms the ligated silver(I) acetylide **II**, the electrophilicity of which is modulated by the hemilabile amide substituent.



Scheme 3-1. Synthesis of AgOAc complexes of ligands **5e** and **5g** (top) and ball and stick plots of **6e** (CCDC 843618) and **6g** (CCDC 882589) (bottom).



Scheme 3-2. Proposed catalytic cycle for the homogeneous Ag(I)-catalyzed AAC reaction.

Nucleophilic attack on **II** by the azide generates the intermediate **IIIA**, shown as the $16e^-$ species. The role of the hemilabile nature of the ligand comes into play again from **IIIA** by complexation of the amide forming an $18e^-$ intermediate, which transmits polarization of negative charge through the filled d orbitals into the acetylide π^* -orbitals effecting cyclization onto the tethered azide. This process can proceed through the transient silver metallacycle shown as **IIIB**, from which the nitrogen migrates to carbon carrying both electrons to yield metalated triazole **IV**, leading to product **3** on protonation and regenerating the active catalyst **I**. A similar catalytic cycle, without ancillary ligand effects, was postulated for the CuAAC process in accord with DFT calculations.^[6c]

3.3 Conclusion

We report a chemically robust and effective general homogeneous catalyst for the AgAAC reaction. A pronounced ligand effect is observed and a significant role is attributed to the hemi-labile nature of ligand **5g** in both the stability and efficiency of the catalyst **6g**. The catalyst is effective at loadings as low as 0.5 mol-% and is stable thermally over repeated catalytic cycles showing no silver metal precipitation. A mechanism is proposed involving continuous coordination of the phosphane donor of the ligand to silver and proceeding through intermediates that allow coordination and polarization of the acetylide/azide to effect the stepwise cyclization. Further studies to probe the mechanism and extension of reaction scope are under investigation.

3.4 References

- [1]. (a) H. C. Kolb, M. G. Finn, K. B. Sharpless, *Angew. Chem. Int. Ed.* **2001**, *40*, 2004-2021. (b) C. W. Tornøe, C. Christensen, M. Meldal, *J. Org. Chem.* **2002**, *67*, 3057-3064. (c) V. V. Rostovtsev, L. G. Green, V. V. Fokin, K. B. Sharpless, *Angew. Chem. Int. Ed.* **2002**, *41*, 2596-2599.

- [2]. For selected application of click reactions in materials and bioconjugate chemistry see: (a) M. Juricek, P. H. J. Kouwer, A. E. Rowan, *Chem. Comm.* **2011**, 47, 8740-8749. (b) W. R. Algar, D. E. Prasuhn, M. H. Stewart, T. L. Jennings, J. B. Blanco-Canosa, P. E. Dawson, I. L. Medintz, *Bioconj. Chem.* **2011**, 22, 825-858. (c) A. Bernardin, A. Cazet, L. Guyon, P. Delannoy, F. Vinet, D. Bonnafe, I. Texier, *Bioconj. Chem.* **2010**, 21, 583-588. (d) J. M. Casas-Solvas, E. Ortiz-Salmerón, I. Fernández, L. García-Fuentes, F. Santoyo-González, A. Vargas-Berenguel, *Chem. Eur. J.* **2009**, 15, 8146-8162. (e) J. F. Lutz, *Angew. Chem. Int. Ed.* **2007**, 46, 1018-1025.
- [3]. For selective publications see: (a) Q. Wang, C. Hawker, *Chem. Asian J.* **2011**, 6, 2568-2569 (entire thematic review issue). (b) X. Li *Chem. Asian J.* **2011**, 6, 2606-2616. (c) E. M. Sletten, C. R. Bertozzi, *Acc. Chem. Res.* **2011**, 44, 666-676. (d) M. D. Best, M. M. Rowland, H. E. Bostic, *Acc. Chem. Res.* **2011**, 44, 686-698. (e) K. A. Winans, C. R. Bertozzi, *Chem. Biol.* **1998**, 5, R313-R315. (f) K. J. Yarema, L. K. Mahal, R. E. Bruehl, E. C. Rodriguez, C. R. Bertozzi, *J. Biol. Chem.* **1998**, 276, 31168-31179. (g) E. Saxon, C. R. Bertozzi, *Science*, **2000**, 287, 2007-2010. (h) Q. Wang, T. R. Chan, R. Hilgraf, V.V Fokin, K. B. Sharpless, M. G. Finn, *J. Am. Chem. Soc.* **2003**, 125, 3192-3193. (i) R. Breinbauer, M. Kohn, *ChemBioChem* **2003**, 4, 1147-1149. (j) V. D. Bock, H. Hiemstra, J. H. Van, Maarseveen, *Eur. J. Org. Chem.* **2005**, 51-68. (k) A. Wang, N. W. Nairn, R. S. Johnson, D. A. Tirrell, K. Grabstein, *Chem. Bio. Chem.* **2008**, 9, 324-330. (l) F. Amblard, J. H. Cho, R. F. Schinazi, *Chem. Rev.* **2009**, 109, 4207-4220. (m) T. Fekner, X. Li, M. M. Lee, M. K. Chan, *Angew. Chem. Int. Ed.* **2009**, 48, 1633-1635.
- [4]. For a selection of recent reviews and contributions see: (a) B. Dervaux, F. E. Du Prez, *Chem. Sci.* **2012**, 3, 959-966. (b) L. Ackermann, H. K. Potukuchi, *Org. Biomol. Chem.* **2010**, 8, 4503-4513. (c) J. E. Hein, V. V. Fokin, *Chem. Soc. Rev.* **2010**, 39, 1302-1315. (d) M. Meldal, C. W.

- Tornøe, *Chem. Rev.* **2008**, *108*, 2952-3015. (e) S. Diez-Gonzalez, *Catal. Sci. Technol.* **2011**, *1*, 166-178.
- [5]. For select mechanistic and theoretical investigations see: (a) O. R. Valentin, V. F. Valery, M. G. Finn, *Angew. Chem. Int. Ed.* **2005**, *44*, 2210-2215. (b) B. F. Straub, *Chem. Comm.* **2007**, 3868-3870. (c) B. R. Buckley, S. E. Dann, D. P. Harris, H. Heaney, E. C. Stubbs, *Chem. Comm.* **2010**, 2274-2276. (d) I. P. Silvestri, F. Andemarian, G. N. Khairallah, S. W. Yap, T. Quach, S. Tsegay, C. M. Williams, R. A. R. O'Hair, P. S. Donnelly, S. J. Williams, *Org. Biomol. Chem.* **2011**, *9*, 6082-6088. (e) C. Shao, X. Wang, J. Xu, J. Zhao, Q. Zhang, Y. Hu, *J. Org. Chem.* **2010**, *75*, 7002-7005. (f) M. G. Finn, V. V. Fokin, *Copper Catalyzed Azide-Alkyne Cycloaddition* pp 235-260, in *Catalysis Without Precious Metals*, R. M. Bullock (Ed.), Wiley VCH, Weinheim, 2010. (g) S. I. Presolski, V. Hong, S. H. Cho, M. G. Finn. *J. Am. Chem. Soc.* **2010**, *132*, 14570-14576.
- [6]. (a) Gold acetylide: D. V. Partyka, L. Gao, T. S. Teets, J. B. Updegraff III, N. Deligonul, T. G. Gray, *Organometallics* **2009**, *28*, 6171-6182. (b) V. Aucagne, D. A. Leigh, *Org. Lett.* **2006**, *8*, 4505-4507. (c) F. Himo, T. Lovell, R. Hilgraf, V. V. Rostovtsev, L. Noodleman, K. B. Sharpless, V. V. Fokin, *J. Am. Chem. Soc.* **2005**, *127*, 210-216. (d) V. D. Bock, H. Hiemstra, J. H. van Maarseveen, *Eur. J. Org. Chem.* **2006**, 51-68.
- [7]. (a) F. Dumoulin, V. Ahsen, *J. Porphyrins Phthalocyanines* **2011**, *15*, 481-504. (b) M. Wenska, M. Alvira, P. Steunenbergh, Å. Stenberg, M. Murtola, R. Strömberg, *Nucleic Acids Research*, **2011**, *39*, 9047-9059. (c) W. H. Binder, R. Sachsenhofer, *Macro. Rapid Commun.* **2007**, *28*, 15-54. (d) S. Cantel, J. A. Halperin, M. Chorev, M. Scrima, A. M. D'Ursi, J. J. Levy, R. D. DiMarchi, A. LeChevalier, P. Rovero, A. M. Papini, *Advances in Experimental Medicine and Biology*, **2009**, *611*, 175-176. (e) M. A. Kamaruddin, P. Ung, M. I. Hossain, B. Jarasrassamee, W. O'Malley, P. Thompson, D. Scanlon, H-C.

- Cheng, B. Graham, *Bioorg. Med. Chem. Lett.* **2011**, 21, 329-331. (f) E. Boiddelier, L. Salmon, J. Ruiz, D. Astruc, *Chem. Comm.* **2008**, 5788-5790. (g) P. Zhao, M. Grillaud, L. Salmon, J. Ruiz, D. Astruc, *Adv. Synth. Catal.* **2012**, 354, 1001-1011. (h) Z. Gonda, Z. Novak, *Dalton Trans.* **2010**, 39, 726-729. (i) T. R. Chan, R. Hilgraf, K. B. Sharpless, V. V. Fokin, *Org. Lett.* **2004**, 6, 2853-2855. (j) V. O. Rodionov, S. I. Presolski, D. D. Diaz, V. V. Fokin, M. G. Finn, *J. Am. Chem. Soc.* **2007**, 129, 12705-12712.
- [8]. J. McNulty, K. Keskar, R. Vemula, *Chem. Eur. J.* **2011**, 17, 14727-14730.
- [9]. C. J. Burrows, J. G. Muller, *Chem. Rev.* **1998**, 98, 1109-1052.
- [10]. (a) H. J. Johnston, G. Hutchison, F. M. Christensen, S. Peters, S. Hankin, V. Stone, *Critical Rev. in Toxicol.* **2010**, 40, 328-346. (b) J. J. Liu, P. Galettis, A. Farr, L. Maharaj, H. Samarasinha, A. C. McGechan, B. C. Baguley, R. J. Bowen, S. J. Berners-Price, M. J. McKeage, *J. Inorg. Biochem.* **2008**, 102, 303-310.
- [11]. (a) G. Adjabeng, T. Brenstrum, C. S. Frampton, A. J. Robertson, J. Hillhouse, J. McNulty, A. Capretta, *J. Org. Chem.* **2004**, 69, 5082-5086. (b) T. Brenstrum, D. A. Gerritsma, G. M. Adjabeng, C. S. Frampton, J. Britten, A. J. Robertson, J. McNulty, A. Capretta, *J. Org. Chem.* **2004**, 69, 7635-7639. (c) G. Adjabeng, T. Brenstrum, J. Wilson, C. S. Frampton, A. Robertson, J. Hillhouse, J. McNulty, A. Capretta, *Org. Lett.* **2003**, 5, 953-955.
- [12]. F. Alonso, Y. Moglie, G. Radivoy, M. Yus, *Eur. J. Org. Chem.* **2010**, 1875-1884.
- [13]. M. Maddani, K. R. Prabhu, *Tetrahedron Lett.* **2008**, 49, 4526-4530.
- [14]. B. Pal, P. Jaisankar, V. S. Giri, *Syn Commun.* **2004**, 34, 1317-1323.
- [15]. J. Ritschel, F. Sasse, M. E. Maier, *Eur. J. Org. Chem.* **2007**, 78-87.

- [16]. A. Lüth, W. Löwe, *Eur. J. Med. Chem.* **2008**, *43*, 1478-1488.
- [17]. J. McNulty, J. J. Nair, S. Cheekoori, V. Larichev, A. Capretta, A. J. Robertson, *Chem. Eur. J.* **2006**, *12*, 9314-9322.
- [18]. L. Benati, G. Bencivenni, R. Leardini, M. Minozzi, D. Nanni, R. Scialpi, P. Spagnolo, G. Zanardi, *J. Org. Chem.* **2006**, *71*, 5822-5825.
- [19]. D. V. Allen, D. Venkataraman, *J. Org. Chem.* **2003**, *68*, 4590-4593.
- [20]. K. Keskar (M.S. Thesis **2008**-McMaster University, Unpublished results).
- [21]. J. McNulty, K. Keskar, *Tetrahedron Lett.* **2008**, *49*, 49, 7054-7057
- [22]. D. J. Ager, M. B. East, A. Eisenstadt, S. A. Laneman, *Chem. Commun.* **1997**, 2359-2360.
- [23]. W. Dai, Y. Zhang, *Tetrahedron Lett.* **2005**, *46*, 1377-1381.
- [24]. L. Brammer, J. C. Mareque Rivas, C. D. Spilling, *J. Organometallic Chem.* **2000**, *609*, 36-43.
- [25]. S. Chassaing, A. Sido, A. Alix, M. Kumarraja, P. Pale, J. Sommer, *Chem. Eur. J.* **2008**, *14*, 6713-6721.
- [26]. K. Kamata, Y. Nakagawa, K. Yamaguchi, N. Mizuno, *J. Am. Chem. Soc.* **2008**, *130*, 15304-15310.
- [27]. F. Friscourt, G-J. Boons, *Org. Lett.* **2010**, *12*, 21, 4936-4939.
- [28]. X. Meng, X. Xu, T. Gao, B. Chen, *Eur. J. Org. Chem.* **2010**, 5409-5414.
- [29]. P. Appukkuttan, W. Dehaen, V. V. Fokin, E. Van der Eycken, *Org. Lett.* **2004**, *6*, 4223-4225.
- [30]. M. Liu, O. Reiser, *Org. Lett.* **2011**, *13*, 5, 1102-1105.

- [31]. D. Wang, N. Li, M. Zhao, W. Shi, C. Ma, B. Chen, *Green Chem.* **2010**, 12, 2120-2123.

3.5 Experimental Section

All reactions were carried out under nitrogen atmosphere in oven dried glassware. Toluene (dry) was distilled over sodium/benzophenone. AgOAc (purity \geq 99.0%) and AgOTf (purity = 99.95%) were purchased from Fluka Chemicals, Switzerland and Sigma-Aldrich, Canada respectively. DMSO (dry) was obtained from Sigma-Aldrich (Sure-seal) and dichloromethane was distilled over calcium hydride. Phenyl acetylenes were obtained commercially from Sigma-Aldrich or AlfaAesar. Melting points were recorded in open capillary using a calibrated Büchi melting point B540 apparatus. Thin layer chromatography (TLC) was carried out using aluminium sheets pre-coated with silica gel 60F₂₅₄ (Merck) and was visualized under 254 nm UV light. ¹H and ¹³C spectra were recorded on a AV 600 spectrometer in CDCl₃ with TMS as internal standard. Chemical shifts (δ) are reported in ppm downfield of TMS and coupling constants (*J*) are expressed in hertz (Hz).

General procedure for the preparation of starting azides (2a-2f):^[12]

Sodium azide (1.0 g, 15.3 mmol, 1 equiv.) was dissolved in DMSO (25 mL) by stirring in a flame-dried 100-mL round-bottom flask under nitrogen for 12 h. A solution of corresponding benzyl bromide/chloride (13.8 mmol, 0.9 equiv.) was added, and the reaction was stirred for 10 h. Water (20 mL) was added slowly to quench the reaction (exothermic process) and, the mixture was stirred until it cooled to room temperature. The mixture was poured into water (50 mL) and extracted with diethyl ether (3 x 30 mL). The organic layer was separated, washed with brine, dried with sodium sulphate, filtered, and concentrated in vacuo to afford azide **2a-2h** as oils.

1-(Azidomethyl)benzene (2a):^[12] ¹H NMR (200 MHz, CDCl₃) δ 7.43-7.25 (m, 5H), 4.35 (s, 2H) ppm.

1-(Azidomethyl)-4-methoxybenzene (2b):^[13] ¹H NMR (600 MHz, CDCl₃) δ 7.28 (d, *J* = 8.6 Hz, 2H), 6.94 (d, *J* = 8.6 Hz, 2H), 4.30 (s, 2H), 3.85 (s, 3H) ppm.

1-(Azidomethyl)-4-chlorobenzene (2c):^[14] ¹H NMR (600 MHz, CDCl₃) δ 7.39 (d, *J* = 8.3 Hz, 2H), 7.28 (d, *J* = 8.3 Hz, 2H), 4.35 (s, 2H) ppm.

1-(azidomethyl)-3-bromobenzene (2d):^[15] ¹H NMR (600 MHz, CDCl₃) δ 7.51 (d, *J* = 1.9 Hz, 2H), 7.28 (d, *J* = 1.4 Hz, 2H), 4.35 (s, 2H) ppm.

Methyl 2-azidoacetate (2e):^[16] ¹H NMR (600 MHz, CDCl₃) δ 3.91 (s, 2H), 3.83 (s, 3H) ppm.

1-(2-azidoethyl)benzene (2f):^[17] ¹H NMR (600 MHz, CDCl₃) δ 7.37 (t, *J* = 7.4 Hz, 2H), 7.33 – 7.28 (m, 1H), 7.28 – 7.24 (m, 2H), 3.55 (t, *J* = 7.3 Hz, 2H), 2.94 (t, *J* = 7.3 Hz, 2H) ppm.

General procedure for the preparation of starting azides (Figure 3-2, 2g-2i):^[18]

In a 100-mL round-bottom flask, 4-methoxyaniline (1.0 g, 8.1 mmol, 1 eq.) was dissolved in water (2.5 mL) that contained concentrated HCl (4.1 mL). This solution was cooled to below 5 °C in an ice bath and diazotized with a solution of NaNO₂ (0.850 g, 12.1 mmol, 1.5 equiv.) with distilled water (2.5 mL). The mixture was stirred in an ice bath for 1 h. A solution of NaN₃ (1.05 g, 16.2 mmol, 2 equiv.) in water (6 mL) was added at 0 °C, and stirred for 30 min. The mixture was allowed to warm up to room temperature and stirred for an additional 3 h. The reaction mixture was extracted with ethyl acetate EtOAc (2 X 50 mL). The combined organic layers was dried over anhydrous Na₂SO₄, filtered and concentrated under reduced pressure. The crude 4-

methoxyazidobenzene was further purified by flash column chromatography over a short plug of silica gel (5% EtOAc:hexanes) to afford a yellow liquid in 80% yield. An identical procedure was followed for the synthesis of **2g** and **2i**.

4-Chlorophenyl Azide (Figure 3-2, 2g):^[18] ¹H-NMR (600 MHz, CDCl₃) δ 7.32 (d, J = 8.2 Hz, 2H), 6.96 (d, J = 8.2 Hz, 2H) ppm.

4-Methoxyphenyl Azide (Figure 3-2, 2h):^[18] ¹H-NMR (600 MHz, CDCl₃) δ 6.96 (d, J = 8.8 Hz, 2H), 6.89 (d, J = 8.8 Hz, 2H), 3.80 (s, 3H) ppm.

Azidobenzene (Figure 3-2, 2i):^[18] ¹H NMR (400 MHz, CDCl₃) δ 7.34 (t, J= 8.0 Hz, 2H), 7.12 (t, J= 7.2 Hz, 1H), 7.02 (d, J= 7.6 Hz, 2H) ppm.

Synthesis of (2-methoxyphenyl)diphenylphosphine (Table 3-1, 5b):^[19]

To a clear solution of 1-iodo-2-methoxybenzene (0.100 g, 0.42 mmol) in THF (2.0 mL) was added *n*-BuLi (1.6 M in hexanes, 0.530 mL, 0.854 mmol,) at -78 °C under a nitrogen atmosphere. The resulting solution was stirred at -78 °C for 1 h. A solution of chlorodiphenylphosphine (76.0 µL, 0.427 mmol) in THF (2.0 mL) was added at -78 °C. Then the mixture was warmed to room temperature and stirred for an additional 3 h. Water was added to quench the reaction, and the mixture was extracted with diethyl ether (3 X 15 mL). The organic layers were combined, washed with brine, dried over Na₂SO₄, and concentrated. The resulting residue was purified by column chromatography on silica gel to obtain (0.075 g, 60%) as crystalline white solid. M.p. 120-122 °C (ref.^[19] m.p. 124-126 °C). ¹H NMR (200 MHz, CDCl₃); δ = 6.40-7.40 (m, 14H, ArH), 3.65 (s, 3H, OMe) ppm. ³¹P NMR (80 MHz, CDCl₃); δ = -16.74 ppm.

Synthesis of [2-(Diphenylphosphino)phenyl]methanol (Table 3-1, 5c):^[20]

To a suspension of 2-(diphenylphosphino) benzoic acid (0.100 g, 0.32 mmol) in THF (2.0 mL) was added lithium aluminum hydride (0.027 g, 0.71 mmol). The resulting reaction mixture was stirred at room temperature for 2 h. The reaction

mixture was then quenched by adding saturated solution of sodium potassium tartrate. The mixture was extracted with ethyl acetate (3 X 15 mL). The organic layers were combined, washed with brine, dried over Na₂SO₄ and concentrated. The resulting residue was purified by column chromatography on silica gel to give **5c**^[21] (0.076 g) as a colourless oil in 80% yield. ¹H NMR (200 MHz, CDCl₃); δ = 7.46-7.57 (m, 1H, ArH), 7.14-7.39 (m, 12H, ArH), 6.83-6.95 (m, 1H, ArH), 4.82 (s, 1H), 2.04 (bs. S, 1H, -OH) ppm. ³¹P NMR (80 MHz, CDCl₃); δ = -16.29 ppm.

Synthesis of Methyl 2-(Diphenylphosphino)benzoate (Table 3-1, **5d):**^[20]

In an 50-mL flame-dried pear shaped Schlenk flask equipped with a magnetic stirbar, rubber septum and an argon inlet, cesium carbonate (0.190 g, 0.58 mmol, 1.25 equiv.) and CuI (10 mol-% with respect to diphenylphosphine) were charged and the vessel was sealed with a rubber septum. Toluene (5.0 mL), the methyl-2-bromobenzoate (0.1 g, 0.46 mmol, 1.0 equiv.), and diphenylphosphine (0.72 g, 0.38 mmol, 0.8 equiv.) were injected into the tube through the septum. The rubber septum was replaced with the dry argon flushed reflux condenser. The reaction mixture was then heated at 110 °C for 24 h. The reaction mixture was then cooled to room temperature and filtered with dichloromethane to remove any insoluble residues. The filtrate was concentrated *in vacuo*; the residue was purified by flash chromatography on silica gel to obtain **5d**^[22] as a colourless solid in 60% yield. M.p. 97.5-99 °C (ref.^[22] m.p. 96 °C). ¹H NMR (200 MHz, CDCl₃); δ = 8.10-8.12 (m, 1H), 7.32-7.37 (m, 12H), 6.96-6.99 (m, 1H), 3.78 (s, 3H) ppm. ³¹P NMR (80 MHz, CDCl₃); δ = -4.41 ppm.

Synthesis of *N,N*-Diisopropyl-2-diphenylphosphino)benzamide (Table 3-1, **5e):**^[20]

Into a flame-dried flask, containing a magnetic stirring bar, was weighed *N, N*-diisopropylbenzamide (0.100 g, 0.48 mmol, 1.0 equiv.) under an argon

atmosphere and anhydrous THF (2 mL) was added. The flask was stirred for 15 min at -78 °C whereupon *sec*-BuLi (1.4 M solution in cyclohexane, 0.417 mL, 0.58 mmol, 1.2 equiv.) was added drop wise followed by TMEDA (0.088 mL, 0.58 mmol, 1.2 equiv.). Resultant solution stirred at -78 °C for 30 min. Chlorodiphenylphosphine (0.090 mL, 0.48 mmol, 1 equiv.) was added dropwise at -78 °C. The reaction mixture stirred for an additional 1 h at -78 °C then allowed to reach room temperature with continuous stirring. The reaction mixture was quenched with saturated solution of NH₄Cl and extracted with ethyl acetate. The organic phase was washed with water followed by brine, dried over sodium sulphate and concentrated in vacuo. Purification through column chromatography (hexane/ethyl acetate) gave **5e**^[23] as a colourless solid in 91% yield. M.p. 95-97 °C; ¹H NMR (200 MHz, CDCl₃): δ = 1.07 (m, 6H), 1.59 (d, 6H), 3.51 (m, 1H), 3.71 (d, 1H), 7.13-7.43 (m, 14H) ppm. ¹³C NMR (51 MHz, CDCl₃): δ 20.4, 20.7, 20.8, 45.9, 51.1, 125.1, 125.2, 125.7, 128.2, 128.4, 128.5, 129.2, 133.4, 133.5, 133.7, 134.1, 134.2, 134.9, 137.1, 137.6, 145.6, 145.8, 169.9 ppm. ³¹P (80 MHz, CDCl₃): δ -14.13 ppm. HRMS (M⁺) calcd. For C₂₅H₂₈NOP: 389.1894, found 389.1909.

Synthesis of [(2-*N,N*-Dimethylaminomethyl)phenyl]diphenylphosphine (Table 3-1, **5f):^[24]**

The ligand was synthesized according to the published procedure with slight modification. To a solution of *n*BuLi in hexane (1.6 M solution in hexanes, 10.2 mL, 16.3 mmol, 1.2 equiv.) at room temperature was added dimethylbenzylamine (1.84 g, 13.6 mmol, 1.0 equiv.). The reaction mixture was diluted with freshly distilled diethyl ether (15 mL) and allowed to stand for 24 h. The lithiated benzylamine deposited on the flask as a mass of yellow crystals leaving orange solution. The crystalline mass was resuspended in solution with vigorous stirring. The solution was cooled in ice water bath and diphenylchlorophosphine (3.0 mL, 16.3 mmol, 1.2 equiv.) was added slowly. The reaction mixture was stirred for 1h in an ice bath and then warmed to room

temperature over 20 min. The mixture was recooled in ice, and the reaction was cautiously quenched by the slow addition of water. The reaction mixture was partitioned between 2M HCl and diethyl ether. The HCl extracts were adjusted to pH 12 with NaOH. The resultant aqueous solution was extracted with CH₂Cl₂. The CH₂Cl₂ extracts were dried, filtered and concentrated in vacuo to give orange oil. The crude product was crystalized by adding ethanol (8.0-10.0 mL) and cooling at -20 °C to give **5f** in 90% yield. ¹H NMR (200 MHz, CDCl₃): δ = 2.08 (s, 6H), 3.64 (s, 2H), 6.90 (m, 1H), 7.13-7.31 (m, 12H), 7.48 (m, 1H) ppm. ³¹P (80 MHz, CDCl₃): δ = -15.43 ppm.

Synthesis of *N,N*-Diisopropyl-2-(di-*tert*-butylphosphino) benzamide (Table 3-1, **5g):^[23]**

To a flame-dried flask with a stirring bar was added the *N,N*-diisopropylbenzamide (0.454 mg, 2.2 mmol) and THF (4 mL) under argon atmosphere. The resultant solution was cooled to -78 °C and *n*BuLi (1.6 M in hexanes, 1.66 mL, 2.65 mmol) was added dropwise. The reaction mixture was stirred for 30 min at -78 °C. Chloro-di-*tert*-butylphosphine (0.585 mL, 2.65 mmol) was added to the reaction mixture followed by stirring at -78 °C for 2h. The reaction mixture was further stirred at 1h at room temperature. The reaction mixture was filtered through a pad of Celite, and the filtrate was concentrated under reduced pressure to give crude product, which was purified by flash chromatography to afford **5g** as white solid in 78% yield. ¹H NMR (600 MHz, CDCl₃): δ = 7.66 (d, *J* = 7.4 Hz, 1H), 7.24 (t, *J* = 7.4 Hz, 1H), 7.18 (t, *J* = 7.3 Hz, 1H), 7.05 (d, *J* = 5.9 Hz, 1H), 3.57 (hept, *J* = 6.6 Hz, 1H), 3.38 (hept, *J* = 6.8 Hz, 1H), 1.47 (dd, *J* = 9.6, 6.8 Hz, 6H), 1.17 – 1.04 (m, 21H), 0.95 (d, *J* = 6.6 Hz, 3H) ppm. ³¹P NMR (243 MHz, CDCl₃) δ = 23.09 ppm.

Synthesis of *N,N*-Diisopropyl-2-(di-cyclohexylphosphino)benzamide (Table 3-1, 5h):^[23]

To a flame dried flask with a stirring bar was added the *N,N*-diisopropylbenzamide (0.454 mg, 2.2 mmol) and THF (4 mL) under argon atmosphere. The resultant solution was cooled to -78 °C and *n*BuLi (1.6 M in hexanes, 1.66 mL, 2.65 mmol,) was added dropwise. The reaction mixture was stirred for 30 min at -78 °C. Chlorodicyclohexylphosphine (0.585 mL, 2.65 mmol) was added to the reaction mixture followed by stirring at -78 °C for 2h. The reaction mixture was further stirred at 1h at room temperature. The reaction mixture was filtered through a pad of Celite, and the filtrate was concentrated under reduced pressure to give crude product, which was purified by flash chromatography to afford **5h** as white solid in 75% yield. ¹H NMR (600 MHz, CDCl₃): δ = 7.62 – 7.41 (m, 1H), 7.32 (s, 2H), 7.15 (s, 1H), 3.56 (d, *J* = 20.2 Hz, 1H), 3.52 – 3.35 (m, 1H), 2.11-1.03 (m, 34H) ppm. ³¹P NMR (243 MHz, CDCl₃): δ = -9.22 ppm.

Synthesis of 1, 3, 5, 7-Tetramethyl-2, 4, 8-Trioxa-6-(2'- *N, N*-diisopropylbenzamide)-6-Phospha-adamantane (Table 3-1, 5i):

A mixture containing 1,3,5,7-tetramethyl-2,4,8-trioxa-6-phospha-adamantane (0.152 g, 0.70 mol, 2 equiv.), 2-bromo-*N, N*-diisopropylbenzamide (0.100 g, 0.35 mol, 1 equiv.), triethylamine (0.106 g, 0.70 mol, 2 equiv.) and nickel acetate tetrahydrate (0.272 g, 1.09 mmol, 3.1 equiv.) and toluene (2.0 mL) was heated to reflux under nitrogen atmosphere with magnetic stirring. During this time the nickel acetate dissolved, generating a reddish brown solution. After 60h at reflux, the mixture was filtered through pad of Celite. The organic solvent was evaporated to yield crude mass, which was purified by flash chromatography (10-15% EtOAc: hexanes) to yield a colourless, crystalline solid in 60% yield. M.p. 180-183 °C. ¹H NMR (600 MHz, CDCl₃): δ = 8.26 (d, *J* = 7.8 Hz, 1H), 7.38 (t, *J* = 7.4 Hz, 1H), 7.33 (td, *J* = 7.6, 1.5 Hz, 1H), 7.16 (ddd,

$J = 7.4, 3.0, 1.3$ Hz, 1H), 3.55 – 3.43 (m, 2H), 2.06 – 1.97 (m, 2H), 1.92 (dd, $J = 25.1, 13.1$ Hz, 1H), 1.60 (d, $J = 6.8$ Hz, 3H), 1.57 – 1.52 (m, 4H), 1.45 (s, 3H), 1.41 (s, 3H), 1.36 (d, $J = 12.7$ Hz, 3H), 1.34 (d, $J = 12.7$ Hz, 3H), 1.19 (d, $J = 6.7$ Hz, 3H), 1.03 (d, $J = 6.6$ Hz, 3H) ppm. ^{31}P NMR (243 MHz, CDCl_3): $\delta = -35.84$ ppm. ^{13}C NMR (151 MHz, CDCl_3): $\delta = 169.9$ (d, $J = 4.7$ Hz), 148.6 (d, $J = 37.75$ Hz), 133.9 (d, $J = 2.8$ Hz), 130.3 (d, $J = 33.22$ Hz), 129.9, 127.8, 125.6 (d, $J = 8.7$ Hz), 96.8, 96.1, 73.9 (d, $J = 4.5$ Hz), 73.7 (d, $J = 16.61$ Hz), 51.0, 45.9, 45.8, 36.4, 28.6 (d, $J = 21.3$ Hz), 28.1, 27.8, 26.6 (d, $J = 10.9$ Hz), 20.7, 20.7, 20.5, 20.2. HRMS (M^+) calcd. For $\text{C}_{23}\text{H}_{34}\text{NO}_4\text{P}$: 419.2223, found 419.2225.

General Procedure for the Preparation of Ligand/AgOAc Complex (1:1):^[8]

To an oven dried-flask was added the corresponding ligand (0.100 g, 1.00 equiv.), silver acetate (1.0 equiv.) and freshly distilled dichloromethane (5.0 mL), and the solution stirred at room temperature for 10-12 h in the dark. The resultant homogenous reaction mixture was filtered through a pad of Celite to remove any insoluble impurities. The organic layer was evaporated, further treated with dry pentane (2.0 mL), and concentrated. The complex obtained was dried under high vacuum to yield the silver acetate complex.

Table 3-1, 6a: Yield: 99%. ^1H NMR (600 MHz, CDCl_3): $\delta = 7.49 - 7.38$ (m, 15H), 2.09 (s, 3H) ppm. ^{31}P NMR (243 MHz, CDCl_3): $\delta = 16.28$ (brs) ppm.

Table 3-1, 6b: Yield: 99%. ^1H NMR (600 MHz, CDCl_3): $\delta = 7.57 - 7.34$ (m, 11H), 7.00 – 6.86 (m, 2H), 6.79 – 6.65 (m, 1H), 3.78 (s, 3H), 2.09 (s, 3H) ppm. ^{31}P NMR (243 MHz, CDCl_3): $\delta = 2.12$ (d, $J = 670.6$ Hz) ppm.

Table 3-1, 6c: Yield: 82%. ^1H NMR (600 MHz, CDCl_3): $\delta = 7.56$ (d, $J = 6.8$ Hz, 1H), 7.45 (t, $J = 7.3$ Hz, 3H), 7.42 – 7.29 (m, 8H), 7.22 (t, $J = 7.5$ Hz, 1H), 6.84 (t, $J = 8.5$ Hz, 1H), 4.75 (s, 2H), 1.93 (s, 3H) ppm. ^{31}P NMR (243 MHz, CDCl_3): $\delta = 4.21$ (s) ppm.

Table 3-1, 6d: Yield: 99%. ^1H NMR (600 MHz, CDCl_3) δ 8.17 (ddd, $J = 7.7, 4.2, 1.1$ Hz, 1H), 7.56 (t, $J = 7.6$ Hz, 1H), 7.50 – 7.36 (m, 11H), 6.99 – 6.87 (m, 1H), 3.73 (s, 3H), 2.08 (s, 3H) ppm. ^{31}P NMR (243 MHz, CDCl_3): $\delta = 17.77$ (d, $J = 833.49$ Hz) ppm.

Table 3-1, 6e: Data previously reported.^[8]

Table 3-1, 6f: Yield: 99%. ^1H NMR (600 MHz, CDCl_3): $\delta = 7.49 - 7.38$ (m, 6H), 7.36 (dd, $J = 10.5, 4.0$ Hz, 4H), 7.31 (t, $J = 7.5$ Hz, 1H), 7.24 – 7.11 (m, 2H), 6.84 – 6.73 (m, 1H), 3.26 (s, 2H), 2.09 (s, 6H), 2.04 (s, 3H) ppm. ^{31}P NMR (243 MHz, CDCl_3): $\delta = 5.29$ (d, $J = 690.12$ Hz) ppm.

Table 3-1, 6g: Yield: 99%. ^1H NMR (600 MHz, CDCl_3): $\delta = 7.81$ (d, $J = 5.8$ Hz, 1H), 7.44 (d, $J = 6.3$ Hz, 1H), 7.37 (t, $J = 6.5$ Hz, 1H), 7.20 (d, $J = 1.0$ Hz, 1H), 3.60 – 3.35 (m, 2H), 1.98 (s, 3H), 1.76 (d, $J = 6.1$ Hz, 3H), 1.44 (d, $J = 6.3$ Hz, 3H), 1.39 – 1.24 (m, 21H), 1.06 (d, $J = 6.0$ Hz, 3H) ppm. ^{31}P NMR (243 MHz, CDCl_3): $\delta = 46.63$ (d, $J = 692.55$ Hz) ppm. M.p. >170 °C (Complex decomposes slightly at this temperature), melts at 190-200 °C.

Development of X-ray crystals of 6g (Table 3-1): Compound **6g** was dissolved in dichloromethane followed by slow addition of pentane (10X) over it. Crystals were developed after slow evaporation of solvents.

Table 3-1, 6h: Yield: 99%. ^1H NMR (600 MHz, CDCl_3): $\delta = 7.59$ (t, $J = 7.1$ Hz, 1H), 7.51 – 7.41 (m, 2H), 7.25 (dd, $J = 3.5, 1.4$ Hz, 1H), 3.67 – 3.40 (m, 2H), 2.39 – 2.24 (m, 1H), 2.14 – 1.96 (m, 6H), 1.87 (t, $J = 13.8$ Hz, 1H), 1.82 (d, $J = 6.7$ Hz, 3H), 1.71 (m, 4H), 1.62 (d, $J = 11.8$ Hz, 1H), 1.51 (d, $J = 6.7$ Hz, 5H), 1.42 – 1.17 (m, 12H), 1.13 (d, $J = 6.4$ Hz, 4H) ppm. ^{31}P NMR (243 MHz, CDCl_3): $\delta = 23.84$ (d, $J = 711.99$ Hz) ppm.

Table 3-1, 6i: Yield: 85%. ^1H NMR (600 MHz, CDCl_3): $\delta = 8.44$ (t, $J = 6.6$ Hz, 1H), 7.57 – 7.51 (m, 1H), 7.47 (t, $J = 7.6$ Hz, 1H), 7.31 – 7.27 (m, 1H), 3.64 – 3.48 (m, 2H), 2.70 (dd, $J = 14.0, 6.4$ Hz, 1H), 2.12 – 1.97 (m, 5H), 1.89 – 1.72

(m, 4H), 1.57 – 1.43 (m, 17H), 1.34 (m, 3H), 1.15 (m, 3H) ppm. ^{31}P NMR (243 MHz, CDCl_3): δ = -9.29 (d, J = 721.71 Hz) ppm.

General Procedure for the Ag(I) Complex Catalyzed Synthesis of 1,2,3-Triazoles:

To a mixture of phenyl acetylene (0.010 g, 0.09 mmol, 1 equiv.) and benzyl/aryl azide (0.14 mmol, 1.5 equiv.) in toluene (1 mL) was added sequentially catalyst (**6g**) (2-2.5 mol-%) and caprylic acid (20 mol-%). The mixture was then stirred with heating at 90 °C for 24h. The reaction mixture was diluted and extracted with ethyl acetate (2 X 20 mL), washed with sodium hydrogen carbonate (5 mL) and brine, dried over anhydrous sodium sulphate, and concentrated under reduced pressure. The resulting residue was purified through silica gel column chromatography (10-20% ethyl acetate/hexanes) to afford the desired product.

1-Benzyl-4-phenyl-1H-1,2,3-triazole (Figure 3-2, 3a):^[5e] ^1H NMR (600 MHz, CDCl_3): δ = 7.79 (dd, J = 8.2, 1.1 Hz, 2H), 7.65 (s, 1H), 7.43 – 7.34 (m, 5H), 7.34 – 7.27 (m, 3H), 5.57 (s, 2H) ppm. ^{13}C NMR (151 MHz, CDCl_3): δ = 148.2, 134.6, 130.5, 129.1, 128.8, 128.2, 128.0, 125.7, 119.4, 54.2 ppm.

1-(4-Methoxybenzyl)-4-phenyl-1H-1,2,3-triazole (Figure 3-2, 3b):^[25] ^1H NMR (600 MHz, CDCl_3): δ = 7.79 – 7.71 (m, 2H), 7.58 (s, 1H), 7.35 (t, J = 7.6 Hz, 2H), 7.27 (d, J = 7.4 Hz, 1H), 7.23 (d, J = 8.7 Hz, 2H), 6.87 (d, J = 8.7 Hz, 2H), 5.47 (s, 2H), 3.77 (s, 3H) ppm. ^{13}C NMR (151 MHz, CDCl_3): δ = 159.9, 148.0, 130.5, 129.6, 128.7, 128.1, 126.5, 125.6, 119.2, 114.5, 55.3, 53.8 ppm.

1-(4-Chlorobenzyl)-4-phenyl-1H-1,2,3-triazole (Figure 3-2, 3c):^[25] ^1H NMR (600 MHz, CDCl_3): δ = 7.84 – 7.76 (m, 2H), 7.66 (s, 1H), 7.43 – 7.38 (m, 2H), 7.38 – 7.34 (m, 2H), 7.32 (dt, J = 9.1, 4.3 Hz, 1H), 7.25 (s, 2H), 5.55 (s, 2H) ppm. ^{13}C NMR (151 MHz, CDCl_3): δ = 149.0, 135.5, 133.8, 131.0, 130.0, 130.0, 129.5, 128.9, 126.3, 120.0, 54.1 ppm.

1-(3-Bromobenzyl)-4-phenyl-1*H*-1,2,3-triazole (Figure 3-2, 3d):^[5e] ¹H NMR (600 MHz, CDCl₃): δ = 7.87 – 7.80 (m, 2H), 7.72 (s, 1H), 7.53 (d, *J* = 7.7 Hz, 1H), 7.50 (s, 1H), 7.44 (t, *J* = 7.6 Hz, 2H), 7.39 – 7.33 (m, 1H), 7.32 – 7.23 (m, 2H), 5.58 (s, 2H) ppm. ¹³C NMR (151 MHz, CDCl₃): δ = 148.4, 136.8, 131.9, 131.0, 130.7, 130.3, 128.8, 128.3, 126.5, 125.7, 123.1, 119.4, 53.4 ppm.

1-Benzyl-4-(4-fluorophenyl)-1*H*-1,2,3-triazole (Figure 3-2, 3e):^[26] ¹H NMR (600 MHz, CDCl₃): δ = 7.77 (dd, *J* = 8.9, 5.3 Hz, 2H), 7.61 (s, 1H), 7.42 – 7.35 (m, 3H), 7.33 – 7.30 (m, 2H), 7.09 (t, *J* = 8.7 Hz, 2H), 5.57 (s, 2H) ppm. ¹³C NMR (151 MHz, CDCl₃): δ = 162.8 (d, *J* = 247.3 Hz), 147.5, 134.7, 129.3, 129.0, 128.2, 127.5 (d, *J* = 8.1 Hz), 126.9 (d, *J* = 2.7 Hz), 119.3, 115.93 (d, *J* = 21.7 Hz), 54.4.

1-Benzyl-4-(4-bromophenyl)-1*H*-1,2,3-triazole (Figure 3-2, 3f):^[27] ¹H NMR (600 MHz, CDCl₃): δ = 7.70 (m, 3H), 7.58 – 7.53 (m, 2H), 7.45 – 7.38 (m, 3H), 7.34 (d, *J* = 6.3 Hz, 2H), 5.60 (s, 2H) ppm. ¹³C NMR (151 MHz, CDCl₃): δ = 147.3, 134.6, 132.1, 129.6, 129.3, 129.0, 128.2, 127.3, 122.2, 119.6, 54.4.

1-Benzyl-4-*m*-tolyl-1*H*-1,2,3-triazole (Figure 3-2, 3g):^[25] ¹H NMR (600 MHz, CDCl₃): δ = 7.66 (s, 1H), 7.64 (s, 1H), 7.57 (d, *J* = 7.7 Hz, 1H), 7.42 – 7.34 (m, 3H), 7.33 – 7.30 (m, 2H), 7.28 (t, *J* = 7.7 Hz, 1H), 7.13 (d, *J* = 7.6 Hz, 1H), 5.58 (s, 2H), 2.38 (s, 3H) ppm. ¹³C NMR (151 MHz, CDCl₃): δ = 148.4, 138.6, 134.8, 130.4, 129.3, 129.1, 128.9 (d, *J* = 13.9 Hz), 128.2, 126.5, 122.9, 119.6, 54.4, 21.5.

1-Benzyl-4-(2-chlorophenyl)-1*H*-1,2,3-triazole (Figure 3-2, 3h):^[28] ¹H NMR (600 MHz, CDCl₃): δ = 8.18 (dd, *J* = 7.9, 1.6 Hz, 1H), 8.04 (s, 1H), 7.37 – 7.27 (m, 5H), 7.26 – 7.22 (m, 2H), 7.19 (m, 1H), 5.54 (s, 2H) ppm. ¹³C NMR (151 MHz, CDCl₃): δ = 144.4, 134.6, 131.1, 130.1, 129.8, 129.2, 129.1, 129.0, 128.7, 127.9, 127.1, 123.1, 54.2 ppm.

Ethyl 2-(4-Phenyl-1*H*-1,2,3-triazol-1-yl)acetate (Figure 3-2, 3i):^[5c] ¹H NMR (600 MHz, CDCl₃): δ = 7.94 (s, 1H), 7.90 – 7.85 (m, 2H), 7.46 (t, *J* = 7.7 Hz, 2H), 7.38 (t, *J* = 7.4 Hz, 1H), 5.26 (s, 2H), 3.86 (s, 3H) ppm. ¹³C NMR (151 MHz, CDCl₃): δ = 166.7, 148.3, 130.3, 128.8, 128.3, 125.8, 120.9, 53.1, 50.8 ppm.

1-(2-Phenylethyl)-4-phenyl-1*H*-1,2,3-triazole (Figure 3-2, 3j):^[29] ¹H NMR (600 MHz, CDCl₃): δ = 7.79 (dd, *J* = 8.3, 1.1 Hz, 2H), 7.49 (s, 1H), 7.43 (t, *J* = 7.7 Hz, 2H), 7.38 – 7.31 (m, 3H), 7.31 – 7.26 (m, 1H), 7.17 (d, *J* = 7.4 Hz, 2H), 4.67 (t, *J* = 7.3 Hz, 2H), 3.29 (t, *J* = 7.2 Hz, 2H) ppm. ¹³C NMR (151 MHz, CDCl₃): δ = 147.4, 137.0, 130.6, 128.8, 128.8, 128.7, 128.1, 127.1, 125.7, 119.9, 51.7, 36.8 ppm.

1-Benzyl-4-butyl-1*H*-1,2,3-triazole (Figure 3-2, 3k):^[30] ¹H NMR (600 MHz, CDCl₃): δ = 7.32 – 7.25 (m, 3H), 7.19 (m, 2H), 7.11 (s, 1H), 5.42 (s, 2H), 2.65 – 2.57 (m, 2H), 1.62 – 1.50 (m, 2H), 1.35 – 1.22 (m, 2H), 0.84 (t, *J* = 7.4 Hz, 3H) ppm. ¹³C NMR (151 MHz, CDCl₃): δ = 149.1, 135.2, 129.2, 128.8, 128.2, 120.7, 54.2, 31.7, 25.6, 22.5, 14.0.

1-(4-Chlorobenzyl)-4-butyl-1*H*-1,2,3-triazole (Figure 3-2, 3l): ¹H NMR (600 MHz, CDCl₃): δ = 7.36 – 7.31 (m, 2H), 7.18 (m, 3H), 5.46 (s, 2H), 2.74 – 2.64 (m, 2H), 1.67 – 1.57 (m, 2H), 1.43 – 1.31 (m, 2H), 0.91 (t, *J* = 7.4 Hz, 3H) ppm. ¹³C NMR (151 MHz, CDCl₃): δ = 149.2, 134.8, 133.6, 129.4, 120.5, 53.3, 31.6, 25.4, 22.4, 13.9. HRMS (*M*⁺) calcd. For C₁₃H₁₆ClN₃: 249.1034, found 249.1033. M.P. 52-54 °C

1-(4-Chlorophenyl)-4-(4-fluorophenyl)-1*H*-1,2,3-triazole (Figure 3-2, 3m): ¹H NMR (600 MHz, DMSO): δ = 9.33 (s, 1H), 8.03 – 7.94 (m, 4H), 7.77 – 7.68 (m, 2H), 7.36 (t, *J* = 8.9 Hz, 2H) ppm. ¹³C NMR (151 MHz, DMSO): δ = 162.0 (d, *J* = 245.0 Hz), 146.5, 135.3, 132.9, 129.9, 127.4, 127.3, 126.6 (d, *J* = 2.5 Hz), 126.6, 121.6, 119.6, 116.0, 115.9. HRMS (*M*⁺) calcd. For C₁₄H₉ClFN₃: 273.0479, found 273.0469. M.p. 205-208 °C

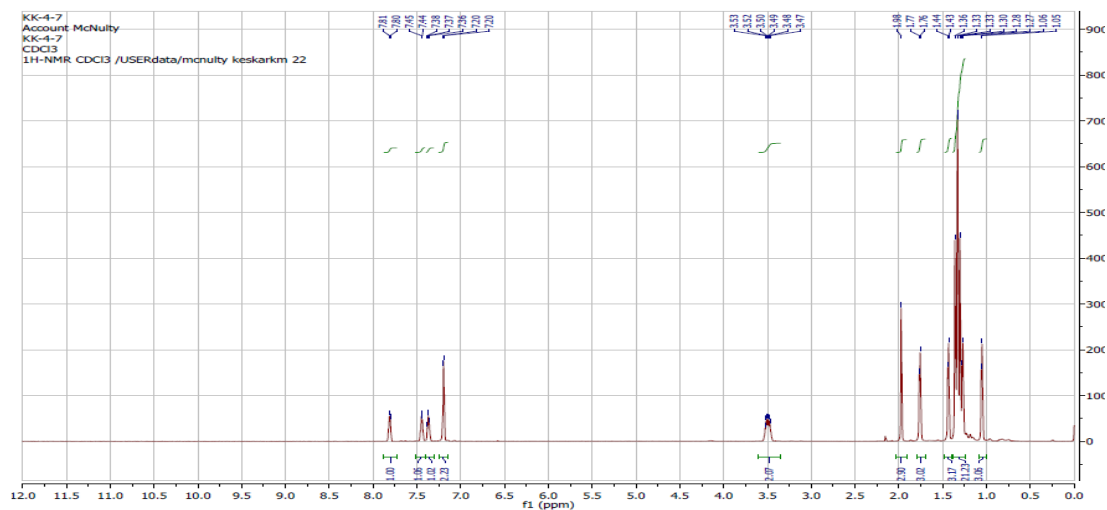
1-(4-Chlorophenyl)-4-phenyl-1H-1,2,3-triazole (Figure 3-2, 3n): ^{131}H NMR (600 MHz, DMSO): δ = 9.34 (s, 1H), 8.01 (d, J = 8.9 Hz, 2H), 7.95 (dd, J = 8.2, 1.1 Hz, 2H), 7.73 (d, J = 8.9 Hz, 2H), 7.51 (t, J = 7.7 Hz, 2H), 7.42 – 7.37 (m, 1H) ppm. ^{13}C NMR (151 MHz, DMSO): δ = 147.4, 135.4, 132.9, 129.9, 129.0, 128.3, 125.3, 121.6, 119.7.

1-(4-Methoxyphenyl)-4-phenyl-1H-1,2,3-triazole (Figure 3-2, 3o): ^{131}H NMR (600 MHz, CDCl_3): δ = 8.14 (s, 1H), 7.93 (d, J = 6.6 Hz, 2H), 7.71 (dd, J = 7.0, 1.7 Hz, 2H), 7.48 (t, J = 6.8 Hz, 2H), 7.39 (s, 1H), 7.07 (dd, J = 6.9, 1.8 Hz, 2H), 3.91 (s, 3H) ppm. ^{13}C NMR (151 MHz, CDCl_3): δ = 160.0, 148.3, 130.7, 130.5, 129.0, 128.4, 125.9, 122.3, 117.9, 114.9, 55.7.

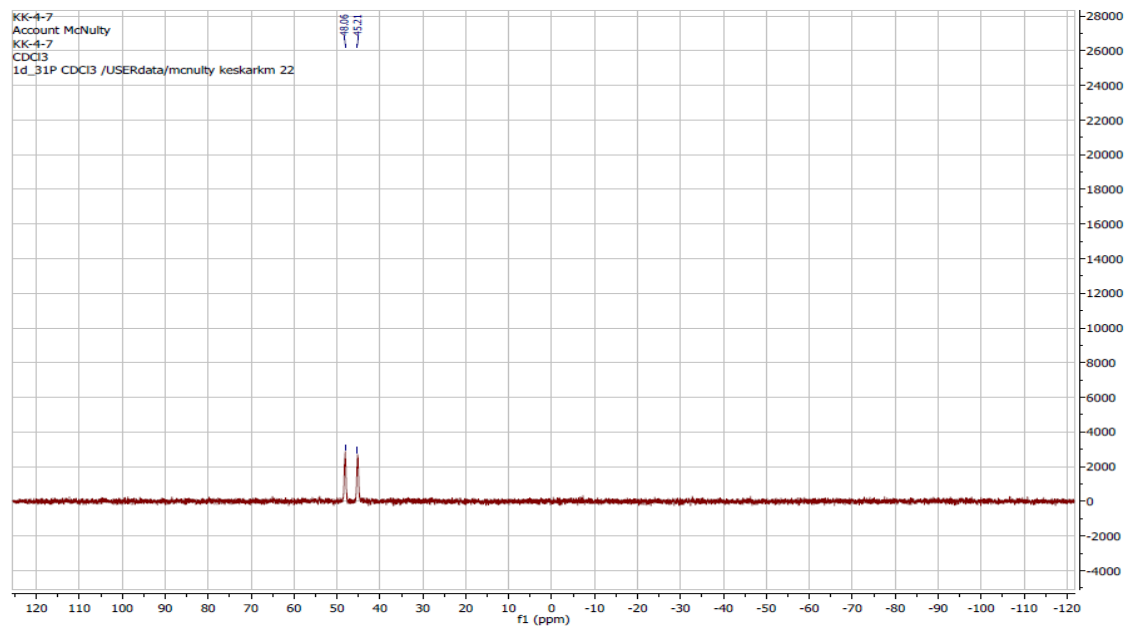
4-(4-Fluorophenyl)-1-phenyl-1H-1,2,3-triazole (Figure 3-2, 3p): ^1H NMR (600 MHz, DMSO): δ = 9.30 (s, 1H), 8.00 (dd, J = 8.9, 5.5 Hz, 2H), 7.97 – 7.93 (m, 2H), 7.69 – 7.62 (m, 2H), 7.54 (dd, J = 10.6, 4.2 Hz, 1H), 7.36 (t, J = 8.9 Hz, 2H) ppm. ^{13}C NMR (151 MHz, DMSO): δ = 161.9 (d, J = 244.9 Hz), 146.4, 136.6, 129.9, 128.7, 127.3 (d, J = 8.2 Hz), 126.8, 120.0, 119.5, 116.0, 115.8. HRMS (M^+) calcd. For $\text{C}_{14}\text{H}_{10}\text{FN}_3$: 239.0850, found 239.0859. M.P. 198-200 °C.

3.6 NMR Spectra: (Only new ^1H , ^{13}C and ^{31}P NMR spectras are displayed)*

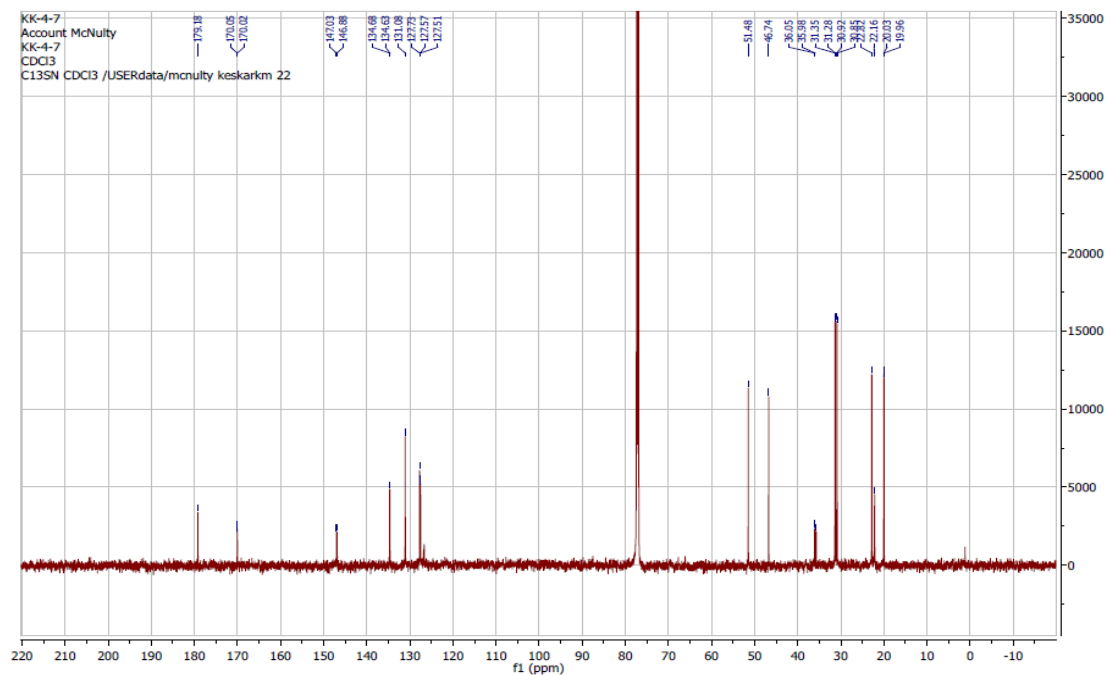
^1H NMR complex (Table 3-1, 6g):



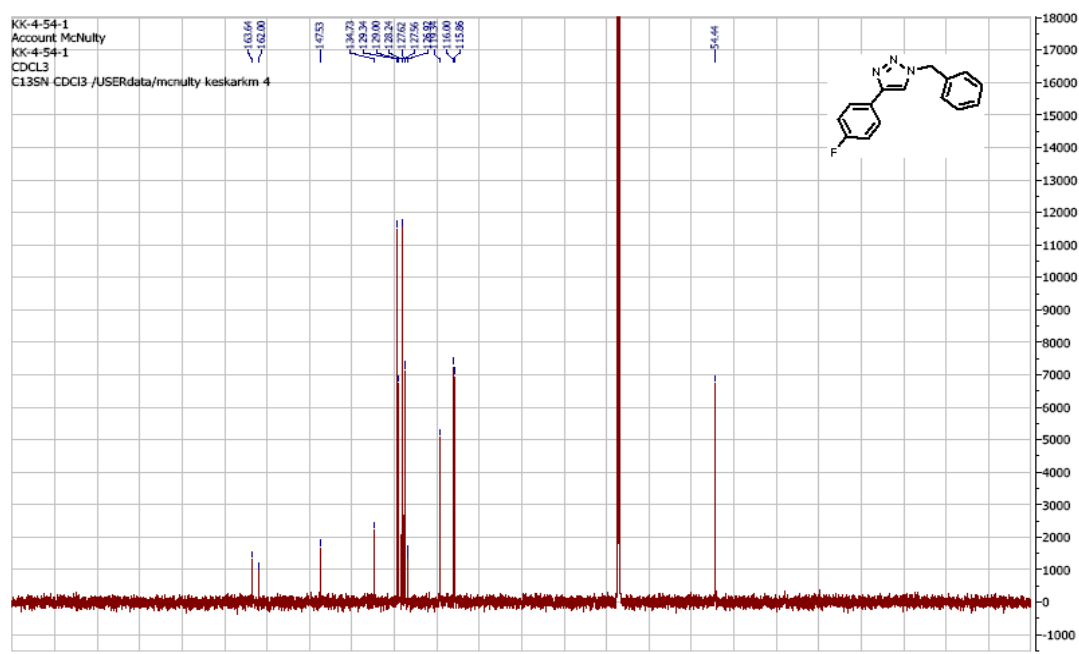
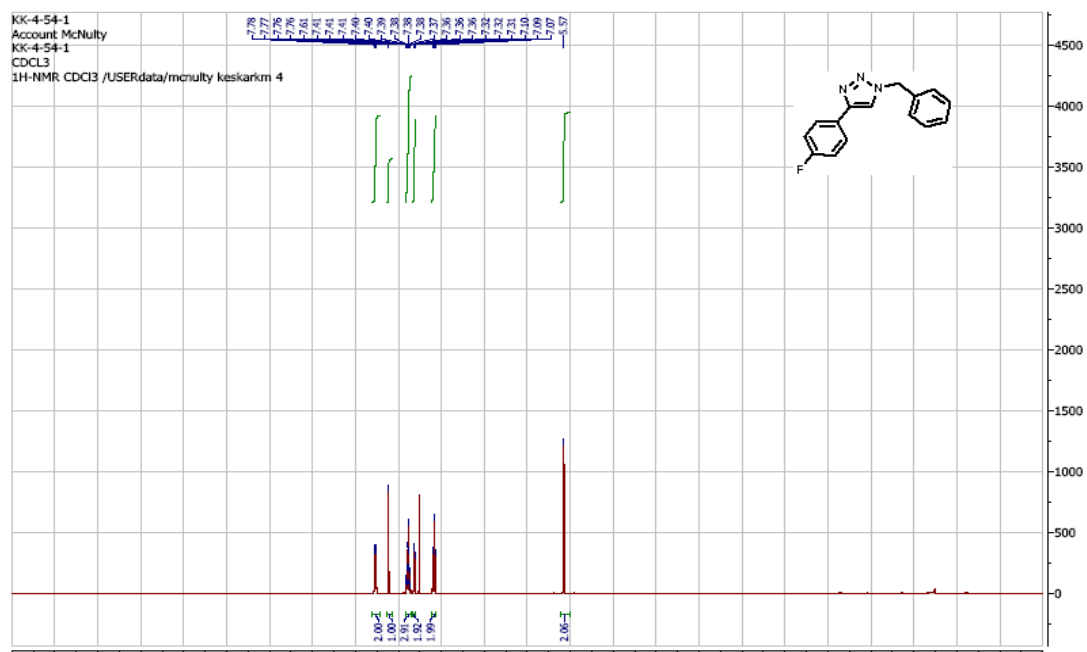
^{31}P NMR of complex (Table 3-1, 6g):



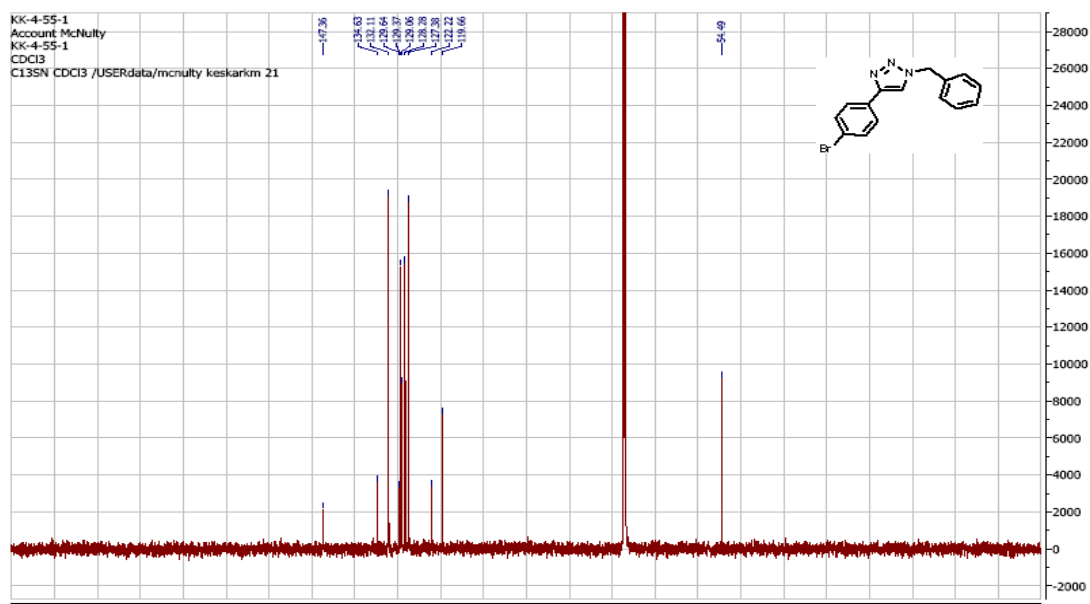
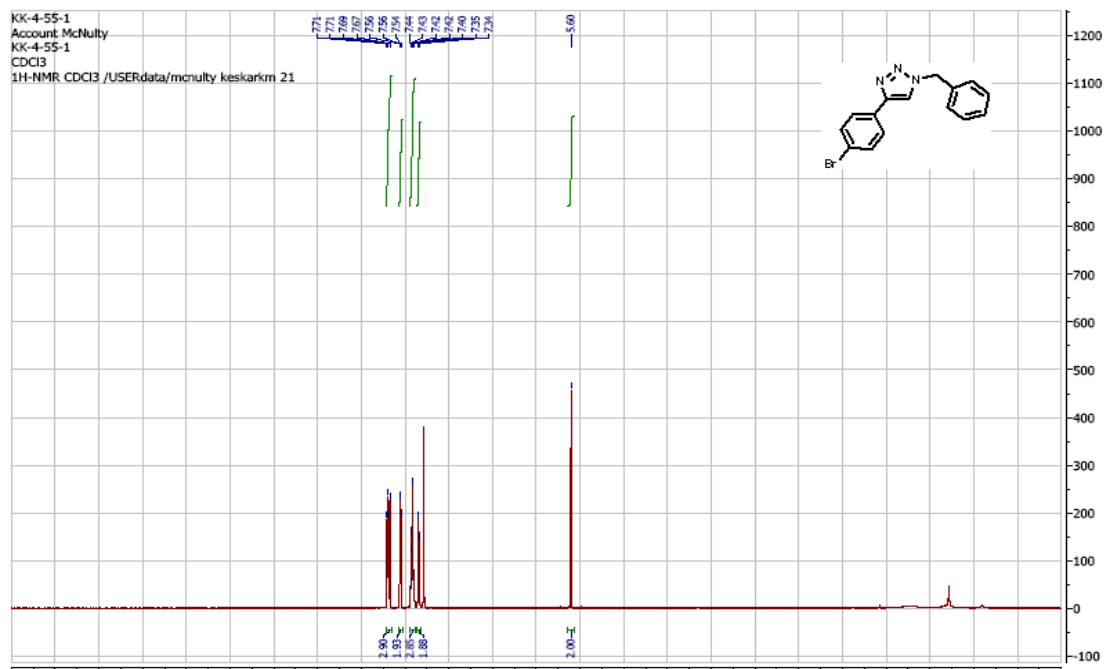
^{13}C NMR of complex (Table 3-1, 6g):



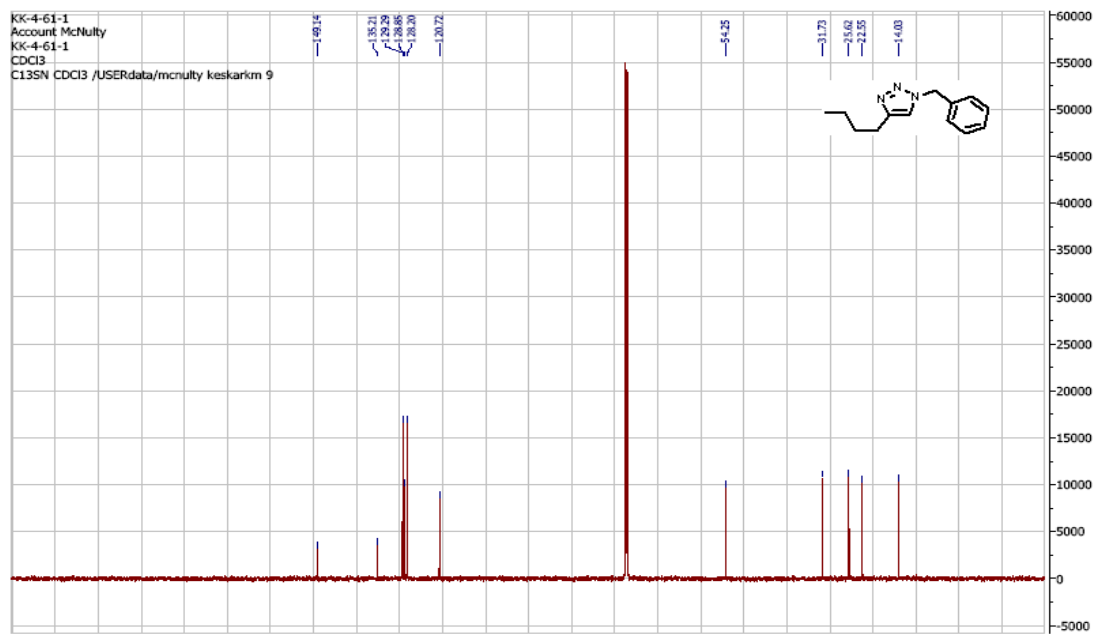
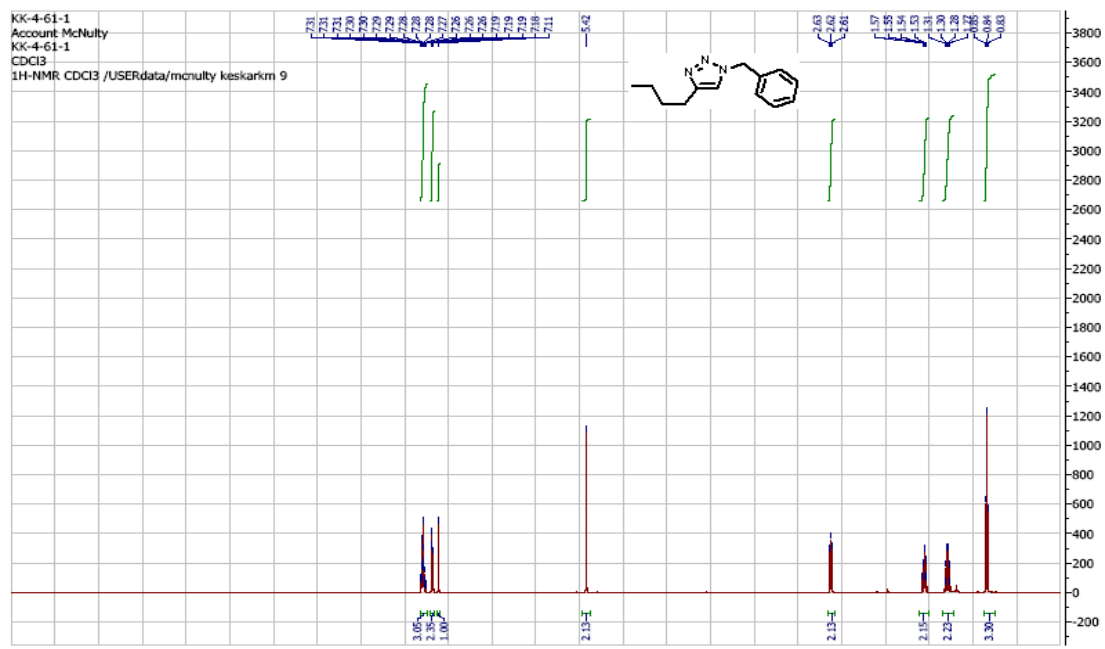
1-Benzyl-4-(4-fluorophenyl)-1H-1,2,3-triazole(Figure 3-2, 3e):



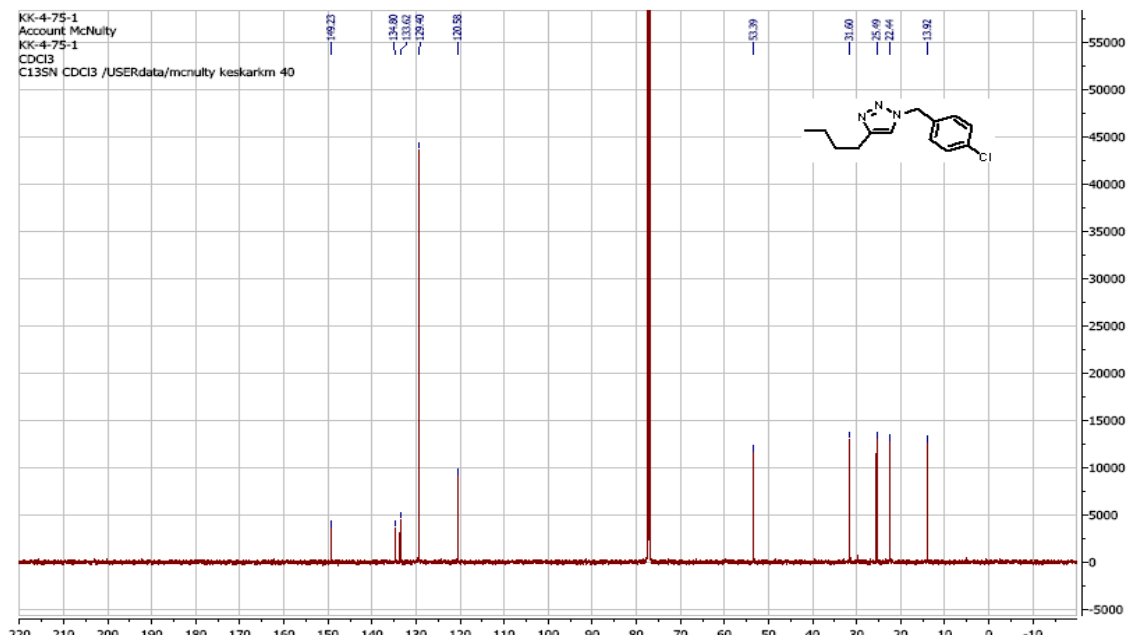
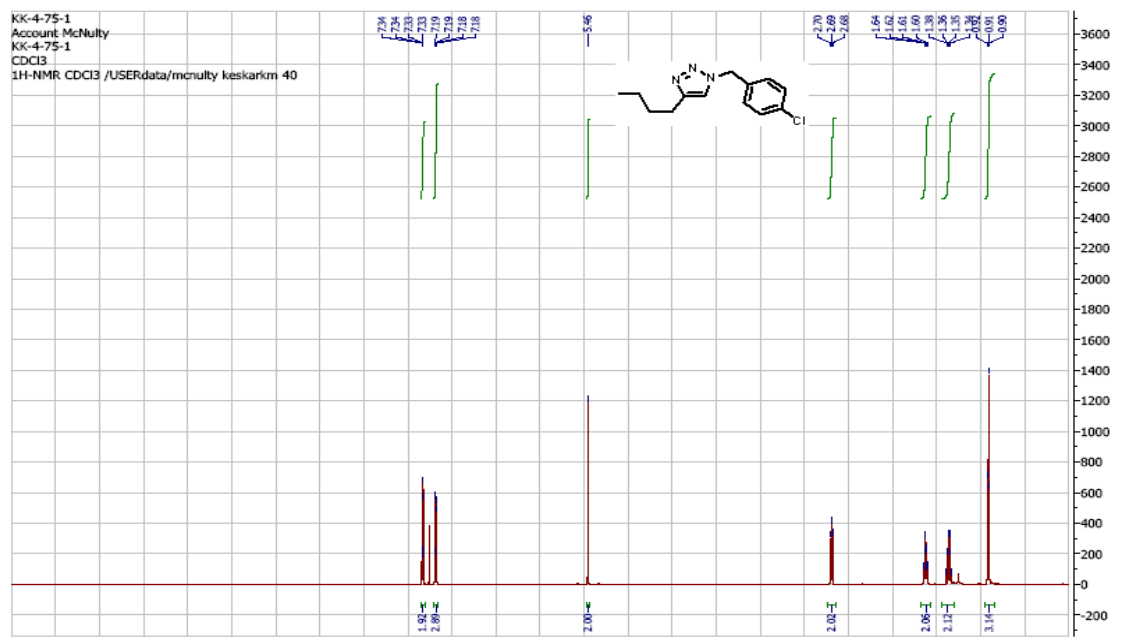
1-Benzyl-4-(4-bromophenyl)-1H-1,2,3-triazole(Figure 3-2, 3f):



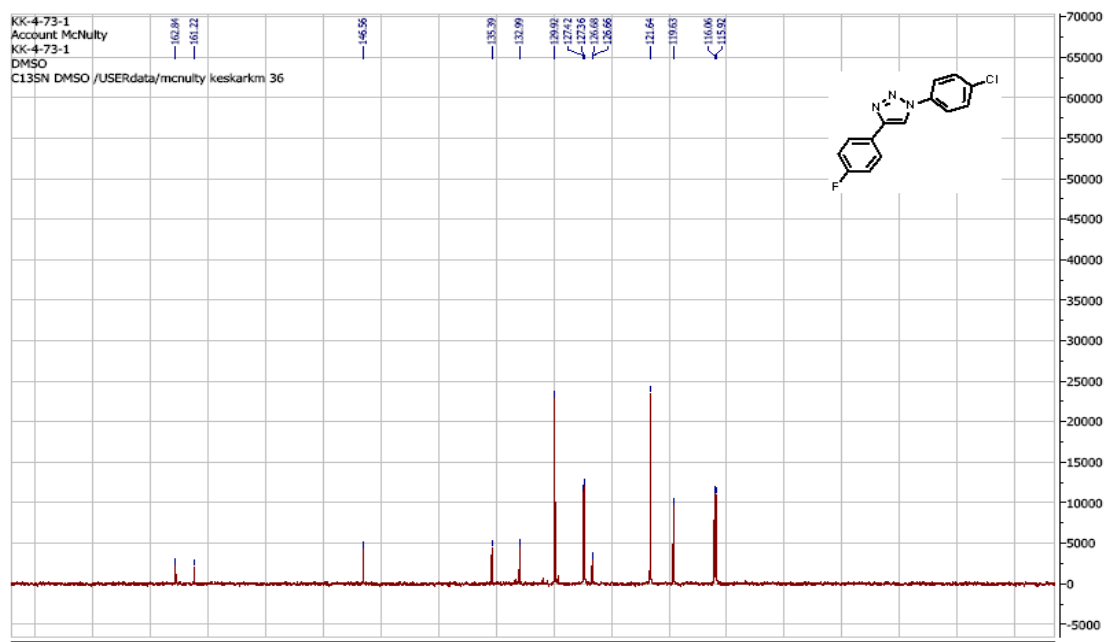
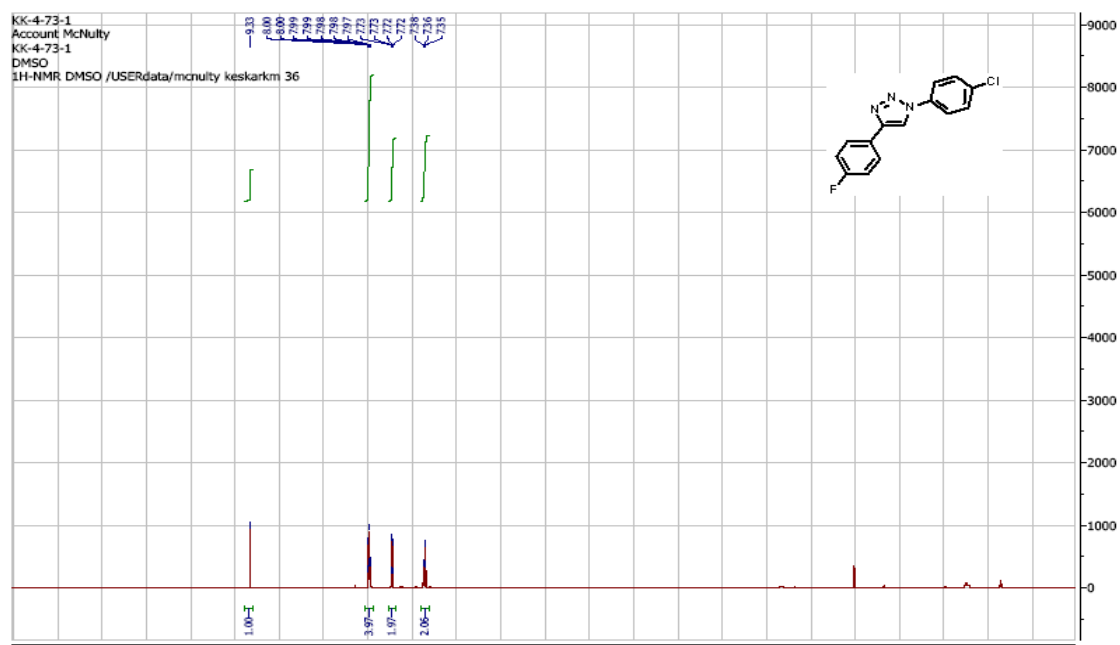
1-Benzyl-4-butyl-1H-1,2,3-triazole(Figure 3-2, 3k):



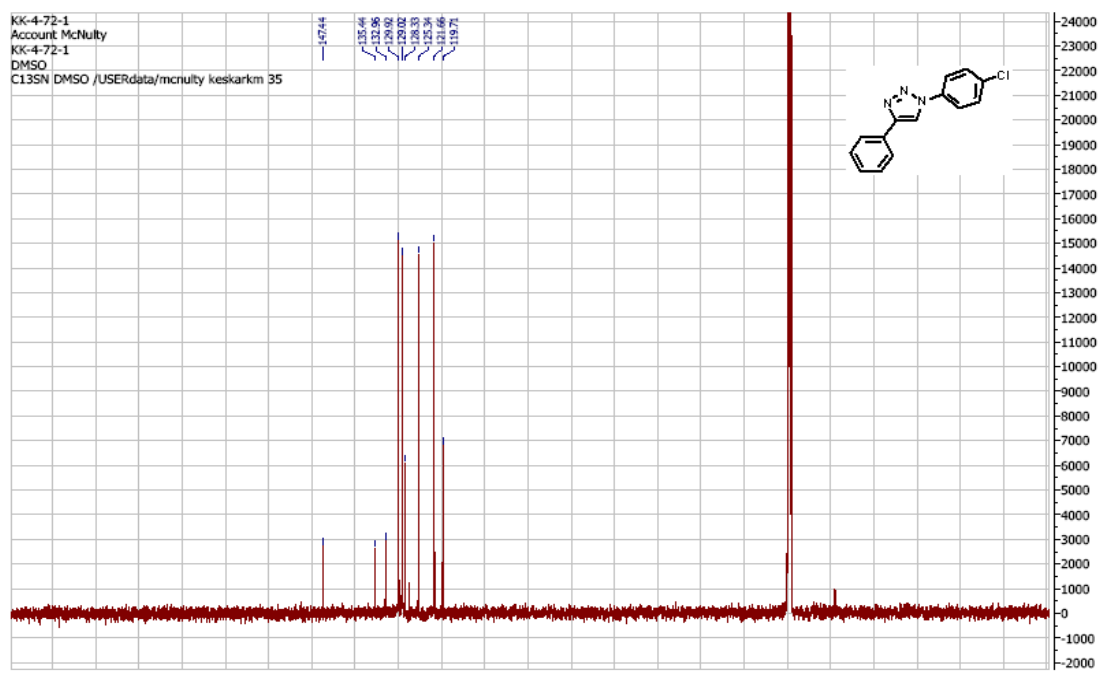
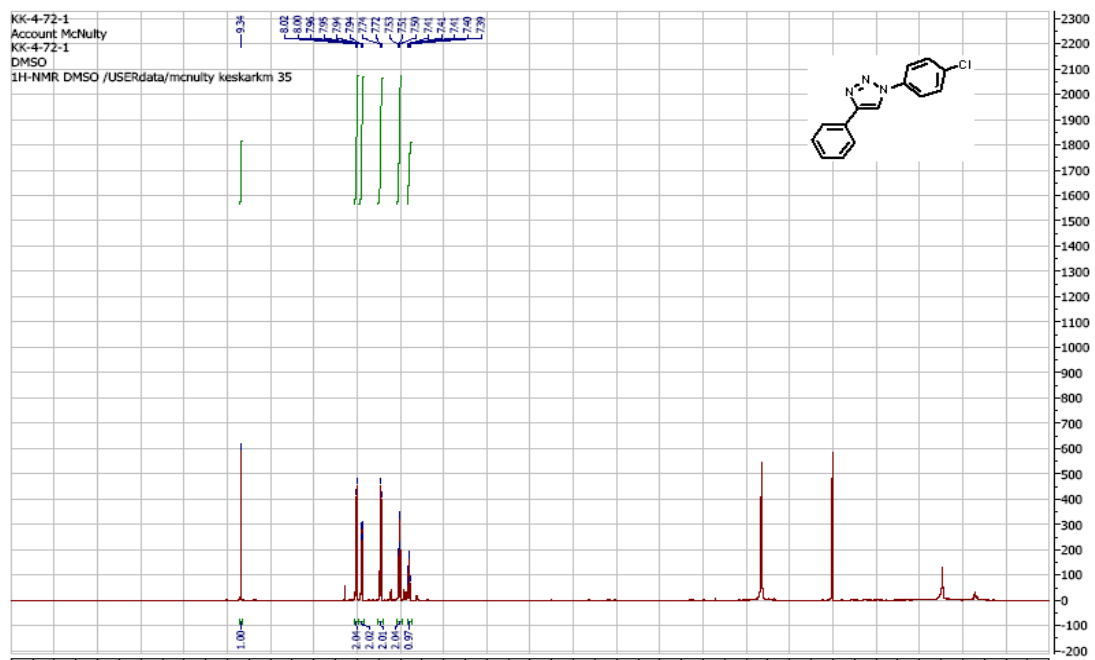
1-(4-Chlorobenzyl)-4-butyl-1H-1,2,3-triazole (Figure 3-2, 3I):



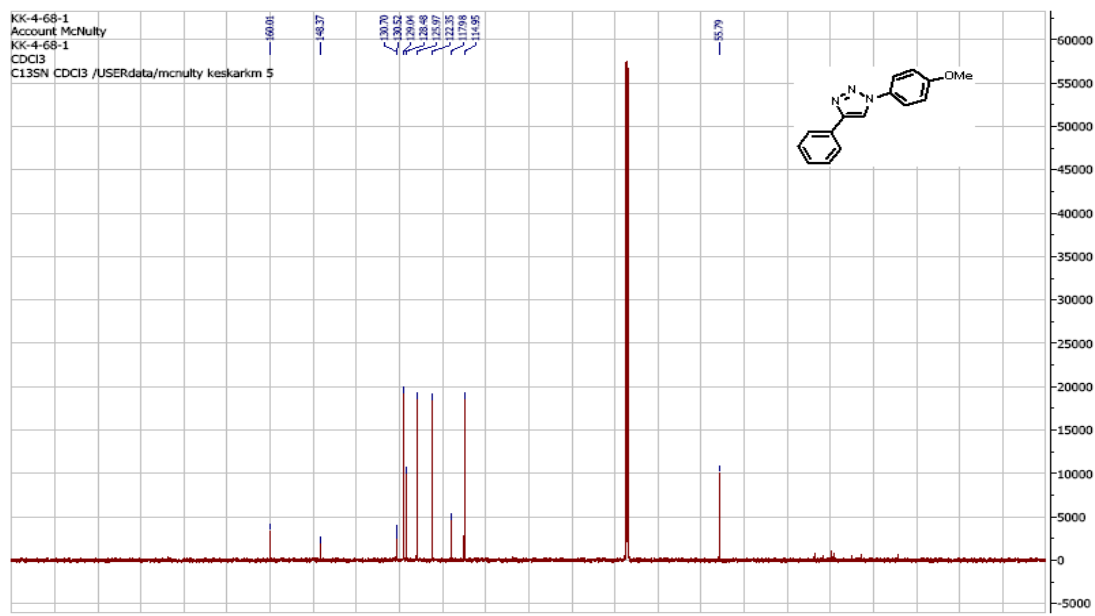
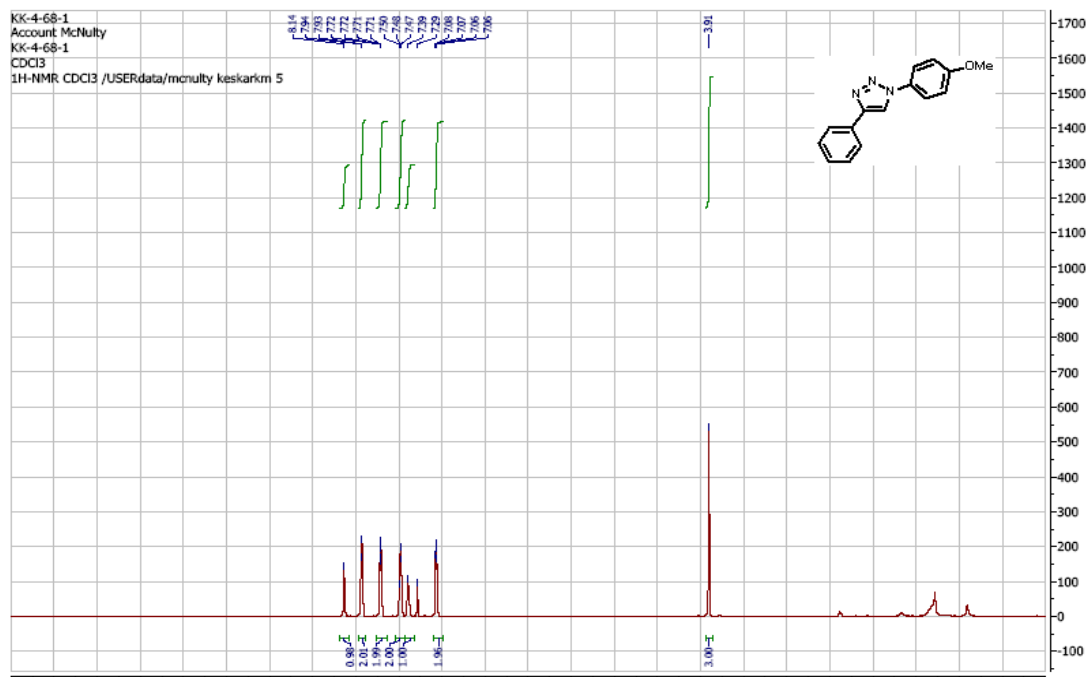
1-(4-Chlorophenyl)-4-(4-fluorophenyl)-1H-1,2,3-triazole (Figure 3-2, 3m):



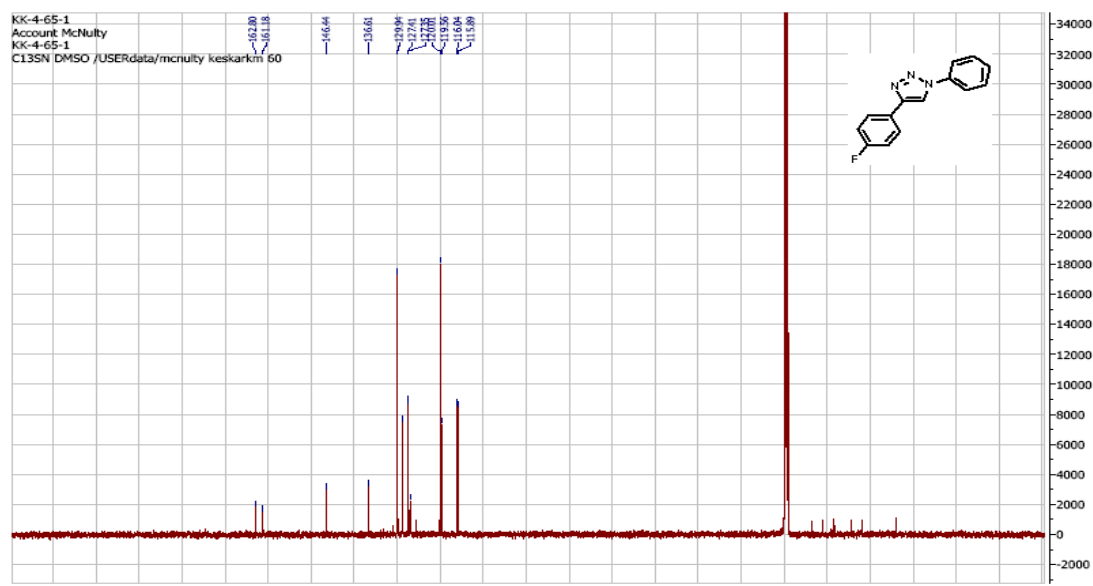
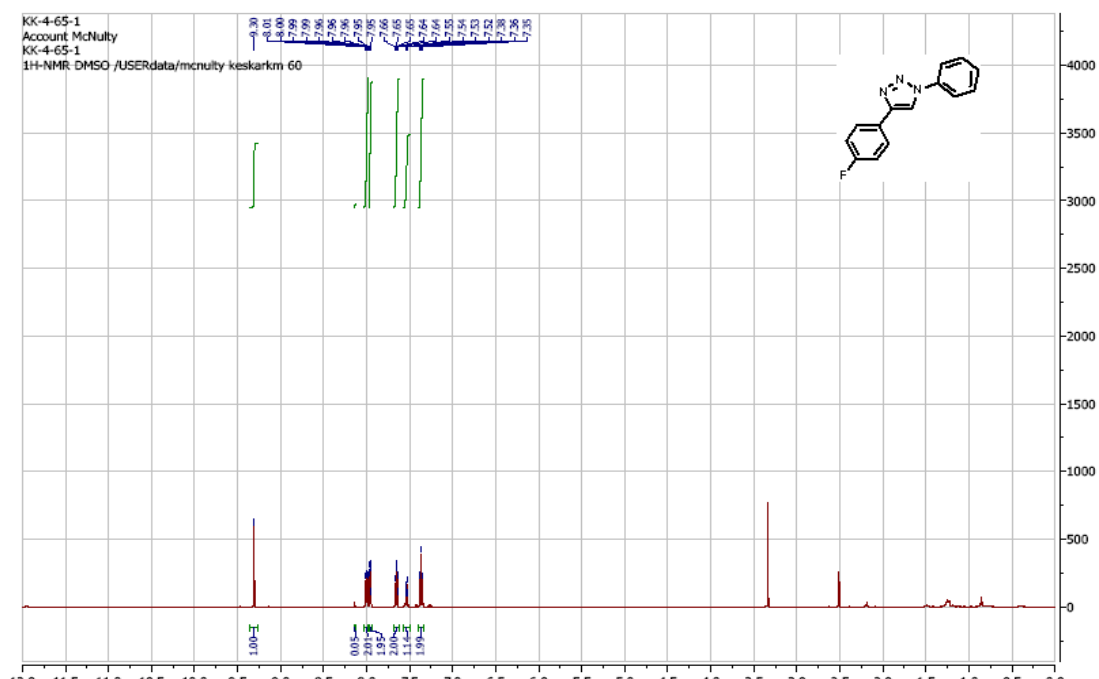
1-(4-Chlorophenyl)-4-phenyl-1H-1,2,3-triazole(Figure 3-2, 3n):



1-(4-Methoxyphenyl)-4-phenyl-1H-1,2,3-triazole (Figure 3-2, 3o):



4-(4-Fluorophenyl)-1-phenyl-1H-1,2,3-triazole (Figure 3-2, 3p):



*All other triazole ^1H and ^{13}C spectras can be found in chapter 2, Section 2.6.

JOHN WILEY AND SONS LICENSE
TERMS AND CONDITIONS

Sep 30, 2014

This is a License Agreement between Kunal Keskar ("You") and John Wiley and Sons ("John Wiley and Sons") provided by Copyright Clearance Center ("CCC"). The license consists of your order details, the terms and conditions provided by John Wiley and Sons, and the payment terms and conditions.

All payments must be made in full to CCC. For payment instructions, please see information listed at the bottom of this form.

License Number	3462580088731
License date	Sep 05, 2014
Licensed content publisher	John Wiley and Sons
Licensed content publication	European Journal of Organic Chemistry
Licensed content title	A Robust, Well-Defined Homogeneous Silver(I) Catalyst for Mild Intramolecular Hydroamination of 2-Ethynylanilines Leading to Indoles
Licensed copyright line	Copyright © 2014 WILEY-VCH Verlag GmbH & Co. KGaA, Weinheim
Licensed content author	James McNulty, Kunal Keskar
Licensed content date	Jan 23, 2014
Start page	1622
End page	1629
Type of use	Dissertation/Thesis
Requestor type	Author of this Wiley article
Format	Print and electronic
Portion	Full article
Will you be translating?	No
Title of your thesis / dissertation	"Advances in Late Transition Metal Catalysis, Olefination Reactions and Applications"
Expected completion date	Dec 2014
Expected size (number of pages)	300

Chapter IV: A Robust, Well-Defined Homogeneous Silver(I) Catalyst for Mild Intramolecular Hydroamination of 2-Ethynylanilines Leading to Indoles

4.1 Introduction

The development of transition-metal catalyzed alkene and alkyne hydroamination reactions has continued to transform the synthesis of aliphatic and heterocyclic amines over the last decade.^[1] Initial work on non-Michael-type hydroamination reactions focused on the use of base-catalyzed approaches to higher amines. However, these processes involve use of strong base often under forcing thermal conditions and are of limited scope.^[2] A wide range of both Lewis acidic and late transition metal homogeneous and heterogeneous catalysts^[1] have now been developed to effect hydroamination reactions. In particular, late transition metal complexes of both d^8 and d^{10} electronic configuration are employed. Despite these improvements, many processes require thermal conditions and substrate scope is still largely limited to activated olefins and intramolecular hydroamination processes.

Although heterogeneous and homogeneous catalytic processes based on Cu(I), Au(I), Au(III), Pd(0), Pd(II), Zn(II) and Hg(II) have been developed to effect hydroamination reactions,^[1,3] very few reports on the use of Ag(I) catalysts^[4] have appeared. Consequently, the development of Ag(I) catalytic systems was recently termed “somewhat neglected” with some understatement.^[1b] The homogeneous silver(I) situation contrasts sharply with the use of homogeneous ligated gold(I)-complexes, applications of which have expanded greatly in recent years. Despite the expected lower π -acidity of isoelectronic silver(I) species, the ready availability and significantly lower cost of precursor silver salts are driving factors in our current research program aimed at identifying robust, useful homogeneous silver(I) catalysts. As a case in point, the intramolecular hydroamination of *N*-protected 2-ethynylanilines (**1a**,

Table 4-1) has emerged as a valuable route to functionalized indoles and this process has been reported catalyzed by Cu salts,^[3a,b] Et₂Zn,^[3c] ZnBr₂,^[3e] Hg(OAc)₂,^[3d] and Rh(I) species.^[3f] Conditions required for this cyclization are often harsh requiring high temperature and addition of base is required along with the catalyst to perform reaction at room temperature.^[3b] No reports on the homogeneous catalysis of this reaction using silver(I) species has been reported. One example of a case involving an unprotected aniline was reported using heterogeneous silver(I) triflate,^[4a] whereas the intramolecular hydroamination of 6-amino-1-hexyne to its cyclic imine derivative was reported using silver tetrafluoroborate and a homogeneous triphos-ligated silver(I) catalyst.^[4i] This reaction, pioneered by Müller and co-workers, serves as the most comprehensive study on the late transition metal-catalyzed *5-endo-dig* hydroamination processes.^[4i,4j]

Table 4-1. Silver salt-promoted intramolecular hydroamination.^a

Entry	Ag Salt	Conv. (%)
1	Ag ₂ SO ₄	0
2	Ag ₂ CO ₃	26
3	AgOSO ₂ CF ₃	3
4	AgNO ₃	2
5	Ag ₂ O	83
6	Ag- <i>p</i> -toluenesulfonate	0
7	AgOAc	94
8 ^a	L ₂ AgOAc (Complex D)	>99

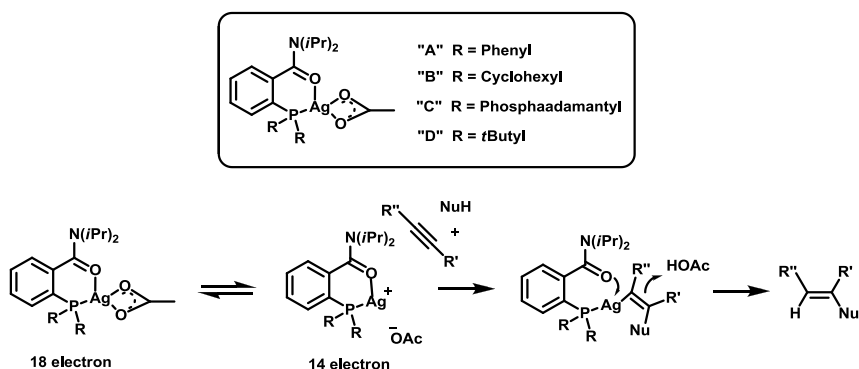
L₂AgOAc
"Complex D"

^[a] Reactions run with complexes (A-C) showed inferior results with some Ag(0) precipitation

The use of silver(I) salts or complexes in hydroamination and other areas of catalysis has “lagged behind”^[5] other coinage metals for several reasons. The facile precipitation of silver metal under many conditions and the rapid precipitation of silver halides in the presence of common halide counter-anions serve to limit the scope of silver(I) species in catalysis.

4.2 Results and Discussion

We recently reported the first examples of silver(I) catalyzed Huisgen cycloaddition reactions involving the use of homogeneous silver(I) species to initiate the necessary alkyne activation.



Scheme 4-1. Postulated reactivity of homogeneous silver(I)-promoted alkyne hydroamination.

We prepared silver(I) acetate complexes **A** to **D** (**Scheme 4-1**) from the corresponding 2-dialkylphosphino-*N,N*-diisopropyl benzamides. The hemilabile ligand was found to play a pivotal role in effecting this cycloaddition through polarization effects on reaction intermediates during the catalytic cycle.^[6b] On this basis of this π -acid reactivity, we postulated reactivity along the lines outlined in **Scheme 4-1** that might lead to homogeneous silver-promoted alkyne hydroamination. In this paper we describe the success of this protocol and development of a very robust and efficient homogeneous catalyst for the

intramolecular hydroamination reaction of 2-ethynylaniline derivatives. This protocol is carried out at room temperature and does not require the use of any basic additives. This readily enabled the construction of a mini-library of indole derivatives, including a sensitive, problematic^[3c] silylated indole derivative (vinylsilane).

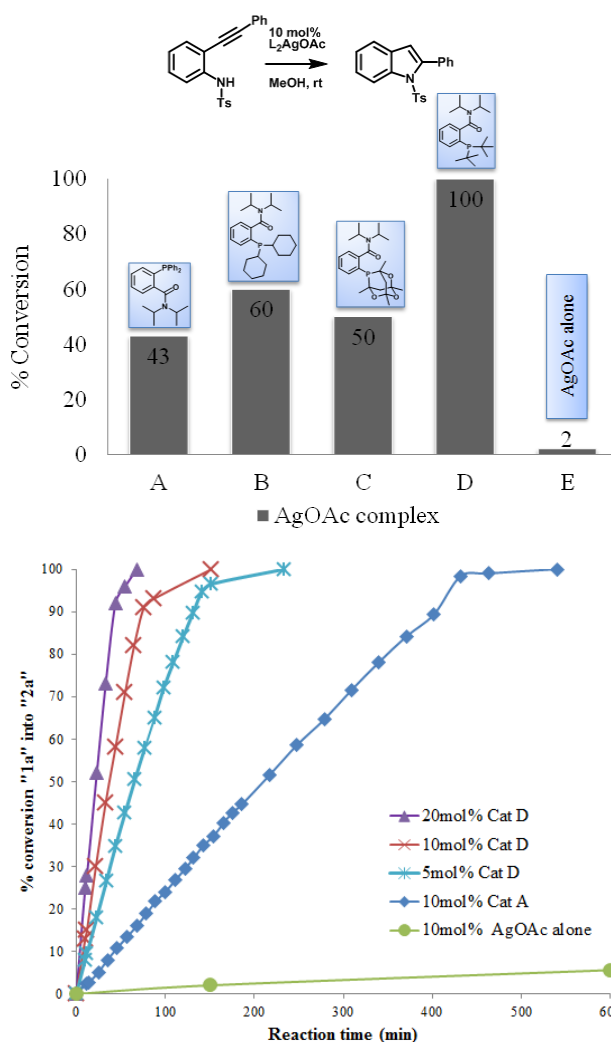
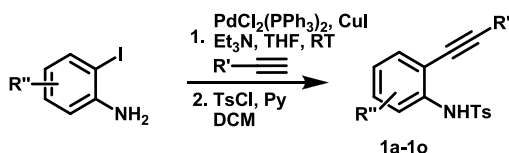


Figure 4-1. Ligand optimization (top) identifying complex **D** as optimal (100% conversion after 2.5 h) and kinetic data for complexes **A**, **D** (three concentrations) and comparison with the heterogeneous AgOAc promoted reaction, room temp. in methanol.

The base reaction of the *N*-tosyl-2-ethynylaniline **1a** is shown atop **Table 4-1**. A range of heterogeneous silver salts were first screened under standard thermal hydroamination conditions in toluene at 100 °C. The reactions were initially performed in deuterated toluene to allow simple monitoring by ¹H-NMR spectroscopy. The use of silver oxide (**Table 4-1**, Entry 5) and silver acetate (**Table 4-1**, Entry 7) alone provided corresponding indole adduct in 83% and 94% conversion respectively. Notably, the use of silver salts containing weakly coordinating anions here proved ineffective, in contrast to the intramolecular hydroamination reported on 6-amino-1-hexyne.^[4] Although a clear explanation for the dichotomy of these heterogeneously catalyzed reactions is not obvious, we note that these reactions were conducted in acetonitrile on a different substrate containing a free amine. Our attention immediately became focused on the homogeneous ligated silver(I) species (**Table 4-1**, catalyst **D** shown). This hydroamination reaction was far superior and seen to proceed at much faster rate, (*vide infra*) fully generating desired indole within 20 min (**Table 4-1**, Entry 8). Catalyst **D** was found to possess superior stability relative to complexes **A**, **B** and **C**. **Figure 4-3** in the experimental section shows the actual reactions with silver acetate after 30 mins (a) and 12 h (b) performed in toluene at 100 °C as well as the reaction with catalyst **D** (c) also after 12 h in toluene at 100 °C. Absolutely no silver metal precipitation is observed in the homogeneous reaction promoted by complex **D**, in contrast to the heterogeneous silver salt-promoted versions. In addition to catalyst thermal stability, we noted also that complexes **A-D** are non-hydrated or solvated, they are readily soluble in most organic solvents and show no silver chloride deposition when shaken with brine. Similar stability was noted during the Huisgen catalyzed process described above.^[6] The hydroamination reaction was investigated at or, near room temperature in various other solvents. Despite the homogeneous nature of these reactions, no conversion is observed in standard organic solvents such as toluene, dioxane, cyclohexane and

dichloromethane at room temperature or at 50 °C after 15 minutes. However, to our delight, the reaction with 10.0 mol% catalyst was found to be successful in dipolar solvents methanol, acetonitrile and dimethylformamide (DMF) at 50 °C, leading to >95% conversion in 15 min. The reaction performed in methanol proved very efficient *even at room temperature*, giving >99% conversion in 2.5 h. A catalyst screen identified complex **D** as the most active homogeneous catalyst for the cyclization, (**Figure 4-1**, top). Reactions in DMF and acetonitrile were also efficient at 22 °C, providing full conversion within 1.5-2.5h.

The catalyst loading could also be lowered to 1.0 mol% in DMF or methanol, leading to full conversions in about 13 h and 20 h respectively, demonstrating a significant rate effect on catalyst concentration. Kinetic data of the cyclization reaction followed in methanol using catalyst **A** (10.0 mol%), catalyst **D** at three different concentrations (5, 10 and 20 mol%) and the heterogeneous silver acetate promoted cyclization (10.0 mol%) are shown in **Figure 4-1**, bottom. The data show a clear rate acceleration for the homogeneous versions of the reaction as well as demonstrating the pronounced ligand accelerating effect comparing complexes **A** to **D**. The initial rate of reaction was precisely doubled employing catalyst **D** at 10.0 and 20.0 mol% demonstrating the reaction to be first order in catalyst concentration, a result in accord with previous intramolecular hydroamination reactions promoted with rare-earth metal^{1b]} and copper(I) catalysts.^[4j] The reaction performed in methanol was also advantageous in terms of work-up as the product indole often precipitates during the course of reaction. All subsequent experiments were conducted in either dry methanol or DMF.



Scheme 4-2. General method for preparation of aminoalkynes.

Table 4-2. Scope of the homogeneous intramolecular hydroamination of 2-alkylanilines promoted with 1.0 mol-% complex **D** at room temperature.

$\text{1a-1o} \xrightarrow[\text{DMF, 13-15 h, r.t.}]{\text{L}_2\text{AgOAc (1.0 mol-\%)}} \text{2a-2o}$

Entry	Substrate	Product	% Isolated yield	Entry	Substrate	Product	% Isolated yield
1			99	8			90
2			90	9			94
3			90	10			95
4			99	11			95
5			93	12			99
6			94	13			98
7			92	14			95
				15			95

The scope of the silver-promoted hydroamination was investigated employing starting materials **1a-o**, which were prepared from commercially available substituted 2-iodoanilines, following a two-step Sonogashira and *N*-tosylation protocol (**Scheme 4-2**).

The reaction conditions developed for substrate **1a** using catalyst **D** proved to be very general and **Table 4-2** summarizes the scope of variations investigated. The reactions were conducted in dry methanol or DMF (shown in **Table 4-2**) at room temperature using only 1.0 mol% of catalyst **D**. No additional base was required to effect high conversions in all cases investigated.

The reaction allows conversion of both electron rich, electron deficient aromatic systems to the corresponding 2-substituted indole derivative in high yields. In order to challenge the sensitivity of the new catalytic process, we prepared the trimethylsilyl-alkyne **1o**. We were delighted to find the homogeneous silver-catalyzed reaction in DMF permitted smooth hydroamination leading to the sensitive 2-trimethylsilyl-indole **2o**, which could be isolated in very high yield for the first time.^[3c] This result is illustrative of the mild and chemoselective π -acidity of these catalysts as trimethylsilyl-functionalized alkynes normally proceed quickly to the desilylated silver acetylides in the presence of silver salts.^[7]

Other electron withdrawing protecting groups on nitrogen worked equally well giving high yields of corresponding 2-substituted indole derivatives. For e.g. *N*-phenylsulphonyl-2-ethynylaniline (**13h**), *N*-methylsulphonyl-2-ethynylaniline (**21h**) worked equally well with 1.0 mol% catalyst **D** in DMF at room temperature. However, other protecting groups like -COPh, -COCH₃, -Boc, -COCF₃ along with free -NH failed to provide corresponding indole derivatives under similar condition.

We envision a catalytic cycle along the lines of that postulated in **Figure 4-2**. Loss of acetate from the catalyst precursor leads to the electrophilic 14-electron species **I** which tethers to the alkyne leading to **II** and reversibly to the *ortho*-amino substituent, suggesting a key role for the hemilabile ligand **II** to **III**. A standard pathway for the heterogeneous ligand-free cycle is outlined proceeding directly from **II** to **V**, for which the data (**Table 4-1**) show this to be

relatively slow. The mechanism for ligand accelerated catalysis follows the cycle through intermediates II, III, IV and V. Loss of the weak amide donor from II opens a more electrophilic site for coordination of the amine. Re-coordination of the amide (W =weak donor) in III leads to polarization of the silver-nitrogen bond (III to IV) initiating the cyclization leading to organosilver intermediate V through a stepwise process. Final proto-demetalation yields the indole derivative and regenerated the active catalyst.

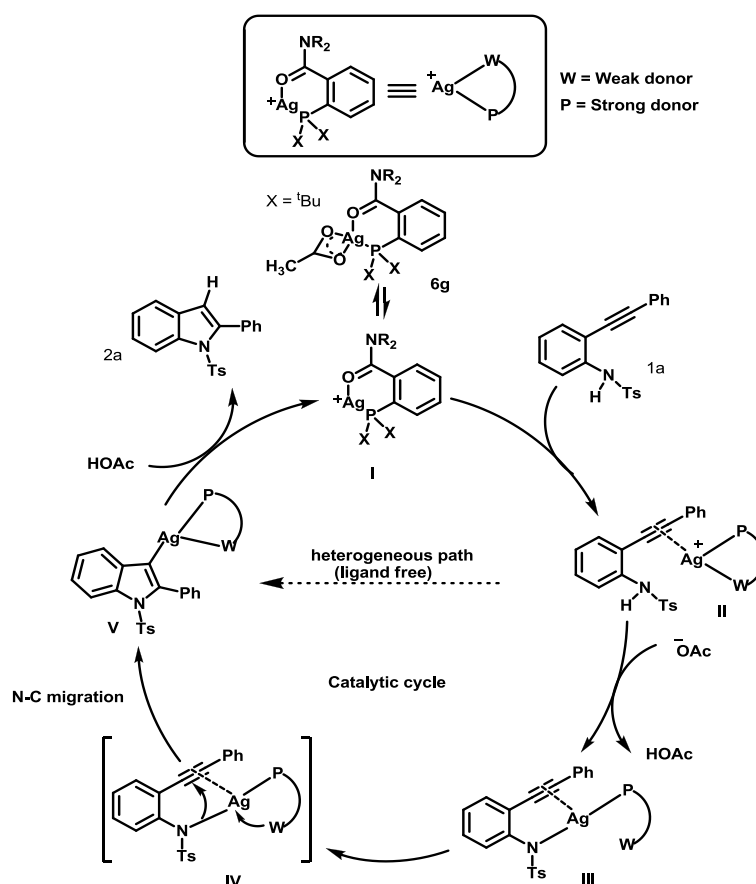


Figure 4-2. Postulated catalytic cycle for the hemilabile ligand accelerated intramolecular hydroamination promoted by catalyst **D**.

Interestingly, the only prior report on a homogeneous silver(I) catalyzed hydroamination, that of 6-amino-1-hexyne leading to the cyclic imine derivative,

resulted in poor (26% yield) conversion to the cyclized product using a triphos-ligated silver complex. The use of bidentate ligands was described as giving rise to even worse outcomes (5% yield). The reaction was observed to be most efficient using silver tetrafluoroborate alone (44-56% yield),^[4i] a process that also results in silver metal deposition. This situation contrast sharply to the present results using the hemilabile silver acetate complex **D**. The complex is very stable and catalytically active, allowing high conversion of 2-alkynyl anilines to indoles at room temperature in DMF as described (**Table 4-2**). Finally, although the homogeneous silver-mediated hydroamination reported here leads to *N*-tosyl protected indoles, we note that *N*-tosyl-indole derivatives can be readily deprotected using tetrabutyl ammonium fluoride under mild conditions, in contrast to aliphatic tosylamines.^[8]

4.3 Conclusion

We describe the first examples of homogeneous intramolecular hydroamination of 2-alkynylanilines employing well-defined silver(I) catalysts leading to substituted indoles. The reactions are promoted with low loadings (1.0 mol%) of catalyst and are conveniently conducted at room temperature in methanol or DMF. The reactions were shown to be first-order in catalyst and a mechanism was postulated highlighting the role of the hemilabile ligand in promoting the cyclization. In addition, the enhanced thermal and chemical stability of these silver(I) complexes makes them ideal to probe chemical reactivity (π -acidity) in the area of homogeneous catalysis without fear of silver metal or halide precipitation, problems that have plagued the development of silver catalysis in general. The role of these silver species in promoting Huisgen chemistry,^[6] and now hydroamination, bodes well for the future of silver(I) catalysis. It is our hope that the use of complexes such as **D** should allow this field of homogeneous silver(I) catalysis to catch-up^[5] with its competing technologies and to undergo significant advances of this previously neglected^[1b] synthetic field.

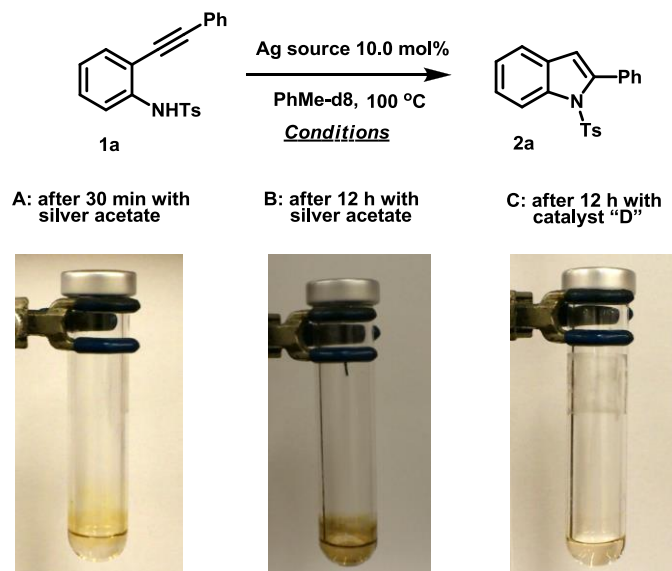
4.4 References

- [1]. N. T. Patil, R. D. Kavthe, V. S. Shinde, *Tetrahedron*, **2012**, 68, 9079-8146. (b) T. E. Müller, K. C. Hulzsch, M. Yus, F. Foubelo, M. Tada, *Chem. Rev.* **2008**, 108, 3795-3892.
- [2]. R. J. Schlott, J. C. Falk, K. W. Narducy, *J. Org. Chem.*, **1972**, 37, 4243-4245. (b) J. Seayad, A. Tillack, C. G. Hartung, M. Beller, *Adv. Synth. Catal.* **2002**, 344, 795–813.
- [3]. For comprehensive reviews on transition-metal catalyzed hydroamination see ref. 1. For select reports on hydroamination reactions of 2-ethynylanilines see: (a) K. Hiroya, S. Itoh, T. Sakamoto, *J. Org. Chem.* **2004**, 69, 1126-1136. (b) K. Hiroya, S. Itoh, T. Sakamoto, *Tetrahedron*. **2005**, 61, 10958-10964. (c) Y. Yin, W. Ma, Z. Chai, G. Zhao, *J. Org. Chem.* **2007**, 72, 5731-5736. (d) T. Kurisaki, T. Naniwa, H. Yamamoto, H. Imagawa, M. Nishizawa, *Tetrahedron Lett.* **2007**, 48, 1871-1874. (e) K. Okuma, J.-I. Seto, K.-I. Sakaguchi, S. Ozaki, N. Nagahora, K. Shioji, *Tetrahedron Lett.* **2009**, 50, 2943-2945. (f) A. Boyer, N. Isono, S. Lackner, M. Lautens, *Tetrahedron*. **2010**, 66, 6468-6482.
- [4]. For previous reports on silver-catalyzed hydroamination reactions see: (a) B. C. J. van Esseveldt, F. L. van Delft, Jan M. M. Smits, R. de Gelder, H. E. Schoemaker, F. P. J. T. Rutjes *Adv. Synth. Catal.* **2004**, 346, 823-834. (b) R. S. Robinson, M. C. Dovey, D. Gravestock, *Tetrahedron Lett.* **2004**, 45, 6787–6789. (c) D. K. Barange, T. C. Nishad, N. K. Swamy, V. Bandameedi, D. Kumar, B. R. Sreekanth, K. Vyas, M. Pal, *J. Org. Chem.* **2007**, 72, 8547–8550. (d) A. M. Prior, R. S. Robinson, R. S., *Tetrahedron Lett.* **2008**, 49, 411–414. (e) T. Tsuchimoto, K. Aoki, T. Wagatsuma, Y. Suzuki, *Eur. J. Org. Chem.* **2008**, 4035-4040. (f) S. R. Beeren, S. L. Dabb, B. A. Messerle, *J. Organomet. Chem.* **2009**, 694, 309-312. (g) T. Xu, G. Liu, *Org. Lett.* **2012**, 14, 5416-5419. (h) D. Rambabu, P. V. N. S. Murthy, K. R. S. Prasad, A. Kandale, G. S. Deora, M. V. B. Rao, M. Pal, *Tetrahedron Lett.* **2012**, 53,

- 6577-6583. (i) T. E. Müller, A. K. Pleier, J., *Chem. Soc. Dalton Trans.* **1999**, 583-587. (j) T. E. Müller, M. Grosche, E. Herdtweck, A. K. Pleiner, E. Walter, Y. K. Yan, *Organometallics*, **2000**, *19*, 170-183. (k) D. W. Knight, PCT Int. Appl. WO100479 (2006). For other silver catalyzed processes leading to indoles see: (l) C. H. Oh, S. Karmakar, H. Park, Y. Ahn, J. W. Kim., *J. Am. Chem. Soc.* **2010**, *132*, 1792-1793. (m) D. D. Vachhani, V. P. Mehta, S. G. Modha, K. Van Hecke, L. Van Meervelt, E. V. Van der Eycken, *Adv. Synth. Catal.* **2012**, *354*, 1593-1599.
- [5]. P. A. Wender, preface in M. Harmata (Ed), *Silver in Organic Chemistry*, J. Wiley and Son, Hoboken, N.J., 2010.
- [6]. J. McNulty, K. Keskar, R. Vemula, *Chem. Eur. J.* **2011**, *17*, 14727-14730. (b) J. McNulty, K. Keskar, *Eur. J. Org. Chem.* **2012**, *28*, 5462-5470.
- [7]. U. Halbes-Letinois, J.-M. Weibel, P. Pale, *Chem. Soc. Rev.* **2007**, *36*, 759-769.
- [8]. (a) A. Yasuhara, T. Sakamoto, *Tetrahedron Lett.* **1998**, *39*, 595-595. (b) S. K. Jackson, M. A. Kerr, *J. Org. Chem.* **2007**, *72*, 1405-1411. (c) S. Krishnan, J. T. Bagdanoff, D. C. Ebner, Y. K. Ramtohul, U. K. Tambar, B. M. Stoltz, *J. Am. Chem. Soc.* **2008**, *130*, 13745-13754.
- [9]. Y. Monguchi, S. Mori, S. Aoyagi, A. Tsutsui, T. Maegawa, H. Sajiki, *Org. Biomol. Chem.* **2010**, *8*, 3338-3342.
- [10]. K. Inamoto, N. Asano, Y. Nakamura, M. Yonemoto, Y. Kondo, *Org. Lett.* **2012**, *14*, 2622-2625.
- [11]. A. Karadeolian, M. Kerr, *J. Org. Chem.* **2010**, *75*, 6830-6841.

4.5 Experimental Section

Figure 4-3. Photographs taken after the hydroamination reaction in toluene showing silver metal deposition in the heterogeneous reactions (**A** and **B**) but not in the homogeneous reaction (**C**).



Dichloromethane was distilled over calcium hydride. Toluene was distilled over sodium metal in the presence of benzophenone indicator. All other solvents including dimethylformamide (>99%) were purchased as sure-seal bottles from Sigma Aldrich and used as-is. ^1H and ^{13}C spectra were obtained on a 600 MHz Bruker NMR spectrometer. Chemical shifts are reported in units of δ (ppm) and coupling constants (J) are expressed in Hz. Mass spectra were run on a Micromass Quattro Ultima spectrometer fitted with a direct injection probe (DIP) with ionization energy set at 70 eV and HRMS (EI) were performed with a Micromass Q-TOF Ultima spectrometer. Thin layer chromatography (TLC) was run using Macherey-Nagel aluminum-backed plates. Melting points were obtained on an Electronic Research Associates Inc. melting point apparatus corrected against an external calibrant. Silver acetate (>99%) was purchased from Fluka. Silver trifluoromethanesulphonate (>98%), Silver oxide (>99%) and Silver paratoluenesulphonate (>99%) were obtained from Sigma Aldrich. Silver nitrate was obtained from International Correspondence Schools, USA. Silver sulfate (ACS quality) was obtained from BDH and Silver carbonate (99%) was purchased from General Chemical Division, USA.

General procedure for synthesis of 2-phenylethynylaniline and *N*-tosyl-2-phenylethynylaniline (Scheme 4-2):

2-phenylethynylaniline and *N*-tosyl- 2-phenylethynylaniline **1a** were prepared according to reported procedure.^[3c] Using same procedure other 2-substituted ethynylanilines and corresponding *N*-tosyl derivatives were prepared.

***N*-(2-((4-bromophenyl)ethynyl)phenyl)-4-methylbenzenesulfonamide**

(Scheme 4-2, 1b): M.p. 99-101 °C. ¹H NMR (600 MHz, CDCl₃) δ 7.66 (d, *J* = 8.3 Hz, 2H), 7.61 (d, *J* = 8.2 Hz, 1H), 7.53 (d, *J* = 8.5 Hz, 2H), 7.37 (dd, *J* = 7.7, 1.3 Hz, 1H), 7.34 – 7.28 (m, 3H), 7.18 (d, *J* = 8.1 Hz, 2H), 7.14 (s, 1H), 7.07 (td, *J* = 7.6, 1.0 Hz, 1H), 2.35 (s, 3H). ¹³C NMR (151 MHz, CDCl₃) δ 144.2, 137.7, 136.2, 133.0, 132.2, 132.0, 130.0, 129.7, 127.3, 124.8, 123.5, 121.1, 120.5, 114.4, 95.0, 85.0, 21.6. HRMS: calcd. for C₂₁H₁₆BrNO₂S[M]⁺ 425.0085; found 425.0085.

***N*-(2-((3-chlorophenyl)ethynyl)phenyl)-4-methylbenzenesulfonamide**

(Scheme 4-2, 1c): ¹H NMR (600 MHz, CDCl₃) δ 7.66 (d, *J* = 8.3 Hz, 2H), 7.63 (d, *J* = 8.2 Hz, 1H), 7.40 (d, *J* = 1.6 Hz, 1H), 7.37 (dt, *J* = 7.7, 1.8 Hz, 2H), 7.36 – 7.30 (m, 3H), 7.19 (d, *J* = 8.0 Hz, 2H), 7.11 (s, 1H), 7.10 – 7.06 (m, 1H), 2.35 (s, 3H). ¹³C NMR (151 MHz, CDCl₃) δ 144.2, 137.7, 136.3, 134.5, 132.3, 131.5, 130.1, 129.9, 129.8, 129.4, 127.3, 124.8, 123.8, 120.9, 114.4, 94.5, 85.0, 21.6. HRMS: calcd. for C₂₁H₁₆ClNO₂S[M]⁺ 381.0581; found 381.0590.

***N*-(4,5-dimethyl-2-(phenylethynyl)phenyl)-4-methylbenzenesulfonamide**

(Scheme 4-2, 1d): M.p. 170-172 °C. ¹H NMR (600 MHz, CDCl₃) δ 7.51 (d, *J* = 8.2 Hz, 2H), 7.37 – 7.29 (m, 3H), 7.25 (dd, *J* = 8.3, 2.3 Hz, 2H), 7.07 (d, *J* = 21.0 Hz, 2H), 6.99 (d, *J* = 8.0 Hz, 2H), 6.36 (s, 1H), 2.51 (s, 3H), 2.29 (s, 3H), 2.23 (s, 3H). ¹³C NMR (151 MHz, CDCl₃) δ 143.5, 138.2, 137.1, 136.8, 133.1, 132.6, 131.6, 130.6, 129.5, 128.6, 128.3, 127.6, 122.7, 121.5, 93.8, 85.6, 21.5, 20.9, 19.6. HRMS: calcd. for C₂₃H₂₁NO₂S[M]⁺ 375.1300; found 375.1293.

N-(2-((2-chlorophenyl)ethynyl)phenyl)-4-methylbenzenesulfonamide

(Scheme 4-2, 1e): M.p. 91-94 °C. ^1H NMR (600 MHz, CDCl_3) δ 7.72 (d, J = 8.4 Hz, 2H), 7.69 (d, J = 8.5 Hz, 2H), 7.53 – 7.48 (m, 2H), 7.40 (dd, J = 7.7, 1.5 Hz, 1H), 7.36 – 7.32 (m, 1H), 7.32 – 7.27 (m, 2H), 7.17 – 7.14 (m, 2H), 7.05 (td, J = 7.6, 1.1 Hz, 1H), 2.32 (s, 3H). ^{13}C NMR (151 MHz, CDCl_3) δ 144.0, 138.4, 136.2, 135.9, 132.8, 131.8, 130.2, 130.0, 129.7, 129.4, 127.5, 126.8, 124.1, 122.3, 119.1, 113.3, 93.3, 89.4, 21.6. HRMS: calcd. for $\text{C}_{21}\text{H}_{16}\text{ClNO}_2\text{S}[\text{M}]^+$ 381.0597; found 381.0590.

N-(2-((4-fluorophenyl)ethynyl)phenyl)-4-methylbenzenesulfonamide

(Scheme 4-2, 1h): ^1H NMR (600 MHz, CDCl_3) δ 7.67 (d, J = 8.3 Hz, 1H), 7.61 (d, J = 8.2 Hz, 1H), 7.47 – 7.42 (m, 1H), 7.36 (dd, J = 7.7, 1.4 Hz, 1H), 7.30 (td, J = 8.2, 1.5 Hz, 1H), 7.18 (d, J = 8.0 Hz, 1H), 7.16 (s, 1H), 7.11 – 7.05 (m, 2H), 2.35 (s, 2H). ^{13}C NMR (151 MHz, CDCl_3) δ 163.0 (d, J = 251.3 Hz), 144.2, 137.7, 136.2, 133.7 (d, J = 8.5 Hz), 132.1, 129.8 (d, J = 15.3 Hz), 127.4, 124.7, 120.4, 118.2, 116.10 (d, J = 22.2 Hz), 114.5, 95.1, 83.6, 21.6. HRMS: calcd. for $\text{C}_{21}\text{H}_{16}\text{FNO}_2\text{S}[\text{M}]^+$ 365.0891; found 365.0886.

N-(5-chloro-2-(hex-1-ynyl)phenyl)-4-methylbenzenesulfonamide (Scheme 4-2, 1m):

^1H NMR (600 MHz, CDCl_3) δ 7.69 (d, J = 8.3 Hz, 2H), 7.59 (d, J = 2.0 Hz, 1H), 7.24 (d, J = 8.0 Hz, 2H), 7.21 (s, 1H), 7.16 (d, J = 8.3 Hz, 1H), 6.95 (dd, J = 8.3, 2.1 Hz, 1H), 2.42 (t, J = 7.1 Hz, 2H), 2.39 (s, 3H), 1.62 – 1.53 (m, 2H), 1.51 – 1.40 (m, 2H), 0.97 (t, J = 7.3 Hz, 3H). ^{13}C NMR (151 MHz, CDCl_3) δ 144.4, 138.7, 136.0, 134.6, 132.8, 129.8, 127.3, 124.4, 119.2, 113.1, 99.0, 74.6, 30.7, 22.2, 21.7, 19.3, 13.7. HRMS: calcd. for $\text{C}_{19}\text{H}_{20}\text{ClNO}_2\text{S}[\text{M}]^+$ 361.0905; found 361.0903.

General procedure for intramolecular hydroamination reaction: (for e.g. Table 4-2, 2a)

Into a screw cap vial containing a telfon-coated stirring bar was added **1a** (0.0020g, 0.0057 mmol) followed by a solution of the catalyst **D** (1.0 mol%) in

dimethylformamide or methanol (0.280 mL). The reaction mixture was allowed to stir at room temperature for 12-28 h. Upon completion of reaction (TLC) solvent was removed under vacuum. The reaction mixture was then extracted with ethyl acetate (3 X 10 mL), washed with water, brine. The organic layer was dried over anhydrous sodium sulfate and concentrated under reduced pressure. The resulting residue was purified through silica gel column chromatography (2-5% ethyl acetate: hexanes) to afford **2a**.

2-phenyl-1-tosyl-1H-indole (Table 4-2, 2a):^[9] ¹H NMR (600 MHz, CDCl₃) δ 8.31 (d, *J* = 8.4 Hz, 1H), 7.50 (dd, *J* = 7.6, 1.8 Hz, 2H), 7.47 – 7.39 (m, 4H), 7.39 – 7.33 (m, 1H), 7.29-7.24 (m, 4H), 7.04 (d, *J* = 8.0 Hz, 2H), 6.54 (s, 1H), 2.29 (s, 3H). ¹³C NMR (151 MHz, CDCl₃) δ 144.6, 142.2, 138.4, 134.8, 132.5, 130.7, 130.4, 129.3, 128.7, 127.6, 126.9, 124.9, 124.4, 120.8, 116.8, 113.7, 21.6.

2-(4-bromophenyl)-1-tosyl-1H-indole (Table 4-2, 2b): M.p. 142-144 °C. ¹H NMR (600 MHz, CDCl₃) δ 8.30 (d, *J* = 8.4 Hz, 1H), 7.59 – 7.52 (m, 2H), 7.44 (d, *J* = 7.7 Hz, 1H), 7.40 – 7.36 (m, 3H), 7.29 – 7.24 (m, 3H), 7.05 (d, *J* = 8.1 Hz, 2H), 6.54 (s, 1H), 2.29 (s, 3H). ¹³C NMR (151 MHz, CDCl₃) δ 144.8, 141.0, 138.5, 134.6, 131.8, 131.5, 130.9, 130.5, 129.4, 126.8, 125.2, 124.6, 123.2, 120.9, 116.8, 114.1, 21.6. HRMS: calcd. for C₂₁H₁₆BrNO₂S[M]⁺ 425.0083; found 425.0085.

2-(3-chlorophenyl)-1-tosyl-1H-indole (Table 4-2, 2c): M.p. 47-50 °C. ¹H NMR (600 MHz, CDCl₃) δ 8.30 (d, *J* = 8.4 Hz, 1H), 7.45 (d, *J* = 7.7 Hz, 1H), 7.44 – 7.42 (m, 1H), 7.42 – 7.38 (m, 2H), 7.32-7.24 (m, 2H), 7.28 (dd, *J* = 7.9, 2.2 Hz, 3H), 7.07 (d, *J* = 8.4 Hz, 2H), 6.57 (s, 1H), 2.30 (s, 3H). ¹³C NMR (151 MHz, CDCl₃) δ 144.9, 140.5, 138.4, 134.7, 134.2, 133.5, 130.4, 130.0, 129.4, 128.9, 128.8, 128.8, 126.9, 125.3, 124.5, 121.0, 116.7, 114.3, 21.6. HRMS: calcd. for C₂₁H₁₆ClNO₂S[M]⁺ 381.0599; found 381.0590.

5,6-dimethyl-2-phenyl-1-tosyl-1H-indole (Table 4-2, 2d): M.p. 146-150 °C. ¹H NMR (600 MHz, CDCl₃) δ 7.48 (dd, *J* = 7.8, 1.6 Hz, 2H), 7.41 – 7.34 (m, 3H), 7.01 (s, 1H), 6.97 – 6.90 (m, 5H), 6.41 (s, 1H), 2.81 (s, 3H), 2.37 (s, 3H), 2.30 (s, 3H). ¹³C NMR (151 MHz, CDCl₃) δ 146.1, 144.2, 139.1, 135.5, 134.6, 133.1, 132.8, 130.6, 129.9, 129.0, 128.5, 127.9, 127.4, 118.7, 116.6, 21.7, 21.5, 21.2. HRMS: calcd. for C₂₃H₂₁NO₂S[M]⁺ 375.1295; found 375.1293.

2-(2-chlorophenyl)-1-tosyl-1H-indole (Table 4-2, 2e): M.p. 48-52 °C. ¹H NMR (600 MHz, CDCl₃) δ 8.27 (d, *J* = 8.4 Hz, 1H), 7.51 (d, *J* = 7.7 Hz, 1H), 7.49 – 7.47 (m, 1H), 7.43 (d, *J* = 8.4 Hz, 2H), 7.41 – 7.31 (m, 4H), 7.28 (d, *J* = 7.9 Hz, 1H), 7.11 (d, *J* = 8.2 Hz, 2H), 6.63 (s, 1H), 2.31 (s, 3H). ¹³C NMR (151 MHz, CDCl₃) δ 144.8, 137.5, 137.3, 135.4, 135.2, 133.1, 131.7, 130.2, 129.9, 129.5, 127.1, 125.8, 125.1, 124.0, 121.1, 115.8, 113.9, 21.7. HRMS: calcd. for C₂₁H₁₆ClNO₂S[M]⁺ 381.0591; found 381.0590.

2-m-tolyl-1-tosyl-1H-indole (Table 4-2, 2f):^[9] ¹H NMR (600 MHz, CDCl₃) δ 8.30 (d, *J* = 8.4 Hz, 1H), 7.44 (d, *J* = 7.6 Hz, 1H), 7.37 – 7.33 (m, 1H), 7.33 – 7.27 (m, 5H), 7.26 – 7.22 (m, 2H), 7.04 (d, *J* = 8.1 Hz, 2H), 6.53 (s, 1H), 2.42 (s, 3H), 2.29 (s, 3H). ¹³C NMR (151 MHz, CDCl₃) δ 144.6, 142.4, 138.3, 137.1, 134.9, 132.4, 131.1, 130.6, 129.5, 129.2, 127.5, 127.5, 127.0, 124.8, 124.3, 120.7, 116.7, 113.4, 21.6, 21.5.

2-p-tolyl-1-tosyl-1H-indole (Table 4-2, 2g):^[9] ¹H NMR (600 MHz, CDCl₃) δ 8.30 (d, *J* = 8.4 Hz, 1H), 7.43 (d, *J* = 7.7 Hz, 1H), 7.40 (d, *J* = 8.0 Hz, 2H), 7.36 – 7.32 (m, 1H), 7.30 – 7.26 (m, 4H), 7.26 – 7.22 (m, 3H), 7.04 (d, *J* = 8.2 Hz, 2H), 6.51 (s, 1H), 2.44 (s, 3H), 2.28 (s, 3H). ¹³C NMR (151 MHz, CDCl₃) δ 144.5, 142.4, 138.7, 138.3, 134.8, 130.8, 130.3, 129.7, 129.3, 128.4, 126.9, 124.7, 124.4, 120.7, 116.8, 113.4, 21.6, 21.5.

2-(4-fluorophenyl)-1-tosyl-1H-indole (Table 4-2, 2h): M.p. 112-115 °C. ¹H NMR (600 MHz, CDCl₃) δ 8.31 (d, *J* = 8.4 Hz, 1H), 7.48 – 7.42 (m, 3H), 7.39 – 7.33 (m, 1H), 7.28 (d, *J* = 7.5 Hz, 1H), 7.26-7.24 (m, 2H), 7.11 (t, *J* = 8.7 Hz,

2H), 7.05 (d, $J = 8.2$ Hz, 2H), 6.52 (s, 1H), 2.29 (s, 3H). ^{13}C NMR (151 MHz, CDCl_3) δ 163.2 (d, $J = 248.9$ Hz), 144.8, 141.0, 138.3, 134.8, 132.2 (d, $J = 8.1$ Hz), 130.5, 129.4, 128.5, 126.8, 125.0, 124.5, 120.8, 116.7, 114.7 (d, $J = 21.8$ Hz), 113.7, 21.6. HRMS: calcd. for $\text{C}_{21}\text{H}_{16}\text{FNO}_2\text{S}[\text{M}]^+$ 365.0884; found 365.0886.

methyl 2-phenyl-1-tosyl-1H-indole-5-carboxylate (Table 4-2, 2i):^[10] ^1H NMR (600 MHz, CDCl_3) δ 8.36 (d, $J = 8.8$ Hz, 1H), 8.17 (d, $J = 1.2$ Hz, 1H), 8.04 (dd, $J = 8.8, 1.7$ Hz, 1H), 7.50 – 7.46 (m, 2H), 7.46 – 7.45 (m, 1H), 7.44 – 7.39 (m, 2H), 7.27 (d, $J = 8.3$ Hz, 3H), 7.05 (d, $J = 8.0$ Hz, 2H), 6.60 (s, 1H), 3.94 (s, 3H), 2.30 (s, 3H). ^{13}C NMR (151 MHz, CDCl_3) δ 167.3, 145.0, 143.4, 140.95, 134.8, 131.9, 130.5, 130.3, 129.5, 129.1, 127.7, 126.9, 126.3, 126.0, 122.9, 116.3, 113.4, 52.3, 21.6.

(1-tosyl-1H-indol-2-yl)methanol (Table 4-2, 2j):^[11] ^1H NMR (600 MHz, CDCl_3) δ 8.05 (d, $J = 8.4$ Hz, 1H), 7.71 (d, $J = 8.4$ Hz, 2H), 7.48 (d, $J = 7.7$ Hz, 1H), 7.32 – 7.28 (m, 1H), 7.23 (t, $J = 7.5$ Hz, 1H), 7.20 (d, $J = 8.3$ Hz, 2H), 6.64 (s, 1H), 4.91 (s, 2H), 3.31 (brs, 1H), 2.33 (s, 3H). ^{13}C NMR (151 MHz, CDCl_3) δ 145.2, 140.3, 137.0, 135.6, 130.0, 129.2, 126.5, 125.0, 123.8, 121.2, 114.4, 111.2, 58.6, 21.6.

6-chloro-2-phenyl-1-tosyl-1H-indole (Table 4-2, 2k):^[10] ^1H NMR (600 MHz, CDCl_3) δ 8.35 (d, $J = 1.8$ Hz, 1H), 7.48 – 7.43 (m, 3H), 7.43 – 7.39 (m, 2H), 7.36 (d, $J = 8.3$ Hz, 1H), 7.28 – 7.23 (m, 3H), 7.07 (d, $J = 8.1$ Hz, 2H), 6.50 (s, 1H), 2.31 (s, 4H). ^{13}C NMR (151 MHz, CDCl_3) δ 145.0, 142.8, 138.7, 135.1, 134.7, 132.0, 130.7, 130.5, 129.5, 129.0, 127.6, 127.0, 125.0, 121.4, 116.8, 112.9, 21.7.

2-butyl-1-tosyl-1H-indole (Table 4-2, 2l):^[9] ^1H NMR (600 MHz, CDCl_3) δ 8.16 (d, $J = 8.3$ Hz, 1H), 7.61 (d, $J = 8.4$ Hz, 2H), 7.40 (d, $J = 7.5$ Hz, 1H), 7.24 (dd, $J = 8.3, 1.2$ Hz, 1H), 7.21 – 7.19 (m, 1H), 7.18 (d, $J = 8.2$ Hz, 2H), 6.38 (s, 1H), 2.98 (t, $J = 7.7$ Hz, 2H), 2.33 (s, 3H), 1.73 (dt, $J = 15.3, 7.6$ Hz, 2H), 1.48-1.40

(m, 2H), 0.96 (t, $J = 7.4$ Hz, 3H). ^{13}C NMR (151 MHz, CDCl_3) δ 144.7, 142.6, 137.3, 136.4, 131.0, 129.9, 126.4, 123.9, 123.5, 120.1, 114.9, 108.7, 31.1, 28.8, 22.6, 21.6, 14.0.

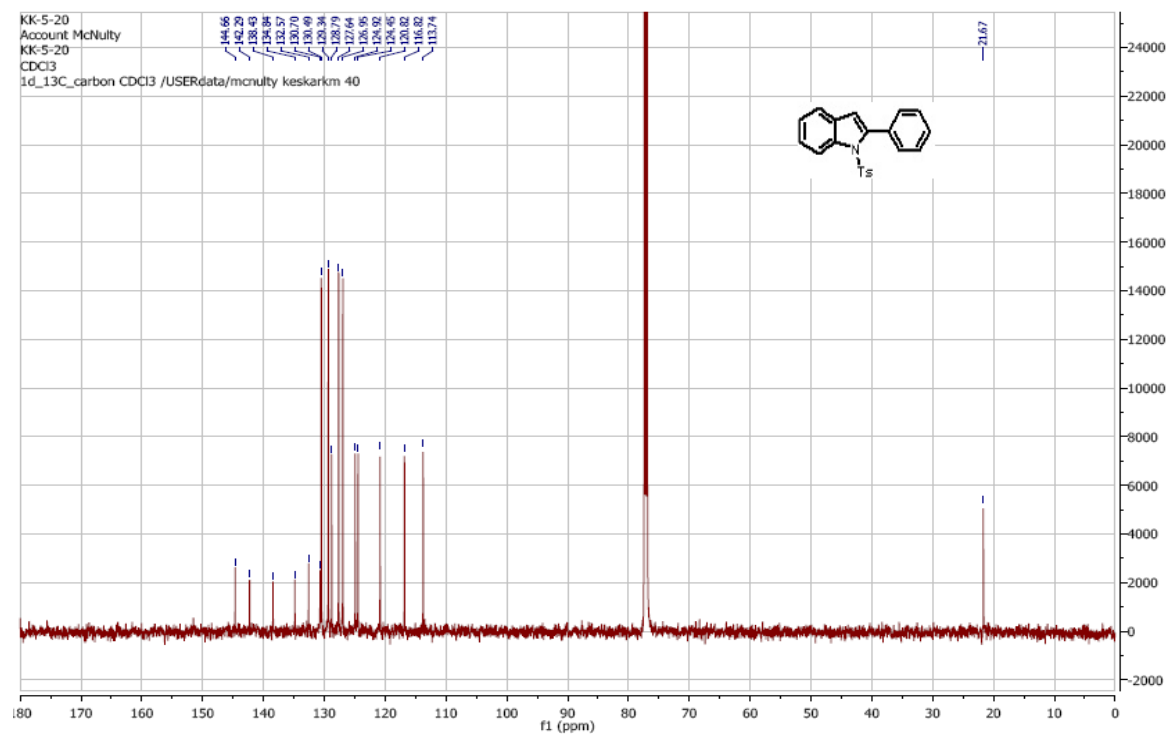
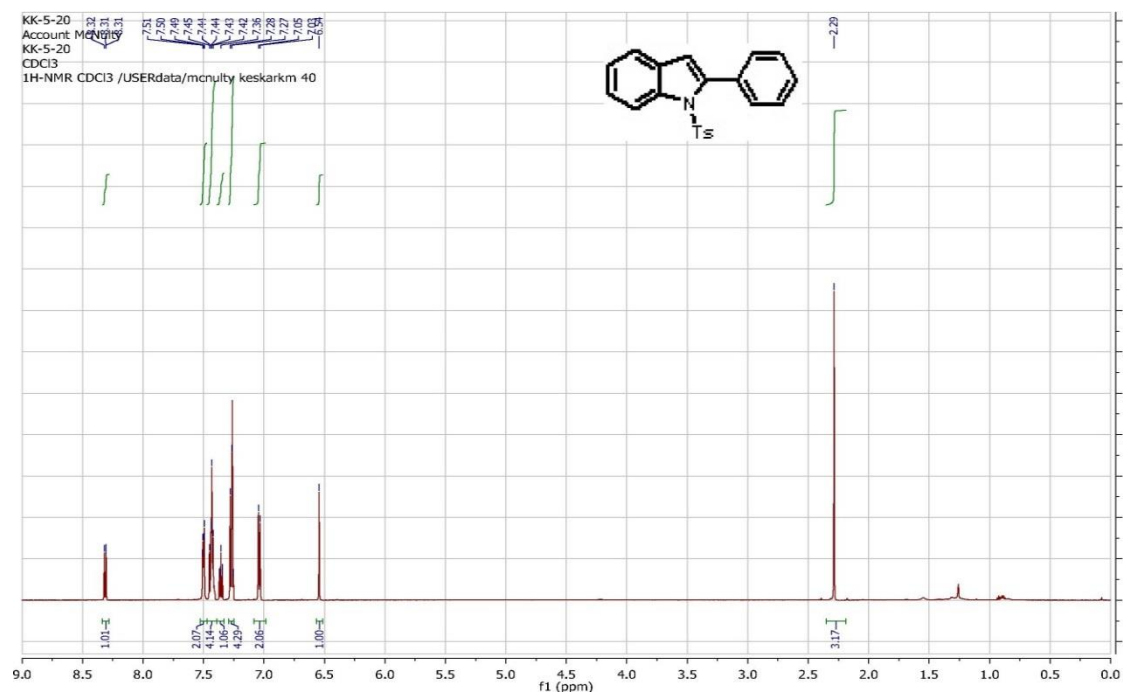
2-butyl-6-chloro-1-tosyl-1H-indole (Table 4-2, 2m): M.p. 95-98 °C. ^1H NMR (600 MHz, CDCl_3) δ 8.21 (d, $J = 1.7$ Hz, 1H), 7.62 (d, $J = 8.4$ Hz, 2H), 7.31 (d, $J = 8.3$ Hz, 1H), 7.21 (d, $J = 8.2$ Hz, 2H), 7.18 (dd, $J = 8.3, 1.8$ Hz, 1H), 6.34 (d, $J = 0.6$ Hz, 1H), 2.95 (t, $J = 7.4$ Hz, 2H), 2.35 (s, 3H), 1.70 (dt, $J = 15.3, 7.6$ Hz, 2H), 1.49 – 1.36 (m, 2H), 0.95 (t, $J = 7.4$ Hz, 3H). ^{13}C NMR (151 MHz, CDCl_3) δ 145.0, 143.3, 137.6, 136.2, 130.0, 129.8, 128.4, 126.4, 124.1, 120.8, 115.1, 108.1, 30.9, 28.7, 22.5, 21.7, 14.0. HRMS: calcd. for $\text{C}_{19}\text{H}_{20}\text{ClNO}_2\text{S}[\text{M}]^+$ 361.0893; found 361.0903.

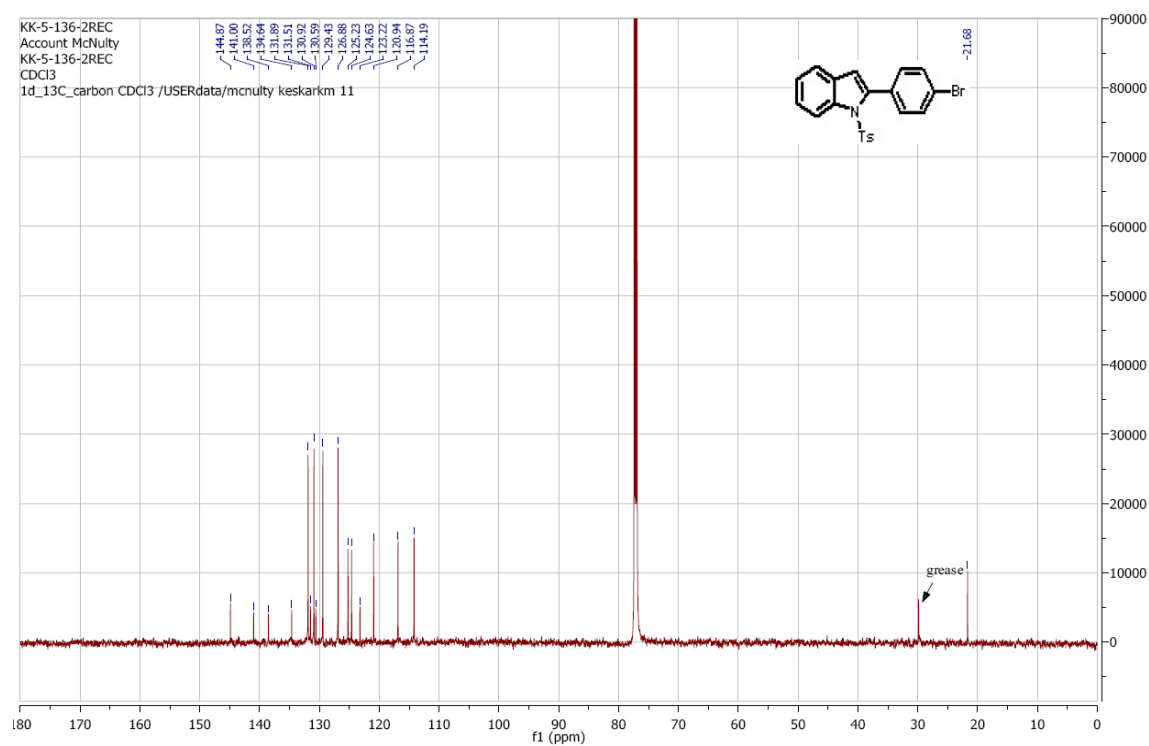
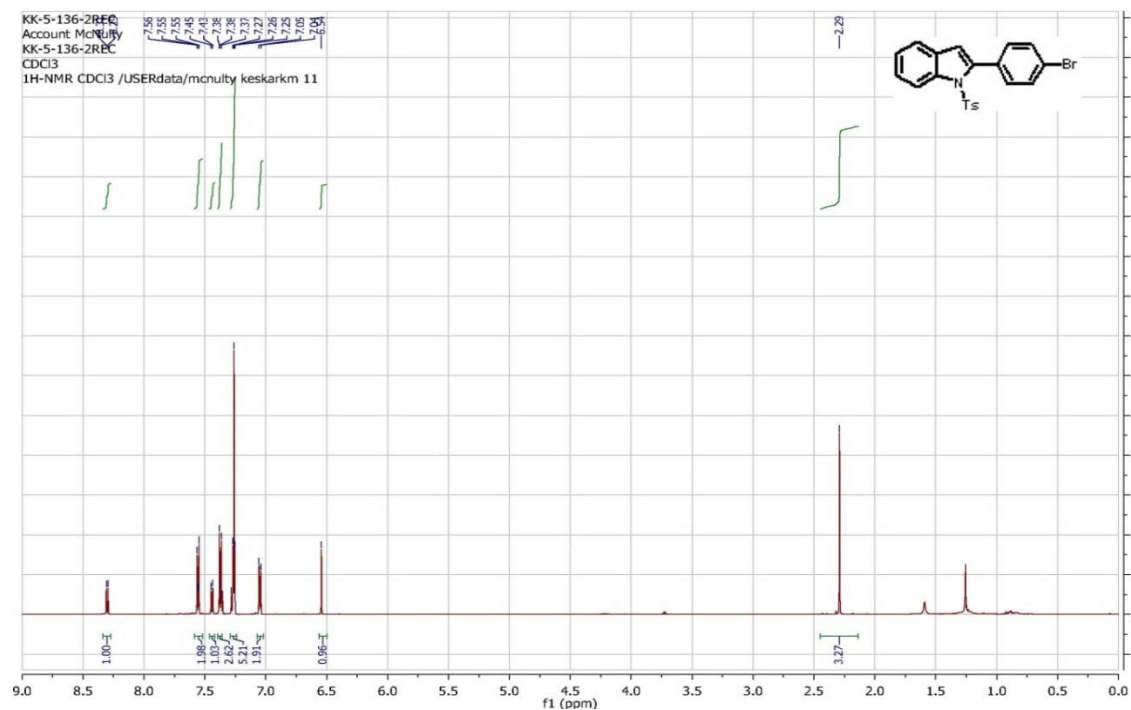
5-fluoro-2-phenyl-1-tosyl-1H-indole (Table 4-2, 2n): ^1H NMR (600 MHz, CDCl_3) δ 8.26 (dd, $J = 8.9, 4.5$ Hz, 1H), 7.49 (dd, $J = 7.8, 1.7$ Hz, 2H), 7.47 – 7.40 (m, 3H), 7.24 (d, $J = 8.4$ Hz, 2H), 7.11 – 7.07 (m, 2H), 7.05 (d, $J = 8.5$ Hz, 2H), 6.50 (s, 1H), 2.30 (s, 3H). ^{13}C NMR (151 MHz, CDCl_3) δ 160.3 (d, $J = 240.9$ Hz), 144.8, 144.1, 134.7, 134.5, 132.1, 131.8, 130.4, 129.4, 129.0, 127.7, 126.9, 118.0 (d, $J = 9.3$ Hz), 113.4, 112.7 (d, $J = 25.1$ Hz), 106.3 (d, $J = 24.0$ Hz), 21.6.

1-tosyl-2-(trimethylsilyl)-1H-indole (Table 4-2, 2o): ^1H NMR (600 MHz, CDCl_3) δ 7.87 (d, $J = 8.3$ Hz, 1H), 7.56 (d, $J = 8.3$ Hz, 2H), 7.51 (d, $J = 7.7$ Hz, 1H), 7.23 (t, $J = 7.3$ Hz, 1H), 7.18 (t, $J = 7.6$ Hz, 1H), 7.17 (d, $J = 8.3$ Hz, 2H), 6.95 (s, 1H), 2.32 (s, 3H), 0.46 (s, 9H). ^{13}C NMR (151 MHz, CDCl_3) δ 144.4, 143.1, 138.7, 136.4, 130.9, 129.8, 126.5, 125.0, 123.3, 121.7, 121.1, 114.2, 21.6, 0.7. HRMS: calcd. for $\text{C}_{18}\text{H}_{21}\text{NO}_2\text{SSi}[\text{M}]^+$ 343.1070; found 343.1062.

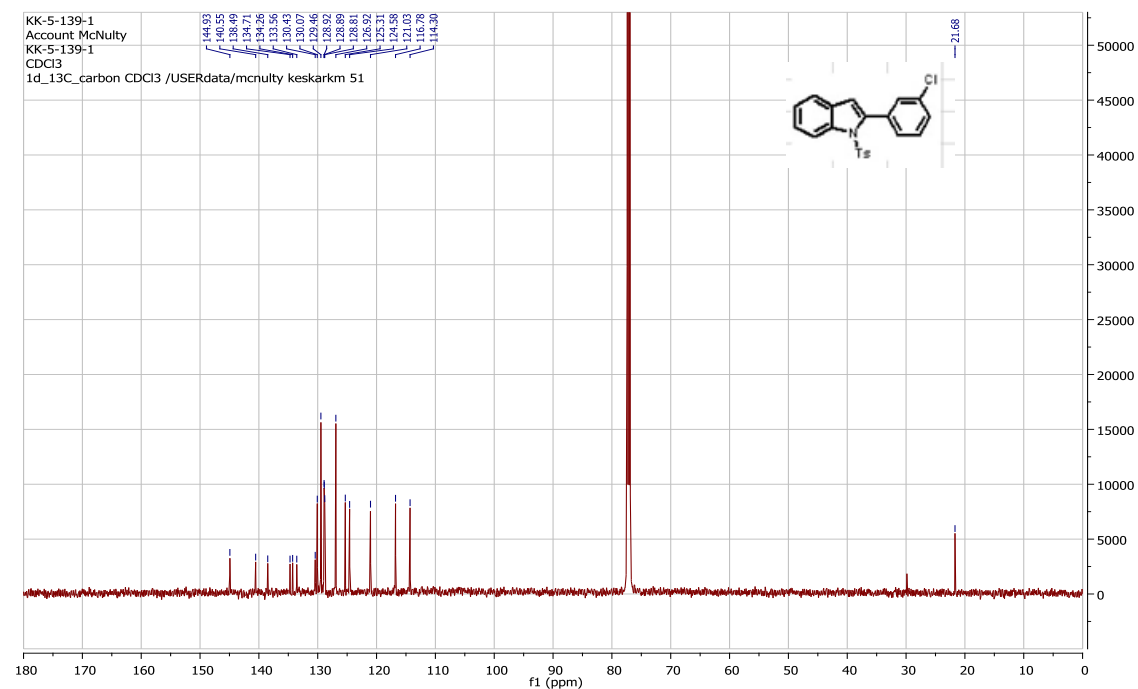
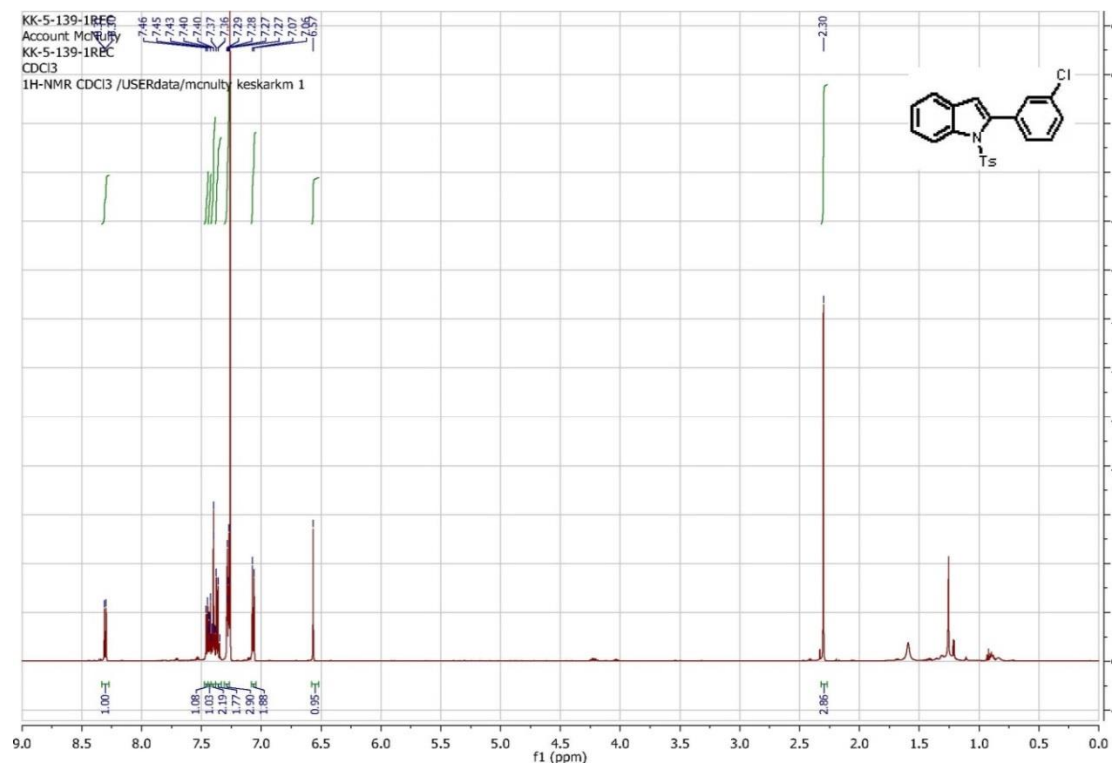
4.6 NMR Spectra

2-phenyl-1-tosyl-1H-indole (Table 4-2, 2a): (^1H and ^{13}C NMR)

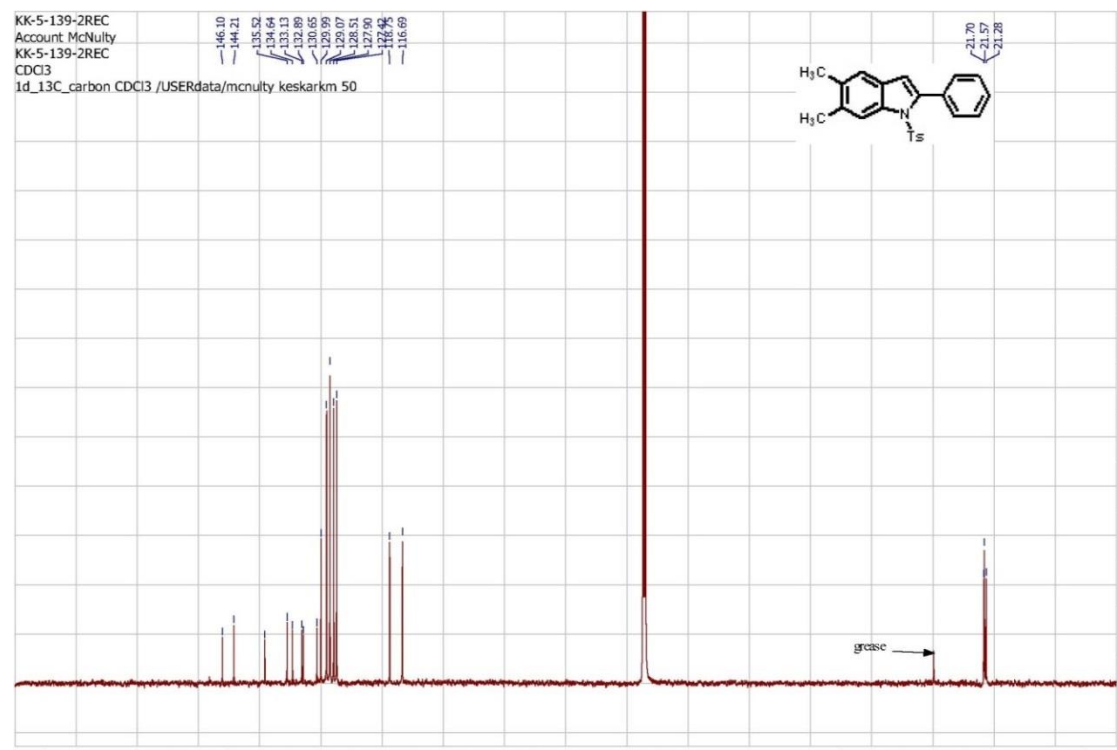
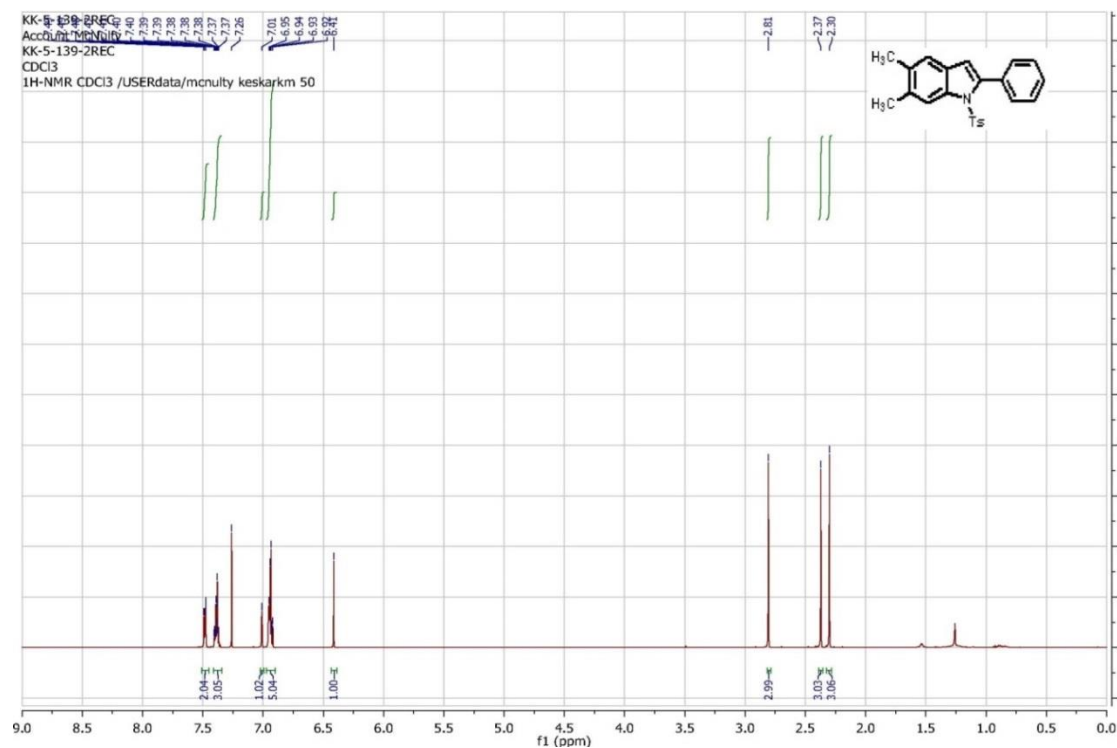


2-(4-bromophenyl)-1-tosyl-1H-indole (Table 4-2, 2b): (¹H and ¹³C NMR)

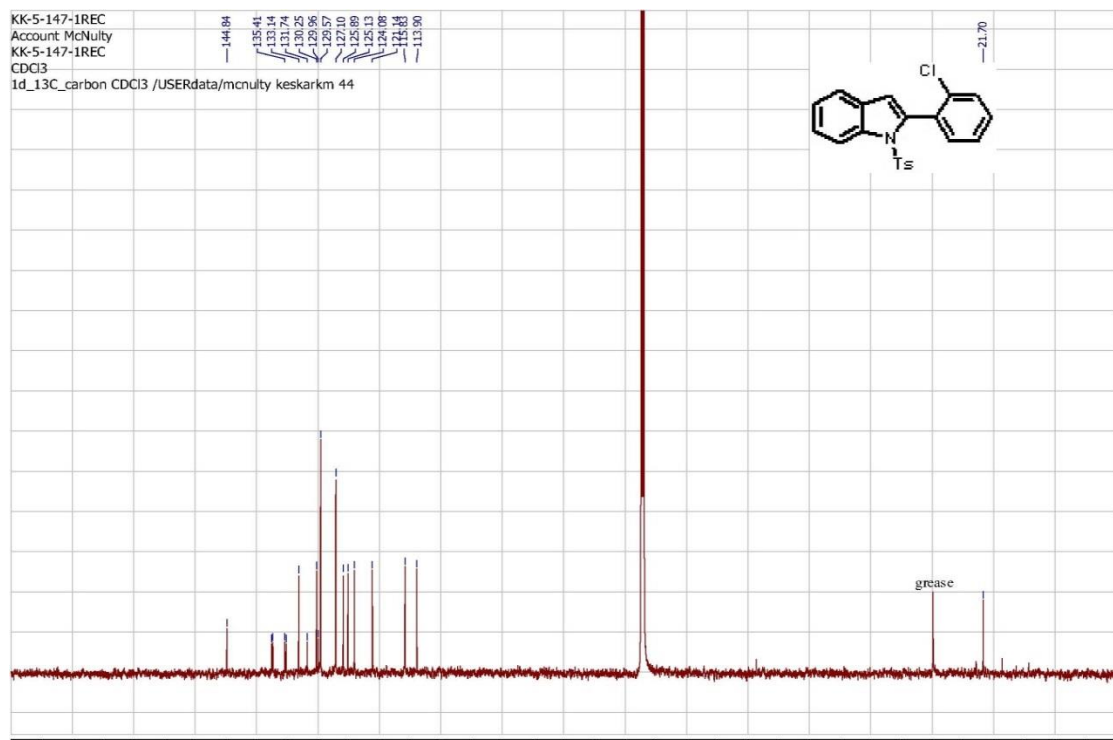
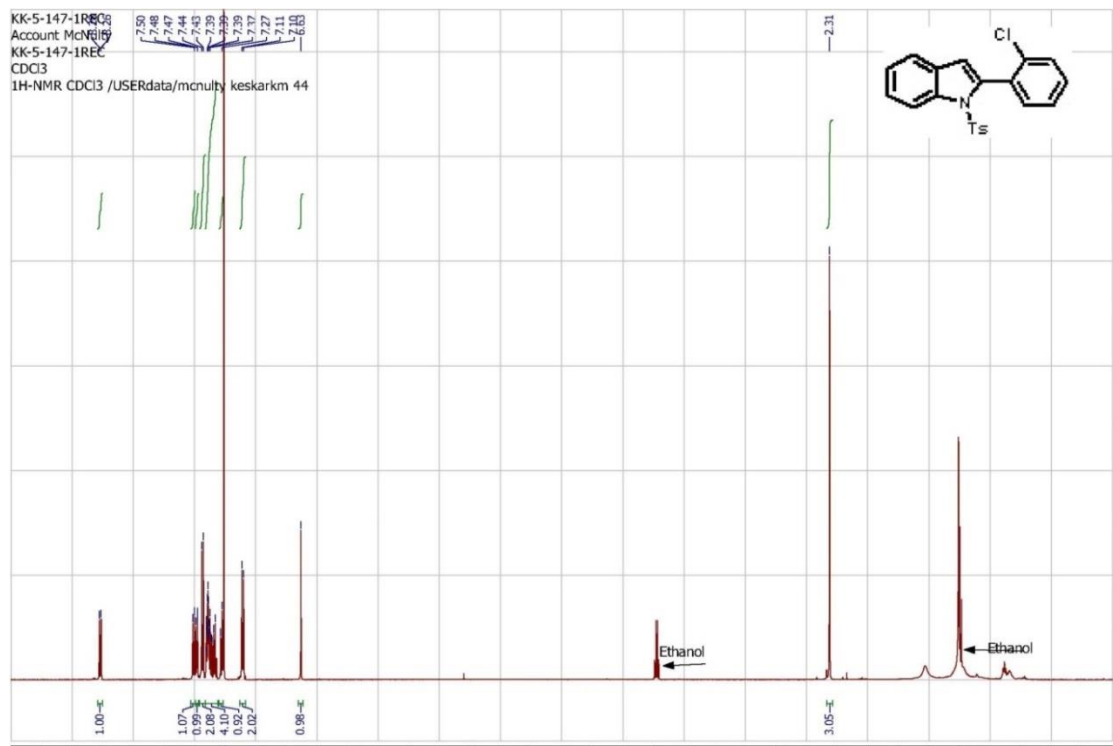
2-(3-chlorophenyl)-1-tosyl-1H-indole (Table 4-2, 2c): (^1H and ^{13}C NMR)



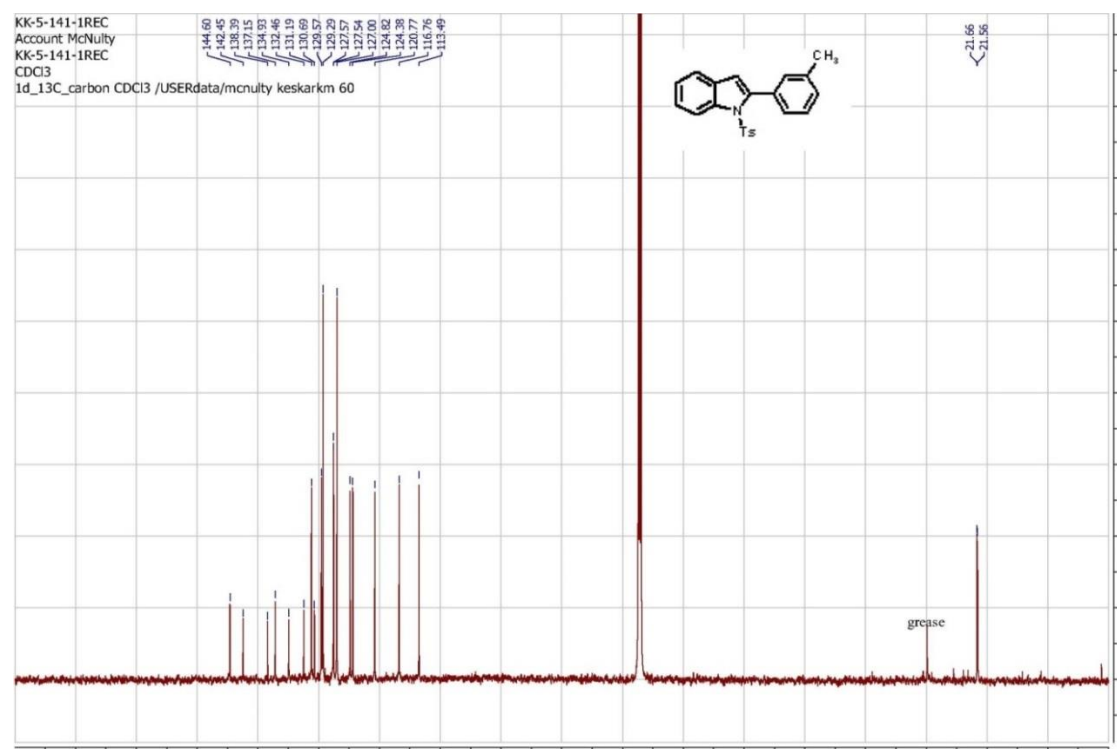
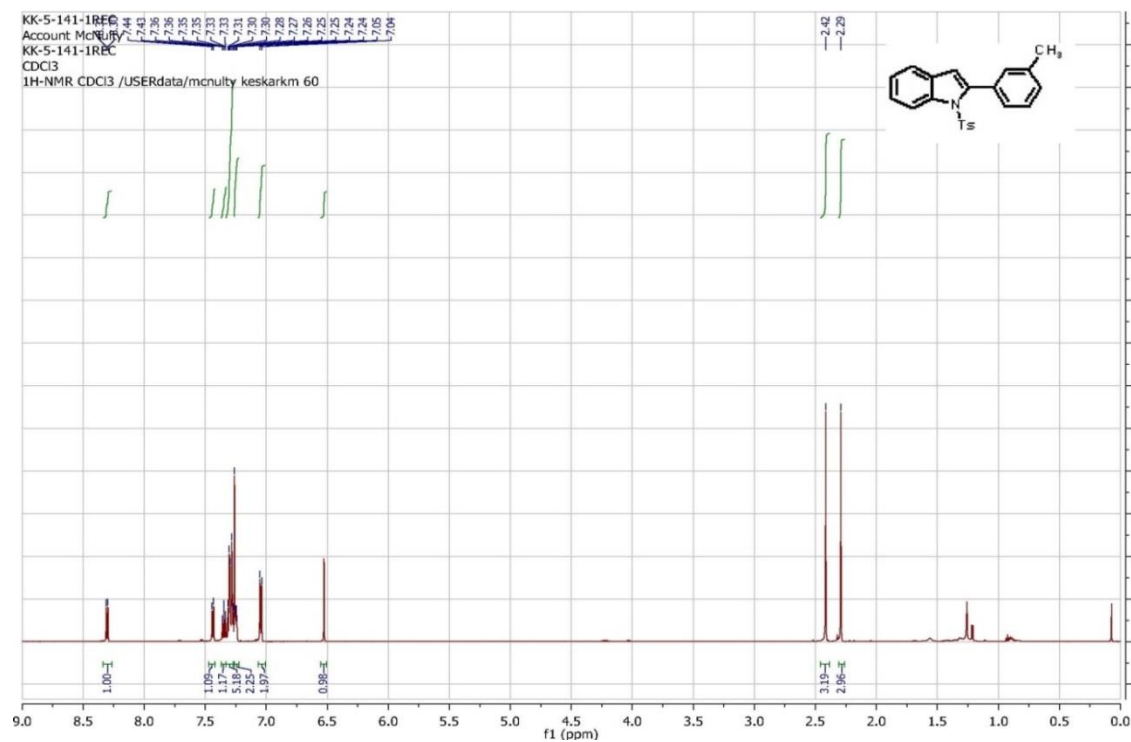
5,6-dimethyl-2-phenyl-1-tosyl-1H-indole (Table 4-2, 2d): (^1H and ^{13}C NMR)



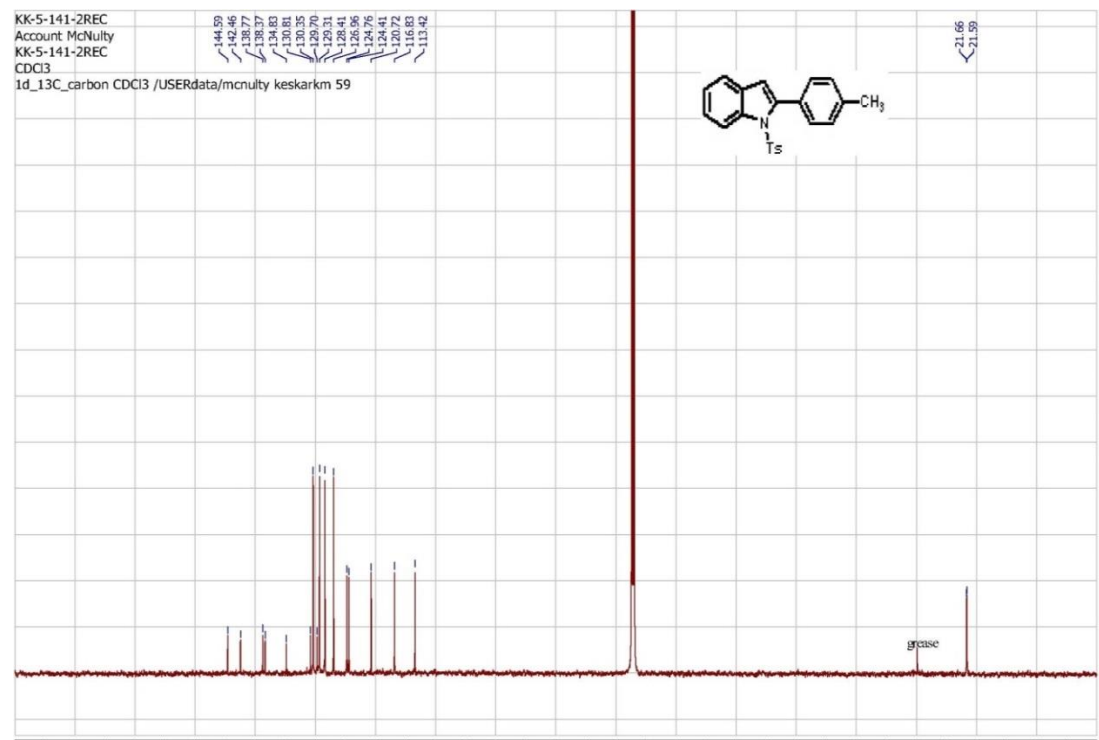
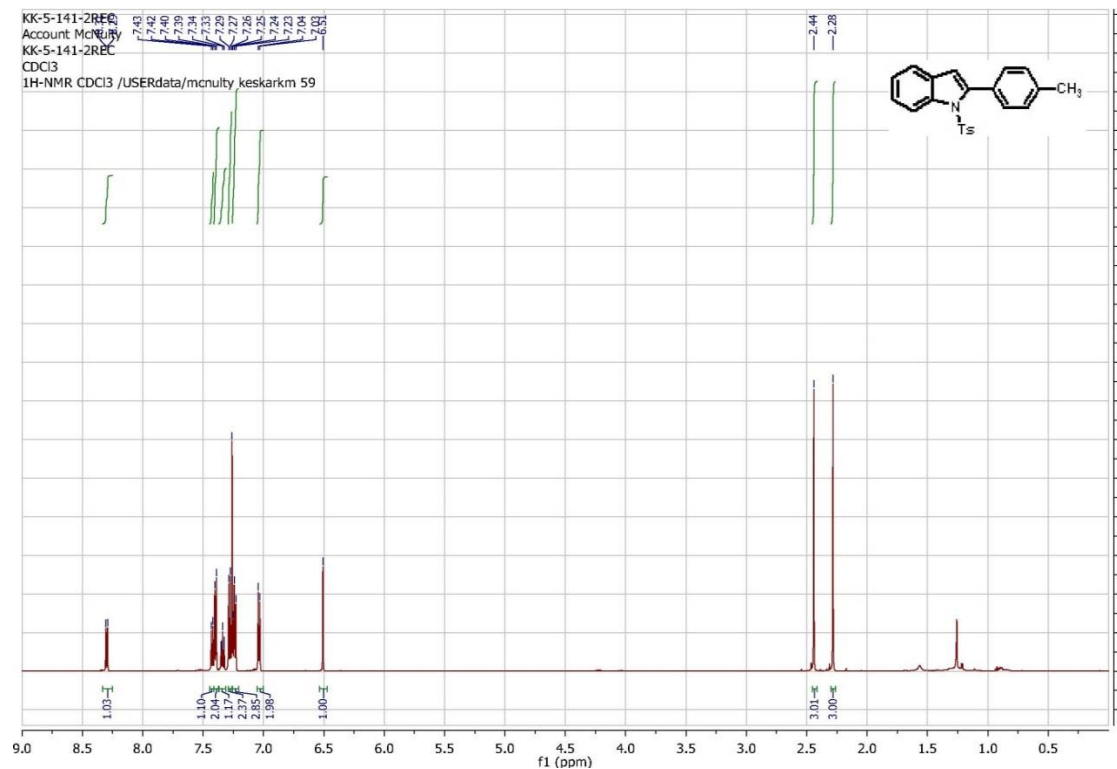
2-(2-chlorophenyl)-1-tosyl-1H-indole (Table 4-2, 2e): (^1H and ^{13}C NMR)



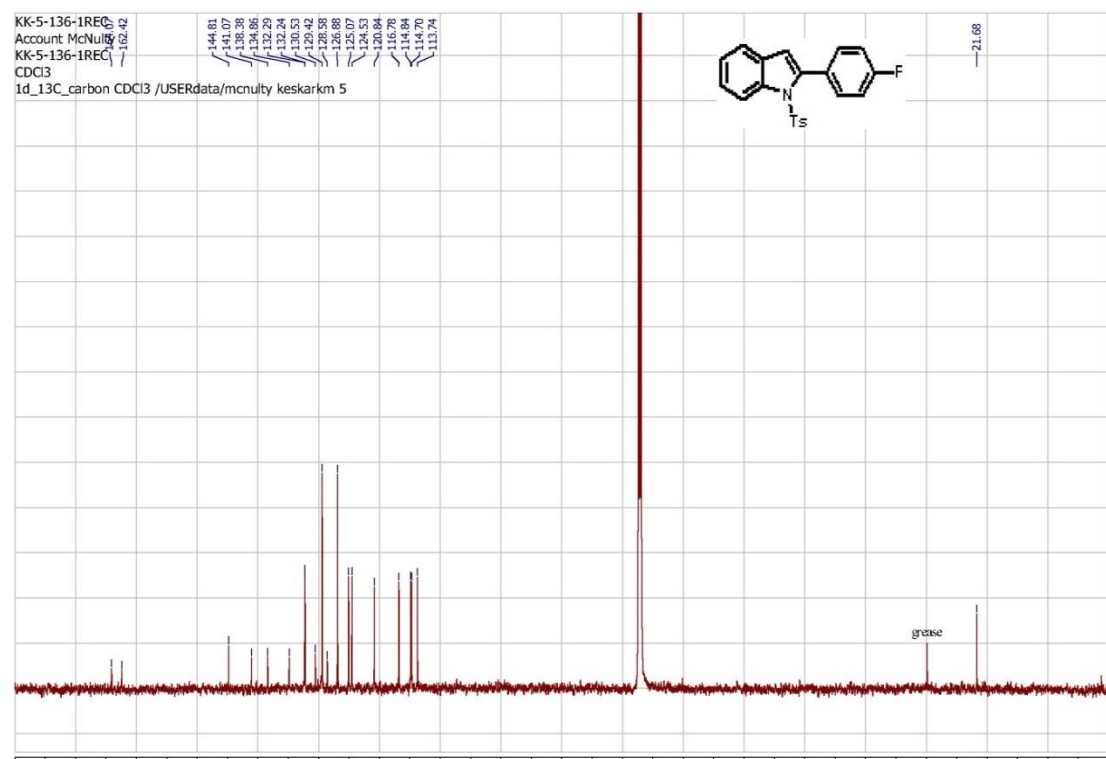
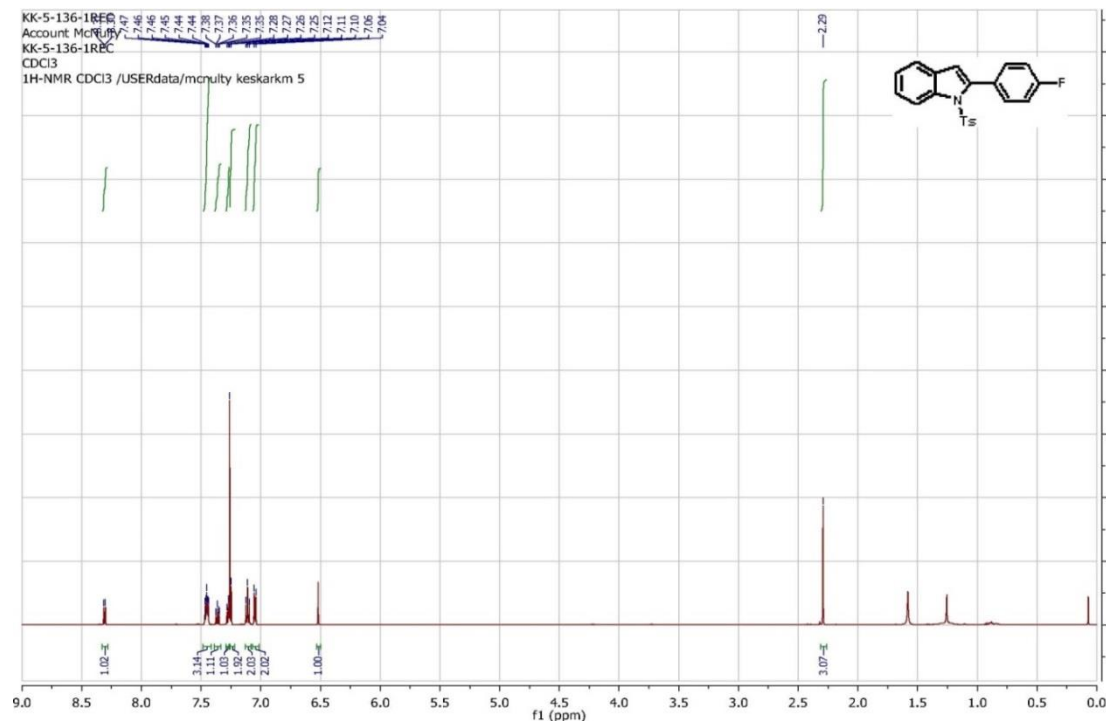
2-m-tolyl-1-tosyl-1H-indole (Table 4-2, 2f): (^1H and ^{13}C NMR)



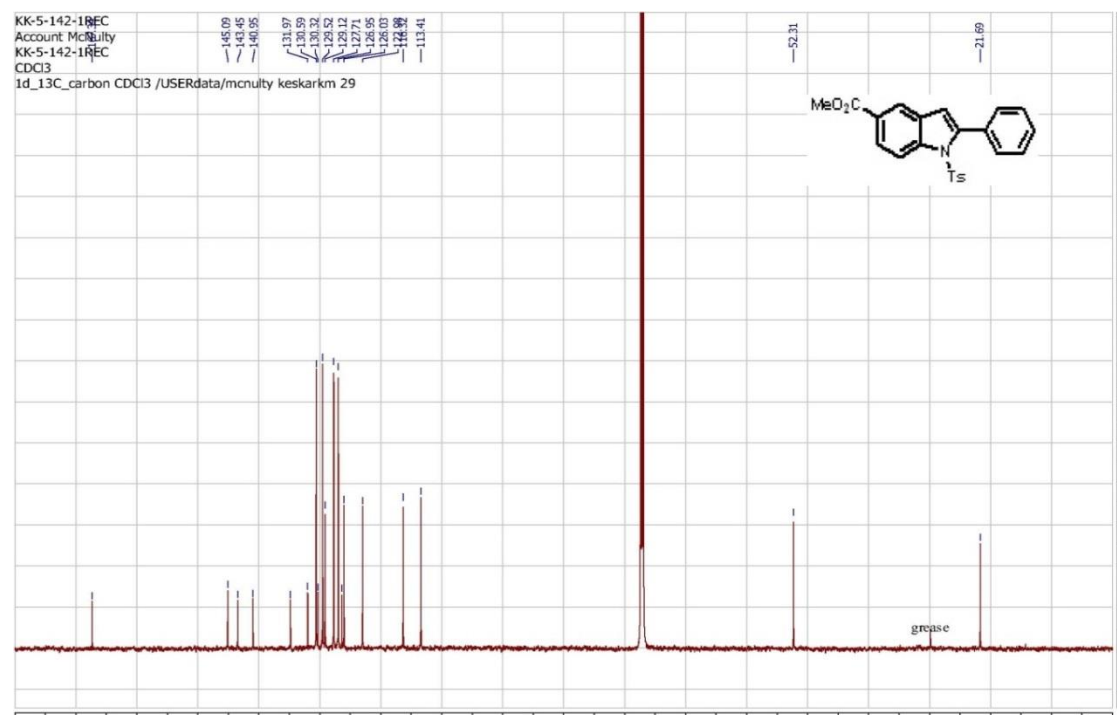
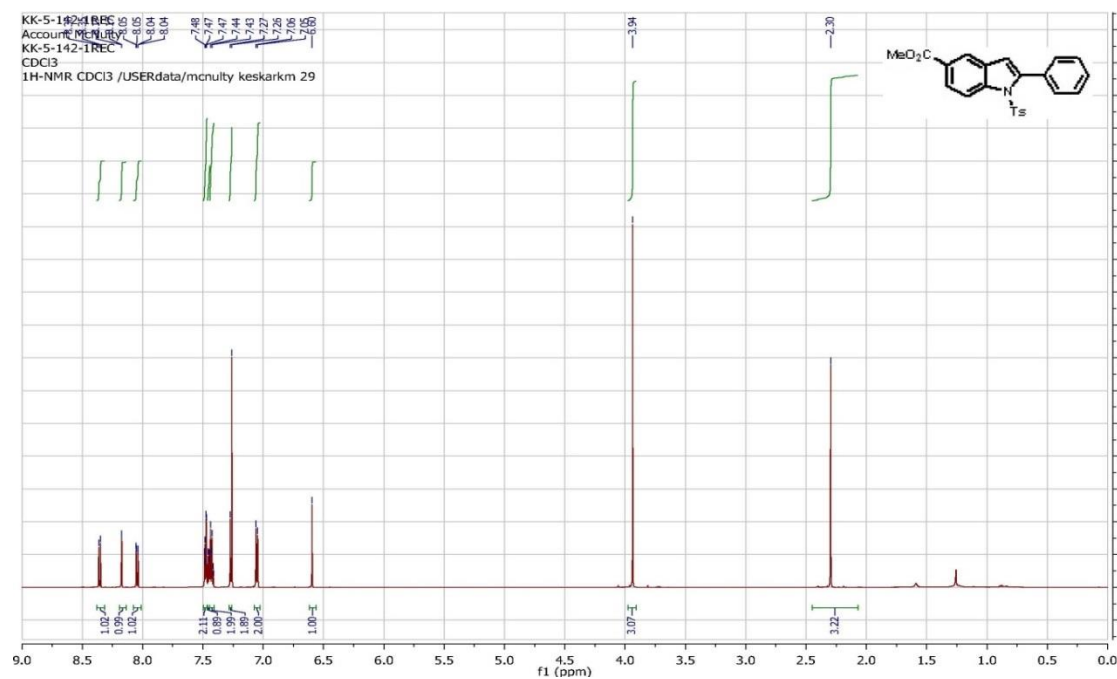
2-p-tolyl-1-tosyl-1H-indole (Table 4-2, 2g): (^1H and ^{13}C NMR)



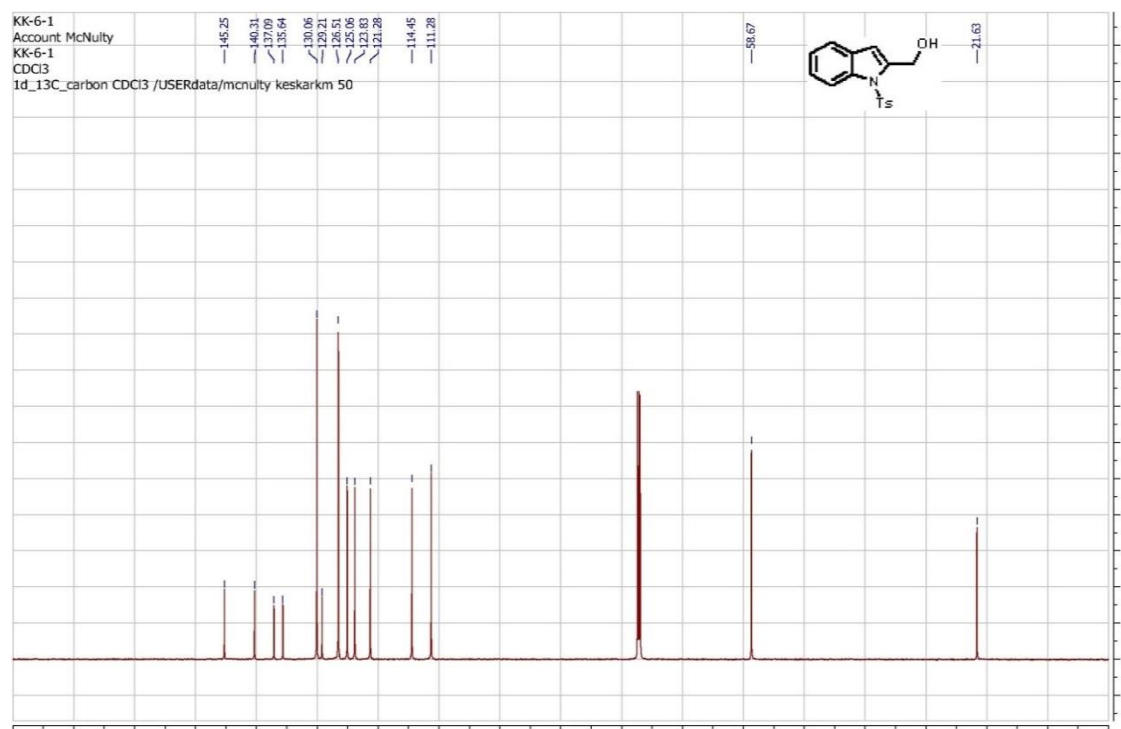
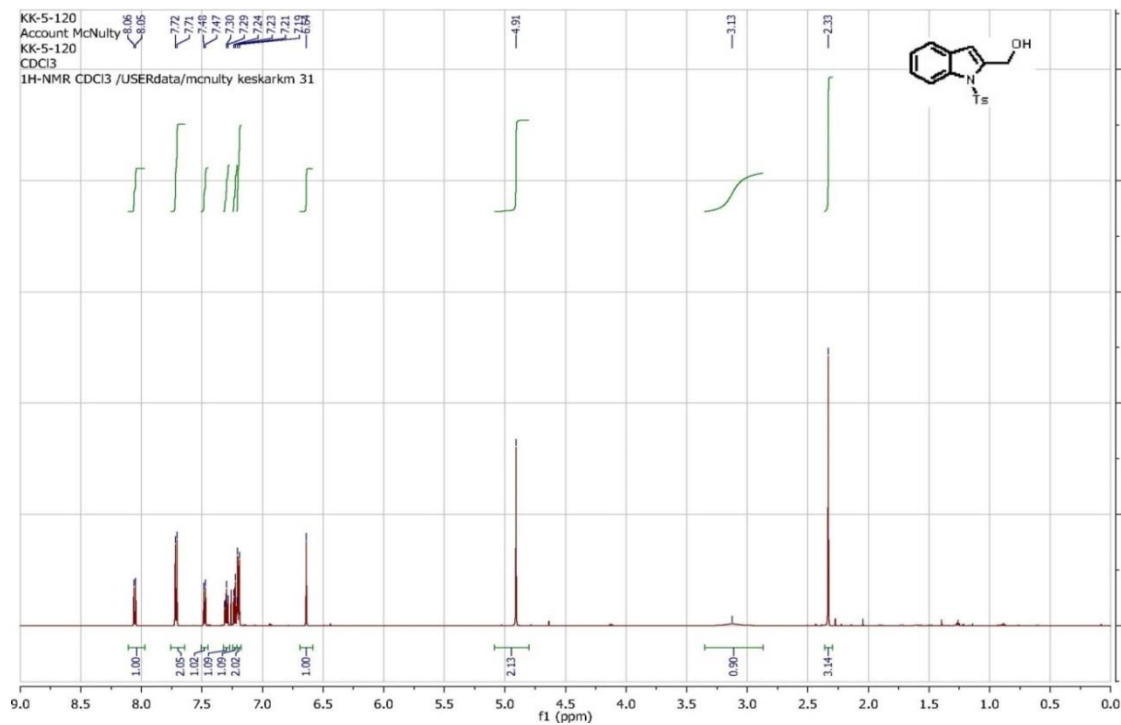
2-(4-fluorophenyl)-1-tosyl-1H-indole (Table 4-2, 2h): (^1H and ^{13}C NMR)



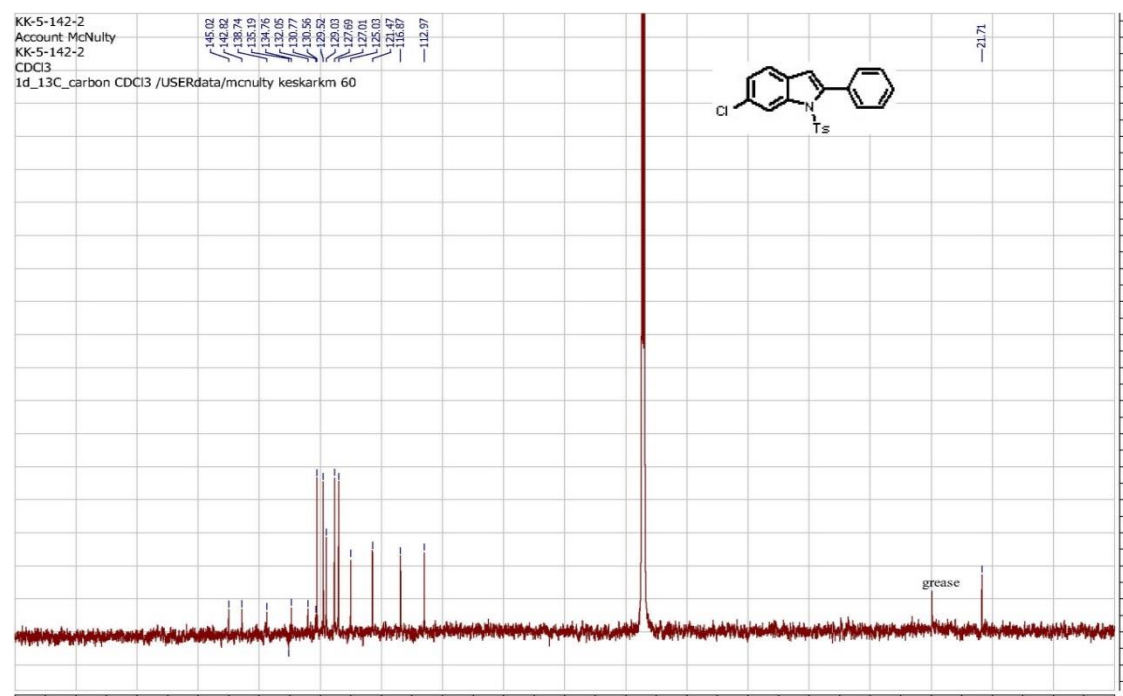
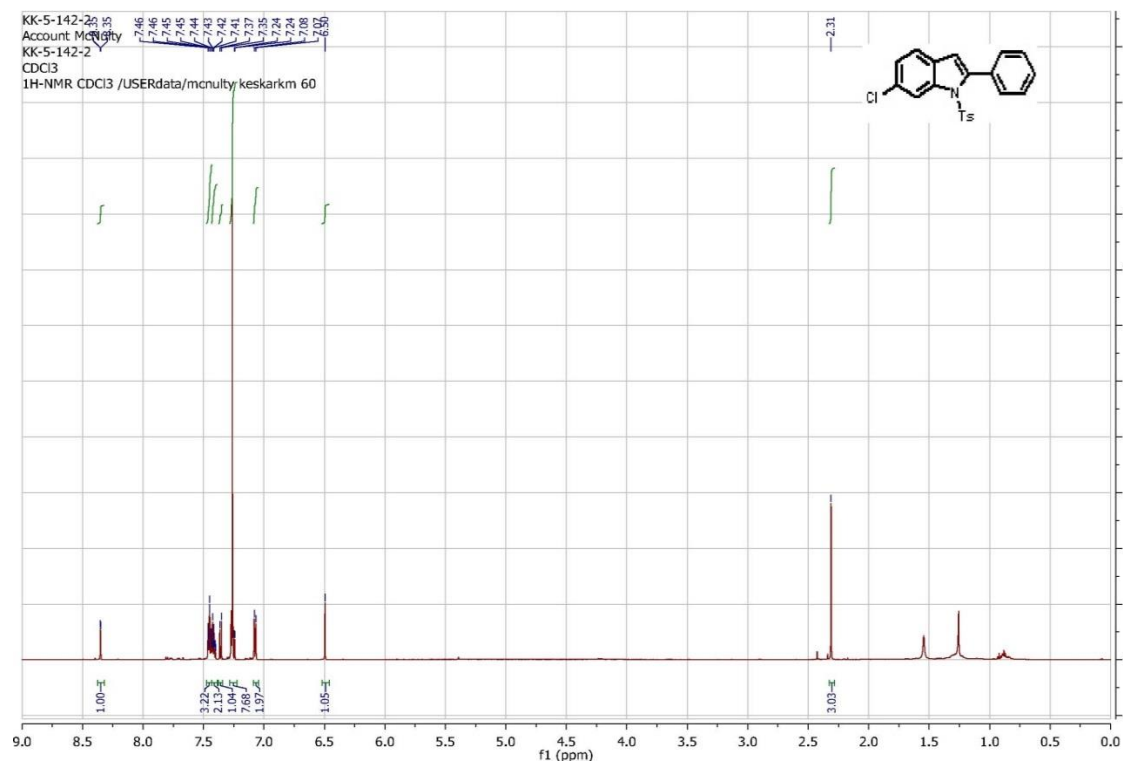
methyl 2-phenyl-1-tosyl-1H-indole-5-carboxylate (Table 4-2, 2i): (^1H and ^{13}C NMR)



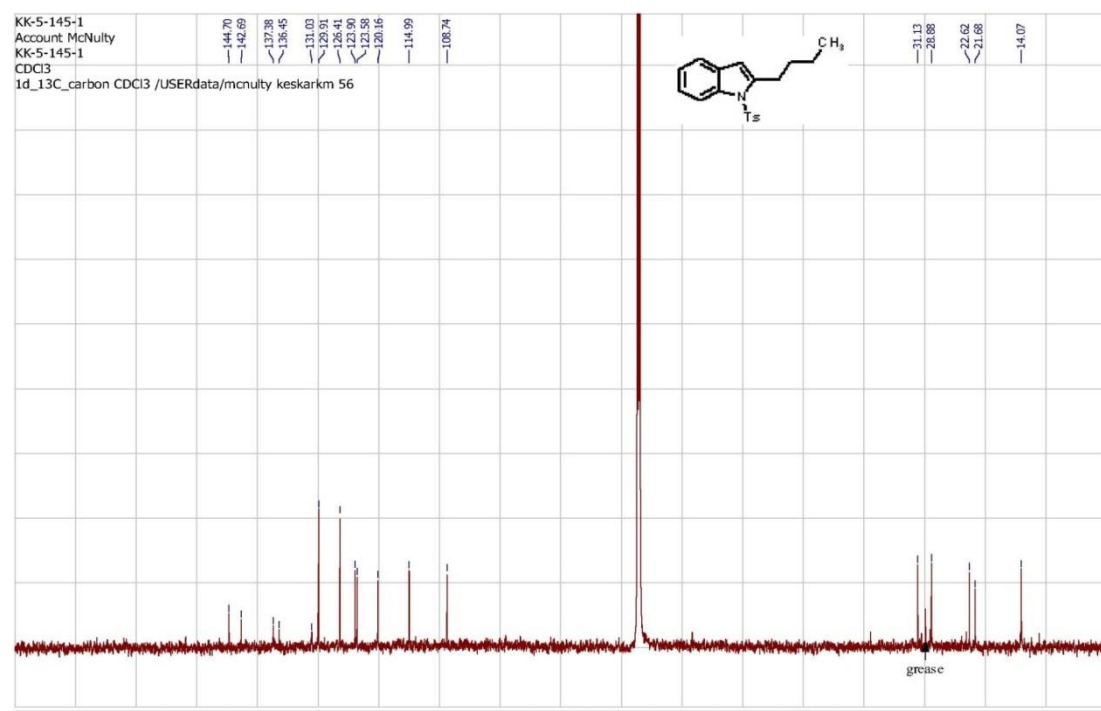
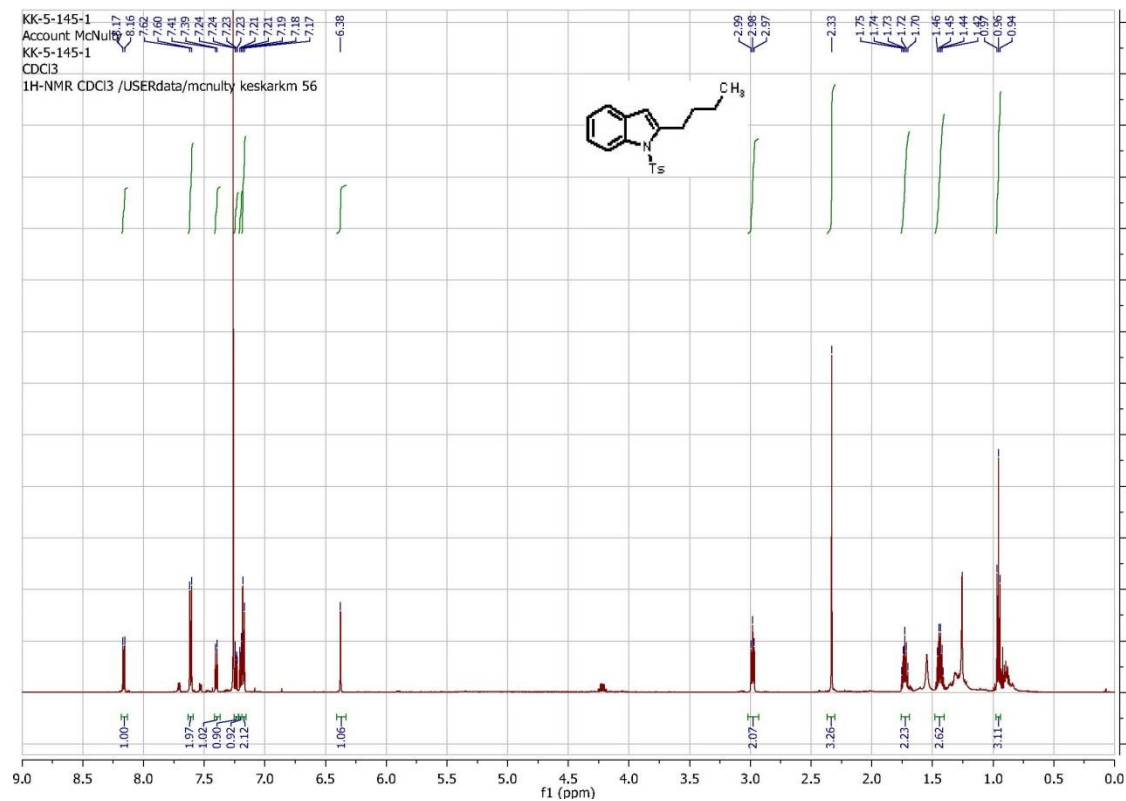
(1-tosyl-1H-indol-2-yl)methanol (Table 4-2, 2j): (^1H and ^{13}C NMR)



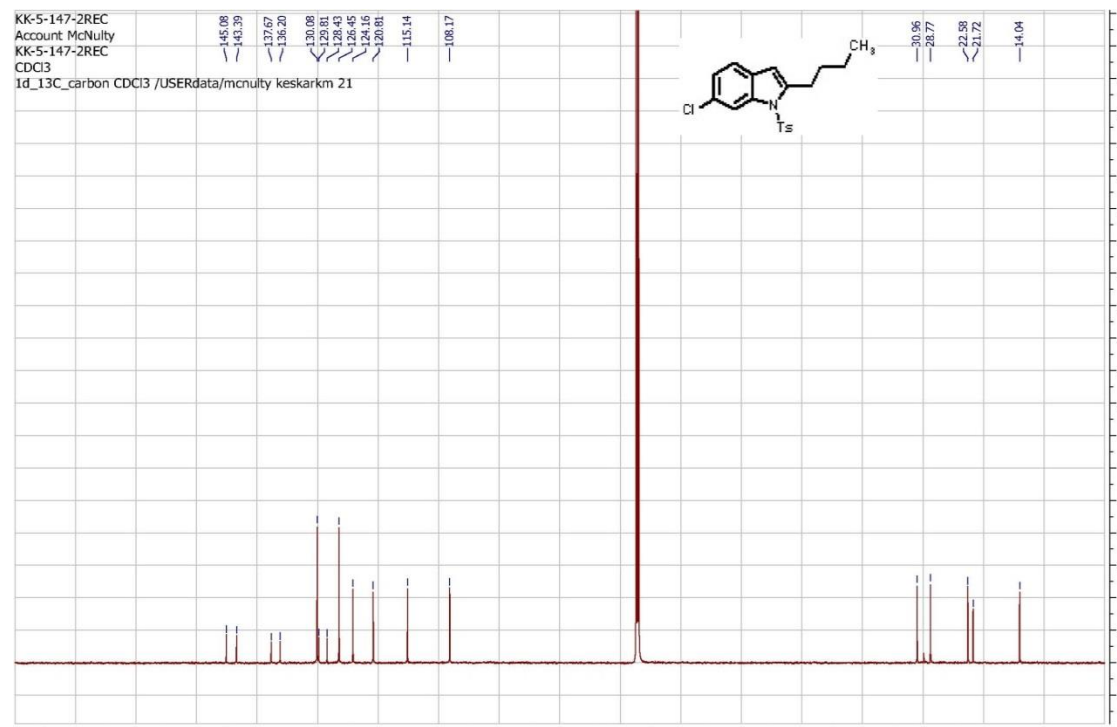
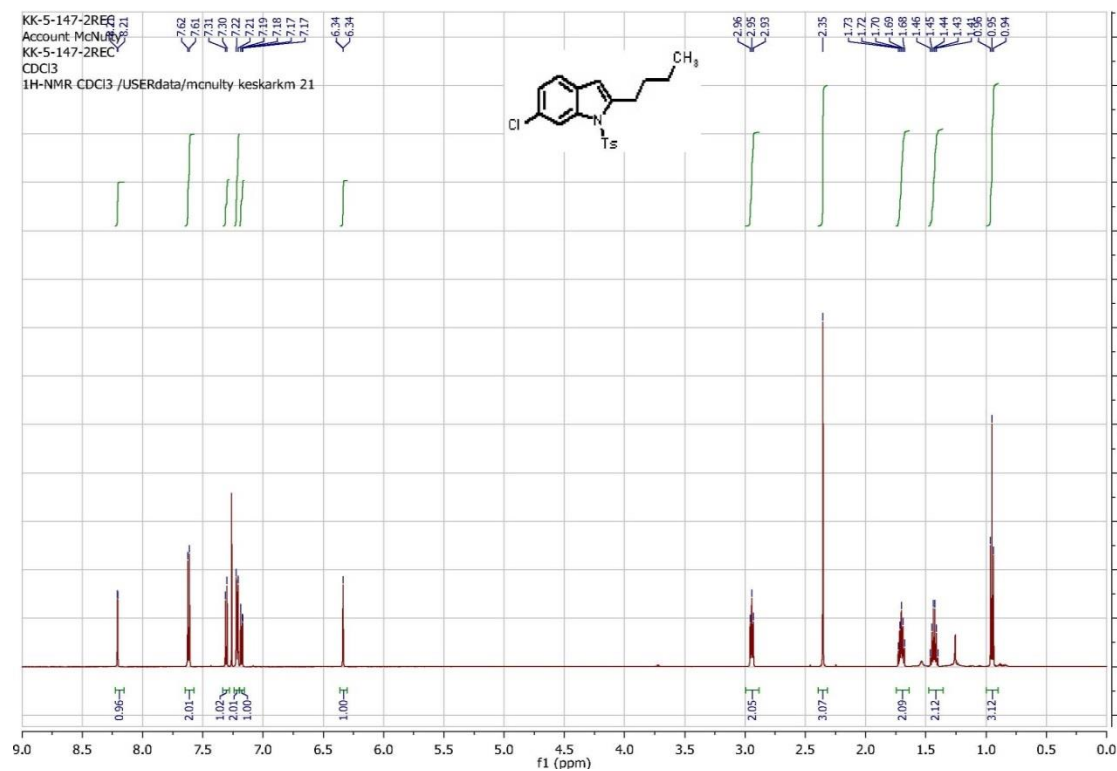
6-chloro-2-phenyl-1-tosyl-1H-indole (Table 4-2, 2k): (^1H and ^{13}C NMR)



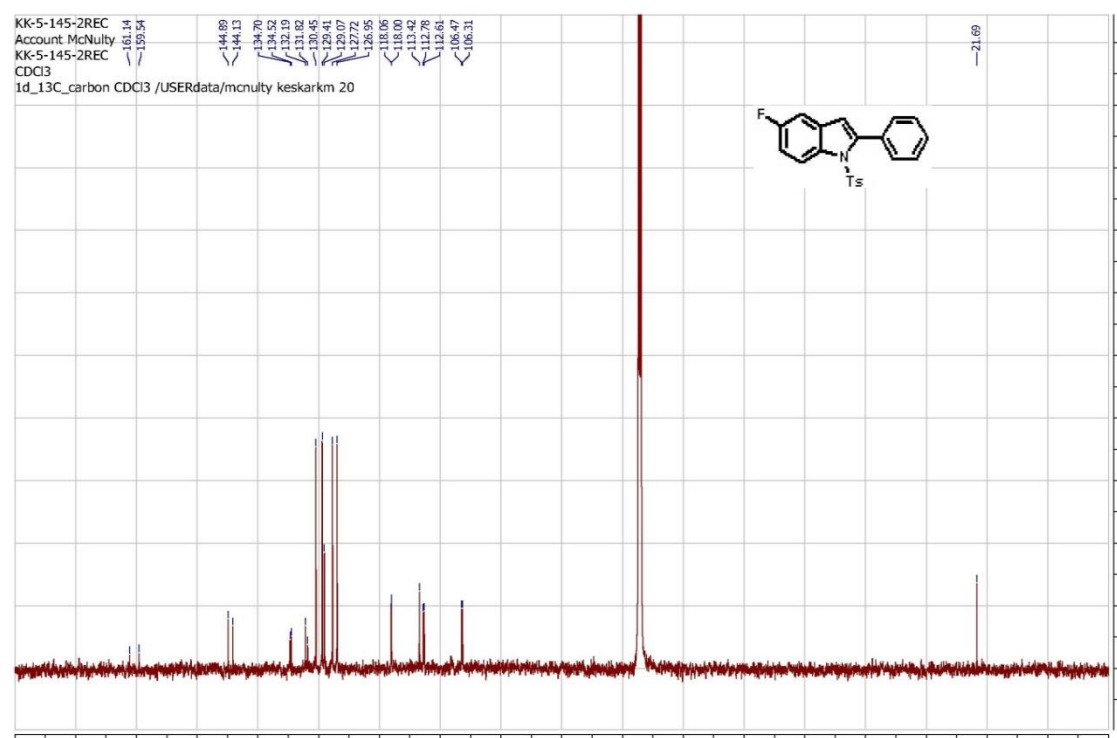
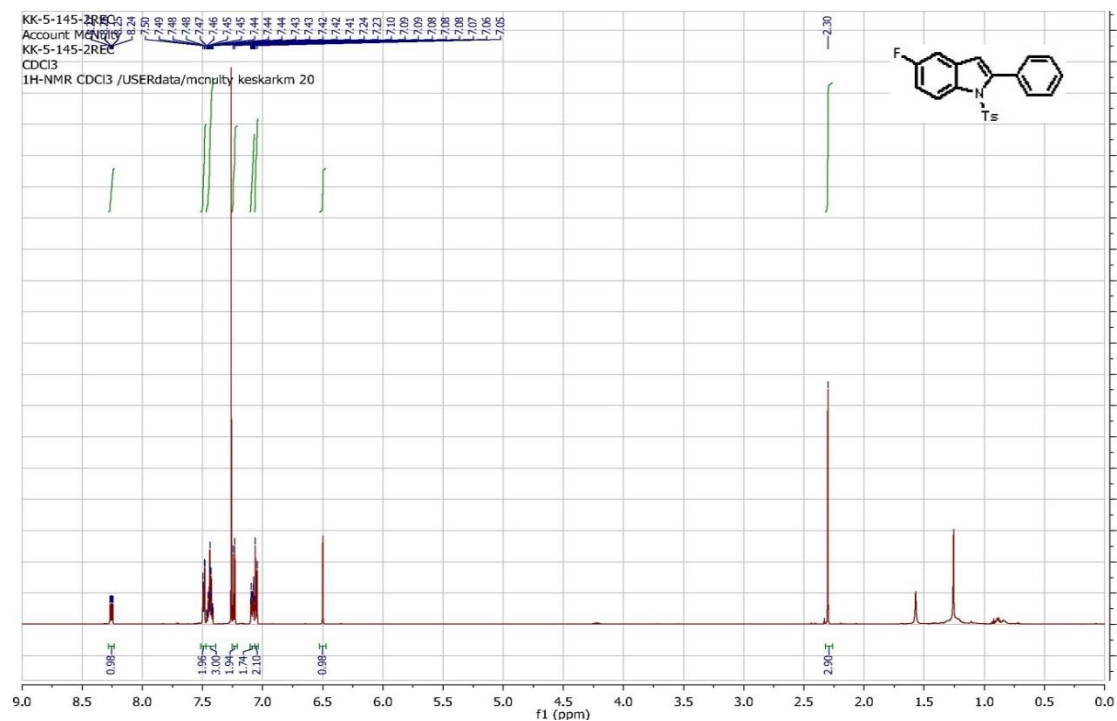
2-butyl-1-tosyl-1H-indole (Table 4-2, 2I): (^1H and ^{13}C NMR)



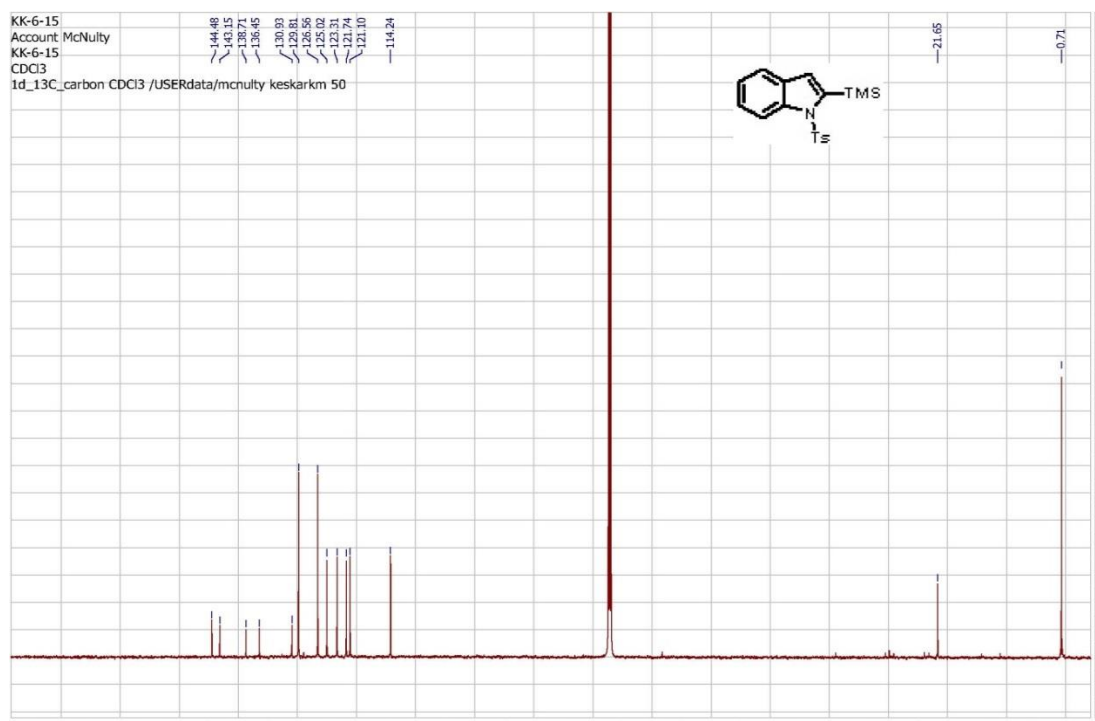
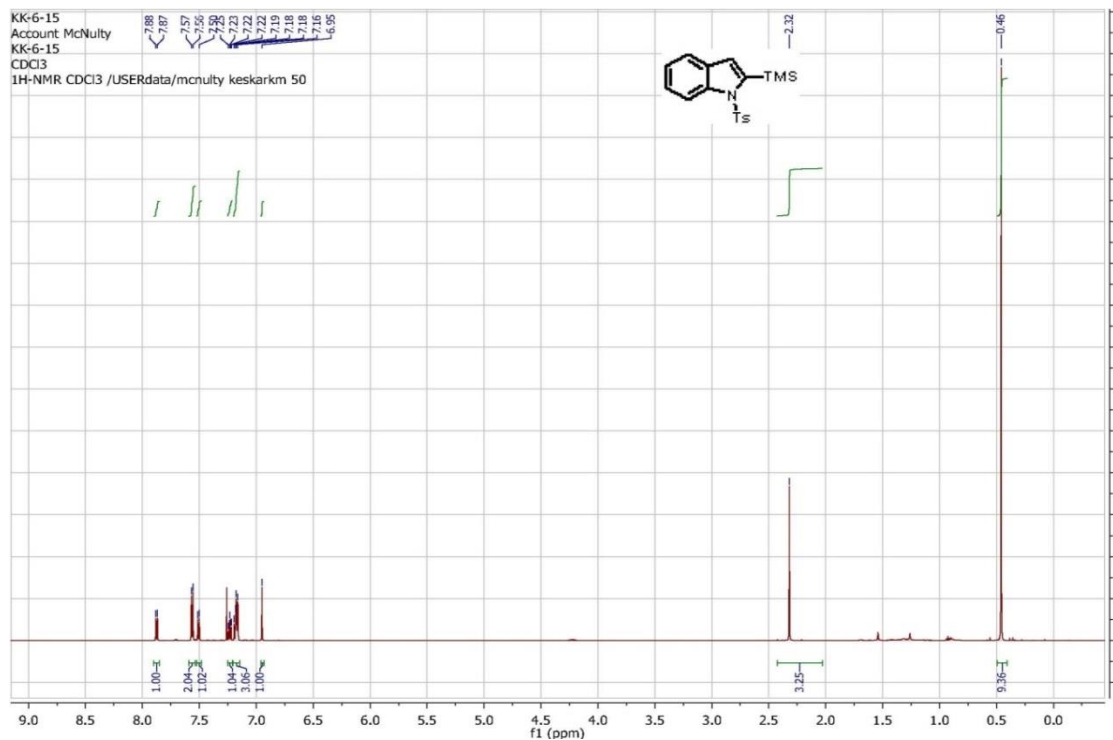
2-butyl-6-chloro-1-tosyl-1H-indole (Table 4-2, 2m): (^1H and ^{13}C NMR)



5-fluoro-2-phenyl-1-tosyl-1H-indole (Table 4-2, 2n): (^1H and ^{13}C NMR)



1-tosyl-2-(trimethylsilyl)-1H-indole (Table 4-2, 2o): (^1H and ^{13}C NMR)



Chapter V: Phthalide: a direct building-block towards P,O and P,N hemilabile ligands: Application in the palladium-catalyzed Suzuki-Miyaura cross-coupling of aryl chlorides.

Reproduced from Reference IV-(List of publications) with permission from the The Royal Society of Chemistry

5.1 Introduction

Hemilabile P,O and P,N functionalized ligands^{1a,b} have emerged^{1a,b} and continue to advance as important effectual ligands with applications to an expanding array of metal catalyzed cross-coupling reactions as well as hydrogenation and cycloaddition reactions. The success of hemilabile ligands in filling methodological gaps in transition metal catalysis has inspired the development of efficient routes toward new hemilabile ligand types, select examples of which are listed in **Figure 5-1**. Guram and co-workers developed the P,O and P,N-type ligands **A** and **B** for Suzuki–Miyaura cross-coupling of aryl chlorides.^{1c} Kwong and co-workers introduced the indolylphosphines **C**^{1d,e} while Pfaltz and co-workers have extensively utilized phosphine-oxazoline ligand **D** in hydrogenation and other processes.^{1f} Stradiotto and co-workers have introduced similar hemilabile ligands for aryl chloride amination^{1g} and alkyne hydroamination.^{1h}

Our group has been involved in the design and application of useful phosphine ligands over the last decade.² We recently reported the synthesis and application of the P,O and P,N-type ligands **E** and **F** (**Figure 5-1**) for Suzuki–Miyaura coupling reactions,³ including successful reaction of deactivated, *ortho*-substituted aryl chlorides. Silver(I) complexes of the hemilabile ligand **G** were demonstrated to be highly effective in promoting the first examples of homogeneous silver catalyzed azide-alkyne cycloaddition reactions.⁴ An extensive structure-activity study with ligands of type **G** revealed

the importance of the hemilabile ligand in promoting the catalytic cycle through on-again, off-again polarization of intermediates.⁴

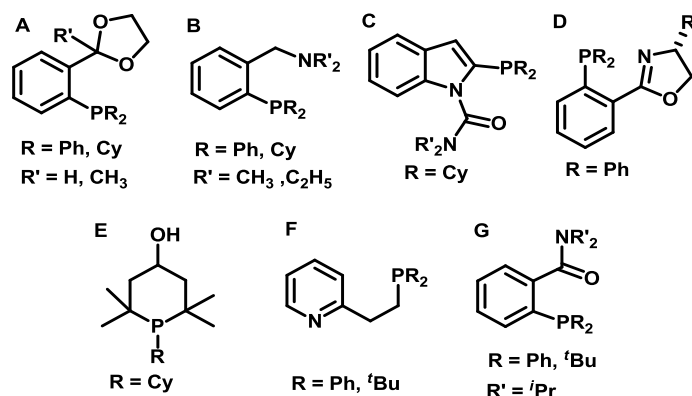
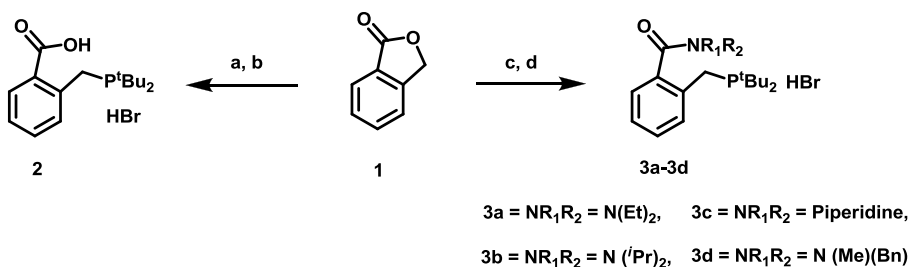


Figure 5-1. Hemilabile Examples of P,O and P,N type ligands employed in metal-mediated cross-coupling and other processes.

The P,O ligands **E** are available in only two synthetic steps from commodity materials and the P,N ligand **F** in only one step, involving free radical addition of a secondary phosphine to 2-vinyl pyridine. Our criteria are that the ligands should be available in a few steps from commodity materials and, in view of air-sensitivity of many phosphines, involve robust conditions in the preparation, isolation and handling of the ligand. It occurred to us that the commodity lactone phthalide **1** could serve as a pivotal building block in the synthesis of new P,N and/or P,O ligands as homologues of ligand type **G**, should opening of the lactone be feasible through treatment with either a Bronsted or Lewis acid and a secondary phosphine (**Scheme 5-1**). Secondary and tertiary phosphine HBr⁵ and HBF₄ salts⁶ have proven to be useful air-stable phosphine equivalents. In this paper, we report our success opening this phthalide route toward stable HBr salts of new hemilabile ligands and application in the Pd-mediated Suzuki-Miyaura cross-coupling reaction.

5.2 Results and Discussion

Phthalide **1** was observed to readily enter into reaction with commercial hydrogen bromide (33%) in acetic acid yielding α -bromo-*ortho*-toluic acid in good yield without need of purification.⁷ Treatment of the resulting α -bromo-*ortho*-toluic acid with ditertiarybutyl phosphine in acetone yielded the carboxylic acid functionalized ligand **2** in the form of its air stable HBr salt in 70% overall isolated yield from **1**. For the synthesis of the amide functionalized ligands **3a-3d**, (Scheme 5-1) a Lewis acid catalyzed ring opening approach was investigated.



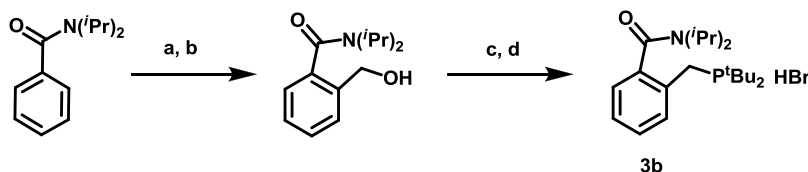
(a) HBr-HOAc 70 °C, then. (b) ^tBu₂PH, acetone, reflux, 70%. (c) AlCl₃, R₁R₂NH, 88-94%. (d) PBr₃, CH₂Cl₂, 0 °C, then ^tBu₂PH, acetone, reflux, 99%.

Scheme 5-1. Synthesis of P,O and P,N-type hemilabile ligands from **1**.

Phthalide readily opened with a catalytic amount of aluminium trichloride in the presence of a variety of secondary amines, such as diethylamine, piperidine and *N*-methyl-*N*-benzyl amine, yielding the desired amides.⁸ Very hindered amines such as *N,N* diisopropylamine failed to react and an alternative approach (vide infra) was developed to access ligand **3b**. The ring opening approach yielded the amides **3a**, **3c** and **3d** exclusively as the primary *ortho*-benzylic alcohols, providing the handle for attachment of the phosphine moiety. The alcohols were converted to their benzylic bromide derivatives quantitatively with PBr₃ in dichloromethane and subsequently reacted with ditertiarybutyl phosphine in acetone to yield ligands **3a**, **3c** and **3d** (Scheme 5-1). These

ligands are obtained in isolated yields of between 88-94% from phthalide over this two-step (**1** to **3a**, **3c** and **3d**) sequence (**Scheme 5-1**).

We previously demonstrated the *N,N* diisopropylamide functionalized hemilabile ligand (**Figure 5-1**, type **G**) to be most effective in the Ag-mediated Huisgen reaction.⁴ In order to build a comprehensive ligand series for screening purposes, we developed an alternative process for the synthesis of ligand **3b** as shown (**Scheme 5-2**). Commercially available *N,N*-diisopropylbenzamide was subjected to directed *ortho*-lithiation and formylated with DMF yielding the *ortho*-aldehyde cleanly. The formyl derivative was stirred overnight with NaBH₄ in methanol at room temperature to give the benzylic alcohol intermediate in good yield,⁹ which was then converted to ligand **3b** quantitatively under the conditions reported above.



(a) *s*-BuLi (1.1 equiv), THF, then DMF (quench). (b) NaBH₄, MeOH, 0 °C, 70%. (c) PBr₃, CH₂Cl₂, 0 °C, (d) ^tBu₂PH, acetone, reflux, 99%.

Scheme 5-2. Synthesis of ligand **3b** from *N,N*-diisopropylbenzamide.

The palladium catalyzed Suzuki-Miyaura cross-coupling reaction of aryl halides with aryl-boron derivatives represents a simple and effective route towards synthesis of substituted biaryls.¹⁰ Biaryl substructures are well represented among important classes of organic compounds with applications in pharmaceutical, agrochemical and materials chemistry.¹¹

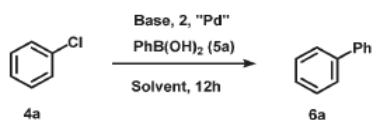
Aryl iodides and bromides are the most common halide partners used in Suzuki cross-coupling reactions. Although more readily available, aryl chlorides are

more challenging and individual cases often require optimized reaction conditions with a particular ligand and Pd source.

In general, sterically hindered, electron-rich mono- or bidentate phosphines have proved to be useful in effecting these catalytic cycles.¹² The employment of *N*-heterocyclic carbene ligands¹³ and, more recently, the use of hemilabile P,O and P,N-type ligands,^{1,3} has proven effective in Pd-catalyzed Suzuki-Miyaura reaction of challenging aryl chlorides.

The general utility of ligands **2** and **3a-3d** was investigated employing the Pd-catalyzed Suzuki-Miyaura cross-coupling reaction of chlorobenzene **4a** with phenylboronic acid **5a** as a starting point. We screened the carboxylic acid P,O-ligand **2** under a variety of conditions (**Table 5-1**). Not surprisingly, choice of base was observed to be critical with CsF proving optimal, yielding biphenyl in good yield (76%). Stronger bases (K₃PO₄, Et₃N, Cs₂CO₃, NaO^tBu) proved ineffective for the coupling reaction giving poor or trace (TLC detectable) conversion (**Table 5-1**).¹⁴

Table 5-1. Suzuki-Miyaura cross coupling reaction of chlorobenzene with Pd-complexes of ligand **2**.



Entry	Base	"Pd"	Solvent	Isolated yield (%)
1	K ₃ PO ₄	Pd(OAc) ₂	PhMe	Trace
2	K ₃ PO ₄	Pd(OAc) ₂	Dioxane	Trace
3	K ₃ PO ₄	Pd ₂ (dba) ₃	PhMe	52
4	CsF	Pd ₂ (dba) ₃	PhMe	76
5	Et ₃ N	Pd ₂ (dba) ₃	PhMe	Trace
6	Cs ₂ CO ₃	Pd ₂ (dba) ₃	PhMe	37
7	NaO ^t Bu	Pd ₂ (dba) ₃	PhMe	13
8	K ₂ CO ₃	Pd ₂ (dba) ₃	PhMe	28

Reaction conditions: **4a** (0.040 g, 0.355 mmol, 1.0 equiv.), **5a** (0.052 g, 0.426 mmol, 1.2 equiv.), base (1.065 mmol, 3.0 equiv.), Pd(OAc)₂ (2.0 mol%) or, Pd₂(dba)₃ (2.0 mol% (4.0 mol% Pd)), ligand **2** (3.0 mol%), solvent (2.5 mL), 110 °C.

Table 5-2. Screening phthalide-derived ligands **3a-3d** in the Suzuki-Miyaura cross-coupling reaction.

Reaction scheme: 4-chlorobenzene (**4a**) + PhB(OH)₂ (**5a**) → biphenyl-4-ylbenzene (**6a**)

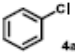
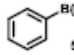
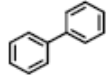
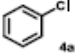
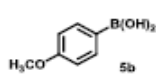
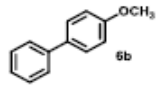
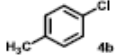
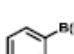
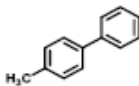
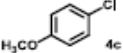
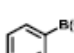
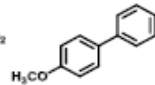
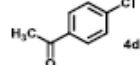
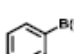
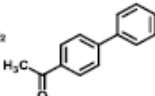
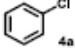
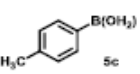
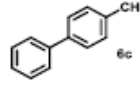
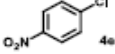
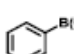
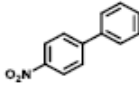
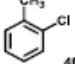
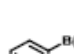
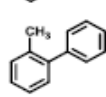
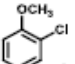

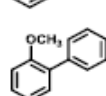
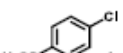
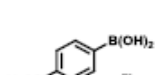
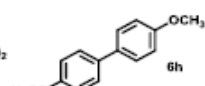
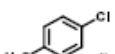
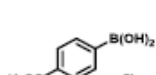
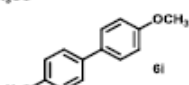
Conditions: Base, "L", "Pd"; PhB(OH)₂ (**5a**); Solvent, 12h

Entry	Base	"Pd"	"L"	Solvent	Isolated yield (%)
1	Et ₃ N	Pd(OAc) ₂	3a	PhMe	Trace
2	K ₃ PO ₄	Pd(OAc) ₂	3a	PhMe	44
3	Cs ₂ CO ₃	Pd ₂ (dba) ₃	3a	PhMe	61
4	CsF	Pd ₂ (dba) ₃	3a	PhMe	76
5	NaO ^t Bu	Pd ₂ (dba) ₃	3a	PhMe	43
6	K ₂ CO ₃	Pd ₂ (dba) ₃	3a	PhMe	83
7	K ₃ PO ₄	Pd ₂ (dba) ₃	3a	PhMe	87
8	Cs ₂ CO ₃	Pd(OAc) ₂	3b	PhMe	15
9	Cs ₂ CO ₃	Pd(OAc) ₂	3b	PhMe	18
10	K ₃ PO ₄	Pd(OAc) ₂	3b	PhMe	55
11	K ₂ CO ₃	Pd(OAc) ₂	3b	PhMe	18
12	Na ₂ CO ₃	Pd(OAc) ₂	3b	PhMe	10
13	Et ₃ N	Pd(OAc) ₂	3b	PhMe	Trace
14	CsF	Pd(OAc) ₂	3b	PhMe	39
15	NaO ^t Bu	Pd(OAc) ₂	3b	PhMe	33
16	NaOAc	Pd(OAc) ₂	3b	PhMe	9
17	K ₃ PO ₄	Pd(OAc) ₂	3b	Dioxane	30
18	K ₃ PO ₄	Pd ₂ (dba) ₃	3b	PhMe	88
19	K ₃ PO ₄	Pd ₂ (dba) ₃	3b	PhMe	74 ^a
20	K ₃ PO ₄	Pd ₂ (dba) ₃	3c	PhMe	96
21	K ₃ PO ₄	Pd ₂ (dba) ₃	3d	PhMe	91

Reaction conditions: for entries 1–18, 20–21: **4a** (0.040 g, 0.355 mmol, 1.0 equiv.), **5a** (0.052 g, 0.426 mmol, 1.2 equiv.), base (1.065 mmol, 3.0 equiv.), Pd(OAc)₂ (2.0 mol%) or, Pd₂(dba)₃ (2.0 mol% (4.0 mol% Pd)), **3a-3d** (3.0 mol%), solvent (2.5 mL).^a Entry 19: **4a** (0.040 g, 0.355 mmol, 1.0 equiv.), **5a** (0.052 g, 0.426 mmol, 1.2 equiv.), base (1.065 mmol, 3.0 equiv.), Pd₂(dba)₃ (2.0 mol% (4.0 mol% Pd)), **3a-3d** (5.0 mol%), solvent (2.5 mL), 110 °C.

These results indicate that the free acid is required on the ligand and that salts are not effective, perhaps due to low solubility or aggregation in organic media. We next surveyed the utility of the amide functionalized ligand series **3a-3d** in the standard reaction varying the ligand, base and palladium source (**Table 5-2**).

Table 5-3. SM cross coupling reaction of aryl halides with ligand **3c**.

$\text{Ar-Cl} + \text{Ar'-B(OH)}_2 \xrightarrow[\text{PhMe, 12h}]{\text{Pd}_2(\text{dba})_3, 2 \text{ mol}\% \text{ ligand } 3\text{c}, 3 \text{ mol}\% \text{ K}_3\text{PO}_4, 3 \text{ equiv}}$ Ar-Ar'				
Entry	Ar-Cl 4a-4g	Ar'-B(OH) ₂ 5a-5c	Product 6a-6i	Isolated Yield (%)
1.				96
2.				92
3.				98
4.				90
5.				99
6.				90
7.				99
8.				90
9.				90
10.				83
11.				85

General reaction conditions: aryl chloride (0.040 g, 0.355 mmol, 1.0 equiv), aryl boronic acid (0.052 g, 0.426 mmol, 1.2 equiv), K₃PO₄ (0.226 g, 1.065 mmol, 3.0 equiv), Pd₂(dba)₃ (6.5 mg, 2.0 mol %), ligand **3c** (4.5 mg, 3.0 mol %), PhMe (2.5 mL), 110 °C.

The air-stable ligands are introduced into the reaction as their HBr salts and converted *in-situ* to the free phosphine base through addition of slight excess of

the required base.^{5,6} Overall, Pd₂(dba)₃ proved to be a more effective Pd-source than Pd(II) acetate, while potassium phosphate proved to be the superior base. In one key control experiment, we determined that addition of excess ligand was detrimental. For example, a Pd:ligand ratio of 1:0.75 (**Table 5-2, entry 18, 88% isolated**) was employed compared with a Pd:ligand ratio of 1:1.25 (**Table 5-2, entry 19, 74% isolated**). Direct comparison of the ligand effect (**Table 5-2, entries 7, 18, 20 and 21**) demonstrated use of ligand **3c** to be most effective. This reaction went to full conversion and biphenyl **6a** was isolated in 96% after column chromatography.

The overall optimized reaction condition identified from this screen was selected in order to probe the efficiency of Pd-complexes of ligand **3c** in the general Suzuki-Miyaura reaction with more challenging aryl chlorides. Overall, palladium complexes of ligand **3c** proved to have broad substrate scope, the overall results of this investigation are presented in **Table 5-3**. The standard reaction condition was employed and no attempt was made to optimise individual entries in **Table 5-3**.

Electron rich and sterically hindered aryl chlorides underwent efficient cross-coupling with various aryl boronic acids leading to high isolated yield of biaryls (83-99%). Activated (electron deficient) aryl chlorides (**Table 5-3, entry 5, 7**) expectedly gave excellent yields (99%) with phenyl boronic acid. Most gratifying were the results observed with deactivated (methyl and methoxy substituted) and sterically hindered *ortho*-substituted aryl chlorides (**Table 5-3, entries 8-11**). These substrates were observed to proceed to high conversion with Pd-complexes of ligand **3c**, and the corresponding biaryls were isolated in high (83-90%) overall yield.

5.3 Conclusion

We have shown the economical, readily available lactone phthalide to be a useful building block for the rapid construction of new hemilabile phosphine

ligands. In particular, Pd-complexes of the piperidinamide ligand **3c** proved to be highly effective in the Suzuki-Miyaura Cross-Coupling reaction of activated, deactivated as well as sterically hindered aryl chlorides. The cost and air-sensitivity of many hemilabile ligands currently employed present economical and technical challenges. Ligand **3c** is readily available in two steps from phthalide and directly produced as its air stable HBr salt, allowing easy isolation, storage and handling. Many variations of the chemistry disclosed can be considered to rapidly access useful ligands from phthalide. Further study of these processes and applications to metal-mediated reactions, including application of ligand **2** in aqueous chemistry, are under investigation.

5.4 References

- [1]. (a) P. Braunstein and F. Naud, *Angew. Chem. Int. Ed.*, 2001, **40**, 680; (b) Z. Weng, S. Teo and T. S. A. Hor, *Acc. Chem. Res.*, 2007, **40**, 676; (c) X. Bei, H. W. Turner, W. H. Weinberg and A. S. Guram, *J. Org. Chem.*, 1999, **64**, 6797; (d) C. M. So, C. C. Chiu, C. P. Lau, F. Y. Kwong, *J. Org. Chem.* 2008, **73**, 7803; (e) C. M. So, C. P. Lau, A. S. C. Chan, F. Y. Kwong, *J. Org. Chem.* 2008, **73**, 7731; (f) D. Rageot and A. Pfaltz, *Helv. Chem. Acta*, 2012, **95**, 2176; (g) B. J. Tardiff, M. Stradiotto, *Eur. J. Org. Chem.* 2012, 3972; (h) C. B. Lavery, R. McDonald, M. Stradiotto, *Chem. Comm.* 2012, **48**, 7277.
- [2]. (a) A. Robertson, C. Bradaric, C. S. Frampton, J. McNulty and A. Capretta, *Tetrahedron Lett.*, 2001, **42**, 2609; (b) G. Adjabeng, T. Brenstrum, J. Wilson, C. S. Frampton, A. J. Robertson, J. Hillhouse, J. McNulty and A. Capretta, *Org. Lett.*, 2003, **5**, 953; (c) S. A. Ohnmacht, T. Brenstrum, K. H. Bleicher, J. McNulty and A. Capretta, *Tetrahedron Lett.*, 2004, **45**, 5661; (d) D. A. Gerritsma, T. Brenstrum, J. McNulty and A. Capretta, *Tetrahedron Lett.*, 2004, **45**, 8319; (e) T. Brenstrum, J. Clattenburg, J. Britten, S. Zavorine, J. Dyck, A. J. Robertson, J. McNulty and A. Capretta, *Org. Lett.*, 2006, **8**, 103;

- (f) J. McNulty, J. J. Nair, M. Sliwinski and A. J. Robertson, *Tetrahedron Lett.*, 2009, **50**, 2342.
- [3]. (a) E. Ullah, J. McNulty and A. Robertson, *Tetrahedron Lett.*, 2009, **50**, 5599; (b) E. Ullah, J. McNulty, V. Larichev, A. J. Robertson, *Eur. J. Org. Chem.* 2010, 6824; (c) E. Ullah, J. McNulty, C. Kennedy and A. Robertson, *Org. Biomol. Chem.*, 2011, **9**, 4421.
- [4]. (a) J. McNulty, K. Keskar and R. Vemula, *Chem. Eur. J.*, 2011, **17**, 14727; (b) J. McNulty, K. Keskar, *Eur. J. Org. Chem.*, 2012, 5462.
- [5]. (a) J. McNulty and D. McLeod, *Tetrahedron Lett.*, 2011, **52**, 5467; (b) P. Das, D. McLeod and J. McNulty, *Tetrahedron Lett.*, 2011, **52**, 199; (c) P. Das and J. McNulty, *Eur. J. Org. Chem.*, 2010, 3587; (d) J. McNulty, P. Das and D. McLeod, *Chem. Eur. J.*, 2010, **16**, 6756.
- [6]. M. R. Netherton and G. C. Fu, *Org. Lett.* 2001, **3**, 4295.
- [7]. G. Pifferi and E. Testa, *Tetrahedron*, 1966, **22**, 2107.
- [8]. (a) P. Lesimple and D.C.H. Bigg, *Synthesis*, 1991, **4**, 306; (b) C. Adams, J. Papillon, J. M. Ksander, 2007, *PCT Int. Appl.*, 2007117982. (c) A. Padwa and C. K. Eidell, *ARKIVOC*, 2003, **14**, 62.
- [9]. T. Kawasaki and T. Kimachi, *Tetrahedron*, 1999, **55**, 6847.
- [10]. N. Miyaura, *Top. Curr. Chem.*, 2002, **219**, 11; (b) A. Suzuki, *J. Organomet. Chem.*, 2002, **653**, 83; (c) N. Miyaura, *J. Organomet. Chem.*, 2002, **653**, 54; (d) A. Suzuki, *J. Organomet. Chem.*, 1999, **576**, 147; (e) S. Kotha, K. Lahiri and D. Kashinath, *Tetrahedron*, 2002, **58**, 9633; (f) N. Miyaura and A. Suzuki, *Chem. Rev.* 1995, **95**, 2457.
- [11]. (a) B. H. Kaae, P. Krogsgaard-Larsen and T. N. Johansen, *J. Org. Chem.*, 2004, **69**, 1401; (b) M. Hocek, A. Hol'ý, I. Votruba and H. Dvořáková, *J.*

Med. Chem., 2000, **43**, 1817; (c) N. Zou, J.-F. Liu and B. Jiang, *J. Comb. Chem.*, 2003, **5**, 754; (d) T. Laird, *Org. Proc. Res. & Dev.* 2006, **10**, 851; (e) J. Hassan, M. Sevignon, C. Gozzi, E. Schulz and M. Lemaire, *Chem. Rev.* 2002, **102**, 1359; (f) S. D. Roughley and A. M. Jordan, *J. Med. Chem.* 2011, **54**, 3451.

[12]. For a selection of previous reports on activation of aryl chlorides see: (a) S. L. Buchwald and D. L. Surrey, *Angew. Chem., Int. Ed.*, 2008, **47**, 2; (b) T. M. Barder, S. D. Walker, J. R. Martenille and S. L. Buchwald, *J. Am. Chem. Soc.*, 2005, **127**, 4685; (c) E. R. Strieter and S. L. Buchwald, *Angew. Chem., Int. Ed.*, 2006, **45**, 925; (d) T. M. Barder and S. L. Buchwald, *Angew. Chem., Int. Ed.*, 2004, **43**, 1871. (e) R. Martin and S. L. Buchwald, *Acc. Chem. Res.*, 2008, **41**, 1461. (f) J. P. Wolfe, R. A. Singer, B. H. Yang and S. L. Buchwald, *J. Am. Chem. Soc.*, 1999, **121**, 9550; (g) J. P. Wolfe, H. Tomori, J. P. Sadighi, J. J. Yin and S. L. Buchwald, *J. Org. Chem.*, 2000, **65**, 1158; (h) E. R. Streiter, D. G. Blackmond and S. L. Buchwald, *J. Am. Chem. Soc.*, 2003, **125**, 13978; (i) A. F. Littke, C. Dai and G. C. Fu, *J. Am. Chem. Soc.*, 2000, **122**, 4020; (j) J. F. Hartwig, M. Kawatsura, S. I. Hauck, K. H. Shaughnessy and L. M. Alcazar-Roman, *J. Org. Chem.*, 1999, **64**, 5575; (k) N. E. Leadbeater, *Chem. Commun.*, 2005, 2881; (l) J. P. Wolfe and S. L. Buchwald, *J. Org. Chem.*, 2000, **65**, 1144; (m) D. W. Old, J. P. Wolfe and S. L. Buchwald, *J. Am. Chem. Soc.*, 1998, **120**, 9722; (n) X. Huang, K. W. Anderson, D. Zim, L. Jiang, A. Klupers and S. L. Buchwald, *J. Am. Chem. Soc.*, 2003, **125**, 6653; (o) A. Aranyos, D. W. Old, A. Kiyomori, J. P. Wolfe, J. P. Sadighi and S. L. Buchwald, *J. Am. Chem. Soc.*, 1999, **121**, 4369; (p) K. Billingsley and S. L. Buchwald, *J. Am. Chem. Soc.*, 2007, **129**, 3358; (q) G. C. Fu, *Acc. Chem. Res.*, 2008, **41**, 1555.

[13]. (a) W. A. Herrmann, *Angew. Chem. Int. Ed.* 2002, **41**, 1290–1309; (b) O. Navarro, R. A. Kelly and S. P. Nolan, *J. Am. Chem. Soc.* 2003, **125**, 16194–16195; (c) G. Altenhoff, R. Goddard, C. W. Lehman and F. Glorius, *J. Am.*

- Chem. Soc.* 2004, 126, 15195-15201; (d) J. Nasielski, N. Hadei, G. Achonduh, E. A. B. Kantchev, C. J. O'Brien, A. Lough, and M. G. Organ, *Chem. Eur. J.*, 2010, **16**, 10844; (e) L. Jiang, F. Shan, Z. Li and D. Zhao, *Molecules*, 2012, **17**, 12121.
- [14]. Cesium fluoride has been shown to be an effective mild base in other cross-coupling reactions bearing orthogonal acidic hydrogen atoms, see: (a) M. Wasa, K. M. Engle and Jin-Quan Yu, *J. Am. Chem. Soc.*, 2009, **131**, 9886; (b) J. P. Wolfe and S. L. Buchwald, *J. Org. Chem.*, 2000, **65**, 1144.
- [15]. R. Ghosh, N. N. Adarsh, A. Sarkar, *J. Org. Chem.*, 2010, **75**, 5320.
- [16]. W-M. Dai, Y. Li, Y. Zhang, C. Yue and J. Wu, *Chem. Eur. J.*, 2008, **14**, 5538.
- [17]. M. L. Kantam, P. Srinivas, J. Yadav, P. R. Likhar, S. Bhargava, *J. Org. Chem.*, 2009, **74**, 4882.

5.5 Experimental Section

All fine chemicals were obtained from Sigma-Aldrich and used as obtained. Dichloromethane was distilled over calcium hydride. Toluene was distilled over sodium metal in the presence of benzophenone indicator. HBr-AcOH (33% by wt) was used as obtained from Sigma Aldrich. ^1H and ^{13}C and ^{31}P NMR spectra were obtained on a 600 MHz Bruker NMR spectrometer. Chemical shifts are reported in units of δ (ppm) and coupling constants (J) are expressed in Hz. Mass spectra were run on a Micromass Quattro Ultima spectrometer fitted with a direct injection probe (DIP) with ionization energy set at 70 eV and HRMS (EI) were performed with a Micromass Q-TOF Ultima spectrometer. Thin layer chromatography (TLC) was run using Macherey-Nagel aluminum-backed plates. Melting points were obtained on an Electronic Research Associates Inc. melting point apparatus corrected against an external calibrant.

Synthesis of 2-((di-tert-butylphosphino)methyl)benzoic acid hydrobromide (Scheme 5-1, 2):

Into a flame-dried flask with a stirring bar was added HBr-AcOH (10.0 mL, 33% by wt). A mixture of phthalide (0.500 g) in glacial acetic acid was slowly added to it and the reaction mixture allowed to stir at room temperature for 2 h and 1.5 h at 70 °C. The reaction mixture was stirred overnight. The reaction mixture was poured on ice-water (100.0 mL) to obtain precipitate. The precipitate was filtered and dried under high vacuum to obtain α -bromo-*o*-toluic acid as white solid in 70% yield having spectroscopic properties in accord with the literature (^1H NMR (600 MHz, DMSO) δ 7.89 (m, 1H), 7.59 – 7.56 (m, 2H), 7.45 (m, 2H), 5.08 (s, 2H)).⁷ To a flame-dried schlenk flask with a stirring bar was added α -bromo-*o*-toluic acid (0.570 g, 2.65 mmol) followed by degassed acetone (25.0 mL). Under argon atmosphere, di-*t*-butylphosphine (0.490 mL, 2.65 mmol) was added to the flask. The schlenk flask was then flushed with two times with argon atmosphere and closed under argon atmosphere. The reaction mixture was then heated to reflux overnight. Upon cooling the reaction flask, acetone was removed under vacuum and diethyl ether (20.0 mL) was added to the flask to obtain 2-((di-tert-butylphosphino)methyl)benzoic acid hydrobromide **2** as a colourless amorphous solid in quantitative yield. Melting point: 205-208 °C. ^1H NMR (600 MHz, CD_2Cl_2) δ 8.22 (d, J = 7.8 Hz, 1H), 7.67 (d, J = 7.7 Hz, 1H), 7.64 (t, J = 7.5 Hz, 1H), 7.53 (d, J = 7.4 Hz, 1H), 7.10 (d, J = 484.71 Hz, 1H), 4.33 (dd, J = 14.9, 6.6 Hz, 2H), 1.52 (s, 9H), 1.50 (s, 9H). ^{31}P NMR (243 MHz, CD_2Cl_2) δ 38.25 (d, J = 484.4 Hz). ^{31}P NMR ^1H decoupled (243 MHz, CD_2Cl_2) δ 38.37. ^{13}C NMR (151 MHz, CD_2Cl_2) δ 168.4, 133.8, 133.6 (d, J = 6.5 Hz), 133.3, 132.2, 129.7, 129.7, 34.1 (d, J = 33.6 Hz), 28.3, 23.4 (d, J = 39.5 Hz). HRMS: calcd. For $\text{C}_{16}\text{H}_{25}\text{O}_2\text{P}$ $[\text{M}]^+$ 281.1682; found 281.1670.

Synthesis of 2-((di-tert-butylphosphino)methyl)-*N,N*-diethylbenzamide hydrobromide (Scheme 5-1, 3a):

Into a flame-dried flask with magnetic stirring bar was added AlCl_3 (1.3 g). Dichloroethane (5.0 mL) was added to the flask. A mixture of diethylamine (1.95 mL, 2.5 equiv) in dichloroethane (3.0 mL) was added to the flask maintaining the temperature below 25 °C. The reaction mixture was stirred for 30 min at rt. Phthalide (1.0 g, 1.0 equiv) was added to the flask slowly in portions. The reaction mixture was stirred for 50 min at rt. Afterwards ice and water was added to the flask and reaction mixture was stirred for additional 30 min. Reaction mixture was filtered through celite pad and aqueous phase was extracted with dichloromethane, washed with brine and dried to give crude product which was purified using a quick flask chromatography (EtOAc : Hexanes, gradient elution) gave *N,N*-diethyl-2-(hydroxymethyl)benzamide as orange oil in 88% yield.⁸ ^1H NMR (600 MHz, CDCl_3) δ 7.46 (dd, J = 7.6, 0.7 Hz, 1H), 7.40 (td, J = 7.5, 1.3 Hz, 1H), 7.32 (td, J = 7.5, 1.3 Hz, 1H), 7.24 (dd, J = 7.5, 1.1 Hz, 1H), 4.53 (s, 2H), 3.59 (q, J = 7.1 Hz, 2H), 3.45 (brs, 1H), 3.24 (q, J = 7.1 Hz, 2H), 1.29 (t, J = 7.1 Hz, 3H), 1.10 (t, J = 7.1 Hz, 3H). ^{13}C NMR (151 MHz, CDCl_3) δ 171.3, 138.6, 136.0, 129.7, 129.5, 127.4, 125.7, 63.7, 43.4, 39.3, 14.0, 12.7.

Into a flame-dried flask with a magnetic stirring bar was added *N,N*-diethyl-2-(hydroxymethyl)benzamide (0.110 g, 0.530 mmol, 1.0 equiv). Freshly distilled dichloromethane (3.0 mL) was added to the flask. The reaction mixture was cooled to 0 °C and PBr_3 (0.250 mL, 2.65 mmol, 5.0 equiv) was added to it. The reaction mixture was stirred at 0 °C for 3 h. Dichloromethane was removed under vacuum and the water (2.0 mL) was added to the flask. The reaction mixture was extracted with ethyl acetate, washed with brine, dried over sodium sulphate. The solvent was evaporated under high vacuum and the crude sample, was obtained as oil. A sample of 2-(bromomethyl)-*N,N*-diethylbenzamide allowed to dry under high vacuum for 30 min and then

dissolved in 1.0 mL degassed acetone where upon it was added to a flame-dried, argon flushed schlenk flask with a stirring bar. Additional degassed acetone (2.0 mL) was added to the flask. Under an argon atmosphere, di-*t*-butylphosphine (0.093 mL, 0.504 mmol, 0.95 equiv) was added to the flask. The schlenk flask was then vented under vacuum and flushed with argon twice and closed under argon. The reaction mixture was then heated to reflux overnight. Upon cooling the reaction flask, acetone was removed under vacuum and diethyl ether (20.0 mL) was added to the flask. Resultant colourless crystalline solid was filtered to obtain 2-((di-*tert*-butylphosphino)methyl)-*N,N*-diethylbenzamide hydrobromide **3a** in quantitative yield. Melting point: 163-165 °C. ^1H NMR (600 MHz, CDCl_3) δ 8.38 (d, J = 484.9 Hz, 1H), 8.24 (d, J = 7.8 Hz, 1H), 7.52 (t, J = 7.6 Hz, 1H), 7.37 (t, J = 7.6 Hz, 1H), 7.24 (d, J = 7.6 Hz, 1H), 4.01 (s, 1H), 3.60 (q, J = 7.1 Hz, 2H), 3.19 (q, J = 7.0 Hz, 2H), 2.62 (s, 1H), 1.56 (s, 9H), 1.54 (s, 9H), 1.29 (t, J = 7.1 Hz, 3H), 1.12 (t, J = 7.1 Hz, 3H). ^1H NMR (600 MHz, CD_2Cl_2) δ 8.52 (d, J = 485.7 Hz, 1H), 8.17 (d, J = 7.9 Hz, 1H), 7.54 (td, J = 7.7, 1.2 Hz, 1H), 7.43 (t, J = 7.6 Hz, 1H), 7.29 (d, J = 7.6 Hz, 1H), 4.23-3.93 (brs, 2H), 3.59 (q, J = 7.1 Hz, 2H), 3.20 (q, J = 7.1 Hz, 2H), 1.56 (s, 9H), 1.53 (s, 9H), 1.29 (t, J = 7.1 Hz, 3H), 1.13 (t, J = 7.1 Hz, 3H). ^{31}P NMR (243 MHz, CDCl_3) δ 36.4 (d, J = 483.1 Hz). ^{31}P NMR ^1H decoupled (243 MHz, CDCl_3) δ 36.5. ^{13}C NMR (151 MHz, CDCl_3) δ 169.9, 136.1 (d, J = 5.9 Hz), 132.5 (d, J = 5.2 Hz), 130.4, 128.2, 127.2 (d, J = 7.6 Hz), 126.5, 43.7, 39.5, 33.8 (d, J = 32.9 Hz), 28.1, 19.7 (d, J = 37.5 Hz), 14.2, 13.1. HRMS: calcd. For $\text{C}_{18}\text{H}_{29}\text{NOP} [\text{M}]^+$ 306.2001; found 306.1987 (Loss of one C_2H_5 group).

Similar procedure was followed to obtain ligand **3c** and **3d** (Scheme 5-1).

(2-(hydroxymethyl)phenyl)(piperidin-1-yl)methanone:⁸ Yield 90%. ^1H NMR (600 MHz, CDCl_3) δ 7.47 (d, J = 7.5 Hz, 1H), 7.41 (t, J = 7.5 Hz, 1H), 7.34 (t, J = 7.4 Hz, 1H), 7.25 (d, J = 7.5 Hz, 1H), 4.56 (m, 2H), 3.77 (s, 2H), 3.50 (s, 1H), 3.33 (s, 2H), 1.71 (s, 4H), 1.52 (s, 2H). ^{13}C NMR (151 MHz, CDCl_3) δ 170.3, 139.1, 135.6, 129.9, 129.6, 127.4, 126.3, 64.1, 48.7, 43.0, 26.6, 25.7, 24.5.

Scheme 5-1, 3c: Yield 99%. Melting point: 178-180 °C. ^1H NMR (600 MHz, CDCl_3) δ 8.29 (d, $J = 483.2$ Hz, 1H), 8.18 (d, $J = 7.9$ Hz, 1H), 7.52 (t, $J = 7.7$ Hz, 1H), 7.37 (t, $J = 7.6$ Hz, 1H), 7.25 (d, $J = 7.6$ Hz, 1H), 4.54 (brs, 1H), 3.98 (brs, 1H), 3.62 (brs, 2H), 3.32 (t, $J = 5.5$ Hz, 2H), 1.85-1.64 (m, 6H), 1.58 (s, 9H), 1.56 (s, 9H). ^{31}P NMR (243 MHz, CDCl_3) δ 36.6 (d, $J = 483.0$ Hz). ^{31}P NMR ^1H decoupled (243 MHz, CDCl_3) δ 36.7. ^{13}C NMR (151 MHz, CDCl_3) δ 168.6, 135.5, 132.8 (d, $J = 5.2$ Hz), 130.5, 128.2, 127.9 (d, $J = 7.9$ Hz), 127.0, 48.6, 42.9, 28.1, 26.7, 25.8, 24.3, 19.9 (d, $J = 37.3$ Hz). HRMS: calcd. For $\text{C}_{17}\text{H}_{25}\text{NOP}$ $[\text{M}]^+$ 290.1678; found 290.1674 (Loss of one ^tBu group).

N-benzyl-2-(hydroxymethyl)-N-methylbenzamide:⁸ Yield 94%. Rotamer mixture. Major: ^1H NMR (600 MHz, CDCl_3) δ 7.48 (dd, $J = 7.5, 1.8$ Hz, 1H), 7.45 - 7.40 (m, 3H), 7.39-7.32 (m, 3H), 7.31 (t, $J = 5.7$ Hz, 1H), 7.15 (d, $J = 7.3$ Hz, 1H), 4.81 (s, 2H), 4.60 (s, 2H), 3.67 (brs, 1H), 2.86 (s, 3H). Minor: ^1H NMR (600 MHz, CDCl_3) δ 7.48 (dd, $J = 7.5, 1.8$ Hz, 1H), 7.45 - 7.40 (m, 3H), 7.39-7.32 (m, 3H), 7.31 (t, $J = 5.7$ Hz, 1H), 7.15 (d, $J = 7.3$ Hz, 1H), 4.60 (s, 2H), 4.51 (s, 2H), 3.67 (s, 1H), 3.10 (s, 3H). ^{13}C NMR (151 MHz, CDCl_3) δ 172.4, 171.8, 139.2, 139.0, 136.7, 136.1, 135.4, 135.2, 130.1, 130.0, 129.8, 128.9, 128.8, 128.2, 127.8, 127.7, 127.5, 127.5, 126.9, 126.6, 126.3, 64.1, 55.3, 50.6, 36.8, 33.1.

Scheme 5-1, 3d: Yield 99%. Melting point: 168-171 °C. Rotamer mixture. Major: ^1H NMR (600 MHz, CDCl_3) δ 8.58 (d, $J = 485.9$ Hz, 1H), 8.17 (d, $J = 7.7$ Hz, 1H), 7.58 - 7.49 (m, 1H), 7.43 - 7.27 (m, 6H), 7.09 (d, $J = 7.3$ Hz, 1H), 4.83 (s, 2H), 3.96 (s, 2H), 2.91 (s, 3H), 1.55 (s, 9H), 1.53 (s, 9H). Minor: ^1H NMR (600 MHz, CDCl_3) δ 8.63 (d, $J = 485.9$ Hz, 1H), 8.11 (d, $J = 7.9$ Hz, 1H), 7.58 - 7.49 (m, 1H), 7.43 - 7.27 (m, 6H), 7.09 (d, $J = 7.3$ Hz, 1H), 4.53 (s, 2H), 3.74 (s, 2H), 3.23 (s, 3H), 1.57 (s, 9H), 1.54 (s, 9H). ^{31}P NMR ^1H decoupled (243 MHz, CDCl_3) δ 34.8, 34.2. ^{31}P NMR (243 MHz, CDCl_3) δ 34.7 (d, $J = 485.38$ Hz), 34.1 (d, $J = 485.38$ Hz). ^{13}C NMR (151 MHz, CDCl_3) Major: ^{13}C NMR (151 MHz, CDCl_3) δ 170.0, 136.6, 136.3, 135.3 (d, $J = 5.20$ Hz), 132.5, 130.7, 128.9, 128.8, 128.3, 128.2, 127.8, 127.3, 126.9, 50.9, 37.4, 33.8 (d, $J = 32.71$ Hz),

28.0, 19.3 (d, $J = 38.68$ Hz). HRMS: calcd. For $C_{23}H_{31}NOP$ $[M]^+$ 368.2161; found 368.2143 (Loss of one methyl group).

Synthesis of 2-((di-tert-butylphosphino)methyl)-*N,N*-diisopropylbenzamide hydrobromide (Scheme 5-2, 3b):

Into a flame-dried flask with a magnetic stirring bar was added *N,N*-diisopropylbenzamide (I) (1.0 g, 4.87 mmol, 1.0 equiv). Freshly distilled THF (4.0 mL) was added to the flask. *s*-BuLi (3.82 mL, 1.1 equiv, 1.4 M solution in cyclohexane) was added to the flask at -78 °C. After 60 min, DMF (1.80 mL, 19.4 mmol, 4.0 equiv) was added to the flask and stirred for 30 min at rt. To the reaction mixture 15.0 mL water was added and reaction mixture was extracted with diethyl ether, washed with brine and solvent was dried over sodium sulphate. The solvent was removed under vacuum to give off white solid which was recrystallized from pentane to give light yellow solid. The crude aldehyde was dissolved in 15.0 mL methanol at 0 °C and $NaBH_4$ (0.185 g, 4.87 mmol, 1.0 equiv) was added by portions. The reaction mixture was stirred at 0 °C for 30 min, followed by overnight at rt. The reaction mixture was quenched and solvent was evaporated under vacuum. The crude reaction mixture was extracted with ethyl acetate, washed with brine and dried over sodium sulphate. The solvent evaporation and a quick flash column afforded 2-(hydroxymethyl)-*N,N*-diisopropylbenzamide in 70% yield.⁹ 1H NMR (600 MHz, $CDCl_3$) δ 7.45 (d, $J = 7.6$ Hz, 1H), 7.45 (d, $J = 7.6$ Hz, 1H), 7.39 (t, $J = 7.5$ Hz, 1H), 7.39 (t, $J = 7.5$ Hz, 1H), 7.33 (t, $J = 7.5$ Hz, 1H), 7.19 (d, $J = 7.5$ Hz, 1H), 7.19 (d, $J = 7.5$ Hz, 1H), 4.67 (d, $J = 11.7$ Hz, 1H), 4.45 (d, $J = 12.0$ Hz, 1H), 3.92 – 3.80 (m, 1H), 3.63 (d, $J = 29.0$ Hz, 1H), 3.61 – 3.53 (m, 1H), 3.61 – 3.50 (m, 1H), 1.59 (m, 6H), 1.16 (m, 6H). ^{13}C NMR (151 MHz, $CDCl_3$) δ 171.3, 138.3, 137.6, 129.9, 129.1, 127.5, 125.0, 64.0, 51.3, 46.1, 20.9, 20.6, 20.4, 20.3.

Into a flame-dried flask with a magnetic stirring bar was added *N,N*-diisopropyl-2-(hydroxymethyl)benzamide (0.103 g, 0.437 mmol, 1.0 equiv). Freshly distilled

dichloromethane (3.0 mL) was added to the flask. The reaction mixture was cooled to 0 °C and PBr₃ (0.206 mL, 2.12 mmol, 5.0 equiv) was added to it. The reaction mixture was stirred at 0 °C for 3 h. Dichloromethane was removed under vacuum and the water (2.0 mL) was added to the flask. The reaction mixture was extracted with ethyl acetate, washed with brine, dried over sodium sulphate. The solvent was evaporated under high vacuum and the crude sample, was obtained as an oil. Crude sample of 2-(bromomethyl)-*N,N*-diisopropylbenzamide allowed to dry under high vacuum for 30 min and then dissolved in 1.0 mL degassed acetone where upon it was added to a flame-dried, argon flushed schlenk flask with a stirring bar. Additional degassed acetone (2.0 mL) was added to the flask. Under argon atmosphere, di-*t*-butylphosphine (0.076 mL, 0.415 mmol, 0.95 equiv) was added to the flask. The schlenk flask was then flushed with two times with argon atmosphere and closed under argon atmosphere. The reaction mixture was then heated to reflux overnight. Upon cooling the reaction flask, acetone was removed under vacuum and diethyl ether (20.0 mL) was added to the flask to obtain 2-((di-*tert*-butylphosphino)methyl)-*N,N*-diisopropylbenzamide hydrobromide **3b** in quantitative yield. Melting point: 172-175 °C. ¹H NMR (600 MHz, CDCl₃) δ 8.39 (d, *J* = 480.54 Hz, 1H), 8.28 (d, *J* = 7.8 Hz, 1H), 7.42 (t, *J* = 7.5 Hz, 1H), 7.28 (t, *J* = 7.4 Hz, 1H), 7.08 (d, *J* = 7.5 Hz, 1H), 4.50-4.33 (m, 1H), 3.51 (td, *J* = 6.0 Hz, 1H), 3.45 – 3.28 (m, 1H), 1.63-1.31 (m, 24H), 1.11-0.95 (m, 6H). ³¹P NMR ¹H decoupled (243 MHz, CDCl₃) δ 36.1. ³¹P NMR (243 MHz, CDCl₃) δ 36.0 (d, *J* = 483.1 Hz). ¹³C NMR (151 MHz, CDCl₃) δ 169.8, 137.6, 132.4, 130.0, 128.5, 126.1, 125.5, 51.1, 46.1, 34.1 (d, *J* = 32.3 Hz), 33.5 (d, *J* = 33.2 Hz), 21.4, 20.9, 20.4, 20.2, 19.8 (d, *J* = 37.2 Hz). HRMS: calcd. For C₂₂H₃₈NOP [M]⁺ 363.2703; found 363.2691

General procedure for Suzuki-Miyaura coupling reaction:

Into an oven dried Schlenk flask equipped with a magnetic stirring bar were added under argon the aryl halide (0.040 g, 0.355 mmol), boronic acid (0.065 g,

0.426 mmol), Pd₂(dba)₃ (0.0065 g, 2.0 mol%), ligand **3c** (0.0045 g, 3.0 mol%), and K₃PO₄ (0.226 g, 1.065 mmol, Aldrich, ReagentPlus, 99%). The flask was capped, evacuated, and flushed with argon three times. Toluene (2.5 mL) was introduced and the reaction mixture was immersed in a pre-heated oil bath at the indicated temperature for 110 °C for 12 h. (**Table 3, entry 2**). The reaction mixture was then diluted with ethyl acetate, filtered through silica and the solvent was removed at reduced pressure. The crude product was then purified by column chromatography on silica gel to get pure biphenyl (**6a**).

Biphenyl (Table 5-3, 6a): ¹H NMR (600 MHz, CDCl₃) δ 7.64 (dd, *J* = 8.3, 1.2 Hz, 2H), 7.52 – 7.46 (m, 2H), 7.42 – 7.36 (m, 1H). ¹³C NMR (151 MHz, CDCl₃) δ 141.2, 128.7, 127.2, 127.1.^{3c}

4-Methoxybiphenyl (Table 5-3, 6b): ¹H NMR (600 MHz, CDCl₃) δ 7.47 (dd, *J* = 8.1, 0.9 Hz, 2H), 7.46 – 7.44 (m, 2H), 7.33 (t, *J* = 7.8 Hz, 2H), 7.22 (t, *J* = 7.4 Hz, 1H), 6.90 (d, *J* = 8.7 Hz, 2H), 3.76 (s, 3H). ¹³C NMR (151 MHz, CDCl₃) δ 158.1, 139.8, 132.7, 127.6, 127.1, 125.7, 125.6, 113.1, 54.3.^{3c}

4-Methylbiphenyl (Table 5-3, 6c): ¹H NMR (600 MHz, CDCl₃) δ 7.63 (dd, *J* = 8.3, 1.2 Hz, 2H), 7.55 (d, *J* = 8.1 Hz, 2H), 7.48 (t, *J* = 7.7 Hz, 2H), 7.39 – 7.35 (m, 1H), 7.30 (d, *J* = 7.9 Hz, 2H), 2.45 (s, 3H). ¹³C NMR (151 MHz, CDCl₃) δ 141.2, 138.4, 137.0, 129.5, 128.7, 127.0, 127.0, 21.1.^{3c}

1-(biphenyl-4-yl)ethanone (Table 5-3, 6d): ¹H NMR (600 MHz, CDCl₃) δ 7.94 (d, *J* = 8.4 Hz, 2H), 7.62 – 7.56 (m, 2H), 7.55 – 7.51 (m, 2H), 7.38 (dd, *J* = 10.4, 4.8 Hz, 2H), 7.31 (ddd, *J* = 7.4, 6.1, 1.1 Hz, 1H), 2.54 (s, 3H). ¹³C NMR (151 MHz, CDCl₃) δ 197.7, 145.7, 139.8, 135.8, 128.9, 128.9, 128.2, 127.2, 127.2, 26.6.^{3c}

4-nitrobiphenyl (Table 5-3, 6e): ¹H NMR (600 MHz, CDCl₃) δ 8.36 – 8.30 (m, 2H), 7.78 – 7.74 (m, 2H), 7.66 (dd, *J* = 5.2, 3.2 Hz, 2H), 7.56 – 7.50 (m, 2H),

7.48 (ddd, $J = 7.6, 3.8, 1.2$ Hz, 1H). ^{13}C NMR (151 MHz, CDCl_3) δ 146.6, 146.0, 137.7, 128.1, 127.8, 126.7, 126.3, 123.0.¹⁵

2-methylbiphenyl (Table 5-3, 6f): ^1H NMR (600 MHz, CDCl_3) δ 7.46 (m, 2H), 7.39 (m, 3H), 7.35 – 7.26 (m, 4H), 2.33 (s, 3H). ^{13}C NMR (151 MHz, CDCl_3) δ 142.0, 141.9, 135.3, 130.3, 129.8, 129.2, 128.0, 127.2, 126.7, 125.7, 20.4.¹⁶

2-methoxybiphenyl (Table 5-3, 6g): ^1H NMR (600 MHz, CDCl_3) δ 7.45 (dd, $J = 8.2, 1.2$ Hz, 2H), 7.35 – 7.30 (m, 2H), 7.26 – 7.22 (m, 3H), 6.95 (td, $J = 7.5, 1.1$ Hz, 1H), 6.91 (dd, $J = 8.7, 0.8$ Hz, 1H), 3.73 (s, 3H). ^{13}C NMR (151 MHz, CDCl_3) δ 155.4, 137.5, 129.8, 128.5, 127.5, 126.9, 125.8, 119.7, 110.2, 54.5.¹⁶

4,4'-dimethoxybiphenyl (Table 5-3, 6h): ^1H NMR (600 MHz, CDCl_3) δ 7.40 (d, $J = 8.8$ Hz, 2H), 6.88 (d, $J = 8.8$ Hz, 2H), 3.76 (s, 3H). ^{13}C NMR (151 MHz, CDCl_3) δ 157.6, 126.7, 113.1, 54.3.¹⁷

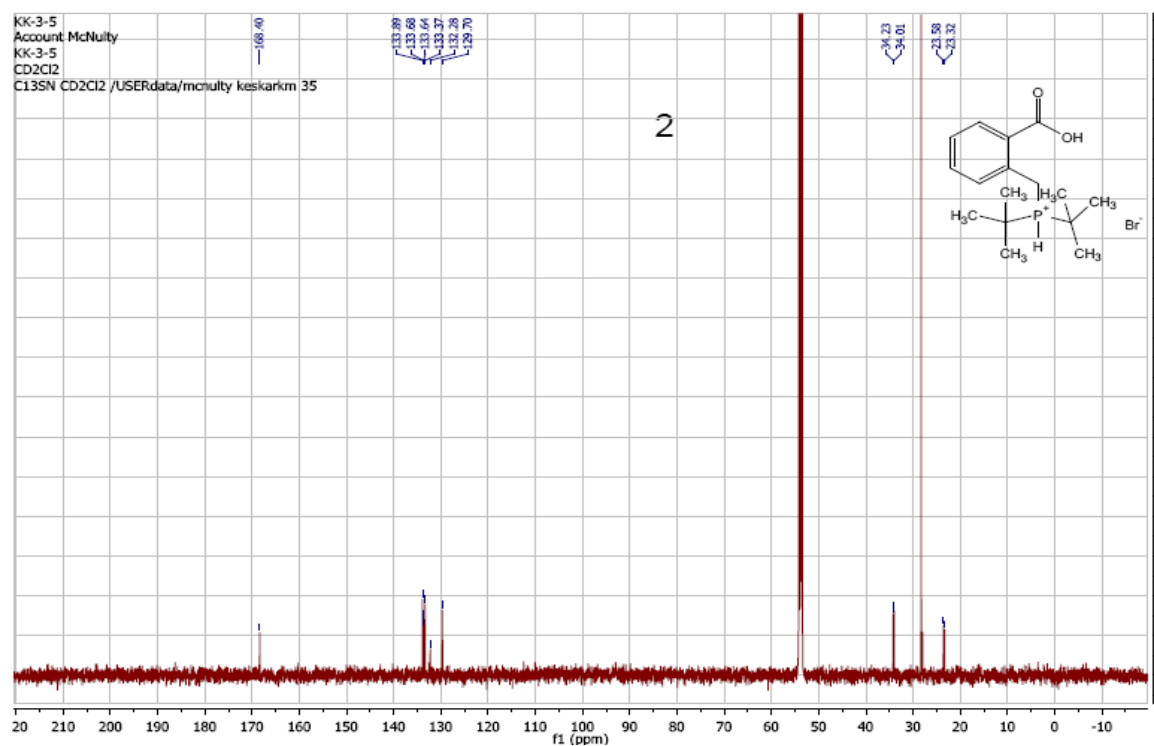
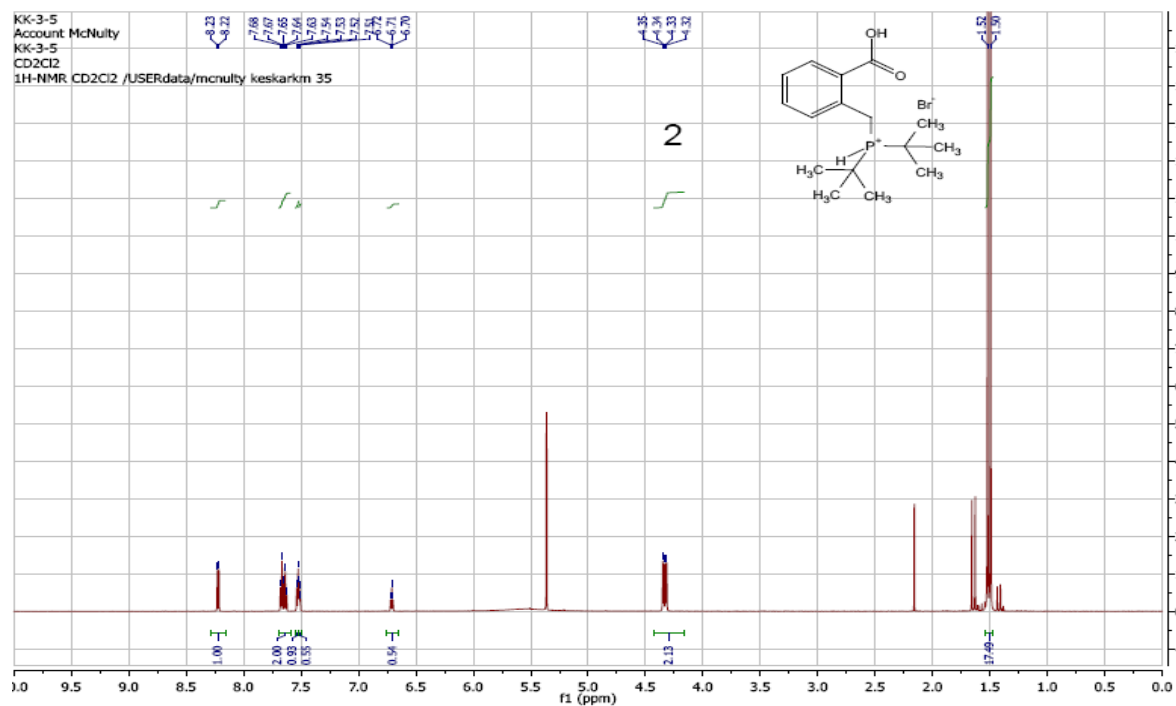
4-methoxy-4'-methylbiphenyl (Table 5-3, 6i): ^1H NMR (600 MHz, CDCl_3) δ 7.43 (d, $J = 8.8$ Hz, 2H), 7.37 (d, $J = 8.1$ Hz, 2H), 7.14 (d, $J = 7.8$ Hz, 2H), 6.88 (d, $J = 8.8$ Hz, 2H), 3.76 (s, 3H), 2.30 (s, 3H). ^{13}C NMR (151 MHz, CDCl_3) δ 157.9, 136.9, 135.3, 132.7, 128.4, 126.9, 125.5, 113.1, 54.2, 20.0.¹⁷

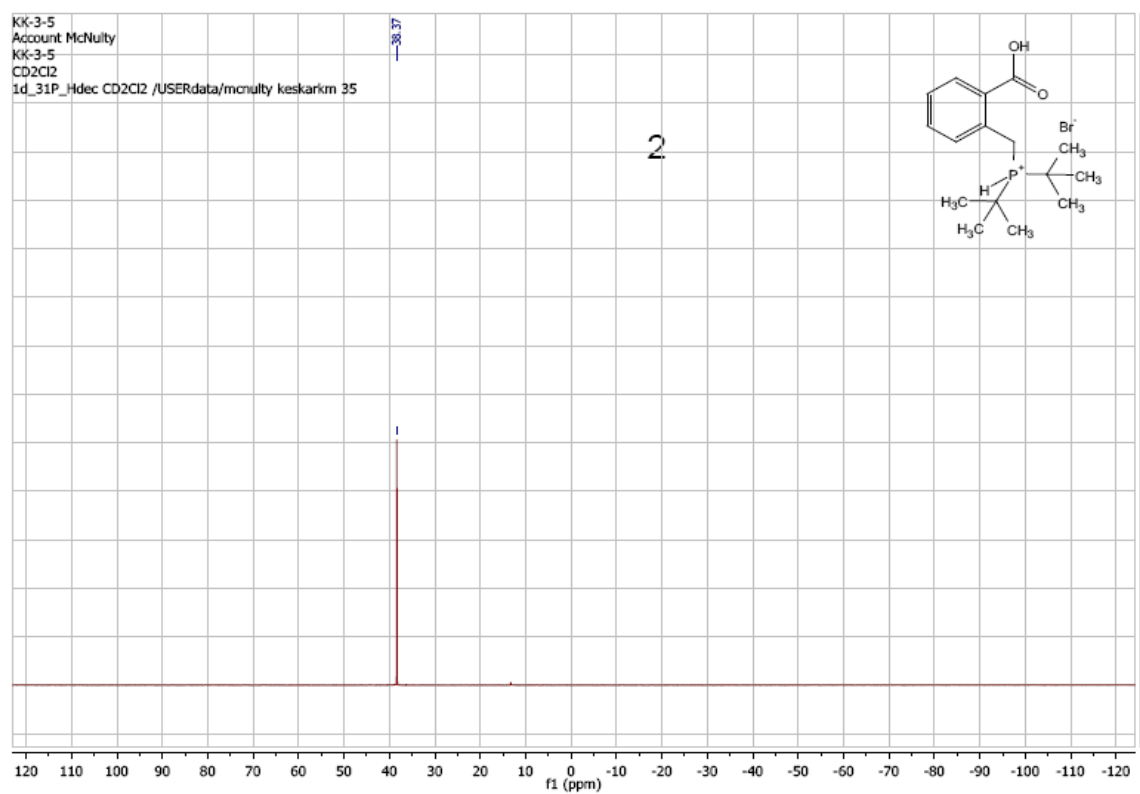
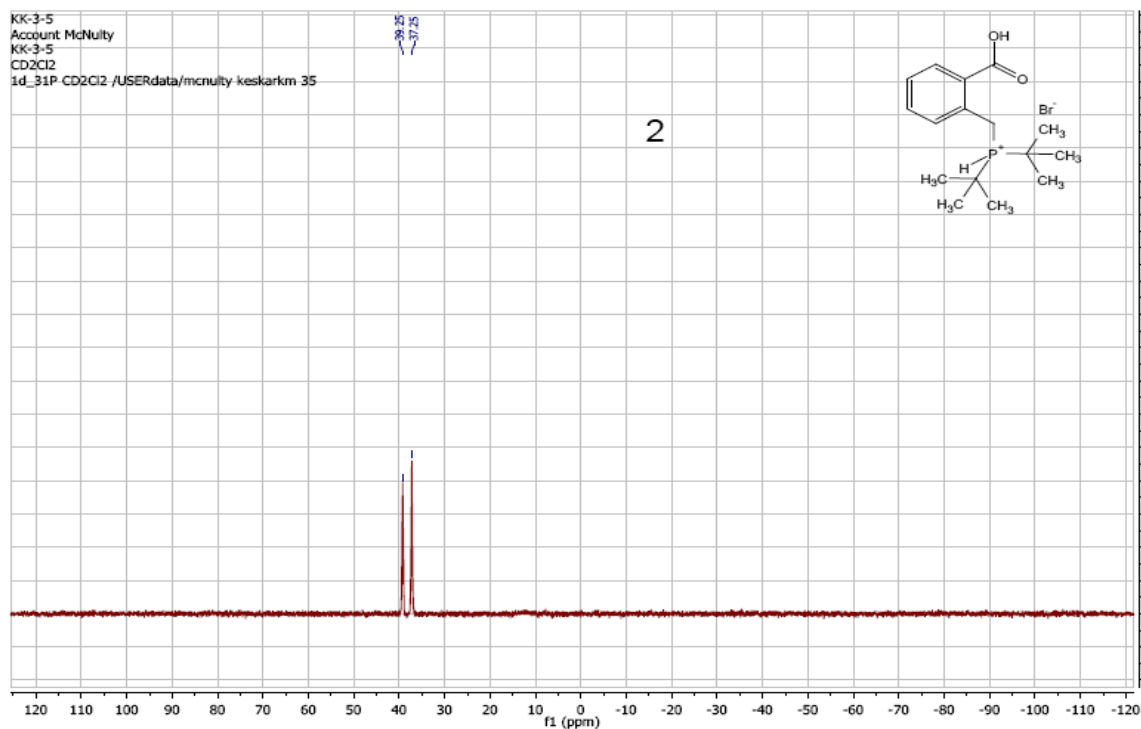
5.6 NMR Spectra:

^1H , ^{13}C and ^{31}P spectra of the new ligands are below. ^1H -NMR spectra for biphenyls is included in the thesis however ^{13}C -NMR spectra are not due to pages limit. These can be found online. (Reference IV- List of Publications)

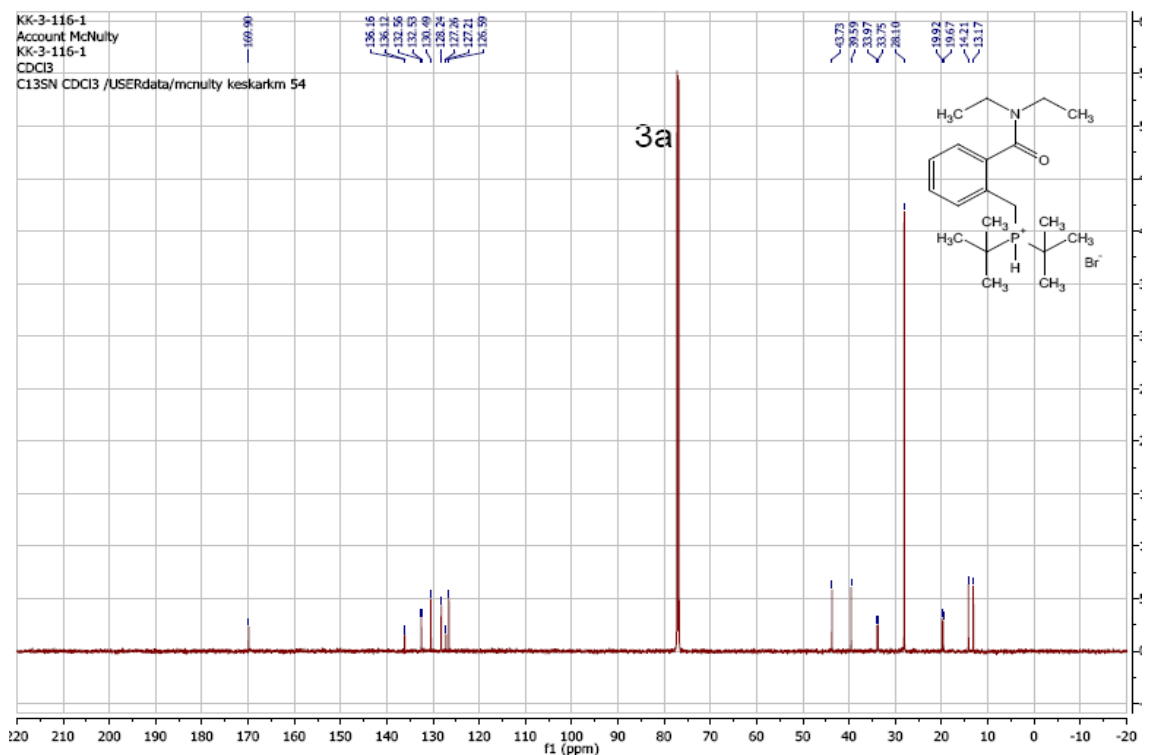
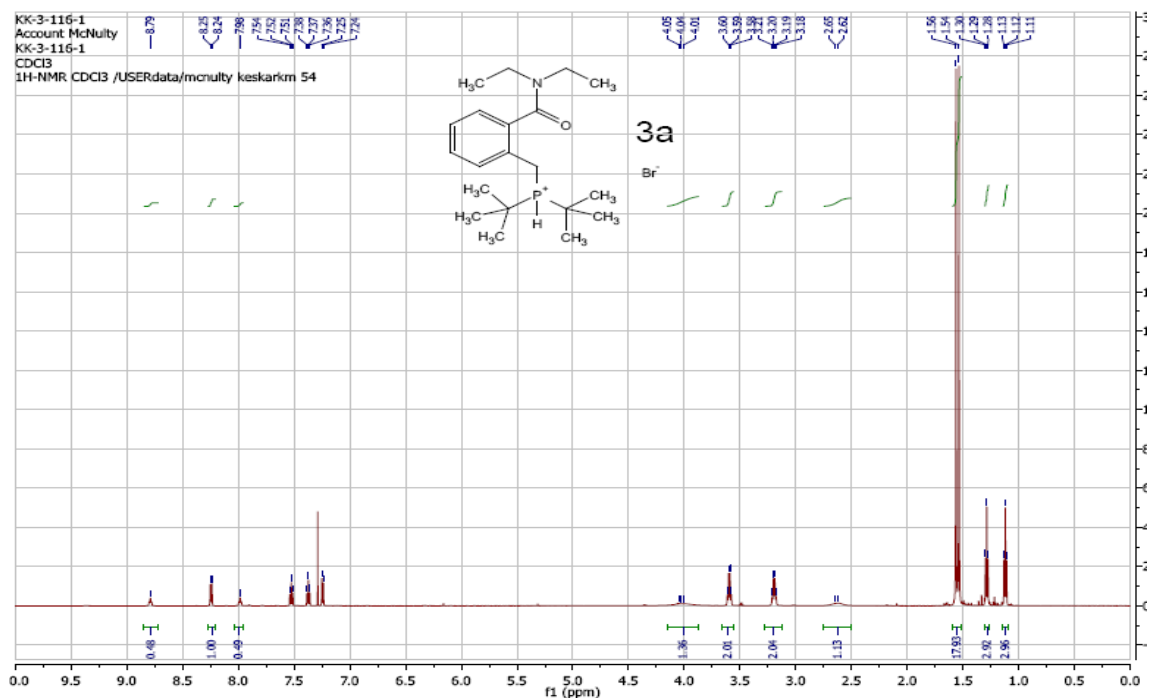
(See next page for ^1H , ^{13}C and ^{31}P spectra,)

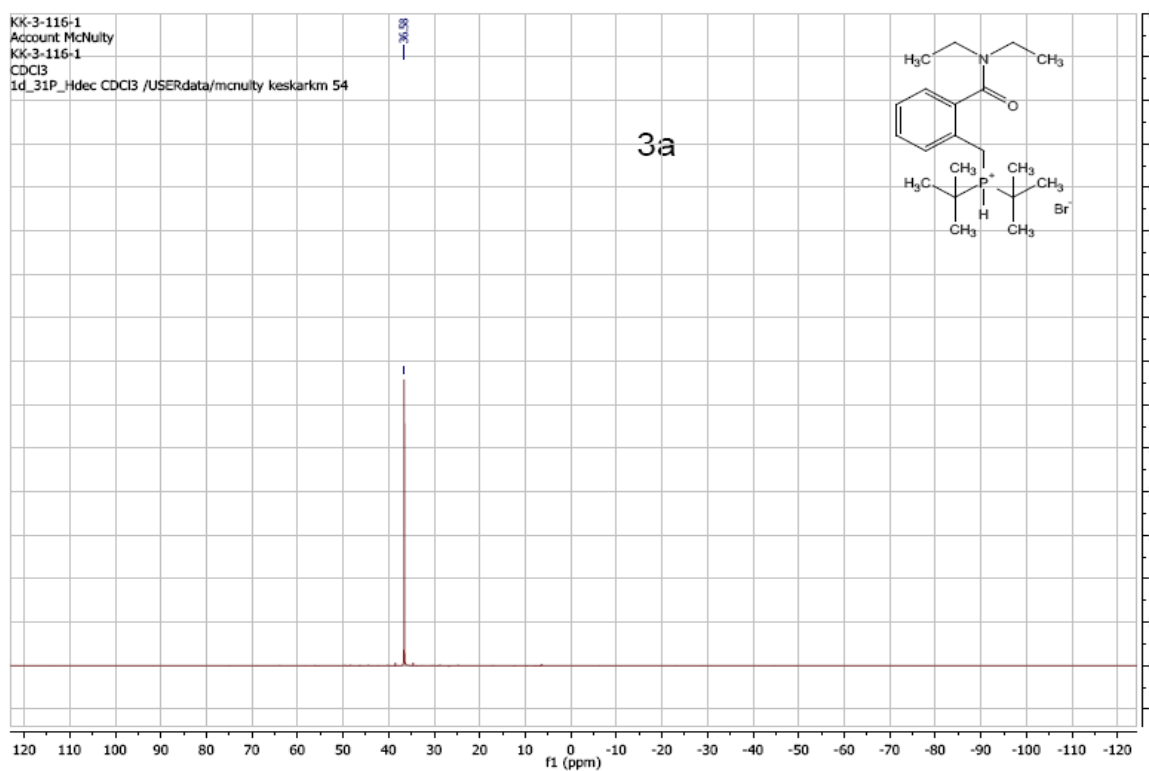
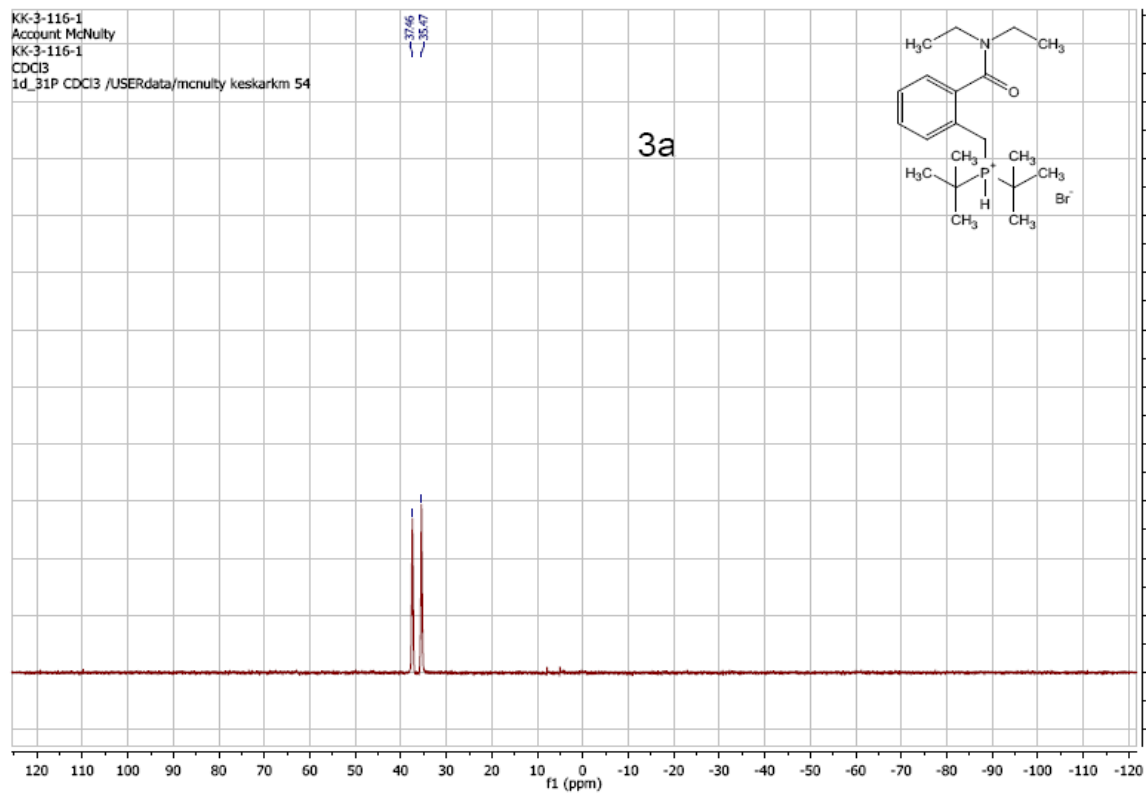
2-((di-tert-butylphosphino)methyl)benzoic acid hydrobromide (Scheme 5-1, 2):



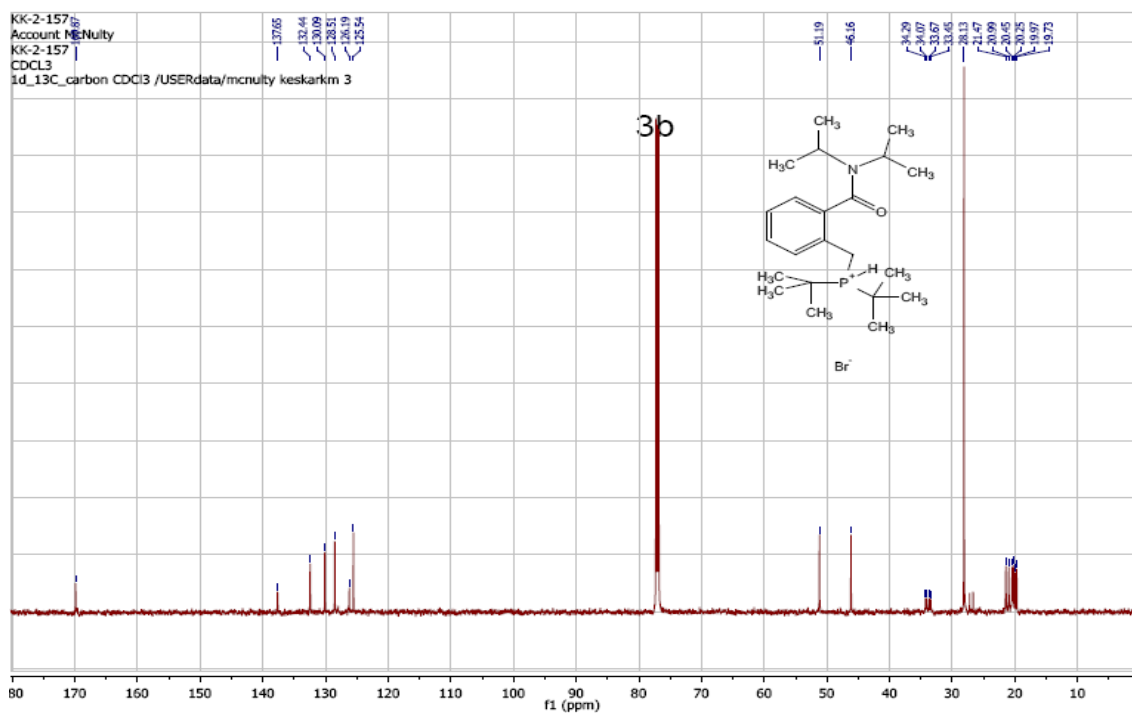
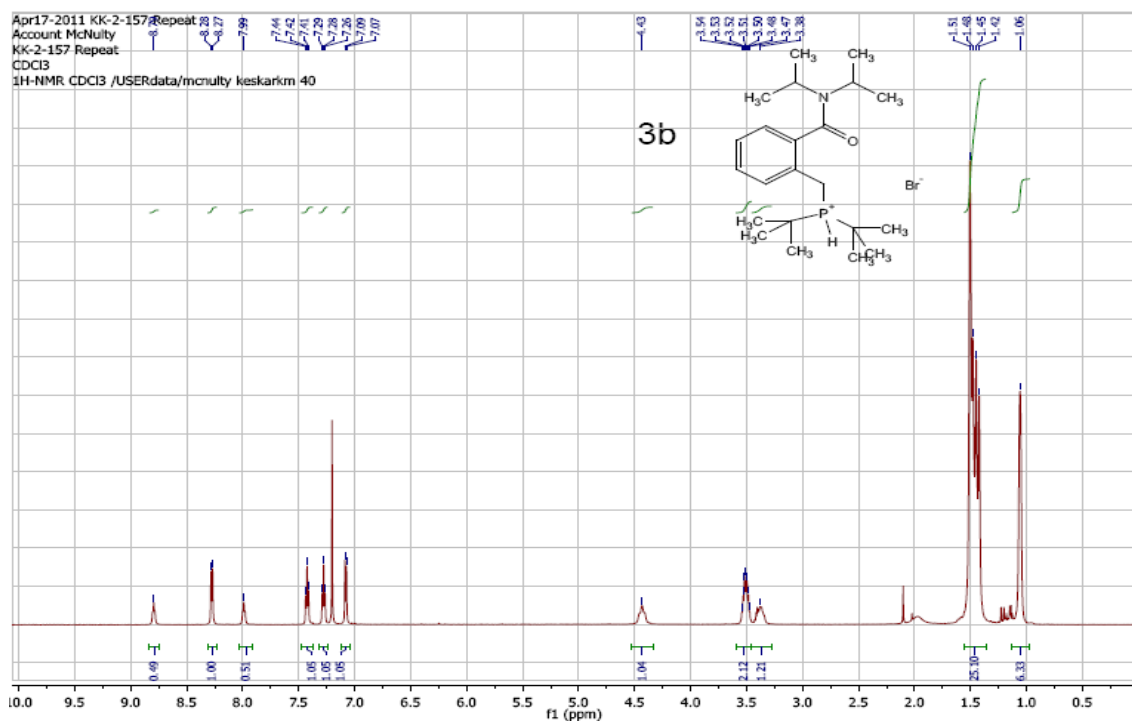


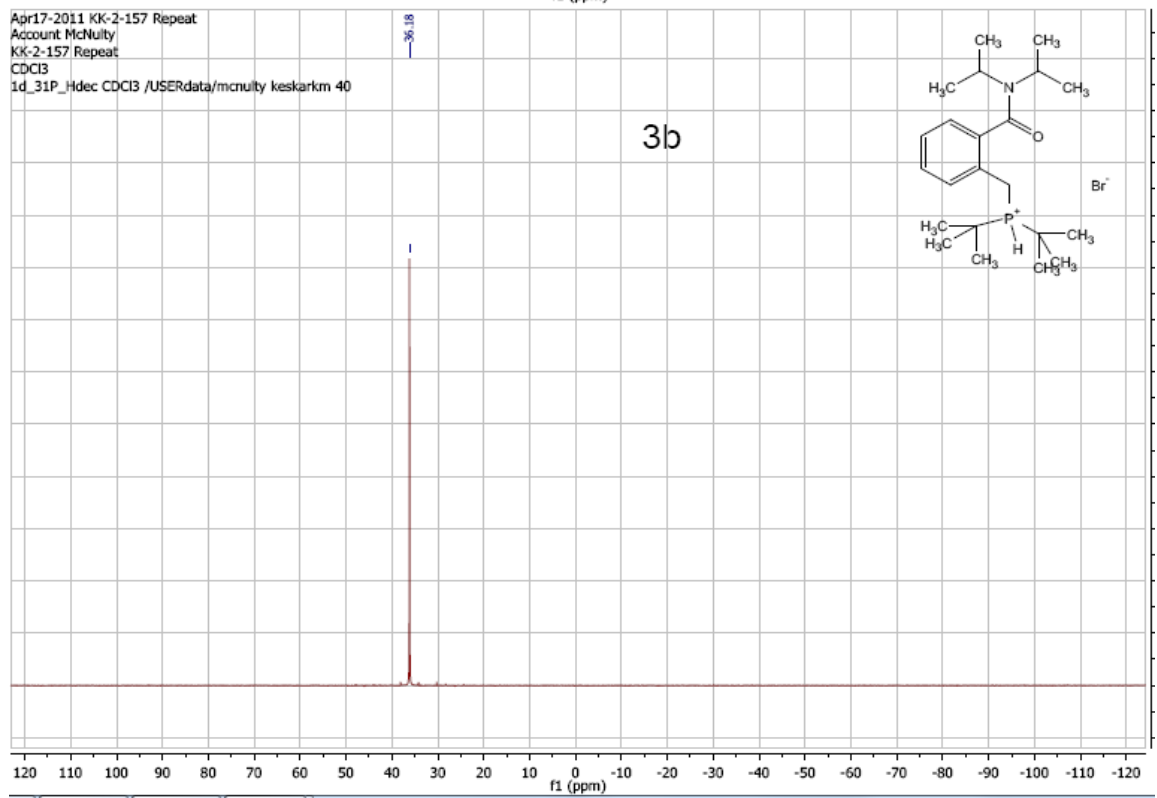
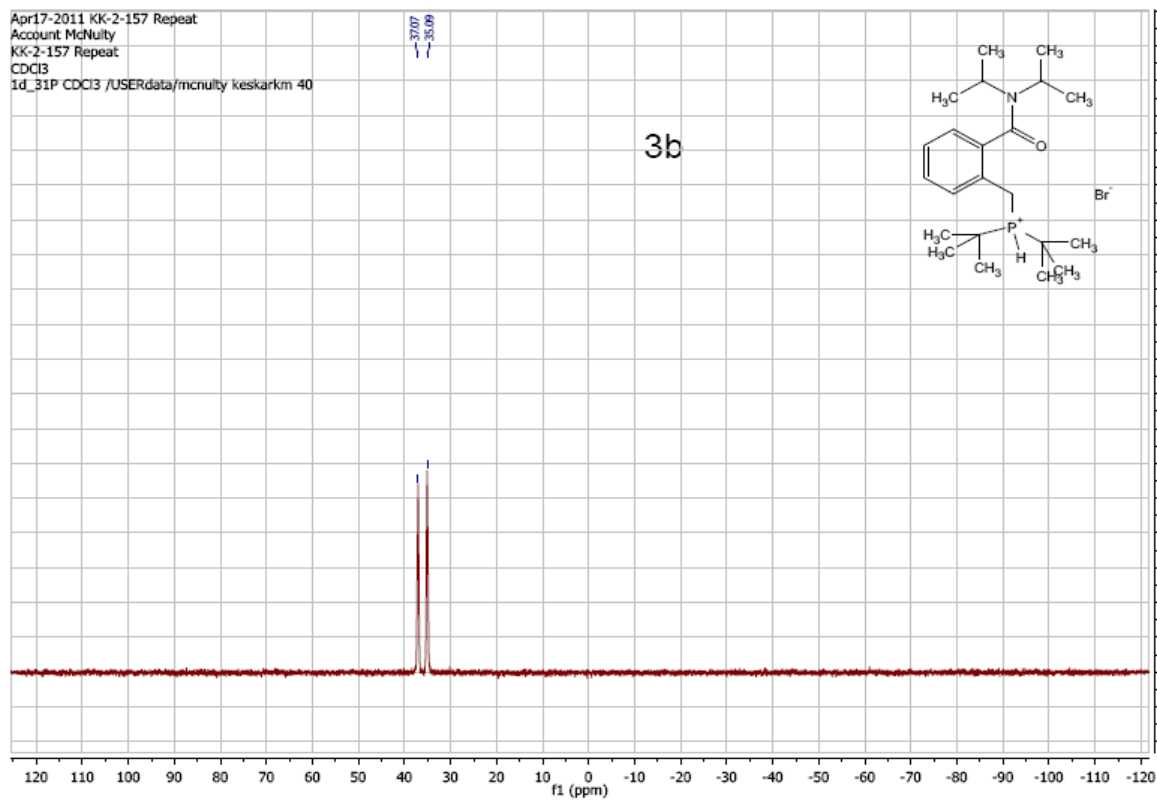
2-((di-tert-butylphosphino)methyl)-*N,N*-diethylbenzamide hydrobromide
(Scheme 5-1, 3a):



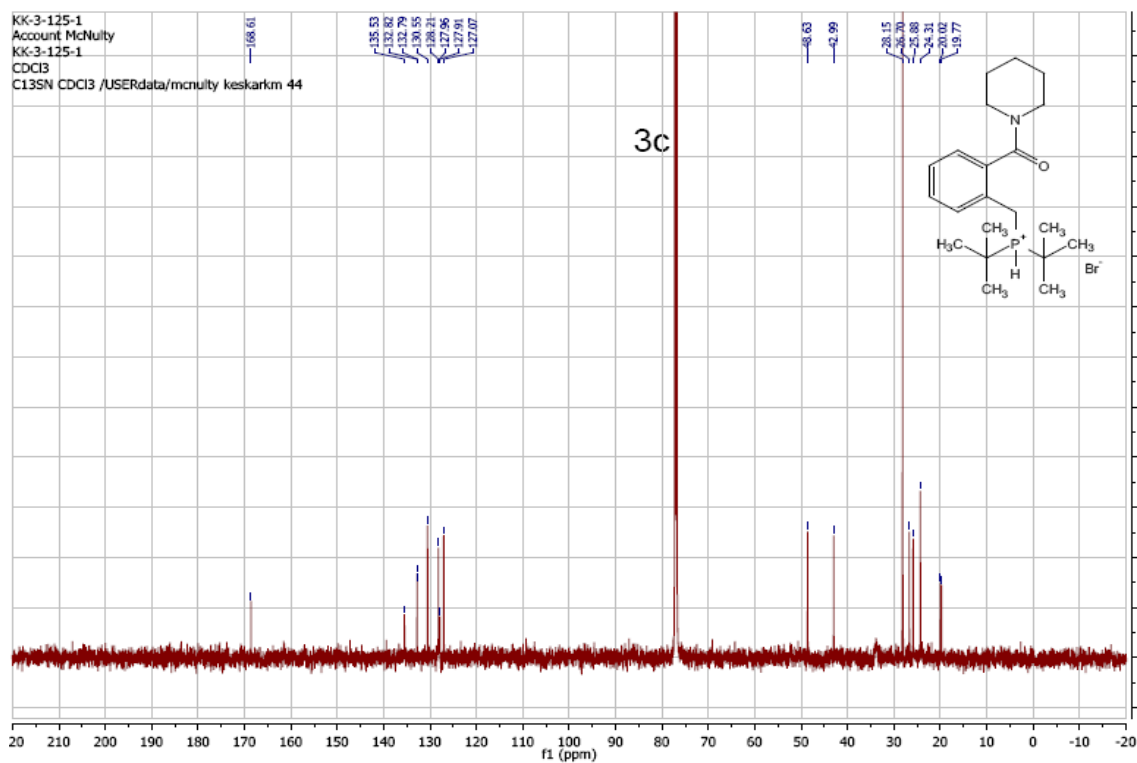
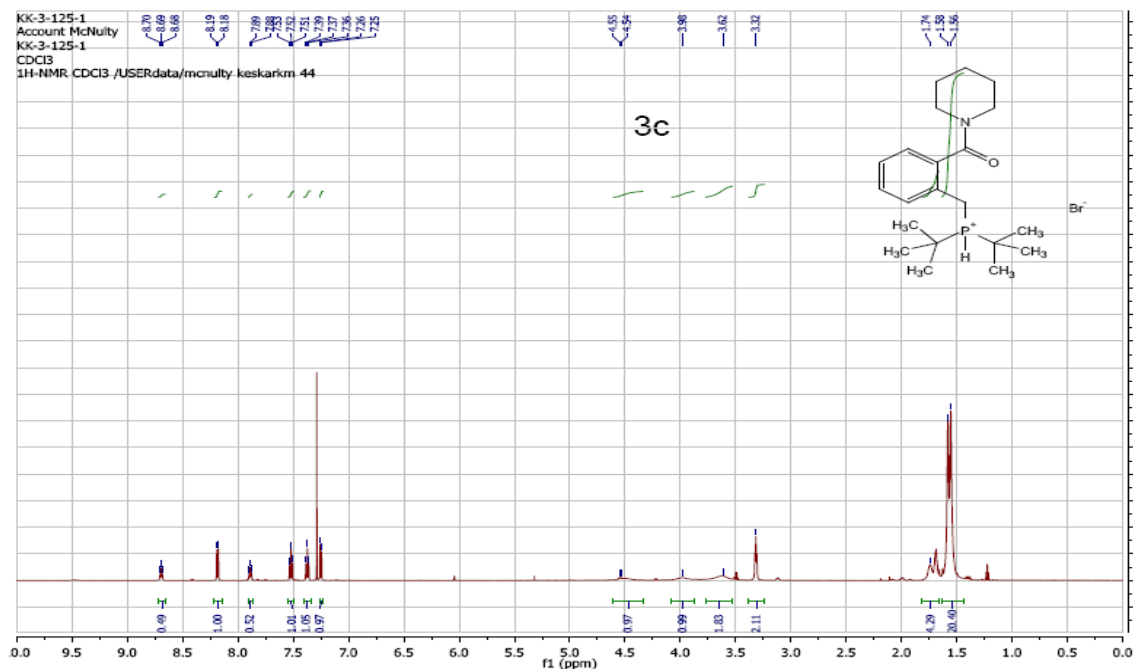


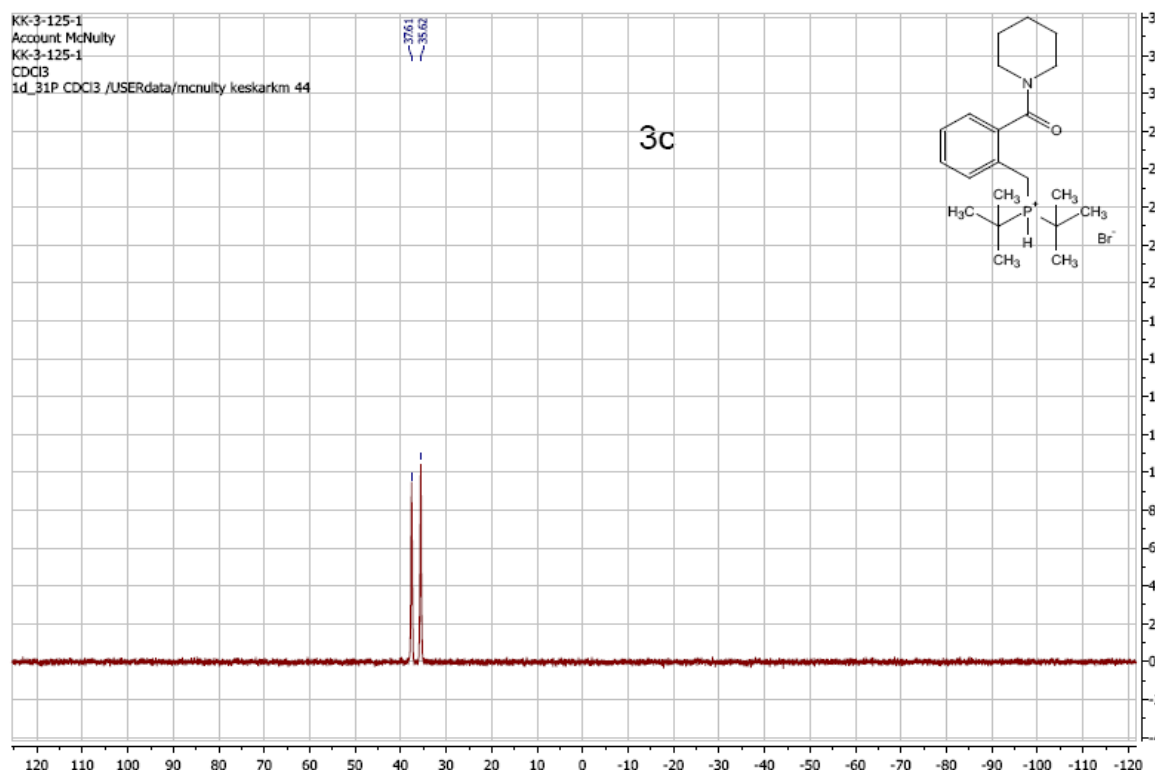
2-((di-tert-butylphosphino)methyl)-*N,N*-diisopropylbenzamide hydrobromide
(Scheme 5-1, 3b):



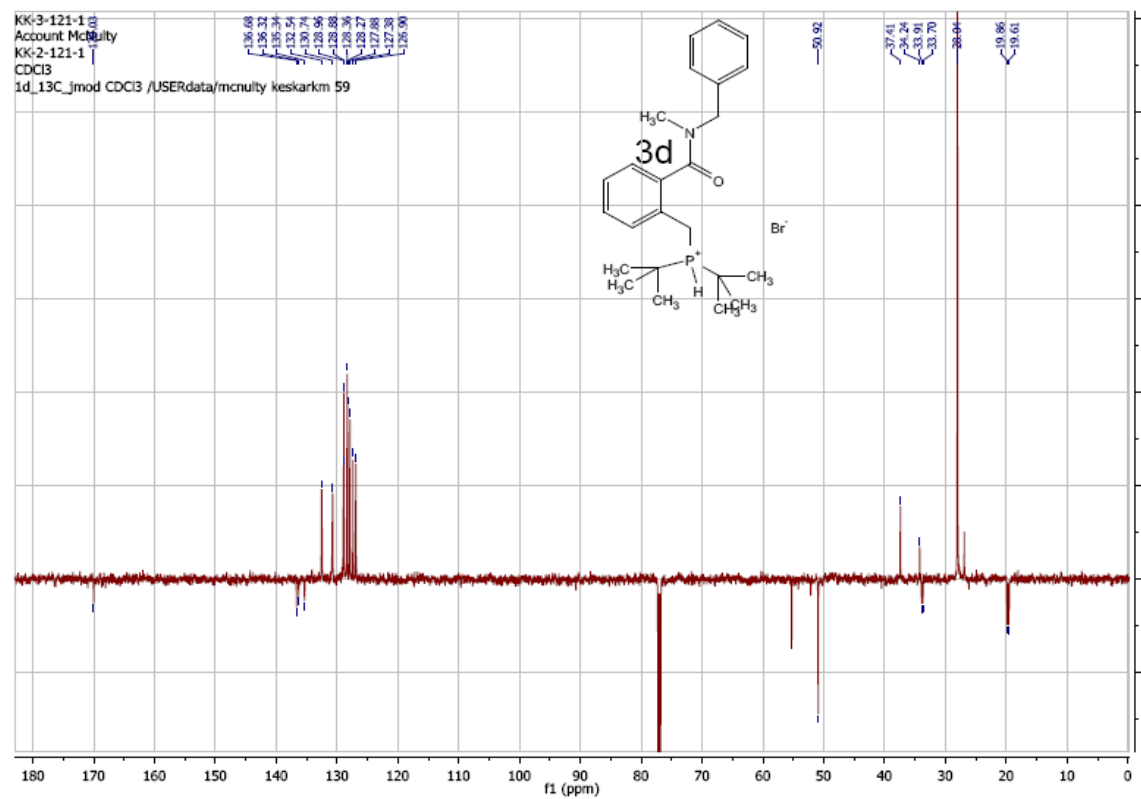
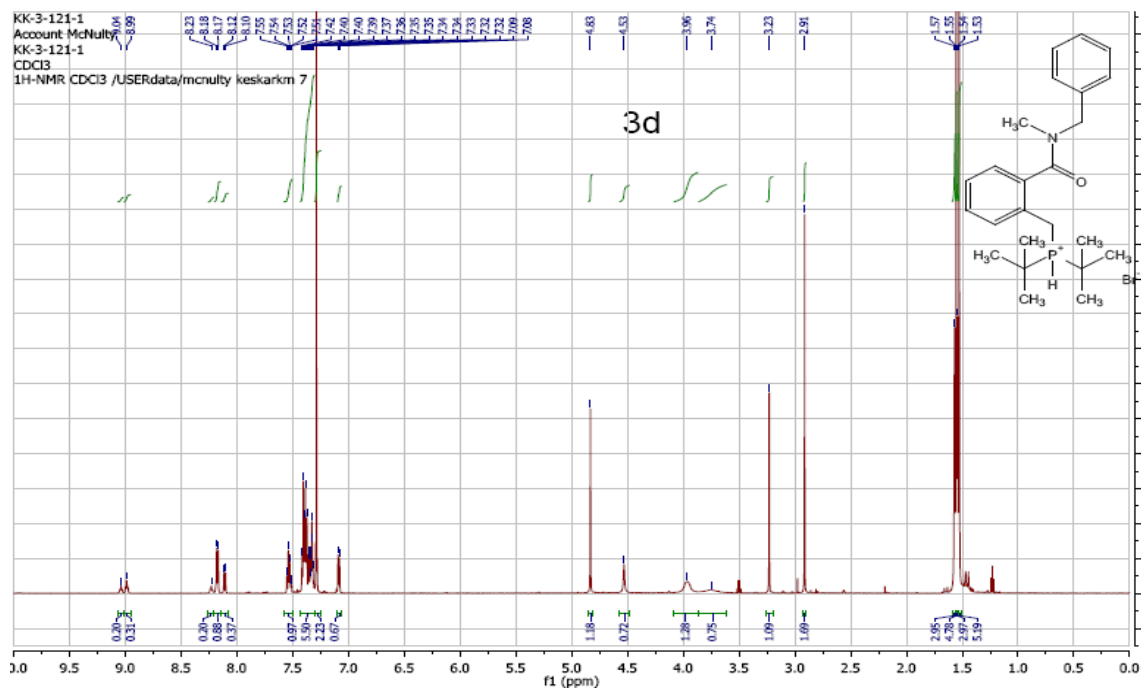


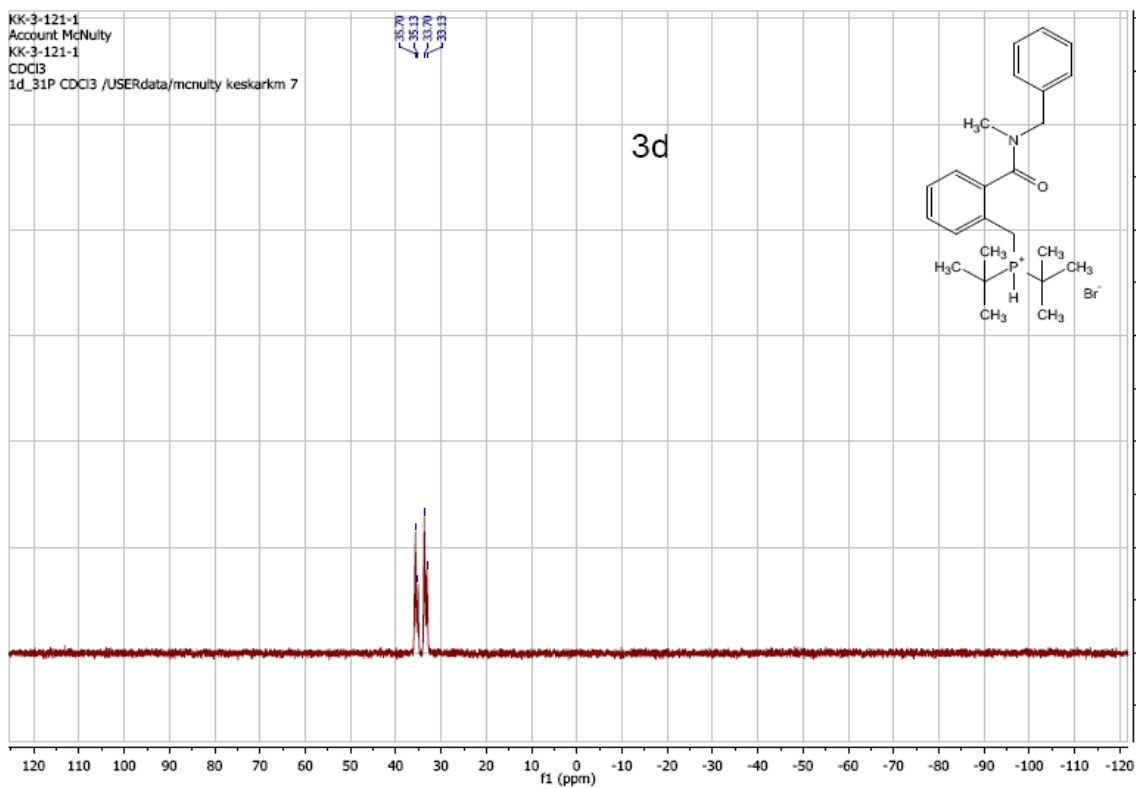
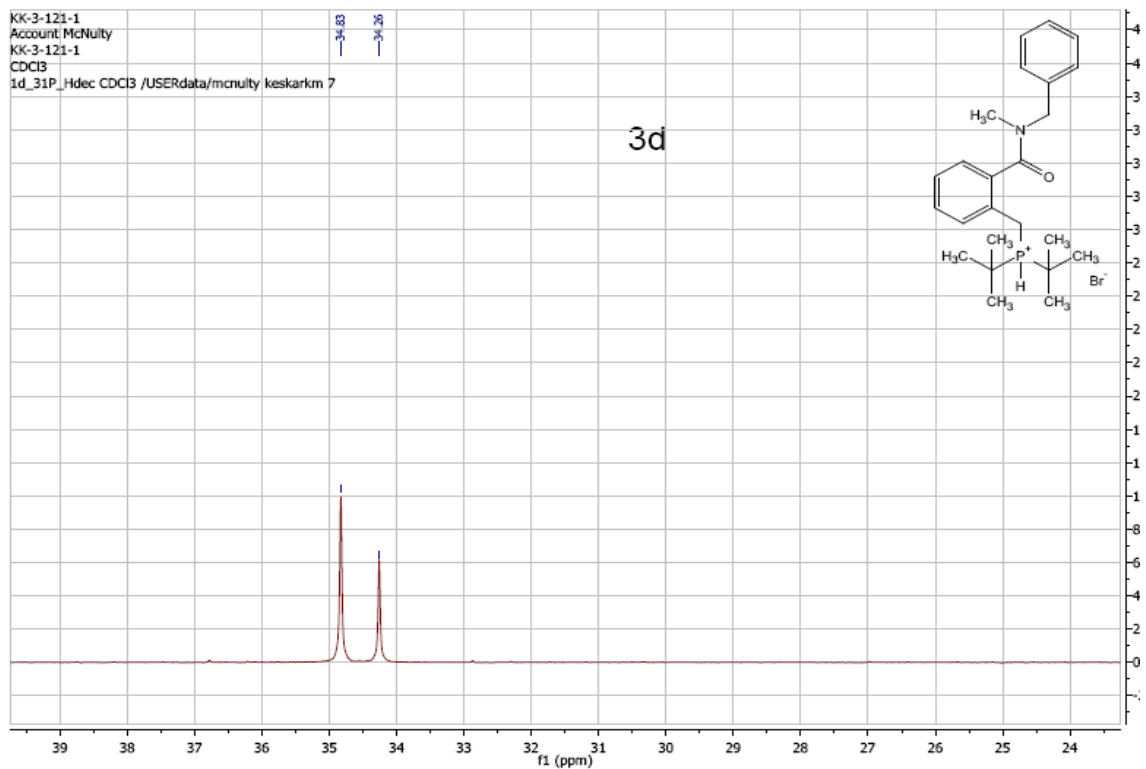
(Scheme 5-1, 3c):



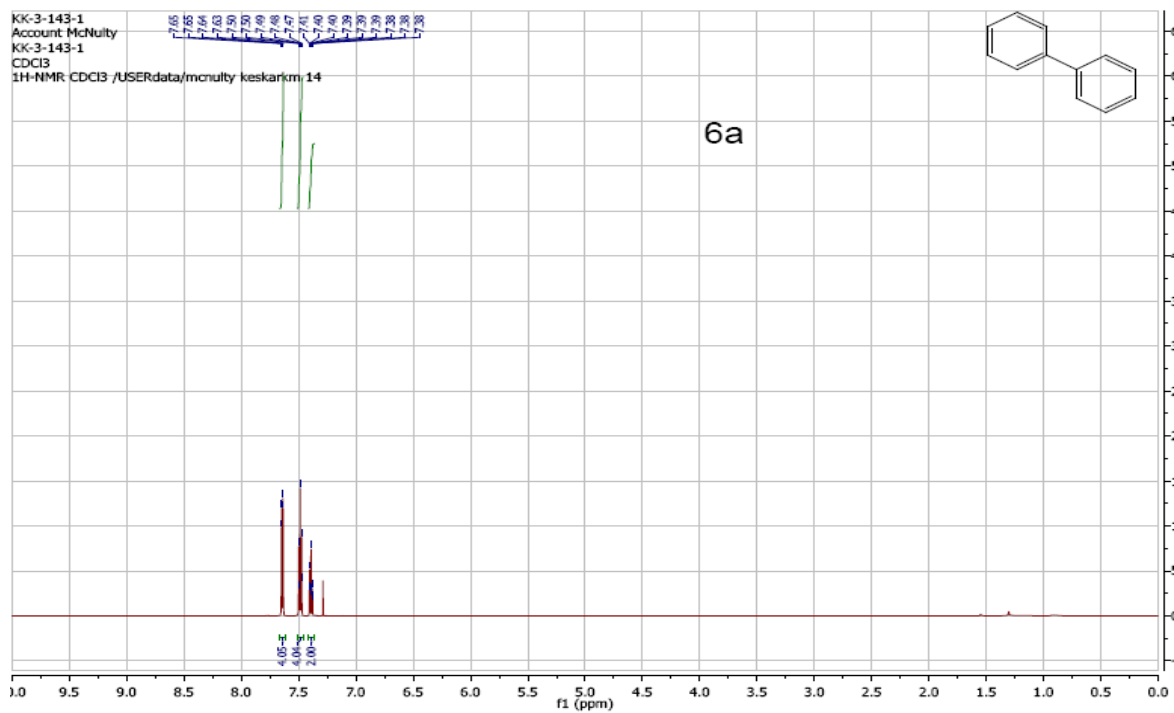


(Scheme 5-1, 3d):

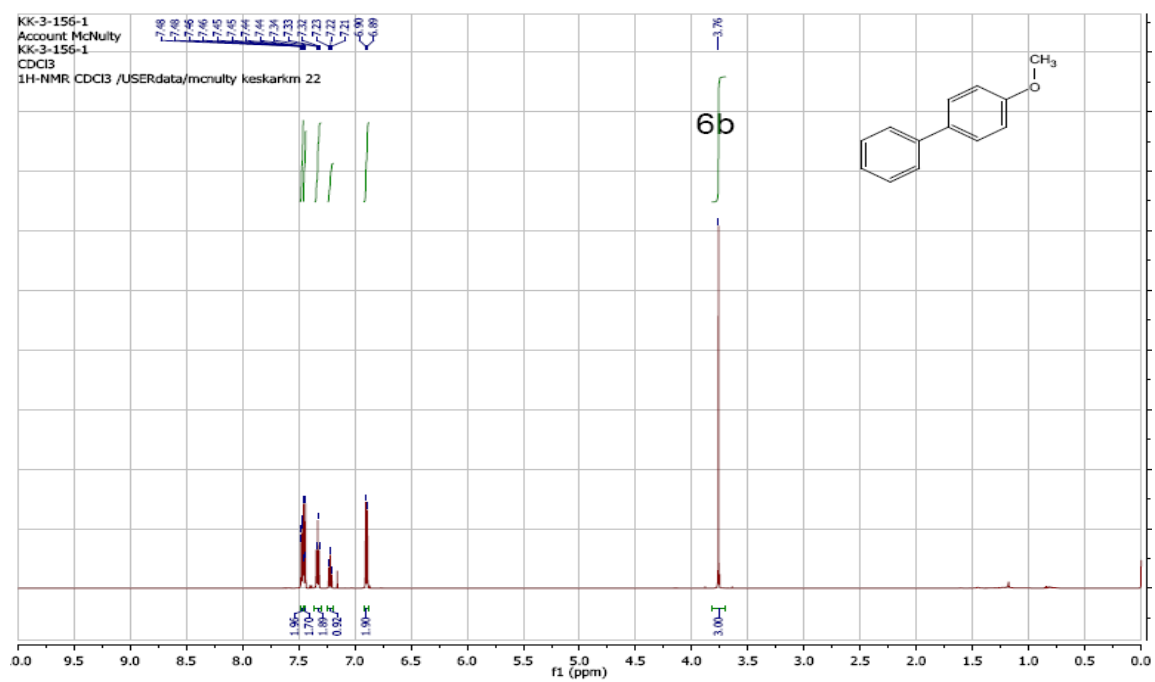




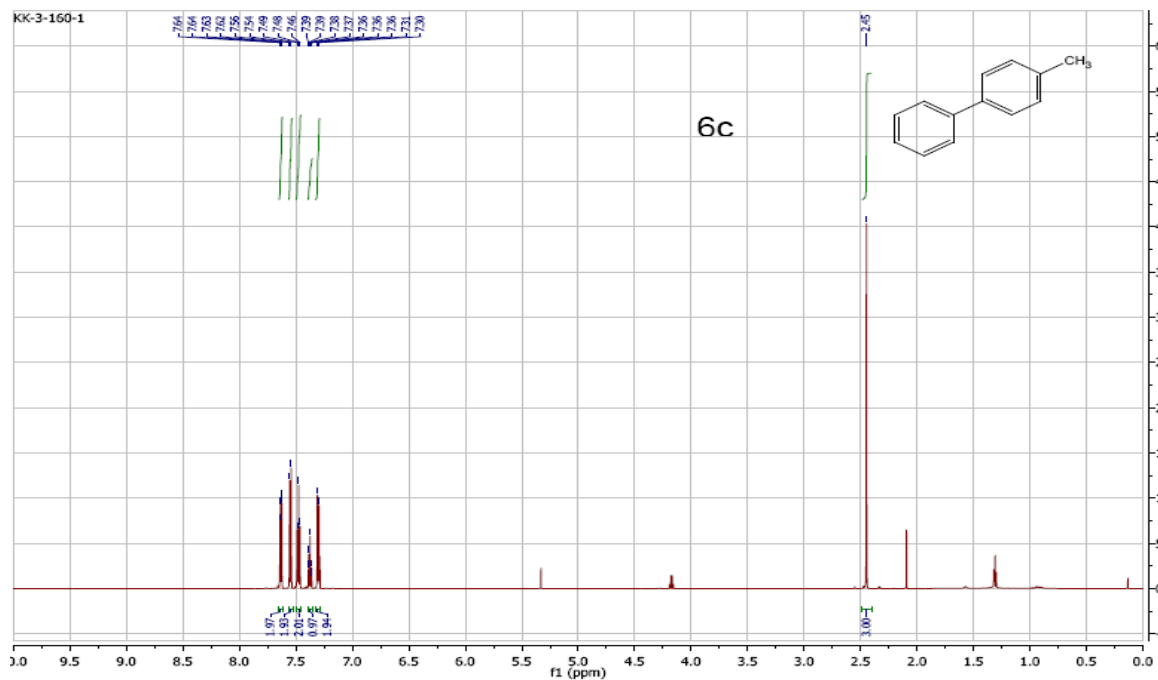
Biphenyl (Table 5-3, 6a):



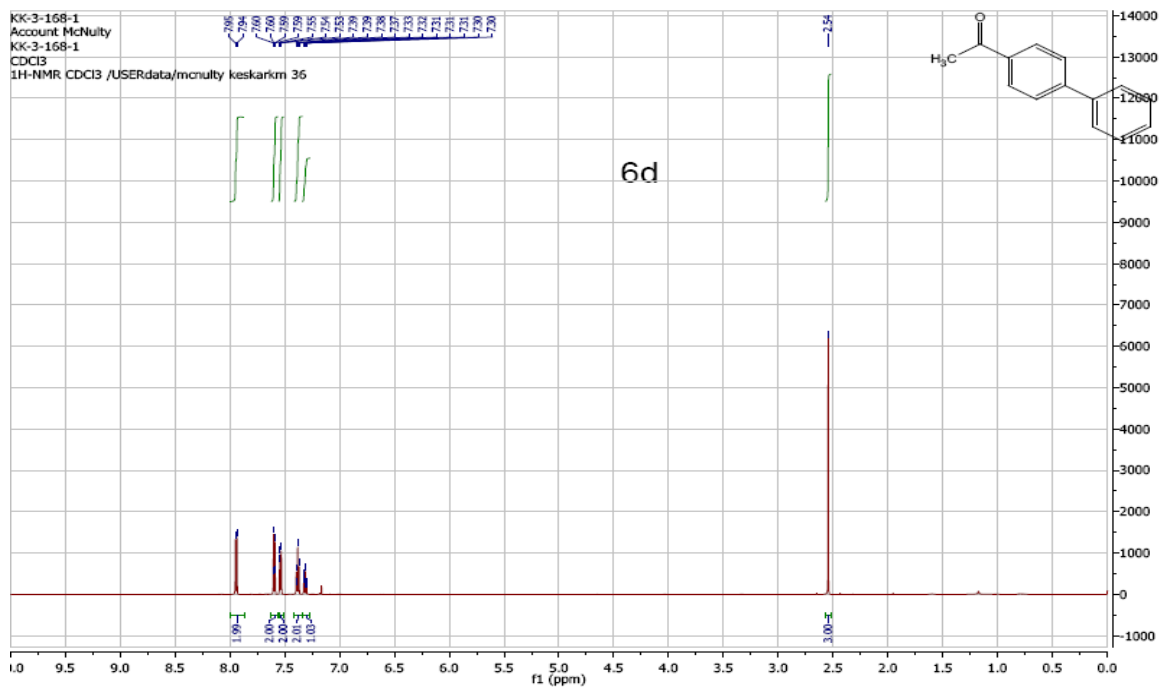
4-Methoxybiphenyl (Table 5-3, 6b):



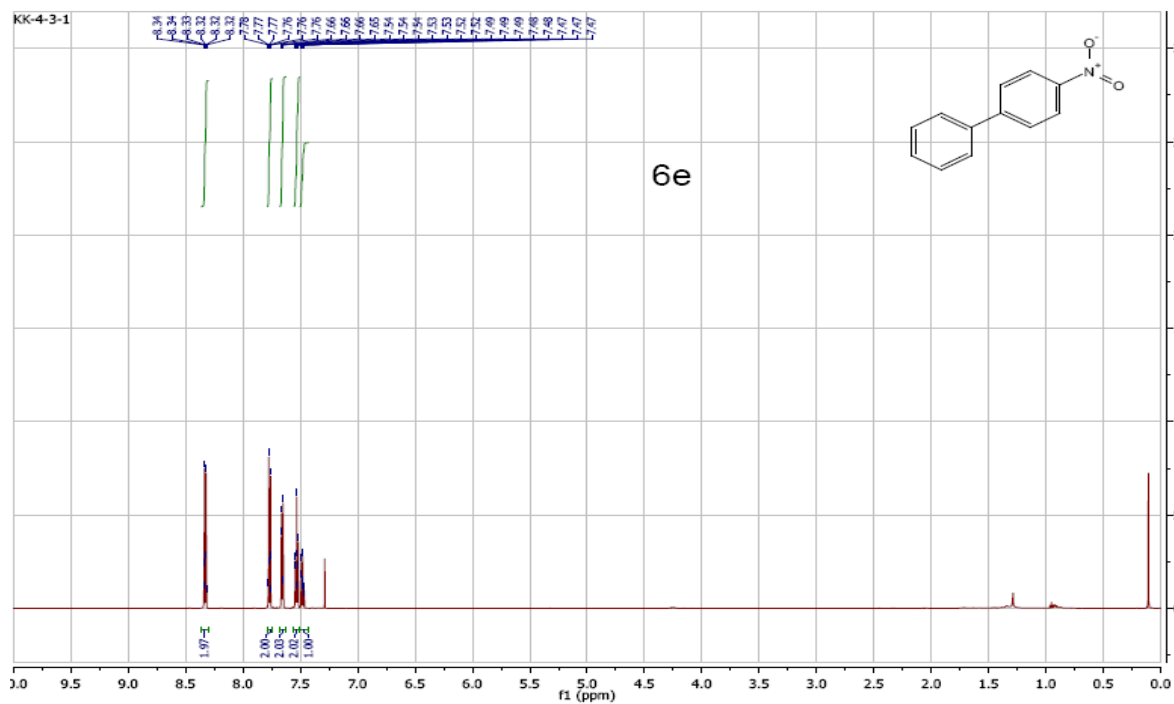
4-Methylbiphenyl (Table 5-3, 6c):



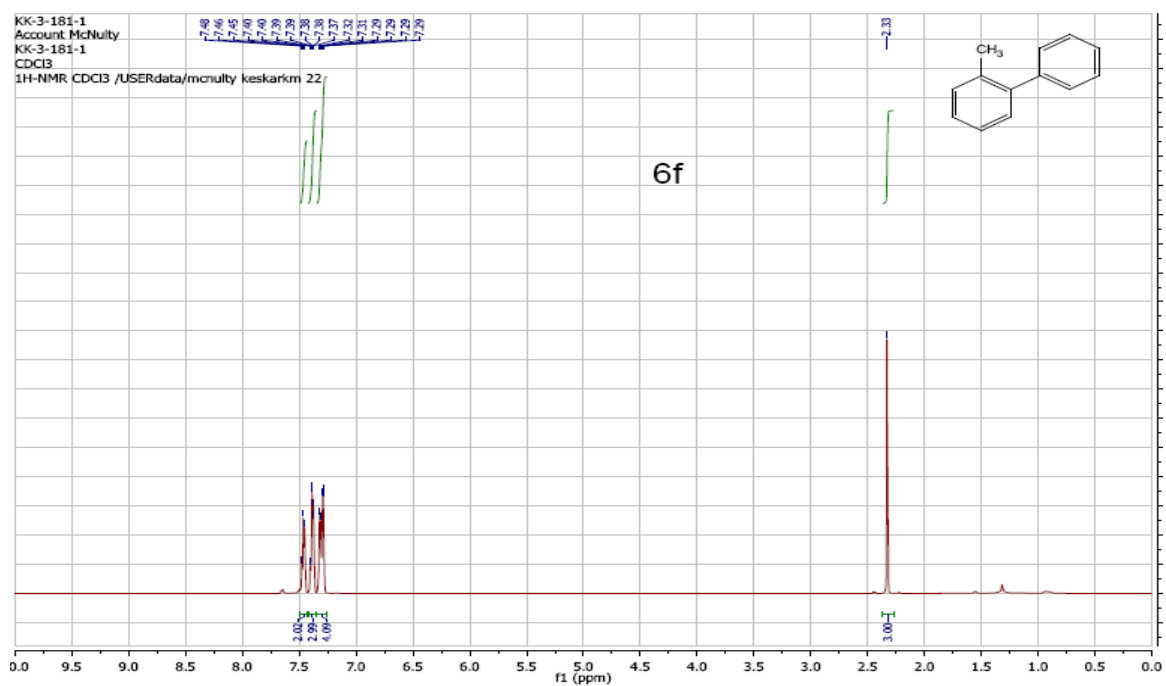
1-(biphenyl-4-yl)ethanone (Table 5-3, 6d):



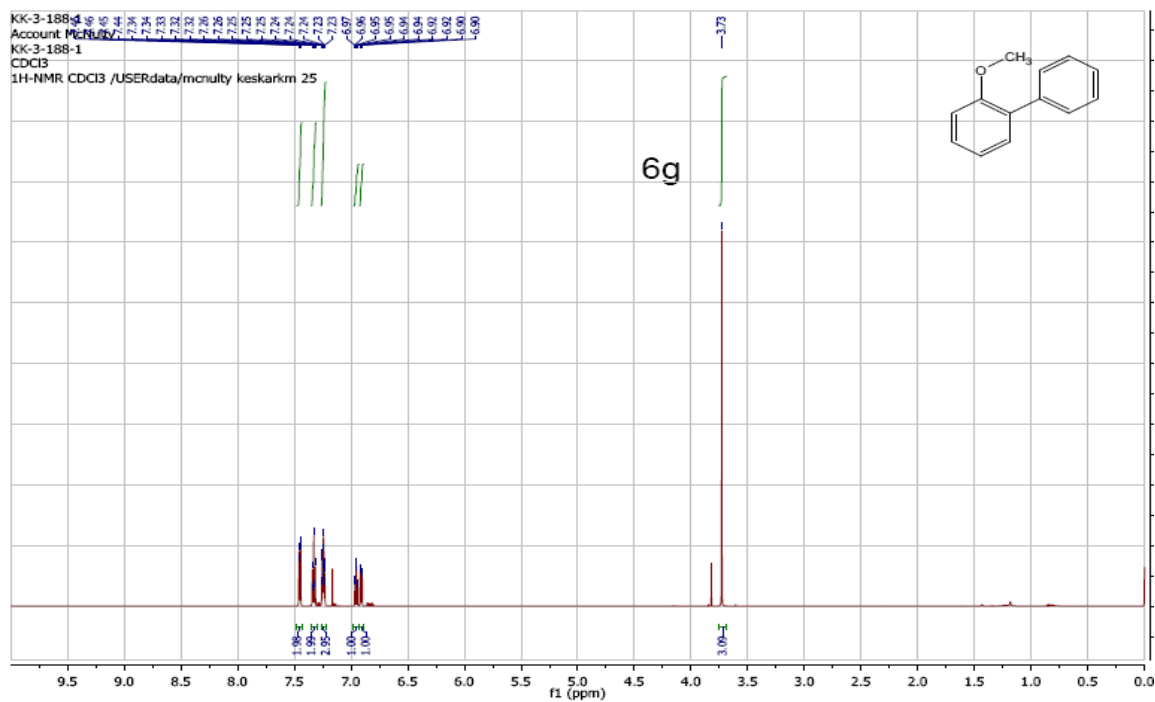
4-nitrobiphenyl (Table 5-3, 6e):



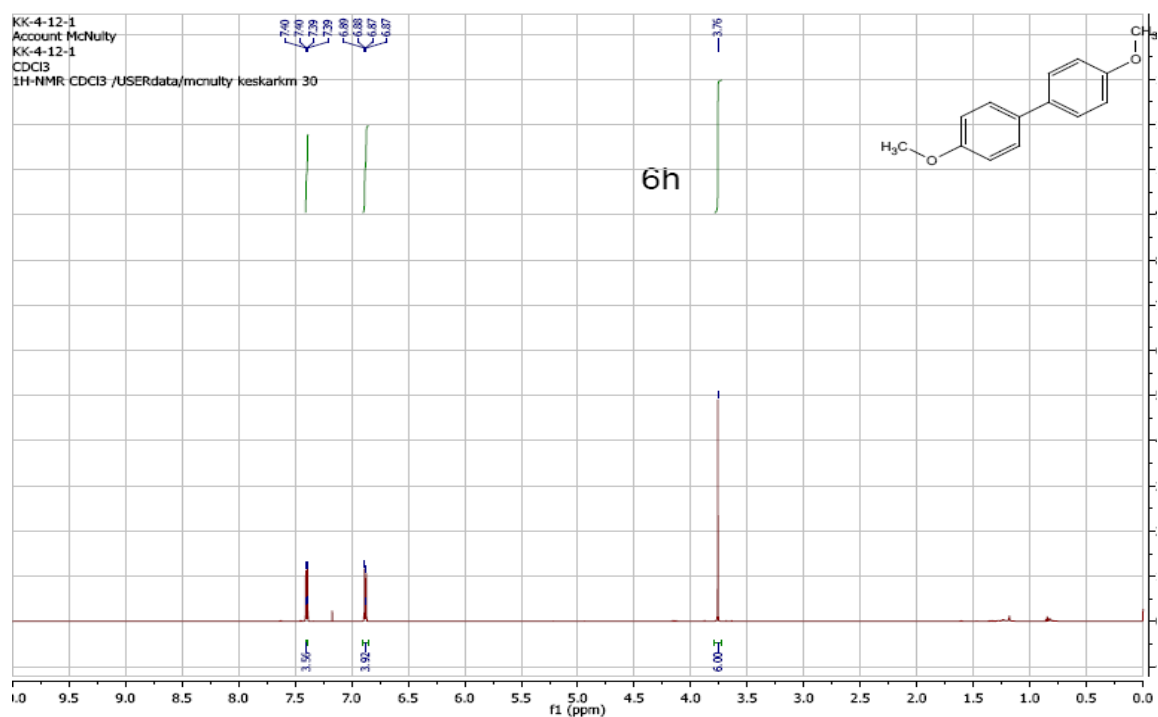
2-methylbiphenyl (Table 5-3, 6f):



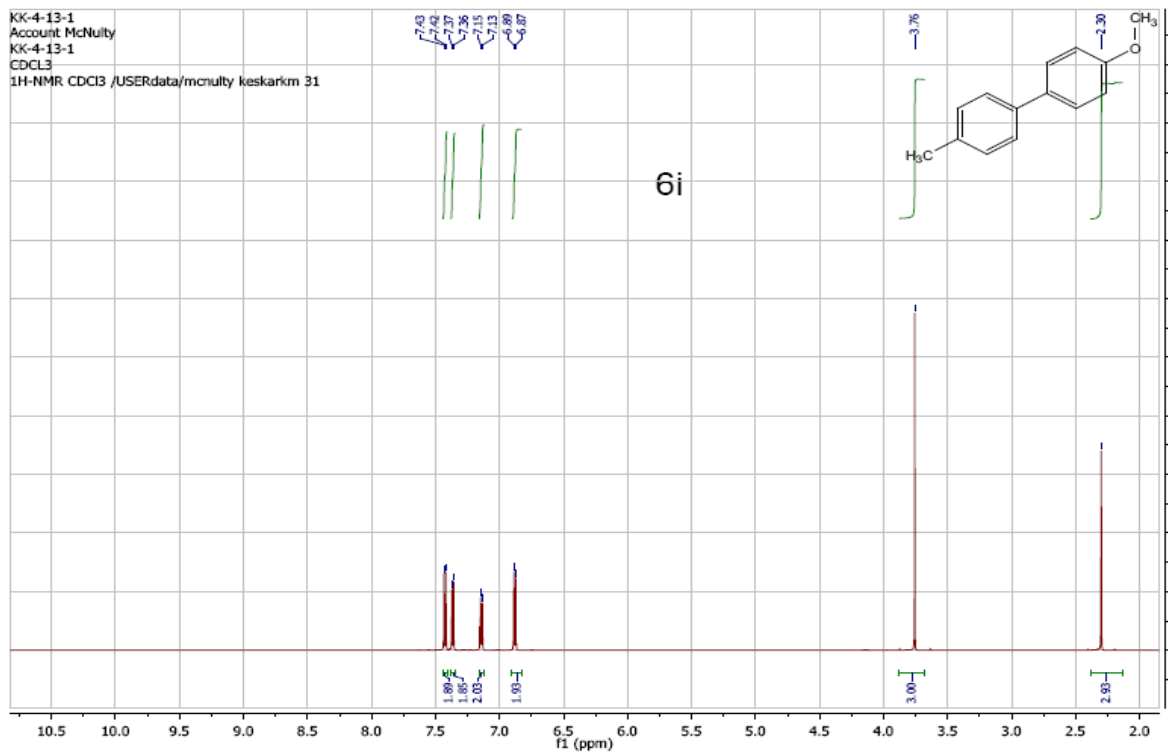
2-methoxybiphenyl (Table 5-3, 6g):



4,4'-dimethoxybiphenyl (Table 5-3, 6h):



4-methoxy-4'-methylbiphenyl (Table 5-3, 6i):



ELSEVIER LICENSE
TERMS AND CONDITIONS

Sep 30, 2014

This is a License Agreement between Kunal Keskar ("You") and Elsevier ("Elsevier") provided by Copyright Clearance Center ("CCC"). The license consists of your order details, the terms and conditions provided by Elsevier, and the payment terms and conditions.

All payments must be made in full to CCC. For payment instructions, please see information listed at the bottom of this form.

Supplier	Elsevier Limited The Boulevard, Langford Lane Kidlington, Oxford, OX5 1GB, UK
Registered Company Number	1982084
Customer name	Kunal Keskar
Customer address	1280 Main St W Hamilton, ON L8S 4M1
License number	3464201236826
License date	Sep 08, 2014
Licensed content publisher	Elsevier
Licensed content publication	Bioorganic & Medicinal Chemistry Letters
Licensed content title	Discovery of a new class of cinnamyl-triazole as potent and selective inhibitors of aromatase (cytochrome P450 19A1)
Licensed content author	James McNulty, Kunal Keskar, Denis J. Crankshaw, Alison C. Holloway
Licensed content date	Available online 7 August 2014
Licensed content volume number	n/a
Licensed content issue number	n/a
Number of pages	1
Start Page	None
End Page	None
Type of Use	reuse in a thesis/dissertation
Intended publisher of new work	other
Portion	full article
Format	both print and electronic

Are you the author of this Elsevier article?	Yes
Will you be translating?	No
Title of your thesis/dissertation	"Advances in Late Transition Metal Catalysis, Olefination Reactions and Applications"
Expected completion date	Dec 2014
Estimated size (number of pages)	
Elsevier VAT number	GB 494 6272 12

Chapter VI: Discovery of a new class of cinnamyl-triazole as potent and selective inhibitors of aromatase (cytochrome P450 19A1)

6.1 Introduction

Aromatase inhibitors (AI's), such as exemestane **1**, anastrozole **2** and letrozole **3**, have emerged over the last few decades as alternatives to the selective estrogen receptor modulating agent tamoxifen **4**, in the treatment of hormone-dependent breast cancer. Approximately 75% of postmenopausal breast cancer patients have hormone-dependent (estrogen-dependent) breast cancer,¹ now the leading cancer amongst women.² Tamoxifen **4** (**Figure 6-1**) served as the standard anti-estrogen in treating such tumors for many years.^{3a-f} Tamoxifen and its metabolites function as selective estrogen receptor modulators (SERMs).^{3f} Their partial antagonist action in breast tissue prevents estrogen binding and resulting downstream effects that include cancer cell proliferation and the activation of survival and anti-apoptosis pathways.^{3d-e}

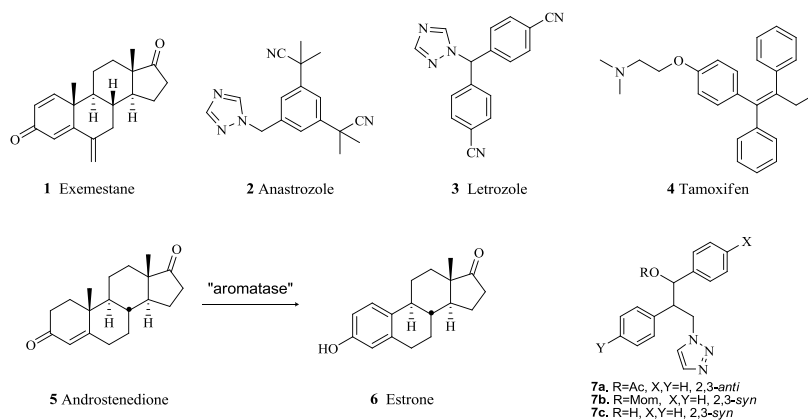


Figure 6-1. Structures of currently used AIs **1-3**, and the SERM agent tamoxifen **4**. Example of aromatase conversion of **5** to **6** and structure of recently described potent AIs **7** employing aryl halide ketone bioisosteres.

Als are inhibitors of human cytochrome P450 19A1 enzyme complex (CYP19A1), the rate-limiting enzyme involved in the oxidative decarboxylation of the C19 methyl group in androgens such as testosterone and androstenedione **5** leading to the estrogens estradiol and estrone **6** respectively (**Figure 6-1**).⁴ Irreversible Type-I aromatase inhibitors (steroidal) such as exemestane **1** as well as reversible, nonsteroidal type-II inhibitors exemplified by anastrozole **2** and letrozole **3**, are currently approved Als for the treatment of metastatic estrogen-dependent breast cancer.^{1a,5a-e}

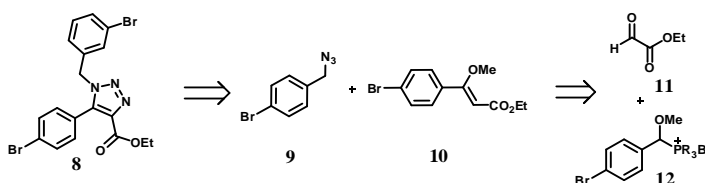


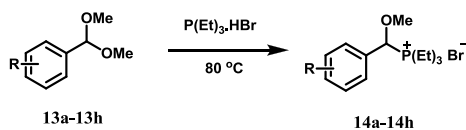
Figure 6-2. Cinnamyl-triazole core structure **8** and retrosynthetic analysis based on the Wittig reaction of alkoxyphosphonium salt **12**.

Despite their clinical success, current Als are associated with issues such as osteoporosis, joint pain, reproductive problems and androgenic side effects. These compounds also partly inhibit cytochromes 1A1, 1A2, 2D6, 2C8/9 and 3A4, all of which are involved in the metabolism of xenobiotics, thus increasing the likelihood of drug-drug interactions. These factors necessitate the discovery and development of structurally novel, potent and selective Als for the next generation treatment of ER positive breast cancer. Natural products and structural analogues have proven to be valuable sources in the search for lead compounds as nonsteroidal Als. In particular, natural products from the cinnamic and coumaric acid pathways, including cinnamates, chalcones, flavanones/flavones, isoflavones and stilbenes⁶ have been shown to be privileged structures amongst naturally occurring Als. Work in our own laboratories resulted in the discovery of natural flavones^{6c} that exhibited potent aromatase inhibitory activity as well as a series of alkaloids and synthetic

derivatives that demonstrated selective activity against aromatase and other cytochrome P450s.⁷ This work resulted in the discovery^{8a} of potent triazole-containing AIs based on a common 5-component pharmacophore **7** (**Figure 6-1**). A key aspect of the optimization in this work was the inclusion of aryl bromide residues as carbonyl-mimics at positions corresponding the keto groups on androstenedione.^{8b} The use of aryl halides as ketone bioisosteres resulted in increased aromatase inhibition to 20 nM. In continuance of this work, we desired to explore a rapidly accessible system capable of mimicking the androstendione core and allowing incorporation of aryl halide groups at the critical positions. Consideration of both natural product and synthetic AI structures led us to postulate the cinnamyl-triazole core molecule **8** (**Figure 6-2**) as a potential new lead for developing AIs. In this letter, we report the synthesis of an initial mini-panel of compounds based on this cinnamyl-triazole core and discovery of their potent aromatase activities.

6.2 Results and Discussion

The principal method for preparing 1,2,3-triazoles is the copper(I) catalyzed 1,3-dipolar stepwise cycloaddition of an azide onto an alkyne (Click Reaction).¹¹ The direct synthesis of 1,2,3-triazoles under metal-free thermal cycloaddition conditions (Huisgen reaction) is less explored. In addition to alkynes, access to 1,2,3-triazoles from the cycloaddition of azides onto heteroatom-substituted alkenes is an alternative route to functionalized triazoles. Examples of such “alkyne equivalents” include enol ethers, enamines, vinylogous amides, vinyl amides, and vinyl sulfoxides. The cycloadditions of azides onto functionalized alkenes typically requires higher temperatures than alkynes, but such alkenes do possess advantages such easy access from carbonyl compounds and high regioselectivity in the cycloaddition due to the polarized nature of the alkene.

**Scheme 6-1.** Synthesis of alkoxyphosphonium salts **14a-14h**.**Table 6-1.** Conversion of α -methoxy phosphonium salts to β -methoxycinnamate “alkyne equivalents”.

Entry	Alpha-alkoxy P salts	Beta-alkoxy acrylate Isolated yield(%)
1	 14a	 15a 80
2	 14b	 15b 85
3	 14c	 15c 82
4	 14d	 15d 80
5	 14e	 15e 85
6	 14f	 15f 88
7	 14g	 15g 52
8	 14h	 15h 40

Following a recently described method for the synthesis of α -alkoxyphosphonium salts (**Scheme 6-1**), from the reaction of a dialkylacetal and a trialkylphosphine hydrobromide salt,^{9a} we prepared the series of α -methoxybenzyl phosphonium salts **14a-h** (**Scheme 6-1**). These salts were obtained in high yield (92-98%) without need of chromatographic purification through simply removing methanol under high vacuum. We next investigated α -methoxy ylide formation and olefination of the range of substituted phosphonium salts with ethyl glyoxylate. Dark red solutions of the ylides were generated in THF at -78 °C using lithium bistrimethylsilylazide. Efficient olefination occurred in all cases upon addition of ethyl glyoxylate and the corresponding methoxycinnamate **15a-h** were purified by silica gel chromatography and isolated in 40–88% yields and good (*E*) selectivity. (*E*: *Z* ratio ranging between 70:30 to 80:20.) as summarized in **Table 6-1**. These β -alkoxycinnamates are relatively stable to air but are readily hydrolyzed to the corresponding β -keto esters in high yield upon treatment with acids.

Thermal cycloaddition of the series of methoxycinnamates with benzylic azides occurred smoothly in a sealed tube at 150 °C, leading to the desired triazoles **16a-h** in fair to excellent yield. The cycloadditions were seen to be completely regioselective, leading only to the 1,4,5 trisubstituted 1,2,3-triazoles. Regiochemical assignments are in accord with earlier examples confirmed via X-ray crystallographic analysis.¹⁰ⁱ The well-known Cu-catalyzed azide alkyne cycloaddition leads to 1,4-triazoles and requires employment of a terminal alkyne.¹¹ Thus in addition to complete regiocontrol, the use of vinyl ethers allows access to functionalized triazoles that are not available from the conventional click process.

The series of eight novel cinnamyltriazoles **16a-h** described in **Table 6-2** were screened for activity against recombinant human aromatase via kinetic monitoring of the conversion of *O*-dibenzylfluorescein benzyl ester (DBF) substrate to fluorescein by-product.^{8a} Fluorometric measurement of emission

was made at 535 nm after excitation at 485 nm utilizing ketoconazole as a positive control. The overall results of the screening are shown in **Table 6-2**. To our delight, several analogs proved to be potent inhibitors, displaying a 100-fold range in potencies ranging from the μM range down to 20 nM, **Table 6-2**. The most interesting examples proved to be the dibromo compound **16c** and the corresponding bromo-chloro-analog **16f** that exhibited potencies of 20 and 30 nM respectively. The positions of halogenation approximate the location of the carbonyl groups in natural substrates such as androstendione. These results add further to the previous postulate of arylbromide/chloride residues as bioisosteres^{8b} in the development of stable analogs as potent AI's. In addition to potency, the discovery of this new pharmacophore is significant in view of the rapid synthetic entry to the series in only four chemical steps following the sequence aldehyde to dimethylacetal **13**, to alkoxyphosphonium salt **14**, to methoxycinnamate **15** and finally triazole **16**. The final thermal Huisgen reaction with benzylic (or other) azide as the fourth (last) step leading to **16** allows significant late-stage diversity for further optimization in this new lead series.

6.3 Conclusion

In summary, we report a new natural product-inspired heteroaromatic 1,4,5-substituted cinnamyltriazole pharmacophore, examples of which display potent aromatase inhibitory activity. The core structure can be rapidly prepared in four linear steps from readily available aldehydes and the synthesis incorporates a regiospecific, diversity oriented thermal Huisgen reaction as the last step. The most potent AIs within this new series incorporate aryl halide residues at positions mimicking the carbonyl substituents of the natural enzyme substrates. Further development of potent and selective AIs based on this novel pharmacophore are currently under investigation.

Table 6-2. Regiocontrolled thermal Huisgen cycloaddition of benzyl azides onto β -methoxycinnamates leading to potent AIs.

R $\xrightarrow[\text{Sealed Tube, 150 } ^\circ\text{C}]{\text{BnN}_3}$

Entry	Beta-alkoxy acrylate	Benzyl azide	Click Product	Isolated Yield (%)	K _i (uM)	pK _i
1	15b	N_3	16a	95	1.41	5.85
2	15f	N_3	16b	95	0.64	6.20
3	15f	N_3	16c	96	0.02	7.66
4	15d	N_3	16d	57	0.71	6.15
5	15e	N_3	16e	40	0.71	6.15
6	15a	N_3	16f	40	0.03	7.60
7	15a	N_3	16g	44	0.36	6.45
8	15b	N_3	16h	48	0.15	6.84

6.4 References

1. (a) Goss, P.E.; Strasser, K. *J. Clin. Oncol.* **2001**, *19*, 881; (b) Brueggemeier, R. W.; Hackett, J. C.; Diaz-Cruz, E. S. *Endocr. Rev.* **2005**, *26*, 331; (c) Schneider, R.; Barakat, A.; Pippen, J.; Osborne, C. *Breast. Canc. Targ. Therap.* **2011**, *3*, 113; (d) Litton, J. K.; Arun, B. K.; Brown, P. H.; Hortobagyi, G. N. *Expt. Opin. Pharmacother.* **2012**, *13*, 325; (e) Ingle, J. N. *Steroids*, **2011**, *76*, 765.
2. Breast cancer is also the most frequently diagnosed cancer in women comprising 30% of all new cases and is the second most lethal cancer amongst women. The rate of incidence increased significantly in recent years to 230,480 cases in 2011, with a mortality rate of 20%. (a) International Agency for Research on Cancer. *World Cancer Report 2008*. Lyon, France: International Agency for Research on Cancer; 2008; (b) Siegel, R.; Ward, E.; Brawley, O.; Jemal, A. *CA Canc. J. Clin.* **2011**, *61*, 212; (c) American Cancer Society. *Cancer Facts & Figures 2010*, 3-9; American Cancer Society, Atlanta, 2010.
3. (a) Cole, M. P.; Jones, C. T.; Todd, I. D. *Br. J. Cancer* **1971**, *25*, 270; (b) Baum, M.; Brinkley, D. M.; Dossett, J. A.; McPherson, K.; Patterson, J. S.; Rubens, R. D.; Smiddy, F. G.; Stoll, B. A.; Wilson, A.; Lea, J. C.; Richards, D.; Ellis, S. H. *Lancet* **1983**, *2*, 450; (c) Furr, B. J.; Jordan, V. C. *Pharmacol. Ther.* **1984**, *25*, 127; (d) Jordan, V. C. *Nature Rev. Drug Dis.* **2003**, *2*, 205; (e) Jordan, V. C. *Br. J. Pharmacol.* **2006**, *147*, 269; (f) McDonnell, D. P.; Wardell, S. E. *Curr. Opinion in Pharmacol.* **2010**, *10*, 620.
4. (a) Simpson, E. R; Clyne, C.; Rubin, G.; Boon, W. C.; Robertson, K.; Britt, K.; Speed, C.; Jones, M. *Annu. Rev. Physiol.* **2002**, *64*, 93; (b) Simpson, E. R; Mahendroo, M. S.; Means, G. D.; Kilgore, M. W.; Hinshelwood, M. M.; Graham-Lorence, S.; Amarneh, B.; Ito, Y.; Fisher, C. R.; Michael, M. D. *Endocr. Rev.* **1994**, *15*, 342; (c) James, V. H; McNeill, J. M.; Lai, L. C.;

- Newton, C. J.; Ghilchik, M. W.; Reed, M. J. *Steroids* **1987**, 50, 269; (d) Miller, W. R.; O'Neill, J. *Steroids* **1987**, 50, 537; (e) Reed, M. J.; Owen, A. M.; Lai, L. C.; Coldham, N. G.; Ghilchik, M. W.; Shaikh, N. A.; James, V. H. *Int. J. Cancer* **1989**, 44, 233; (f) Bulun, S. E.; Price, T. M.; Aitken, J.; Mahendroo, M. S.; Simpson, E. R. *J. Clin. Endocrinol. Metab.* **1993**, 77, 1622.
5. (a) Ingle, J. N. *Clin. Cancer Res.* **2001**, 7, 4392; (b) Buzdar, A. U.; Howell, A. *Clin. Cancer Res.* **2001**, 7, 2620; (c) Murray, R. *Cancer Chemother. Pharmacol.* **2001**, 48, 259; (d) Hamilton, A.; Volm, M. *Oncology* **2001**, 15, 965; (e) Buzdar, A. U. *Semin. Oncol.* **2001**, 28, 291.
 6. (a) Balunas, M. J.; Su, B.; Brueggemeier, R. W.; Kinghorn, A. D. *Anticancer Agents Med. Chem.* **2008**, 8, 646; (b) Bonfield, K.; Amato, E.; Bankemper, T.; Agard, H.; Steller, J.; Keeler, J. M.; Roy, D.; McCallum, A.; Paula, S.; Ma, L., *Bioorganic & Med. Chem.* **2012**, 20, 2603. (c) McNulty, J.; Nair, J. J.; Bollareddy, E.; Keskar, K.; Thorat, A.; Crankshaw, D. J.; Holloway, A. C.; Khan, G.; Wright, G. D.; Ejim, L. *Phytochemistry* **2009**, 70, 2040; (d) Wang, Y.; Lee, K. W.; Chan, F. L.; Chen, S.; Leung, L. K. *Toxicol. Sci.* **2006**, 92, 71; (e) Balunas, M. J.; Kinghorn, A. D. *Planta Med.*, **2010**, 76, 1087.
 7. (a) McNulty, J.; Nair, J. J.; Singh, M.; Crankshaw, D. J.; Holloway, A. C. *Bioorg. Med. Chem. Lett.* **2009**, 19, 5607; (b) McNulty, J.; Nair, J. J.; Singh, M.; Crankshaw, D. J.; Holloway, A. C.; Bastida, J. *Bioorg. Med. Chem. Lett.* **2009**, 19, 3233; (c) McNulty, J.; Nair, J. J.; Singh, M.; Crankshaw, D. J.; Holloway, A. C. *Bioorg. Med. Chem. Lett.* **2010**, 20, 2335; (d) McNulty, J.; Nair, J. J.; Singh, M.; Crankshaw, D. J.; Holloway, A. C.; Bastida, J. *Nat. Prod. Comm.* **2010**, 5, 1195; (e) McNulty, J.; Thorat, A.; Vurgun, N.; Nair, J. J.; Makaji, E.; Crankshaw, D. J.; Holloway, A.C.; Pandey, S. *J. Nat. Prod.*, **2011**, 74, 106; (f) McNulty, J.; Nair, J. J.; Griffin, C.; Pandey, S. *J. Nat. Prod.* **2008**, 71, 357; (g) McNulty, J.; Nair, J. J.; Bastida, J.; Pandey, S.; Griffin, C. *Phytochemistry* **2009**, 70, 913.

8. (a) McNulty, J.; Nair, J. J.; Vurgun, N.; DiFrancesco, B.; Brown, C. E.; Holloway, A.; Crankshaw, D.; Tsoi, B. *Bioorg. & Med. Chem. Lett.* **2012**, 22, 718. (b) McNulty, J.; Nielsen, A. J.; Brown, C. E.; DiFrancesco, B.; Vurgun, N.; Nair, J. J.; Crankshaw, D.; Holloway, A. C., *Bioorg. & Med. Chem. Lett.* **2013**, 23, 6060.
9. (a) Das, P.; McNulty, J. *Eur. J. Org. Chem.* **2010**, 3587; (b) McNulty, J.; Keskar, K. *Eur. J. Org. Chem.* **2011**, 6902.
10. (a) Scarpati, R.; Sica, D.; Lionetti, A. *Gazz. Chim. Ital.* **1963**, 93, 90. (b) Chabala, J. C.; Christensen, B. G.; Ratcliffe, R. W.; *Tetrahedron Lett.* **1985**, 26, 5407. (c) Häbich, D.; Barth, W. *Heterocycles.* **1989**, 29, 2083. (d) Peng, W-M.; Zhu, S-Z. *J. Fluorine Chem.* **2002**, 116, 81. (e) Pocar, D.; Stradi, R.; Rossi, L. M. *J. Chem. Soc., Perkin Trans. 1*, **1972**, 619. (f) Nomura, Y.; Takeuchi, Y.; Tomoda, S.; Ito, M. M. *Bull. Chem. Soc. Jpn*, **1981**, 46, 1800. (g) Palacios, F.; Ochoa de Retana, A. M.; Pagalday, J.; Sanchez, J. M. *Heterocycles*, **1995**, 40, 543. (h) Palacios, F.; Ochoa de Retana, A. M.; Pagalday, J.; Sanchez, J. M. *Org. Prep. Proced. Int.* **1995**, 27, 603. (i) Peng, W.; Zhu, S. *Synlett*, **2003**, 187. (j) Peng, W.; Zhu, S. *Tetrahedron*, **2003**, 59, 4395. (k) Kadaba, P. K. *J. Org. Chem.* **1992**, 57, 3075. (l) Sasaki, T.; Eguchi, S.; Yamaguchi, M.; Esaki, T. *J. Org. Chem.* **1981**, 46, 1800. (m) Freeze, S.; Norris, P. *Heterocycles*, **1999**, 51, 1807. (n) Huisgen, R.; Möbius, L.; Mueller, G.; Stangl, H.; Szeimies, G.; Vernon, J. M. *Chem. Ber*, **1965**, 98, 3992. (o) Wu, L.; Chen, Y.; Luo, J.; Sun, Q.; Peng, M.; Lin, Q. *Tetrahedron Lett.* **2014**, 55, 3847; (p) Huisgen, R.; Möbius, G.; Szeimies, G. *Chem. Ber.* **1965**, 98, 1138. (q) Rogue, D.; Neill, J.; Antoon, J.; Stevens, E. P. *Synthesis.* **2005**, 2497.
11. (a) Kolb, H. C.; Finn, M. G.; Sharpless, K. B. *Angew. Chem. Int. Ed.* **2001**, 40, 2004. (b) McNulty, J.; Keskar, K.; Vemula, R. *Chem. Eur. J.* **2011**, 17, 14727. (c) McNulty, J.; Keskar, K. *Eur. J. Org. Chem.* **2012**, 5462.

12. Barluenga, J.; López, L. A.; Löber, O.; Tomás, M.; García-Granda, S.; Alvarez-Rúa, C. and Borge, J. *Angew. Chem. Int. Ed.*, **2001**, *40*, 3392.
13. Fan, R. L. and Hudlicky, T. *Tetrahedron Lett.*, **1989**, *30*, 5533.
14. Majireck, M. M. and Weinreb, S. M. *J. Org. Chem.*, **2006**, *71*, 8680.

6.5 Experimental Section

Tetrahydrofuran (THF) was distilled over sodium metal in the presence of benzophenone indicator. ^1H and ^{13}C spectra were obtained on a 600 or, 200 MHz Bruker NMR spectrometer. Chemical shifts are reported in units of δ (ppm) and coupling constants (J) are expressed in Hz. Mass spectra were run on a Micromass Quattro Ultima spectrometer fitted with a direct injection probe (DIP) with ionization energy set at 70 eV and HRMS (EI) unless mentioned, were performed with a Micromass Q-TOF Ultima spectrometer. Thin layer chromatography (TLC) was run using Macherey-Nagel aluminum-backed plates. Melting points were obtained on an Electronic Research Associates Inc. melting point apparatus corrected against an external calibrant.

General experimental procedure for synthesis of α -methoxyphosphonium salts (Scheme 6-1, 14a-14h):

Into a flame-dried flask, containing a magnetic stirring bar was weighed the corresponding dimethyl acetal (2.0 mmol, 1 equiv.) under argon. Triethylphosphane hydrobromide (2.0 mmol, 1 equiv.) was added to the flask before being stirred for 50 min. at 80 °C under argon. Solvent was removed and the resulting mixture was placed under high vacuum for 50 min. to give the α -methoxyphosphonium salt.^{9a}

α -Methoxy-4-chlorobenzyl-triethylphosphonium bromide^{9a} (Scheme 6-1, 14a):

¹H NMR (600 MHz, CDCl₃) δ 7.61 (dd, J = 8.5, 1.9 Hz, 2H), 7.36 (d, J = 8.4 Hz, 2H), 6.53 (d, J = 10.0 Hz, 1H), 3.39 (s, 3H), 2.59 – 2.43 (m, 3H), 2.38 – 2.23 (m, 3H), 1.15 (dt, J = 17.7, 7.7 Hz, 9H). ¹³C NMR (151 MHz, CDCl₃) δ 136.0 (d, J = 2.5 Hz), 130.1, 129.7, 129.2 (d, J = 3.9 Hz), 75.3 (d, J = 64.7 Hz), 59.1 (d, J = 12.4 Hz), 10.5 (d, J = 45.6 Hz), 6.1 (d, J = 5.5 Hz). ³¹P-NMR (80 MHz, CDCl₃): δ 38.55.

α -Methoxy-benzyl-triethylphosphonium bromide^{9a} (Scheme 6-1, 14b):

¹H NMR (600 MHz, CDCl₃) δ 7.51 (d, J = 7.6 Hz, 2H), 7.38 – 7.25 (m, 3H), 6.26 (d, J = 9.5 Hz, 1H), 2.51 – 2.33 (m, 3H), 2.32 – 2.15 (m, 3H), 1.08 (dt, J = 17.7, 7.7 Hz, 9H). ¹³C NMR (151 MHz, CDCl₃) δ 131.1, 129.8, 129.2, 127.4 (d, J = 4.0 Hz), 75.7 (d, J = 64.5 Hz), 58.7 (d, J = 12.6 Hz), 10.2 (d, J = 45.9 Hz), 5.8 (d, J = 5.4 Hz). ³¹P-NMR (80 MHz, CDCl₃): 38.46.

α -Methoxy-2-chlorobenzyl-triethylphosphonium bromide (Scheme 6-1, 14c):

¹H NMR (200 MHz, CDCl₃) δ 7.62 – 7.29 (m, 4H), 5.85 (d, J = 8.6 Hz, 1H), 3.36 (s, 3H), 2.87 – 2.54 (m, 3H), 2.54 – 2.20 (m, 3H), 1.15 (dt, J = 18.1, 7.6 Hz, 9H). ¹³C NMR (50 MHz, CDCl₃) δ 133.6 (d, J = 5.6 Hz), 131.8 (d, J = 2.5 Hz), 131.0, 129.0, 128.9, 128.5 (d, J = 1.8 Hz), 73.4 (d, J = 64.9 Hz), 59.6 (d, J = 11.8 Hz), 10.8 (d, J = 45.2 Hz), 6.1 (d, J = 5.8 Hz). ³¹P-NMR (80 MHz, CDCl₃): 42.31. HRMS (ES): calcd. for C₁₄H₂₃OPCl [M]⁺ 273.1176; found 273.1175.

α -Methoxy-4-methylbenzyl-triethylphosphonium bromide (Scheme 6-1, 14d):

¹H NMR (200 MHz, CDCl₃) δ 7.52 (d, J = 8.0 Hz, 2H), 7.31 – 7.19 (m, 2H), 6.41 (d, J = 9.5 Hz, 1H), 3.43 (s, 3H), 2.70 – 2.23 (m, 6H), 2.36 (s, 3H), 1.19 (dt, J =

17.5, 7.7 Hz, 9H). ^{13}C NMR (50 MHz, CDCl_3) δ 140.3 (d, J = 3.1 Hz), 130.2 (d, J = 1.8 Hz), 128.2, 127.8 (d, J = 4.7 Hz), 76.1 (d, J = 65.1 Hz), 58.9 (d, J = 12.7 Hz), 21.3, 10.5 (d, J = 45.8 Hz), 6.1 (d, J = 5.8 Hz). ^{31}P -NMR (80 MHz, CDCl_3): 37.77. HRMS (ES): calcd. for $\text{C}_{15}\text{H}_{26}\text{OP}$ $[\text{M}]^+$ 253.1728; found 253.1721.

α -Methoxy-3,4-methylenedioxybenzyl-triethylphosphonium bromide^{9a}
(Scheme 6-1, 14e):

^1H NMR (200 MHz, CDCl_3) δ 7.36 – 7.22 (m, 1H), 7.06 (s, 1H), 6.87 (d, J = 8.0 Hz, 1H), 6.54 (d, J = 9.5 Hz, 1H), 6.02 (d, J = 1.1 Hz, 2H), 3.45 (s, 3H), 2.65 – 2.31 (m, 6H), 1.21 (dt, J = 17.4, 7.7 Hz, 9H). ^{13}C NMR (50 MHz, CDCl_3) δ 149.1, 148.8, 124.9, 122.7 (d, J = 5.9 Hz), 109.3 (d, J = 2.3 Hz), 107.3 (d, J = 3.4 Hz), 101.7, 76.1 (d, J = 66.0 Hz), 59.0 (d, J = 12.9 Hz), 10.6 (d, J = 45.6 Hz), 6.2 (d, J = 5.8 Hz). ^{31}P -NMR (80 MHz, CDCl_3): 37.65.

α -Methoxy-4-bromobenzyl-triethylphosphonium bromide (Scheme 6-1, 14f):

^1H NMR (200 MHz, CDCl_3) δ 7.72 – 7.44 (m, 4H), 6.70 (d, J = 10.3 Hz, 1H), 3.44 (s, 3H), 2.75 – 2.50 (m, 3H), 2.48 – 2.19 (m, 3H), 1.19 (dt, J = 17.6, 7.7 Hz, 9H). ^{13}C NMR (50 MHz, CDCl_3) δ 132.7 (d, J = 1.9 Hz), 130.7, 129.6 (d, J = 4.6 Hz), 124.4 (d, J = 3.8 Hz), 75.5 (d, J = 64.7 Hz), 59.3 (d, J = 12.5 Hz), 10.6 (d, J = 45.6 Hz), 6.2 (d, J = 5.8 Hz). ^{31}P -NMR (80 MHz, CDCl_3): 37.99. HRMS (ES): calcd. for $\text{C}_{14}\text{H}_{23}\text{OPBr}$ $[\text{M}]^+$ 317.0673; found 317.0670.

α -Methoxy-triethyl[(2*E*)-3-phenyl-2-propenyl]phosphonium bromide^{9a}
(Scheme 6-1, 14g):

^1H NMR (200 MHz, CDCl_3) δ 7.53 -7.40 (m, 2H), 7.39 – 7.29 (m, 3H), 7.18 (dd, J = 14.6, 4.2 Hz, 1H), 6.25 – 5.97 (m, 2H), 3.52 (s, 3H), 2.83 – 2.28 (m, 6H), 1.32 (dt, J = 17.5, 7.7 Hz, 9H). ^{13}C NMR (50 MHz, CDCl_3) δ 139.0 (d, J = 11.5 Hz), 134.6 (d, J = 2.1 Hz), 129.4, 128.9, 127.1, 118.3 (d, J = 2.6 Hz), 75.4 (d, J

= 67.0 Hz), 59.0 (d, J = 12.1 Hz), 10.9 (d, J = 45.9 Hz), 6.4 (d, J = 5.7 Hz). ^{31}P -NMR (80 MHz, CDCl_3): 38.28.

α -Methoxy-triethyl[(2*E*)-2-methyl-3-phenyl-2-propenyl]phosphonium bromide^{9a} (Scheme 6-1, 14h):

^1H NMR (200 MHz, CDCl_3) δ 7.49 – 7.33 (m, 4H), 7.30 – 7.23 (m, 1H), 7.20 – 7.10 (m, 1H), 5.99 (d, J = 10.8 Hz, 1H), 3.49 (s, 3H), 2.82 – 2.47 (m, 6H), 2.06 (s, 3H), 1.57 – 1.10 (m, 9H). ^{13}C NMR (50 MHz, CDCl_3) δ 135.6, 135.0, 134.8, 129.4, 128.6, 128.0, 80.5 (d, J = 63.9 Hz), 58.8 (d, J = 13.1 Hz), 15.3, 11.4 (d, J = 45.1 Hz), 6.4 (d, J = 5.9 Hz). ^{31}P -NMR (80 MHz, CDCl_3): 37.76.

General experimental procedure for synthesis of β -methoxy cinnamates (Table 6-1, 15a-15h):

Into a flame-dried flask, containing a magnetic stirring bar was weighed the corresponding α -methoxy-phosphonium bromide (1.0 mmol, 1.0 eq) under Ar. Dry THF (1.0 mL) was added into the flask to make a 1M solution. The flask was stirred at 0 °C for 15 min whereupon LHMDs (1.1 mmol, 1.1 eq, 1.0 M stock, THF) was added slowly. After 35 min, a 1.0 M solution (in THF) of ethyl glyoxylate (1.05 mmol, 1.05 eq) was added to the reaction flask maintained at 0 °C. The flask was kept at 0 °C for 1.5 h and then slowly warmed to room temperature where it was stirred for a further 1.5 h. The resulting mixture was concentrated to remove solvent. At the end of the reaction, the solvent was removed with a rotary evaporator. Water was added (10 mL) to the residue, and the resulting mixture was extracted with dichloromethane (3 x 15 mL). The combined organic layers were dried over MgSO_4 , filtered, and concentrated. The product was purified using silica gel column chromatography eluted with 10% ethyl acetate in hexane to yield the corresponding β -methoxy cinnamate.

Ethyl 3-(4-chlorophenyl)-3-methoxyacrylate (Table 6-1, 15a):

(28:72 *cis:trans*), ^1H NMR (200 MHz, CDCl_3); δ (ppm): 7.52 – 7.32 (m, 4H), 5.56 (s, 1H, *cis* isomer), 5.27 (s, 1H, *trans* isomer), 4.21 (q, $J = 7.1$ Hz, 2H, *cis* isomer), 4.06 (q, $J = 7.1$ Hz, 2H, *trans* isomer), 3.86 (s, 3H, *cis* isomer), 3.80 (s, 3H, *trans* isomer), 1.31 (t, $J = 7.1$ Hz, 3H, *cis* isomer), 1.18 (t, $J = 7.1$ Hz, 3H, *trans* isomer). ^{13}C NMR (151 MHz, CDCl_3) δ (ppm): (*trans* isomer) 170.1, 166.6, 135.7, 133.5, 130.3, 128.0, 92.9, 59.8, 56.4, 14.2. HRMS: calcd. for $\text{C}_{12}\text{H}_{13}\text{ClO}_3$ $[\text{M}]^+$ 240.0552; found 240.0553.

Ethyl 3-methoxy-3-phenylacrylate¹² (Table 6-1, 15b):

(31:69 *cis:trans*), ^1H NMR (200 MHz, CDCl_3); δ (ppm): ^1H NMR (200 MHz, CDCl_3) δ 7.63 – 7.31 (m, 5H), 5.54 (s, 1H, *cis* isomer), 5.27 (s, 1H, *trans* isomer), 4.22 (q, $J = 7.1$ Hz, 2H, *cis* isomer), 4.05 (q, $J = 7.1$ Hz, 2H, *trans* isomer), 3.84 (s, 3H, *cis* isomer), 3.81 (s, 3H, *trans* isomer), 1.32 (t, $J = 7.1$ Hz, 3H, *cis* isomer), 1.15 (t, $J = 7.1$ Hz, 3H, *trans* isomer). ^{13}C NMR (50 MHz, CDCl_3); δ (ppm): (*trans* isomer) 171.2, 166.6, 135.0, 129.5, 128.5, 127.5, 92.34, 59.4, 56.2, 14.0.

Ethyl 3-(2-chlorophenyl)-3-methoxyacrylate (Table 6-1, 15c):

(22:78 *cis:trans*), ^1H NMR (200 MHz, CDCl_3); δ (ppm): δ 7.44 – 7.28 (m, 4H), 5.40 (s, 1H, *trans* isomer), 5.06 (s, 1H, *cis* isomer), 4.18 (q, $J = 7.1$ Hz, 2H, *cis* isomer), 4.01 (q, $J = 7.1$ Hz, 2H, *trans* isomer), 3.83 (s, 3H, *trans* isomer), 3.61 (s, 3H, *cis* isomer) 1.10 (t, $J = 7.1$ Hz, 3H, *trans* isomer), 1.27 (t, $J = 7.1$ Hz, 3H, *cis* isomer). ^{13}C NMR (50 MHz, CDCl_3); δ (ppm): (*trans* isomer) 168.5, 166.2, 135.3, 132.4, 130.2, 129.9, 129.3, 126.4, 94.9, 59.7, 56.6, 14.1. HRMS (CI): calcd. for $\text{C}_{12}\text{H}_{13}\text{ClO}_3$ $[\text{M}]^+$ 241.0631; found 241.0726.

Ethyl 3-methoxy-3-*p*-tolylacrylate (Table 6-1, 15d):

(37:63 *cis:trans*), ^1H NMR (200 MHz, CDCl_3); δ (ppm): δ 7.44 (d, $J = 8.0$ Hz, 1H), 7.34 (d, $J = 8.0$ Hz, 1H), 7.22 (m, 2H), 5.53 (s, 1H, *cis* isomer), 5.24 (s, 1H, *trans* isomer), 4.21 (q, $J = 7.1$ Hz, 2H, *cis* isomer), 4.06 (q, $J = 7.1$ Hz, 2H, *trans* isomer), 3.85 (s, 3H, *cis* isomer), 3.80 (s, 3H, *trans* isomer), 2.38 (s, 3H), 1.32 (t, $J = 7.1$ Hz, 3H, *cis* isomer), 1.18 (t, $J = 7.1$ Hz, 3H, *trans* isomer). ^{13}C NMR (50 MHz, CDCl_3) δ 171.6, 166.9, 139.8, 132.3, 128.7, 128.4, 92.1, 59.6, 56.3, 21.5, 14.3. HRMS: calcd. for $\text{C}_{13}\text{H}_{16}\text{O}_3$ $[\text{M}]^+$ 220.1099; found 220.1095.

Ethyl 3-(benzo[d][1,3]dioxol-5-yl)-3-methoxyacrylate (Table 6-1, 15e):

(38:62 *cis:trans*), ^1H NMR (200 MHz, CDCl_3); δ (ppm) 7.04 – 6.99 (m, 1H, *trans* isomer), 6.98 – 6.90 (m, 1H, *trans* isomer), 6.82 (dd, $J = 8.0, 2.0$ Hz, 1H, *trans* isomer), 6.02 (s, 2H, *cis* isomer), 5.98 (s, 2H, *trans* isomer), 5.49 (s, 1H, *cis* isomer), 5.21 (s, 1H, *trans* isomer), 4.20 (q, $J = 7.1$ Hz, 2H, *cis* isomer), 4.07 (q, $J = 7.1$ Hz, 2H, *trans* isomer), 3.85 (s, 3H, *cis* isomer), 3.78 (s, 3H, *trans* isomer), 1.31 (t, $J = 7.1$ Hz, 3H, *cis* isomer), 1.20 (t, $J = 7.1$ Hz, 3H, *trans* isomer). ^{13}C NMR (50 MHz, CDCl_3) δ 170.7, 166.8, 148.8, 146.9, 128.6, 123.3, 109.5, 107.7, 101.3, 92.0, 59.6, 56.3, 14.2. HRMS: calcd. for $\text{C}_{13}\text{H}_{14}\text{O}_5$ $[\text{M}]^+$ 250.0848; found 250.0841.

Ethyl 3-(4-bromophenyl)-3-methoxyacrylate (Table 6-1, 15f):

(30:70 *cis:trans*), ^1H NMR (200 MHz, CDCl_3); δ (ppm): 7.61 – 7.47 (m, 2H), 7.44-7.29 (m, 2H), 5.56 (s, 1H, *cis* isomer), 5.27 (s, 1H, *trans* isomer), 4.21 (q, $J = 7.1$ Hz, 2H, *cis* isomer), 4.06 (q, $J = 7.1$ Hz, 2H, *trans* isomer), 3.86 (s, 3H, *cis* isomer), 3.80 (s, 3H, *trans* isomer), 1.31 (t, $J = 7.1$ Hz, 3H, *cis* isomer), 1.18 (t, $J = 7.1$ Hz, 3H, *trans* isomer). ^{13}C NMR (50 MHz, CDCl_3); δ (ppm): (*trans* isomer) 170.1, 166.6, 133.9, 130.9, 130.5, 124.1, 92.8, 59.8, 56.4, 14.2. HRMS: calcd. for $\text{C}_{12}\text{H}_{13}\text{BrO}_3$ $[\text{M}]^+$ 284.0039; found 284.0048.

Ethyl 3-(styryl)-3-methoxyacrylate¹³ (Table 6-1, 15g):

¹H NMR (200 MHz, CDCl₃); δ (ppm): *trans* isomer 8.13 (d, *J* = 16.1 Hz, 1H), 7.72 – 7.48 (m, 2H), 7.44 – 7.17 (m, 4H), 5.17 (s, 1H), 4.21 (q, *J* = 7.1 Hz, 2H), 3.78 (s, 3H), 1.33 (t, *J* = 7.1 Hz, 3H). ¹³C NMR (50 MHz, CDCl₃) δ 167.5, 166.8, 136.2, 135.3, 129.0, 128.7, 127.7, 120.3, 92.4, 59.7, 55.5, 14.5. (Trace amount of *cis* isomer was isolated)

Ethyl 3-(1-((*Z*)-prop-1-enyl)benzene)-3-methoxyacrylate (Table 6-1, 15h):

(32:68 *cis:trans*), ¹H NMR (200 MHz, CDCl₃); δ (ppm): 7.47 – 7.22 (m, 5H), 6.58 (s, 1H), 5.52 (s, 1H, *cis* isomer), 5.09 (s, 1H, *trans* isomer), 4.31 – 4.03 (m, 2H), 3.90 (s, 3H, *cis* isomer), 3.73 (s, 3H, *trans* isomer), 2.10 (d, *J* = 1.4 Hz, 3H, *trans* isomer), 2.04 (d, *J* = 1.1 Hz, 3H, *cis* isomer), 1.41 – 1.14 (m, 3H). ¹³C NMR (50 MHz, CDCl₃, *trans* isomer) δ 174.8, 167.1, 136.8, 133.1, 131.4, 129.2, 128.2, 127.1, 91.5, 59.7, 56.2, 16.9, 14.4.

General procedure for synthesis of ethyl 1-benzyl-5-(4-aryl)-1*H*-1,2,3-triazole-4-carboxylate: (Table 6-2, 16a-16h)

For ethyl 1-benzyl-5-(4-phenyl)-1*H*-1,2,3-triazole-4-carboxylate: In a screw-cap vial having stir bar, the ethyl 3-methoxy-3-phenylacrylate (0.015 g, 0.072 mmol) and aryl azide (0.1 mL) were added, the vial was flushed with argon and sealed. The sealed vial was heated in oil bath at 150 °C until disappearance of cinnamate (92-96 h). The crude reaction mixture was column chromatographed with 30% ethyl acetate in hexanes to give title compound.

Ethyl 1-benzyl-5-phenyl-1*H*-1,2,3-triazole-4-carboxylate¹⁴: (Table 6-2, 16a)

¹H NMR (200 MHz, CDCl₃); δ (ppm): 7.51 – 7.40 (m, 3H), 7.28 – 7.18 (m, 5H), 7.02 – 6.99 (m, 2H), 5.44 (s, 2H), 4.30 (q, *J* = 7.1 Hz, 2H), 1.26 (t, *J* = 7.1 Hz, 3H). ¹³C NMR (50 MHz, CDCl₃); δ (ppm): 161.0, 141.4, 137.2, 134.7, 130.3,

130.1, 129.8, 128.9, 128.5, 127.6, 126.0, 61.1, 52.3, 14.2. HRMS (M)⁺ calcd. for C₁₈H₁₇N₃O₂: 307.1326, found 307.1321.

Ethyl 1-benzyl-5-(4-bromophenyl)-1H-1,2,3-triazole-4-carboxylate: (Table 6-2, 16b)

¹H NMR (600 MHz, CDCl₃); δ (ppm): 7.56 (d, *J* = 8.5 Hz, 2H), 7.31-7.23 (m, 3H), 7.04 (d, *J* = 8.5 Hz, 2H), 7.00 (dd, *J* = 7.4, 1.9 Hz, 2H), 5.42 (s, 2H), 4.30 (q, *J* = 7.1 Hz, 2H), 1.28 (t, *J* = 7.1 Hz, 3H). ¹³C NMR (151 MHz, CDCl₃); δ (ppm): 160.9, 140.3, 137.4, 134.5, 131.9, 131.5, 129.0, 128.7, 127.5, 124.9, 124.9, 61.3, 52.4, 14.2. HRMS (M)⁺ calcd. for C₁₈H₁₆BrN₃O₂: 385.0416, found 385.0426.

Ethyl-1-(3-bromobenzyl)-5-(4-bromophenyl)-1H-1,2,3-triazole-4-carboxylate: (Table 6-2, 16c)

¹H NMR (600 MHz, CDCl₃); δ (ppm): 7.60 (d, *J* = 8.5 Hz, 2H), 7.42 (d, *J* = 8.0, 1H), 7.15 (t, *J* = 7.9 Hz, 1H), 7.13 (t, *J* = 1.6 Hz, 1H), 7.05 (d, *J* = 8.5 Hz, 2H), 6.94 (d, *J* = 7.7 Hz, 1H), 5.39 (s, 2H), 4.31 (q, *J* = 7.1 Hz, 2H), 1.31 (t, *J* = 7.1 Hz, 3H). ¹³C NMR (151 MHz, CDCl₃); δ (ppm): 160.8, 140.3, 137.5, 136.5, 132.1, 131.9, 131.4, 130.7, 130.6, 126.1, 125.1, 124.7, 123.1, 61.4, 51.7, 14.2. HRMS (M)⁺ calcd. for C₁₈H₁₅Br₂N₃O₂: 462.9538, found 462.9531.

Ethyl 1-benzyl-5-p-tolyl-1H-1,2,3-triazole-4-carboxylate: (Table 6-2, 16d)

¹H NMR (600 MHz, CDCl₃); δ (ppm): 7.27-7.25 (m, 3H), 7.24 (d, *J* = 7.8 Hz, 1H), 7.09 (d, *J* = 8.1 Hz, 2H), 7.02 (dd, *J* = 6.8, 2.7 Hz, 2H), 5.42 (s, 2H), 4.30 (q, *J* = 7.1 Hz, 2H), 2.41 (s, 3H), 1.28 (t, *J* = 7.1 Hz, 3H). ¹³C NMR (151 MHz, CDCl₃); δ (ppm): 161.1, 141.6, 140.4, 137.1, 134.9, 129.8, 129.3, 128.9, 128.5, 127.6, 122.9, 61.1, 52.1, 21.6, 14.2. HRMS (M)⁺ calcd. for C₁₉H₁₉N₃O₂: 321.1473, found 321.1477.

Ethyl-5-(benzo[d][1,3]dioxol-6-yl)-1-benzyl-1H-1,2,3-triazole-4-carboxylate: (Table 6-2, 16e)

^1H NMR (600 MHz, CDCl_3); δ (ppm): 7.29 – 7.27 (m, 3H), 7.04 (dd, $J = 6.6, 2.9$ Hz, 2H), 6.85 (d, $J = 8.5$ Hz, 1H), 6.66-6.65 (m, 2H), 6.04 (s, 2H), 5.44 (s, 2H), 4.33 (q, $J = 7.1$ Hz, 2H), 1.31 (t, $J = 7.1$ Hz, 3H). ^{13}C NMR (151 MHz, CDCl_3); δ (ppm): 161.1, 149.3, 147.9, 141.1, 137.2, 134.8, 128.9, 128.5, 127.5, 124.1, 119.0, 110.3, 108.6, 101.8, 61.2, 52.2, 14.3. HRMS (M) $^+$ calcd. for $\text{C}_{19}\text{H}_{17}\text{N}_3\text{O}_4$: 351.1227, found 351.1219.

Ethyl-1-(3-bromobenzyl)-5-(4-chlorophenyl)-1H-1,2,3-triazole-4-carboxylate: (Table 6-2, 16f)

^1H NMR (600 MHz, CDCl_3); δ (ppm): 7.45-7.43 (m, 3H), 7.16-7.11 (m, 4H), 6.94 (dd, $J = 7.7, 0.6$ Hz, 1H), 5.39 (s, 2H), 4.31 (q, $J = 7.1$ Hz, 2H), 1.29 (t, $J = 7.1$ Hz, 3H). ^{13}C NMR (151 MHz, CDCl_3); δ (ppm): 161.0, 140.5, 137.8, 137.1, 136.7, 132.1, 131.4, 130.9, 130.8, 129.4, 126.3, 124.5, 123.3, 61.6, 51.9, 14.4. HRMS (M) $^+$ calcd. for $\text{C}_{18}\text{H}_{15}\text{BrClN}_3\text{O}_2$: 419.0036, found 419.0036.

Ethyl 1-benzyl-5-(4-chlorophenyl)-1H-1,2,3-triazole-4-carboxylate: (Table 6-2, 16g)

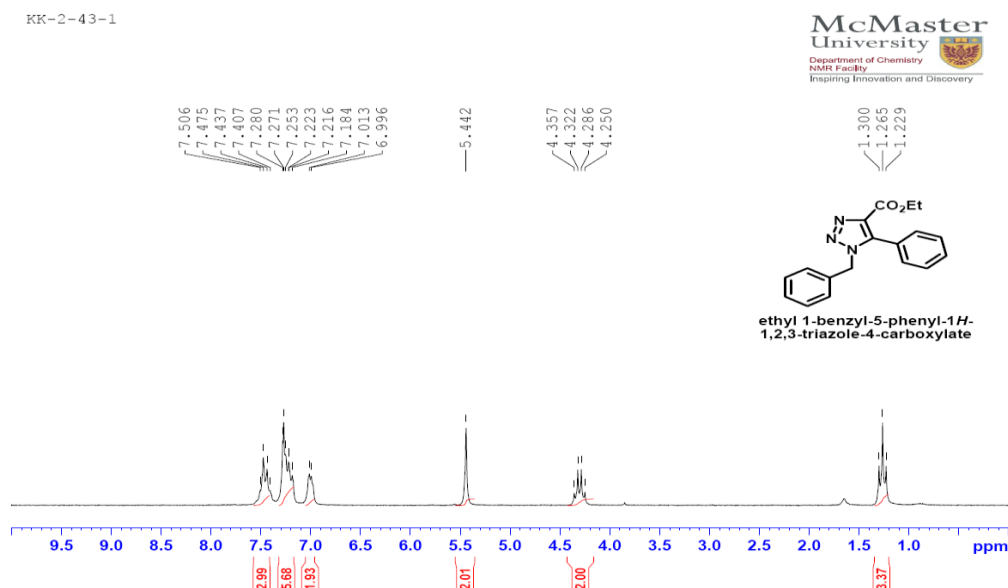
^1H NMR (200 MHz, CDCl_3); δ (ppm): 7.41 (d, $J = 8.3$ Hz, 2H), 7.28-7.26 (m, 3H), 7.11 (d, $J = 8.4$ Hz, 2H), 7.01-6.99 (m, 2H), 5.43 (s, 2H), 4.30 (q, $J = 7.1$ Hz, 2H), 1.28 (t, $J = 7.1$ Hz, 3H). ^{13}C NMR (50 MHz, CDCl_3); δ (ppm): 161.2, 141.6, 137.4, 134.8, 130.4, 130.3, 130.0, 129.1, 128.8, 128.7, 128.7, 127.7, 126.2, 61.3, 52.4, 14.3. HRMS (M) $^+$ calcd. for $\text{C}_{18}\text{H}_{16}\text{ClN}_3\text{O}_2$: 341.0932, found 341.0931.

Ethyl 1-(3-bromobenzyl)-5-phenyl-1H-1,2,3-triazole-4-carboxylate: (Table 6-2, 16h)

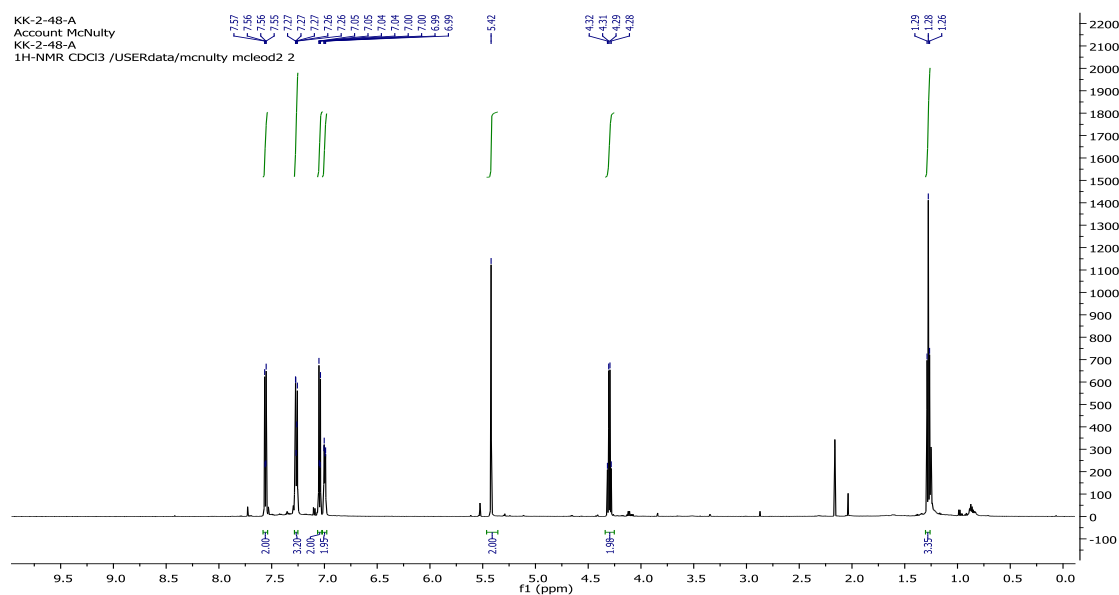
^1H NMR (600 MHz, CDCl_3); δ (ppm): 7.53-7.50 (m, 1H), 7.48 – 7.44 (m, 2H), 7.40 (d, $J = 8.0$ Hz, 1H), 7.18 (dd, $J = 8.2, 1.3$ Hz, 2H), 7.13 (t, $J = 7.9$ Hz, 1H), 7.10 (t, $J = 1.6$ Hz, 1H), 6.93 (dd, $J = 7.7, 0.6$ Hz, 1H), 5.39 (s, 2H), 4.30 (q, $J = 7.1$ Hz), 1.26 (t, $J = 7.1$ Hz, 3H). ^{13}C NMR (151 MHz, CDCl_3); δ (ppm): 160.9, 141.4, 137.4, 136.7, 131.8, 130.8, 130.5, 130.4, 129.8, 128.8, 126.3, 125.9, 122.9, 61.2, 51.6, 14.2. HRMS (M) $^+$ calcd. for $\text{C}_{18}\text{H}_{16}\text{BrN}_3\text{O}_2$: 385.0424, found 385.0426.

6.6 NMR Spectra

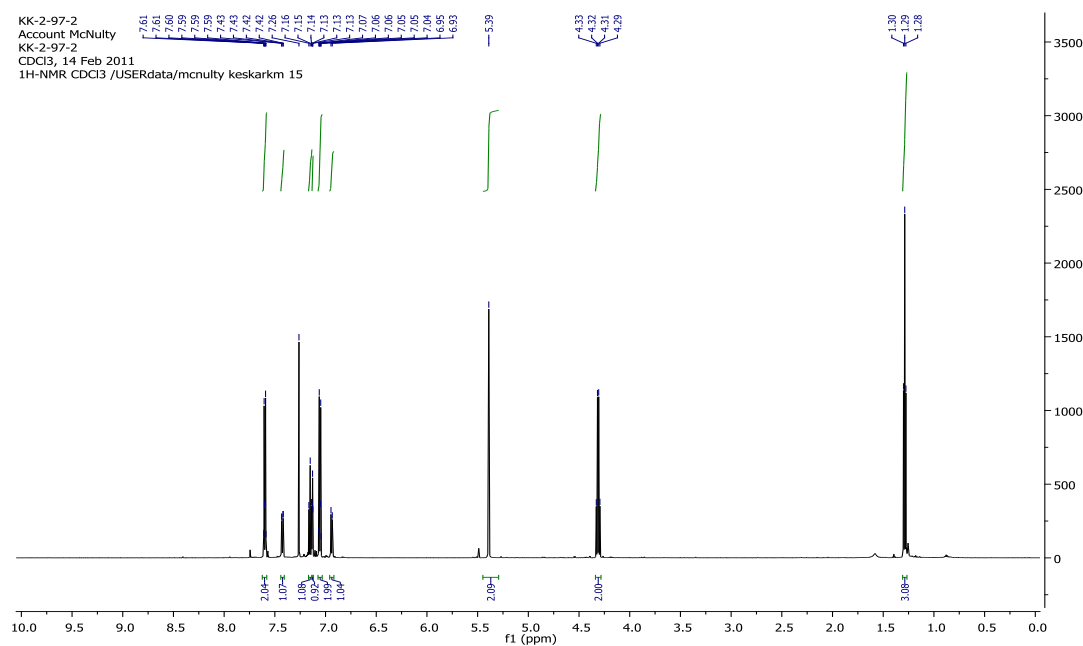
^1H -NMR Spectra's are of 1,4,5 trisubstituted cinnamyltriazoles are included in the thesis. ^{13}C -NMR Spectra can be found online in the publisher article. (Reference V- List of Publications)

Ethyl 1-benzyl-5-phenyl-1H-1,2,3-triazole-4-carboxylate: (Table 6-2, 16a)

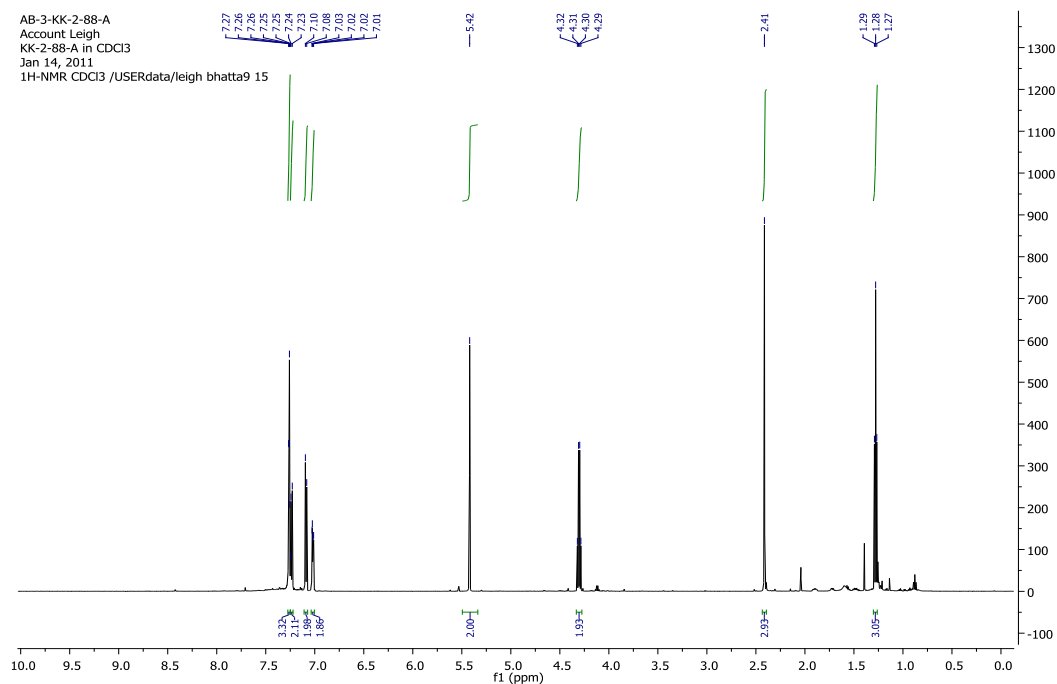
Ethyl 1-benzyl-5-(4-bromophenyl)-1H-1,2,3-triazole-4-carboxylate: (Table 6-2, 16b)



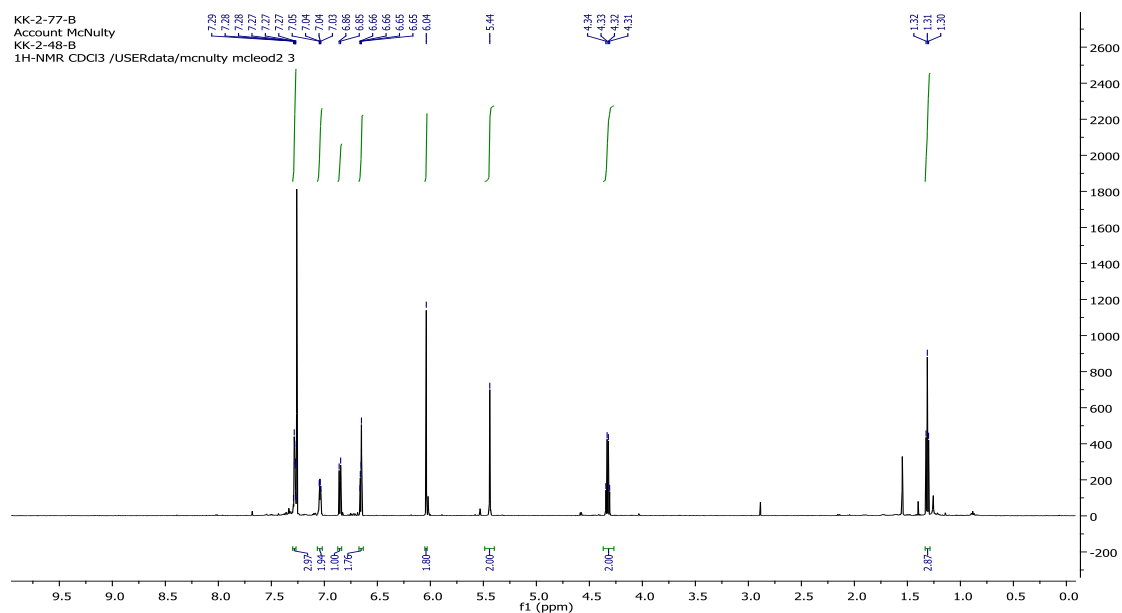
Ethyl 1-(3-bromobenzyl)-5-(4-bromophenyl)-1H-1,2,3-triazole-4-carboxylate: (Table 6-2, 16c)



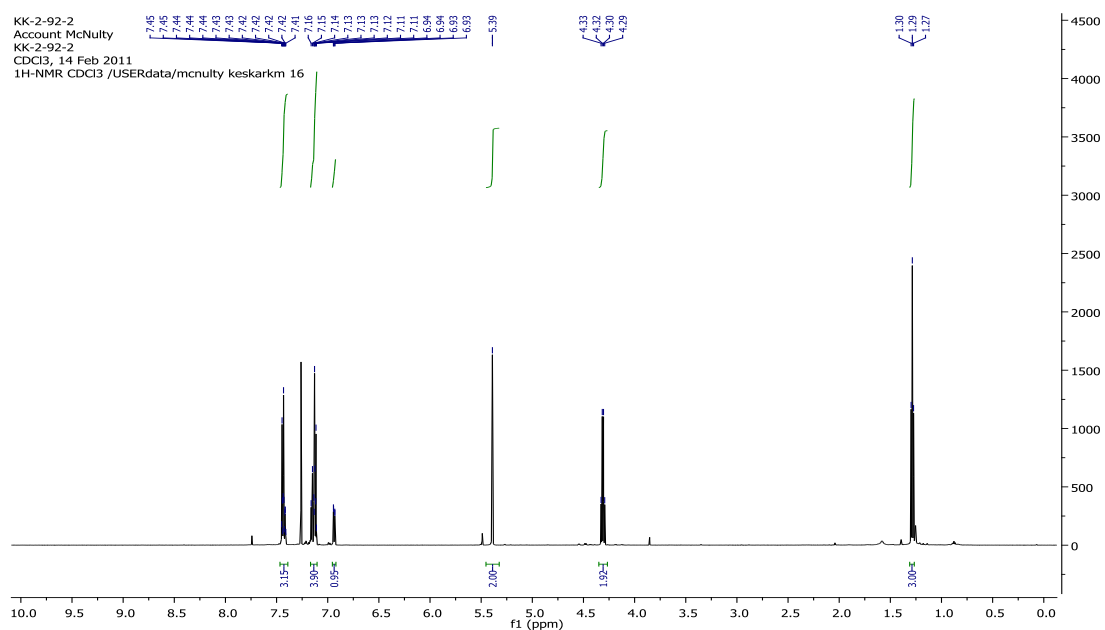
Ethyl 1-benzyl-5-p-tolyl-1H-1,2,3-triazole-4-carboxylate: (Table 6-2, 16d)



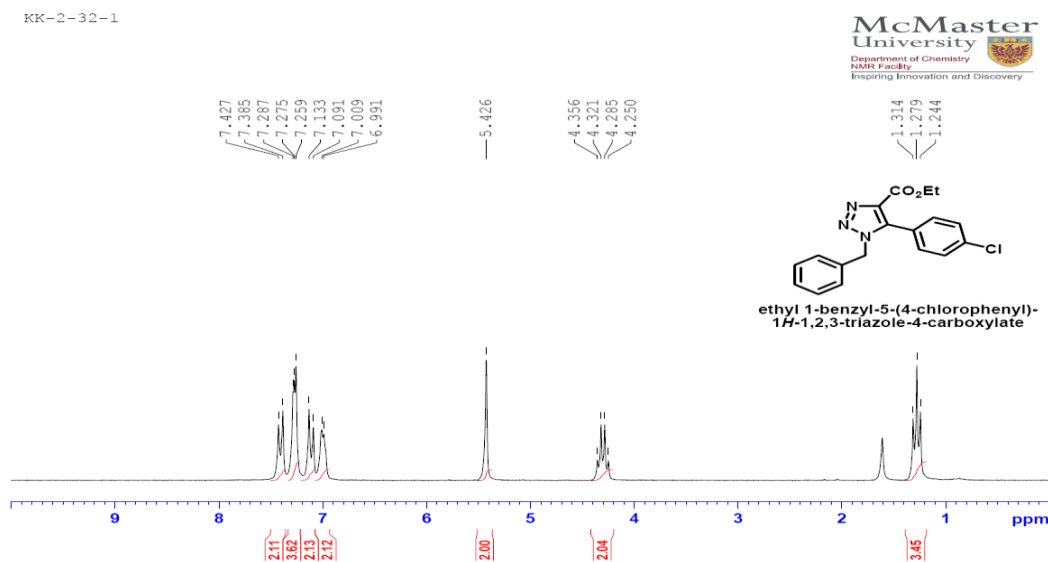
Ethyl 5-(benzo[d][1,3]dioxol-6-yl)-1-benzyl-1H-1,2,3-triazole-4-carboxylate:
(Table 6-2, 16e)



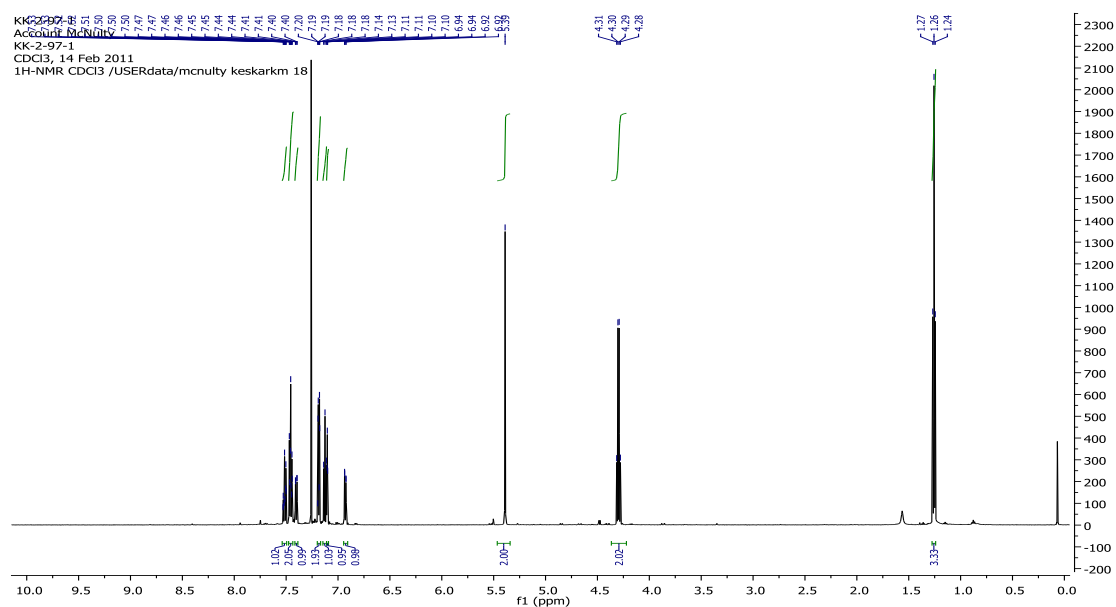
Ethyl 1-(3-bromobenzyl)-5-(4-chlorophenyl)-1H-1,2,3-triazole-4-carboxylate:
(Table 6-2, 16f)



Ethyl 1-benzyl-5-(4-chlorophenyl)-1H-1,2,3-triazole-4-carboxylate: (Table 6-2, 16g)



Ethyl 1-(3-bromobenzyl)-5-phenyl-1H-1,2,3-triazole-4-carboxylate: (Table 6-2, 16h)



JOHN WILEY AND SONS LICENSE
TERMS AND CONDITIONS

Sep 30, 2014

This is a License Agreement between Kunal Keskar ("You") and John Wiley and Sons ("John Wiley and Sons") provided by Copyright Clearance Center ("CCC"). The license consists of your order details, the terms and conditions provided by John Wiley and Sons, and the payment terms and conditions.

All payments must be made in full to CCC. For payment instructions, please see information listed at the bottom of this form.

License Number	3462580188747
License date	Sep 05, 2014
Licensed content publisher	John Wiley and Sons
Licensed content publication	European Journal of Organic Chemistry
Licensed content title	A Tandem "On-Palladium" Heck–Jeffery Amination Route Toward the Synthesis of Functionalized Indole-2-carboxylates
Licensed copyright line	Copyright © 2011 WILEY-VCH Verlag GmbH & Co. KGaA, Weinheim
Licensed content author	James McNulty, Kunal Keskar
Licensed content date	Sep 27, 2011
Start page	6902
End page	6908
Type of use	Dissertation/Thesis
Requestor type	Author of this Wiley article
Format	Print and electronic
Portion	Full article
Will you be translating?	No
Title of your thesis / dissertation	"Advances in Late Transition Metal Catalysis, Olefination Reactions and Applications"
Expected completion date	Dec 2014
Expected size (number of pages)	300

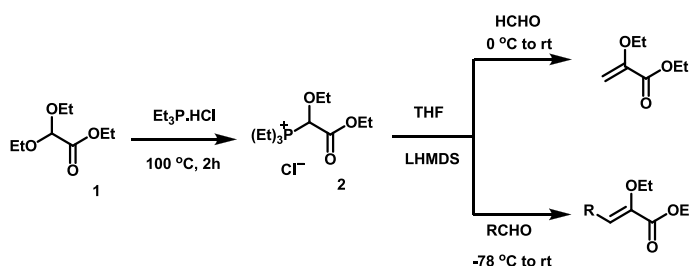
Chapter VII: A Tandem “on-palladium” Heck-Jeffery Amination Route Toward the Synthesis of Functionalized Indole-2-carboxylates

7.1 Introduction

The indole nucleus occupies a privileged position amongst the nitrogen heterocycles, a consequence of its occurrence in the amino acid tryptophan. Indole derivatives are significant in terms of the varied structures and wide ranging biological activities demonstrated by both indole-containing secondary metabolites and wholly synthetic derivatives. The provenance of the indole nucleus in many of the classic alkaloid skeletons (aspidospermae, corynanthe, iboga, ergot etc) and simpler tryptophan degradation products (gramine, serotonin etc) inspired an early interest in both the structure and synthesis of indole derivatives,^[1] a trend that continues unabated.^[2] Recent approaches towards indole synthesis are for the most part based on transition-metal promoted routes,^[3] some of which converge on intermediates common to the classic syntheses.^[1] The myriad of biological activities documented for both natural and synthetic indole derivatives continues to expand and includes toxicity, anticancer, antiviral, antimicrobial, neurological, and hormonal (plant and mammalian) activities.^[4] These factors have assured a continued focus on the synthesis of functionalized indoles and their biological evaluation. The recent interest in indole-2-carboxylic acid derivatives as non-nucleoside reverse transcriptase^[5a] and integrase^[5b] inhibitors for HIV treatment, in conjunction with a report from our group^[6] relating to the synthesis of vinyl ethers prompted us to investigate a possible tandem Pd-mediated Heck-Jeffery amination process as a direct route to such indole derivatives. In this communication we report the successful annulation of 2-iodoanilines onto an alkoxyacrylate yielding functionalized indole-2-carboxylates via an on-palladium tandem Heck-Jeffery amination (HJA) process.

7.2 Results and Discussion

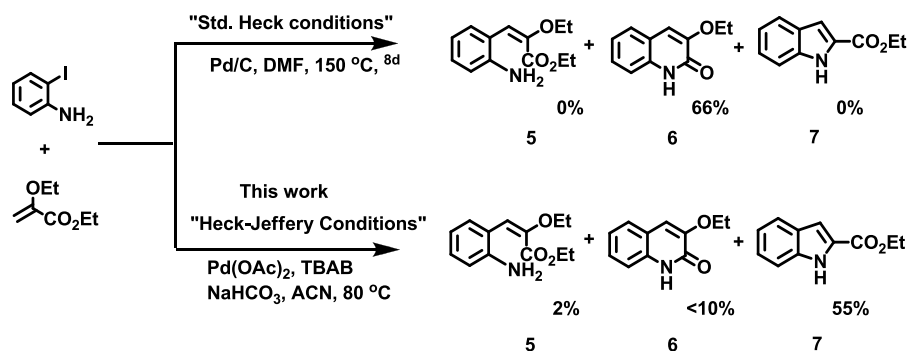
We recently described a general route towards the synthesis of vinyl ethers involving the reaction of α -alkoxy functionalized ylides with carbonyl compounds.^[6] Therein it was shown that the reaction of a dialkyl acetal with a trialkylphosphine hydrobromide yielded the α -alkoxyphosphonium salt derived of the acetal. Ylide generation and olefination allowed access to a wide range of functionalized vinyl ethers and alkoxy-1,3-dienes. As an extension of this work, we have now successfully converted ethyl glyoxylate-diethylacetal (**1**, **Scheme 7-1**) into the functionalized phosphonium salt **2**. Salt **2** was also obtainable from the corresponding chloroacetal. Ylide generation from **2** and trapping with formaldehyde allowed us to access the α -alkoxy acrylate **3** as well as to various α -alkoxy cinnamates **4** (see experimental section, **scheme 7-5**) through trapping of the ylide with aromatic aldehydes.



Scheme 7-1. Synthesis of α -alkoxyacrylates and cinnamates using functionalized ylides.

While the Heck reaction of *ortho*-haloanilines and acrylate esters is known to provide access to *ortho*-aminocinnamates in moderate yield,^[7] it is well known that nucleophilic^[8a] and Pd-mediated^[8c-d] Heck-type addition to α -alkoxyacrylates such as **3** is sluggish due to electronic deactivation of the olefin. The only report of such a process using an *ortho*-iodo aniline^[8d] was shown to yield a quinolinone **6** (**Scheme 7-2**) through intramolecular *N*-acylation of the intermediate Heck-adduct **5**. This result and others^[7]

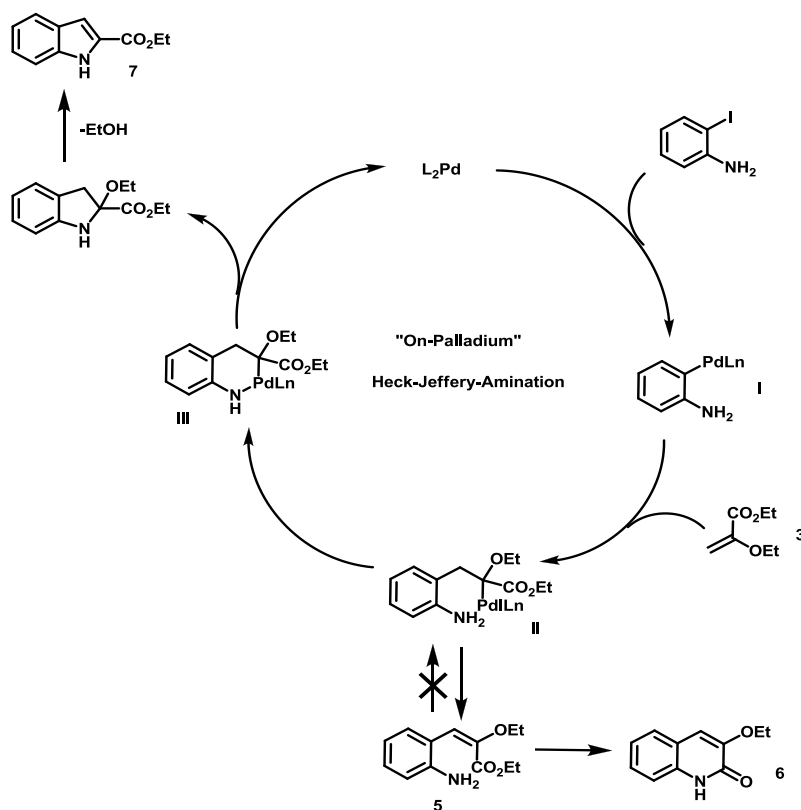
demonstrate that under normal Heck conditions reductive elimination to yield the cinnamate precedes a possible intramolecular *N*-insertion, thus precluding a direct indole synthesis.



Scheme 7-2. Annulation of ortho-iodoanilines with alkoxy acrylate **3** via a standard Heck and the tandem “on-palladium” Heck-Jeffery-amination process (isolated yields given).

These results led us to postulate a catalytic cycle as depicted in **Scheme 7-3**, in which, under Jeffery-type conditions (Pd(II) precursor, no ligand, TBAB etc),^[7a] an intramolecular ligand exchange (**II** to **III**), followed by reductive elimination (loss of HI/base not shown) and elimination of ethanol would deliver the indole **7** directly.

The development of such a tandem HJA process to functionalized *ortho*-iodoanilines and vinyl ethers would allow for a direct “on-palladium” route to indole-2-carboxylates. A Heck-Jeffery route to indoles has been reported from *N*-acyl enamines, involving a subsequent enamine hydrolysis and Reissert-type ring closure.^[9a] This process does not involve an intramolecular ligand exchange. The intramolecular trapping of Heck-type intermediates via aminopalladation is a known process in the synthesis of pyrrolidines, but to our knowledge has not been applied towards the synthesis of indoles.^[9b]



Scheme 7-3. Proposed catalytic cycle for annulation of *ortho*-iodoanilines with alkoxy acrylate **3** via the tandem "On-palladium" Heck-Jeffery-amination process.

The reaction of *ortho*-iodoaniline with α -ethoxyacrylate **3**, investigated under standard Heck conditions (**Scheme 7-2**) furnished only the quinolinone **6**, with no trace of the corresponding indole-2-carboxylate ester, as previously reported.^[8d] We experimented with various parameters of the reaction under Jeffery-type conditions^[7a] and determined that the desired indole-2-carboxylate derivative was formed under a narrow subset of conditions. A summary of various conditions attempted is reported in **Table 7-1**. For comparison, these reactions were stopped after 24h and the isolated yield of ethyl indole-2-carboxylate determined. Although the reaction was sluggish, it was found best performed in dipolar aprotic solvents using Pd(OAc)₂ as catalyst. The reaction

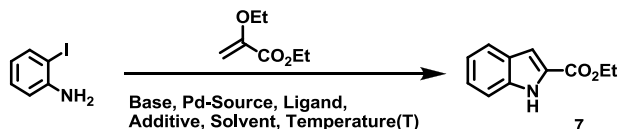
requires base and sodium hydrogen bicarbonate proved most effective, although is perhaps not critical (**Table 7-1**, entries 1-3).

No reaction occurs at room temperature while heating in acetonitrile at 80 °C as solvent proved slightly superior to DMF. Further experiments (**Table 7-1**, entries 4-9) allowed us to identify satisfactory conditions (**Table 7-1**, entry 9). Several failed optimization attempts provided circumstantial evidence indicating the lack of involvement of a Pd⁰-species as the active catalyst, differing from a straightforward Heck reaction^[7c] For example, the reaction failed completely when conducted in an ionic liquid solvent (entries 10 and 11, IL-109 = trihexyl(tetradecyl)phosphonium bistriflimide), a media known to be highly effective in Pd⁰-mediated amination^[6b] and Heck processes.^[6e]

Furthermore, the addition of ligands including *P*-phenylphosphadamantane (CYTOP 292),^[6c] triphenylphosphine or bidentate bis(*di**tert*-butylphosphino)-*o*-xylene^[6d] with Pd(OAc)₂ (**Table 7-1**, entries 12-16) proved to shut down the catalytic cycle completely. The direct use of Pd⁰ catalyst precursors proved also to be ineffective. Extension of the reaction time of the optimized protocol (**Table 7-1**, entry 9) to 96h gave maximum yield of ethyl indole-2-carboxylate **7a** as shown in **Scheme 7-2, bottom**. Under these conditions, annulation of 2-iodoaniline onto the alkoxyacrylate occurred yielding indole-2-carboxylate **7a** as the major product, contrasting sharply to the Heck process^[8d] (**Scheme 7-2, top**) that yields the quinolinone. Formation of a small amount of the quinolinone **6** and a trace amount of the cinnamate **5** under the HJA conditions most likely represents “leakage” from the catalytic cycle via Heck-type β-hydride elimination from intermediate **II**. This step could potentially be reversible via an aminopalladation process. In order to test this hypothesis, we desired to investigate the reversibility of this elimination step and show that **5** is not converted to the indole under these conditions through re-entry to the catalytic cycle or by other means.

Table 7-1. Optimization of the Heck-Jeffery-amination process for the synthesis of indole-2-carboxylate **7**.^a

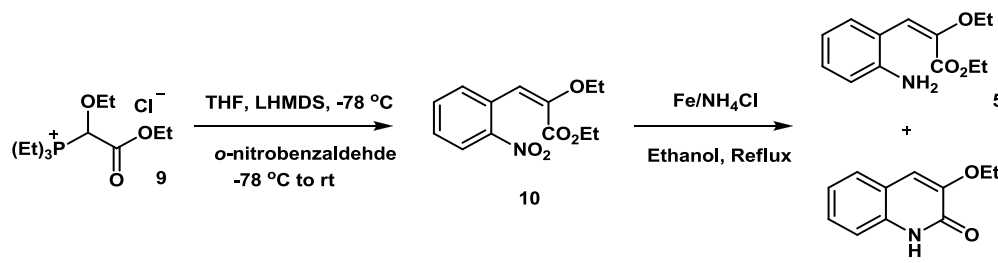
Typical reaction condition- Iodoaniline 0.18 mmol), ethyl 2-ethoxyacrylate (0.27 mmol), TBAB (0.36 mmol), Pd source 10.0 mol%, L = 5.0 mol%, Base (3 eq), Solvent (1.5 mL)



Entry	Base	Pd-Source	Ligand	Additive	Solvent	(T)	Yield (%)
1	NaHCO ₃	Pd(OAc) ₂	none	TBAB	DMF	95	29
2	K ₂ CO ₃	Pd(OAc) ₂	none	TBAB	DMF	95	20
3	Cs ₂ CO ₃	Pd(OAc) ₂	none	TBAB	DMF	95	Trace
4	NaHCO ₃	Pd(OAc) ₂	none	TBAB	ACN	80	30
5	NaHCO ₃	Pd(OAc) ₂	none	TBAB, 5 Å MS	ACN	80	<10
6	NaHCO ₃	Pd(OAc) ₂	none	TBAB	ACN	RT	NR
7	NaHCO ₃	Pd(OAc) ₂	none	TBAB	DMF	150	17
8	NaHCO ₃	Pd(OAc) ₂	none	TBAB, AgSO ₄	ACN	80	<10
9	NaHCO ₃	Pd(OAc) ₂	none	TBAB	ACN	80	38 ^a
10	NaHCO ₃	Pd(OAc) ₂	none	TBAB	CYPHOS IL-109	120	NR
11	NaHCO ₃	Pd(OAc) ₂	none	none	CYPHOS IL-109	120	NR
12	NaHCO ₃	Pd(OAc) ₂	CYTOP-292	TBAB	ACN	80	<5
13	NaHCO ₃	Pd(OAc) ₂	CYTOP-292	TBAB	DMF	150	Trace
14	Et ₃ N	Pd(OAc) ₂	CYTOP-292	TBAB	DMF	150	NR
15	Et ₃ N	Pd(OAc) ₂	PPh ₃	TBAB	DMF	150	NR
16	Et ₃ N	Pd(OAc) ₂	Bidentate Ligand ^b	TBAB	DMF	150	NR
17	NaHCO ₃	Pd ₂ dba ₃	none	TBAB	DMF	95	Trace

^a24 h reaction with 2.8 eq of acrylate. ^b1,2-bis((di-tert-butylphosphinomethyl)benzene.

To this end, we synthesized the *ortho*-amino cinnamate **5** independently through the route shown in **Scheme 7-4**. Olefination of 2-nitrobenzaldehyde **8** with the functionalized ylide **9** (derived from **2**) yielded the 2-nitrocinnamate **10**. Dissolving metal reduction (Fe, NH₄Cl) of **10** gave the aniline **5** (12%) as well as quinolinone **6** (48%). Compounds **5** and **6** were readily separated on silica-gel chromatography. Compound **5** was treated under standard Heck conditions with Pd(OAc)₂ and found to slowly convert to **6**, with no trace of the indole-2-carboxylate being observed. Treatment of **5** under the Heck-Jeffery conditions described (**Scheme 7-2**) slowly (over 48h) yielded quinolinone **6** (60%), unreacted cinnamate **5** (30%) and a trace of the indole **7** observed only by thin layer chromatography. We attribute the trace indole formation to hydrolysis of the enol ether in **10** followed by Reissert-type closure. These results indicate that under the Heck-Jeffery conditions, elimination from intermediate **II** to give **5** is essentially irreversible and that indole formation is in accord with the “on-palladium” catalytic cycle indicated in **Scheme 7-3**.



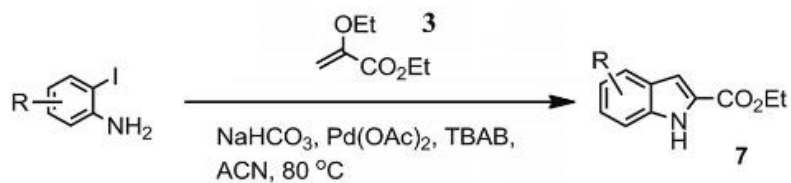
Scheme 7-4. Independent synthesis of the α-ethoxy cinnamate **5** and conversion to **6** thermally and under Heck-Jeffery-amination conditions.

The scope of this new route to valuable indole-2-carboxylate derivatives^[5] was investigated with a mini-panel of readily available *ortho*-iodoanilines and is summarized in **Table 7-2**. The HJA process allowed general conversion to the corresponding indole-2-carboxylate derivative in 48 to 77% isolated yields, always accompanied by 5 to 10% of the corresponding quinolinone, produced

via the “leakage” pathway. The indole-2-carboxylate derivatives were easily separable from the quinolinones on silica-gel and the numbers reported in **Table 7-1** are final isolated yields. The annulation also proved chemoselective in the presence of lesser reactive aryl halides, allowing access to useful chloro- and fluoro- functionalized indole-2-carboxylates.

Lastly, several of our results have brought into question the accepted mechanism of the Heck-Jeffery reaction. The dichotomy (i.e **Scheme 7-2**) between the standard Pd⁰-mediated Heck reaction of vinyl ethers such as **3** and that described herein under the “on-palladium” Heck-Jeffery amination process is indicative of the involvement of a distinct catalytic species for the HJA process. Proposed catalytic cycles involving Jeffery conditions typically invoke Pd⁰/Pd(II) intermediates,^[7a] although they invariably require Pd(II) precursors. The present HJA process requires a Pd(II) precursor, Pd⁰-pre catalysts and/or addition of ligands do not promote this direct indole formation, but instead result in exit from the catalytic cycle via intermediate **II** giving quinolinone **6**.^[8d] The HJA process proceeds slowly under conditions where typical Pd⁰-mediated pathways would be expected to be rapid and the normal Heck-type adducts should be formed.

The present results also show that the normal Heck adducts do not re-enter the catalytic cycle, indole formation likely occurs via an independent on-palladium route. One explanation may be that excess halide anion present during the HJA process (requires TBAB) hinders β-hydride elimination (**Scheme 7-3**, **II** to **5**) on the standard Pd^{II} intermediate, a process known in the Heck reaction itself,^[10e] leaving little option but intramolecular ligand exchange, leading to the indole-2-carboxylate. However this explanation does not account for the lack of reactivity under conditions of low halide concentration (**Table 7-1**, entry 8), or in ionic liquids containing non-nucleophilic counter anions (**Table 7-1**, entries 10 and 11).

Table 7-2. Synthesis of functionalized Indole-2-carboxylates.

Entry	Iodoaniline	Indole-2-carboxylates	Isolated yield (%)
1. (7a)			55%
2. (7b)			54%
3. (7c)			57%
4. (7d)			48%
5. (7e)			77%
6. (7f)			52%
7. (7g)			63%
8. (7h)			50% ^[a]
9.			trace ^[b]

[a] Based on recovered starting iodoaniline. [b] Ethyl 2-ethoxy-3-phenylacrylate was used as the acrylate source.

Additionally, this does not satisfactorily account for the inability of direct Pd^0 sources to promote the HJA process as described nor why Pd^0 sources under standard $\text{Pd}^0/\text{Pd}^{\text{II}}$ Heck conditions gives only quinolinones (**Scheme 7-2, top**),^[8d] not indole-2-carboxylates.

Another possible explanation for this dichotomy is that while the standard Heck process proceeds via $\text{Pd}^0/\text{Pd}^{\text{II}}$ intermediates, the on-palladium HJA reaction proceeds via a different cycle possibly involving $\text{Pd}^{\text{II}}/\text{Pd}^{\text{IV}}$ intermediates, **Scheme 7-3** ($\text{L} = \text{AcO}^-$). Such catalytic cycles have been proposed and deemed to be “unlikely” in the Heck reaction.^[7c] The increased electrophilicity of the Pd-centre on intermediate **II** under such conditions, may be expected to favour intramolecular ligand exchange onto the appended *ortho*-amino group, and thus account for the successful direct annulation to the indole derivatives. Known catalytic processes involving $\text{Pd}^{\text{II}}/\text{Pd}^{\text{IV}}$ intermediates typically proceed under oxidative conditions,^[10] at least one report on the intramolecular trapping of Heck adducts on-Pd via a $\text{Pd}^{\text{II}}/\text{Pd}^{\text{IV}}$ pathway is known.^[10d] The present HJA process would require a direct oxidative addition of an aryl iodide to a Pd^{II} catalyst to access the Pd^{IV} intermediate.

7.3 Conclusion

In conclusion, we report the successful annulation of *ortho*-iodoanilines onto an α -ethoxy acrylate resulting in a general synthesis of indole-2-carboxylate derivatives. The reaction appears to be mechanistically distinct from a standard Heck reaction. Under Heck-Jeffery conditions, evidence is presented consistent with an all “on-palladium” mechanism, involving a critical intramolecular amination, or ligand exchange step, (**II-III**, **Scheme 7-3**) that intervenes and effectively competes with the standard Heck process (**II-5**). Further investigation into the mechanism, scope and application of the method is in progress.

7.4 References

- [1]. Fischer, E.; Jourdan, F. *Chem. Ber.* **1883**, 16, 2241-2245. (b) Van Order, R. B.; Lindwall, H. G. *Chem. Rev.* **1942**, 30, 69-96. (c) Madelung, W. *Chem. Ber.* **1912**, 45, 1128-1134. (d) Reissert, A. *Chem. Ber.* **1897**, 30, 1030-1053. (e) Sundberg, R. J. *The Chemistry of Indoles*, Academic Press, New York, 1970.
- [2]. For a selection of recent syntheses of functionalized indoles see: (a) Newman, S. G.; Lautens, M. *J. Am. Chem. Soc.*, **2010**, 132, 11416-11417. (b) Cacchi, S.; Fabrizi, G.; Goggiamani, A.; Perboni, A.; Sferrazza, A.; Stabile, P. *Org. Lett.*, **2010**, 12, 3279-3281. (c) Ohta, Y.; Chiba, H.; Oishi, S.; Fujii, N.; Ohno, H. *J. Org. Chem.*, **2009**, 74, 7052-7058. (d) Zhou, L.; Doyle, M. P. *J. Org. Chem.*, **2009**, 74, 9222-9224. (e) Li, X.; Du, Y.; Liang, L.; Li, X.; Pan, Y.; Zhao, K. *Org. Lett.*, **2009**, 11, 2643-2646. (f) Kraus, G. A.; Guo, H. *Org. Lett.*, **2008**, 10, 3061-3063. (g) Cui, S. L.; Wang, J.; Wang, Y. G. *J. Am. Chem. Soc.*, **2008**, 130, 13526-13527. (h) Sakai, N.; Annaka, K.; Fujita, A.; Sato, A.; Konakahara, T. *J. Org. Chem.*, **2008**, 73, 4160-4165. (i) Stokes, B. J.; Dong, H.; Leslie, B. E.; Pumphrey, A. L.; Driver, T. G. *J. Am. Chem. Soc.*, **2007**, 129, 7500-7501. (j) Chen, Y.; Xie, X.; Ma, D. *J. Org. Chem.*, **2007**, 72, 9329-9334. (k) Liu, F.; Ma, D. *J. Org. Chem.*, **2007**, 72, 4844-4850. (l) Sridharan, V.; Perumal, S.; Avendaño, C.; Menéndez, J. C. *Synlett*, **2006**, 91-95. (m) Jia, Y.; Zhu, J. *J. Org. Chem.*, **2006**, 71, 7826-7834. (n) Fayol, A.; Fang, Y. Q.; Lautens, M. *Org. Lett.*, **2006**, 8, 4203-4206. (o) Yue, D.; Yao, T.; Larock, R. C. *J. Org. Chem.*, **2006**, 71, 62-69. (p) Willis, M. C.; Brace, G. N.; Holmes, I. P. *Angew. Chem. Int. Ed.*, **2005**, 44, 403-406. (q) Fang, Y. Q.; Lautens, M. *Org. Lett.*, **2005**, 7, 3549-3552.
- [3]. For recent reviews on transition metal mediated approaches to indole synthesis see: (a) Cacchi, S.; Fabrizi, G.; Goggiamani, A. *Org. Biomol. Chem.*, **2011**, 9, 641-652. (b) Cacchi, S.; Fabrizi, G. *Chem. Rev.* **2011**, 111,

- PR215-PR283 (c) Zeni, G.; Larock, R. C. *Chem. Rev.* **2006**, *106*, 4644-4680. (d) Cacchi, S.; Fabrizi, G. *Chem. Rev.* **2005**, *105*, 2873-2920.
- [4]. (a) Nemes, A. Monoterpenoid Indole Alkaloids, CNS and Anticancer Drugs, in *Analogue-Based Drug Discovery II*, Fischer, J; Ganellin, C. R. (Ed.s), J. Wiley, 2010. (b) Hesse, M. in *Alkaloids, Nature's Curse or Blessing?*, Wiley-VCH, 2002. (c) Ishikura, M.; Yamada, K. *Nat. Prod. Rep.* **2009**, *26*, 803-852.
- [5]. For biologically active indole-2-carboxylic acid derivatives see: (a) Mayes, B. A.; Chaudhuri, N. C.; Hencken, C. P.; Jeannot, F.; Latham, G. M.; Mathieu, S.; McGarry, F. P.; Stewart, A. J.; Wang, J.; Moussa, A., *Org. Proc. Res. & Dev.* **2010**, *14*, 1248-1253. (b) Sechi, M.; Derudas, M.; Dallochio, R.; Dessi, A.; Bacchi, A.; Sannia, L.; Carta, F.; Palomba, M.; Ragab, O.; Chan, C.; Shoemaker, R.; Sei, S.; Dayam, R.; Neamati, N. *J. Med. Chem.* **2004**, *47*, 5298-5310.
- [6]. (a) Das, P.; McNulty, J. *Eur. J. Org. Chem.*, **2010**, 3587-3591. (b) McNulty, J.; Cheekoori, S.; Bender, T. P.; Coggan, J. A. *Eur. J. Org. Chem.* **2007**, 1423-1428. (c) McNulty, J.; Nair, J. J.; Capretta, A. *Tetrahedron Lett.*, **2009**, *50*, 4087-4091. (d) McNulty, J.; Nair, J. J.; Sliwinski, M.; Robertson, A. *J. Tetrahedron Lett.*, **2009**, *50*, 2342-2346. (e) Gerritsma, D. A.; Robertson, A.; McNulty J.; Capretta, A. *Tetrahedron Lett.* **2004**, *45*, 7629-7632.
- [7]. (a) Jeffery, T. *Tetrahedron*, **1996**, *52*, 10113-10130. (b) Basu, B.; Das, S.; Das, P.; Mandal, B.; Banerjee, D.; Almqvist, F. *Synthesis*, **2009**, 1137-1146. (c) Beccalli, E. M.; Borsini, E.; Brenna, S.; Galli, S.; Rigamonti, M.; Brogginni, G. *Chem. Eur. J.* **2010**, *16*, 1670-1678.
- [8]. (a) Quick, J.; Jenkins, R. *J. Org. Chem.*, **1978**, *43*, 2275-2277. (b) Cacchi, S.; Ciattini, P. G.; Morera, E.; Ortar, G. *Tetrahedron Lett.*, **1987**, *28*, 3039-3042. (c) Merlic, C. A.; Semmelhack, M. F. *J. Organomet. Chem.*, **1990**, *391*, C23-

- C27. (d) Sakamoto, T.; Kondo, Y.; Yamanaka, H. *Heterocycles*, **1988**, 27, 453-456.
- [9]. (a) Tullberg, E.; Schacher, F.; Peters, D.; Frejd, T. *Synthesis*, **2006**, 1183-1189. (b) Minatti, A.; Muniz, K. *Chem. Soc. Rev.* **2007**, 36, 1142-1152.
- [10]. (a) Racowski, J. M.; Dick, A. R.; Sanford, M. S. *J. Am. Chem. Soc.*, **2009**, 131, 10974-10983. (b) Deprez, N. R.; Sanford, M. S. *J. Am. Chem. Soc.*, **2009**, 131, 11234-11241. (c) Mei, T-S.; Wang, X.; Yu, J-Q. *J. Am. Chem. Soc.*, **2009**, 131, 10806-10807. (d) Kalyani, D.; Satterfield, A. D.; Sanford, M. S. *J. Am. Chem. Soc.*, **2010**, 132, 8419-8427. (e) Lu, X. *Topics In Catal.*, **2005**, 35, 73-86.
- [11]. Koenig, S. G.; Dankwardt, J. W.; Liu, Y.; Zhao, H.; Singh, S. P. *Tetrahedron Lett.* **2010**, 51, 6549-6551.
- [12]. Sanz, R.; Escribano, J.; Pedrosa, M. R.; Aguado, R.; Arnáiz, F. J. *Adv. Synth. Catal.* **2007**, 349, 713-718.
- [13]. Shou, W. G.; Li, J.; Guo, T.; Lin, Z.; Jia, G. *Organometallics*. **2009**, 28, 6847-6854.
- [14]. Najer, H.; Giudicelli, R.; Loiseau, J.; Menin, J. *Bulletin de la Societe Chimique de France*. **1963**, 12, 2831-2840.
- [15]. Cai, Q.; Li, Z.; Wei, J.; Ha, C.; Pei, D.; Ding, K. *Chem. Commun.* **2009**, 7581-7583.
- [16]. Boon, W. R. *J. Chem. Soc. 1*, **1949**, S231.
- [17]. Brodin, R.; Boigegrain, R.; Bignon, E.; Molimard, J-C.; Olliero, D. *PCT Int. Appl.* **1999**, WO 99155525 A1 19990401.
- [18]. Metz, W- Jr.; Ding, F. *PCT Int. Appl.*, **2006**, 2006023467.

- [19]. Bach, K. K.; El-Seedi, H. R.; Jensen, H. M.; Nielsen, H. B.; Thomsen, I.; Torssell, K. B. G. *Tetrahedron*, **1994**, *50*, 7543-7556.
- [20]. Stevens, C. L.; Sherr, A. E. *J. Org. Chem.* **1952**, *17*, 1177-1181.
- [21]. Aitken, R. A.; Thom, G. L., *Synthesis*, **1989**, *12*, 958-959.

7.5 Experimental section

All reactions were carried out under argon atmosphere in oven dried glassware. Acetonitrile and DMF were obtained from Sigma-Aldrich. Iodoaniline derivatives were obtained from Sigma-Aldrich, AlfaAesar and AB Chem, Canada. THF was distilled over sodium/benzophenone. Melting points were recorded in open capillary tubes using a calibrated Büchi B540 apparatus. Thin layer chromatography (TLC) was carried out using aluminium sheets pre-coated with silica gel 60F₂₅₄ (Merck) and was visualized under 254/360 nm UV. ¹H and ¹³C spectra were recorded on a AV 600 spectrometer in CDCl₃ with TMS as internal standard. Chemical shifts (δ) are reported in ppm downfield of TMS and coupling constants (*J*) are expressed in Hertz (Hz).

Synthesis of 1,2-diethoxy-2-oxo-triethylphosphonium chloride (Scheme 7-1, 2):

Into a flame dried flask, containing a magnetic stirring bar, were weighed sequentially ethyl 2,2-diethoxyacetate **1** (0.274 g, 1.56 mmol, 1.0 eq) and triethyl phosphine chloride (0.091 g, 0.59 mmol, 0.6 eq). The reaction mixture was sealed and heated at 100 °C 2 h. Ethanol was removed and resulting mixture was placed under high vacuum for 50 min to give the phosphonium salt **2** in 85% yield as an oil. The title compound was also prepared in gram quantities according to a literature procedure.^[19] ¹H NMR (200 MHz, CDCl₃); δ (ppm): 6.22 (d, *J* = 13.9 Hz, 1H), 4.29 (dd, *J* = 13.7, 6.9 Hz, 2H), 4.11-3.82 (m, 2H), 2.61 (dd, *J* = 12.2, 6.5 Hz, 6H), 1.40-1.18 (m, 15H). ¹³C NMR (50 MHz, CDCl₃); δ (ppm): 167.2, 167.1, 72.4 (d, *J* = 62 Hz), 70.8 (d, *J* = 9.0 Hz), 63.1,

15.2, 14.1, 12.1, 11.2, 6.2, 6.1. ^{31}P NMR (81 MHz, CDCl_3); 43.05 ppm. HRMS (M) $^+$ calc for $\text{C}_{12}\text{H}_{26}\text{O}_3\text{P}$: 249.1617, found 249.1620.

Synthesis of ethyl 2-ethoxyacrylate (Scheme 7-1, **3**):^[20]

Into a flame dried flask, containing a magnetic stirring bar was weighed the phosphonium salt **2** (0.284 g, 1.0 mmol) under argon atmosphere. Dry THF (1.0 mL) was added into the flask. The flask was stirred at 0 °C for 15 min whereupon NaHMDS (1.04 mL, 1.05 mmol, 1.0 M stock, THF) was added slowly. After 35 min, paraformaldehyde (0.030 g, 1.0 eq) was added to the reaction flask maintained at 0 °C. The flask was kept at 0 °C for further 2 h and then slowly warmed to room temperature during overnight. The resulting mixture was concentrated to remove solvent. Water was added and resultant mixture was extracted with ethyl acetate (3 X 20 mL). The combined organic layers were dried over sodium sulphate, filtered and concentrated. The product was purified using silica gel column chromatography with 5% ethyl acetate in hexane to yield **3** as colorless oil in 85-90% yield. ^1H NMR (600 MHz, CDCl_3); δ (ppm): 5.30 (d, J = 2.40 Hz, 1H), 4.57 (d, J = 2.40 Hz, 1H), 4.25 (q, J = 7.10 Hz, 2H), 3.81 (q, J = 7.00 Hz, 2H), 1.38 (t, J = 7.00 Hz, 3H), 1.31 (t, J = 7.10 Hz, 3H). ^{13}C NMR (151 MHz, CDCl_3); δ (ppm): 163.4, 151.5, 93.7, 64.1, 61.4, 14.2.

Ethyl α -ethoxycinnamate (Scheme 7-5, **4a):**^[21] 42:58 *cis:trans*, ^1H NMR (200 MHz, CDCl_3); δ (ppm): 7.86 – 7.73 (m, 1H), 7.45 – 7.11 (m, 4H), 7.00 (s, 1H, *cis* isomer), 6.11 (s, 1H, *trans* isomer), 4.32 (q, J = 7.1 Hz, 2H, *cis* isomer), 4.13 (q, J = 7.2 Hz, 2H, *trans* isomer), 3.96 (q, J = 7.0 Hz, 2H, *trans* and *cis* isomer), 1.41 (t, J = 7.0 Hz, 3H for *trans* isomer, 6H for *cis* isomer), 1.09 (t, J = 7.1 Hz, 3H, *trans* isomer). ^{13}C NMR (50 MHz, CDCl_3); δ (ppm): (*E* isomer) 164.8, 147.7, 135.1, 130.2, 128.4, 128.1, 109.0, 64.6, 61.4, 14.5, 13.7.

Ethyl α -ethoxy-5-phenylpent-2-enoate (Scheme 7-5, **4b):** 43:57 *cis:trans*, ^1H NMR (200 MHz, CDCl_3); δ (ppm): 7.30-7.20 (m, 5H), 6.31 (t, J = 7.4 Hz, 1H, *cis* isomer), 5.24 (t, J = 7.4 Hz, 1H, *trans* isomer), 4.47 – 4.02 (m, 2H), 3.92 – 3.48

(m, 2H), 2.90-2.65 (m, 4H), 1.49 – 1.14 (m, 6H). ^{13}C NMR (50 MHz, CDCl_3); δ (ppm): 164.0, 145.4, 141.6, 128.5, 128.4, 125.9, 114.7, 64.3, 60.9, 36.4, 28.6, 15.4, 14.5, 14.3. HRMS: calcd. For $\text{C}_{15}\text{H}_{20}\text{O}_3$ $[\text{M}]^+$ 248.1412; found 248.1419.

Ethyl α -ethoxy-3,4,5-trimethoxycinnamate (Scheme 7-5, 4c): 39:61 *cis:trans*, ^1H NMR (200 MHz, CDCl_3); δ (ppm): (*E* isomer) 6.44 (s, 2H), 6.03 (s, 1H), 4.15 (q, $J = 7.1$ Hz, 2H), 3.94 – 3.90 (m, 2H), 3.82 (s, 9H), 1.42 (t, $J = 7.0$ Hz, 3H), 1.13 (t, $J = 7.1$ Hz, 3H). (*Z* isomer) 7.11 (s, 2H), 6.91 (s, 1H), 4.31 (q, $J = 7.1$ Hz, 2H), 4.05 (d, $J = 7.1$ Hz, 2H), 3.88 (s, 9H), 1.39 (dt, $J = 7.1, 5.2$ Hz, 6H). ^{13}C NMR (50 MHz, CDCl_3); δ (ppm): 164.9, 152.9, 147.9, 136.9, 130.6, 108.4, 106.7, 105.4, 64.6, 61.4, 60.9, 56.0, 14.5, 13.8. HRMS: calcd. For $\text{C}_{16}\text{H}_{22}\text{O}_6$ $[\text{M}]^+$ 310.1416; found 310.1423.

Ethyl α -ethoxy-4-methoxycinnamate (Scheme 7-5, 4d):^[21] 38:62 *cis:trans*, ^1H NMR (200 MHz, CDCl_3); δ (ppm): (*E* isomer) 7.15 (d, $J = 8.5$ Hz, 2H), 6.83 (d, $J = 8.7$ Hz, 2H), 6.09 (s, 1H), 4.16 (q, $J = 7.1$ Hz, 2H), 3.99 – 3.85 (m, 2H), 3.80 (s, 3H), 1.41 (t, $J = 7.0$ Hz, 3H), 1.14 (t, $J = 7.1$ Hz, 3H). (*Z* isomer) 7.77 (d, $J = 8.8$ Hz, 2H), 6.95 (d, $J = 10.6$ Hz, 2H), 6.88 (s, 1H), 4.30 (dd, $J = 14.2, 7.1$ Hz, 2H), 3.99 (dd, $J = 14.1, 7.1$ Hz, 2H), 3.84 (s, 3H), 1.37 (td, $J = 7.1, 1.4$ Hz, 6H). ^{13}C NMR (50 MHz, CDCl_3); δ (ppm): 164.8, 158.6, 146.6, 129.7, 127.2, 113.5, 109.7, 64.6, 61.2, 55.3, 14.5, 13.8.

Ethyl α -ethoxy-4-chlorocinnamate (Scheme 7-5, 4e):^[21] 37:63 *cis:trans*, ^1H NMR (200 MHz, CDCl_3); δ (ppm): (*E* isomer) 7.25 (d, $J = 7.2$ Hz, 2H), 7.12 (d, $J = 8.3$ Hz, 2H), 6.03 (s, 1H), 4.15 (q, $J = 7.1$ Hz, 2H), 3.93 (q, $J = 6.9$ Hz, 2H), 1.43 (t, $J = 6.9$ Hz, 3H), 1.13 (t, $J = 7.1$ Hz, 3H). (*Z* isomer) 7.73 (d, $J = 8.5$ Hz, 2H), 7.33 (d, $J = 8.6$ Hz, 2H), 6.92 (s, 1H), 4.31 (q, $J = 7.1$ Hz, 2H), 4.02 (dd, $J = 5.7$ Hz, 2H), 1.39 (m, 6H). ^{13}C NMR (50 MHz, CDCl_3); δ (ppm): 164.5, 148.1, 145.23, 133.7, 129.9, 128.3, 107.9, 64.7, 61.6, 14.6, 13.8.

Synthesis of Ethyl α -ethoxy-2-nitrocinnamate (Scheme 7-4, 10):

Into a flame dried flask, containing a magnetic stirring bar, was weighed salt **2** (0.284 g, 1.0 mmol, 1.0 eq) under argon. Dry THF (1.0 mL) was added and the contents cooled and stirred at -78 °C for 15 min whereupon LHMDs (1.04 mL, 1.05 mmol, 1.0 M stock, THF) was added slowly. After 35 min, 2-nitrobenzaldehyde (0.150 g, 1.0 eq) was added to the reaction flask maintained at -78 °C. The flask was kept at -78 °C for a further 2 h and allowed to slowly warm to room temperature overnight. The resulting mixture was concentrated to remove solvent. Water was added and the mixture extracted with ethyl acetate (3 x 20 mL). The combined organic phase was dried over sodium sulphate, filtered and concentrated. The product was purified using silica gel column chromatography (gradient, 5-10% ethyl acetate in hexane) to yield 2-nitrocinnamate **10** as a colorless oil in 72% yield (*E*: *Z* ratio = 3:1). ¹H NMR (600 MHz, CDCl₃); δ (ppm): (*E* isomer) 8.05 (dd, *J* = 8.2, 1.2 Hz, 1H), 7.52 (td, *J* = 7.5, 1.1 Hz, 1H), 7.45-7.39 (m, 1H), 7.31-7.24 (m, 1H), 6.46 (s, 1H), 4.01 (m, 4H), 1.46 (t, *J* = 7.0 Hz, 3H), 0.96 (t, *J* = 7.1 Hz, 3H). ¹³C NMR (151 MHz, CDCl₃); δ (ppm): 163.40, 148.14, 147.54, 132.76, 132.09, 131.85, 128.01, 124.57, 107.17, 64.90, 61.36, 14.44, 13.65. (*Z* isomer) 8.00-7.94 (m, 2H), 7.62-7.57 (m, 1H), 7.47-7.40 (m, 1H), 7.29 (s, 1H), 4.32 (q, *J* = 7.1 Hz, 2H), 3.95 (q, *J* = 7.0 Hz, 2H), 1.37 (t, *J* = 7.1 Hz, 3H), 1.21 (t, *J* = 7.0 Hz, 3H). ¹³C NMR (151 MHz, CDCl₃); δ (ppm): 163.9, 148.5, 146.8, 132.8, 131.9, 128.8, 128.7, 124.6, 117.8, 68.5, 61.7, 15.4, 14.3.

Synthesis of Ethyl α -ethoxy-2-aminocinnamate (Scheme 7-4, 5) and its cyclization to (Scheme 7-4, 6):

Into a flame dried flask, containing a magnetic stirring bar, was weighed compound **10** (0.087 g, 0.33 mmol, 1eq), under argon. Dry ethanol (5.0 mL) was added to the flask. Iron powder (0.368 g, 6.8 mmol), NH₄Cl (0.529 g, 9.9 mmol) was added to the flask. The resultant mixture was refluxed for 48 h. The

reaction mixture was cooled to room temperature and filtered through celite pad, washed with excess ethanol. Ethanol was evaporated under vacuum and crude reaction mixture was purified using silica gel column chromatography with 10-15% and 50% ethyl acetate in hexanes to yield the aniline **5** as well as quinolinone **6** in 60% yield. (aniline: quinolinone = 20:80) ^1H NMR (600 MHz, $\text{DMSO}-d_6$); δ (ppm): (Quinolinone) 11.87 (s, 1H), 7.55 (dd, $J = 7.8, 1.1$ Hz, 1H), 7.31 (ddd, $J = 8.4, 7.2, 1.4$ Hz, 1H), 7.25 (d, $J = 8.1$ Hz, 1H), 7.19 (s, 1H), 7.16-7.10 (m, 1H), 4.04 (q, $J = 7.0$ Hz, 2H), 1.37 (t, $J = 7.0$ Hz, 3H). ^{13}C NMR (151 MHz, $\text{DMSO}-d_6$); δ (ppm): 157.3, 147.8, 133.9, 126.8, 126.2, 121.8, 119.8, 114.4, 111.8, 63.7, 14.3. (aniline: obtained as *E*: *Z* = 2:1) ^1H NMR (600 MHz, CDCl_3); δ (ppm): (*E* isomer) 7.56 (dd, $J = 7.7, 1.1$ Hz, 1H), 7.18-7.11 (m, 2H), 6.80-6.75 (m, 1H), 6.74-6.69 (m, 1H), 4.33 (q, $J = 7.1$ Hz, 2H), 4.18 (br s, 2H), 3.90 (q, $J = 7.0$ Hz, 2H), 1.39 (t, $J = 7.1$ Hz, 3H), 1.28 (t, $J = 7.0$ Hz, 3H). ^{13}C NMR (151 MHz, CDCl_3); δ (ppm): 164.7, 145.2, 143.9, 131.1, 130.0, 121.0, 118.7, 118.3, 116.4, 68.5, 61.3, 15.3, 14.4.

General procedure for the Heck-Jeffery amination indole-2-carboxylate synthesis:

Into a flame-dried Schlenk tube, containing a magnetic stirring bar, was weighed the corresponding 2-iodoaniline (0.040 g, 0.18 mmol 1.0 eq), ethyl 2-ethoxyacrylate (0.052 g, 0.36 mmol, 2.0 eq), TBAB (0.118 g, 0.36 mmol, 2.0 eq), NaHCO_3 (0.092 g, 1.09 mmol, 6.0 eq.), $\text{Pd}(\text{OAc})_2$ (0.0061 g, 15 mol%) and dry acetonitrile (1.8-2.0 mL). The reaction mixture was stirred at 80 °C for 96 hours monitored by TLC. The reaction mixture was allowed to cool to room temperature. Solvent was evaporated under vacuum and crude reaction mixture was extracted with ethyl acetate and washed with brine. The combined organic extracts were dried over sodium sulphate, filtered, and concentrated. The product was purified using silica gel column chromatography using 2-5% ethyl acetate in hexanes to yield corresponding ethyl 1H-indole-2-carboxylate. Data are summarized below for the entries in **Table 1**.

Ethyl 1H-indole-2-carboxylate (Table 7-2, 7a):^[11] M.P.: 123-125 °C (Lit M.P. 121-123 °C)^[12]. ¹H NMR (600 MHz, CDCl₃); δ (ppm): 8.92 (br s, 1H), 7.69 (d, *J* = 8.12 Hz, 1H), 7.42 (d, *J* = 8.12 Hz, 1H), 7.32 (m, 1H), 7.23 (m, 1H), 7.15 (m, 1H), 4.42 (q, *J* = 7.20 Hz, 2H), 1.42 (t, *J* = 7.20 Hz, 3H). ¹³C NMR (151 MHz, CDCl₃); δ (ppm): 162.1, 136.9, 127.6, 125.4, 122.7, 120.9, 111.9, 108.7, 61.1, 14.5.

Ethyl 6-chloro-1H-indole-2-carboxylate (Table 7-2, 7b):^[12] M.P. 169-171 °C (Lit M.P. 163-165 °C)^[12]. ¹H NMR (600 MHz, CDCl₃); δ (ppm): 9.07 (br s, 1H), 7.59 (d, *J* = 8.50 Hz, 1H), 7.42 (s, 1H), 7.19 (s, 1H), 7.12 (dd, *J* = 8.50 Hz, 1.8 Hz, 1H), 4.20 (q, *J* = 7.10 Hz, 2H), 1.42 (t, *J* = 7.10 Hz, 3H). ¹³C NMR (151 MHz, CDCl₃); δ (ppm): 161.9, 137.1, 131.4, 128.3, 126.1, 123.6, 122.0, 111.84, 108.7, 61.3, 14.5.

Ethyl 6-methoxy-1H-indole-2-carboxylate (Table 7-2, 7c):^[13] M.P. 131-133 °C (Lit M.P. 135-136 °C)^[14]. ¹H NMR (600 MHz, CDCl₃); δ (ppm): 8.88 (br s, 1H), 7.54 (d, *J* = 8.6 Hz, 1H), 7.16 (m, 1H), 6.83 (s, 1H), 6.82 (dd, *J* = 8.6 Hz, 2.2 Hz, 1H), 4.39 (q, *J* = 7.18 Hz, 2H), 3.86 (s, 3H), 1.41 (t, *J* = 7.18 Hz, 3H). ¹³C NMR (151 MHz, CDCl₃); δ (ppm): 162.1, 159.0, 138.0, 126.5, 123.5, 122.0, 112.4, 109.1, 93.8, 60.9, 55.6, 14.5.

Ethyl 5-fluoro-1H-indole-2-carboxylate (Table 7-2, 7d):^[11] M.P. 147-149 °C (Lit M.P. 147-148 °C)^[11]. ¹H NMR (600 MHz, CDCl₃); δ (ppm): 9.00 (br s, 1H), 7.36 (dd, *J* = 8.9, 4.3 Hz, 1H), 7.32 (dd, *J* = 9.2, 2.4 Hz, 1H), 7.18 (m, 1H), 7.09 (td, *J* = 9.02, 2.48 Hz, 1H), 4.42 (q, *J* = 7.10 Hz, 2H), 1.42 (t, *J* = 7.10 Hz, 3H). ¹³C NMR (151 MHz, CDCl₃); δ (ppm): 161.8, 158.3 (d, *J* = 237.59 Hz), 129.2, 127.8 (d, *J* = 10.4 Hz), 114.5 (d, *J* = 26.89 Hz), 112.9 (d, *J* = 9.59 Hz), 108.5 (d, *J* = 5.25 Hz), 106.9 (d, *J* = 23.26 Hz), 61.3, 14.5.

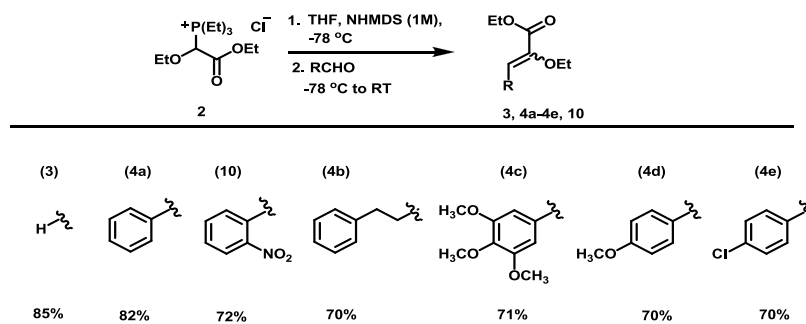
Ethyl 5-chloro-1H-indole-2-carboxylate (Table 7-2, 7e):^[12] M.P. 167 °C (Lit M.P. 167-169 °C)^[12]. ¹H NMR (600 MHz, CDCl₃); δ (ppm): 9.12 (br s, 1H), 7.66 (d, *J* = 1.83 Hz, 1H), 7.35 (d, *J* = 8.35 Hz, 1H), 7.27 (dd, *J* = 8.73, 1.92 Hz, 1H),

7.15 (m, 1H), 4.42 (q, $J = 7.10$ Hz, 2H), 1.42 (t, $J = 7.10$ Hz, 3H). ^{13}C NMR (151 MHz, CDCl_3); δ (ppm): 161.9, 135.2, 128.8, 128.5, 126.5, 125.9, 121.8, 113.1, 108.0, 61.4, 14.5.

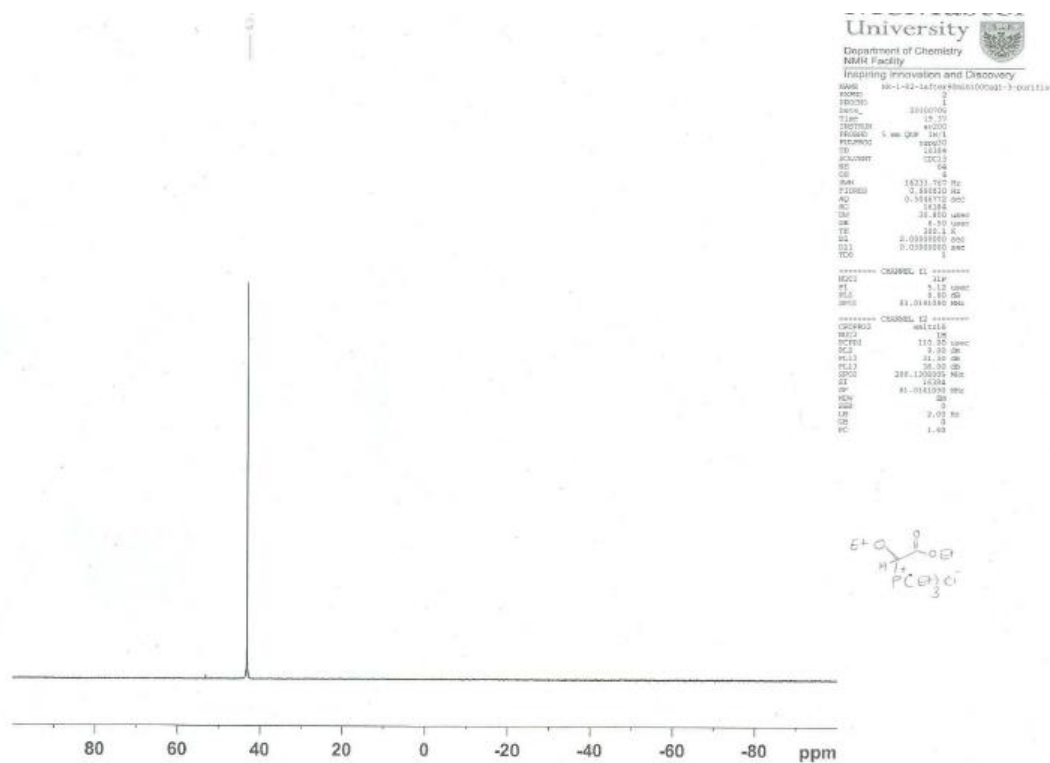
Ethyl 5-methyl-1H-indole-2-carboxylate (Table 7-2, 7f):^[15] M.P. 161-162 °C (Lit M.P. 163 °C)^[16]. ^1H NMR (600 MHz, CDCl_3); δ (ppm): 8.85 (br s, 1H), 7.46 (d, $J = 0.64$ Hz, 1H), 7.31 (d, $J = 8.46$ Hz, 1H), 7.15 (m, 2H), 4.41 (q, $J = 7.10$ Hz, 2H), 2.44 (s, 3H), 1.42 (t, $J = 7.10$ Hz, 3H). ^{13}C NMR (151 MHz, CDCl_3); δ (ppm): 162.2, 135.3, 130.2, 127.9, 127.6, 127.4, 121.9, 111.6, 108.2, 61.0, 21.5, 14.5.

Ethyl 5,6-dimethyl-1H-indole-2-carboxylate (Table 7-2, 7g):^[17] M.P. 162-165 °C. ^1H NMR (600 MHz, CDCl_3); δ (ppm): 8.71 (br s, 1H), 7.43 (s, 1H), 7.18 (s, 1H), 7.12 (dd, $J = 2.00, 0.84$ Hz, 1H), 4.39 (q, $J = 7.18$ Hz, 2H), 2.37 (s, 3H), 2.34 (s, 3H), 1.41 (t, $J = 7.18$ Hz, 3H). ^{13}C NMR (151 MHz, CDCl_3); δ (ppm): 162.2, 136.1, 135.3, 129.9, 126.8, 126.1, 122.3, 112.3, 112.0, 108.2, 60.9, 20.9, 20.2, 14.5.

Ethyl 5-cyano-1H-indole-2-carboxylate (Table 7-2, 7h):^[18] M.P. 179-180 °C, ^1H NMR (600 MHz, CDCl_3); δ (ppm): 9.20 (s, 1H), 8.08 (s, 1H), 7.54 (dd, $J = 8.6, 1.3$ Hz, 1H), 7.50 (d, $J = 8.6$ Hz, 1H), 7.28 (d, $J = 1.2$ Hz, 1H), 4.44 (q, $J = 7.1$ Hz, 2H), 1.43 (t, $J = 7.1$ Hz, 3H). ^{13}C NMR (151 MHz, CDCl_3); δ (ppm): 161.4, 138.0, 129.9, 128.6, 127.7, 127.3, 120.0, 113.0, 109.0, 104.5, 61.7, 14.4.



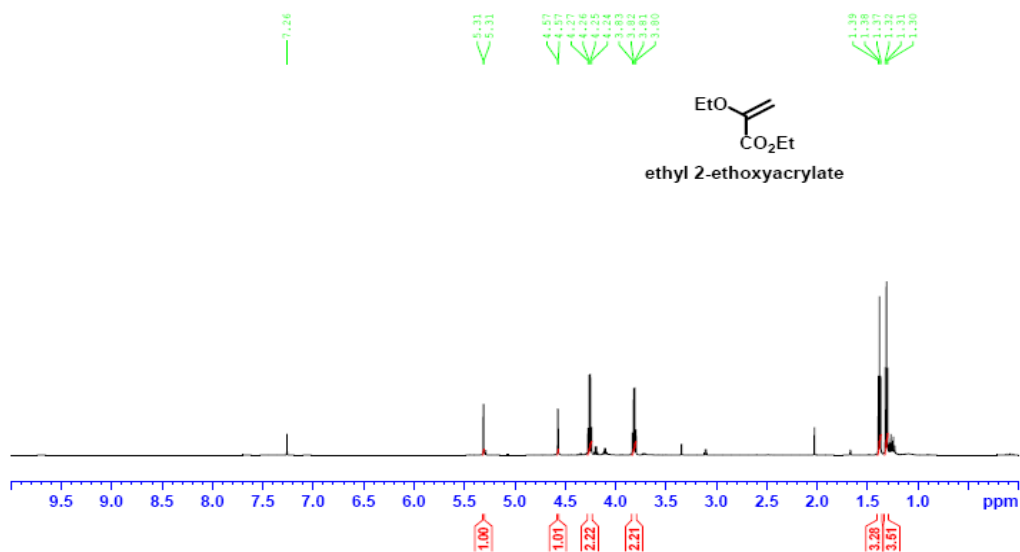
Scheme 7-5. Scope of olefination reaction with phosphonium salt **2**.

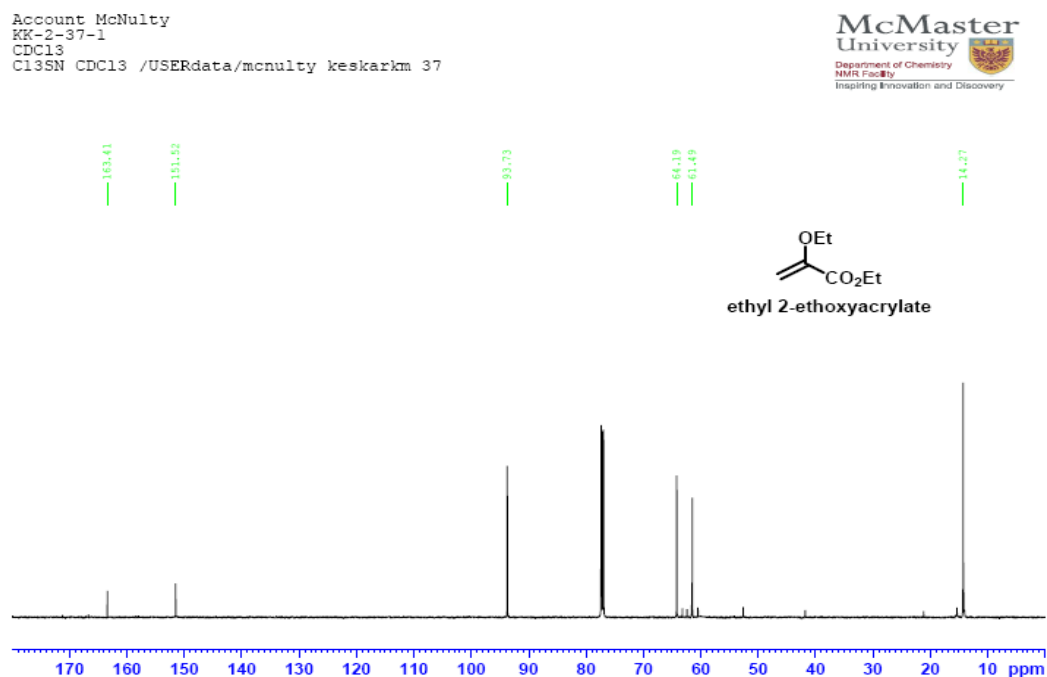


ethyl 2-ethoxyacrylate (Scheme 7-1, 3):

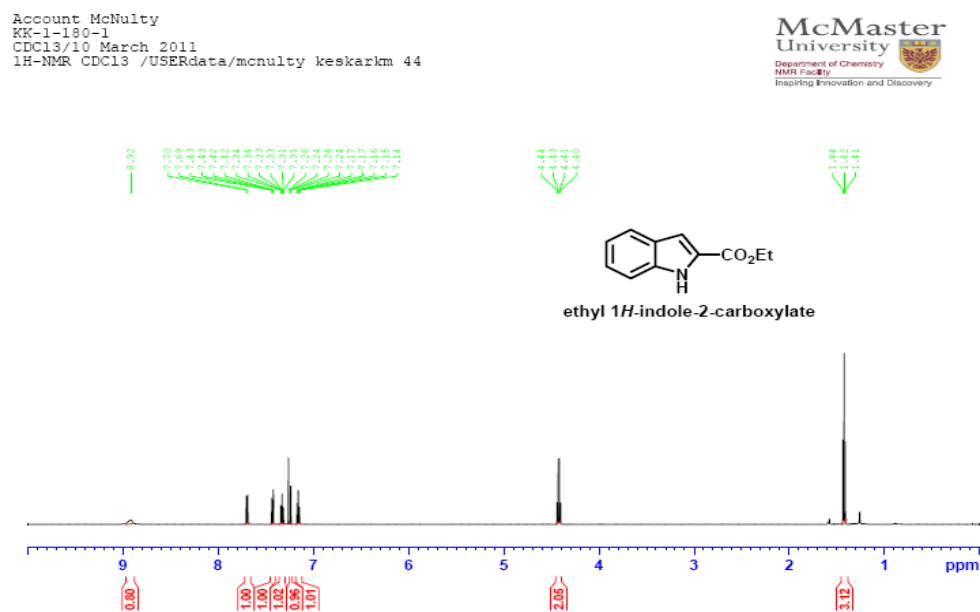
Account McNulty
KK-2-37-1
CDC13
1H-NMR CDC13 /USERdata/mcnulty keskarkm 37

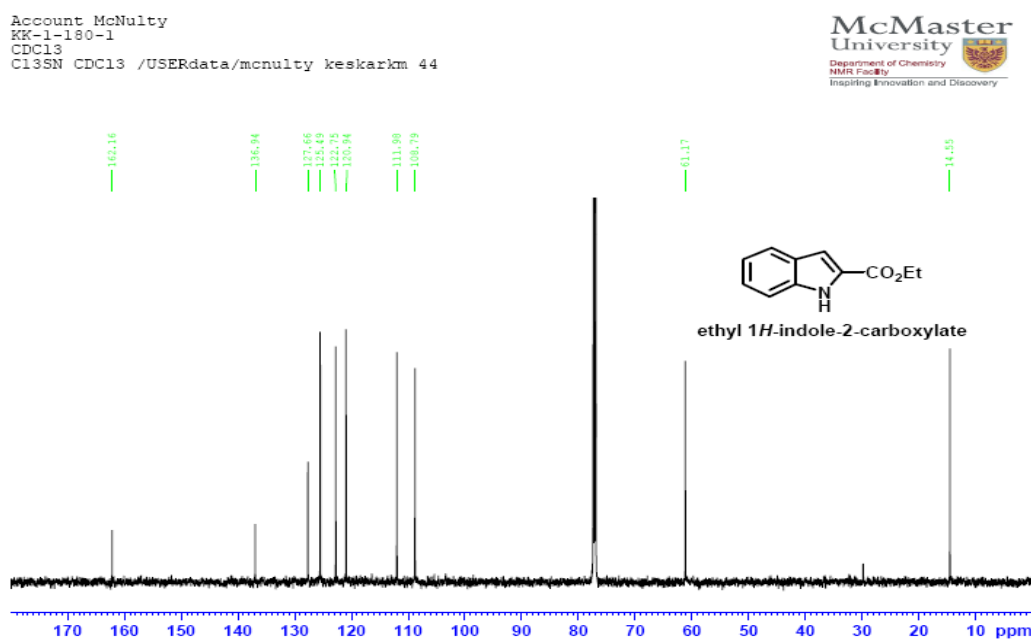
McMaster
University
Department of Chemistry
NMR Facility
Inspiring Innovation and Discovery



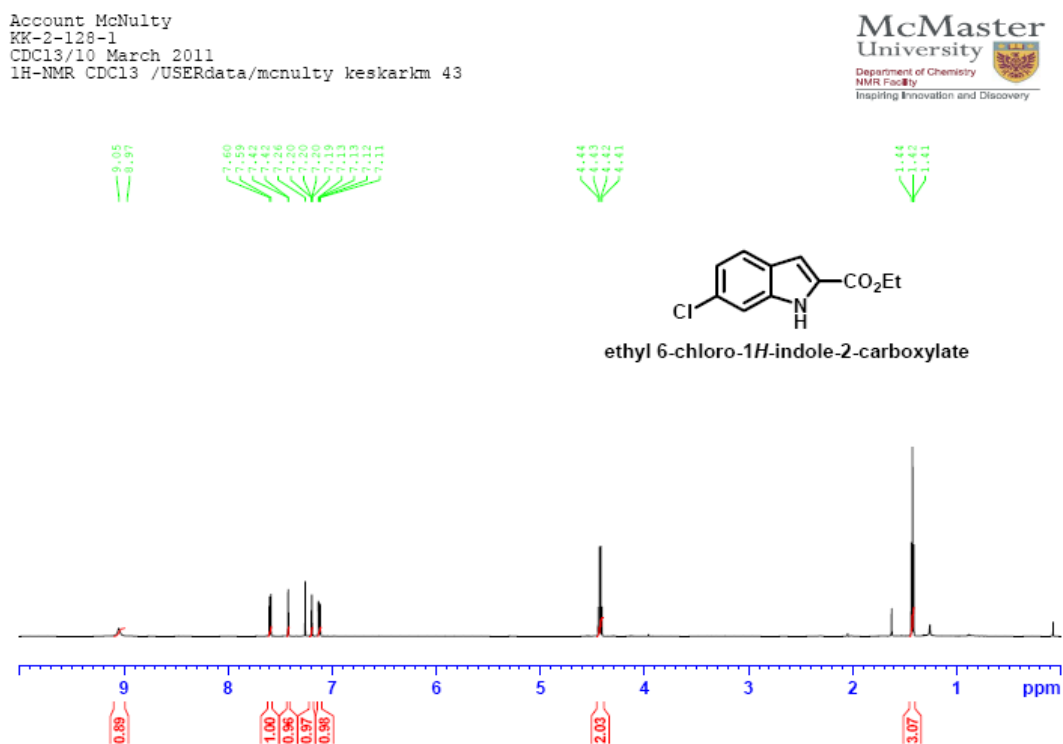


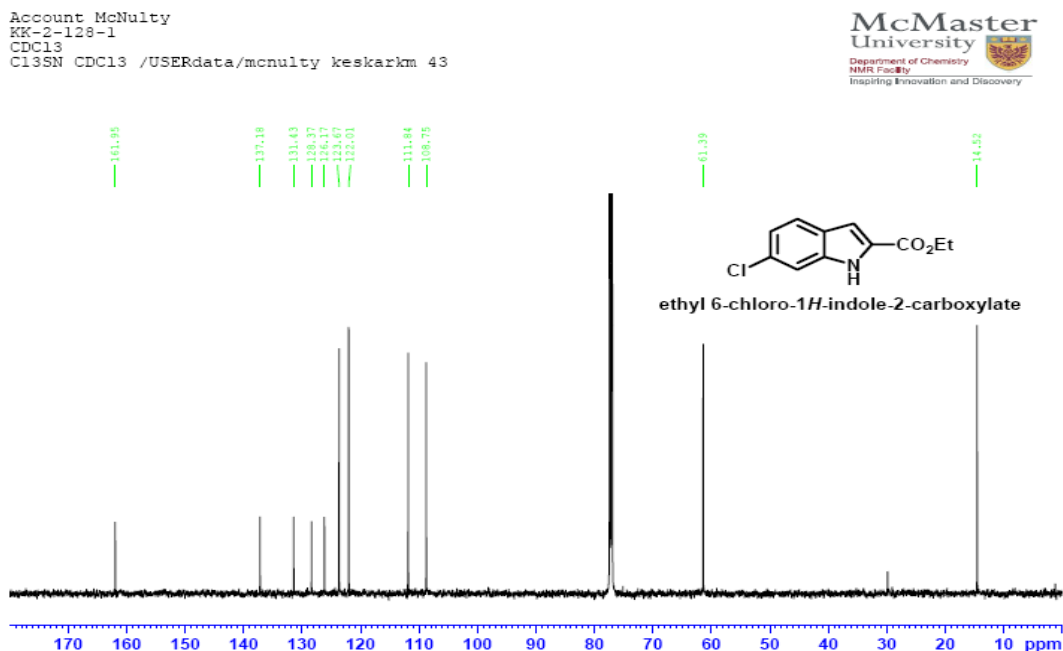
Ethyl 1H-indole-2-carboxylate (Table 7-2, 7a):



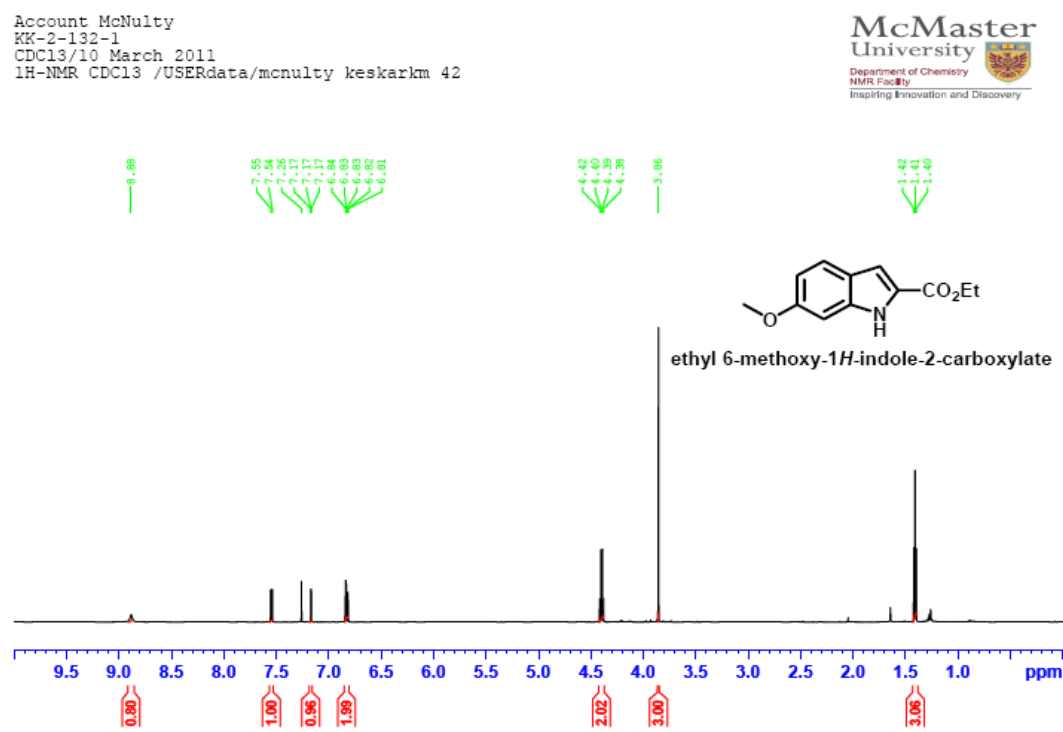


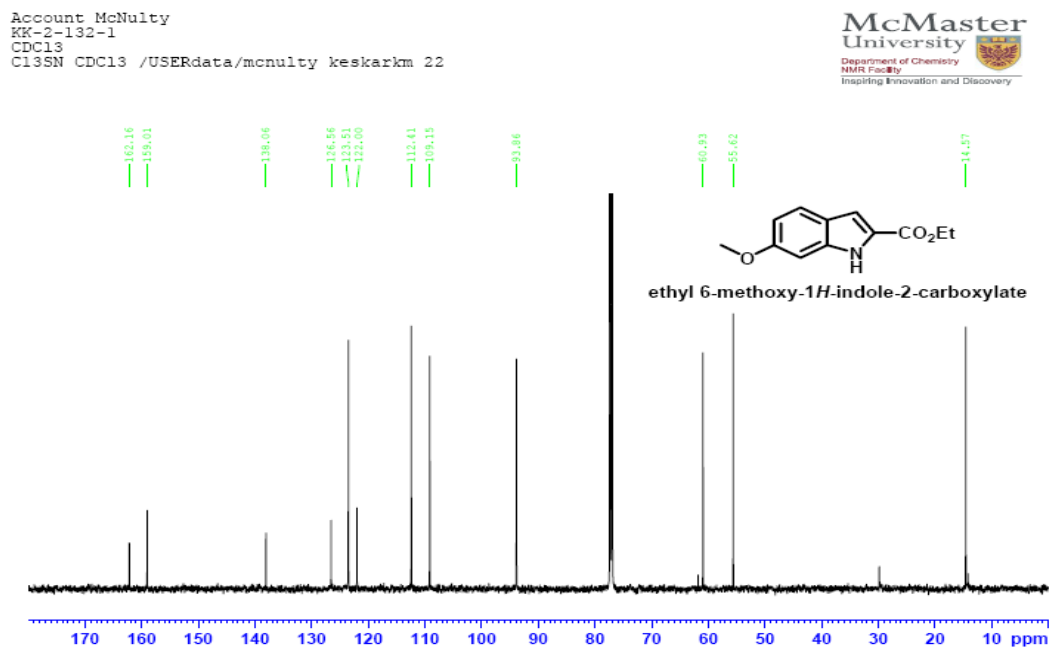
Ethyl 6-chloro-1*H*-indole-2-carboxylate (Table 7-2, 7b):



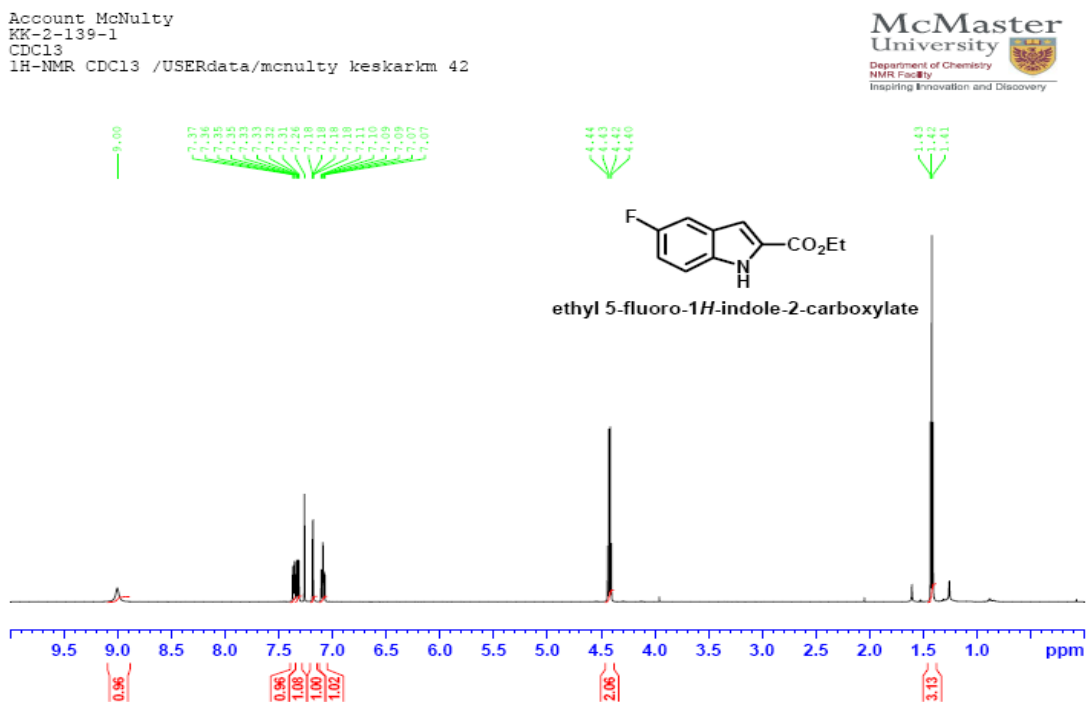


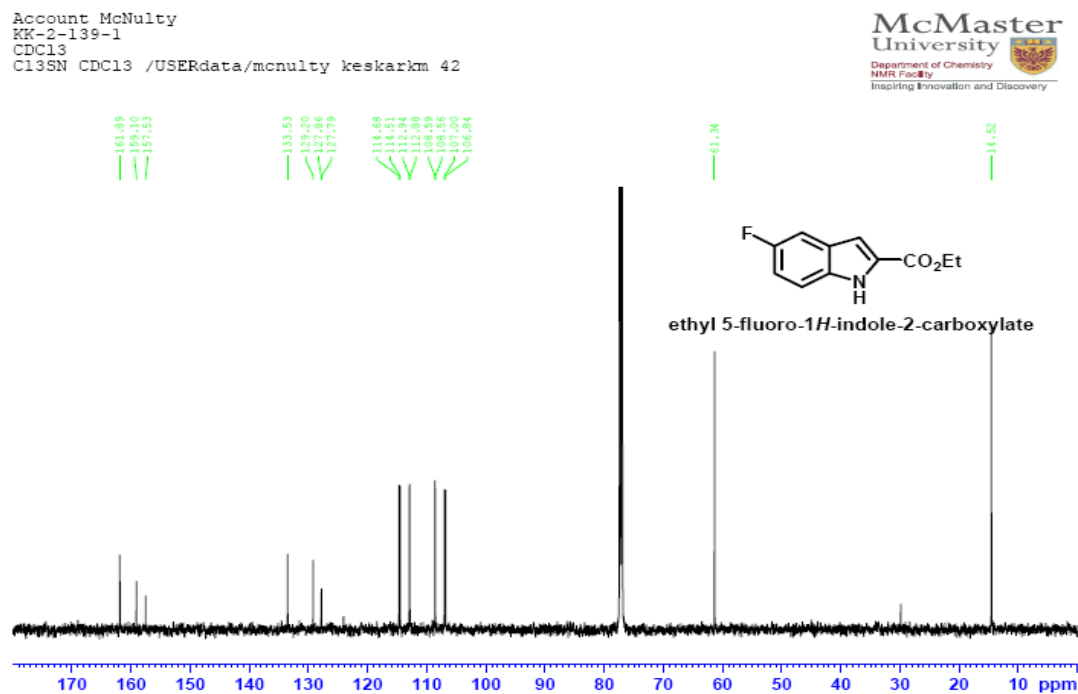
Ethyl 6-methoxy-1H-indole-2-carboxylate (Table 7-2, 7c):



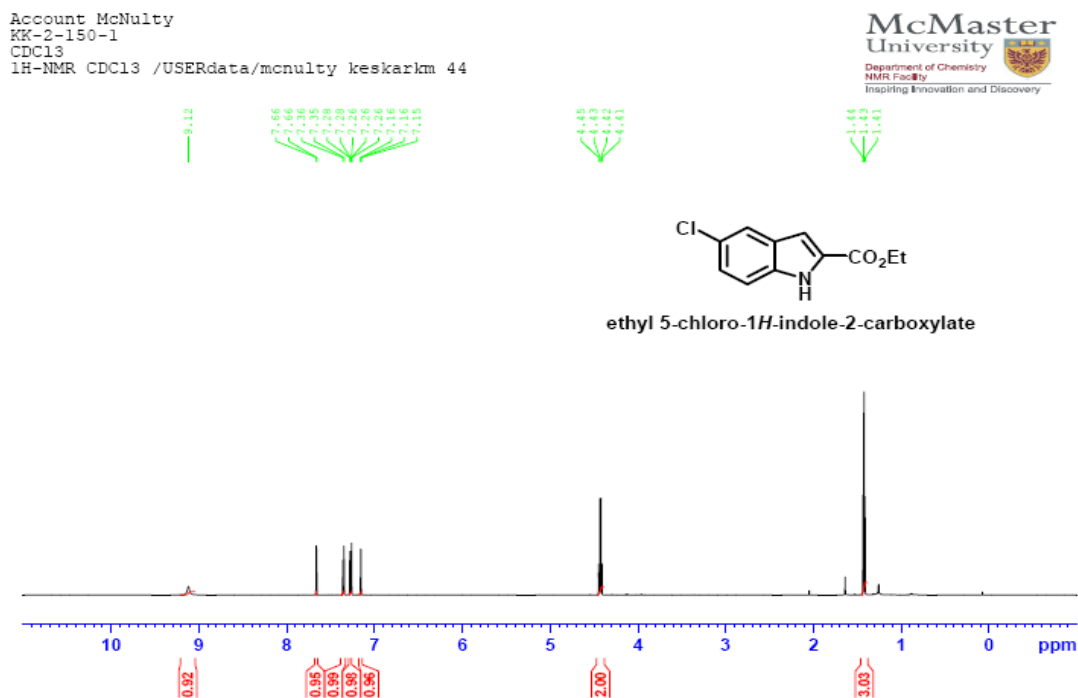


Ethyl 5-fluoro-1H-indole-2-carboxylate (Table 7-2, 7d):

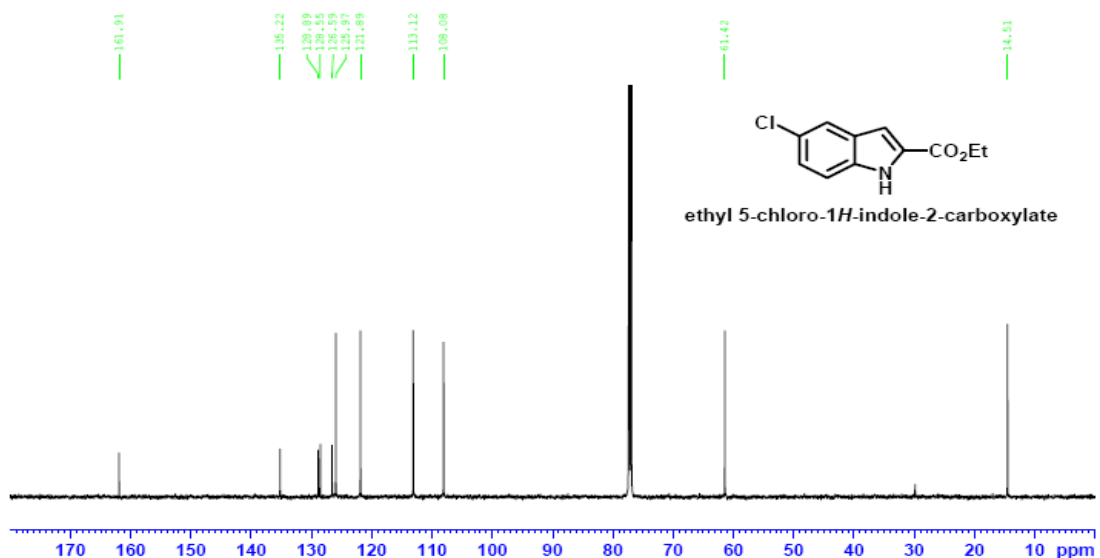




Ethyl 5-chloro-1H-indole-2-carboxylate (Table 7-2, 7e):

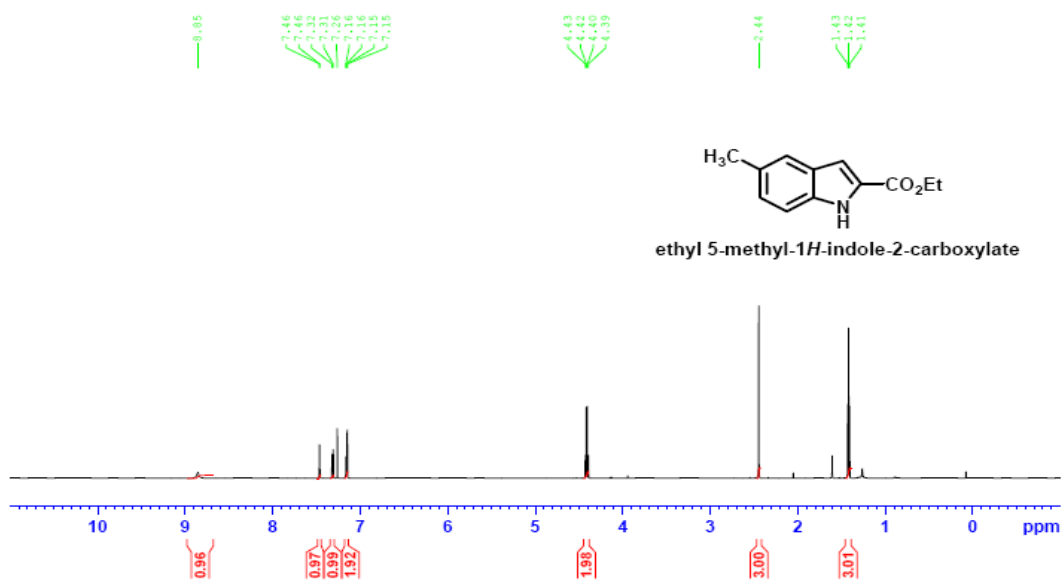


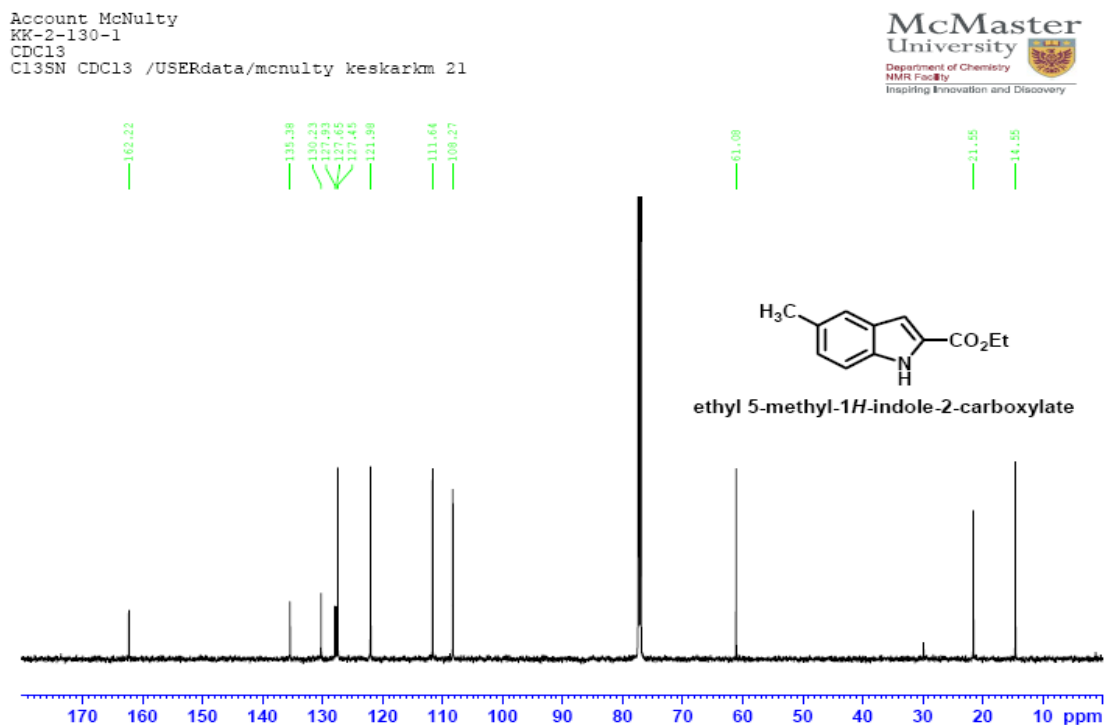
Account McNulty
KK-2-150-1
CDC13
C13SN CDC13 /USERdata/mcnulty keskarkm 44



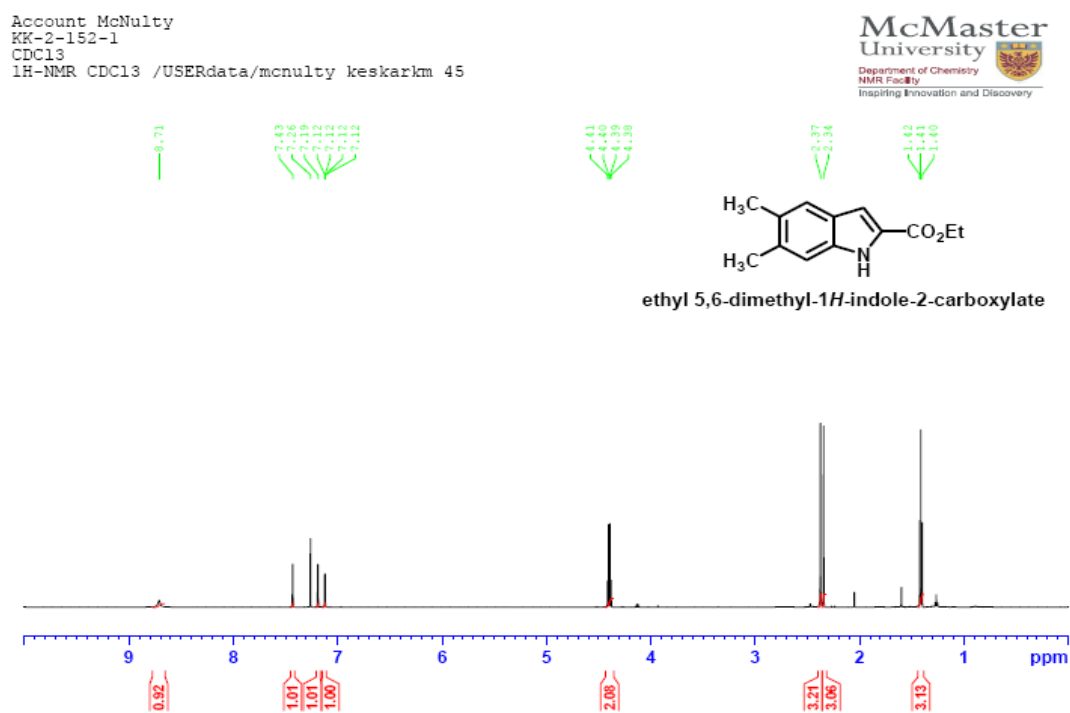
Ethyl 5-methyl-1H-indole-2-carboxylate (Table 7-2, 7f):

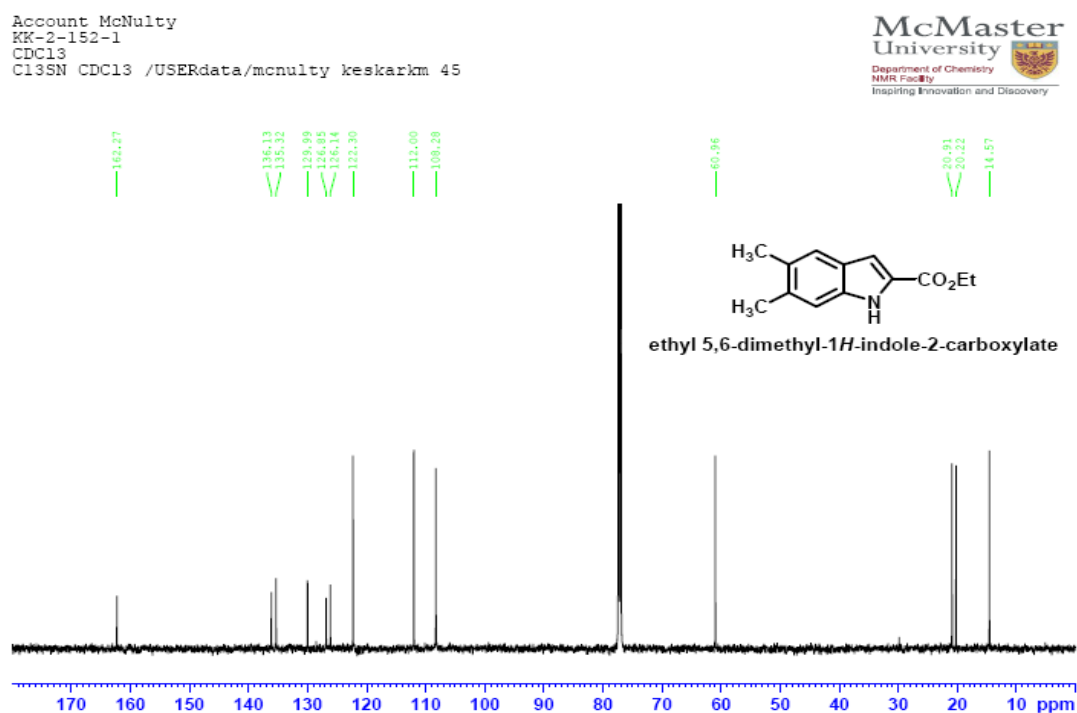
Account McNulty
KK-2-130-1
CDC13/10 March 2011
1H-NMR CDC13 /USERdata/mcnulty keskarkm 41



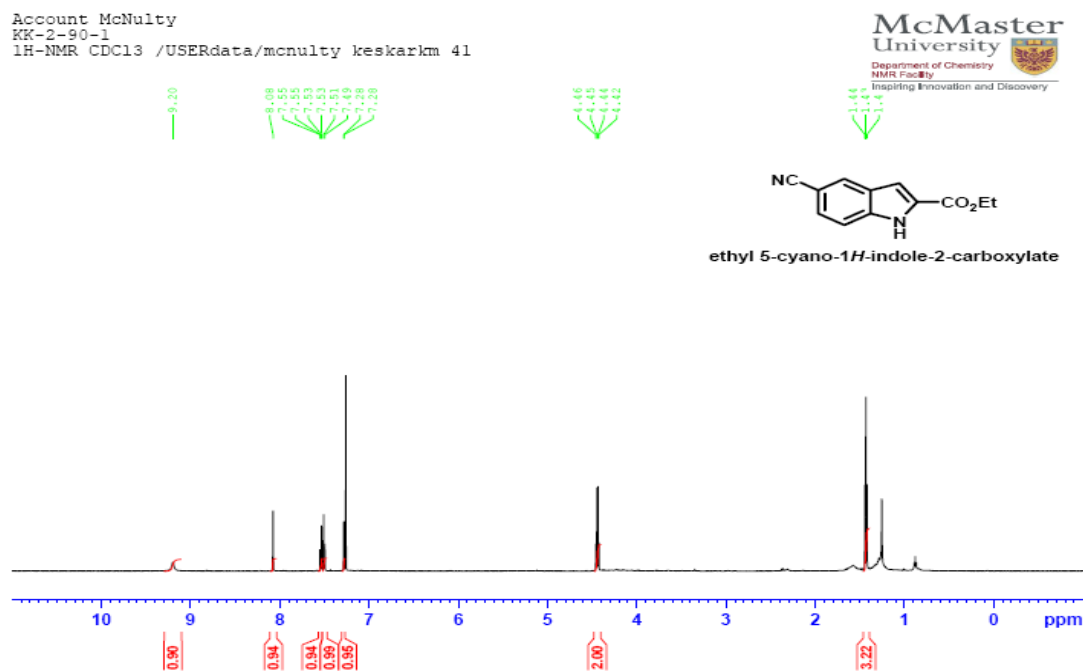


Ethyl 5,6-dimethyl-1H-indole-2-carboxylate (Table 7-2, 7g):





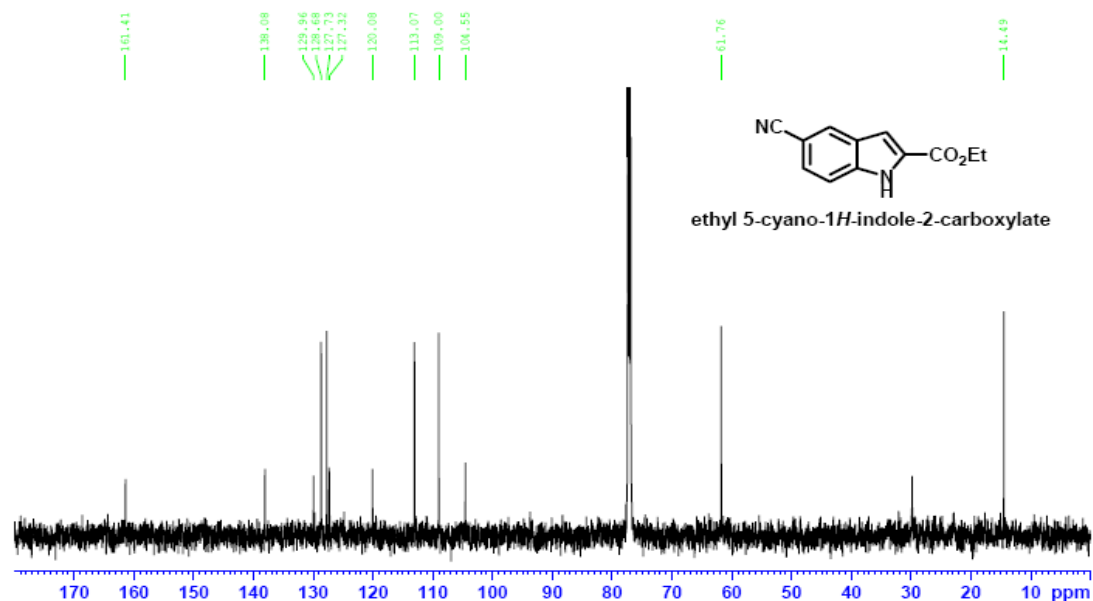
Ethyl 5-cyano-1H-indole-2-carboxylate (Table 7-2, 7h):



Account McNulty

KK-2-90-1

C13SN CDC13 /USERdata/mcnulty keskarkm 41



**Chapter VIII: Total synthesis of the cyanobacterial metabolite nostodione
A: discovery of its antiparasitic activity against *Toxoplasma gondii***

*Reproduced from Reference VII-(List of publications) with permission from the The Royal
Society of Chemistry*

8.1 Introduction

Cyanobacteria (blue-green algae) isolated from marine, freshwater and terrestrial environments have proven to be a prolific source of biologically active secondary metabolites with a wide range of therapeutic potential.¹ The indole-containing natural product nostodione A (**1**) (**Figure 8-1**) was first isolated from the terrestrial cyanobacterium *Nostoc commune* in 1994 and shown to inhibit mitotic spindle formation.² The same compound was subsequently isolated from the freshwater cyanobacteria *Scytonema hofmanni* and shown to possess proteasome inhibitory activity.³ Nostodione A exists as a thermodynamic mixture of the (*E*)- and (*Z*)-conformational isomers shown (**Figure 8-1**). The compound is believed to be biosynthesized from prenostodione,^{4a} an oxidative coupling product of 4-hydroxyphenylpyruvic acid from L-tyrosine and L-tryptophan.^{4b} Nostodione A belongs to a small family of alkaloids that have been isolated from cyanobacteria in recent years including scytonemin (**2**), a dimer of prenostodione (**Figure 8-1**).⁵ In addition to the anti-mitotic and proteosomal activities described above, these highly UV-absorbing molecules are believed to serve a protective function against solar radiation within the cyanobacterial colony and are of interest as potential sunblock ingredients. The chemical synthesis of isoprenostodione was recently reported,^{6a} while a single report of the synthesis of both nostodione A (**1**)^{6b} and the dimeric scytonemin (**2**)^{6c} have been reported by Mårtensson and co-workers. An enzymatic approach to the Scytonemin monomer has also recently been reported.^{6d}

We became interested in the synthesis and biological evaluation of nostodione A (**1**) for several reasons. Our research groups recently initiated a joint program

aimed at the discovery of novel small-molecules exhibiting biological activity against the parasite *Toxoplasma gondii*, the protozoan responsible for toxoplasmosis.⁷ From a structural viewpoint, nostodione A resembles several known oxidized, condensed indole alkaloids such as indirubin, tryptanthrin⁸ and the pyrroloiminoquinones,⁹ examples of which display activity to *T. gondii*, **Figure 8-1**.

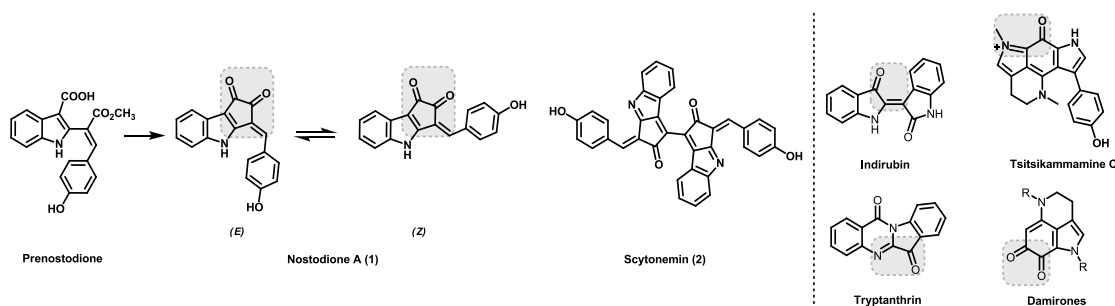


Figure 8-1. Structure of the cyanobacterial secondary metabolite nostodione A (1) and related biosynthetic alkaloids.

8.2 Results and Discussion

Synthetic access to nostodione A would allow for a wider screening of its biological activity allowing a complete assessment of its therapeutic potential. In this paper we report a diversity-oriented approach towards the synthesis of nostodione A itself, as well as the synthesis of a mini-library of analogues and the discovery of cytotoxicity and anti-invasion activity of these derivatives to *T. gondii* infection.

Our retrosynthetic analysis of nostodione A (1) is outlined in **Figure 8-2**. In order to conduct structure-activity evaluation of analogues of (1) we considered a Horner-Wadsworth-Emmons (HWE)-type disconnection of the 4-hydroxystyryl unit in (1) leading to the β -ketophosphonate (3) and 4-hydroxybenzaldehyde, or protected derivative thereof. In the synthetic direction, β -ketophosphonate (3) was envisioned as an ideal nexus that would allow construction of an

assemblage of nostodione A analogues via a diversity-oriented HWE reaction (with ArCHO or RCHO) in the last step.

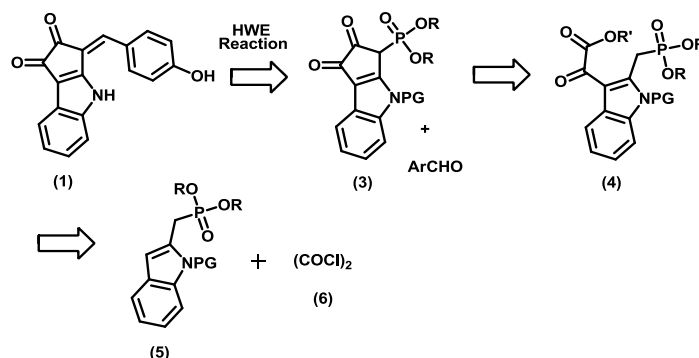
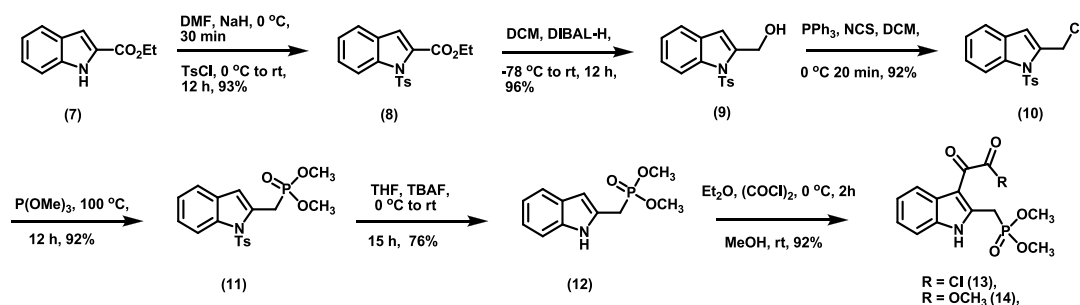


Figure 8-2. Retrosynthetic analysis of nostodione A (1).

It was envisioned that the β -ketophosphonate (3) could be accessed through an intramolecular α -phosphonate acylation-type reaction¹⁰ from the 3-oxalylindole derivative (4), in turn, the product of acylation of the indole (5) with oxalyl chloride. Compound (5) was projected to be the product of a Michaelis-Arbuzov reaction of a 2-halomethylindole derivative, ultimately derived from commercially available indole-2-carboxylic acid derivatives.

The synthesis thus began with ethyl-indole-2-carboxylate (7), as shown in **Scheme 8-1**. In exploratory studies, we determined that formation of the necessary 2-halomethylindole derivatives was complicated in the presence of the free indole NH. Protection as the *N*-tosyl derivative (8) followed by reduction of the ester led efficiently to the desired alcohol (9). Conversion to the chloromethyl derivative (10) now occurred smoothly and this reactive intermediate underwent clean Michaelis-Arbuzov alkylation with trimethylphosphite yielding phosphonate (11). Attempts at C3-acylation on intermediate (11) with oxalyl chloride met with failure, which we attributed to *N*-tosyl-induced electronic deactivation at this position.



Scheme 8-1. Synthesis of the 3-oxalyl-indole-2-phosphonomethyl intermediates (13) and (14).

Removal of the *N*-tosyl substituent was accomplished under mild conditions using TBAF.¹¹ Direct acylation on the deprotected phosphonate (12) now occurred smoothly with oxalyl chloride in diethyl ether yielding initially the monoacyl chloride derivative (13). Attempts at intramolecular acylation initially proved extremely challenging and a summary of select examples en-route to optimization of this reaction is collected in **Table 8-1**.

Table 8-1. Optimization of the intramolecular phosphonate acylation.

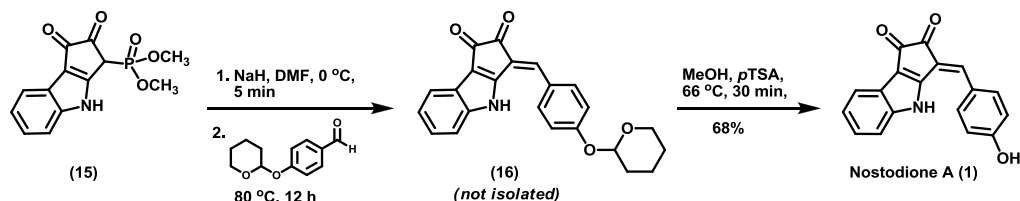
The reaction scheme shows the intramolecular acylation of phosphonate intermediates (13) and (14) to form product (15). The reaction conditions are Base (2.5 equiv), Solvent, and Temperature. The products are (15) where R = Cl (13) and R = OCH₃ (14).

Entry	R/R'	Base	Solvent	Temperature (°C)	Isolated yield (%)
1	-Cl/H	LHMDS	THF	rt	not clean
2	-Cl/H	NaH	THF	rt	not clean
3	-OCH ₃ /H	LHMDS	THF	reflux	38
4	-OCH ₃ /H	LDA	THF	reflux	not clean
5	-OCH ₃ /H	KO ^t Bu	THF	reflux	22
6	-OCH ₃ /H	NaH	THF	reflux	55-60
7	-OCH ₃ /H	NaH	PhMe	reflux	NR
8	-OCH ₃ /H	NaH	THF+HMPA(1:1)	rt/reflux	NR
9	-OCH ₃ /H	NaH	THF+DMF(1:1)	rt/reflux	trace
10	-OCH ₃ /PMB	NaH/LHMDS /KO ^t Bu	THF/DMF	rt/ reflux	NR

Attempted intramolecular acylation on the immediate acid chloride (**13**) proved futile with a number of bases and solvents (**Table 8-1**, entries 1 and 2). The acid chloride was converted to the ester (**14**) in order to probe the intramolecular ester acylation according to an intermolecular precedent.¹⁰ Initial efforts of acylation in refluxing tetrahydrofuran (THF) with lithium hexamethyldisilylamide (LHMDS) as base gave moderate yield (38%) of the β -ketophosphonate (**15**), (**Table 8-1**, entry 3). Surprisingly reaction with other bases such as LDA or KO^tBu yielded little or no conversion to the cyclic phosphonate. However, to our delight, yields improved up to 60% when sodium hydride (NaH) was used as base in refluxing THF (**Table 8-1**, entries 4-9). Increasing the reaction temperature further in a sealed tube or switching to other solvents (e.g. toluene, NaH 0% conversion) or addition of polar aprotic solvent such as DMF or HMPA did not benefit the cyclization. Conversion of (**14**) to the PMB protected derivative and attempted intramolecular cyclization (**Table 8-1**, entry 10) under a variety of conditions also did not proceed, indicating that protecting groups on nitrogen are not tolerated. It is unclear why the combination of NaH/THF works best in this case, base solubility does not appear to be an issue however it appears that formation of the dianion is very important to achieve the desired intramolecular cyclization. Under these conditions (**Table 8-1**, entry 6) a reasonable isolated yield (55-60%) of the crucial cyclic β -ketophosphonate (**15**) could be obtained reproducibly from this reaction.

With β -ketophosphonate (**15**) now on hand, we began initial studies on the critical HWE reaction as summarized in **Scheme 8-2**. Protection of 4-hydroxybenzaldehyde with dihydropyran gave the unstable 4-tetrahydropyranyl ether. This was reacted with the dianion generated from (**15**) and the HWE reaction proceeded smoothly to give the THP-protected derivative of nostodione A (**16**) which was immediately deprotected, completing the synthesis of nostodione A in 68% isolated yield from (**15**). Synthetic nostodione

A was isolated as a yellow pigment with m.p. 285 °C (decomp), lit. mp 280 °C (decomp)² and spectroscopic data in accord with the literature values including an (*E*):(*Z*) ratio of 4:1 (acetone) for both our synthetic material and the natural product.^{2,6c} This synthesis constitutes the second reported total synthesis of nostodione A and was achieved in only 8 chemical steps and 21.6% overall yield from commercial ethyl indole-2-carboxylate (**7**).



Scheme 8-2. Completion of the synthesis of nostodione A (**1**) employing the HWE strategy.

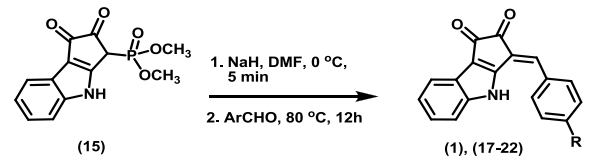
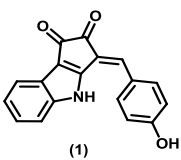
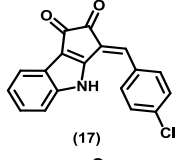
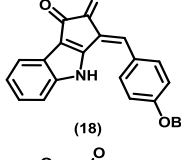
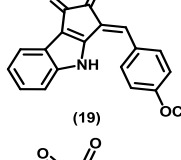
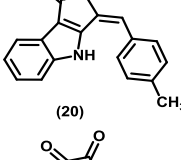
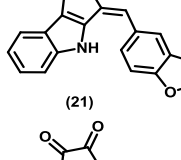
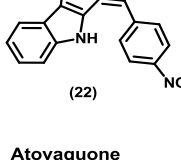
We were now positioned to exploit the diversity-oriented HWE reaction from (**15**) as described. The HWE reaction proved successful with a variety of substituted benzaldehydes and allowed for the assembly of the mini-library of aryl ring structural analogues (**17**) to (**22**) summarized in **Table 8-2**. NMR analysis of the series of analogues uncovered a prominent substituent effect on the (*E*):(*Z*) ratio of these nostodione A derivatives. The (*E*)-isomer content was observed to be predominant in all cases, including those containing either electron donating or withdrawing groups (ratio of (*E*)-isomer in DMSO-*d*₆: 4-CH₃ (88%), 3,4-methylenedioxy (95%), 4-NO₂ (>98%), 4-OBn (94%), 4-OCH₃ (94%), 4-Cl (83%)). These results indicate that the free phenolic group in (**1**) may play a unique role in stabilizing the (*Z*)-isomer of nostodione A.

With nostodione A itself and the mini-panel of synthetic analogues available, we now assessed their antiprotozoal activity.^{1e} We employed a published colorimetric assay¹² to assess both in vitro cell cytotoxicity and anti-Toxoplasma capabilities of the nostodione mini-library. Briefly, diluted compounds were

added to human foreskin fibroblast (HFF; ATCC) cells growing in 96-well tissue culture plates. Beginning at 320 μM , the compounds were serially diluted across the plate by dilutions of 0.5 log₁₀. *T. gondii* RH-2F tachyzoites that constitutively express β -galactosidase (β -gal) were then added to most wells, leaving 2 wells in each column parasite-free for cytotoxicity testing. The substrate for β -gal, chlorophenol red- β -D-galactopyranoside (CPRG), was added to the *Toxoplasma* wells after 4 days of incubation at 37 °C/ 5% CO₂. Further incubation for 20h was followed by addition of the cell viability reagent, CellTiter 96 Aqueous One Solution Reagent (Promega Corp., WI) to the uninfected cytotoxicity wells. Color reactions in all wells were then read in a Vmax microplate reader (Molecular Devices, CA) after 3h of incubation. The amount of absorbance (570-650 nm) in wells containing drug, *Toxoplasma*, and CPRG was compared to that in parasite control wells. In the cytotoxicity wells, the bio-reduction of the cell viability reagent by viable cells into a soluble, colored formazan product was captured by reading the plates at 490-650 nm. The median and 90% inhibitory concentrations (IC₅₀, IC₉₀ respectively) and the median cytotoxic dose (TD₅₀) were calculated using CalcuSyn software (Biosoft, Cambridge, U.K.). For each compound, a therapeutic index (TI) was calculated with the formula $\text{TI} = \text{TD}_{50} / \text{IC}_{50}$. This number reflects the specific activity of a compound against *Toxoplasma*. Atovaquone, a broad spectrum anti-parasitic drug used therapeutically to treat many parasitic protozoan diseases including malaria, was used as the assay positive control. The overall biological activity data obtained is summarized in **Table 8-2**.

Nostodione A (**1**) proved to have quite low specific activity against *T. gondii* displaying an IC₅₀ of 85 μM and a TI of 1. Of the structural analogues of nostodione A, the lowest IC₅₀ values were displayed by the mono-substituted 4-alkoxy-substituted derivatives alone (**Table 8-2**, entries 3 and 4). The 4-benzyloxy- and 4-methoxy- derivatives exhibited IC₅₀ values of 4.6 μM and of 5.6 μM respectively.

Table 8-2. Assembly of nostodione A mini-panel (1) and (17)-(22) via the HWE strategy and anti-toxoplasmosis biological activity.

<div style="text-align: center;">  <p>(15) (1), (17-22)</p> </div>						
Entry	Nostodione A and analogues	Isolated yield (%)	IC ₅₀ (μM)	IC ₉₀ (μM)	TD ₅₀ (μM)	TI
1	 (1)	68	85	183	108	1
2	 (17)	82	21.6	114	172	8
3	 (18)	68	4.6	30	≥320	70
4	 (19)	72	5.6	44	25	5
5	 (20)	55	27.8	103	161	6
6	 (21)	42	19	78	23	1
7	 (22)	44	50.6	166	219	4
8	Atovaquone		0.2	0.6	21	111

In contrast, the 4-methyl- and 3,4-methylenedioxy derivatives were less potent, as were those containing electron withdrawing groups 4-chloro- and 4-nitro (**Table 8-2**, entries 2, 5, 6 and 7). More importantly, the 4-benzyloxy-containing derivative (**18**) demonstrated low cytotoxicity with a therapeutic index of >70, significantly less cytotoxic than the methoxy-containing analog (**19**). The results also show clearly that the substituent effect on biological activity is not a simple electronic effect, demonstrating no discernible quantitative structure-activity correlation. The results point to the 4-benzyloxy substituent as a key fragment on the anti-toxoplasmosis pharmacophore of nostodione A that is amenable to further optimization of both potency and selectivity.

A preliminary evaluation of direct effects of the compounds on extracellular tachyzoites was performed. The commonly used red/green invasion assay^{12b} allowed us to evaluate nostodione A and the mini-panel of structural analogues for inhibition of host cell invasion by the tachyzoites using fluorescent labels to distinguish tachyzoites that had actively penetrated (green bars) the cells from those that were attached but unable to enter (red bars) the host cells. A decrease in the number of penetrated parasites (**Figure 8-3**, green bars) relative to the vehicle [DMSO (VHL)] is indicative of invasion inhibition. As shown in **Figure 8-3** all of the compounds tested (20 μ M) significantly inhibited tachyzoite invasion of the host cell. Further, in this assay, an effect on attachment is defined as a difference in the total numbers of both penetrated and attached parasites relative to same of the vehicle.^{12b} With the exception of the 4-methyl derivative (**20**), all of the test compounds significantly inhibited tachyzoite attachment. The inhibition of attachment and the inhibition of penetration are not necessarily interconnected. It is possible to inhibit invasion while not inhibiting attachment as is displayed by the 4-methyl derivative. Such activity has been reported for inhibitors of actin polymerization such as cytochalasin D.^{12b} Compounds (20 μ M) were tested for activity directly on extracellular tachyzoites using an established method.^{12b} Green bars represent

invaded/intracellular parasites; red bars depict attached/extracellular parasites. Data are mean values \pm SEM of three independent experiments. *Tachyzoite invasion was significantly lower ($P \leq 0.05$, two-tailed Student's *t*-test) than the VHL control. ** Tachyzoite attachment to host cell was significantly decreased ($P \leq 0.05$, two-tailed Student's *t*-test) relative to VHL control.

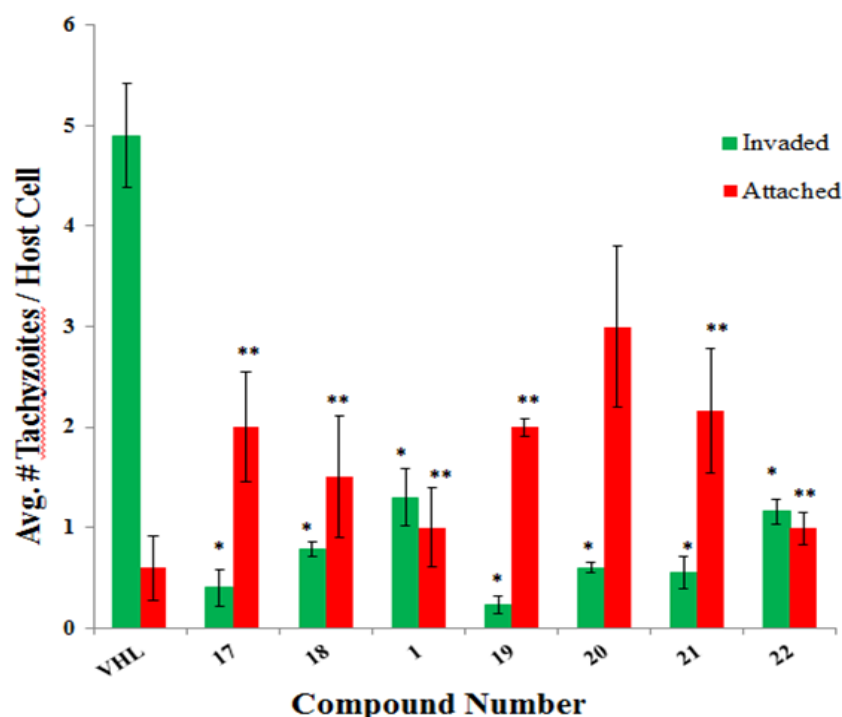


Figure 8-3. Quantification of invasion inhibition of nostodione A and mini panel using red/green assay.

8.3 Conclusion

In conclusion, we report the total synthesis of the cyanobacterial natural product nostodione A in 8 chemical steps and 21.6% overall yield from commercially available ethyl indole-2-carboxylate. The synthetic strategy employed a diversity-oriented late stage Horner-Wadsworth-Emmons olefination allowing for the assembly of a mini-panel of structural analogues. The antiparasitic

biological activity of nostodione A and analogues is reported for the first time. The late stage HWE synthetic paradigm permitted the discovery of a valuable lead anti-toxoplasmosis pharmacophore incorporating a 4-benzyloxy substituent on the nostodione A phenolic substituent. Further elaboration on this lead compound toward the development of a novel potent and selective anti-toxoplasmosis agent and investigation of related antiprotozoal activity of nostodione A and analogues from functionalized indole-2-carboxylates¹³ is currently in progress. These interesting preliminary results also indicate diversity in the structure-activity relationships (SAR) of the compounds relevant to the inhibition of host cell attachment and invasion by *T. gondii* tachyzoites. Further biological studies to delineate the nature of such SARs in more detail are in progress.

8.4 References

1. M. Burja, B. Banaigs, E. Abou-Mansour, J. G. Burgess and P. C. Wright, *Tetrahedron*, **2001**, 57, 9347.
2. A. Kobayashi, S. Kajiyama, K. Inawaka, H. Kanzaki and K. Kawazu, *Z. Naturforsch*, **1994**, 49c, 464.
3. S. S. Hee, G. Chlipala and J. Orjala, *J. Microbiol. Biotechnol.*, **2008**, 18, 1655.
4. (a) A. Ploutno and S. Carmeli, *J. Nat. Prod.*, **2001**, 64, 544. (b) E. P. Balskus and C. T. Walsh, *J. Am. Chem. Soc.*, **2009**, 131, 14648.
5. P. J. Proteau, W. H. Gerwick, F. Garcia-Pichel and R. Castenholz, *Experientia*, **1993**, 49, 825.
6. (a) J. C. Badenock, J. J. Jordan and G. W. Gribble, *Tetrahedron Lett.*, **2013**, 54, 2759. (b) A. Ekebergh, A. Börje and J. Mårtensson, *Org. Lett.*, **2012**, 14, 6274. (c) A. Ekebergh, I. Karlsson, R. Mete, Y. Pan, A. Börje and J.

- Mårtensson. *Org. Lett.*, **2011**, 13, 4458. (d) S. Malla and M. O. A. Sommer, *Green Chem.*, **2014**, 16, 3255.
7. J. McNulty, R. Vemula, C. Bordón, R. Yolken and L. Jones-Brando, *Org. & Biomolec. Chem.*, **2014**, 12, 255.
8. B. Krivogorsky, P. Grundt, R. Yolken and L. Jones-Brando, *Antimicrob. Agents & Chemother.*, **2008**, 52, 4466.
9. R. A. Davis, M. S. Buchanan, S. Duffy, V. M. Avery, S. A. Charman, W. N. Charman, K. L. White, D. M. Shackleford, M. D. Edstein, K. T. Andrews, D. Camp and R. J. Quinn, *J. Med. Chem.*, **2012**, 55, 5851.
10. (a) K. M. Maloney and J. Y. L. Chung, *J. Org. Chem.*, **2009**, 74, 7574. (b) T. Maegawa, K. Otake, K. Hirosawa, A. Goto and H. Fujioka, *Org. Lett.*, **2012**, 14, 4798. (c) A. Samarat, V. Fargeas, J. Villières, J. Lebreton and H. Amri, *Tetrahedron Lett.*, **2001**, 42, 1273.
11. (a) A. Yasuhara and T. Sakamoto, *Tetrahedron Lett.*, **1998**, 39, 595. (b) S. K. Jackson and M. A. Kerr, *J. Org. Chem.*, **2007**, 72, 1405. (c) S. Krishnan, J. T. Bagdanoff, D. C. Ebner, Y. K. Ramtohl, U. K. Tambar and B. M. Stoltz, *J. Am. Chem. Soc.*, **2008**, 130, 13745.
12. (a) L. Jones-Brando, E. F. Torrey and R. Yolken, *Schizophr. Res.*, **2003**, 62, 237. (b) C. P. Hencken, L. Jones-Brando, C. Bordón, R. Stohler, B. T. Mott, R. Yolken, G. H. Posner and L. E. Woodard, *J. Med. Chem.*, **2010**, 53, 3594.
13. J. McNulty and K. Keskar, *Eur. J. Org. Chem.*, **2011**, 6902.
14. J. McNulty and K. Keskar, *Eur. J. Org. Chem.*, **2014**, 1622.

8.5 Experimental Section

Dichloromethane (DCM) was distilled over calcium hydride. Toluene (PhMe), Tetrahydrofuran (THF) was distilled over sodium metal in the presence of benzophenone indicator. All other solvents including dimethylformamide (DMF) (>99%) were purchased as sure-seal bottles from Sigma Aldrich. ^1H and ^{13}C spectra were obtained on a 600 MHz Bruker NMR spectrometer. Chemical shifts are reported in units of δ (ppm) and coupling constants (J) are expressed in Hz. Solvent residual peak from CDCl_3 (^1H = 7.26 ppm, ^{13}C = 77.16 ppm) and DMSO-d_6 (^1H = 2.50 ppm, ^{13}C = 39.52 ppm) were used as reference peaks for recording the chemical shifts. Mass spectra were run on a Micromass Quattro Ultima spectrometer fitted with a direct injection probe (DIP) with ionization energy set at 70 eV and HRMS (EI) were performed with a Micromass Q-TOF Ultima spectrometer. Thin layer chromatography (TLC) was run using Macherey-Nagel aluminum-backed plates. Melting points were obtained on an Electronic Research Associates Inc. melting point apparatus corrected against an external calibrant. SiliaFlash® P60 [Particle size 40-63 μm (230-400 mesh)] from Silicycle, Canada was used for all the silica gel column chromatography.

Ethyl 1-tosyl-1H-indole-2-carboxylate (Scheme 8-1, 8):

Into a flame-dried flask with a stirring bar was added ethyl indole-2-carboxylate (1.0 g, 1.0 equiv, 5.28 mmol). Dimethylformamide (8.0 mL) was added to the flask under inert atmosphere. Sodium hydride (0.32 g, 1.5 equiv, 60% dispersion in mineral oil) was added to the flask in portions while maintaining the temperature at 0 °C. The reaction mixture was stirred for 30 min at 0 °C. 4-Toluenesulfonyl chloride (2.01 g, 2.0 equiv, 10.5 mol) was added to the flask slowly in portions. The reaction mixture was stirred for 30 min at 0 °C and then overnight (12 h) at room temperature. Reaction mixture was diluted with excess water and extracted with ethyl acetate (3 X 100 mL). The organic layer was washed with brine and dried over sodium sulfate to give crude product which

was purified using silica-gel flash chromatography (10-15% of EtOAc : hexanes, gradient elution) to yield Ethyl 1-tosyl-1H-indole-2-carboxylate. Yield = 93%. ^1H NMR (600 MHz, CDCl_3) δ 8.13 (d, J = 8.5 Hz, 1H), 7.95 (d, J = 8.4 Hz, 2H), 7.58 (d, J = 7.8 Hz, 1H), 7.45 (ddd, J = 8.4, 7.3, 1.1 Hz, 1H), 7.32 – 7.25 (m, 3H), 7.17 (s, 1H), 4.44 (q, J = 7.1 Hz, 2H), 2.39 (s, 3H), 1.42 (t, J = 7.2 Hz, 3H). ^{13}C NMR (151 MHz, CDCl_3) δ 161.5, 145.0, 138.2, 135.8, 132.0, 129.6, 128.3, 127.5, 127.0, 124.1, 122.5, 116.6, 115.5, 62.0, 21.7, 14.2.

(1-tosyl-1H-indol-2-yl)methanol (Scheme 8-1, 9):

Into a flame-dried flask with a stirring bar was added Ethyl 1-tosyl-1H-indole-2-carboxylate (1.0 g, 1.0 equiv, 2.91 mmol). Dichloromethane (8.00 mL) was added to the flask under inert atmosphere. The reaction mixture was cooled to -78 °C whereupon; DIBAL (7.28 mL, 2.5 equiv, 1M solution in cyclohexane) was added drop wise to the flask. The reaction mixture was stirred at -78 °C for additional 2 h. The reaction mixture was then allowed to warm to room temperature and stirred overnight (12 h). The reaction mixture was diluted with diethyl ether and cooled to 0 °C. Slowly water (0.30 mL) was added to the reaction mixture followed by 15% aqueous sodium hydroxide (0.30 mL). Additional water (0.72 mL) was added and then allowed the reaction mixture to warm to room temperature and stir for 15 minutes. Anhydrous magnesium sulphate was added to the flask and further reaction mixture was stirred for 15 minutes. The reaction mixture was filtered and washed with dichloromethane to remove salts. The filtrate was concentrated to give crude product which was purified using silica-gel flash chromatography (15-30% of EtOAc : hexanes, gradient elution) to yield (1-tosyl-1H-indol-2-yl)methanol.¹³ Yield = 96%. ^1H NMR (600 MHz, CDCl_3) δ 8.05 (d, J = 8.4 Hz, 1H), 7.71 (d, J = 8.4 Hz, 2H), 7.48 (d, J = 7.7 Hz, 1H), 7.32 – 7.28 (m, 1H), 7.23 (t, J = 7.5 Hz, 1H), 7.20 (d, J = 8.3 Hz, 2H), 6.64 (s, 1H), 4.91 (s, 2H), 3.31 (brs, 1H), 2.33 (s, 3H). ^{13}C NMR (151 MHz, CDCl_3) δ 145.2, 140.3, 137.0, 135.6, 130.0, 129.2, 126.5, 125.0, 123.8, 121.2, 114.4, 111.2, 58.6, 21.6.

2-(chloromethyl)-1-tosyl-1H-indole (Scheme 8-1, 10):

Into a flame-dried flask with a stirring bar was added (1-tosyl-1H-indol-2-yl)methanol (1.0 g, 1.0 equiv, 3.31 mmol). Dichloromethane (8.00 mL) was added to the flask under inert atmosphere. The reaction mixture was cooled to 0 °C. Triphenylphosphine (1.74 g, 2.0 equiv, 6.63 mmol) was added to the flask. N-Chlorosuccinimide (0.755 g, 1.7 equiv, 5.64 mmol) was then added slowly to the flask at 0 °C. (*The reaction was monitored by using TLC*). The reaction mixture was stirred approximately for 20 min at 0 °C. Upon completion of reaction, the reaction mixture was diluted with water and extracted with ethyl acetate (3 X 100 mL). The organic layer was washed with brine and dried over sodium sulfate to give crude product which was purified using silica-gel flash chromatography (10-15% of EtOAc : hexanes, gradient elution) to yield 2-(chloromethyl)-1-tosyl-1H-indole. Yield = 92%. M.p.: 53-55 °C. ¹H NMR (600 MHz, CDCl₃) δ 8.00 (dd, *J* = 8.5, 0.7 Hz, 1H), 7.69 (d, *J* = 8.4 Hz, 2H), 7.40 (d, *J* = 7.8 Hz, 1H), 7.24 (ddd, *J* = 8.5, 7.3, 1.2 Hz, 1H), 7.18 – 7.14 (m, 1H), 7.12 (d, *J* = 8.1 Hz, 2H), 6.71 (d, *J* = 0.5 Hz, 1H), 4.99 (s, 2H), 2.25 (s, 3H). ¹³C NMR (151 MHz, CDCl₃) δ 145.2, 137.3, 136.4, 135.7, 129.9, 128.8, 126.9, 125.5, 123.9, 121.3, 114.8, 113.1, 39.0, 21.6. HRMS: calcd. For C₁₆H₁₄ClNO₂S [M]⁺ 319.0430; found 319.0434.

Dimethyl (1-tosyl-1H-indol-2-yl)methylphosphonate (Scheme 8-1, 11):

Into a 10-20 mL Biotage microwave vial with a stirring bar was added 2-(chloromethyl)-1-tosyl-1H-indole (1.0 g, 1.0 equiv, 3.12 mmol). Trimethyl phosphite (1.94 mL, 5 equiv, 15.6 mmol) was added to the vial. The reaction mixture was sealed and heated to 100 °C overnight (12h). The reaction mixture was diluted with water and extracted with ethyl acetate (3 X 100 mL). The organic layer was washed with brine and dried over sodium sulfate. The solvent was removed using rotary evaporator (*caution! Use proper ventilation.*) to give crude product which was purified using silica-gel flash chromatography (50-

90% of EtOAc : hexanes, gradient elution) to yield dimethyl (1-tosyl-1H-indol-2-yl)methylphosphonate. Yield = 92%. ^1H NMR (600 MHz, CDCl_3) δ 8.10 (d, J = 8.4 Hz, 1H), 7.62 (d, J = 8.4 Hz, 2H), 7.43 (d, J = 7.7 Hz, 1H), 7.27 (t, J = 7.7 Hz, 1H), 7.23 – 7.19 (m, 1H), 7.17 (d, J = 8.1 Hz, 2H), 6.81 (d, J = 3.5 Hz, 1H), 3.81 – 3.76 (m, 2H), 3.77 (s, 3H), 3.75 (s, 3H), 2.31 (s, 3H). ^{13}C NMR (151 MHz, CDCl_3) δ 145.1, 137.1, 135.6, 130.8 (d, J = 5.7 Hz), 129.9, 129.6, 126.5, 124.6, 123.9, 120.7, 115.1, 112.7 (d, J = 6.8 Hz), 53.2, 53.2, 25.4 (d, J = 142.8 Hz), 21.6. ^{31}P NMR (243 MHz, CDCl_3) δ 26.50. HRMS: calcd. For $\text{C}_{18}\text{H}_{20}\text{NO}_5\text{PS}$ $[\text{M}]^+$ 393.0795; found 393.0800.

Dimethyl (1H-indol-2-yl)methylphosphonate (Scheme 8-1, 12):

Into a flame-dried flask with a stirring bar was added dimethyl (1-tosyl-1H-indol-2-yl)methylphosphonate (0.200 g, 1.0 equiv, 0.50 mmol). THF (5.0 mL) was added to the flask under inert atmosphere. The reaction mixture was cooled to 0 °C. Tetra-*n*-butylammonium fluoride (4.06 mL, 8.0 equiv, 4.06 mmol, 1M solution in THF) was added drop wise to the flask. The reaction mixture was then allowed to warm to room temperature and stirred overnight (15 h). The reaction mixture was diluted with excess water and extracted with ethyl acetate (3 X 50 mL). The organic layer was washed with brine and dried over sodium sulfate and evaporated using rotary evaporator to give crude product which was purified using silica-gel flash chromatography (0-3% of MeOH : DCM, gradient elution) to yield dimethyl (1H-indol-2-yl)methylphosphonate. Yield = 76%. M.P.: 112-114 °C. ^1H NMR (600 MHz, CDCl_3) δ 8.97 (s, 1H), 7.54 (d, J = 7.8 Hz, 1H), 7.34 (dd, J = 8.1, 0.6 Hz, 1H), 7.15 (t, J = 7.6 Hz, 1H), 7.10 – 7.06 (m, 1H), 6.36 (s, 1H), 3.72 (s, 3H), 3.70 (s, 3H), 3.37 (d, J = 20.9 Hz, 2H). ^{13}C NMR (151 MHz, CDCl_3) δ 136.5, 128.4, 128.0 (d, J = 10.5 Hz), 121.9, 120.1, 119.9, 111.0, 102.6 (d, J = 10.7 Hz), 53.3, 53.3, 25.6 (d, J = 140.6 Hz). ^{31}P NMR (243 MHz, CDCl_3) δ 27.24. HRMS: calcd. For $\text{C}_{11}\text{H}_{14}\text{NO}_3\text{P}$ $[\text{M}]^+$ 239.0714; found 239.0711.

**Methyl-2-(2-((dimethoxyphosphoryl)methyl)-1H-indol-3-yl)-2-oxoacetate
(Scheme 8-1, 14):**

Into a flame-dried flask with a stirring bar was added dimethyl (1H-indol-2-yl)methylphosphonate (0.053 g, 1.0 equiv, 0.22 mmol). Freshly distilled diethyl ether (20.0 mL) was added to the flask under inert atmosphere. The reaction mixture was sonicated for 5 min and then cooled to 0 °C. Oxalyl chloride (0.047 mL, 2.5 equiv, 0.55 mmol) was added drop wise to the flask. The reaction mixture was stirred at 0 °C for additional 2.0 h. Methanol (excess) was added to the flask and then the reaction mixture was then allowed to warm to room temperature and stirred for additional 2.0 h. Diethyl ether was removed under reduced pressure and the crude reaction mixture was purified using silica-gel flash chromatography (0-4% of MeOH : DCM, gradient elution) to yield methyl 2-(2-((dimethoxyphosphoryl)-methyl)-1H-indol-3-yl)-2-oxoacetate. Yield = 92%. ¹H NMR (600 MHz, CDCl₃) δ 10.82 (s, 1H), 7.67 (d, *J* = 8.0 Hz, 1H), 7.24 – 7.22 (m, 1H), 7.21 – 7.19 (m, 1H), 7.18 – 7.14 (m, 1H), 4.02 (s, 3H), 3.99 (d, *J* = 21.7 Hz, 2H), 3.79 (s, 3H), 3.77 (s, 3H). ¹³C NMR (151 MHz, CDCl₃) δ 181.9, 166.1, 139.6 (d, *J* = 9.6 Hz), 135.5, 125.8, 123.8, 123.0, 119.6, 112.0, 110.3, 53.6, 53.6, 52.8, 24.4 (d, *J* = 136.8 Hz). ³¹P NMR (243 MHz, CDCl₃) δ 26.14. HRMS: calcd. For C₁₄H₁₆NO₆P [M]⁺ 325.0715; found 325.0711.

**Dimethyl 1,2-dioxo-1,2,3,4-tetrahydrocyclopenta[b]indol-3-ylphosphonate
(Table 8-1, 15):**

Into a flame-dried two necked round bottom flask with a stirring bar and a reflux condenser was added methyl 2-(2-((dimethoxyphosphoryl)methyl)-1H-indol-3-yl)-2-oxoacetate (0.105 g, 1.0 equiv, 0.32 mmol). Freshly distilled THF (40.0 mL) was added to the flask under inert atmosphere. The reaction mixture was cooled to 0 °C. Sodium hydride (0.031 g, 2.5 equiv, 0.80 mmol, 60% dispersion in mineral oil) was added to the flask. The reaction mixture was heated at reflux approximately 12 h (overnight, check TLC) in oil bath. During this time the

solution develops an intense red color. Excess THF was distilled off under reduced pressure and the crude reaction mixture was purified using silica-gel flash chromatography [2-15% of MeOH: DCM, gradient elution, slow column] to yield dimethyl 1,2-dioxo-1,2,3,4-tetrahydrocyclopenta[b]indol-3-ylphosphonate. Yield = 55-60%. ^1H NMR (600 MHz, DMSO) δ 12.98 (s, 1H), 7.84 (d, J = 7.7 Hz, 1H), 7.64 (d, J = 8.1 Hz, 1H), 7.42 (t, J = 7.6 Hz, 1H), 7.34 (t, J = 7.3 Hz, 1H), 5.01 (d, J = 26.4 Hz, 1H), 3.79 (d, J = 11.2 Hz, 3H), 3.70 (d, J = 11.1 Hz, 3H). ^{13}C NMR (151 MHz, DMSO) δ 194.7, 175.4, 158.5 (d, J = 9.0 Hz), 140.0, 125.6, 123.6, 123.0 (d, J = 5.6 Hz), 120.9, 120.6, 113.7, 53.7 (d, J = 6.1 Hz), 53.5 (d, J = 6.5 Hz), 43.9 (d, J = 136.6 Hz). ^{31}P NMR (243 MHz, DMSO) δ 17.00. HRMS (ES): calcd. For $\text{C}_{13}\text{H}_{13}\text{NO}_5\text{P}$ $[\text{M}]^+$ 294.0525; found 294.0531. [Very slow column performed; otherwise product (**15**) often contaminates with the starting material (**14**) which can be determined by ^{31}P spectroscopy (ranging from 8-15%). In the event of such contamination, yield correction was applied based upon ^{31}P spectroscopy.]

Nostodione A (Scheme 8-2, 1):

Into a flame-dried two necked round bottom flask with a stirring bar and a reflux condenser was added dimethyl 1,2-dioxo-1,2,3,4-tetrahydrocyclopenta[b]indol-3-ylphosphonate (0.034 g, 1.0 equiv, 0.11 mmol). DMF (3.5 mL) was added to the flask under inert atmosphere. The reaction mixture was cooled to 0 °C. Sodium hydride (0.012 g, 2.5 equiv, 0.29 mmol, 60% dispersion in mineral oil) was added to the flask. The reaction mixture was stirred for 5 min at 0 °C. 4-(tetrahydro-2H-pyran-2-yloxy)benzaldehyde (0.048 g, 2 equiv, 0.23 mmol) was added to the flask. The reaction mixture was then heated at reflux approximately 12 h (overnight) in oil bath. Excess DMF was distilled off under vacuum. The crude reaction mixture was dissolved in dichloromethane and passed through a short packed silica gel bed. Dichloromethane was evaporated under reduced pressure. The crude material was re-dissolved in dry MeOH (5.0 mL) and *p*-toluenesulphonic acid (10 mol%) was added to the flask. The

reaction mixture was refluxed for 30 minutes. Methanol was evaporated under reduced pressure and the crude reaction mixture was purified using silica-gel flash chromatography (0-5% of MeOH : DCM, gradient elution) to yield Nostodione A (1).^{6b} Yield = 68%. M.p.: decompose at >285°C. ¹H NMR (600 MHz, DMSO, *Major isomer*) δ 12.21 (s, 1H), 10.26 (br s, 1H), 7.83 (d, J = 7.8 Hz, 1H), 7.73 (d, J = 8.2 Hz, 2H), 7.66 (d, J = 8.1 Hz, 1H), 7.41 (ddd, J = 8.1, 7.2, 0.9), 7.33 (ddd, J = 8.1, 7.2, 0.9), 7.29 (s, 1H), 6.96 (d, J = 8.6 Hz, 2H). ¹³C NMR (151 MHz, DMSO) δ 193.60, 176.93, 159.85, 158.91, 141.25/140.77, 131.86, 128.71, 126.34, 124.59, 123.84, 123.80, 121.01, 120.74, 119.41/119.06, 116.42, 114.34.

¹H NMR (600 MHz, DMSO, *Minor isomer*) δ 12.93 (s, 1H), 10.35 (s, 1H), 8.08 (d, J = 8.7 Hz, 2H), 7.76 (d, J = 7.8 Hz, 1H), 7.57 (d, J = 8.1 Hz, 1H), 7.38 (ddd, J = 8.2, 7.2, 1.1), 7.29 (ddd, J = 8.0, 7.1, 0.8), 7.23 (s, 1H), 6.90 (d, J = 8.7 Hz, 2H). ¹³C NMR (151 MHz, DMSO) δ 192.53, 175.98, 164.56, 160.47, 141.25/140.77, 134.07, 131.91, 126.01, 125.25, 123.60, 121.65, 121.08, 119.66, 119.41/119.06, 115.70, 113.17. HRMS: calcd. For C₁₈H₁₁NO₃ [M]⁺ 289.0731; found 289.0739.

Representative procedure for synthesis of Nostodione A analogues:

Into a flame-dried two necked round bottom flask with a stirring bar and a reflux condenser was added dimethyl 1,2-dioxo-1,2,3,4-tetrahydrocyclopenta[b]indol-3-ylphosphonate (0.040 g, 1.0 equiv, 0.13 mmol). DMF (4.5 mL) was added to the flask under inert atmosphere. The reaction mixture was cooled to 0 °C. Sodium hydride (0.014 g, 2.5 equiv, 0.34 mmol) was added to the flask. The reaction mixture was stirred for 5 min at 0 °C. Corresponding aldehyde (2 equiv) was added to the flask. The reaction mixture was then heated at reflux approximately 12 h (overnight) in oil bath. Excess DMF was distilled off under vacuum. The crude reaction mixture was purified using silica-gel flash

chromatography (MeOH : DCM, gradient elution) to yield corresponding analogue.

3-(4-chlorobenzylidene)cyclopenta[b]indole-1,2(3H,4H)-dione (Table 8-2, entry 2, 17):

Isomeric ratio: 83:17. M.p.: decomposes at >290 °C. Major isomer: ¹H NMR (600 MHz, DMSO) δ 12.20 (s, 1H), 7.87 (d, *J* = 7.8 Hz, 1H), 7.82 (d, *J* = 8.3 Hz, 2H), 7.65 (d, *J* = 8.3 Hz, 1H), 7.63 (d, *J* = 8.5 Hz, 2H), 7.47 – 7.43 (m, 1H), 7.38 (s, 1H), 7.37-7.33 (m, 1H). Minor isomer: ¹H NMR (600 MHz, DMSO) δ 13.08 (s, 1H), 8.08 (d, *J* = 8.6 Hz, 2H), 7.82 (d, *J* = 8.3 Hz, 1H, overlap with major isomer), 7.63 (d, *J* = 8.5 Hz, 1H, overlap with major isomer), 7.57 (d, *J* = 8.6 Hz, 2H), 7.45 – 7.42 (m, 1H), 7.34-7.31 (m, 1H), 7.29 (s, 1H). ¹³C NMR (151 MHz, DMSO) δ 193.01(major), 192.28(minor), 176.90(major), 175.96(minor), 162.77, 157.33, 140.89, 140.86, 135.01, 134.53, 132.84(minor), 132.76, 132.42, 130.96(major), 129.52(major), 129.00(minor), 128.63(minor), 127.02(major), 126.71(minor), 126.37(major), 125.35, 124.06(major), 123.79(minor), 123.08, 121.43(minor), 121.34, 121.06(major), 120.70, 114.19(major), 113.40(minor). HRMS: calcd. For C₁₈H₁₀ClNO₂ [M]⁺ 307.0403; found 307.0400.

3-(4-(benzyloxy)benzylidene)cyclopenta[b]indole-1,2(3H,4H)-dione (Table 8-2, entry 3, 18):

Isomeric ratio: 94:06. M.p.: decomposes at > 247 °C. Major isomer: ¹H NMR (600 MHz, DMSO) δ 12.25 (s, 1H), 7.85 (d, *J* = 7.8 Hz, 1H), 7.79 (d, *J* = 8.6 Hz, 2H), 7.66 (d, *J* = 8.2 Hz, 1H), 7.50 (d, *J* = 7.3 Hz, 2H), 7.45 – 7.42 (m, 2H), 7.44-7.40 (m, 1H), 7.38 – 7.35 (m, 1H), 7.34 (s, 1H), 7.33-7.32 (m, 1H), 7.22 (d, *J* = 8.6 Hz, 2H), 5.23 (s, 2H). Major isomer: ¹³C NMR (151 MHz, DMSO) δ 193.24, 177.01, 160.09, 158.16, 140.73, 136.66, 131.47, 128.53, 128.14, 128.03, 127.81, 126.60, 126.32, 124.15, 123.98, 120.84, 120.80, 120.43, 115.80, 114.16, 69.51. HRMS: calcd. For C₂₅H₁₇NO₃ [M]⁺ 379.1203; found 379.1208.

3-(4-methoxybenzylidene)cyclopenta[b]indole-1,2(3H,4H)-dione (Table 8-2, entry 4, 19):

Isomeric ratio: 94:06. M.p.: decomposes with melt at 290-294 °C. Major isomer: ¹H NMR (600 MHz, DMSO) δ 12.22 (s, 1H), 7.84 (d, *J* = 7.8 Hz, 1H), 7.79 (d, *J* = 8.6 Hz, 2H), 7.66 (d, *J* = 8.2 Hz, 1H), 7.44 – 7.39 (m, 1H), 7.34-7.31 (m, 2H) *including the olefinic -H*, 7.14 (d, *J* = 8.8 Hz, 2H), 3.88 (s, 3H). ¹³C NMR (151 MHz, DMSO) δ 193.27, 176.99, 160.97, 158.24, 140.80, 131.44, 128.17, 126.56, 126.13, 124.12, 123.94, 120.81, 120.41, 115.01, 114.17, 55.47. HRMS: calcd. For C₁₉H₁₃NO₃ [M]⁺ 303.0907; found 303.0895.

3-(4-methylbenzylidene)cyclopenta[b]indole-1,2(3H,4H)-dione (Table 8-2, entry 5, 20):

Isomeric ratio: 88:12. M.p.: decomposes with melt > 308-310 °C. Major isomer: ¹H NMR (600 MHz, DMSO) δ 12.20 (s, 1H), 7.85 (d, *J* = 7.8 Hz, 1H), 7.70 (d, *J* = 8.0 Hz, 2H), 7.67 (d, *J* = 8.2 Hz, 1H), 7.45 – 7.41 (m, 1H), 7.39 (d, *J* = 7.9 Hz, 2H), 7.36 – 7.32 (m, 2H) *including the olefinic -H*, 3.33 (s, 1H). ¹³C NMR (151 MHz, DMSO) δ 193.19, 176.95, 157.78, 140.78, 140.21, 130.94, 130.10, 129.35, 128.07, 126.74, 124.69, 123.98, 121.63, 120.91, 120.73, 114.24, 21.18. HRMS: calcd. For C₁₉H₁₃NO₂ [M]⁺ 287.0946; found 287.0946.

3-(benzo[d][1,3]dioxol-5-ylmethylene)cyclopenta[b]indole-1,2(3H,4H)-dione (Table 8-2, entry 6, 21):

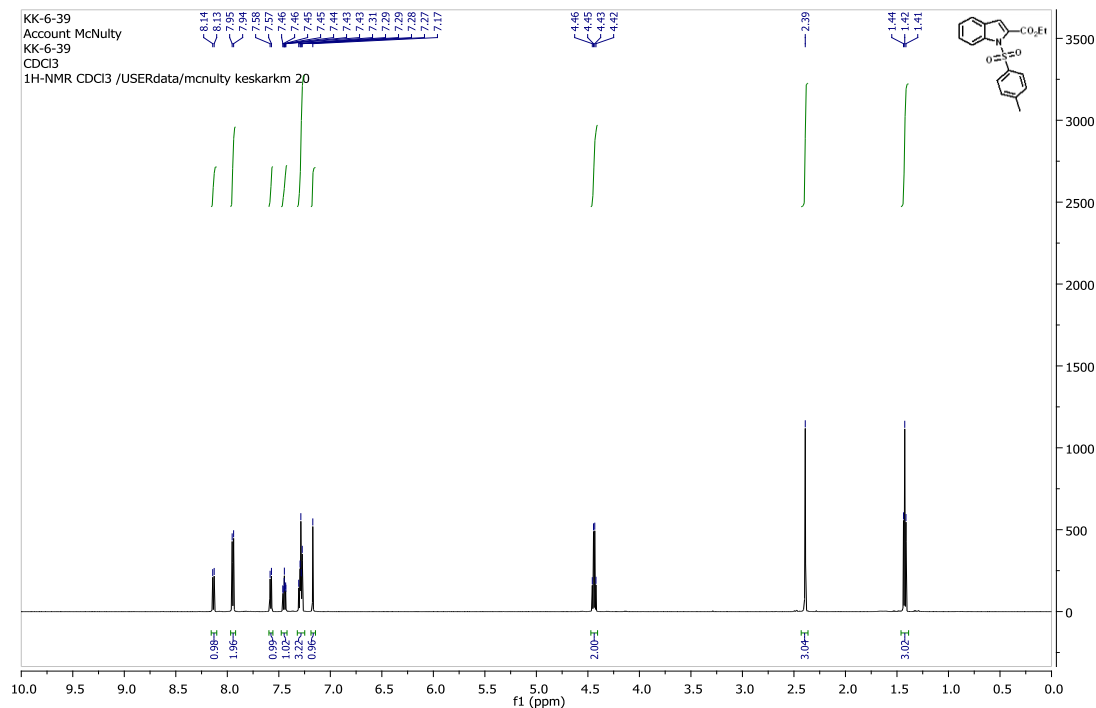
Isomeric ratio: 95:05. M.p.: decomposes with melt > 320 °C. Major isomer: ¹H NMR (600 MHz, DMSO) δ 12.25 (s, 1H), 7.84 (d, *J* = 7.8 Hz, 1H), 7.66 (d, *J* = 8.2 Hz, 1H), 7.42 (t, *J* = 7.7 Hz, 1H), 7.38-7.35 (m, 2H), 7.33 (t, *J* = 7.5 Hz, 1H), 7.30 (s, 1H), 7.11 (d, *J* = 7.9 Hz, 1H), 6.16 (s, 2H). ¹³C NMR (151 MHz, DMSO) δ 193.21, 176.94, 158.09, 149.21, 148.06, 140.82, 128.18, 127.78, 126.64, 124.96, 124.35, 123.95, 120.97, 120.87, 120.81, 114.15, 109.31, 108.92, 101.80. HRMS: calcd. For C₁₉H₁₁NO₄ [M]⁺ 317.0685; found 317.0688.

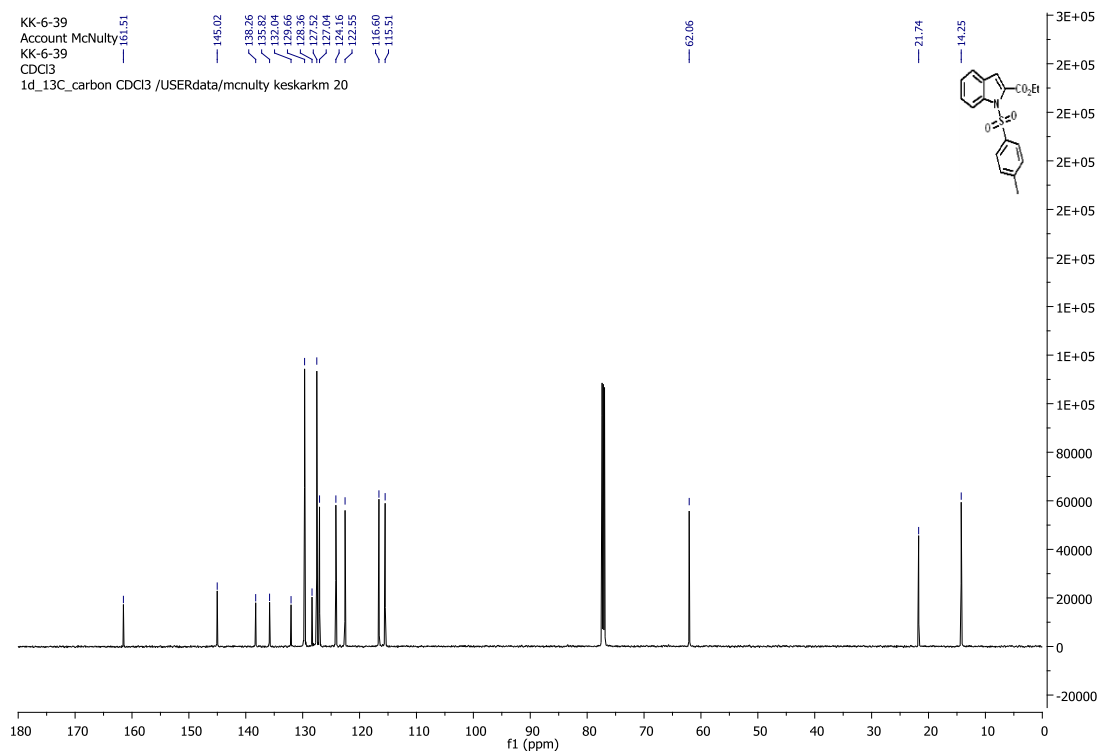
3-(4-nitrobenzylidene)cyclopenta[b]indole-1,2(3H,4H)-dione (Table 8-2, entry 7, 22):

Reaction carried out at room temperature. Isomeric ratio: >98: 02. M.p.: decomposes with melt > 300 °C. Major isomer: ^1H NMR (600 MHz, DMSO) δ 12.21 (s, 1H), 8.39 (d, J = 8.7 Hz, 2H), 8.05 (d, J = 8.6 Hz, 2H), 7.90 (d, J = 7.8 Hz, 1H), 7.65 (d, J = 8.2 Hz, 1H), 7.50 – 7.44 (m, 2H)) *including the olefinic -H*, 7.36 (t, J = 7.6 Hz, 1H). ^{13}C NMR (151 MHz, DMSO) δ 192.81, 176.83, 156.77, 147.54, 141.24, 140.83, 130.31, 127.41, 126.46, 125.28, 124.68, 124.48, 124.14, 123.48, 121.26, 120.68, 114.28. HRMS: calcd. For $\text{C}_{18}\text{H}_{10}\text{N}_2\text{O}_4$ $[\text{M}]^+$ 318.0645; found 318.0641.

8.6 NMR Spectra

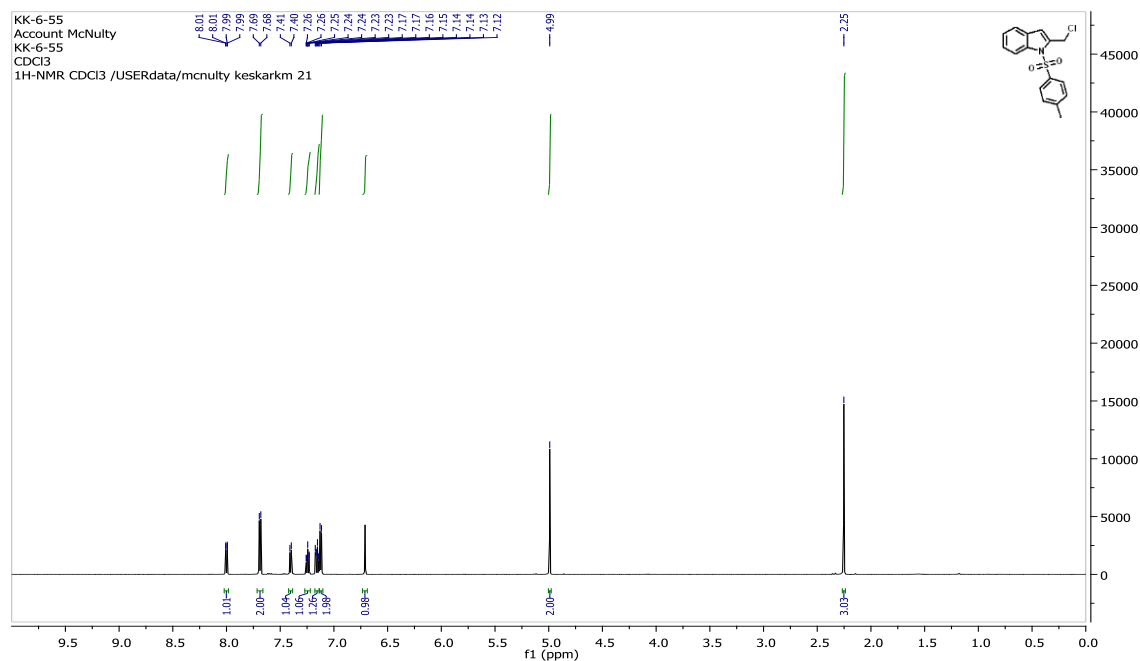
Ethyl 1-tosyl-1H-indole-2-carboxylate (Scheme 8-1, 8):

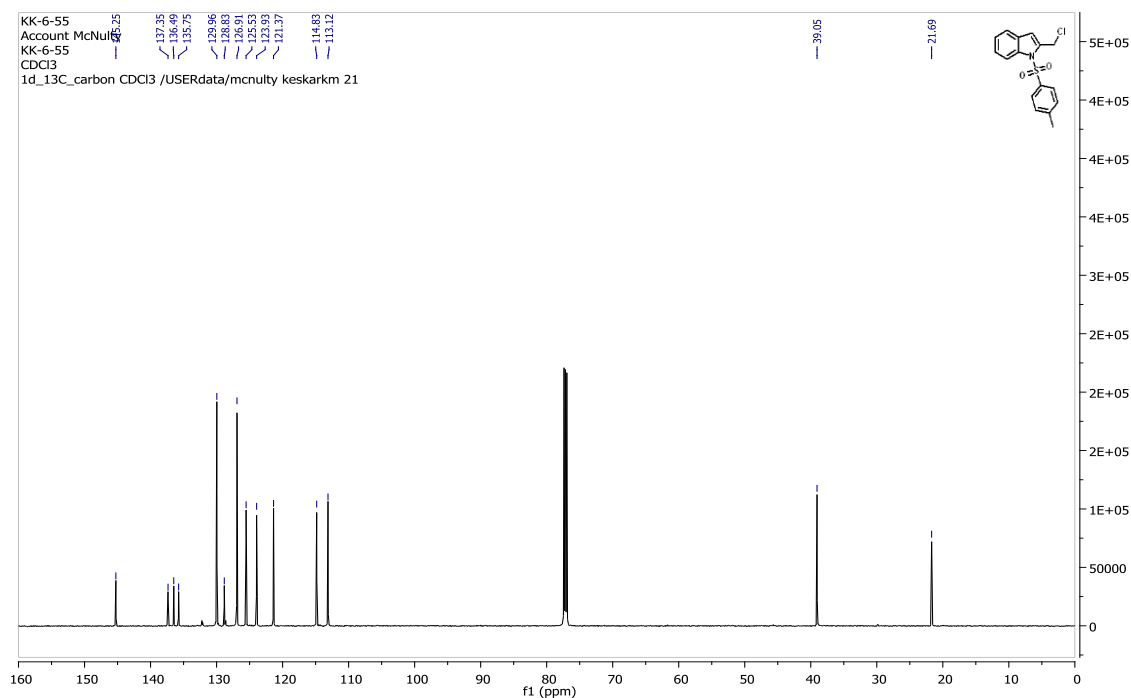




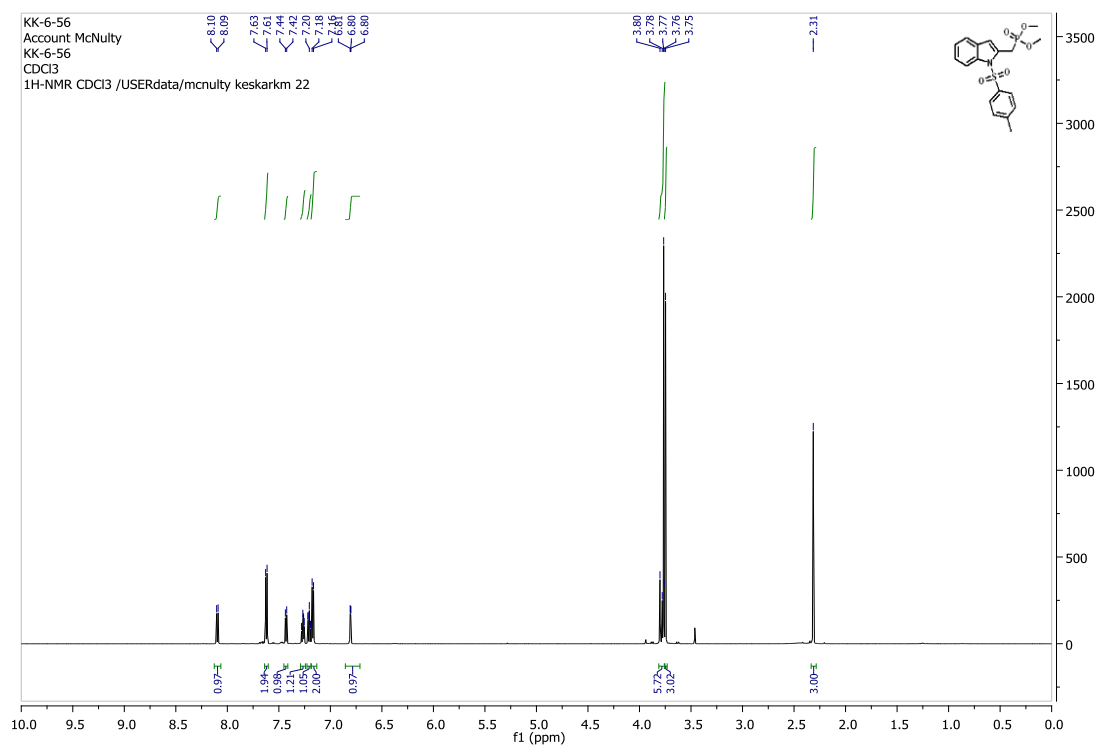
(1-tosyl-1H-indol-2-yl)methanol (9): See spectra in ref **14**

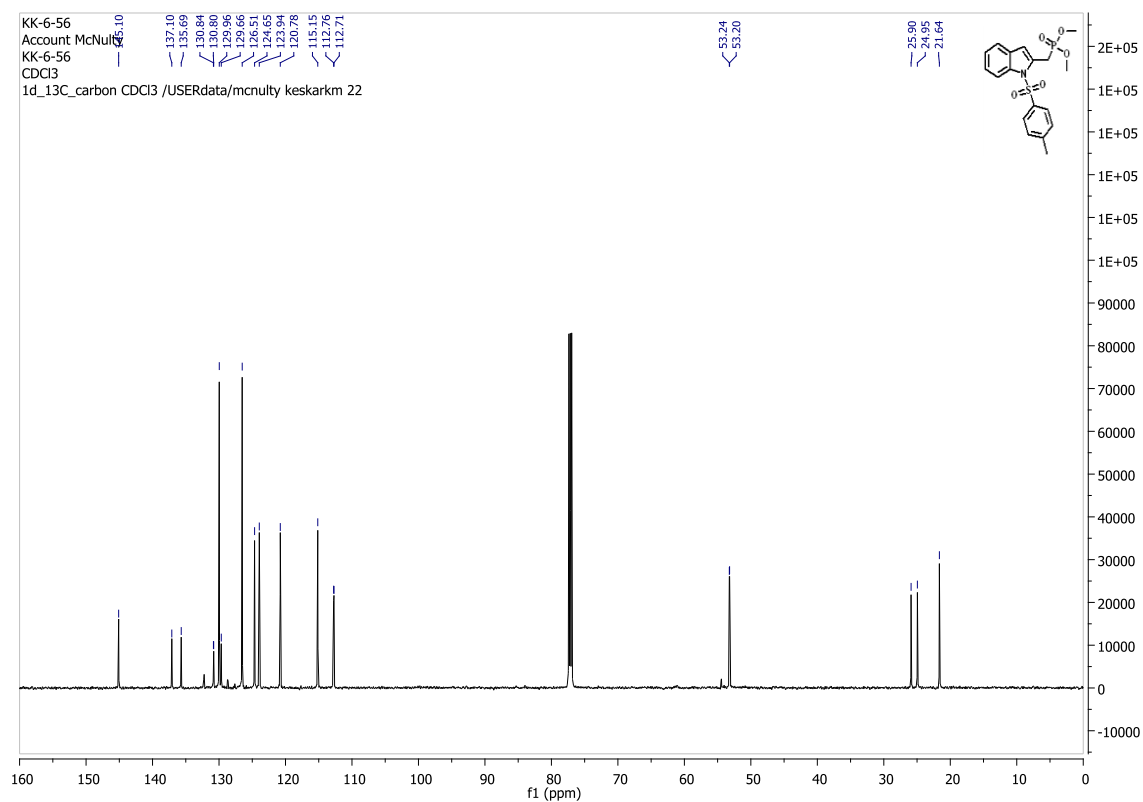
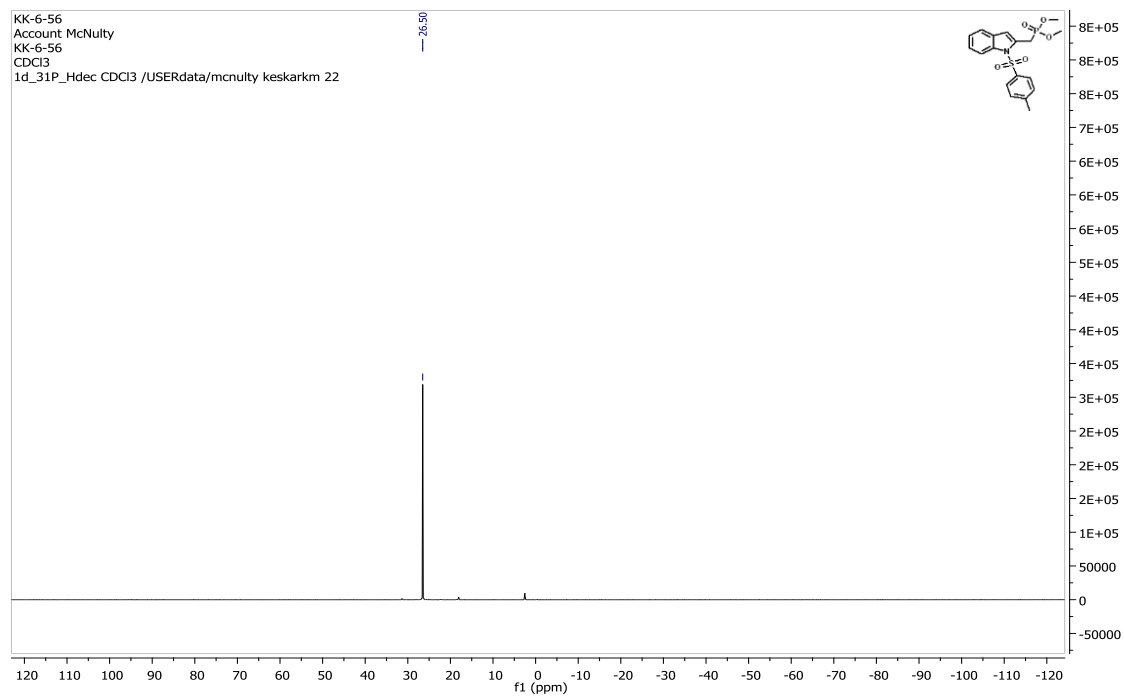
2-(chloromethyl)-1-tosyl-1H-indole (Scheme 8-1, 10):



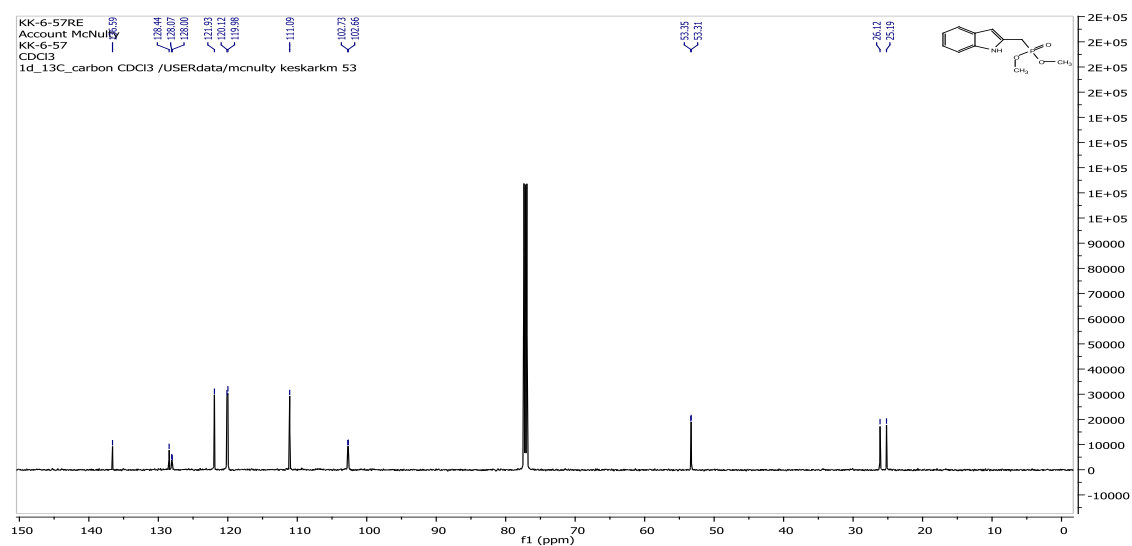
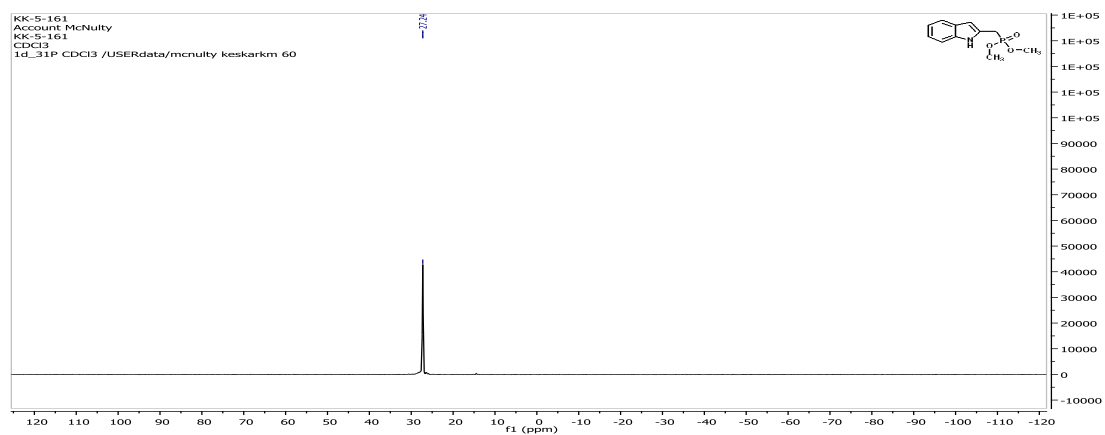
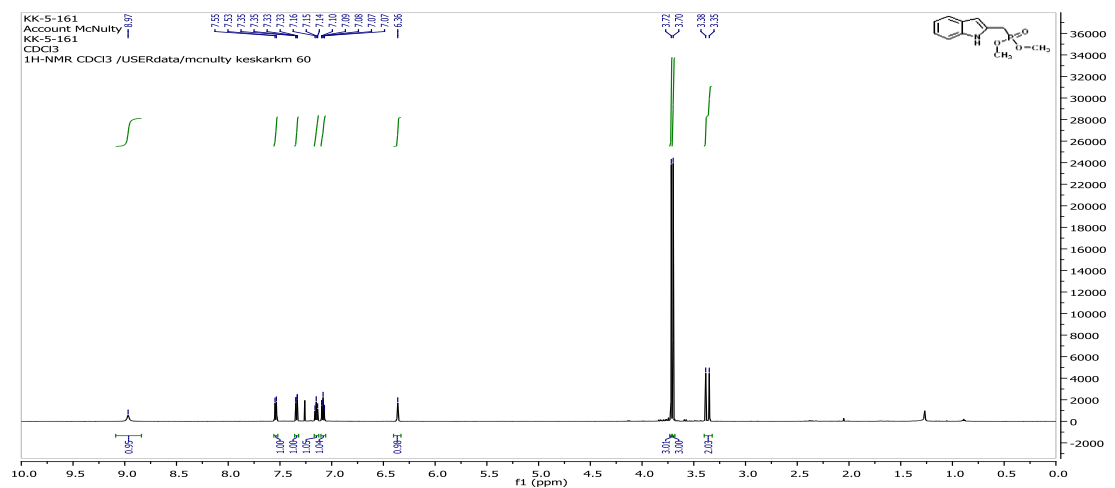


Dimethyl (1-tosyl-1H-indol-2-yl)methylphosphonate (Scheme 8-1, 11):

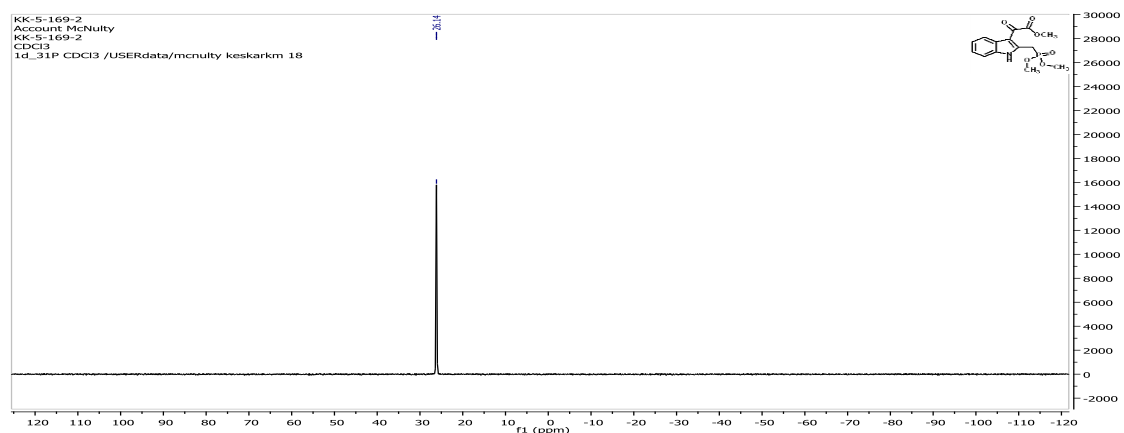
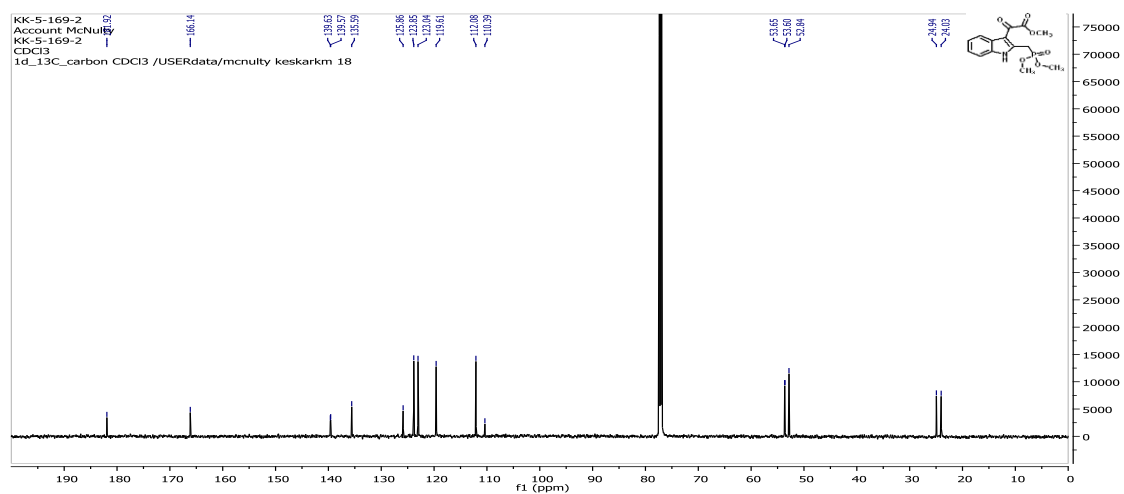
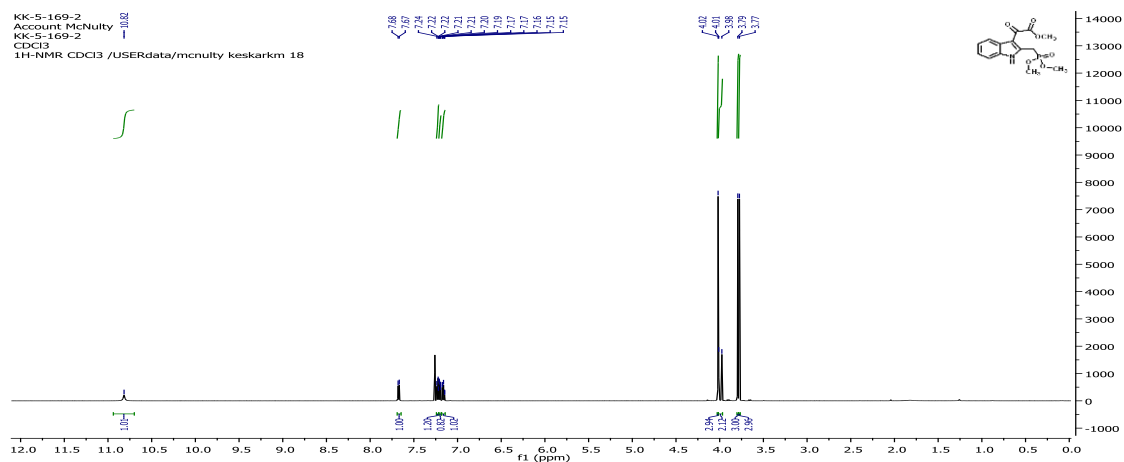




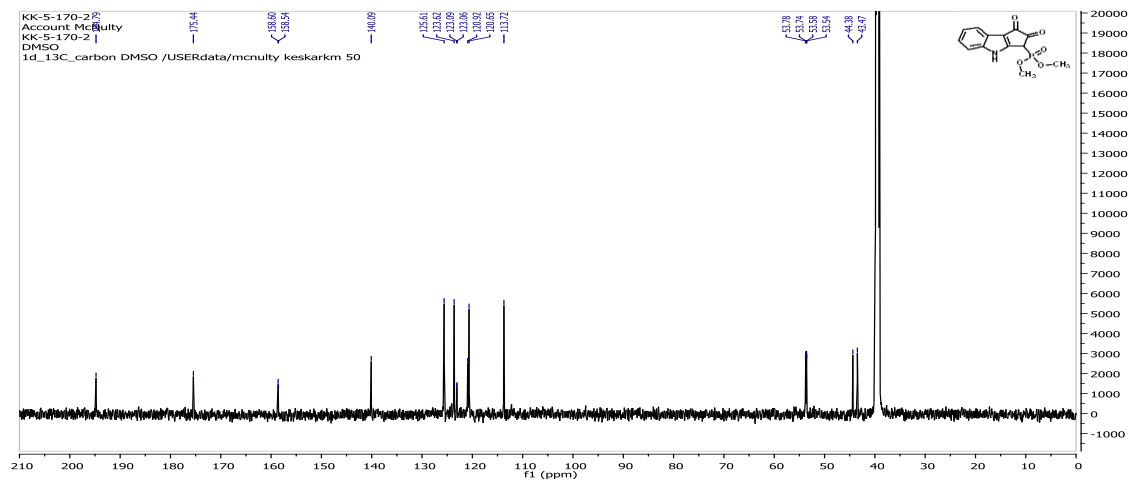
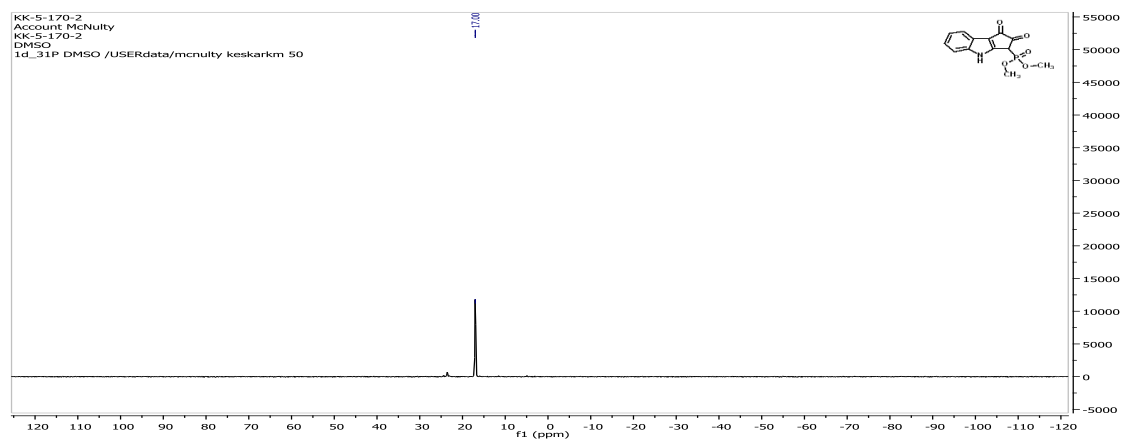
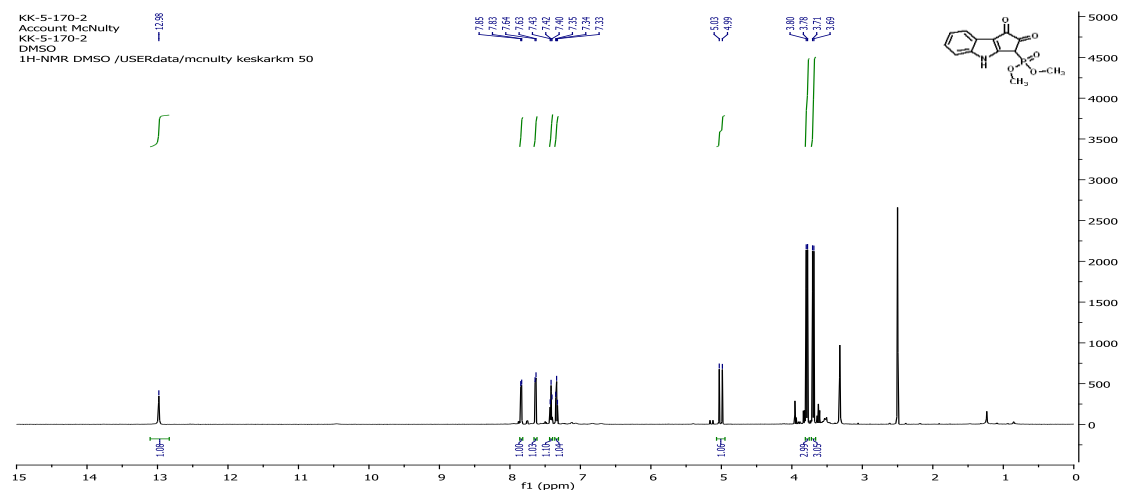
Dimethyl (1H-indol-2-yl)methylphosphonate (Scheme 8-1, 12):



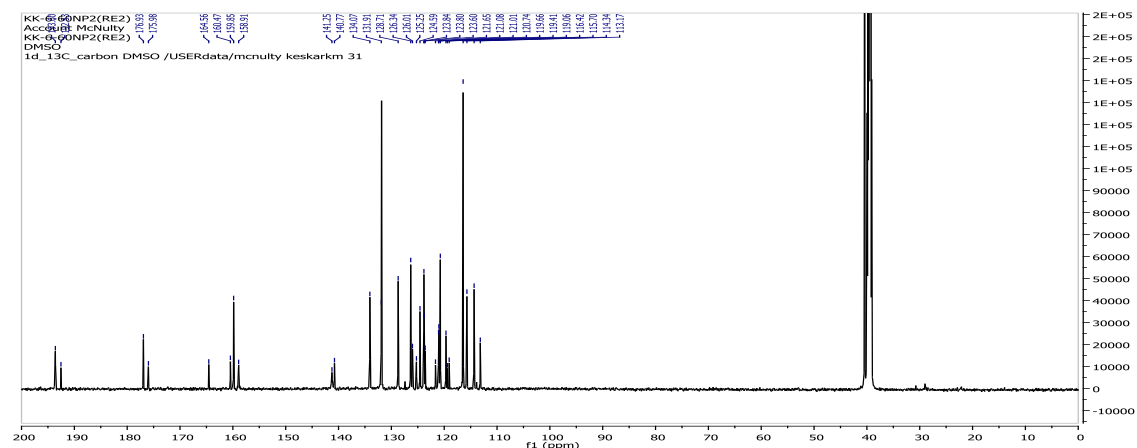
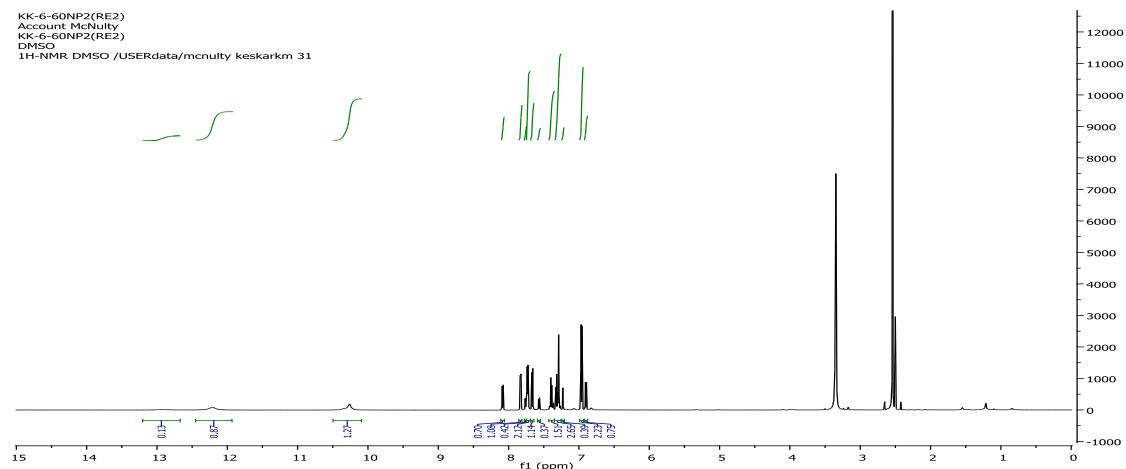
Methyl 2-(2-((dimethoxyphosphoryl)methyl)-1H-indol-3-yl)-2-oxoacetate
(Scheme 8-1, 14):



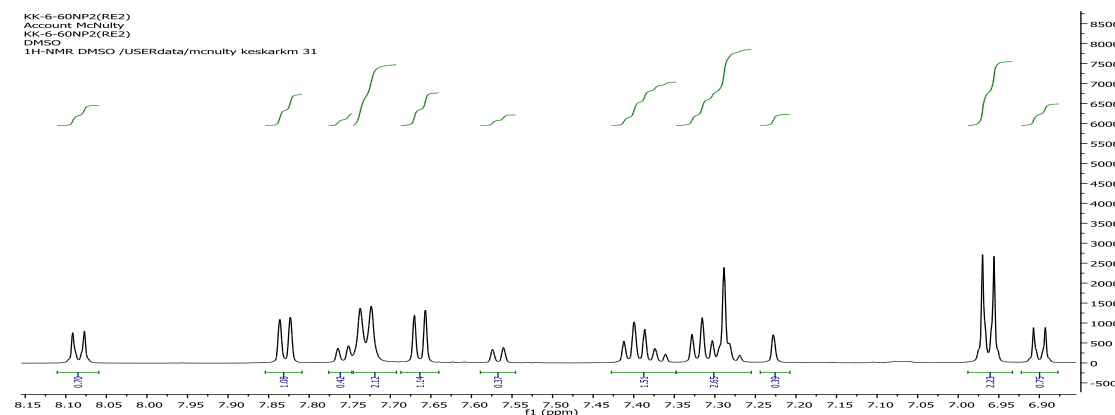
Dimethyl 1,2-dioxo-1,2,3,4-tetrahydrocyclopenta[b]indol-3-ylphosphonate
(Table 8-1, 15):



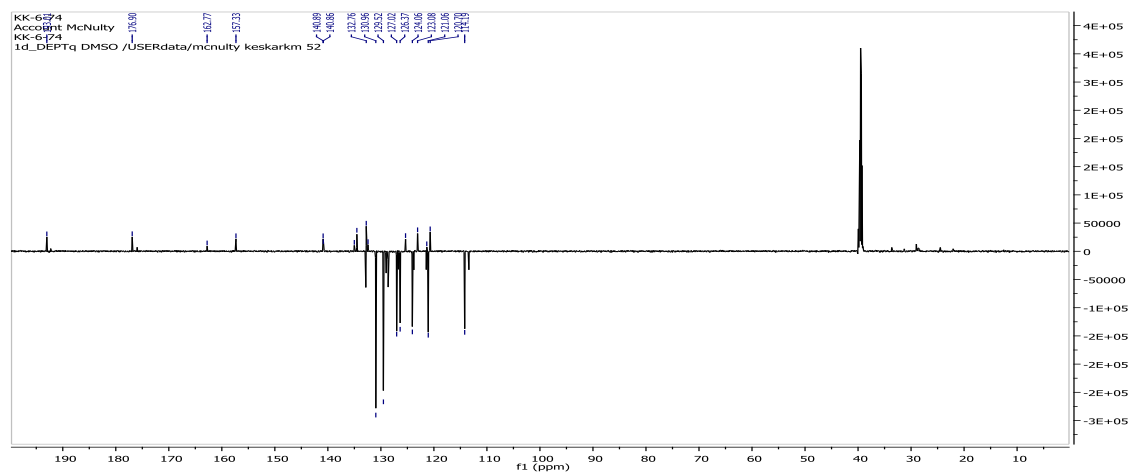
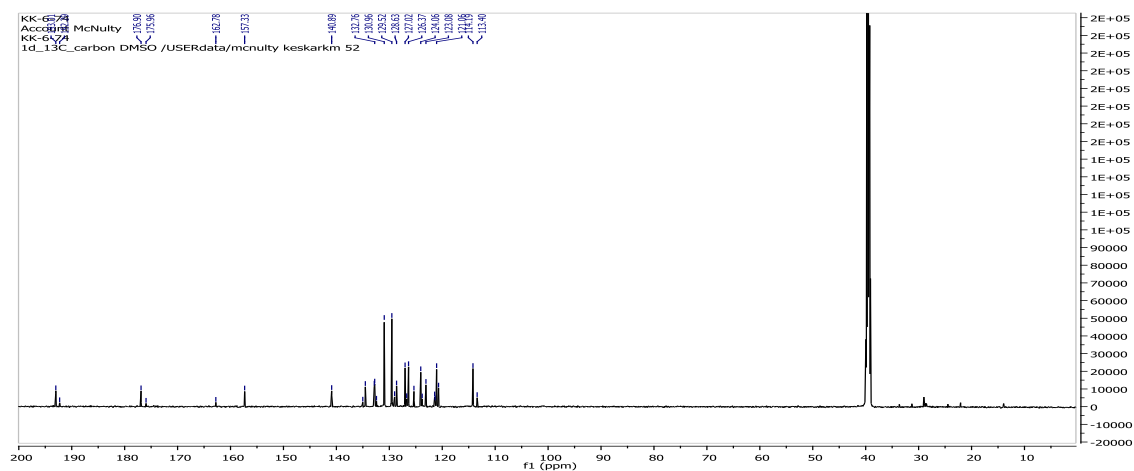
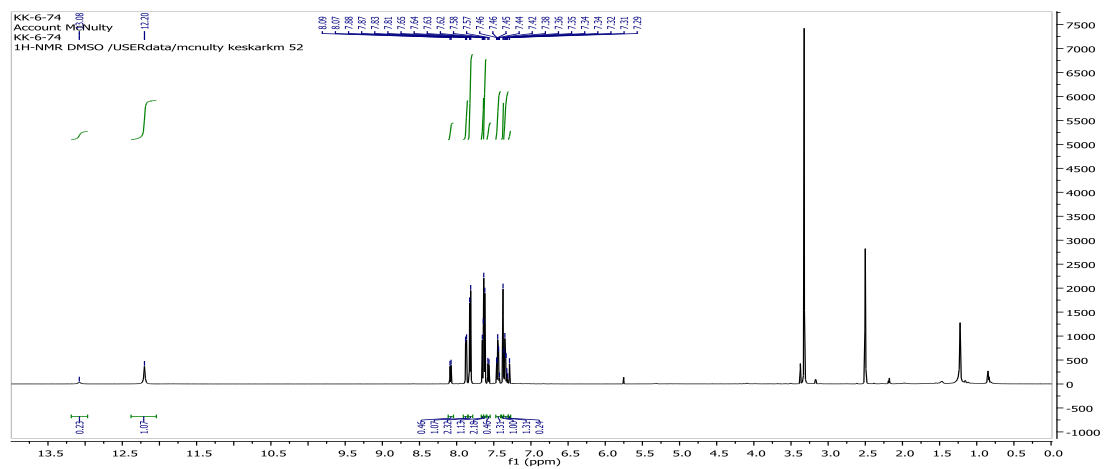
Nostodione A (Scheme 8-2, 1):



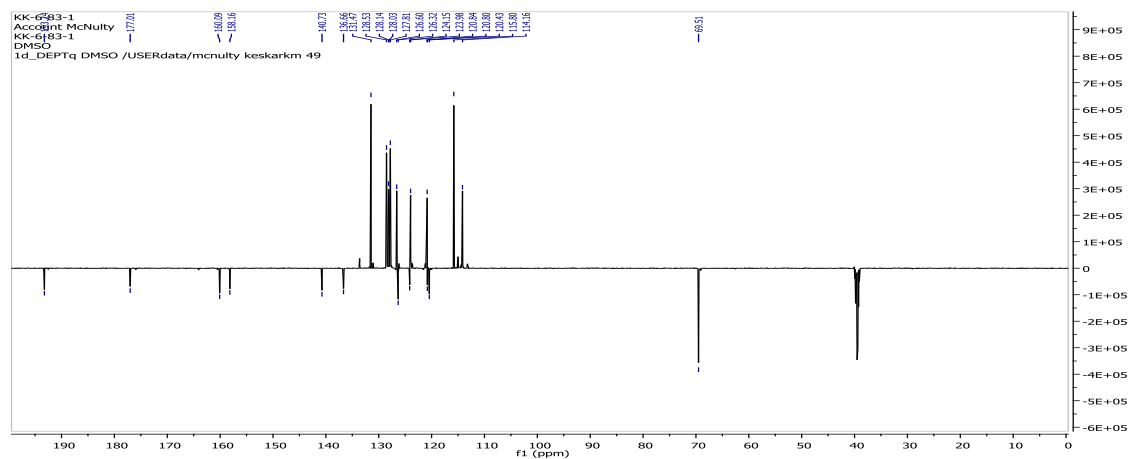
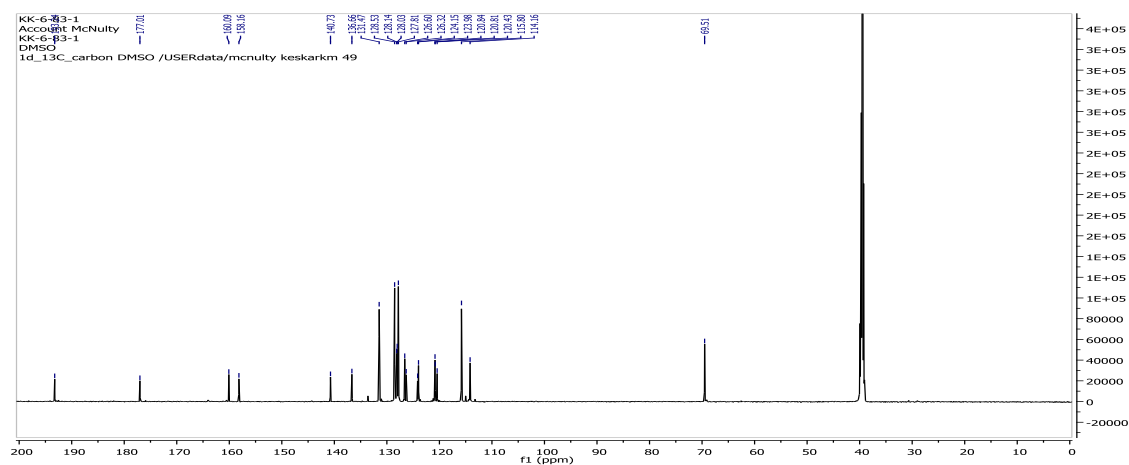
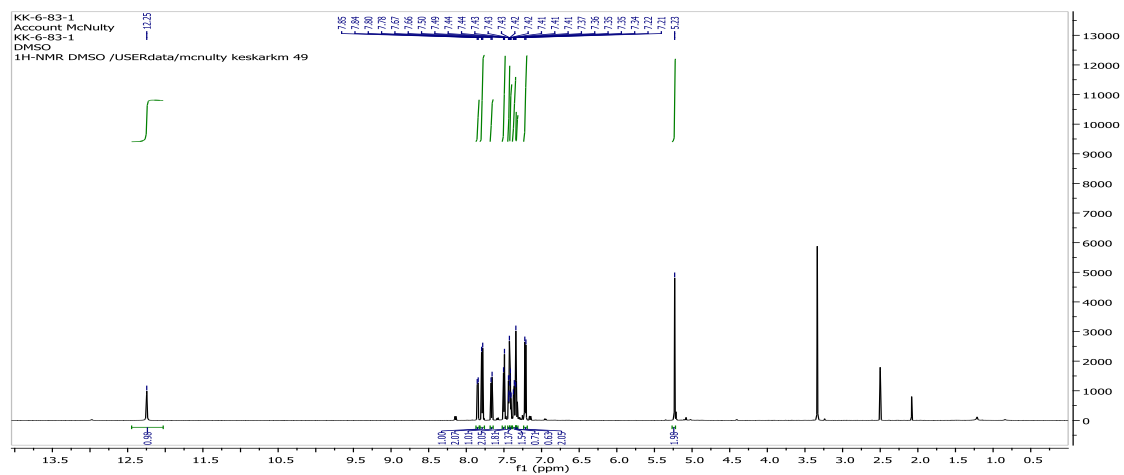
Nostodione A (1): (Aromatic Region zoomed ¹H-NMR)



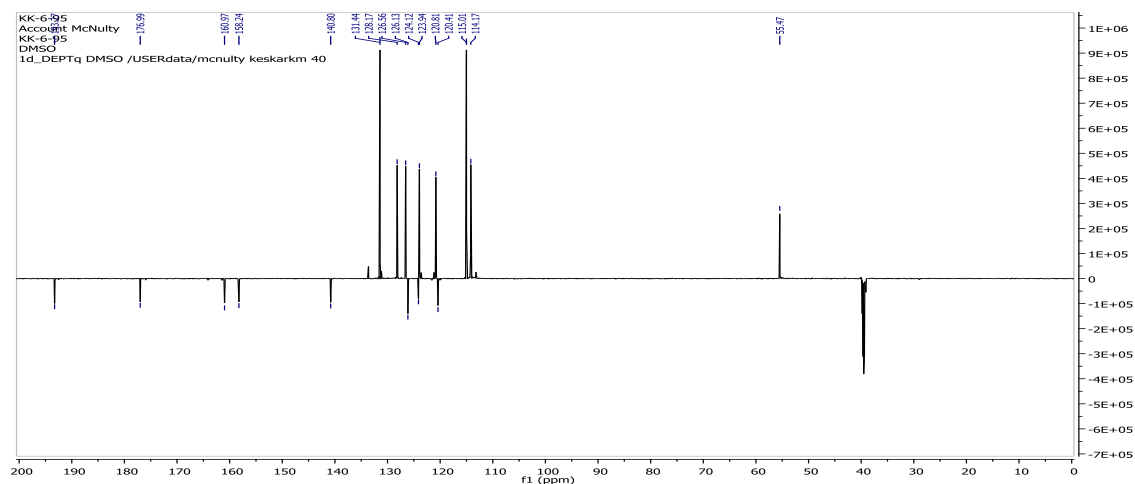
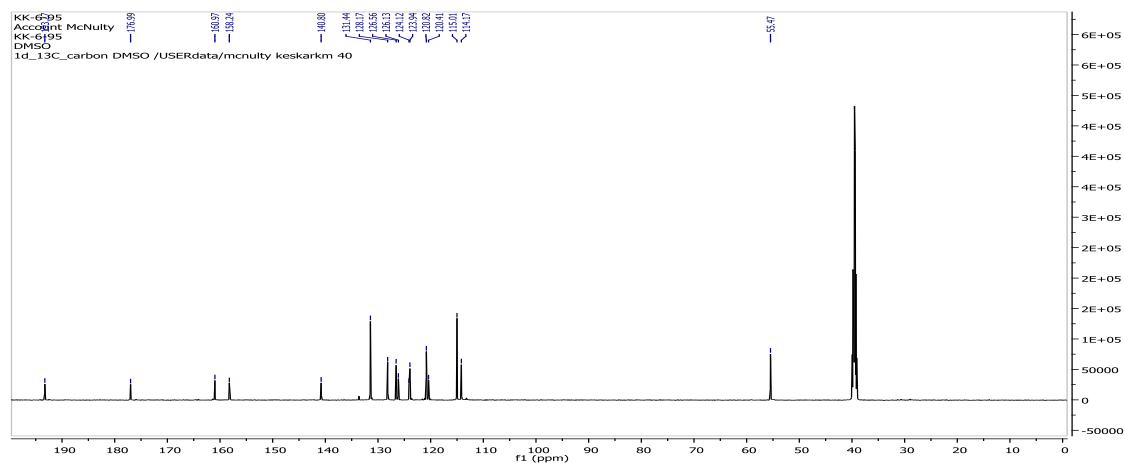
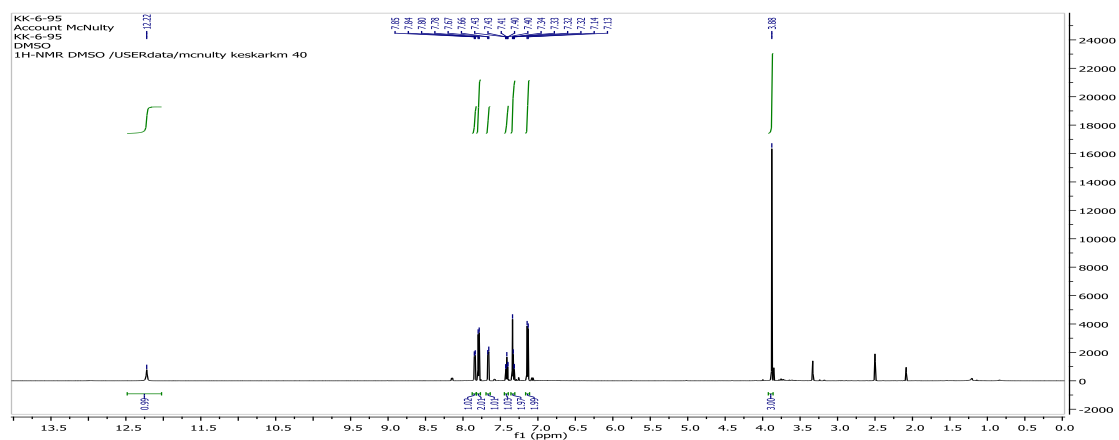
3-(4-chlorobenzylidene)cyclopenta[b]indole-1,2(3H,4H)-dione (Table 8-2, entry 2, 17):



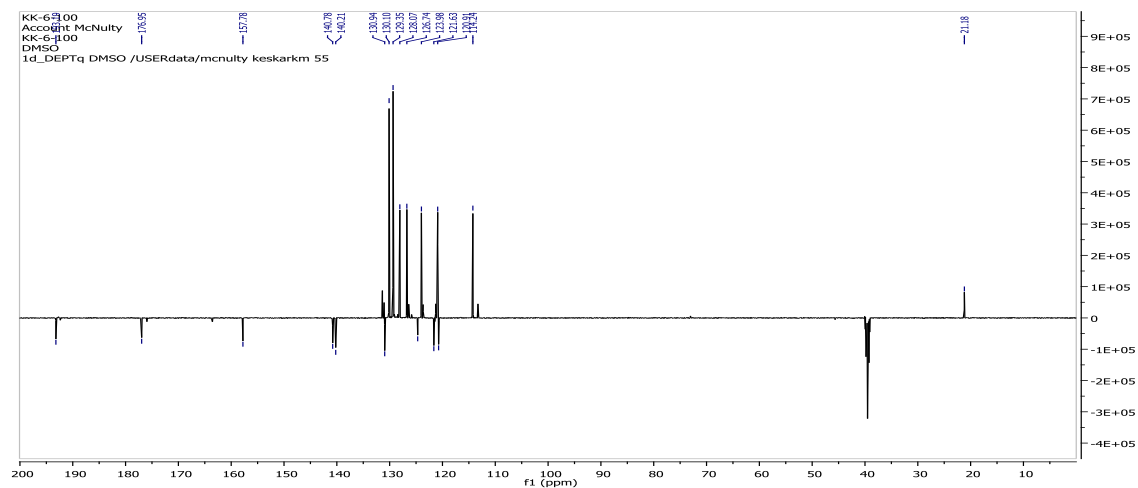
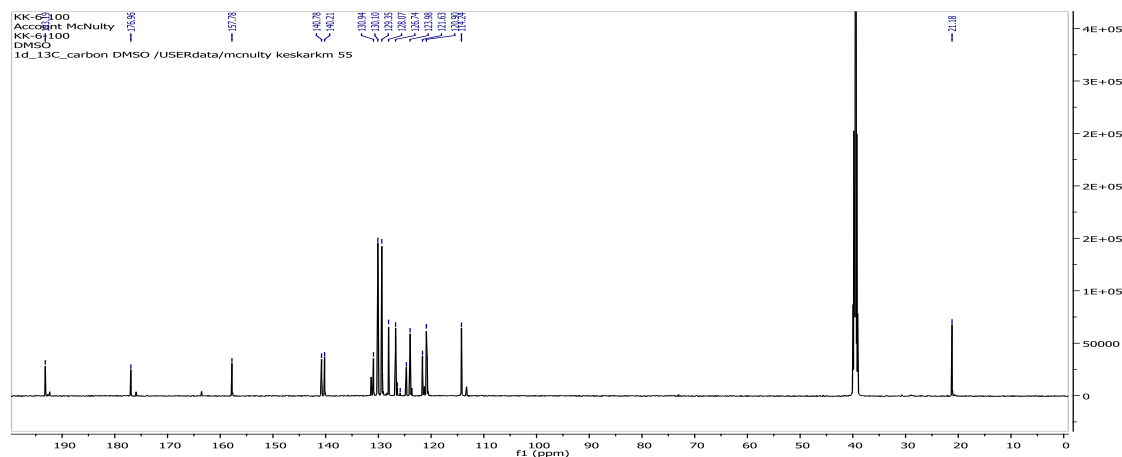
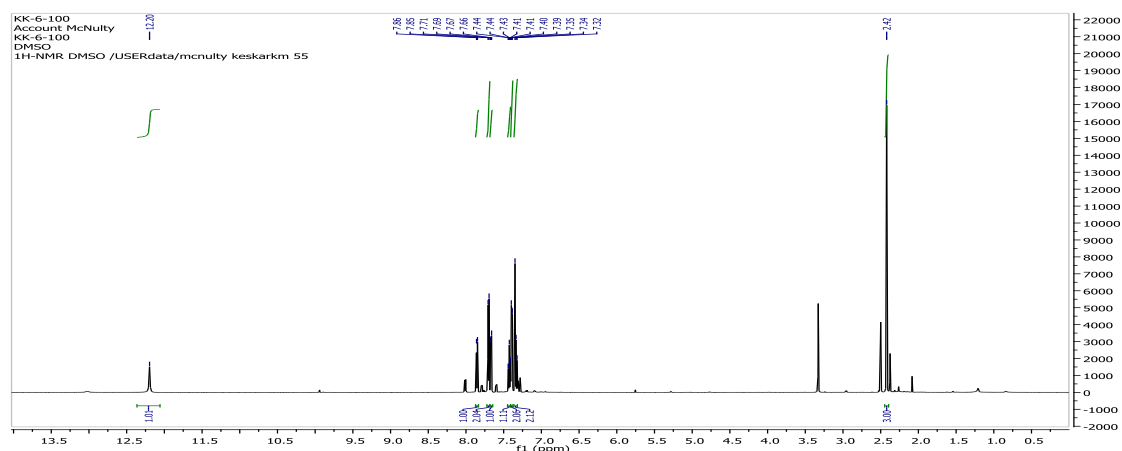
3-(4-(benzyloxy)benzylidene)cyclopenta[b]indole-1,2(3H,4H)-dione (Table 8-2, entry 3, 18):



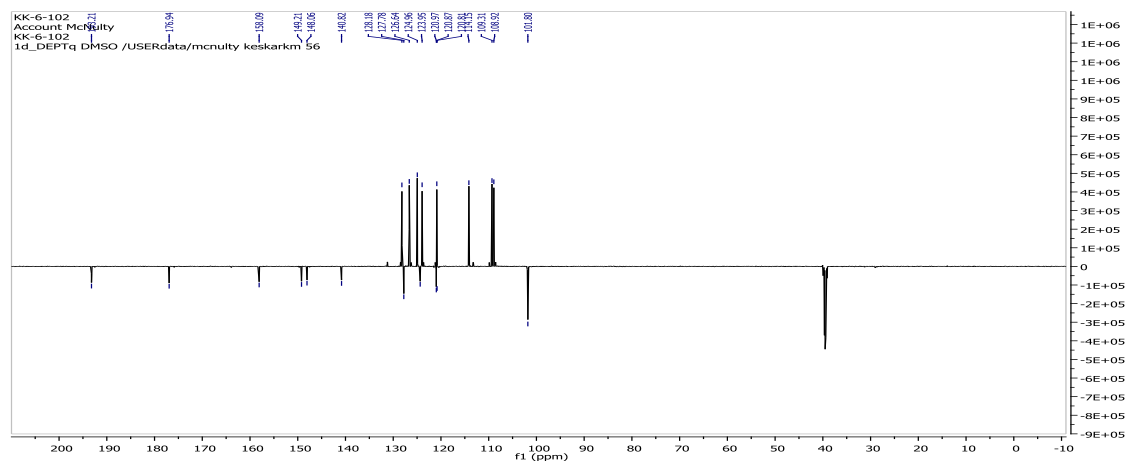
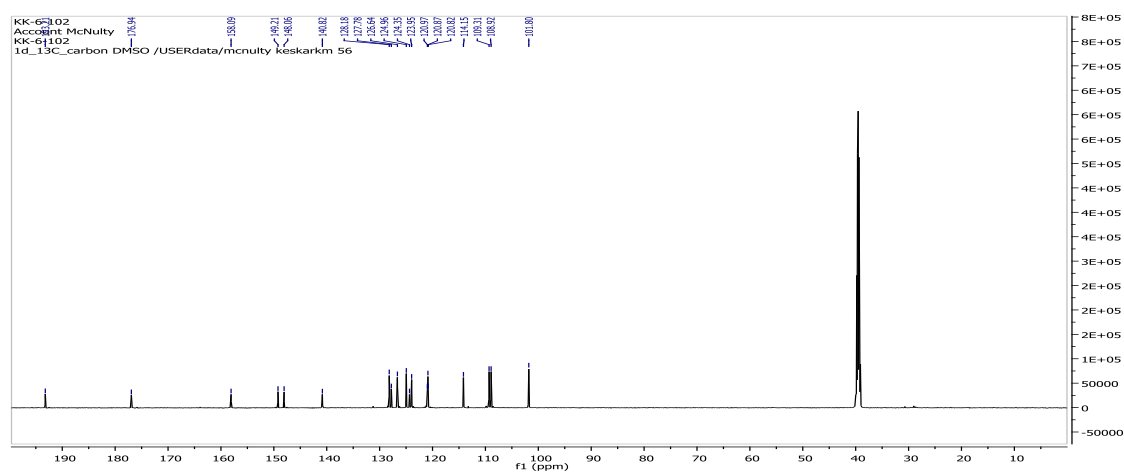
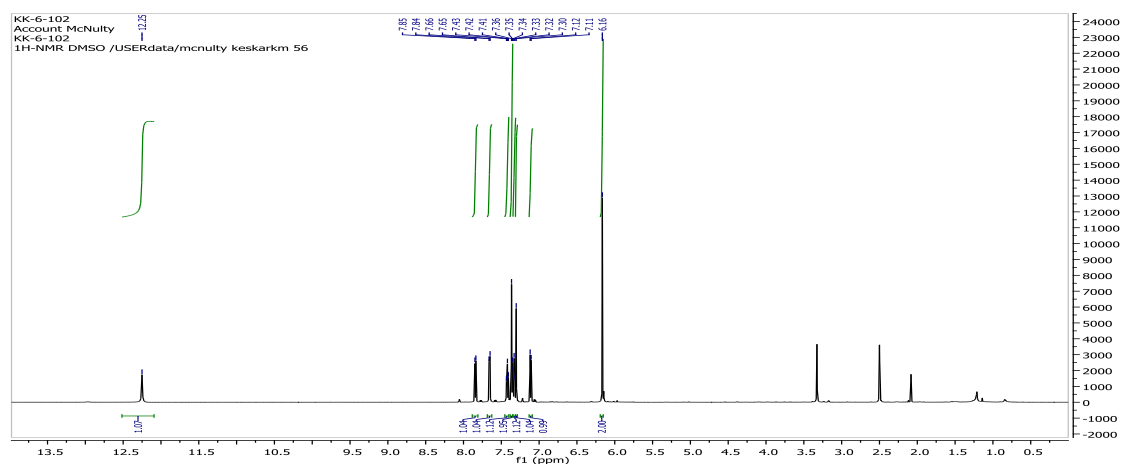
3-(4-methoxybenzylidene)cyclopenta[b]indole-1,2(3H,4H)-dione (Table 8-2, entry 4, 19):



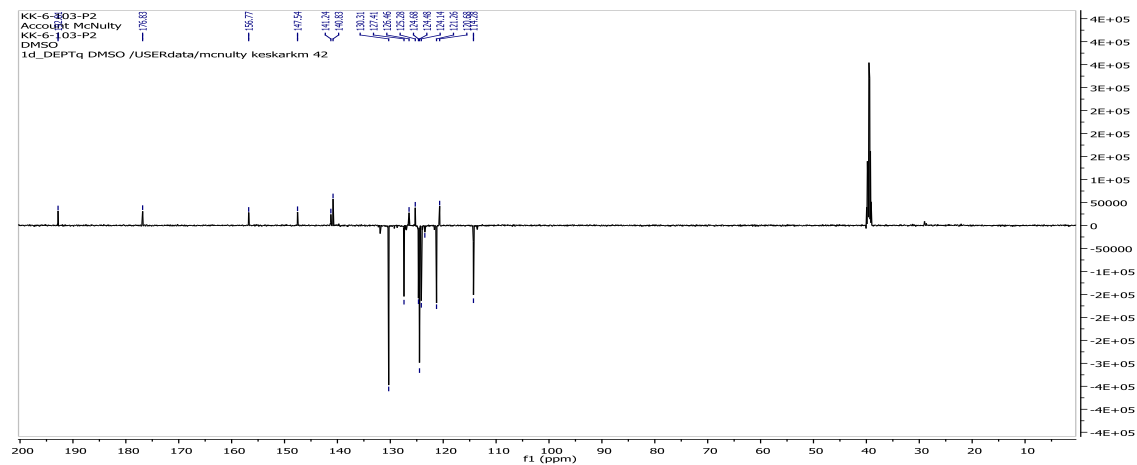
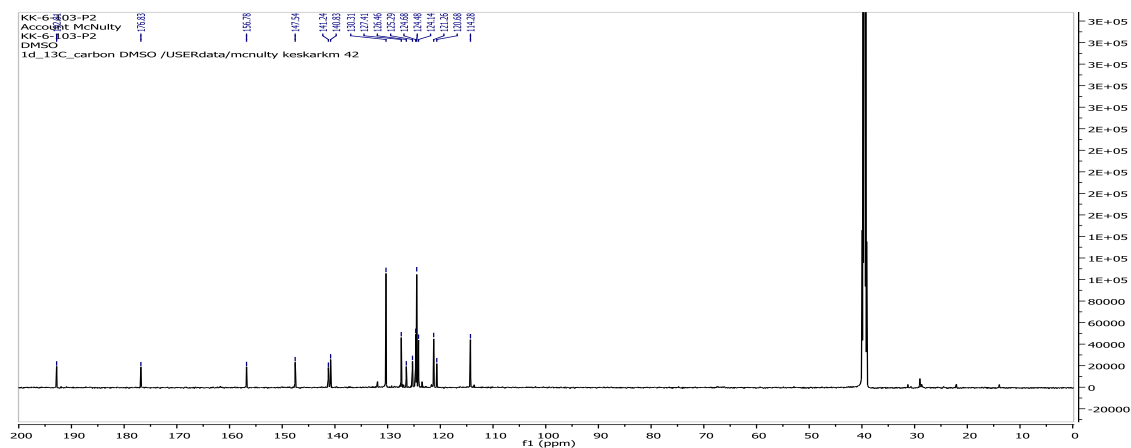
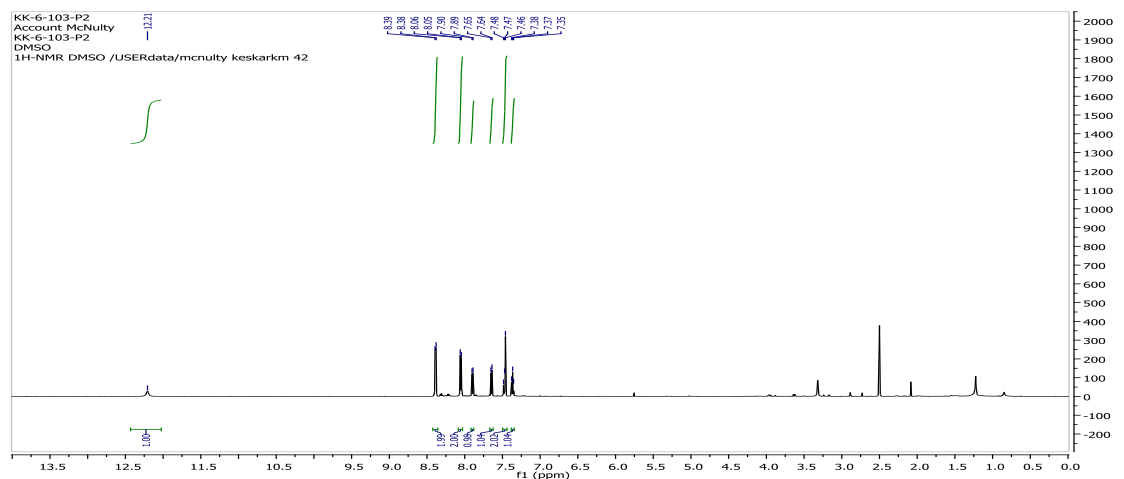
3-(4-methylbenzylidene)cyclopenta[b]indole-1,2(3H,4H)-dione (Table 8-2, entry 5, 20):

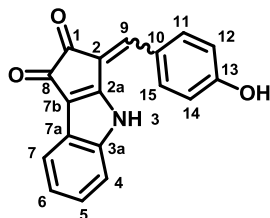


3-(benzo[d][1,3]dioxol-5-ylmethylene)cyclopenta[b]indole-1,2(3H,4H)-dione
(Table 8-2, entry 6, 21):



3-(4-nitrobenzylidene)cyclopenta[b]indole-1,2(3H,4H)-dione (Table 8-2, entry 7, 22):

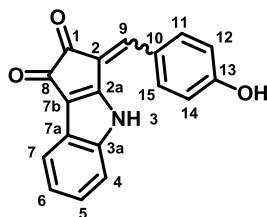


Nostodione A (Scheme 8-2, 1): ^1H -NMR and ^{13}C -NMR signals comparison

Comparison of ^1H -NMR and ^{13}C -NMR signals (δ) between reported^{6b} (Mårtensson), current synthetic approach and natural² nostodione A (**1**) in DMSO- d_6 : Major isomer

Position	Synthetic ^{6b}	Current Approach	Natural ²	Synthetic ^{6b}	Current Approach	Natural ²
1				193.4	193.60	193.5
2				119.1/119.4	119.06/119.41	119.2
2a				158.6	158.91	158.6
3	12.22 (br s)	12.21 (br s)	12.23 (s)			
3a				140.8/140.9	141.25/140.77	140.9
4	7.67 (dt, J = 8.1, 1 Hz)	7.66 (d, J = 8.1 Hz)	7.67 (d, J = 8.0 Hz)	114.2	114.34	114.3
5 ^a	7.40 (ddd, J = 8.3, 7.2, 1.3 Hz)	7.41 (ddd, J = 8.1, 7.2, 0.9)	7.41 (dd, J = 8.0, 7.9 Hz)	126.4	126.34	126.6
6 ^a	7.32 (ddd, J = 7.9, 7.2, 0.9 Hz)	7.33 (ddd, J = 8.1, 7.2, 0.9)	7.33 (dd, J = 7.9, 7.8 Hz)	123.9	123.84	124.1
7	7.84 (dt, J = 7.8, 1.1 Hz)	7.83 (d, J = 7.8 Hz)	7.83 (d, J = 7.8 Hz)	120.8	120.74	120.9

7a				120.9	121.01	121.0
7b				123.7	123.80	123.8
8				177.0	176.93	177.2
9	7.31 (s)	7.29 (s)	7.29 (s)	128.9	128.71	129.1
10				124.5	124.59	124.6
11,15	7.70 (AA'XX')	7.73 (d, $J = 8.2$ Hz)	7.69 (d, $J = 8.7$ Hz)	131.8	131.86	131.9
12,14	6.97(AA'XX')	6.96 (d, $J = 8.6$ Hz)	6.96 (d, $J = 8.7$ Hz)	116.5	116.42	116.7
13				159.9	159.85	160.1
13-OH	10.28 (br s)	10.26 (br s)	10.30 (s)			



Comparison of ^1H -NMR and ^{13}C -NMR signals (δ) between reported^{6b} (Mårtensson), current synthetic approach and natural² nostodione A (**1**) in DMSO- d_6 : Minor isomer

Position	Synthetic ^{6b}	Current Approach	Natural ²	Synthetic ^{6b}	Current Approach	Natural ²
1				192.5	192.53	192.7
2				119.1/ 119.4	119.06/1 19.41	119.2
2a				164.6	164.56	164.7

3	12.96 (br s)	12.93 (br s)	13.02 (s)			
3a				140.8/ 140.9	141.25/1 40.77	140.9
4	7.58 (dt, $J = 8.1, 1.0$ Hz)	7.57 (d, $J = 8.1$ Hz)	7.56 (d, $J = 8.1$ Hz)	113.2	113.17	113.3
5 ^a	7.37 (ddd, $J = 8.2, 7.3, 1.2$ Hz)	7.38 (ddd, $J = 8.2, 7.2, 1.1$)	7.37 (dd, $J = 8.1, 7.9$ Hz)	126.0	126.01	126.1
6 ^b	7.28 (ddd, $J = 7.9, 7.3, 0.9$ Hz)	7.29 (ddd, $J = 8.0, 7.1, 0.8$)	7.27 (dd, $J = 7.9, 7.7$ Hz)	123.6	123.60	123.7
7	7.76 (dt, $J = 7.8, 1.0$ Hz)	7.76 (d, $J = 7.8$ Hz)	7.76 (d, $J = 7.7$ Hz)	121.1	121.08	121.2
7a				121.7	121.65	121.8
7b				119.5	119.66	119.5
8				176.0	175.98	176.1
9	7.23 (s)	7.23 (s)	7.26 (s)	131.9	131.91	132.1
10				125.3	125.25	125.4
11,15	8.08 (AA'XX')	8.08 (d, $J = 8.7$ Hz)	8.08 (d, $J = 8.7$ Hz)	134.1	134.07	134.2
12,14	6.90 (AA'XX')	6.90 (d, $J = 8.7$ Hz)	6.89 (d, $J = 8.7$ Hz)	115.7	115.70	115.9
13				160.5	160.47	160.6
13-OH	10.35 (br s)	10.35 (br s)	10.35 (s)			

CHAPTER IX: Conclusion

In conclusion, we reported the synthesis and reactivity of two new well defined silver(I) acetate complexes ligated to 2-diphenylphosphino-*N,N*-diisopropylcarboxamide and 2-ditertiarybutyl-phosphino-*N,N*-diisopropyl-carboxamide ligands. Both of these complexes are stable at room temperature and completely soluble in organic solvents. We reported the first purely silver(I) catalyzed AAC reaction (AgAAC) of azides on to terminal alkynes with these homogeneous catalysts. The complex prepared from 2-ditertiarybutyl-phosphino-*N,N*-diisopropyl-carboxamide was found to possess superior reactivity and excellent thermal stability. The regioselective synthesis of a range of 1,4 substituted triazoles was achieved in excellent yield with catalyst loadings as low as 0.5 mol-%. We proposed a reaction mechanism involving continuous coordination of the phosphorous donor of the ligand to silver and proceeding through intermediates that allow coordination and polarization of the acetylide/azide to affect a stepwise mechanism.

We also described the first well-defined homogeneous intramolecular hydroamination reaction of 2-alkylanilines employing well defined silver(I) catalyst derived from 2-ditertiarybutyl-phosphino-*N,N*-diisopropylcarboxamide ligand. These reactions were found to occur smoothly at room temperature in methanol and dimethylformamide with loading as low as 1 mol-%. Exceptional thermal stability for this silver(I) catalyst was observed when the reaction was conducted in nonpolar solvents at higher temperature, with absolutely no silver metal precipitation. The reaction was shown to be first order in catalyst and the hemilabile nature of the ligand was shown to have a significant impact on the outcome of the reaction. A coherent catalytic cycle was proposed to explain the ligand effects on the mechanism of the reaction.

The rapid construction of a new hemilabile phosphine ligand family was achieved from the economical and readily available lactone phthalide. A

phthalide lactone opening approach allowed the incorporation of different amines in the hemilabile ligand architecture. These new ligands were found to be exceptionally air stable allowing for easy storage and handling. Pd-complexes prepared from these ligands were shown to readily activate hindered, deactivated aryl chlorides permitting efficient Suzuki-Miyaura cross coupling reactions in problematic cases.

We described a novel entry toward the synthesis of α -alkoxy-functionalized phosphonium salts from the direct reaction of acetals with short-chain trialkylphosphine hydrobromide salts. The synthesis of a range of both methoxycinnamates and α -alkoxy acrylates (*vide infra*) was achieved employing Wittig reactions of α -alkoxy-functionalized ylides. The reactivity of methoxycinnamates was explored by developing methodologies for the synthesis of 1,4,5-trisubstituted 1,2,3-triazoles. The thermal and solvent-less reaction of methoxycinnamates with benzyl azides provided regioselective synthesis of 1,4,5-trisubstituted 1,2,3-triazoles (cinnamyl triazoles) in fair to good yields. These cinnamyl triazoles were found to display potent aromatase inhibitory (AI) activity. Some of the most potent AI's which displayed 0.02 μ M activity, incorporate aryl halide residues at the positions mimicking the carbonyl substituents on the natural enzyme substrate.

The reactivity of the α -alkoxyacrylate was explored by carrying out the synthesis of a wide range of functionalized Indole-2-carboxylates. The reaction of the α -alkoxyacrylate (derived from paraformaldehyde), with *ortho*-iodoanilines proceeded according to the Heck-Jeffery Amination (HJA) protocol providing good yields of a mini-library of aryl-ring functionalized ethyl-2-indolecarboxylates. Several failed attempts under various conditions and investigation of the catalytic cycle with mechanistic probes, provided useful information regarding the mechanism, especially the lack of involvement of Pd(0) species under the HJA reaction conditions and the role of TBAB. Based

on these results, we proposed the possibility of a distinct catalytic cycle involving Pd(II)/Pd(IV), for this protocol.

The total synthesis of the cyanobacterial natural product nostodione A using previously described ethyl-2-indolecarboxylate was accomplished in eight chemical steps with a 21.6% overall yield. A diversity oriented approach involving a crucial intramolecular phosphonate acylation was used for the synthesis of nostodione A and its structural analogs. Late stage HWE reaction allowed us to incorporate a variety of aromatic aldehydes at the final stage of the synthesis and permitted us to assemble a mini-panel of nostodione A structural analogs in good yields for biological studies. Finally, the antiparasitic biological activity of nostodione A was reported for the first time and structure activity relationship allowed us to discover a valuable lead antitoxoplasmosis pharmacophore incorporating a 4-benzyloxy substituent on the nostodione A phenolic substituent.